final report

Project code: B.OJD.0031

Prepared by: R Whittington, D Begg, K Bosward, K de Silva, D Taylor

University of Sydney

Date published: December 2007

PUBLISHED BY

Meat & Livestock Australia Limited

Locked Bag 991

NORTH SYDNEY NSW 2059

Pathogenesis of OJD – Strategic Research Diagnosis and Prevention

Meat & Livestock Australia acknowledges the matching funds provided by the Australian Government to support the research and development detailed in this publication.

Abstract

Johne's disease is a significant international problem because of the direct impact on animal health and welfare and its possible public health implications. It is essential that Australia has the capacity to deal with diseases such as Johne's disease and this necessitates maintenance of expertise to work at international levels of competence. In this project new diagnostic test methods and advanced immunological, molecular biological and proteomic technologies were developed and applied to sheep for the first time. Industry will benefit from this work immediately as a new test for Johne's disease is ready to be validated in 2008. This will provide a result within 48 hours with accuracy equivalent to or greater than radiometric culture of faeces. Advances considered by MLA to have commercial potential are protected by provisional patent for the benefit of the livestock sector. Johne's disease potentially can be detected early in life and removed from a flock before causing harm or spreading. Research will continue to achieve this aim.

Acknowledgements

This report was made possible through the dedication and hard work of a large number of people who contributed to the OJD.031 project and associated projects that provided materials. The authors would like to thank PhD students Kate Bower, Sally Browne, Navneet Dhand, Sanjeev Gumber, Satoko Kawaji, Ian Marsh, Helen McGregor and Ling Zhong, for their contributions to the project and this report, parts of which will appear in other forms in theses. Technical officers Anna Waldron, Craig Kristo, Natalie Schiller, Eileen Risby, Pabitra Dhungyel, Geetanjali Dhand, Nobel Toribio, Rebecca Maurer, Nicole Carter and Reena Mehta worked tirelessly for this project. Lyrissa Di Fiore commenced as a post doctoral fellow with the project and is thanked for her substantial contribution to subprogram 3. David Emery commenced with the project as its Research Manager and provided strategic advice throughout. Marion Saddington provided expert administrative support to the project and supported all staff and students throughout its term.

The authors are very grateful to the following people who kindly provided reagents or resources that made this project possible: Dr Gregers Jungersen, National Veterinary Institute, Technical University of Denmark; Dr Jayne Hope, Institute for Animal Health, Compton, UK; Dr Ingrid Olsen, Department of Animal Health, National Veterinary Institute, Norway; Dr Garry Barcham, Centre for Animal Biotechnology, University of Melbourne; Dr Peter McWaters, CSIRO; Dr Hilary Warren, John Curtin School of Medical Research, Australian National University; Dr John Zaunders; Centre for Immunology, St Vincent's Hospital

Executive Summary

Johne's disease is a significant international problem because of the direct impact on animal health and welfare and its possible public health implications. It is essential that Australia has the capacity to deal with diseases such as Johne's disease and this necessitates maintenance of expertise to work at international levels of competence. This project identified new ways to tackle Johne's disease in the future. New diagnostic test methods and advanced immunological, molecular biological and proteomic technologies were developed and applied to sheep for the first time.

In order to control Johne's disease, more information is needed about the biology or pathogenesis of the disease. The biggest knowledge gaps are in the early stages of disease. The research program was planned following review of current research into tuberculosis, which was the closest relevant example. Throughout biology there is a basic pattern of information encoded in DNA and translated into proteins, which carry out instructions. The latest techniques in genomics and proteomics were applied to study the gene signals and protein effects, respectively. This was done for both the causative bacterium, and the sheep, in order to try to understand the interaction between the two. To enable research in the early stage of infection, a reliable method for experimentally inducing Johne's disease in sheep was developed, a world first.

Cell mediated immune responses play an important role in protecting sheep against *M paratuberculosis*. Many types of cell mediated responses were studied using newly developed methods. The simplest advance in diagnostic tests to measure CMI related to improvements to the existing gamma-interferon test. However, newly developed tests (Cell-ELISA and ELISPOT) for this cytokine were more sensitive. In addition a new assay to measure the cytokine IL-10 found responses as early as 4 months post infection, especially in sheep that had been exposed to *M. paratuberculosis* but not succumbed to disease. The process of apoptosis is believed to be important in the development of mycobacterial disease but there was no consistent difference between infected and uninfected sheep. However, a strong cell proliferative response was detected in the blood as early as 4 months following exposure to *M paratuberculosis*. This has the potential to detect infection in sheep within a few months after exposure. The specificity of all these tests will need to be confirmed to avoid false positive results. Specificity depends on the antigen used in the tests. To improve this aspect over 60 new proteins were discovered using state-of-the-art proteomic approaches. The proteins were specifically associated with the stress/dormancy response of *M. paratuberculosis*, which is thought to enable the organism to persist in the sheep for long periods. Some of the proteins were shown to stimulate an immune response during early infection which might have diagnostic significance. The genes of the sheep that respond during infection were also studied after developing new methods to do so. Many genes were differentially regulated. In a conceptual breakthrough, the genes that code for the molecules on the surface of cells which first recognize invading *M. paratuberculosis* (Toll-like receptors, TLR) were found to be switched on during early infection. These are engaged by microbial pathogens to initiate innate and adaptive immune responses.

Blood remains the most useful type of sample for detection of many types of disease. Proteins in serum were studied in order to find new biomarkers for Johne's disease using mass spectrometry. Analysis using these biomarkers achieved diagnostic sensitivities of 90-93% and specificities of 83-91% in discriminating between infected and unexposed animals. Methods for culture of *M.*

paratuberculosis from blood were also developed, but few sheep were found to have the organism in their blood in the early stages of the infection.

Industry will benefit from this work immediately as a new method for detection of *M. paratuberculosis* in faeces is ready to be validated in 2008. This will provide a result within 48 hours with levels of sensitivity and specificity equivalent to or greater than radiometric culture of faeces. This removes a major impediment to widespread use of faecal samples in diagnosis and surveillance. The other advances will take longer to mature, but all those considered by MLA to have commercial potential are protected by provisional patent for the benefit of the livestock sector. In the medium term the new antigens and the tests applicable to blood samples can be further investigated to ascertain levels of sensitivity and specificity. In the medium term all these new tests can be evaluated in other species including cattle, goats and deer. The new proteins may have application in new-generation vaccines for Johne's disease. They can be produced using genetic engineering and so would be much cheaper than the existing commercial vaccine. Cost is now emerging as a major impediment to widespread use of Gudair ® vaccine.

As a result of this project Johne's disease potentially can be detected early in life and removed from a flock before causing harm or spreading. This is a dramatic change in thinking as current tests are too insensitive to detect infection before it has spread. It may lead to renewed interest in control programs if animal health regulatory authorities and public health agencies deem this to be necessary. If public health concerns persist and impact markets, it will be possible to apply tests to determine prior exposure to *M. paratuberculosis.* This will certainly be possible at flock level and may also be possible at individual animal level with further research.

To achieve these advances, a group of young scientists was assembled at Camden after an international search. They joined technical officers, PhD research students and permanent research staff at the Faculty of Veterinary Science. The University of Sydney added additional scholarships to enable international PhD scholars to join the research program. Eight PhD students undertook studies through direct or indirect involvement with this project. Three have already completed their degrees and are now engaged in employment that services the livestock sector. This is a vital contribution to help redress the skills-shortage in Australia. Biological samples that had been archived from earlier research projects conducted under the National Ovine Johne's Disease Control Program were used. This added value to earlier projects and further reduced the cost of the new research.

Johne's disease remains a difficult problem and without ongoing basic research at an international level will not be successfully controlled. There are parallels between the needs in Johne's disease research and those in tuberculosis in humans, which is caused by a related bacterium, *M tuberculosis:* "the TB vaccine development program include an assortment of tasks such as identifying mechanisms of host defence, improving animal models and conducting Phase 1/II trials over a period of 20 years. There is little certainty in the time span chosen to achieve these goals, but there has been definite progress made in many of the tasks" (Izzo et al (2005) NIH pre-clinical screening program: overview and current status. Tuberculosis 85:25-28). With this background it is vital to note that the aims of Johne's disease research programs worldwide will have the same challenges and difficulties as those for tuberculosis. The current OJD.031 project must be considered as a first step; as the first integrated multidisciplinary project of its kind in the world it has made remarkable progress.

Contents

1 Background

1.1 Context of this project

1.1.1 Historical background

OJD was introduced to Australia in the 1950s and then spread slowly as is typical of a mycobacterial disease. However, by 1994 there were increasingly frequent reports of serious losses in flocks in NSW, leading to calls for a national eradication program. By 2001 ovine Johne's disease was an intractable problem at farm and political levels. Spread of the disease continued despite stringent regulatory measures and in the absence of compensation for affected producers, led to severe divisions within the industry. Research on eradication of the disease by destocking suggested that this would not be possible for many producers. The reasons included difficulties in sourcing healthy replacement stock, lack of tests to accurately certify replacement stock, and uncontrolled spread of the infection from neighbours. There was clearly an urgent need for better diagnostic tests. The main requirement was for a test that could detect infection in young sheep before the onset of faecal shedding. The test needed to be sensitive, specific, accurate and cost effective. In particular it needed to be able to distinguish an active infection from one that had died out as it was believed that some sheep could recover from infection. Accurate identification of early infection at the individual animal level would enable a new approach to eradication, that of test and cull. This had proven to be very effective in reducing the impact of Johne's disease in cattle, but has not led to eradication of the disease because tests (ELISA, faecal culture) were not sufficiently sensitive; early infection was not detected. Test and cull was not possible in sheep for another reason: the high cost of existing tests relative to individual animal value. New automated technology platforms would be needed if tests were to have wide application in the sheep industries. Therefore it was hoped that vaccination would play a large role in reducing losses due to *M. paratuberculosis*.

1.1.2 Vaccination against Johne's disease

Vaccination is now known to be an important, cost-effective preventative measure. Results of a field trial (OJD.009) indicated that inoculation of inactivated *M. paratuberculosis* in oil (the Gudair ® vaccine) induces both antibody and interferon-gamma production and the vaccine was initially registered by the APVMA on this basis. Vaccination with Gudair ® appears to be a useful means of delaying onset of disease in an infected flock and modelling suggests that this will lead to reduced transmission and a marked reduction in within-flock prevalence of infection over a 10 year period. However Gudair ® vaccine does not prevent infection and will not work effectively if given to adult sheep. In general, inactivated vaccines require repeated administration for sustained efficacy but killed mycobacterial cells in oil adjuvant produce severe injection site reactions if doses are repeated. As Gudair ® is useful only if given to lambs it needs to be used over at least a 5 year period before the effects of the disease diminish in all age classes in a flock. There is an urgent need for a better vaccine or therapeutic for ovine Johne's disease. However, the Gudair ® vaccine trial has given indications that the early pathogenesis of infection can be modulated.

In contrast, vaccine strategies for human tuberculosis have focussed on live, attenuated vaccines and there are few surprises in the published approaches. Although still principally conceptual and lacking hard efficacy data, new vaccines involve manipulations or complementation of BCG, novel attenuation of *M. tuberculosis*, or other recombinant, intracellular bacterial vectors expressing promising *M. tuberculosis* antigens. A new Phase 1 clinical trial complementing BCG with MVA85A vaccine has recently commenced. Subunit vaccines using antigen 85 (fibronectin binding protein) and Hsp 60 have induced protection in mice, though not greater than that provided by BCG. Human

vaccine development is hampered by the lack of suitable challenge models, lack of commercial interest from long lead times and ethical and legal complexities of human trials. Therefore, fundamental *M. paratuberculosis* vaccine research with meaningful trials in a well-characterised, outbred sheep model is ideally placed to add substantial value to the human research and clinical efforts. The concept of therapeutic vaccination is appropriate for both tuberculosis and Johne's disease due to putative infection in the immediate post-natal period, that is, many animals have been exposed or are infected before the opportunity to vaccinate.

1.1.3 Human disease and veterinary public health

The resurgence of human tuberculosis in healthy and immunocompromised patients together with the debate over a putative causal association of *M. paratuberculosis* with Crohn's disease have revived efforts to discover new methods of diagnosis, control, treatment and prevention of mycobacterial infections. For food safety, countries exporting livestock or livestock-derived commodities have determined that competitive advantages will accrue to those with reliable market assurance programs (MAPs) to guarantee freedom from *M. paratuberculosis*. Australia is one of these, having declared *official freedom* from *M. bovis* in 1997 after a concerted eradication campaign. The potential impact on meat and milk consumption through public misunderstanding of the Crohn's/Johne's issue is great. Although existing diagnostic tools and regulatory programs will be able to reduce the prevalence of Johne's disease affected flocks and herds over time, freedom from Johne's disease cannot be guaranteed. Better diagnostic tests will be required if this becomes an aim for veterinary public health authorities.

1.1.4 Industry context

In 2001 the National OJD Control Program (NOJDP) was only part way through its six year lifecycle, but MLA recognized that it was heavily focused on existing tools and sought to answer questions deemed to be important in the 1990s, using tools that had been in existence for even longer. It did not provide for basic research, and could not address problems that might arise if basic presumptions about the disease turned out to be incorrect. This led to revision of the business plan and a general call for a basic research program to take advantage of new technologies, particularly DNA-based tests, proteomics, genomics and advanced immunology techniques, in vitro and in vivo models. MLA convened a workshop in November 2001 which led to a series of recommendations; these were used to develop this research program. By 2002 it was clear that OJD could not be eradicated, that prevalence was higher than expected, that spread would likely continue, and that vaccination would be critical to minimise current losses on heavily affected farms. Meanwhile public health concerns about *M. paratuberculosis* promulgated by some sectors of the medical research community necessitated on-going efforts to minimise the occurrence of the organism in agriculture, despite lack of conclusive evidence for a link between Johne's disease in animals and Crohn's disease in man. This is the background against which project OJD.031 commenced.

1.1.5 Knowledge base for Johne's disease

Due to the long incubation period for OJD, most of the knowledge concerning the pathogenesis or actual process of the disease comes from studies on animals in advanced stages of the disease, either naturally infected or infected experimentally with large doses of the organism. Consequently, almost all of the information about earlier stages of infection has been derived indirectly or extrapolated from other diseases caused by mycobacteria in man and animals. From a diagnosis and vaccination perspective, we lack knowledge about the most important stage of the disease.

1.1.6 Tests for Johne's disease

The diagnosis and control of *M. paratuberculosis* is thwarted by an inability to reliably detect early infection. While the specificity of culture tests and ELISA approaches 100%, the sensitivity of most tests is less than 50% on average in individual animals and in the early stages of disease is less than 5-10%. This seriously compromises the negative predictive value of such tests, which are useful mainly as flock tests and even then only if very large numbers of animals are tested. Pooled faecal culture (PFC) is the only cost effective on farm flock test. It has high sensitivity, but is not appropriate for detection of early infection. Animals that have tested negative in PFC may later commence to shed *M. paratuberculosis* in faeces. For this reason repeated testing is required to increase the confidence about a particular flock.

1.1.7 This project builds on a body of research from animals and man

The current suite of tests has been largely adopted from those successfully used for *M. bovis* and *M. tuberculosis;* although unlike these *M. paratuberculosis* is an intestinal pathogen. However, the clinical, biochemical and molecular pathogenesis of uptake, intracellular parasitism and alteration of phagocyte physiology by cellular moieties from *M. tuberculosis* has been widely studied and has much to offer research on *M. paratuberculosis*. New technologies have facilitated this research at a time when multi-drug resistant strains of *M. tuberculosis* are causing a serious resurgence of tuberculosis cases worldwide.

Since diagnostic tests are required for early diagnosis and measures to halt transmission of infection must also prevent shedding of the organism, this research program focuses on the early pathogenesis of OJD in lambs. The advent of new technologies provides unparalleled opportunities to maximise discoveries arising from intimate knowledge of host-pathogen interactions. Given that this basic knowledge is largely lacking for OJD, this program seeks to redress this deficit and apply the newer technologies to crucial stages in the pathogenesis of the infection to optimise the chances to generate improved diagnostic tests and preventative strategies for the sheep industries. The principle that key pathogenetic processes and targets can be subjected to either chemical or immunological attack provides dual possibilities for treatment. It is appreciated that the project is high risk, but the proposal is underpinned by collaborative field studies and research personnel with proven credentials and skills in ruminant-pathogen immunology and isolation, culture and molecular diagnosis of *M. paratuberculosis*.

1.1.8 Research plan

The project was designed around four interacting subprograms, which are illustrated in the following figure.

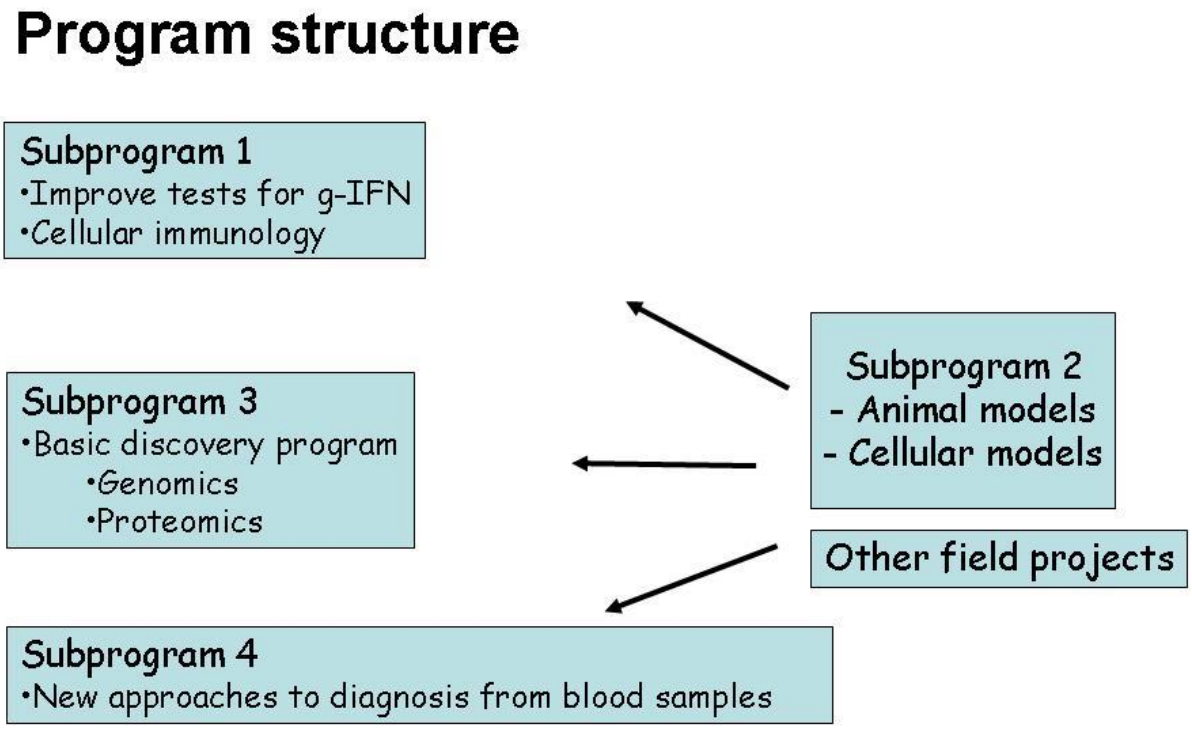

The main body of this final report will follow the subprogram structure illustrated above.

2 Project Objectives

2.1 Primary Objectives

2.1.1 Engage all staff in order to carry out the Project.

2.1.2 Conduct basic research to provide detailed knowledge about the early pathogenesis of OJD.

2.1.3 Identify stages in the disease process at the cellular and molecular levels that provide opportunities for improved diagnostic tests, vaccines and intervention strategies.

2.1.4 Apply new technology platforms including DNA microarray, advanced cellular immunology techniques, genomics and proteomics to the study of Johne's disease.

2.1.5 Apply these new approaches using clinical material from existing field trials in order to capitalise on work in progress in the NOJDCEP.

2.1.6 Apply to Johne's disease, recent research breakthroughs in human mycobacterial diseases such as tuberculosis and leprosy and augment mycobacterial research through rational and instructive use of our livestock models.

Specific subprogram objectives are listed in section 4.

3 Methodology

3.1 Overview

This project utilised a wide range of approaches and technologies which are fully described in this report. However, the methods are highly technical and lengthy and so are provided in the appendices.

4 Results and Discussion

4.1 Overview

In this section a summary of the results of each subprogram is presented. More detailed technical information is provided in the appendices.

4.2 Subprogram 1

4.2.1 SUBPROGRAM 1A

4.2.1.1 Purpose

The purpose of this subprogram is to improve the existing IFN-g assay (Pfizer-CSL) (Bovigam®).

4.2.1.2 Background

Samples must reach lab within too short a period to be practical (12 hrs); there are too many false positive reactions in young cattle and certain cell types are thought responsible for this; the basis of the test as a whole blood assay is poorly understood; the cost of the test is too high (kit $13/test).

4.2.1.3 Objectives/Tasks 2004-2007

1. To test physical and chemical changes to the current test protocol to improve practicality and efficacy
2. To evaluate cells responsible for IFN-g production

4.2.1.4 Results and discussion summary

Objective/task 1

Improvements to the interferon gamma test

The anticoagulant used in blood sample collection greatly affected interferon gamma production, with the greatest interferon production obtained with the use of lithium heparin whilst almost complete abrogation the response occurred with the use of fluoride oxalate and EDTA. In contrast to the studies in cattle, optimum interferon production was obtained after incubation of the blood with the antigen for at least 48 hours as compared to 16 hours in cattle. Interestingly, the finding that 48 hours was required for optimum production in sheep is consistent with that obtained in other species including humans. A field trial study was undertaken to determine if adding the antigen at blood collection and incubating the sample at 37°C during transportation to the laboratory could overcome the losses in interferon production resulting from poor viability of the cells due to aging. The results of the study suggested that this may be possible in some samples however if the *M. paratuberculosis* antigen is to be added to the blood at collection, it is imperative that the blood be transported at 37°C. Significantly lower values were obtained if the samples were transported at ambient temperature. This was not the case for those samples in which pokeweed mitogen was the

additive suggesting that the result was not due to the ambient temperature but was due to an interaction between the cells and the antigen. Possible explanations could include that there is a component of the *M. paratuberculosis* antigen that is having a negative impact on the cell's ability to remain viable or respond to the antigen and that this effect is abrogated at 37°C. The *M. paratuberculosis* antigen utilised in this study is a crude bacterial preparation and further studies should be directed at determining if this effect is repeatable with different sources of PPD or methods of PPD production. In the meantime the test can be improved by incubation for 48 hours, although it remains a research tool. Full methods and results are given in Appendix 1A-1.

Objective/task 2

Evaluation of cells responsible for IFN-γ production in sheep

Identification of the white blood cells that produce interferon gamma (IFN-γ) during *M. paratuberculosis* infections may provide a better understanding of disease development and facilitate development of a better assay to measure IFN-γ. This may allow for the identification of animals exposed to *M. paratuberculosis* that will succumb to disease or develop immunity. Results from this study show that very few cells in peripheral blood of sheep actually produce IFN-γ and it is not possible at this time to identify the types of cells that are producing this cytokine. The reason for this is that the available commercial reagents for double staining of cells for subsequent analysis by flow cytometry appear to strip the cell surface markers from the cells rendering them unidentifiable. This problem appears to be unique to sheep. Full methods and results are provided in Appendix 1A-2.

SUBPROGRAM 1B

4.2.1.5 Purpose

The purpose of this subprogram is to evaluate alternative assay methods for detecting IFN-g and/or other cytokines.

4.2.1.6 Background

The Bovigam ® test format is cumbersome and costly; ELISPOT is reported to be more sensitive than liquid phase assays; FACS and ELISPOT can be semi-automated; cytokines other than IFN-□ may be informative.

4.2.1.7 Objectives/Tasks 2004-2007

1. Develop alternative assay methods for IFN-g in sheep
2. Compare the results of alternative assay methods for IFN-g with other tests for detection of OJD

4.2.1.8 Results and discussion summary

Objective/task 1.

Alternative methods for the detection of IFN-g

The sensitivity of the IFN-γ ELISA to detect *M. paratuberculosis* infected sheep has been poor. To overcome this problem, two alternative assays were developed to detect IFN-g. The ELISPOT assay

has been formatted using the reagents available to detect ovine IFN-g in sheep. The ELISPOT and a derivative assay, the Cell-ELISA, are thought to be more sensitive in the detection of cytokines than an ELISA-based format. These assays differ in the way they measure interferon. The traditional ELISA measures the amount of IFN-g released into the plasma after stimulation of blood with *M. paratuberculosis* antigens. The ELISPOT measures the number of cells producing IFN-g and the Cell-ELISA measures the total amount IFN-g produced by the cells after stimulation with the *M. paratuberculosis* antigens. Full methods and results are provided in Appendix 1B-1.

Objective/task 2.

Comparison of alternative assays for the detection of IFN-g

The two new methods for the detection of IFN-g (ELISPOT and Cell-ELISA) were tested in *M. paratuberculosis* experimentally infected sheep. The two assays were compared to the traditional IFN-g ELISA. The results indicated that all three assays could detect IFN-g at an early stage post inoculation (3 months) but could not distinguish between inoculated animals that developed disease and those that had apparently cleared the infection. Of the ELISPOT and Cell-ELISA assays it appears the Cell ELISA may be the most effective at detecting *M. paratuberculosis* infected sheep. The results indicate new antigens are required to improve IFN-g detection of diseased sheep. The different aspects of IFN-g production measured by these assays may also be used in a synergistic method to improve the detection of *M. paratuberculosis* infected sheep. Full methods and results are provided in Appendix 1B-2.

Detection of *M. paratuberculosis* antigen-specific secretion of IL-10

An ovine IL-10 assay has been developed and optimised and can be used routinely to test cells from blood and other tissues of sheep. Con A and pokeweed mitogen, but not LPS, can be used as a positive control in this assay to ensure that the cells are able to respond to the recall antigen. Unlike the IFN-γ ELISA where the cells are stimulated for 1-2 days it is recommended that cells are cultured with the recall antigen for 6 days for the IL-10 assay. There are several factors which make this IL-10 assay a potentially useful test in assisting diagnosis of OJD. An *M. paratuberculosis* antigen-specific IL-10 response was not seen in the blood or lymph node cells in sheep that have not encountered the mycobacterium. An elevated IL-10 response was observed in blood and lymph node cells associated with sites of infection (ileal lymph node and jejunal lymph node) of sheep that have been exposed to *M paratuberculosis*, but not in a peripheral lymph node of these animals. The ability to detect an IL-10 response in blood cells makes it a potentially useful diagnostic test. Further value is added to the test because a difference in the IL-10 response in control and experimentally challenged sheep can be detected as early as 4 months post infection (p.i.). More encouraging is the finding that early on in disease (4-8 months p.i.), the IL-10 response in peripheral blood mononuclear cells (PBMC) tends to be higher in sheep that have been exposed to *M. paratuberculosis* but do not succumb to disease (at least at 11-13 months p.i.) than in animals that succumb to disease. Further investigation of this phenomenon is warranted. Full methods and results are given in Appendix 1B-3.

4.2.2 SUBPROGRAM 1C

4.2.2.1 Purpose

The purpose of this subprogram is to develop a novel assay for OJD based on apoptosis.

4.2.2.2 Background

There is need for an assay that can discriminate between active infection and infection where *M. paratuberculosis* has been killed by the host.

4.2.2.3 Objectives/Tasks 2004-2007

1. Develop apoptotic assays for sheep
2. Evaluate apoptosis to provide early diagnosis of *M paratuberculosis*-infected sheep, particularly to discriminate between infected and resistant/recovered sheep

4.2.2.4 Results and discussion summary

Objective/task 1

Develop apoptotic assays for sheep

A high throughput flow cytometric method was established to detect apoptosis in ovine peripheral blood or tissue mononuclear cells. Commercially available kits like the TUNEL assay can be used to detect apoptosis in ovine tissues *in situ*. Real time quantitative PCR assays were established using unique ovine specific primers to detect expression of apoptosis related genes in ovine tissues. These assays were applied to study the role of apoptosis in ovine Johne's disease. Full methods and results are provided in Appendix 1C-1.

Objective/task 2

Evaluate apoptosis to provide early diagnosis of *M. paratuberculosis*-infected sheep

The main objective of this study was to examine apoptosis in peripheral blood mononuclear cells (PBMCs) as well as apoptosis in response to recall of the Mptb antigen in sheep. A difference in the level of apoptotic cells in PBMCs of exposed and unexposed sheep was detected soon after exposure to Mptb, but there was no difference between these two groups at later time points: the level of apoptosis was similar in PBMCs from unexposed sheep and those with natural ovine JD infection. In a stimulation assay, Mptb-specific apoptosis detected by cellular caspase activity was variable in cultured PBMCs and it will not be a useful tool in assessing ovine JD. In another trial the analysis indicated that there was no significant relation between infection status of the animals and the level of apoptosis in PBMCs at two time points tested. Therefore Mptb antigen-specific apoptosis in PBMCs detected by caspase activity does not appear to be beneficial in discriminating sheep that will remain free of disease and those that will succumb to ovine JD. However, cells from the ileal lymph nodes (ILN) of Mptb exposed sheep with OJD are more likely to undergo apoptosis when in contact with Mptb antigens than ILN cells from Mptb exposed animals that remain disease-free. The observations of increased apoptosis in gut and lymph node tissues do not have practical diagnostic application as they were not mirrored in peripheral blood, which is more easily accessible in live animals. Full methods and results are provided in Appendix 1C-2.

Two other methods were used to study apoptosis. TUNEL counts of apoptotic cells within the terminal ileum were significantly higher in infected animals compared to exposed negative controls. Similarly pro-apoptotic genes Fas and Bax were significantly up regulated in infected animals compared to controls. The ratio of Bcl2/Bax showed that in these tissues there was an excess of pro-apoptotic Bax, which might make the cells more sensitive to apoptosis. This may help explain the high number of TUNEL positive cells in infected animals. Full methods and results are provided in Appendix 1C-3.

4.3 Subprogram 2

4.3.1 SUBPROGRAM 2A

4.3.1.1 Purpose

The purpose of this subprogram is to establish *in vitro* models to study the interaction between *M. paratuberculosis* and host cells.

4.3.1.2 Background

In vitro models are needed to study the attachment and penetration of *M. paratuberculosis* in the early stage of infection, and the responses of the host; simple, repeatable models are required for genomic and proteomic studies; models available could include explant cultures of gut tissue, immortal cell lines from sheep and other species (monocyte, macrophage and epithelial) and primary cell lines from sheep

4.3.1.3 Objectives/Tasks 2004-2007

1. Establish immortal macrophage/monocyte, epithelial and hybridoma cell lines in culture and determine optimal conditions for *M. paratuberculosis* research
2. Establish methods for primary culture of blood leukocytes of sheep and if appropriate investigate a method for ovine explant tissue culture from surgical, post mortem or abattoir material

4.3.1.4 Results and discussion summary

Objective/task 1

Establishment of cell lines

The initial stage of the project was dedicated to the establishment of stocks of cell lines, the establishment of an *in vitro* infection model and generation of reagents for future studies. A variety of immortal cell lines were acquired and a stock supply created by expanding cell numbers by culture and cryopreserving them for future use. Several hybridoma cell lines were acquired to generate reagents for use in flow cytometric and immunohistochemical techniques. Some antibodies were directly conjugated to a flurochrome (FITC) for use in intracellular staining protocols required for subprogram 1A. *In vitro* infection models were established using immortal cell lines to ascertain optimal conditions for *M. paratuberculosis* research. Initially, human (differentiated U937), murine (RAW264.7) and bovine macrophages (BoMac) were used. The putative bovine cell line BoMac was found not to be of macrophage phenotype while the human myeloid cell line (U937) requires pre-incubation with a differentiating agent (e.g. phorbol esters). Therefore, the murine macrophage cell line RAW264.7 was chosen to study macrophage responses to *in vitro* infection with M paratuberculosis. Studies were carried out to determine engulfment of *M. paratuberculosis* by macrophages and the intracellular survival of the mycobacterium during *in vitro* infection of macrophages. RAW264.7 cells were exposed to medium alone, *M. paratuberculosis* or heat-killed *M. paratuberculosis* (at 10 mycobacteria per macrophage) for up to one week. Macrophages were harvested at days 0, 1, 2, 3, 4 and 7 post-exposure and assessed for viability (by trypan blue exclusion), cell proliferation (by determining total cell number), apoptosis (by detecting caspase activity by flow cytometry) and intracellular presence of *M. paratuberculosis* (by Ziehl Neelsen

staining). Most of the *M. paratuberculosis* were not engulfed by macrophages after 4 hrs of incubation but by 16 hours the majority were inside the cells. Cell proliferation was not affected by the presence of *M. paratuberculosis*. There were some differences in the responses of macrophages to live and heat-killed mycobacteria at day 2 post-infection. Macrophages cultured with live *M. paratuberculosis* had a 1.7 fold higher number of infected cells (macrophages with one or more acid-fast bacilli) than macrophages cultured with heat-killed *M. paratuberculosis*. Interestingly, apoptosis was also greatest in cells incubated with live *M. paratuberculosis* at day 2 post-infection. This experimental model can be used to study other aspects of macrophage-*M. paratuberculosis* interactions. Methods and complete results are provided in the first part of Appendix 2A-1.

Objective/task 2

Primary culture of blood leucocytes

Monocytes can be separated from other mononuclear cells by their ability to adhere to surfaces. Several types of surfaces were tested and tissue culture-treated plastic was found to be as good as other specially treated surfaces. Approximately 1-2% of peripheral blood mononuclear cells (PBMC) are recovered as monocytes by this method. Cells isolated from ovine PBMC by adherence have been confirmed as monocyte/macrophages by their expression of CD14 on 94.5% of the cell population). CD14 is a cell surface marker which is found on monocytes but not on lymphocytes. These cells have been maintained in culture for up to 6 weeks. One recurrent problem with monocyte/macrophage culture is the contamination with fibroblasts. Several methods have been trialled to reduce or remove contaminating cells but none have been successful.

Due to the recovery of low numbers of monocytes by the density gradient method, isolation of monocytes by magnetic cell sorting was also assessed. Direct and indirect methods were tested. In the direct method, monocytes were labelled with an antibody to a cell surface marker which is directly conjugated to a magnetic bead. In the indirect method, monocytes were first labelled with an antibody to a cell surface marker which is conjugated to a fluorochrome. The cells were then stained with an antibody to the fluorochrome which is conjugated to a magnetic bead. Purity of cells separated by this method was only 50% compared to 100% by adherence methods. Therefore, the magnetic cell sorting method was not pursued. Protocols were tested and have been established for isolation of PBMC from larger volumes of blood (200 mL). Approximately 1-2% of PBMC are recovered as monocytes by this method. This reflects the low numbers of monocytes in ovine peripheral blood as similar percentages were found when directly phenotyping blood. Due to the low numbers of monocytes isolated from blood, and the inappropriateness of removing large volumes of blood from sheep, it was decided that it would not be possible to supply adequate numbers of ovine monocytes for ongoing *M. paratuberculosis* research. Use of cattle would overcome this problem as they have more circulating monocytes than sheep. However, monocyte-derived macrophages isolated from peripheral blood from uninfected and naturally infected sheep were infected with *M. paratuberculosis* at 10 bacteria per macrophage. Infected cells were detected by Ziehl-Neelsen staining. There were no significant differences in the ability of cultured macrophages from animals of differing infection status to phagocytose *M. paratuberculosis*. The major hindrance to the progress of this type of study was the inability to isolate large numbers of monocytes from ovine peripheral blood.

The ability of *M. paratuberculosis* to cross an epithelial barrier was initially tested in an *in vitro* model. No acid-fast bacilli were seen when Caco-2 cells were incubated in the absence of *M. paratuberculosis*. In cells exposed to *M. paratuberculosis*, the mycobacteria were mainly found extracellularly. At a multiplicity of infection of 10:1, less than 3% of Caco-2 cells were infected (contained more than one acid-fast bacilli per cell) with *M. paratuberculosis* after 48 hr incubation. Due to the low rate of infection of epithelial cells by *M. paratuberculosis* it was decided not to progress with explant cultures. Methods and complete results are provided in the second part of Appendix 2A-1.

Assays for proliferation of blood leucocytes

Cell mediated immune responses play an important role in protecting against infection caused by intracellular organisms like *M. paratuberculosis*. This work was undertaken to study the proliferation

of mononuclear cell subsets in response to *M. paratuberculosis* antigen in an experimental model of OJD. A high throughput flow cytometric assay was developed for this purpose. A strong cellular immune response was detected in the peripheral circulation of sheep as early as 4 months following exposure to *M. paratuberculosis*. Cell proliferation in response to *M. paratuberculosis* antigen in exposed animals peaked at approximately 8 months post infection $CD4^+$ and $CD8^+$ T cells produced the greatest proliferative response. Within the groups of sheep exposed to *M. paratuberculosis*, we were not able to detect differences in animals that remained free of disease and those that went on to develop OJD. Further analysis of these data sets is required to determine if differences in mononuclear cell proliferation phenotype can be distinguished based on lesion type. Lymphocyte proliferation may be useful as a test for exposure to *M. paratuberculosis.* However, antigen specificity will need to be confirmed to avoid false positive results. Methods and complete results are provided in Appendix 2A-2.

4.3.2 SUBPROGRAM 2B

4.3.2.1 Purpose

The purpose of this subprogram is to provide experimentally infected young sheep and to provide other biological materials for study of the pathogenesis of OJD.

4.3.2.2 Background

It is not possible to obtain clinical material from naturally infected sheep at a consistent stage of infection due to major between-sheep variation in exposure levels and exposure time; sources of *M. paratuberculosis* for infection are not standardised and there are no defined “seed stocks” of *M. paratuberculosis* for long term experimentation; most existing oral infection models have used unrealistically high does of *M paratuberculosis;* it is possible to obtain consistent infection of the gut of sheep using low doses, but repeatability of the model is unknown; surgical biopsy methods and gut loop models have been described for sheep and may be useful.

4.3.2.3 Objectives/Tasks 2004-2007

1. Using natural mating, provide young lambs twice yearly for on-going studies and develop suitable pasture facilities for housing experimental lambs at the University Farms at Camden and Marulan
2. Develop seed stocks of *M paratuberculosis*, confirm the repeatability of seed culture methods and confirm the infectivity of the standardised *M. paratuberculosis* inoculum by sheep inoculation
3. Infect young lambs orally with *M. paratuberculosis* and examine naturally infected sheep to compile a collection of biological samples for testing, then characterise the phenotype of these sheep by sequential testing and post mortem examination for example at about 3 years of age
4. Consider the applicability of surgical models for the study of pathogenesis of *M. paratuberculosis* infection:biopsy, infection delivered at specific intestinal sites in intact lambs, infection delivered into isolated gut loops and lymphatic cannulation models
5. Produce cytokine positive control blood samples for assay standardization by immunizing sheep with killed *M paratuberculosis*

4.3.2.4 Results and discussion summary

Objective/task 1

Lamb production

The University of Sydney farms at Camden provided 128 lambs for the experimental infection models used in this project. Initially lambs were supplied from the Camden farm but due to the worsening of the drought in 2005 and fox predation low lambing percentages were observed. A decision was made to have the lambs supplied from the University farm at Marulan as they could provide the required number of animals for the research to proceed. In addition to this, 46 OJD free ewes were supplied for necropsy as negative controls.

Objective/task 2

Seed stock maintenance

Seed stocks of *M. paratuberculosis* were developed and maintained over the project. These were used for inoculation of the experimental animals. Excess *M. paratuberculosis* not required for the inoculation of the animals was stored and used for other aspect of the project including spiking of blood, infection of *in vitro* cultures and analysis of dormancy in subprograms 3 and 4.

Objective/task 3

Experimental infections of lambs, and collection of biological samples

A critical literature review of experimental infection models for Johne's disease in farm and laboratory animals was conducted (Appendix 2B-1). The factors that appeared to influence the outcome of experimental infections with *M. paratuberculosis* were the species, breed and age of subject used for the infection, the route of infection and the strain, dose and number of doses of *M. paratuberculosis* used to inoculate the subjects. Using information from this review an experimental infection model was developed using an ovine pure clonal strain of *M. paratuberculosis* (Telford 9.2) (Appendix 2B-2). The experimental inoculations resulted in repeatable infection outcomes across multiple trials. The disease outcome from the Telford 9.2 strain was less severe when compared to a gut homogenate strain of *M. paratuberculosis*. During the experimental infection trials regular biological samples were acquired to assess the phenotype of the sheep.

Objective/task 4

Consider the applicability of surgical biopsy for the study of pathogenesis of *M. paratuberculosis* infection

Surgical biopsies were not required to study disease pathogenesis as the regular blood samples and tissues accessed at necropsy provided adequate biological samples to assess the phenotype of the sheep

Objective/task 5

Produce cytokine positive control blood samples for assay standardization by immunizing sheep with killed *M paratuberculosis*

Throughout the project at least two OJD vaccinated animals were maintained at pasture to provide blood samples for cytokines assay development and positive controls for the assays.

Subprogram 3

4.3.3 SUBPROGRAM 3A

4.3.3.1 Purpose

The purpose of this subprogram is to detect *M. paratuberculosis* genes or gene products that are involved in the pathogenesis of OJD.

4.3.3.2 Background

Analysis of bacterial genes activated and proteins expressed during the initiation of infection (epithelial /macrophage uptake) may inform attempts to develop new diagnostics, vaccines or treatments/control methods; identification of reactions and responses from the bacterium which would indicate the failure or success of the infection could be particularly useful; survival and replication in macrophages precedes shedding and antibody responses; nothing is known about how *M. paratuberculosis* replicates and spreads in the host; there is altered bacterial gene expression in intracellular mycobacteria but nothing is known of *M paratuberculosis.*

4.3.3.3 Objectives/Tasks 2004-2007

1. Develop methods for studying the genome and proteome of *M paratuberculosis*
2. Analyse the behaviour of *M. paratuberculosis* in cell cultures and ovine samples using genomic and proteomic techniques

4.3.3.4 Results and discussion summary

Objective/task 1

Detection of *M. paratuberculosis* genes in ovine faeces

A new SYBR Green based real-time quantitative PCR (QPCR) assay based on IS*900* was developed to directly detect and quantify *M. paratuberculosis* DNA in faeces and validated for use on sheep. Both the cattle (C) and sheep (S) strains of *M. paratuberculosis* were detected by the QPCR assay, and no cross reactions were detected with 51 other species of mycobacteria. One copy of IS*900* fragment cloned into plasmid pCR2.1 and 1 fg of *M. paratuberculosis* genomic DNA were consistently detected, while in spiked faecal samples the detection limit was 10 viable *M. paratuberculosiS* (S strain) per one gram of negative ovine faeces. A total of 506 individual ovine faecal samples and 27 pooled ovine faecal samples with known culture results were tested. The QPCR assay identified 68 of 69 BACTEC culture positive individual faeces as positive and there was a strong relation between culture results (time to detection) and DNA quantity detected by the QPCR (r=-0.70). In pooled faecal samples, the results of the QPCR also showed agreement with that of culture (kappa value = 0.59). *M. paratuberculosis* DNA was detected from some culture negative faecal samples from sheep exposed to *M. paratuberculosis*, suggesting that the QPCR has very high analytical sensitivity for *M. paratuberculosis* in faecal samples and detects non-viable *M. paratuberculosis* in ovine faeces. None of the control negative faecal samples were positive in

QPCR. This is the first report of a direct faecal quantitative PCR assay for sheep that has similar sensitivity to a gold standard radiometric culture assay. Full methods and results are provided in Appendix 3A-1.

Protein extraction from *Mycobacterium avium* subsp. *paratuberculosis*: comparison of methods for analysis by sodium dodecyl sulphate polyacrylamide gel electrophoresis, native PAGE and surface enhanced laser desorption/ionization time of flight mass spectrometry

This study was conducted to compare methods for examining the proteome of *M*. *paratuberculosis*. SDS-PAGE, native PAGE and SELDI-TOF-MS were compared and the efficacy of various lysis buffers was assessed. Chaotropic agents (Urea CHAPS and potassium thiocyanate) and non-ionic detergent (Tween20 and Triton X-100) extracts were compared on three different ProteinChip® surfaces along with two energy absorbing molecules (EAM): EAM-1 proprietary formulation (Ciphergen) and sinapinic acid. Urea CHAPS was efficient for extraction of proteins and their detection on all the ProteinChip® surfaces. However, potassium thiocyanate was the most effective buffer, leading to detection of the greatest number of protein peaks on the immobilized metal affinity chromatography (IMAC) surface. Sinapinic acid was more efficient than the EAM-1 proprietary formulation and resulted in additional peaks with higher intensity for both the low and the medium molecular weight range proteins. Intra-chip and inter-chip coefficient of variation for mass/charge varied from 0.01% to 0.07% and 0.00% to 0.08%, respectively. SELDI-TOF-MS was an efficient tool for the protein profiling of *M*. *paratuberculosis* and will be useful for investigation of novel proteins, although SDS-PAGE/2D gel electrophoresis is recommended for study of high molecular weight species. All buffers were suitable for protein extraction for SDS-PAGE, while Tween20 was best for native PAGE. The methods developed here were applied to proteomic studies described below. Full methods and results are given in Appendix 3A-2.

Objective/task 2

Growth pattern and proteome of *M. paratuberculosis* in a temperature flux-induced dormancy model

Phenotypic and genomic data suggest that *M. paratuberculosis* may survive in a dormant state when stressed. The aim of this study was to develop an *in vitro* model to evaluate the proteome of *M. paratuberculosis* during dormancy, based on prior observations that dormancy occurred as a result of temperature flux in the natural environment. Data were obtained for the two genomically distinct strains of M *paratuberculosis*, S and C. The latter was more thermotolerant, surviving for 30 min at 60°C compared to 28 min for the former, but temperature flux was more detrimental to both strains than exposure to the same peak temperature for an equivalent time. Dormancy was induced by repeated exposure to temperature flux in the range 10° to 50°C. 2-D PAGE analysis and tandem mass spectrometry detected 27 differentially expressed spots in the C strain and 11 in the S strain. These proteins represented antioxidant enzymes, fatty acid metabolism, energy production and conversion, ATP and purine biosynthesis, proteolysis, protein synthesis, heat shock protein chaperone, iron storage, cyanate hydrolysis, hypothetical proteins with putative function, hypothetical proteins with unknown function, and phosphate metabolism. The greatest proportion of differentially expressed proteins was involved in fatty acid metabolism (23%). These proteins were induced by exposure to fluctuating temperature but are associated with dormancy and may be required for the survival of *M. paratuberculosis* both in the environment and within the host. Full methods and results are given in Appendix 3A-3.

Survival, dormancy and the proteome of *M. paratuberculosis* during the stress response to hypoxia and nutrient starvation

Few data exist on physiological adaptation of *M*. *paratuberculosis* in either the host or the environment. In this study the proteomic responses of the two distinct strains of *M*. *paratuberculosis* (C and S) to hypoxia and starvation were studied *in vitro*. The growth pattern of *M*. *paratuberculosis* during stress appeared similar to the dormancy response of other mycobacteria. A total of 66 protein spots differentially expressed in response to starvation and/or hypoxic stress were selected and identified, providing first functional assessment of the genomic differences known to exist between these strains. Differentially expressed proteins were classified based on biological function and 13 categories were identified including antioxidant enzymes, amino acid metabolism, fatty acid metabolism, ATP and purine biosynthesis, proteolysis, cell wall synthesis, oxidoreducatse enzymes, protein synthesis, signal recognition, hypothetical proteins with putative function, hypothetical proteins with unknown function, cyanate hydrolysis, phosphate metabolism and cell division. These differentially expressed proteins are potential screening targets for future diagnosis, prevention and control of *M*. *paratuberculosis* infection and their identification will assist understanding the pathogenesis of diseases caused by this organism. Full methods and results are given in Appendix 3A-4.

Evaluation of the immunogenicity of recombinant dormancy-associated proteins during *M. paratuberculosis* infection: implications for pathogenesis and diagnosis

The immunogenicity of recombinant dormancy-associated proteins of *M. paratuberculosis* was characterized in sheep infected with the organism. Five proteins, MAP2411, ClpP, Ppa, MAP0593c and GreA were cloned, expressed and purified as His-tag recombinant proteins from the pET-15b vector in a BL21(DE3)pLysS strain of *E*. *coli*. The humoral immune response of sheep infected with *M*. *paratuberculosis* sampled at different stages of disease was examined. The serological reactivity of these recombinant antigens varied according to the stage of paratuberculosis. MAP2411 was non-immunogenic while GreA, Ppa, ClpP, MAP0593c and combinations of GreA and Ppa, ClpP and MAP0593c, GreA, Ppa, ClpP and MAP0593c reacted with sera of animals in the early stage of disease. These sera were not immunoreactive in a commercial ELISA test that was based on non-defined native antigens. Moreover, MAP0593c and ClpP detected more *M*. *paratuberculosis* infected animals than the Pourquier ELISA. We infer from their immunogenicity that the proteins examined were expressed within macrophages *in vivo*. In a previous study Ppa, ClpP and MAP0593c were expressed *in vitro* during the response to hypoxia, nutrient starvation and thermal flux, suggesting that they may be general stress response effectors in *M. paratuberculosis*. The data in this study not only provide fundamental information on host-mycobacterial interactions through the host immune responses but also have practical implications for the development of future diagnostic tests to detect early immune responses in sheep infected with *M*. *paratuberculosis*. Full methods and results are given in Appendix 3A-5.

SUBPROGRAM 3B

Purpose

The purpose of this subprogram is to detect genes or gene products in the host that are involved in the pathogenesis of OJD.

Background

New tools in genomics and proteomics make it possible to define host genes or gene products which may be responsible for the ability or failure of sheep to resist or recover from *M. paratuberculosis* infection; this knowledge may inform diagnostic test or vaccine/treatment development; *in vitro* models make it possible to study very early infection events; *in vivo* infection models in sheep make it possible to study later stages of infection.

Objectives/Tasks 2004-2007

1. Develop genomic and proteomic tools and methods to analyse host gene expression

2. Analyse host gene/proteome expression in *in vitro* models and in samples from sheep with OJD

4.3.3.5 Results and discussion summary

Objective/task 1

Validation of endogenous reference genes for expression profiling of RAW 264.7 cells infected with *M. paratuberculosis* by quantitative PCR

Reference genes are frequently used to normalize between different biological samples the levels of mRNA measured using quantitative PCR (qPCR). The expression level of many commonly used reference genes has been shown to vary between tissues or cells, or following exposure to various treatments including infection with microbes. The selection of an appropriate reference gene for an individual experiment is therefore a crucial step in the process of accurately determining changes in gene expression. For this purpose, we analysed the expression of nine commonly used reference genes in a murine macrophage cell line, RAW 264.7, for their potential use in the analysis of differential gene expression by quantitative polymerase chain reaction (qPCR) following experimental infection with *M*. *paratuberculosis*. Only one of nine putative reference genes tested, *Casc3a,* was found to be suitable and combinations of two or more reference genes were disadvantageous. Based on data from the study, we recommend an approach for selection of reference genes, conducting assays with technical replicates in duplicate rather than triplicate, determining decision-limit quality control criteria for technical replicates and assessing the significance of gene expression fold differences using $\Delta\Delta Ct$ based on knowledge of the variation in the reference gene. Full methods and results are provided in Appendix 3B-1.

Objective/task 2

Gene expression in the gut of sheep with OJD discovered using DD-PCR after validation of reference genes for the gut

The objective of this part of the study was to examine host gene expression during the sub-clinical to clinical stage of *M. paratuberculosis* infection, to identify known or novel genes regulating the response to infection and to define genes that can be used to identify *M. paratuberculosis* infected animals earlier than currently possible. DD-PCR identified numerous genes that may be differentially regulated. Each was examined in cross validation studies using quantitative real time PCR and four genes were confirmed unequivocally to be differentially regulated in the intestine of the sheep in the response to *M. paratuberculosis* infection. Genes confirmed to be regulated include genes similar to signalling lymphocyte activation molecule (SLAM), serum amyloid A3 (SAA3), translocase of the outer membrane 22 (TOM22) and cathepsin. It appears that these genes have not previously been identified in the context of ovine *M. paratuberculosis* infection. Full methods and results are provided in Appendix 3B-2.

Toll-like receptors

Toll-like receptors (TLR) are engaged by ligands on microbial pathogens to initiate innate and adaptive immune responses. Nothing is known about TLR involvement during infection with *M. paratuberculosis*, the cause of Johne's disease in ruminants, although there is a profound immunopathological response in affected animals. We analysed the expression of ten TLR genes relative to validated reference genes at predilection sites in ileum, jejunum and associated lymph nodes as well as in peripheral blood to determine if TLR expression is altered in response to infection with *M. paratuberculosis* in out-bred sheep. Previously unexposed animals and animals from three naturally infected flocks were used with restricted maximum likelihood linear mixed modelling applied to determine significant differences. These were related to the pathologies observed at different stages of infection in exposed sheep, after allowing for other sources of variation. In most cases there were differences in TLR expression between early paucibacillary and multibacillary groups when compared to uninfected sheep, with most TLRs for the paucibacillary group having lower expression levels than the multibacillary group. Increased expression of TLR 1, 2, 3, 4, 5 and 8 was observed in ileum or jejunum and TLR1, 2, 3, 4, 6, and 8 in mesenteric lymph nodes. While no significant differences were observed in TLR expression in PBMCs, there was a trend for increased expression of TLR1, 2, 6, 7 and 8 in exposed compared to non-exposed animals. Further study of TLR expression in Johne's disease in ruminants is warranted as these observed differences may help explain pathogenesis and may be useful in the future diagnosis of *M. paratuberculosis* infection. Full methods and results are provided in Appendix 3B-3.

Proteomic profiling of ovine serum by SELDI-TOF MS: optimization, reproducibility and feasibility

Surface-enhanced laser desorption/ionization time-of-flight mass spectrometry (SELDI-TOF MS) has the capacity to detect known and unknown immunological molecules in clinical samples such as serum. However, experiments must be rigorously optimised so that spectral data generated from contrasting samples can be interpreted in a biologically relevant context. Here we have determined optimum combinations of ProteinChip® array surfaces, energy absorbing molecules, sample dilutions, instrument settings and reproducibility for SELDI-TOF MS spectral generation from ovine whole sera. Sample dilution had no effect on reproducibility of mass estimates below 15000 Da, but as expected altered the relative intensity of protein peaks. The precision of estimates for peak intensity determined from sera from 8 sheep was 13% - 18% (coefficient of variation) and for mass accuracy was 0.01% - 0.02%. Corresponding values between-chip were 13% - 23% and 0.02% - 0.03%. Concordance correlation analysis suggested moderate to near perfect agreement for intensity and almost perfect agreement for mass within and between chips. Peak intensity was less reproducible for proteins that were more abundant while larger proteins had more variable mass estimates, factors which may influence selection of biomarkers. Routinely collected serum samples stored at -20°C were useful for biomarker identification but must be handled uniformly: a panel of potential biomarkers associated with vaccination with a bacterial antigen was identified with such sera. The information generated in this study will assist studies on whole serum profiling in sheep to facilitate immunological assessment. Full methods and results are provided in Appendix 3B-4.

Identification of serum biomarkers for ovine Johne's Disease using SELDI-TOF-MS

The low-molecular-weight region of the serum proteome is an assortment of intact proteins and fragments of larger proteins including components of the innate and adaptive immune systems, and potentially contains an abundance of diagnostic information. In this study, proteomic profiling of serum using surface-enhanced laser desorption ionisation time-of-flight (SELDI-TOF) MS has been

used to determine the potential of this technology to the discovery of biomarkers for the early diagnosis of ovine Johne's disease. A total of 59 serum samples, representing 30 sheep in various subclinical stages of infection and 29 unexposed, unvaccinated sheep were used to determine putative serum biomarkers for infection with *M. paratuberculosis*. Two independent multivariate statistical algorithms, Classification and Regression Tree (CART) and Linear Discriminant Analysis (LDA), were employed to identify a panel of 21 differentially expressed peptides. Of these, 11 peptides were increased 1.6 to 3.2-fold in infected sheep and 10 peptides had significantly reduced levels, between 1.7 to 4.3-fold, in serum from infected sheep relative to unexposed sheep. CART analysis using these biomarkers achieved sensitivities of 90-93% and specificities of 83-91% in identifying infected and unexposed animals in cross-validation. Full methods and results are provided in Appendix 3B-5.

4.4 Subprogram 4

4.4.1 SUBPROGRAM 4A

4.4.1.1 Purpose

The purpose of this subprogram is to assess the potential for detection of *M. paratuberculosis* in blood as an alternative diagnostic procedure.

4.4.1.2 Background

M. paratuberculosis has been found in blood during the infection, presumably intracellularly; detection of *M. paratuberculosis* in circulating leucocytes during the course of infection would assist diagnosis; several methods are apparent to concentrate or purify infected leucocytes from blood to enhance the sensitivity of detection.

4.4.1.3 Objectives/Tasks 2004-2007

1. Determine whether *M. paratuberculosis* can be detected in blood during infection
2. Evaluate the expression of surface receptors on infected and normal blood leucocytes and evaluate methods to concentrate infected blood-leucocytes using knowledge about receptor expression

4.4.1.4 Results and discussion summary

Objective/task 1

Culture of *M. paratuberculosis* from blood

Culture of pathogenic mycobacteria from blood is of increasing importance to human medicine due to the tendency for these pathogens to cause disease in HIV positive patients. While the growth requirements of *M. tuberculosis* and *M. avium* complex differ from *M. paratuberculosis*, sample processing and culture techniques for these pathogens may be adaptable for culture of *M. paratuberculosis*. A method for detecting viable *M. paratuberculosis* organisms in blood of infected animals by culture has been developed and evaluated on 230 samples. A small number of infected animals appear to have bacteraemia detectable by this method. A method for reducing

environmental contamination from field samples, while causing a minimal effect on *M. paratuberculosis,* has also been developed.

Objective/task 2

Evaluation of the expression of surface receptors on blood cells

This study was designed to examine the cell surface marker expression (phenotype) of blood cells in sheep. Examination of cell surface markers during *M. paratuberculosis* infection may enable identification of animals with susceptibility or resistance to the disease. The results suggested that no single cell surface marker currently able to be measured in sheep in our laboratory could be used for identification of sheep with Johne's disease. Furthermore methods to concentrate infected cells from blood using antibodies against cell surface markers does not appear to be feasible at this time due to the low rate of bacteraemia. Full methods and results are provided in Appendix 4A-2.

SUBPROGRAM 4B

4.4.1.5 Purpose

The purpose of this subprogram is to stimulate infected macrophages to move from intestinal tissue into blood, skin or faeces to increase the sensitivity of diagnostic tests that rely on detection of the organism.

4.4.1.6 Background

Several methods that promote macrophage migration and accumulation are available; stimulation of egress into blood or faeces may enable development of improved diagnostics using these readily procured samples, and using existing tests such as direct-PCR and culture.

4.4.1.7 Objectives/Tasks 2004-2007

1. Analyse the capacity of normal and infected macrophages to migrate and evaluate methods to induce macrophage migration from the intestinal region into blood, skin or faeces of infected sheep
2. Evaluate the sensitivity of PCR and culture to detect *M. paratuberculosis* in blood and/or other samples with and without stimulation of migration

4.4.1.8 Results and discussion summary

Objective/task 1

Migration of normal and infected sheep white blood cells *in vitro* and *in vivo*

Systemic spread of *M. paratuberculosis* during late stage infection is known to occur in sheep. The spread of the bacteria is probably via macrophages in the blood and lymph. To understand the movement of white blood cells during *M. paratuberculosis* infection several experiments were carried out to examine *in vivo* and *in vitro* cell migration. Results from the *in vitro* experiment showed fetal calf serum was inhibitory to white blood cell migration. The *in vivo* experiment showed *M.*

paratuberculosis infected white blood cells moved to all parts of the body. Full methods and results are provided in Appendix 4B-1.

Objective/task 2

Development of a QPCR assay for blood samples

As there may be technical difficulties with routine culture of Mptb from blood, a real time quantitative PCR assay (QPCR) was also developed. A number of QPCR assay formats were assessed for analytical sensitivity and specificity. These assays utilized the *M. paratuberculosis* specific sequences: IS*900*, IS*mav2*, f57, and IS*MAP2.* Primers based on IS*900* were most suitable. Methods for disruption of *M. paratuberculosis* to release its DNA and for removal of inhibitor DNA originating from white blood cells were also optimised. This method can detect 10 organisms in 10 mL of blood. This method is now available for application to stored samples from animal trials. However, it first needs to be compared to a gold standard test; the most appropriate test is culture. As the results of culture using BACTEC suggest that the rate of bacteraemia in sheep is very low, except perhaps at the end of the disease process, additional samples need to be acquired in order to validate the PCR test as it is applied to blood samples. When this has been done the test can be evaluated in archived samples to determine whether it is capable of detecting circulating *M. paratuberculosis* that are not apparent to culture-based methods.

5 Success in Achieving Objectives

5.1 Specific project objectives

5.1.1 Engage all staff in order to carry out the Project

This objective was successfully achieved. Post doctoral Research Fellows were recruited internationally in order to carry out this project. Technical officers and post graduate students were recruited locally and internationally. The University of Sydney provided IPRS scholarships for three international students who worked within or were associated with the project. A list of staff and students is provided in Table 5.1. Not all of those named were present for the entire period. The team represented the largest group ever to be assembled to study Johne's disease in Australia and was probably one of the largest groups in the world at the time. It maintained links with Johne's disease researchers in New Zealand, Europe and the United States throughout the project.

Table 5.1. Staff and students engaged in Project OJD.031

Name	**Position**	**Funding**
Professor Richard Whittington	Chair Farm Animal Health	Faculty
Assoc. Professor David Emery	Associate Prof in Veterinary Parasitology	Faculty
Dr Kate Bosward	Senior Lecturer in Veterinary Pathology	Faculty
Dr Deb Taylor	Post Doctoral Fellow	Project
Dr Kumi de Silva	Post Doctoral Fellow	Project
Dr Doug Begg	Post Doctoral Fellow	Project
Dr Lyrissa Di Fiore	Post Doctoral Fellow	Project
Ms Nicole Carter	Research Assistant	Project
Ms Sally Browne	PhD student	Project
Mrs Ling Zhong	PhD student	MLA scholarship
Mrs Kate Bower	PhD student	MLA scholarship
Ms Satoko Kawaji	PhD student	IPRS scholarship
Mr Navneet Dhand	PhD student	IPRS scholarship
Mr Sanjeev Gumber	PhD student	IPRS scholarship
Ms Helen McGregor	PhD student	MLA scholarship
Mr Ian Marsh	PhD student	MLA scholarship
Ms Natalie Schiller	Technical Officer	MLA OJD.028
Mrs Anna Waldron	FAH Laboratory Manager	Faculty
Mr Craig Kristo	FAH Operations Manager	Faculty
Mrs Geetanjali Dhand	Technical Officer	Faculty
Ms Eileen Risby	Technical Officer	Faculty
Mrs Pabitra Dhungyel	Laboratory attendant	Faculty
Ms Marion Saddington	Administrative Assistant	Faculty
Mr Nobel Toribio	Technical Officer	Faculty
Ms Rebecca Maurer	Technical Officer	Project
Mrs Reena Mehta	Technical Officer	Project

5.1.2 Conduct basic research to provide detailed knowledge about the early pathogenesis of OJD.

This objective was successfully achieved. This project was designed to explore aspects of Johne's disease that had not been considered in Australia before and that, in fact, were not subject to much research internationally. In order to control Johne's disease effectively more knowledge is required about the biology of the disease. At flock level this is known as epidemiology, and studies of this nature were well advanced. At the individual animal level this is known as pathogenesis and there was little being done. The project leader recommended to the international community in 1998 at the 7th International Colloquium on Paratuberculosis that research effort be redirected from study of clinical cases of Johne's disease to intensive investigation of the pathogenesis of the initial or early stages of infection because that is where the main knowledge gaps were. This recommendation appears to have been used by groups in the Australia, USA, Europe and New Zealand to obtain funding to commence research on more fundamental aspects of Johne's disease. However, project OJD.031 was the first of these projects and faced the twofold difficulty of working with sheep for which there were few laboratory reagents for advanced studies, and of working without many veterinary examples to follow. For this reason a basic research program to investigate mycobacterial disease pathogenesis was initiated using the obvious similarities with tuberculosis in man as a starting point. Johne's disease has a very long incubation period, with most infected sheep not showing obvious signs of the infection for 2 to 3 years. For the explicit purpose of study of the early stages of disease, it was deemed appropriate to concentrate effort on the first 18 months of the infection, with particular emphasis on the first 12 months.

5.1.3 Identify stages in the disease process at the cellular and molecular levels that provide opportunities for improved diagnostic tests, vaccines and intervention strategies.

This objective was successfully achieved. Throughout biology a basic pattern exists of encoding of information in genes in DNA, and translation of that information into various actions through mediator proteins. All this occurs at sub-microscopic or molecular levels. Studies were undertaken at the molecular level to determine whether key genes of both sheep and bacterium were involved in early pathogenesis. These were extended to a study of proteins both of the bacterium and of the cells of the sheep. Throughout this research program there was focus on the practical applications of new discoveries to diagnose Johne's disease and prevention of disease through vaccination. This focus led to the discovery of novel proteins and genes which were not previously known to be involved in the pathogenesis of Johne's disease. All have been protected by MLA through provisional patents for the possible future commercial benefit of the livestock sector.

5.1.4 Apply new technology platforms including DNA microarray, advanced cellular immunology techniques, genomics and proteomics to the study of Johne's disease.

This objective was successfully achieved. New technology platforms were used throughout this project. Proteomic techniques included surface-enhanced laser desorption-ionisation time-of-flight mass spectrometry (SELDI-TOF-MS) as a primary discovery tool and two dimensional gel electrophoresis and peptide mass fingerprinting by MALDI-TOF-MS and SDS-PAGE to visualise and identify proteins. Advanced cellular immunology techniques included flow cytometry to enumerate and identify populations of immunological cells in blood and solid tissues, lymphocyte stimulation assays, primary cell culture, ELISPOT and other assays to study cellular and cytokine responses. DNA technology platforms applied for gene discovery included long-distance differential-display

polymerase chain reaction (LD-DD-PCR) and quantitative real time polymerase chain reaction (qPCR). DNA microarray analysis was used but only to compare strains of *M paratuberculosis*. This technology was considered too immature to apply to study of the sheep genome in Johne's disease and there was lack of agreement on how to analyse the results from microarray experiments in sheep when the work commenced in 2003; LD-DD-PCR was applied instead of microarray analysis as it did not require prior knowledge of the sheep genome and it was successful.

5.1.5 Apply these new approaches using clinical material from existing field trials in order to capitalise on work in progress in the NOJDCEP.

This objective was successfully achieved. Throughout this project, carefully archived samples that had been obtained through the previous NOJDP project were utilised. These projects included OJD.020, OJD.002 and OJD.028. Furthermore, careful archiving of samples collected from animals during the present project will ensure that they are able to be used in future research projects.

5.1.6 Apply to Johne's disease, recent research breakthroughs in human mycobacterial diseases such as tuberculosis and leprosy and augment mycobacterial research through rational and instructive use of our livestock models.

This objective was successfully achieved. An extensive literature review of research in tuberculosis and leprosy was undertaken by the project leader in 2001. This formed the basis for the initial research direction in subprograms in this project. Examples include the application of ELISPOT to diagnosis of Johne's disease, proteomic investigations of *M. paratuberculosis*, in vitro cell culture models, apoptosis studies and assessment of gene expression during infection. An extensive literature review of livestock and laboratory animal infection models for Johne's disease was conducted during the project and revealed that there was no suitable model for study of early pathogenesis. None of the models described so far could be considered repeatable or representative of the natural disease. For this reason a new model was developed during the project which meets all of the needs for future research.

5.2 Success in achieving specific research objectives

A large number of specific research objectives were achieved successfully. Each is described above in Section 4 under a specific subprogram.

5.3 Success in achieving implied objectives

Johne's disease is a significant international problem for reasons outlined under background. It is essential that Australia maintains capacity to deal with diseases such as Johne's disease and this necessitates maintenance of a group or groups of people with the necessary expertise to work at international levels of competence. This project enabled the creation of a highly competent research team and led to the training of young scientists and technical staff. Eight PhD students undertook studies through direct or indirect involvement with this project. Three have already completed their degrees and are now engaged in employment that services the livestock sector. This is a vital contribution to help redress the skills-shortage in Australia.

6 Impact on Meat and Livestock Industry – now & in five years time

6.1 Impact on Meat and Livestock Industry – now & in five years time

The impacts of this project can be summarised under three headings: technical advances, conceptual advances and structural advances. The immediate impacts are mainly technical. The long term impacts are technical and conceptual and will lead to structural change in disease control. There are also long term structural impacts in capacity to handle diseases in livestock.

6.1.1 Immediate technical advances

i) New diagnostic test possibilities. The technical advances are very numerous and include discovery of new ways to detect Johne's disease. Immediately, we can proceed to validate a new method for detection of *M. paratuberculosis* in faeces. This will be a rapid test capable of providing a result within 48 hours with levels of sensitivity and specificity equivalent to or greater than radiometric culture of faeces. This removes a major impediment to widespread use of faecal samples in diagnosis and surveillance.

ii) Application of new techniques in research.

6.1.2 Technical advances in 5 years time

i) In the short to medium term new tests applicable to blood samples can be further investigated to ascertain levels of sensitivity and specificity. In particular, the ELISPOT assay for interferon gamma and the ELISA for IL-10 show promise. In the medium term all these new tests can be evaluated in other species including cattle, goats and deer.

ii) New antigens for use in new diagnostic tests. Some of the proteins discovered in this project represent potential breakthroughs for diagnosis of Johne's disease. Over 60 proteins were found to be produced by *M. paratuberculosis* when it is exposed to stress; some of these were shown to be produced within the sheep and were recognised by the immune system of the sheep. These proteins may be suitable for inclusion in novel immunodiagnostic tests for detection of early stage infection. This would remove one of the major impediments to successful application of a test and cull strategy, as all of the existing tests fail to detect many sheep with early stage infection.

iii) New antigens for use in vaccines. The same proteins may have application in new-generation vaccines for Johne's disease. They can be produced using genetic engineering and so would be much cheaper than the existing commercial vaccine. Cost of vaccine is now emerging as a major impediment to widespread use of Gudair ® vaccine.

iv) New research tools. This project has caused the development of a very wide range of new methods for study of Johne's disease at cellular and molecular levels. These will facilitate new discoveries.

6.1.3 Conceptual advances in 5 years time

i) What is Johne's disease and what can be done about it? As a result of this project Johne's disease can no longer be considered a disease of adult animals. It is in fact a life long infection that begins early in life. Conceptually it can be detected early in life and removed form a flock before causing harm or spreading. The technical advances made during this project enable this dramatic change in conceptual approach.

ii) Tests can be developed that will detect animals prior to shedding the bacterium in faeces. This change in thinking may lead to renewed interest in control if animal health regulatory authorities and public health agencies deem this to be necessary. If control is not contemplated in the future, but public health concerns persist and impact markets, it will be possible to apply tests to individual animals to determine their prior exposure to *M. paratuberculosis.* This will certainly be possible at flock level and may also be possible at individual animal level with further research.

6.1.4 Structural impacts in 5 years time

Failure to maintain human capital is a critical risk for the future of the livestock sector in Australia. This project has helped to alleviate this risk in a highly specialised area: animal health and market assurance. This project has directly or indirectly enabled the training of eight PhD students who will remain a highly skilled resource for the livestock sector if employment signals exist to service the sector. Similarly a group of young post doctoral scientists and technical staff has gained invaluable experience in the livestock sector through this project.

7 Conclusions and Recommendations - Section

7.1 Conclusions and Recommendations

7.1.1 Conclusions

1. Johne's disease remains a difficult problem and without ongoing basic research at an international level will not be successfully controlled.

   There are parallels between the needs in Johne's disease research and those in tuberculosis in humans, which is caused by a related bacterium, *M tuberculosis*. Writing recently in the international journal Tuberculosis, Izzo and others (2005) noted that "The model established by the National Institute of Health to achieve their goals in the TB vaccine development program include an assortment of tasks such as identifying mechanisms of host defence, improving animal models and conducting Phase 1/II trials over a period of 20 years. There is little certainty in the time span chosen to achieve these goals, but there has been definite progress made in many of the tasks" (Izzo et al (2005) NIH pre-clinical screening program: overview and current status. Tuberculosis 85:25-28). With this background it is vital to note that the laudable aims of JD research programs worldwide will have the same challenges and difficulties as those for tuberculosis. The current OJD.031 project must be considered as a first step; as the first project of its kind in the world it has made remarkable progress.

2. Good progress has been made in this project, with all of the objectives successfully achieved.

   The application of new technologies in a basic research program has led to important discoveries with immediate and long term potential to greatly improve the way Johne's disease is managed.

7.1.2 Recommendations

1. Considerable basic research on the pathogenesis of Johne's disease will be required to successfully control this disease. Industry should be advised that there is no "quick fix" and the example of tuberculosis in humans should be used as a current example of how difficult the mycobacterial problem can be to solve.

   "The model established by the National Institute of Health to achieve their goals in the TB vaccine development program includes an assortment of tasks such as identifying mechanisms of host defence, improving animal models and conducting Phase 1/II trials over a period of 20 years. There is little certainty in the time span chosen to achieve these goals, but there has been definite progress made in many of the tasks" (Izzo et al (2005) NIH pre-clinical screening program: overview and current status. Tuberculosis 85:25-28). With this background it is vital to note that the laudable aims of Johne's disease research programs worldwide will have the same challenges and difficulties as those for tuberculosis.

2 The direct faecal PCR test developed in this project is suitable for routine use following further validation, improvement to work flow in a routine laboratory setting and implementation/use at other laboratories. This work should proceed immediately.

3. Some of the immunological tests developed during this project appear to have promise and should be evaluated further in both sheep and cattle. Examples include IFN-g ELISPOT, lymphocyte proliferation, IL-10 ELISA and various ELISA-based assays based on novel dormancy-associated antigens.

4. Intellectual property protection should be obtained for key discoveries in this project and maintained until their commercial potential has been fully evaluated. This will require considerable additional research. The discoveries include: dormancy-stress-associated antigens of *M. paratuberculosis* which may be useful in vaccines or diagnostic assays, and; host genes where expression is altered in association with *M. paratuberculosis* infection.

8 Bibliography

Due to the very large number of scientific references required in each subprogram a bibliography is provided separately for each in the appendices.

There were a large number of publications arising from this study and those closely associated with it. They are listed in this section.

Begg D, Bosward K, de Silva K, Di Fiore L, Taylor D and Whittington R (2005). ELISPOT – new methods for detecting IFN-γ. Proceedings of the MLA OJD Harvest Year Conference, 8-9 December, 2005, Adelaide. Meat and Livestock Australia, North Sydney pp. 48-50

Begg D, de Silva K, Di Fiore L, Taylor D and Whittington R (2007). Seeing spots, developing an IFN-gamma ELISPOT assay to detect ovine M. avium subspecies paratuberculosis infection. Proceedings of the 9th International Colloquium on Paratuberculosis, Tsukuba, Japan.

Begg DJ, Taylor D, de Silva K, Di Fiore L and Whittington R (2007). Experimental infection of sheep with M.avium subspecies paratuberculosis: a brief review and introduction to an Australian ovine challenge model. Proceedings of the 9th International Colloquium on Paratuberculosis, Tsukuba, Japan.

Bosward K, Begg D, de Silva K, Di Fiore L, Taylor D, Emery D and Whittington RJ (2006). Optimisation of the interferon-gamma assay to maximise responses to M. ptb. antigen in sheep. In: Manning EJB and Nielsen SS (Eds.) Proceedings of the 8th International Colloquium on Paratuberculosis, Copenhagen, Denmark, August 2005. International Association for Paratuberculosis, Madison p. 549

Bosward KL, Begg D, de Silva K, Di Fiore L, Taylor D and Whittington R (2005). Manipulation of the Interferon – gamma assay to maximise responses to M.ptb antigen in sheep. Proceedings of the MLA OJD Harvest Year Conference, 8-9 December, 2005, Adelaide. Meat and Livestock Australia, North Sydney pp. 32-33

Bower K, Begg D, Di Fiore L, Taylor D and Whittington R (2007). Culture of M. paratuberculosis from blood. Proceedings of the 9th International Colloquium on Paratuberculosis, Tsukuba, Japan.

Browne S, de Silva K, Begg D, Whittington R and Emery D (2007). Apoptosis of mononuclear cells in experimental and natural ovine Johne's disease. Proceedings of the 9th International Colloquium on Paratuberculosis, Tsukuba, Japan.

Browne S, de Silva K, Whittington R and Emery D (2005). Apoptotic responses during the pathogenesis of ovine Johne's disease. Proceedings of the MLA OJD Harvest Year Conference, 8-9 December, 2005, Adelaide. Meat and Livestock Australia, North Sydney pp. 44-47

Browne S, de Silva K, Whittington R and Emery D. Apoptosis in sheep exposed to Mycobacterium avium paratuberculosis. Apoptosis and Immunity Conference, Cairns, May 2005.

Browne S, de Silva K, Whittington R, Emery D (2006). Ovine apoptotic responses to Mycobacterium avium paratuberculosis. In: Manning EJB and Nielsen SS (Eds.) Proceedings of the 8th International Colloquium on Paratuberculosis, Copenhagen, Denmark, August 2005. International Association for Paratuberculosis, Madison p. 149

Cousins DV, Whittington RW (2003). Faecal detection of Mycobacterium paratuberculosis: The Australian experience. 46th Annual Conference of the American Association of Veterinary

Laboratory Diagnosticians; held in conjunction with the United States Animal Health Association Conference 9-16 October, San Diego, CA: pp87.

de Silva K, Begg D, Di Fiore L, Taylor D, Emery D, and Whittington R (2005). Early cellular responses in ovine Johne's disease. Proceedings of the MLA OJD Harvest Year Conference, 8-9 December, 2005, Adelaide. Meat and Livestock Australia, North Sydney pp. 40-43

de Silva K, Begg D, Taylor D, Di Fiore L and Whittington R (2007). Proliferation of lymphocyte subsets in experimental ovine Johne's disease Proceedings of the 9th International Colloquium on Paratuberculosis, Tsukuba, Japan.

de Silva K, Carter N, Taylor D, Di Fiore L, Whittington R and Emery D (2006). Proliferative responses in peripheral blood and lymph node cells in the early stages of ovine Johne's disease. . In: Manning EJB and Nielsen SS (Eds.) Proceedings of the 8th International Colloquium on Paratuberculosis, Copenhagen, Denmark, August 2005. International Association for Paratuberculosis, Madison p. 150

Dhand NK, Eppleston J, Whittington RJ and Toribio JALML (2007). Risk factors for ovine Johne's disease in infected sheep flocks in Australia. Preventive Veterinary Medicine 82: 51-71.

Di Fiore L, Taylor D, de Silva K, Bosward K, Begg D, Emery D and Whittington R (2006). Identification of differentially expressed genes in uninfected and Mycobacterium paratuberculosis (M. ptb.) infected sheep. In: Manning EJB and Nielsen SS (Eds.) Proceedings of the 8th International Colloquium on Paratuberculosis, Copenhagen, Denmark, August 2005. International Association for Paratuberculosis, Madison p. 445

Di Fiore L, Taylor D, de Silva K, Bosward K, McGregor H and Whittington R. (2005) Gene expression signals from the host. Proceedings of the MLA OJD Harvest Year Conference, 8-9 December, 2005, Adelaide. Meat and Livestock Australia, North Sydney pp. 60-61

Emery DL and Whittington RJ (2004). An evaluation of mycophage therapy, chemotherapy and vaccination for control of Mycobacterium avium subsp. Paratuberculosis infection. Veterinary Microbiology 104: 143-155.

Goldsmith K, Begg D, Di Fiore L and Whittington R. (2005) Detection of Mycobacteria from blood. Proceedings of the MLA OJD Harvest Year Conference, 8-9 December, 2005, Adelaide. Meat and Livestock Australia, North Sydney pp. 51-54

Gumber S and Whittington RJ (2007). Comparison of BACTEC 460 and MGIT 960 systems for the culture of Mycobacterium avium subsp. paratuberculosis S strain and observations on the effect of inclusion of ampicillin in culture media to reduce contamination. Veterinary Microbiology 119: 42-52.

Gumber S, Eamens G and Whittington R. (2005) Evaluation of a Pourquier ELISA kit in relation to agar gel immunodiffusion (AGID) test for assessment of the humoral immune response in sheep and goats with and without Mycobacterium paratuberculosis infection. Proceedings of the MLA OJD Harvest Year Conference, 8-9 December, 2005, Adelaide. Meat and Livestock Australia, North Sydney pp. 34-38

Gumber S, Eamens G and Whittington RJ (2006). Evaluation of a Pourquier ELISA kit in relation to agar gel immunodiffusion (AGID) test for assessment of the humoral immune response in sheep and goats with and without Mycobacterium paratuberculosis infection. Veterinary Microbiology 115: 91-101.

Gumber S, Eamens G and Whittington RJ (2006). Validation of ELISA kit for assessment of the humoral immune response in Mycobacterium paratuberculosis infected sheep and goats. In: Manning EJB and Nielsen SS (Eds.) Proceedings of the 8th International Colloquium on Paratuberculosis, Copenhagen, Denmark, August 2005. International Association for Paratuberculosis, Madison p. 554

Gumber S, Taylor DL and Whittington RJ (2007). Protein extraction from Mycobacterium avium subsp. paratuberculosis: Comparison of methods for analysis by sodium dodecyl sulphate polyacrylamide gel electrophoresis, native PAGE and surface enhanced laser desorption/ionization time of flight mass spectrometry. Journal of Microbiological Methods 68:115-127.

Gumber S, Taylor DL, Marsh IB and Whittington RJ (2007). Survival, dormancy and the proteome of Mycobacterium avium subsp. paratuberculosis during the stress response to hypoxia and nutrient starvation. Proceedings of the 9th International Colloquium on Paratuberculosis, Tsukuba, Japan.

Kawaji S, Taylor DL, Mori Y and Whittington RJ (2007). Detection of Mycobacterium avium subsp. paratuberculosis in ovine faeces by direct quantitative PCR has similar or greater sensitivity compared to radiometric culture. Veterinary Microbiology 125: 36-48.

Kawaji S, Taylor DL, Mori Y and Whittington RJ (2007). Detection and quantification of Mycobacterium avium subsp. paratuberculosis in ovine and bovine faeces by direct quantitative PCR. Proceedings of the 9th International Colloquium on Paratuberculosis, Tsukuba, Japan.

Marsh I, Bannantine J, Tizard M and Whittington R. (2005) Genomic and proteomic comparative study of the sheep and cattle strains of Mycobacterium avium subsp. paratuberculosis. Proceedings of the MLA OJD Harvest Year Conference, 8-9 December, 2005, Adelaide. Meat and Livestock Australia, North Sydney pp. 159-173

Marsh I, Whittington R, Reddacliff L and Eamens G. (2005) Hybridisation capture PCR and direct PCR on pooled faecal samples. Proceedings of the MLA OJD Harvest Year Conference, 8-9 December, 2005, Adelaide. Meat and Livestock Australia, North Sydney pp. 21-27

Marsh IB and Whittington RJ (2005). Deletion of an mmpL gene and multiple associated genes from the genome of the S strain of Mycobacterium avium subsp. paratuberculosis identified by representational difference analysis and in silico analysis. Molecular and Cellular Probes 19: 371-384.

Marsh IB, Bannantine JP, Paustian ML, Tizard ML, Kapur V and Whittington RJ (2005). Genomic comparison of Mycobacterium avium subsp. paratuberculosis sheep and cattle strains by using microarray hybridization. Journal of Bacteriology 188: 2290-2293.

Marsh IB, Bannantine JP, Tizard ML and Whittington RJ. (2006) Genomic and proteomic comparative study of the sheep and cattle strains of Mycobacterium avium subsp. paratuberculosis. In: Manning EJB and Nielsen SS (Eds.) Proceedings of the 8th International Colloquium on Paratuberculosis, Copenhagen, Denmark, August 2005. International Association for Paratuberculosis, Madison p. 381-392.

Sevilla I, Singh SV, Garrido JM, Aduriz G, Rodriguez S, Geijo MV, Whittington RJ, Saunders V, Whitlock RH and Juste RA (2005). Molecular typing of Mycobacterium avium subspecies paratuberculosis strains from different hosts and regions. Revue Scientifique et Technique de L Office International Des Epizooties 24: 1061-1066.

Sevilla I, Singh SV, Garrido JM, Aduriz G, Rodriguez S, Geijo MV, Whittington RJ, Saunders V, Whitlock RH and Juste RA (2006). Molecular typing of Mycobacterium avium subsp. paratuberculosis strains from different hosts and regions. In: Manning EJB and Nielsen SS (Eds.) Proceedings of the 8th International Colloquium on Paratuberculosis, Copenhagen, Denmark, August 2005. International Association for Paratuberculosis, Madison p. 456

Singh SV, Sevilla I, Juste RA, Whittington RJ, Kumar V, Gupta VK, Bhatiya AK, Singh AV (2006). Mycobacterium avium subsp. paratuberculosis (bison type) genotype infecting goat population in India. In: Manning EJB and Nielsen SS (Eds.) Proceedings of the 8th International Colloquium on Paratuberculosis, Copenhagen, Denmark, August 2005. International Association for Paratuberculosis, Madison p. 456

Taylor D, de Silva K, Di Fiore L and Whittington R. Gene expression and survival of M. paratuberculosis infected macrophages. In: Manning EJB and Nielsen SS (Eds.) Proceedings of the 8th International Colloquium on Paratuberculosis, Copenhagen, Denmark, August 2005. International Association for Paratuberculosis, Madison p. 162

Taylor D, Gumber S, de Silva K, Goldsmith K, Di Fiore L, Begg D and Whittington R. (2005) Molecular approaches to studying the host-parasite interaction. Proceedings of the MLA OJD Harvest Year Conference, 8-9 December, 2005, Adelaide. Meat and Livestock Australia, North Sydney pp. 62-64

Taylor DL, Zhong L, Di Fiore L, Begg DJ, De Silva K and Whittington RJ (2007). Analysis of Toll-like receptor gene expression in Mycobacterium paratuberculosis infected sheep. Proceedings of the 9th International Colloquium on Paratuberculosis, Tsukuba, Japan.

Taylor, DL, Thomson PC, de Silva K and Whittington RJ (2007). Validation of endogenous reference genes for expression profiling of RAW264.7 cells infected with Mycobacterium avium subsp. paratuberculosis by quantitative PCR. Veterinary Immunology and Immunopathology 115: 43-55.

Whittington R (2005). Johne's disease – an Australian perspective. Proceedings of the Food Safety and Epidemiology Branches of the New Zealand Veterinary Association. NZVA Conference 30 May – 1 June 2005, Wellington. VetLearn, Massey University, Palmerston North. pp 123-142.

Whittington RJ (2003). An overview of diagnostic tests for paratuberculosis. In: Juste RA, Geijo MV, Garrido JM (Eds.) Proceedings of the 7th International Colloquium on Paratuberculosis, Bilbao, Spain, June 2002. International Association for Paratuberculosis, Madison, WI. pp. 131-135

Whittington RJ and Windsor PA (2007). In utero infection of cattle with Mycobacterium avium subsp. paratuberculosis. Proceedings of the 9th International Colloquium on Paratuberculosis, Tsukuba, Japan.

Zhong L, Taylor DL and Whittington RJ (2007). Proteomic analysis for biomarkers for Johne's disease in sheep serum by SELDI-TOP mass spectrometry. Proceedings of the 9th International Colloquium on Paratuberculosis, Tsukuba, Japan.

Zhong L, Taylor DL and Whittington RJ. (2005) Proteomic analysis of sheep serum by SELDI TOF-MS: Identification of putative biomarkers of ovine Johne's disease. Proceedings of the MLA OJD Harvest Year Conference, 8-9 December, 2005, Adelaide. Meat and Livestock Australia, North Sydney pp. 55-59

9 Appendices

9.1 Appendix 1A-1 Subprogram 1 Investigations into the conditions affecting gamma-interferon production in a whole blood assay in sheep

Abbreviations

BJD, Bovine Johnes Disease; Con A, Concanavalin A; EDTA, ethylenediaminetetraacetic acid; ELISA, Enzyme-linked Immunsorbent. Assay; IFN-γ, interferon-gamma; Mptb, Mycobacteria avium subspecies paratuberculosis; OJD, Ovine Johnes Disease; PPD, purified protein derivative; PWM, pokeweed mitogen.

Introduction

The Bovigam® assay (Pfizer/CSL) is a commercially available biphasic whole blood assay utilising an enzyme-linked immunsorbent assay (ELISA) to measure interferon-gamma production. The assay was originally developed for use in cattle in the diagnosis of tuberculosis (Rothel et al., 1992) and has been subsequently used in the diagnosis of Bovine Johnes disease (BJD) (Ref). The assay is especially useful in that it detects the cell mediated immune responses that, in diseases such as Johne's disease, typically occur earlier than the humoral responses which are often associated with onset of clinical disease. The optimal conditions for use of the Bovigam® assay in cattle have been well documented (Rothel et al., 1992). It is recommended that bovine blood samples should be collected into blood tubes in which heparin salts are used as the anticoagulant; that the blood should be assayed within eight hours of collection; and that 16 hours is the optimum incubation time for the whole blood stimulation phase of the assay (Rothel et al., 1992).

In recent years, the assay has been utilised as a research diagnostic test in ovine Johne's Disease (OJD) control programmes. Its capacity to detect infected animals early in the disease process enables it to potentially identify infected sheep prior to bacterial faecal shedding. Removal of such animals from the flock could result in reduction in contamination of pasture and subsequent reduced infection of other sheep. Up until this point however there have been few reports into the optimisation of the assay for use in sheep.

The aims of the current study were therefore to improve the use of the Bovigam® assay in sheep by investigating the effect of different anticoagulants, cell concentrations, blood supplements, blood storage conditions and transit times on production.

Materials and Methods

Sheep

Experiments were conducted on both intensively housed sheep and in field trials. For the initial investigations, two adult Merino sheep were used. The sheep had been vaccinated against OJD (Gudair®, manufacturer) at least 14 days prior to the experiment according to the manufacturer's instructions. Other sheep included the OJD.031A, OJD.028 and OJD.031 trials. For the large scale field trial, 50 approximately seven month old Merino sheep were selected from a property in Trunkey (via Bathurst) in NSW. These sheep had been vaccinated (Gudair®, manufacturer) five months prior to blood collection according to the manufacturer's instructions.

Mptb Antigen

The purified protein derivative (PPD) utilised as the Mptb antigen in these studies (Mptb 316V) was provided by NSW Department of Primary Industries and was prepared according to previous description.

Blood collection

Blood was collected from the jugular vein into ten ml lithium heparin vacutainer tubes for all experiments except for those in which the effect of differing anticoagulant was analysed. In these experiments, blood was also collected into ten ml fluoride oxalate and EDTA vacutainers.

Whole blood culture

Previous studies in cattle (Rothel et al., 1992) in which the blood was diluted in tissue culture media described the non-specific release of in some samples however this finding was not observed in the current study in sheep. Therefore in the current studies all samples were diluted 1:2 in media in order to facilitate adequate mixing with antigen or mitogen. RPMI media (to which had been added FBS, glutamine, Penstrep and 2 mercaptoethalene), was utilised for all experiments. For the initial investigations, 0.5 ml of whole blood was incubated at 37 °C in a humidified atmosphere of 5% CO2 in air in 48 well culture trays with either 0.5 ml RPMI media alone, or RPMI media containing Mptb antigen (at a final concentration of 5µg/ml). Two mitogens, Concanavalin A (Con A, at a final concentration of 10 µg/ml) or pokeweed mitogen (PWM, at a final concentration of 5 µg/ml), were utilised as positive controls to ensure the cells were capable of responding to stimulation. The concentration of Mptb antigen, Con A and PWM were optimised in previous titration assays. For the experiments to determine the optimum incubation time, plates were incubated for 24 to 72 hours. For all subsequent experiments plates were incubated for 48 hours. Following incubation, the supernatant was aspirated from the culture plates and stored in 96 well plastic storage plates at -20 °C until assayed.

ELISA

The whole blood culture method was followed by the Bovigam® sandwich ELISA as previously described by Rothel et al. (1990) and performed according to the manufacturer's instructions. All samples were assayed in duplicate or triplicate wells. Optical densities were measured on a spectrometer at 450 nm (manufacturer, address). Samples were re-assayed if values differed from their means by greater than 10%.

Field trial investigations into the effect of varying transport temperature and time of adding antigen on IFN-□ production

1 Blood collection, transport conditions, whole blood assay and ELISA

Blood was initially collected into ten ml vacutainers containing lithium heparin, mixed and immediately dispensed in one ml alloquots into one of nine polystyrene tubes. Three of the tubes were pretreated with one ml of media alone, three tubes were pretreated with one ml of media containing either Mptb antigen, and three tubes were pretreated with one ml of media containing PWM. The triplicate tubes were then treated in one of three ways:

Group One

For each sheep, three polystryrene tubes containing one of blood in one ml of media alone, one ml of media plus antigen and one ml of media plus mitogen was then transported to the laboratory at ambient temperature which was estimated to have varied between ten and 20ºC. Once at the laboratory, the blood was placed on a bench overnight then incubated in the laboratory incubator at 37°C for 48 hours prior to harvesting the supernatant.

Group Two

For each sheep, three polystryrene tubes containing one of blood in one ml of media alone, one ml of media plus antigen and one ml of media plus mitogen was then transported to the laboratory at in a portable incubator (Cellestis) at 37 °C. Once at the laboratory the blood was placed in a laboratory incubator at 37°C overnight and for a further 48 hours after that prior to harvesting the supernatant.

Group Three

For each sheep, three polystryrene tubes containing one of blood in one ml of media was transported to the laboratory at ambient temperature which was estimated to vary between ten to 20ºC. Once at the laboratory the blood was placed on the laboratory bench overnight. The following morning, either Mptb antigen or PWM was added to two of the three tubes with the final control tubes left as is. All tubes were then placed in the laboratory incubator at 37°C for 48 hours prior to harvesting the supernatant. Once harvested, all supernatants were stored at -20 °C prior to being assayed in the Bovigam® ELISA according to manufacturer's instructions.

2 Statistical analysis

All statistical analysis was performed on Genstat or Minitab version 14. Data were logarithmically transformed prior to analysis of group differences with an analysis of variance and a Chi-squared test. For this experiment, two levels of stringency criteria were utilised to determine if a sample was considered positive or negative. For the more stringent level, the sample was considered positive if the absorbance of the stimulated sample (either PWM or Mptb antigen) was 0.100 absorbance units greater than the absorbance achieved for the non-stimulated control well (media only) for that animal and if the absorbance of the stimulated sample was twice that of the unstimulated sample (i.e. OD Mptb/OD media only ≥ 2 and OD Mptb ≥ OD media only + 0.1). This classification of a sample as a positive reactor was extracted from similar intetpretations reported by researchers who have used the assay for detection of IFN-γ in cattle (Stabel and Whitlock, 2001). For the less stringent criterion level, the sample was considered to be positive if the absorbance of the stimulated sample (either PWM or Mptb antigen) was 0.050 absorbance units greater than the absorbance achieved for the non-stimulated control well (media only) for that animal and if the absorbance of the stimulated sample was 1.3 times that of the unstimulated sample (i.e. OD Mptb/OD media only ≥ 1.3 and OD Mptb = media only + 0.05). This criterion has also been utilised by other researchers.

Results

Effect of anticoagulant

The effect of anticoagulant on production was evaluated in two vaccinated animals. Blood collected into tubes containing lithium heparin resulted in the optimal response with collection of blood into tubes containing potassium EDTA and sodium fluoride resulting in a complete abrogation of the IFN-γ response (Figure 1).

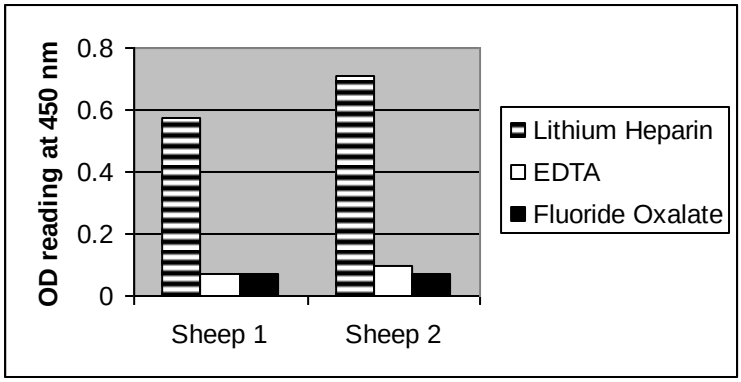

Figure 1. Effect of anticoagulant on IFN-γ production in response to incubation with Mptb antigen in two vaccinated sheep.

Effect of varying duration of incubation.

The effect of varying duration of incubation on IFN-γ production was evaluated in two vaccinated sheep following stimulation in the whole blood assay with Mptb antigen and Con A mitogen. Blood was incubated for 24, 48 or 72 hours prior to harvesting the supernatant. Optimum IFN-γ production was obtained following 48 hours incubation for samples obtained from both sheep that were subsequently stimulated with both antigen and mitogen (Figure 2).

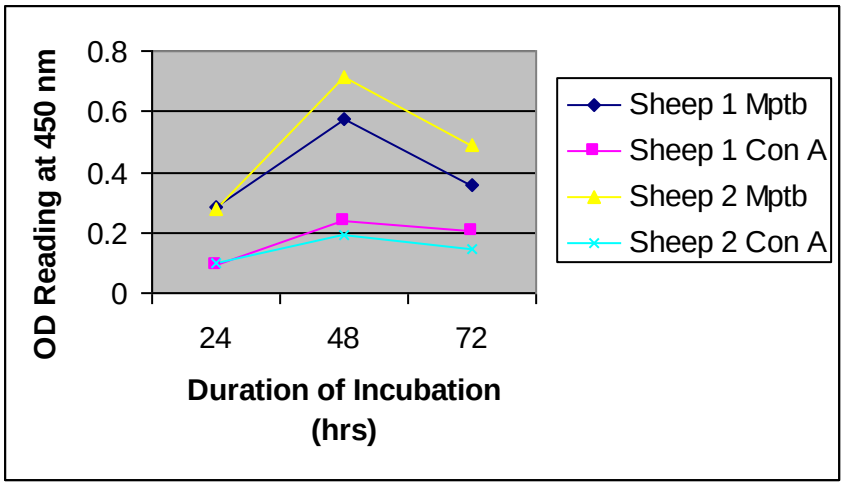

Figure 2. Effect of varying incubation time at 37 °C on IFN-γ production in two vaccinated sheep in response to stimulation with Mptb antigen and Con A mitogen.

Effect of blood storage temperature and duration

The effect on IFN- γ production of varying the temperature at which blood was stored for four, eight or 24 hours prior to incubation in the whole blood assay was evaluated in two vaccinated animals. Adding the antigen at the time of blood collection consistently resulted in lower IFN- γ production than adding that obtained when the antigen was added just prior to incubation irrespective of what temperature the blood was held at or for how long (Figs 3). The longer the delay to incubation, the less IFN-γ produced.

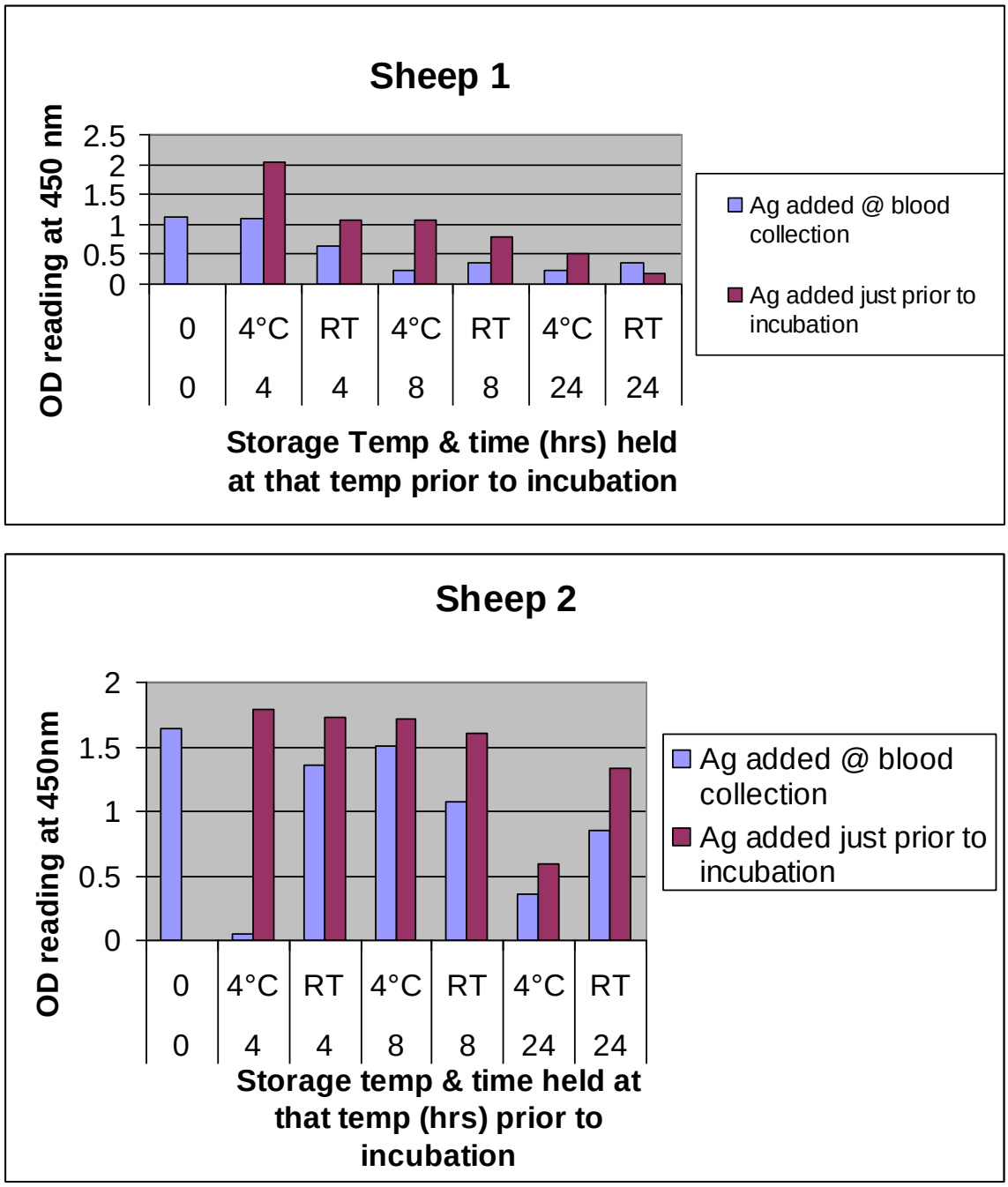

Figure 3. Effects of storage temperatures and time on interferon production

Effect of various media additives

If blood is kept at room temperature during transit additives may be beneficial, although the results were not conclusive (Figure 4). Glucose had a negative impact.

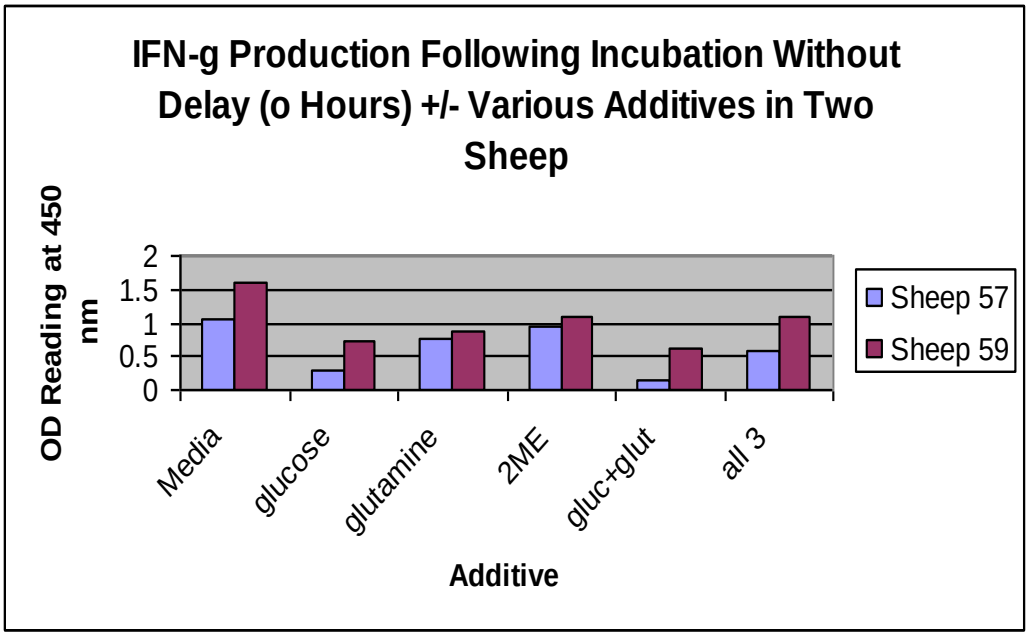

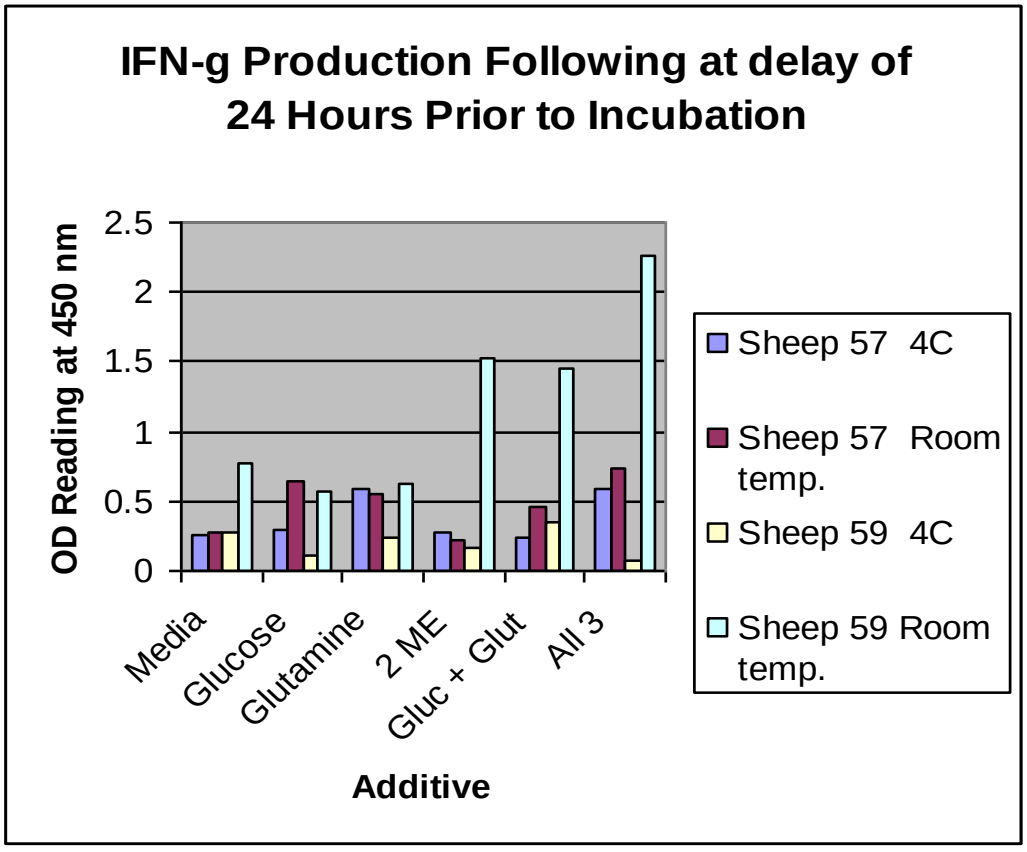

Figure 4. Effect of additives to blood on interferon production.

Effect of total white blood cell concentration and differential cell count

Effect of cell concentration

Decreasing cell concentration in vaccinated sheep

The effect of titrating the total peripheral blood leucocyte by diluting blood with media 1:2 was examined in two vaccinated sheep. In both sheep, with decreasing cell concentration, there was a decreasing IFN-γ response (Figure 5).

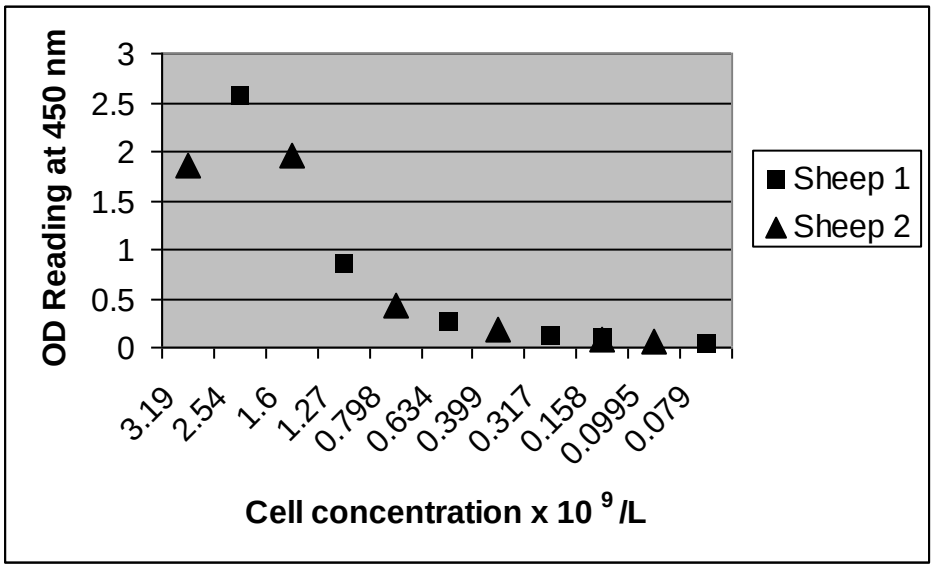

Figure 5. Effect of titrating total white cell concentration on IFN-γ production in two vaccinated sheep.

1b Increasing and decreasing cell concentration in naturally infected sheep

The effect of both concentrating and titrating the peripheral blood leucocyte concentration with media was examined in four naturally infected sheep (OJD.031A sheep). In all four sheep concentrating the peripheral blood concentration two fold resulted in an increase in the IFN-γ production. Subsequent dilution of the sample 1:2 in media resulted in a decreasing IFN-γ response (Figure 6).

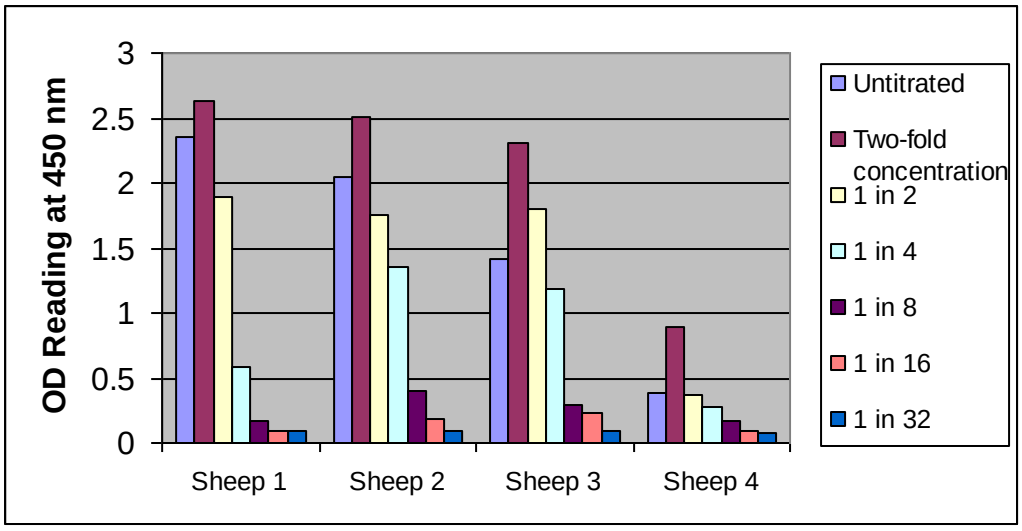

Figure 6. Effect of white blood cell concentration on interferon production.

Field trial experiment

Effect of blood sample treatment on IFN-γ response.

The IFN-γ production in those samples in which Mptb antigen was added at the time of blood collection with subsequent transportation to the laboratory at ambient temperature (Group one) was significantly lower than for the those samples in which the Mptb antigen was added at blood collection with subsequent incubation at 37°C (Group two) or for which the samples were transported at ambient temperature to laboratory with the antigen added added 24 hours after blood collection (Group three). This effect was observed only with the samples stimulated with Mptb antigen and not with those samples stimulated with poke weed mitogen or with the media only controls in which there were no significant differences observed between the three groups (Figure 7).

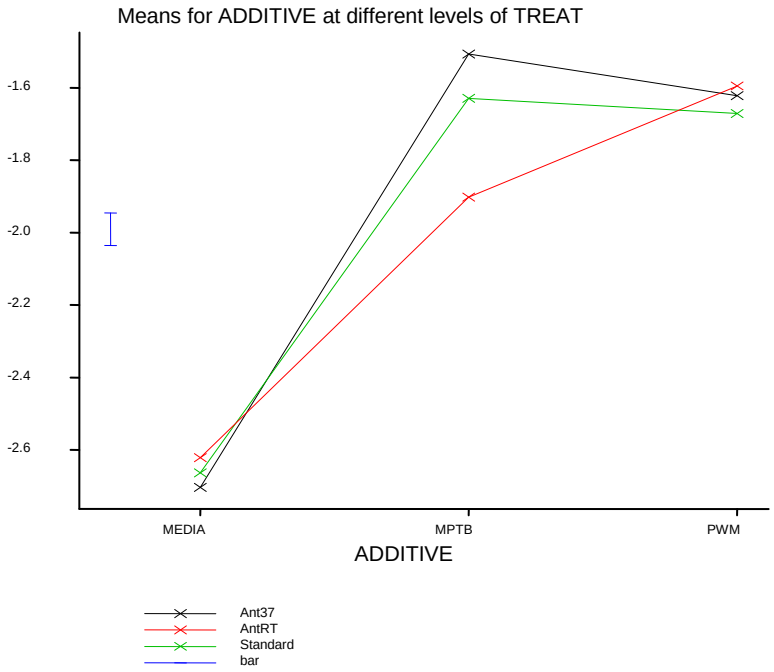

Figure 7. Effect of additives and temperature on interferon production in a field trial ($\log_e$OD)

Effect of treatment on classification of sample as positive or negative.

Two levels of stringency were examined to determine whether adding antigen at blood collection and incubating the sample during transport would result in an IFN-γ level that would be considered a positive reactor that would otherwise have been considered negative. A Chi-squared test revealed no significant differences between the three groups for either level of stringency in terms of the number of samples that would be considered positive reactors. However, when each sheep is analysed individually for its categorisation as positive or negative in response to each treatment, for the more stringent criteria for a sample to be considered positive (i.e. OD Mptb/OD Media only ≥ 2 and OD Mptb ≥ OD Media only + 0.1), 19 out of 46 sheep had a different result based on the treatment the blood received following collection. For nine of those 19 sheep, adding the antigen at blood collection and incubating at ambient temperature would have led to a negative result that would otherwise have been considered positive. For two of those 19 sheep adding antigen at blood collection and incubating at 37 °C led to a positive result that would be otherwise be considered negative if not incubated during transportation. For three of those 19 sheep, adding antigen at blood collection led to a negative result that would otherwise have been considered positive. For the less

stringent criteria for positivity (i.e. OD Mptb/OD Media only ≥ 1.3 and OD Mptb = Media only + 0.05), in 20 out of 43 sheep treatment affected whether the sheep would have been classified as a positive or negative reactor. For 11 of those 20 sheep, adding antigen and incubating at ambient temperature lead to a negative result that would otherwise have been considered positive. For three of those 20 sheep adding antigen and incubating at 37 °C during transportation lead to positive result that would be otherwise negative and for one of those 20 sheep, adding antigen at collection led to a negative result that would have otherwise been positive if the sample had been transported to the laboratory before adding the antigen.

Discussion

The finding that the anticoagulant used in blood sample collection greatly affected IFN- γ production was consistent with that observed when the assay is utilised in cattle (Rothel et al., 1992) and others (Pauly Elasser-Beile See Rothel ref), with the greatest IFN- γ production obtained with the use of Lithium heparin whilst almost complete abrogation the IFN-γ response occurs with the use of Fluoride oxalate and EDTA. In contrast to the studies in cattle, optimum IFN- γ production was obtained after incubation of the blood with the antigen for at least 48 hours as compared to 16 hours in cattle. Interestingly, the finding that 48 hours was required for optimum IFN- γ production in sheep is consistent with that obtained in other species including humans.

The aims of the field trial study was to determine if adding the antigen at blood collection and incubating the sample at 37 °C during transportation to the laboratory could overcome the losses in IFN-γ production resulting from poor viability of the cells due to aging. The results of the study suggested that this may be possible in some samples however if the Mptb antigen is to be added to the blood at collection, it is imperative that the blood be transported at 37°C. Significantly lower IFN-γ values were obtained if the samples were transported at ambient temperature without incubation at 37 °C. This was not the case for those samples in which PWM was the additive suggesting that the result was not a result of the ambient temperature but was due to an interaction between the cells and the antigen. Possible explanations could include that there is a component of the Mptb antigen that is having a negative impact on the cell's ability to remain viable or respond to the antigen and that this effect is abrogated at 37 °C. The Mptb antigen utilised in this study is a crude bacterial preparation and further studies should be directed at determining if this effect is repeatable with different sources of PPD or methods of PPD production.

References

Rothel, J.S., Jones, S.L., Corner, L.A., Cox, J.C., Wood, P.R., 1992. The gamma-interferon assay for diagnosis of bovine tuberculosis in cattle: conditions affecting the production of gamma-interferon in whole blood culture. Aust. Vet. J. 69, 1-4.

9.2 Appendix 1A-2 Subprogram 1 Evaluation of cells responsible for IFN-γ production in sheep vaccinated against Mycobacterium avium subspecies paratuberculosis

Introduction

IFN-γ is thought to play a critical role in protective immunity to mycobacterial infections such as tuberculosis and JD caused by *Mycobacterium avium* subspecies *paratuberculosis* (*M.ptb*) (Flynn et al., 1993; Cunningham et al., 2000; Olsen et al., 2005). IFN-γ plays a central role in type 1 immune responses mediated by T helper 1 (Th1) CD4 cells. Identification of the cells that produce IFN-γ and other cytokines during *M.ptb* may enable improved diagnosis of diseased sheep and the possible identification of animals that will clear the infection. Previous studies in cattle have shown that in the first two years of life there is increased rate of false positive responses to the IFN-γ ELISA assay. The reason for this was found to be non-specific production of IFN-γ by NK cells in response to the *M.ptb* antigens used in the assays (Olsen et al., 2005). The aim of this study was to identify the cell phenotypes that produce IFN-γ in sheep using animals vaccinated against ovine Johne's disease as these usually produce measurable levels of this cytokine.

Methods

Animals

All animals in these experiments were used with the approval of the University of Sydney Animal Care and Ethics Committee. The Merino sheep were maintained at pasture unless otherwise stated. Two sheep were vaccinated with a single dose of Gudair® vaccine (1 mL) in the anterior part of the neck as instructed by the manufacturer.

Intracellular staining for IFN-γ

The following method was used unless otherwise stated. Heparinised blood was centrifuged at 1455 x g for 20 minutes to obtain buffy coats. These were mixed with 3 mL PBS and overlayed onto 2 mL of Ficoll Hypaque (Amersham). The blood layered onto Ficoll tubes were centrifuged at 754 x g for 30 minutes and the interfaces removed into 20 mL of PBS. A cell pellet was obtained by centrifuging at 233 x g for 10 mins This was washed in 10ml of PBS by centrifuging at 233 x g for 10 mins and then resuspended in 5ml of 10% FCS RPMI 1640 (Gibco). Enumeration of the number of viable cells was done using trypan blue and the cell concentration adjusted to 2.5 $X10^6$cell/ml by addition of 10% FCS RPMI 1640. Cells were spilt to three treatments: media control; positive control containing Phorbol-12 Myristate-13 acetate (PMA) 10ng/mL and 1µg/mL of Ionomycin a, and; antigen *M.tpb* (316V EMAI Australia) at 50µg/mL. These were plated into 48 well plates, 1ml per well and incubated at 37^{o}C 5% CO_2. After 6 hours 10 µL of 1mg/mL Brefeldin A (Sigma) was added to each well. At 18 hours the wells were transferred to RIA tubes (BD Biosciences) for staining. Staining was carried out at room temperature in the dark with all centrifugation steps at 233 x g for 5 minutes and all antibodies diluted in FACS buffer (0.1% azide, 1% bovine serum in PBS). RIA tubes were centrifuged to pellet cells to which 50µL FACS buffer or antibody was added and incubated for 10 minutes. The antibodies used were CD4 FITC(17D) at 1/1000, CD5 FITC(CC17)at 1/500 and γδTCR(86D) at 1/500. After surface staining the cells were fixed by addition of 2 mL per tube of BD FACSLYSE (BD biosciences) for 10 minutes then centrifuged and supernatant decanted. Cells were then permeabilised by adding 0.5mL of BD Perm II for 10 minutes, followed by washing cells twice with 2ml of FACS buffer. Intracellular cytokine staining was carried out by addition of 50µL of mouse anti-bovine INF-g (IFN6.19 (A_6B_8) (cell line kindly provided by G. Jungersen Denmark) at 0.25 µg/ml for 10 minutes. Cells were washed once with 1 mL of FACS buffer to remove unbound antibody.

Then 6µL of the secondary labelled antibody goat anti mouse IgG2a APC (Caltag) was added and incubated for 10 minutes. The cells were washed twice with 1 mL of FACS buffer, and to each tube 250 µL of 1% paraformaldehyde was added. A FACSCalibur flow cytometer (BD) was used to read the cells and analysis was carried out using CellquestPro software.

Results

The first assay to measure cytokine producing cells was developed using mitogens to stimulate the cells and IFN-γ was easily detected. However, detection of *M.ptb* specific IFN-γ producing cells was unsuccessful. In the first series of experiments using whole blood, with *M.ptb* antigens to stimulate the cells from an animal vaccinated with Gudair, it was found that the background responses were greater than responses due to *M.ptb* stimulation.

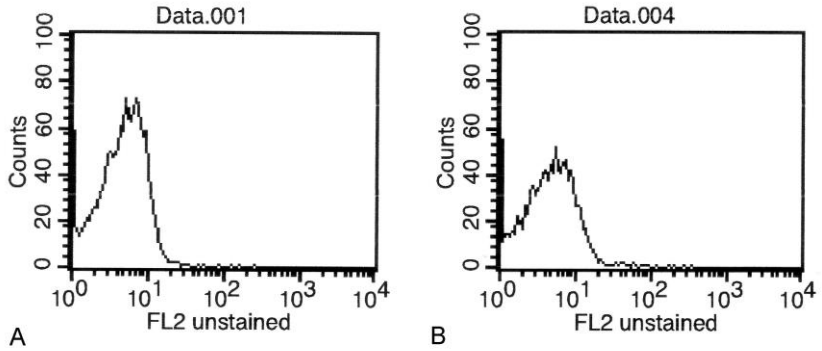

Figure 1: Ficoll density gradient separated and whole blood cells prepared for FACS analysis. A: Ficoll density gradient cells, notice the peak of the graph is narrow with a very small tail to the right. B: Whole blood cells, notice the peak of the graph is wider with a longer tail to the right indicating more background staining.

Stimulated whole blood was compared to Ficoll density gradient separated cells. It was found that the latter produced less background than whole blood (Figure 1).

Although the number of *M.ptb* specific IFN-γ producing cells were very few. Changes in the variables such as the concentration of the *M.ptb* antigen, incubation times and treatment time of the cell with Brefeldin (which stops the cytokine escaping from the cell) did not lead to an increase in the number of *M.ptb* specific IFN-γ producing cells detected (Figure 2).

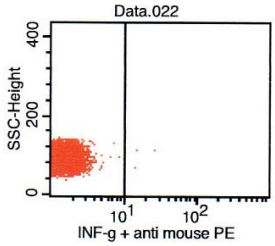

BFA only 4 hours
6.19 stained 0.25μg 10min RT
anti mouse IgG PE 1/2000

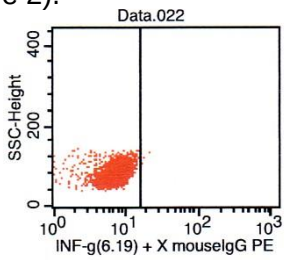

BFA only 24 hours
6.19 stained 0.25μg 10min RT

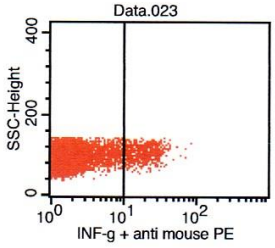

BFA/ionomycin/PMA 4 hours
6.19 stained 0.25μg 10min RT
anti mouse IgG PE 1/2000

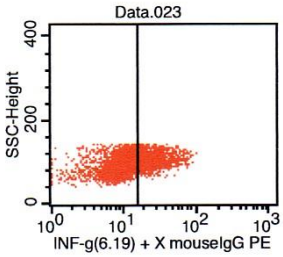

BFA/ionomycin/PMA 24 hours
6.19 stained 0.25μg 10min RT

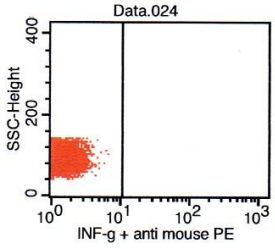

BFA/Mtpb 4 hours
6.19 stained 0.25μg 10min RT
anti mouse IgG PE 1/2000

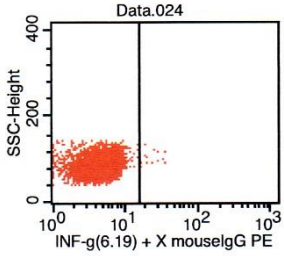

BFA/Mtpb 24 hours
6.19 stained 0.25μg 10min RT

Figure 2. Intracellular staining for IFN-γ production using 4 and 24 hour stimulations. The top two graphs show the unstimulated cells with no IFN-γ production. The middle two graphs show the mitogen stimulated cells with IFN-γ production. The bottom two graphs show the *M.ptb* stimulated cells with no IFN-γ production. The presence of dots in the right hand box indicates IFN-γ producing cells.

The range of *M.ptb* specific IFN-γ producing cells typically recorded was 0.1-1%. It was not until data from the ELISPOT assay was available that this result was confirmed to be meaningful. Data

collected from the ELISPOT also showed that approximately 0.1-1% of cells were producing IFN-γ specific to *M.ptb.*

Due to the low number of IFN-γ producing cells discovered in the above experiment a study was designed using a larger number of cells from a vaccinated sheep to see if it was possible identify the phenotype of the few cells that were producing IFN-γ. The white blood cells after stimulation were stained with the antibody for IFN-γ and subsequently with the phenotypic marker CD-4. However, there was no CD-4 staining. Reversing this antibody staining protocol as suggested by data from another subprogram (1C) did not significantly improve this result (Figure 3).

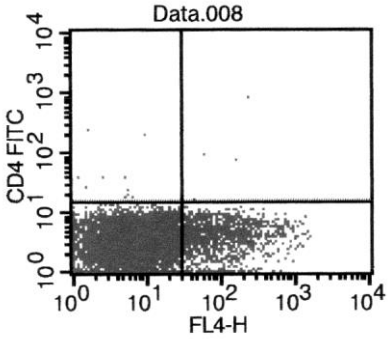

Figure 3. Double staining of white blood cells for the production of IFN-γ (x axis) and the cell surface marker CD-4 (Y axis) in response to the mitogen PMA. The graph shows intracellular IFN-γ production (lower right panel) can be detected but very few CD-4 positive cells can be detected (upper two panels).

A final series of experiments was carried out to discover why the cell phenotype identification procedure was not informative. The experiments used a range of controls and both the CD-4 and CD-5 phenotypic markers. The results from this series of experiments showed that one or several of the chemicals used in the treatment of the cells, (BD Perm II and or BD FACSLYSE) was causing the phenotypic markers on the sheep white blood cells to be lost (Table 1).

Table 1: Intracellular staining with stepwise controls for the determination of loss of cell phenotype markers

Treatment of the cells	Cell phenotype markers	IFN-γ
Normal single staining method	√	√
Brefeldin treatment followed by normal single staining method	√	√
Brefeldin treatment followed by FACS lyse and Perm II treatment and staining	X	√

Discussion

Very few sheep white blood cells produce IFN-γ specifically in response to *M.ptb* antigens and this has made their identification very problematic and time consuming. A series of experiments were designed using a small number of sheep and a large number of cells from each animal to find if it was possible to measure specific cell types producing IFN-γ. The initial experiments were designed to measure IFN-γ production from a phenotype of cells called CD-4, as published literature indicates that this cell type is important in the production of IFN-γ in response to mycobacterial infections (Cowley and Elkins, 2003). The first experiments in this study had shown that very few CD-4 cells were producing IFN-γ. Data gathered from Subprogram 2A gave an indication of normal numbers of CD-4 cells in blood, and so from this data it was realised that the CD-4 counts obtained when cells were also stained for IFN-γ were not correct. An improved experimental design was employed for the analysis of the cells. This showed that CD-4 marker was missing on the white blood cells in which we had measured IFN-γ. Another experiment was designed to test alternative methods of staining the white blood cells for CD-4 and IFN-γ. This was based on information from apoptosis work completed in subprogram 1C which indicated the order in which the cells were stained for two different phenotypic markers such as CD-4 and apoptosis was important. The experiment testing the order of staining the cells did not show any CD-4 expression on the cells. In a similar experiment where CD-5 and IFN-γ double staining was tested it was found that the CD-5 expression on the cells was also lost. It has been deduced from the series of experiments completed to date that there is a problem with the commercial reagents Facs-lyse and/or Perm II when added to sheep blood cells. Discussions with Dr Ingrid Olsen from Norway revealed that this problem does not occur when doing this type of work in goats.

References

Cowley, S. C. and Elkins, K. L. 2003. CD4+ T cells mediate IFN-gamma-independent control of Mycobacterium tuberculosis infection both in vitro and in vivo. J Immunol 171, 4689-99.

Cunningham, J. A., Kellner, J. D., Bridge, P. J., Trevenen, C. L., McLeod, D. R. and Davies, H. D. 2000. Disseminated bacille Calmette-Guerin infection in an infant with a novel deletion in the interferon-gamma receptor gene. Int J Tuberc Lung Dis 4, 791-4.

Flynn, J. L., Chan, J., Triebold, K. J., Dalton, D. K., Stewart, T. A. and Bloom, B. R. 1993. An essential role for interferon gamma in resistance to Mycobacterium tuberculosis infection. J Exp Med 178, 2249-54.

Olsen, I., Boysen, P., Kulberg, S., Hope, J. C., Jungersen, G. and Storset, A. K. 2005. Bovine NK Cells Can Produce Gamma Interferon in Response to the Secreted Mycobacterial Proteins ESAT-6 and MPP14 but Not in Response to MPB70. Infection and Immunity 73, 5628-35.

9.3 Appendix 1B-1 Subprogram 1 ELISPOT: An alternative method for the detection of IFN-γ in M. avium subspecies paratuberculosis infected animals

Introduction

Johne's disease in ruminants is a chronic enteritis caused by infection with *M. avium* subspecies *paratuberculosis* (Mptb). The disease is predominantly spread by the faecal oral route with the infection of animals at a young age. In sheep clinical signs of the disease (weight loss and in the occasional case diarrhoea) develop from 2-5 years of age. One of the confounding issues in the diagnosis of Ovine Johne's disease (OJD) is the infecting strain of Mptb. There are two main strains of Mptb, Cattle (C) and sheep (S), which typically infect their named host species but this is dependant on the geographical location. An example would be sheep where the S strain is more prevalent in Australian and New Zealand while the C strain is more common in India (Sevilla et al., 2005). Typically it is difficult to diagnose Johne's disease in ruminants during the early stages of the infection; only when the animals shed Mptb into the environment and clinical signs start to develop does the sensitivity of the diagnostic tests improve. Current ante-mortem testing for Johne's disease in sheep includes AGID, antibody ELISA and faecal culture. Faecal culture is the current gold standard for the identification of infected animals, although S strain is much more fastidious than the C strain Mptb (Whittington et al., 1999). Interferon gamma (IFN-γ) ELISAs have also been tested but as with the other immunological diagnostic assays for Mptb infection this has poor sensitivity in the early stages of infection (Stewart et al., 2002; Stewart et al., 2004).

The traditional method for detection of IFN-γ from ruminants has been to stimulate whole blood with Mptb antigens, remove the plasma and carry out an ELISA on the plasma. Many research groups typically use kit forms of the assays such as the Bovigam assay (Prionics, Switzerland). The detection of IFN-γ for the diagnosis of Johnes disease using the ELISA has had limited success, depending on the animal species involved and the stage of disease. In sheep the Bovigam assay has been shown to have limited diagnostic potential as the sensitivity is in the range of 50-75% (Stewart et al., 2002; Robbe-Austerman et al., 2006). In cattle IFN-γ ELISAs have had lower specificity in detecting animals younger than 24 months, due to non-specific IFN production by natural killer cells (Olsen and Storset, 2001; Olsen et al., 2005).

In recent years tuberculosis (Tb) detection in humans has improved through the use of IFN-γ assays based on the Enzyme Linked Immuno Spot (ELISPOT) system rather than traditional diagnostic tests such as intradermal skin tests (Lalvani et al., 2001). This assay detects the number of IFN-γ producing cells rather than the total amount of IFN-γ as is measured by traditional cytokine ELISA assays. The ELISPOT has been reported to be 10-200 times more sensitive in the detection of cytokines compared to traditional ELISA (Tanguay and Killion, 1994). Another reason why the ELISPOT has been developed as an alternative form of diagnosis of TB is the ability to discriminate different forms of tuberculosis such as latent or active infections (Codecasa et al., 2006). For these reasons it was decided to develop an IFN-γ ELISPOT for the detection of *M. paratuberculosis* infection in sheep.

Methods

Animals
All animals in these experiments were used with the approval of the University of Sydney Animal Care and Ethics Committee. The Merino sheep were maintained at pasture unless otherwise stated.

Vaccinated sheep
Two sheep were vaccinated with a single dose of Gudair® vaccine (1 mL) subcutaneously to the anterior part of the neck as instructed by the manufacturer.

Naturally exposed or Johne's disease free sheep
Animals were selected from farms in NSW, Australia on which Ovine Johne's disease had been previously identified or found to be free of the disease. The diseased animals were transported to the University of Sydney OJD quarantine shed and held for 2 weeks prior to necropsy. The animals were feed lucerne chaff and grain once daily with water supplied *ad libitum.* Sheep from the OJD free property remained on farm until the day of the necropsy due to their close proximity. A blood sample was taken from each animal prior to being necropsied.

Experimentally infected sheep
Preparation of the Telford *Mycobacterium avium* subspecies *paratuberculosis* inoculum.
Myobacterium paratuberculosis strain Telford 9.2, a pure clonal culture at passage level 5 (including its primary isolation from sheep faeces) was reconstituted from lyophilised stock and inoculated into a BACTEC vial supplemented with egg yolk and mycobactin J (MJ) (Whittington et al., 1999). After culture in BACTEC to achieve maximal growth, the vial was subcultured to 7H10+MJ slopes and incubated for 4-6 weeks at 37^{o}C. Telford 9.2 is an IS1311 S strain, IS900 RFLP type S1 (Marsh et al., 2006; Marsh and Whittington, 2007).

The slopes were harvested into single cell suspensions prepared in PBS with 0.1% V/V Tween 80. Enumeration was conducted using a visual count in a Thoma-ruled counting chamber and by end point titration in BACTEC medium (using a standard three tube most probable number [MPN] method) (Reddacliff et al., 2003). The visual counts were used to prepare the inoculation doses at 10^{9} Mptb organisms/mL of undiluted suspension. One millilitre aliquots of this stock suspension was diluted in 10 mL of PBS for each of the animals to be infected as shown in Table 1.

The remaining undiluted suspension (stock) was retained at 4°C in order to repeat the inoculation one week later. Another MPN was set up on the day of the second dose from the stock suspension stored at 4^{o}C to confirm the viable dose after storage. IS*900* and IS*1311* PCR assays conducted on the stock solution were used to confirm that the infectious material was Mptb S strain.

A fresh suspension was prepared for further inoculation doses (typically one month later).

Table 1: Experimental inoculations of the sheep

Experiment	Treatment	Age of animals at challenge	No of animals	First dose	Second dose	Third dose
1	Telford 9.2	3 months	18	9.3×10^6	9.3×10^6	2.4×10^8
2	Telford 9.2	3 months	12	9.3×10^7	4.3×10^7	9.3×10^6
3	Telford 9.2	4 months	20	9.3×10^7	9.3×10^7	1.5×10^8
3	Control 9.2	4 months	20			

Necropsy: All animals were euthanased using an intravenous injection of barbiturate into the jugular vein. The intestines from the duodenum to the rectum were removed from the animal and placed in a clean tray. The trays were cleaned with warm water and a virucidal disinfectant, Trigene 2 (Medichem International, UK). Samples were then taken from the following sections of the small intestine terminal ileum, posterior jejunum, mid distal jejunum, middle jejunum, mid proximal jejunum and anterior jejunum and ileocecal lymph node. The ileocaecal lymph node and jejunal lymph nodes corresponding to the sections of jejunum sampled were also collected

Histology: Tissue samples were placed in 10% buffered formalin for 48- 72 hours, embedded in paraffin and sectioned at 8µm. Duplicate sections were stained with hematoxylin and eosin or the Ziehl-Neelsen stain. The sections were then graded using the criteria outline by Perez et al (1996) (Perez et al., 1996). Any section graded with a score of one or higher was considered to be positive.

Isolation of *M. paratuberculosis* from faeces and tissue: Samples collected from animals were frozen at -80^{o}C until they were processed. Faecal samples and tissue samples were processed for BACTEC culture as described previously (Whittington et al., 1999). Briefly after decontamination samples were inoculated into Bactec Vials and cultured for 12 weeks at 37^{o}C. After culture any positive samples were confirmed by PCR and REA as previously described (Whittington et al., 1998a; Whittington et al., 1998b).

Purification of peripheral white blood cells for the ELISPOT

Ficoll density gradient centrifugation

A ten millilitre heparinized vaccutainer of blood was centrifuged at 1,455 x *g* for 20 min. The buffy coat of white blood cells was removed and layered on to 2 mL of ficoll paque (GE Healthcare, Sweden δ = 1.077) and centrifuged at 754 x *g* for 30 minutes with no brake. The cloudy layer of white blood cells was removed and washed twice by centrifugation in 10 ml of phosphate buffered saline (PBS). The cells were resuspended in 5 ml of 10% fetal calf serum (Gibco BRL, Grand Island, NY) made up in RPMI 1640 (Gibco BRL) supplemented with L-glutamine and penicillin/streptomycin (Gibco BRL) (complete media). The cells were enumerated using trypan blue and suspended at 2.5 x 10^6 viable cells/mL

Crude White Blood Cell Buffy Coat preparations

A ten millilitre heparinized Vacutainer of blood was centrifuged at 1,455 x *g* for 20 min. The buffy coat of white blood cells was removed and washed twice by centrifugation in 10 ml of phosphate buffered saline (PBS). The cells were enumerated using Turks solution and resuspended in complete media as stated above at 2.5 x 10^6 viable cells/mL

Red blood cell lysis

A ten millilitre heparinized Vacutainer of blood was centrifuged at 1,455 x *g* for 20 min. The buffy coat of white blood cells was removed placed into 5 mL of red blood cell lysis buffer (NH_4CL 8.3g,

$KHCO_3$ 1g, EDTA 3.72g and 10M NaOH 0.4mL in 1L of MQH_20). After a 5 minute incubation, 5 mL of PBS was added to the buffy coat/lysis buffer mixture and centrifuged at 233 x *g* for 10 minutes. The cells were washed with PBS before being enumerated using Trypan blue and resuspended in complete media as stated above at 2.5 x 10^6 viable cells/mL.

ELISPOT assay to detect IFN-γ

The following ELISPOT methodology was used in all assays unless otherwise stated

ELISPOT plates (Millipore) were coated with 50µL of 2 µg/mL of IFN6.19 (immunoglobulin G2a clone 6.19, supplied by Gregers Jungerson Denmark) or MCA2112 (Serotec) and incubated overnight at 4^{o}C. The plates are then hand washed 6 times with phosphate buffered saline (PBS) to remove excess antibody. Purified white blood cells at a concentration of 2.5 x 10^6 cells per mL were diluted to concentrations of 1.25 x 10^6 cells per mL and 6.25 x 10^5 cells per mL with 100 uL of the three dilutions being placed into each well as required into the plate (Millipore). The cells were incubated with 50mL of either culture media (unstimulated), Mptb 316v antigen 30µg/mL (EMAI Australia), Purified protein derivative from *Mycobacterium avium* (PPD-A) 30µg/mL (CSL) and Pokeweed Mitogen (PWM) 10µg/mL (Sigma). The plates were incubated for 18-24 hours at 37^{o}C with 5% CO_2.

The plates were hand washed 6 times using PBS to remove the cells and 50µL of the secondary antibody MCA1783b (Serotec) was added at a concentration of 0.5µg/mL diluted in PBS. The plate was then incubated at 37^{o}C for 1 hour. The plates were washed in PBS and 50uL of 1µg/mL of alkaline phosphatase streptavidin (Vector Laboratories) was added to the wells. The plates were then incubated at 37^{o}C for 1 hour.

The plate was washed 5 times in PBS and 100µL BCIP substrate (Vector Laboratories) was added for 1 hour at room temperature. The BCIP substrate was then removed and the plate was washed 6 times in water.

The plates are allowed to dry and read in a KS ELISPOT reader (Carl Zeiss).

Results were presented as the number of Mptb antigen specific IFN-γ producing cells/ 10^5 white blood cells by taking the number of antigen reactive cells and subtracting the number of unstimulated IFN-γ producing cells/10^5 white blood cells.

IFN-γ ELISA. The assay used was the proprietary Bovigam kit (Pfizer) Briefly 0.5 mL of blood was placed into wells and stimulated with 0.5 mL of Mptb 316v antigen at 20µg/mL. A negative control consisted of the blood having 0.5 mL of media added while the positive control had 0.5 mL PWM added at 10ug/mL. After 48 hours of culture at 37^{o}C with 5% CO_2 the plasma supernatant was collected and stored at -20^{o}C. An analysis of IFN-γ was preformed using the standard protocol outlined for the Bovigam ELISA kit. Results are presented as OD of the Mptb antigen stimulated sample – the OD of the negative control (media stimulated) sample.

Results

Comparisons of antibodies and preparation methods

After the initial optimisation the sensitivity of detecting spots in the IFN-γ ELISPOT assay was found to be affected by several key parameters, including the choice of capture antibody and the method of isolating the white blood cells. The ELISPOT reader was optimised for counting spots from the ELISPOT IFN-γ assay using the MCA2112 capture antibody. The same settings were used to compare two capture antibodies and the different white blood cell isolation methods.

In a direct comparison between the two capture antibodies (MCA2112 and IFN6.19) there were on average 6 fold more resolved spots with IFN6.19 compared with MCA2112, measured across a

range of test conditions. The difference was highly significant (paired t test P<0.001). This was primarily due to spots being more pronounced using the IFN 6.19 antibody which enabled the ELISPOT reader to detect them more readily (Figure 1).

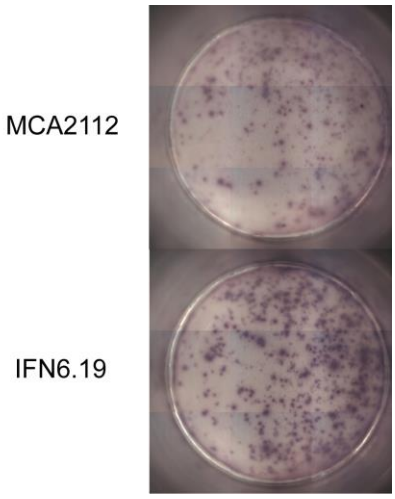

Figure 1: Images of the spots produced when using the capture antibodies MCA2112 or IFN6.19 under the identical conditions in the ovine IFN-γ ELISPOT.

The initial development and optimisation of the IFN-γ ELISPOT was completed on peripheral blood mononuclear cells isolated using Ficoll-paque density gradient centrifugation. This was the standard method to which the other PBMC isolation methods were compared: red blood cell lysis buffer, and; crude white blood cell buffy coats. Both methods produced fewer spots than the Ficoll isolation method using either of the capture antibodies. The percentage reductions of spots measured compared to the Ficoll prepared cells using the MCA2112 capture antibody were 69% $\pm$ 12.5% for the red blood cell lysis method, 76% $\pm$ 22.3% for buffy coat method (n=4) and using the IFN6.19 capture antibody 54% $\pm$ 6.3% red blood cell lysis, 82% $\pm$ 13.1% buffy coat (n=4). As can be seen from Figure 2 the wells using buffy coat prepared cells had a red-brown tinge in the centre due to the red blood cell contamination and increased background colour seen especially when higher concentrations of cells were used. The wells in which the red blood cell lysis buffer cells were prepared did not have background colour but did have fewer spots across the range of cell dilutions tested (Figure 2).

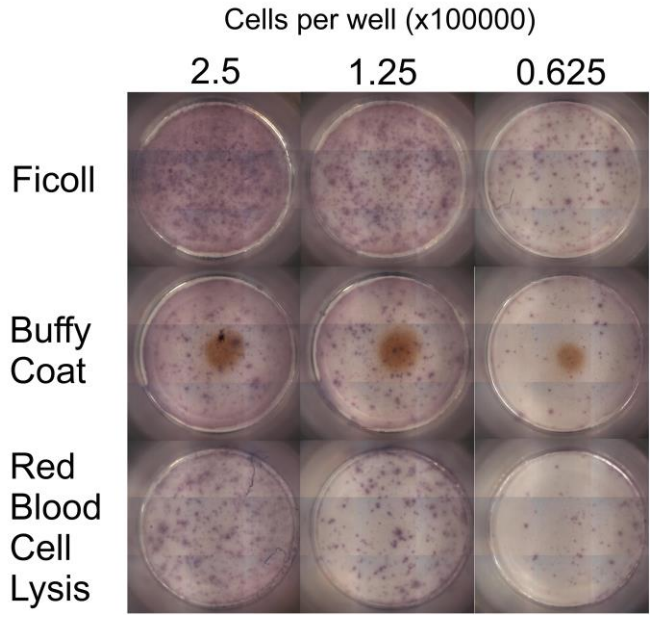

Figure 2: Images of the spots produced when using different peripheral white blood cells purification procedures in the ovine IFN-γ ELISPOT. The capture antibody MCA2112 was used with the purification methods of Ficoll Paque density gradient centrifugation, isolation of the buffy coat via centrifugation and lysis of the red blood cells from buffy coat preparations. All cells were stimulated with PWM

Diagnosis of naturally infected animals

Initial testing on a group of animals from a farm found previously to have OJD showed the IFN-γ ELISPOT assay able to detect strong (>10 Mptb antigen specific IFN-γ producing cells per 10^5 white blood cells) cytokine production from 8/10 Mptb culture positive animals. Animal 981 which was shown to be Mptb culture negative had a strong ELISPOT IFN-γ response (Table 2). The remaining Mptb tissue culture negative animals had minimal IFN-γ responses in both the ELISPOT and Bovigam assays. It can be seen from Table 2 that the two IFN-γ assays gave different results in some animals, 981, 986, 990, were strong responders in the ELISPOT only.

Table 2: Interferon gamma results and infection status as shown by Mptb tissue culture and histology from a group of animals from a farm known to be infected with OJD.

Animal No	ELISPOT*	Bovigam#	Culture	Histology
981	33.2	0.061	-	-
982	0.0	0.001	-	-
983	0.0	0.000	-	-
984	3.6	0.007	-	-
985	27.6	1.904	+	+
986	11.2	0.000	+	+
987	0.4	0.152	+	-
988	60.8	2.830	+	+
989	2.4	2.790	+	+
990	25.6	0.147	+	+
991	0.8	0.000	-	-
992	22.8	1.295	+	+
993	37.6	0.047	+	-
994	11.2	1.821	+	+
995	22.8	0.529	+	-
996	4.4	0.066	-	-

* Number of Mptb antigen specific IFN-γ reactive cells/10^5 white blood cells using the capture antibody MCA2112, the cells were isolated using ficoll density gradient centrifugation.

The Mptb antigen specific IFN-γ OD reading from whole blood stimulated samples tested in the Bovigam assay

Testing the IFN-γ ELISPOT in OJD free animals

The Mptb antigen specific responses in animals not exposed to Mptb was found to vary over time. Figure 3 shows the Mptb antigen specific responses from a group of 20 uninfected animals. While the majority of the animals consistently had low numbers of Mptb antigen specific cells, a few animals had an increasing number over time. At 4 months of age there was a low response as expected, 1.03 $\pm$ 1.2 Mptb specific IFN-γ producing cells per 10^5. At 8 months the average response had slightly decreased (0.66 $\pm$ 1.4). At 12 months of age, the capture antibody was changed to the more sensitive IFN6.19 and there was an increase in the mean number of antigen specific IFN-γ producing cells from the paratuberculosis free sheep (1.4 $\pm$ 3.2). By 17 months of age the animals had an average response of (1.9 $\pm$ 5) but animal 39 clearly had increasing numbers of Mptb antigen specific IFN-γ producing cells.

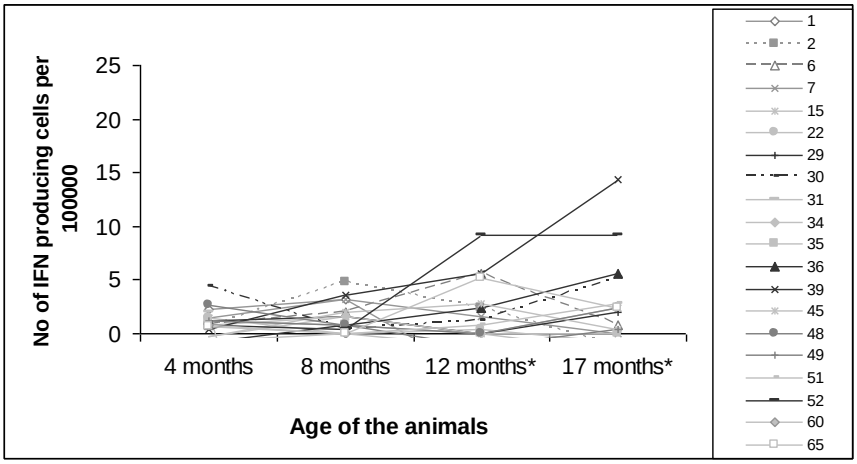

Figure 3: Longitudinal Mptb specific IFN-γ ELISPOT testing on PBMC from a group of 20 OJD free sheep. At 4 and 8 months of age the capture antibody MCA2112 was used while at 12 and 17 months* the antibody was changed to IFN6.19. The PBMC were isolated via ficoll density gradient centrifugation.

Ten merino ewes greater than 3 years of age were selected from the same farm. These animals were found to be negative for OJD by histological analysis and culture of Mptb from their intestinal tissues. Although these animals were classified as OJD negative some of the animals still had Mptb specific responses in the range of 10 reactive cells per 10^5 white blood cells. Significantly most of the animals had a stronger Mycobacterium avium than Mptb antigen (PPDA) response (Figure 4).

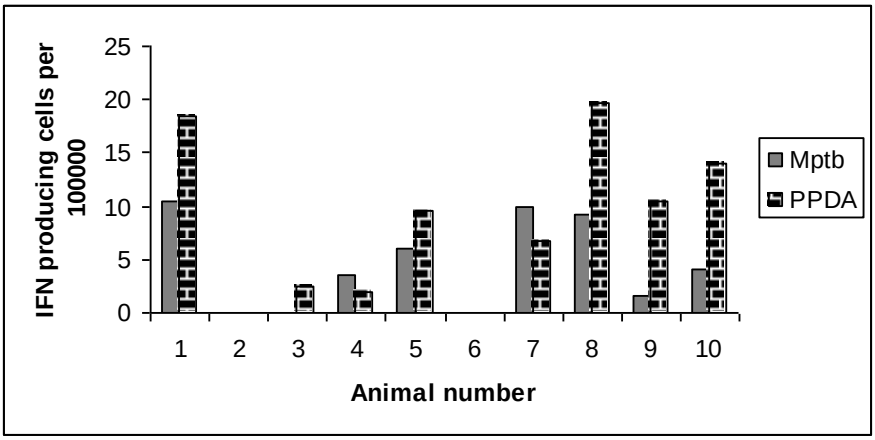

Figure 4: IFN-γ responses from PBMC isolated from 10 OJD free sheep greater than 3 years of age. The animals were found to be free of OJD by histological analysis and tissue culture of intestinal tissues. The assay used the IFN6.19 capture antibody and shows the antigen specific responses to Mptb and Mycobacterium avium (PPDA). The PBMC were isolated via ficoll density gradient centrifugation.

Longitudinal testing of the IFN-γ ELISPOT on blood from experimentally inoculated animals

Sampling of experimental by infected animals over time showed that sheep inoculated with Mptb had more antigen specific IFN-γ producing cells than un-inoculated control animals (Figure 5C). Mptb specific IFN-γ producing cells could be seen as early as 3 months post inoculation although the strength of this response varied over time and between the different experimental infection trials (Figure 5). There was a trend for animals that had apparently cleared the infection to have a lower number of Mptb specific IFN-γ producing white blood cells.

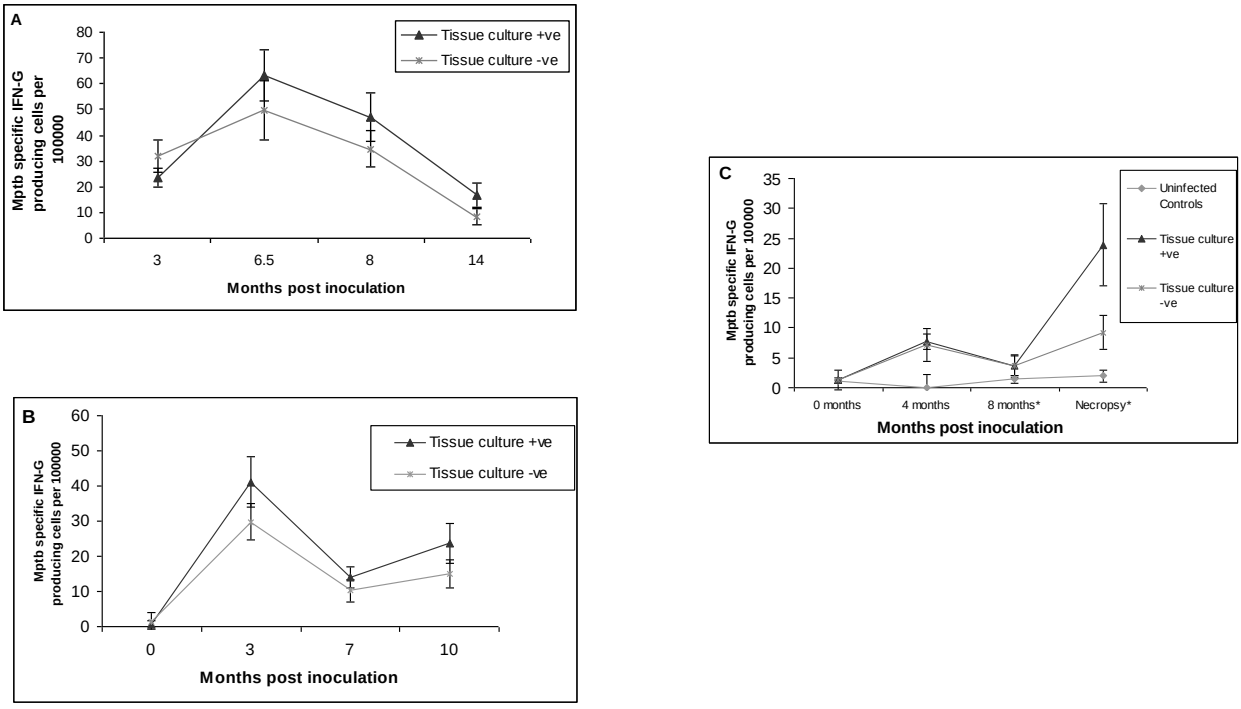

Figure 5: Mptb specific IFN-γ ELISPOT responses from experimentally infected animals over time. A) Average responses from animals inoculated in Experiment 1 that were tissue culture positive or negative. B) Average responses from animals inoculated in Experiment 2 that were tissue culture positive or negative. C) Average responses from animals inoculated in Experiment 3 that were tissue culture positive or negative and also showing a group of un-inoculated animals. Error bars indicate the standard error of the mean.

Discussion

Important aspects that affect the outcome of an ELISPOT assay include the affinity of the capture and detection antibodies and, the activity of the enzyme conjugates and substrates used to generate the spots (Kalyuzhny and Stark, 2001). While there are a limited number of reagents available to veterinary researchers, it was found there were two monoclonal antibodies cross reactive to ovine IFN-γ to enable evaluation of several different capture antibodies. As stated by Kalyuzhny and Stark (2001) the darker the spots and the lighter the background the more accurate the quantification. The selection of the IFN6.19 antibody produced superior spots and therefore improved quantification.

This is possibly due to the IFN6.19 antibody having a higher affinity for ovine IFN-γ than the MCA2112 monoclonal antibody.

The method in which the peripheral white blood cells are prepared was also found to be important. This was analysed as possible future development of the assay will require high throughput and low cost. It was found that Ficoll-paque density gradient centrifugation produced the most easily measured spots in the KS ELISPOT reader while red blood cell lysis of the buffy coat also gave well defined spots. Unfortunately the easiest cell separation method examined, crude buffy coats, produced increased non specific background noise and fewer spots could be enumerated. A reduction in the number of spots when using the red blood cell lysis and buffy coat methods compared to Ficoll separation was not unexpected, as it removes most of the granulocytes, (Neutrophils comprises 10-50%, eosinophils 0-10% and basophils 0-3% of the total leucocyte population in sheep blood) (Feldman et al., 2000). The IFN-γ producing cells are most likely to be T cells (Stabel et al., 2007); granulocytes dilute the number of IFN-γ producing cells resulting in fewer spots being recorded.

It was observed in uninfected animals sampled longitudinally that the number of Mptb specific lymphocytes producing IFN-γ increased over time. A cohort of older animals was necropsied from the same farm. Although these animals did not have an Mptb infection they did have some Mptb specific IFN-γ producing cells, but in general a higher number of *M. avium* specific cells. This could be an indication of exposure to environmental mycobacteria and the poor specificity of the Mptb antigen used. The use of crude antigens has been a problem for the immunological diagnosis of Johne's disease to date but unfortunately there are few commercial antigens available. There is a need for defined specific antigens with which it may be possible to extend the assay to identify animals that are immune, animals that have a latent infection and those that may soon break down into clinical disease state.

The number of Mptb specific reactive cells from infected animals appears to be very low, in the range of 10 to 100 producing cells per 10^5 white blood cells. Some animals may be producing large amounts of IFN-γ from very few cells and this could be an indication of disease status. It has been noted previously as animals move from subclinical to clinical disease there is typically a drop in CMI response (Stabel, 2000), although the IFN-γ response may not always drop as a sheep develops clinical Johne's disease (Begg et al., 2005). As fewer cells may produce IFN-γ but at higher levels per cell there may be a role for assays that measure total IFN-γ as well as the number of IFN-γ producing cells.

As can be seen from Table 2 the IFN-γ ELISPOT showed one sheep (981) to have a high number of Mptb IFN-γ producing cells, but this animal was tissue culture negative and histology negative, in other words apparently free of infection. This response can be explained from data collected from the animal tested as part of the experimental infection studies. It has been shown that animals that are inoculated with Mptb may become immune or over come the infection in some way (Brotherston et al., 1961; Thorel et al., 1992; Gwozdz and Thompson, 2002; Begg and Whittington, 2007). It can be seen from animals that were tissue culture negative in Figure 5, some sheep have possibly eliminated the bacteria or are controlling the infection at lower number than at which tissue culture can detect infection. The number of Mptb specific IFN-γ producing cells from these animals (even though there was trend) was not significantly different from that seen in animals that were tissue culture positive. This indicates the current form of the IFN-γ ELISPOT assay used in this study cannot detect differences between sheep exposed to Mptb but likely to clear the infection and those likely to succumb to disease.

The discovery and use of more Mptb specific antigens may enable better differentiation between animals likely to be immune and those that will succumb to disease or enable identification of sheep that may develop a specific lesion type such as multibacillary or paucibacillary. Research carried out

in tuberculosis has shown that specific antigens from the tuberculosis genome such as Region of Difference 1 (RD1) including culture filtrate protein 10 (CFP-10), early secreted target 6 (ESAT 6) and other proteins such as Rv2031c (also known as HspX, alpha crystalline, or the 16-kDa antigen) as part of ELISPOT IFN-γ tests can allow for the differentiation between active and latent TB patients and people who have been vaccinated with BCG (Lalvani et al., 2001; Goletti et al., 2005; Codecasa et al., 2006; Demissie et al., 2006. However the use of a single RD1 antigen results in a high degree of specificity of the assay but low sensitivity. Improved results are seen when multiple or cocktails of RD1 antigens are used {Pai, 2004 #1504). It was shown by Griffin et al 2005 that by using a number of crude antigens such as purified protein derivatives from Mptb, *M. avium, M. bovis* and protoplasmic antigen from Mptb, a highly sensitive and specific immuno-diagnostic assay could be developed that differentiates between Johne's disease and tuberculosis infections in deer (Griffin et al., 2005a; Griffin et al., 2005b). Since that time numerous studies have been carried out to identify new antigens that may be used in the currently available diagnostic tests such as antibody and IFN-γ ELISAs (Bannantine and Paustian, 2006; Cho and Collins, 2006; Cho et al., 2006; Cho et al., 2007; Leroy et al., 2007; Li et al., 2007).

The difference between assays in identifying animals as strong IFN-γ responders (Table 2) was not surprising and may well aid further diagnosis of diseased animals. The assays measure different outputs; the total amount of IFN-γ released into the plasma for the ELISA compared to the total number of IFN-γ secreting cells measured in the ELISPOT. The different assay outputs may be used concurrently to accurately diagnose Johne's disease in the early stages of subclinical infection. Research carried out comparing IFN-γ whole blood ELISAs and ELISPOT assays in the diagnosis of tuberculosis has shown similar sensivities of these assays (Goletti et al., 2005), although all the patients tested had active Tb. The sensitivity may be different when detecting those with latent disease or in the case of Johne's disease early subclinical infection.

There are a number of documented technical issues related to the use of ELISPOT assays. These include inter operator-variation, especially regarding the enumeration of the cytokine secreting cells and the effect of handling blood samples. Inter-operator variation can be overcome by using a standardised protocol, assay specific controls, a standard automated ELISPOT reader and software parameters (Janetzki et al., 2004; Ryan et al., 2005). Many of the issues with blood sample handling apply to both the traditional IFN-γ ELISA and ELISPOT assays, and reduce the signal. These issues are the interval between blood collection and processing and the storage temperature of blood. The addition of stablisation reagents in the blood tube at sampling (Doherty et al., 2005), or the addition of certain cytokines or antibodies at the time of stimulation (Buza et al., 2004; Jungersen et al., 2005) may overcome this problem. This has yet to be investigated in the ELISPOT assay.

The IFN-γ ELISPOT assay has the potential to improve the diagnosis of Johne's disease in sheep as it has been shown that the assay detects infected animals at a similar or better rate than the IFN-γ ELISA. Further investigations comparing the traditional IFN-γ ELISA with the ELISPOT and other methods of detecting cytokines are warranted. Certain technical issues will also have to be overcome to improve the survival of white blood cells in transported blood and to purify them for ELISPOT. More importantly new antigens will need to be identified and tested to distinguish between animals exposed to Mptb but immune or animals that will succumb to disease.

References

Bannantine, J. P. and Paustian, M. L. 2006. Identification of diagnostic proteins in Mycobacterium avium subspecies paratuberculosis by a whole genome analysis approach. Methods Mol Biol 345, 185-96.

Begg, D. J., O'Brien, R., Mackintosh, C. G. and Griffin, J. F. 2005. Experimental Infection Model for Johne's Disease in Sheep. Infection and Immunity 73, 5603-11.

Begg, D. J. and Whittington, R. J. 2007. Experimental animal infection models for Johne's disease, an infectious enteropathy caused by Mycobacterium avium subsp. paratuberculosis. Vet J.

Brotherston, J. G., Gilmour, N. J. and Samuel, J. 1961. Quantitative Studies of *Mycobacterium johnei* in the Tissues of Sheep. Journal of Comparative Pathology 71, 286 - 299.

Buza, J. J., Hikono, H., Mori, Y., Nagata, R., Hirayama, S., Aodon, g., Bari, A. M., Shu, Y., Tsuji, N. M. and Momotani, E. 2004. Neutralization of interleukin-10 significantly enhances gamma interferon expression in peripheral blood by stimulation with Johnin purified protein derivative and by infection with Mycobacterium avium subsp. paratuberculosis in experimentally infected cattle with paratuberculosis. Infect Immun 72, 2425-8.

Cho, D. and Collins, M. T. 2006. Comparison of the proteosomes and antigenicities of secreted and cellular proteins produced by Mycobacterium paratuberculosis. Clin Vaccine Immunol 13, 1155-61.

Cho, D., Shin, S. J., Talaat, A. M. and Collins, M. T. 2007. Cloning, expression, purification and serodiagnostic evaluation of fourteen Mycobacterium paratuberculosis proteins. Protein Expr Purif 53, 411-20.

Cho, D., Sung, N. and Collins, M. T. 2006. Identification of proteins of potential diagnostic value for bovine paratuberculosis. Proteomics 6, 5785-94.

Codecasa, L., Mantegani, P., Galli, L., Lazzarin, A., Scarpellini, P. and Fortis, C. 2006. An in-house RD1-based enzyme-linked immunospot-gamma interferon assay instead of the tuberculin skin test for diagnosis of latent Mycobacterium tuberculosis infection. J Clin Microbiol 44, 1944-50.

Demissie, A., Leyten, E. M., Abebe, M., Wassie, L., Aseffa, A., Abate, G., Fletcher, H., Owiafe, P., Hill, P. C., Brookes, R., Rook, G., Zumla, A., Arend, S. M., Klein, M., Ottenhoff, T. H., Andersen, P. and Doherty, T. M. 2006. Recognition of stage-specific mycobacterial antigens differentiates between acute and latent infections with Mycobacterium tuberculosis. Clin Vaccine Immunol 13, 179-86.

Doherty, T. M., Demissie, A., Menzies, D., Andersen, P., Rook, G. and Zumla, A. 2005. Effect of sample handling on analysis of cytokine responses to Mycobacterium tuberculosis in clinical samples using ELISA, ELISPOT and quantitative PCR. J Immunol Methods 298, 129-41.

Feldman, B. V., Zinkl, J. G., Jain, N. C. and Schalm, O. W. (2000). Schalms Veterinary Hematology Lippincott Williams and Wilkins.

Goletti, D., Vincenti, D., Carrara, S., Butera, O., Bizzoni, F., Bernardini, G., Amicosante, M. and Girardi, E. 2005. Selected RD1 peptides for active tuberculosis diagnosis: comparison of a gamma interferon whole-blood enzyme-linked immunosorbent assay and an enzyme-linked immunospot assay. Clin Diagn Lab Immunol 12, 1311-6.

Griffin, F., Spittle, E., Mackintosh, C. G., Rodgers, C., Liggett, S. and Cooper, M. (2005a). Serodiagnosis of Johne's disease in red deer (Cervus elaphus). 8th International Colloquium on Paratuberculosis, Copenhagen, Denmark, International Association for Paratuberculosis.

Griffin, J. F., Spittle, E., Rodgers, C. R., Liggett, S., Cooper, M., Bakker, D. and Bannantine, J. P. 2005b. Immunoglobulin G1 enzyme-linked immunosorbent assay for diagnosis of Johne's Disease in red deer (*Cervus elaphus*). Clinical and Diagnostic Laboratory Immunology 12, 1401-9.

Gwozdz, J. M. and Thompson, K. G. 2002. Antigen-induced production of interferon-gamma in samples of peripheral lymph nodes from sheep experimentally inoculated with *Mycobacterium avium* subsp. *paratuberculosis*. Veterinary Microbiology 84, 243-52.

Janetzki, S., Schaed, S., Blachere, N. E., Ben-Porat, L., Houghton, A. N. and Panageas, K. S. 2004. Evaluation of Elispot assays: influence of method and operator on variability of results. J Immunol Methods 291, 175-83.

Jungersen, G., Grell, S. N., Clemensen, A. and Howard, C. J. (2005). Interleukin-12 potentiation of the interferon-gamma test rescues day old blood samples for diagnosis of paratuberculosis PPD specific cellular mediated immune responses. 8th International Colloquium on Paratuberculosis, Copenhagen, Denmark.

Kalyuzhny, A. and Stark, S. 2001. A simple method to reduce the background and improve well-to-well reproducibility of staining in ELISPOT assays. J Immunol Methods 257, 93-7.

Lalvani, A., Pathan, A. A., Durkan, H., Wilkinson, K. A., Whelan, A., Deeks, J. J., Reece, W. H., Latif, M., Pasvol, G. and Hill, A. V. 2001. Enhanced contact tracing and spatial tracking of Mycobacterium tuberculosis infection by enumeration of antigen-specific T cells. Lancet 357, 2017-21.

Leroy, B., Roupie, V., Noel-Georis, I., Rosseels, V., Walravens, K., Govaerts, M., Huygen, K. and Wattiez, R. 2007. Antigen discovery: a postgenomic approach to paratuberculosis diagnosis. Proteomics 7, 1164-76.

Li, L., Munir, S., Bannantine, J. P., Sreevatsan, S., Kanjilal, S. and Kapur, V. 2007. Rapid expression of Mycobacterium avium subsp. paratuberculosis recombinant proteins for antigen discovery. Clin Vaccine Immunol 14, 102-5.

Marsh, I. B., Bannantine, J. P., Paustian, M. L., Tizard, M. L., Kapur, V. and Whittington, R. J. 2006. Genomic comparison of Mycobacterium avium subsp. paratuberculosis sheep and cattle strains by microarray hybridization. J Bacteriol 188, 2290-3.

Marsh, I. B. and Whittington, R. J. 2007. Genomic diversity in Mycobacterium avium: single nucleotide polymorphisms between the S and C strains of M. avium subsp. paratuberculosis and with M. a. avium. Mol Cell Probes 21, 66-75.

Olsen, I., Boysen, P., Kulberg, S., Hope, J. C., Jungersen, G. and Storset, A. K. 2005. Bovine NK Cells Can Produce Gamma Interferon in Response to the Secreted Mycobacterial Proteins ESAT-6 and MPP14 but Not in Response to MPB70. Infection and Immunity 73, 5628-35.

Olsen, I. and Storset, A. K. 2001. Innate IFN-gamma Production in Cattle in Response to MPP14, a Secreted Protein from Mycobacterium avium subsp. Paratuberculosis. Scand J Immunol 54, 306-13.

Perez, V., Garcia Marin, J. F. and Badiola, J. J. 1996. Description and classification of different types of lesion associated with natural paratuberculosis infection in sheep. Journal of Comparative Pathology 114, 107-122.

Reddacliff, L. A., Nicholls, P. J., Vadali, A. and Whittington, R. J. 2003. Use of Growth Indices from Radiometric Culture for Quantification of Sheep Strains of *Mycobacterium avium* subsp. *paratuberculosis*. Applied and Environmental Microbiology 69, 3510-6.

Robbe-Austerman, S., Stabel, J. R. and Palmer, M. V. 2006. Evaluation of the gamma interferon ELISA in sheep subclinically infected with Mycobacterium avium subspecies paratuberculosis using a whole-cell sonicate or a johnin purified-protein derivative. J Vet Diagn Invest 18, 189-94.

Ryan, J. E., Ovsyannikova, I. G., Dhiman, N., Pinsky, N. A., Vierkant, R. A., Jacobson, R. M. and Poland, G. A. 2005. Inter-operator variation in ELISPOT analysis of measles virus-specific IFN-gamma-secreting T cells. Scand J Clin Lab Invest 65, 681-9.

Sevilla, I., Singh, S. V., Garrido, J. M., Aduriz, G., Rodriguez, S., Geijo, M. V., Whittington, R. J., Saunders, V., Whitlock, R. H. and Juste, R. A. 2005. Molecular typing of *Mycobacterium avium* subspecies *paratuberculosis* strains from different hosts and regions. Revue Scientifique et Technique 24, 1061-6.

Stabel, J. R. 2000. Transitions in immune responses to *Mycobacterium paratuberculosis*. Veterinary Microbiology 77, 465-473.

Stabel, J. R., Kimura, K. and Robbe-Austerman, S. 2007. Augmentation of secreted and intracellular gamma interferon following johnin purified protein derivative sensitization of cows naturally infected with Mycobacterium avium subsp. paratuberculosis. J Vet Diagn Invest 19, 43-51.

Stewart, D. J., Stiles, P. L., Whittington, R. J., Lambeth, C., Windsor, P. A., Reddacliff, L., McGregor, H., Dhungyel, O. P., Cousins, D., Francis, B. R., Morcombe, P. W., Butler, R., Salmon, D. D., Roberts, C. F., Sergeant, E., Jasenko, I. and Jones, S. L. (2002). Validation of the interferon-g for diagnosis of ovine Johne's disease: sensitivity and specificity field trials. Seventh International Colloquium on Paratuberculosis, Bilbao, Spain, International Association for Paratuberculosis.

Stewart, D. J., Vaughan, J. A., Stiles, P. L., Noske, P. J., Tizard, M. L., Prowse, S. J., Michalski, W. P., Butler, K. L. and Jones, S. L. 2004. A long-term study in Merino sheep experimentally infected with *Mycobacterium avium* subsp. *paratuberculosis*: clinical disease, faecal culture and immunological studies. Veterinary Microbiology 104, 165-78.

Tanguay, S. and Killion, J. J. 1994. Direct comparison of ELISPOT and ELISA-based assays for detection of individual cytokine-secreting cells. Lymphokine Cytokine Res 13, 259-63.

Thorel, M. F., Vialard, J., Manfroni, F., Bernardot, J., Ostyn, A. and Vandevelde, J. 1992. [Experimental paratuberculosis in sheep after intravenous or oral inoculation: pathogenicity and biologic diagnosis]. Annales de Recherches Vétérinaires 23, 105-15.

Whittington, R., Marsh, I., Choy, E. and Cousins, D. 1998a. Polymorphisms in IS1311, an insertion sequence common to Mycobacterium avium and M. avium subsp. paratuberculosis, can be used to distinguish between and within these species. Mol Cell Probes 12, 349-58.

Whittington, R. J., Marsh, I., McAllister, S., Turner, M. J., Marshall, D. J. and Fraser, C. A. 1999. Evaluation of modified BACTEC 12B radiometric medium and solid media for culture of *Mycobacterium avium* subsp. *paratuberculosis* from sheep. Journal of Clinical Microbiology 37, 1077-83.

Whittington, R. J., Marsh, I., Turner, M. J., McAllister, S., Choy, E., Eamens, G. J., Marshall, D. J. and Ottaway, S. 1998b. Rapid detection of Mycobacterium paratuberculosis in clinical samples from ruminants and in spiked environmental samples by modified BACTEC 12B radiometric culture and direct confirmation by IS900 PCR. J Clin Microbiol 36, 701-7.

9.4 Appendix 1B-2 Subprogram 1 Comparison of alternative assays for the detection of IFN-γ in Johne's diseased sheep

Introduction

The use of immunologically based tests for the diagnosis of Johne's disease has had varied outcomes. Assays such as the ELISA to detect antibody is used widely to detect disease (Dolz et al., 1999; Miller et al., 2000; Whitlock et al., 2000; Whittington et al., 2003; Griffin et al., 2004; Griffin et al., 2005; McKenna et al., 2005b; Eda et al., 2006; Gumber et al., 2006). The sensitivity of these antibody ELISA assays with a high degree of specificity have shown variable sensitivity results depending on the animal species, the antigen and the class of antibody detected (Griffin et al., 2005; McKenna et al., 2005a; Eda et al., 2006; Gumber et al., 2006; Robbe-Austerman et al., 2006a). Another immunological test commonly mentioned is the ELISA assay to detect Interferon gamma (IFN-γ). The first use of this assay was to detect early stage tuberculosis infections. IFN-γ is thought to be one of the first cytokines up-regulated in an animal's immune response to mycobacteria. Therefore the presumption behind IFN-γ testing for Johne's disease was that it would allow for earlier detection of infection and possible disease (Stewart et al., 2002). Data collected to date in sheep indicate the IFN-γ ELISA has approximately the same or slightly better sensitivity than traditional antibody ELISA assays for the detection of *M. paratuberculosis* (*M.ptb*) infected animals (Stewart et al., 2002; Robbe-Austerman et al., 2006b). Alternative methods for the detection of IFN-γ in *M.ptb* infected sheep have been developed in this project including the ELISPOT and Cell ELISA assays. The Cell ELISA assay is a hybrid of the ELISA and ELISPOT assays (Bakhiet et al., 1999). The difference between the three assays is what they measure. The traditional ELISA measures the amount of IFN-γ released into the plasma after stimulation of the blood with *M.ptb* antigens. The ELISPOT measures the number of cells producing IFN-γ and the Cell-ELISA measures the total amount of IFN-γ produced by the cells after stimulation with the *M.ptb* antigens. The ELISPOT assay has been shown to be 10-200 times more sensitive than traditional ELISA assays for the detection of cytokines (Tanguay and Killion, 1994). It was hoped by the utilisation of this increased sensitivity the ability to diagnose *M.ptb* infected sheep may be improved using the different IFN-γ detection methods. The aim of this study was to compare different methods of IFN-γ detection in *M.ptb* experimentally infected sheep using various assays, the traditional ELISA, the ELISPOT and the Cell-ELISA.

Methods

Animals

All animals in these experiments were used with the approval of the University of Sydney Animal Care and Ethics Committee. The Merino sheep were maintained at pasture unless otherwise stated.

Experimentally infected sheep

Preparation of the Telford *Mycobacterium avium* subspecies *paratuberculosis* inoculum.

Myobacterium paratuberculosis strain Telford 9.2, a pure clonal culture at passage level 5 (including its primary isolation from sheep faeces) was reconstituted from lyophilised stock and inoculated into a BACTEC vial supplemented with egg yolk and mycobactin J (MJ) (Whittington et al., 1999). After culture in BACTEC to achieve maximal growth, the vial was subcultured to 7H10+MJ slopes and incubated for 4-6 weeks at 37^{o}C. Telford 9.2 is an IS1311 S strain, IS900 RFLP type S1 (Marsh et al., 2006; Marsh and Whittington, 2007).

The slopes were harvested into single cell suspensions prepared in PBS with 0.1% V/V Tween 80. Enumeration was conducted using a visual count in a Thoma-ruled counting chamber and by end point titration in BACTEC medium (using a standard three tube most probable number [MPN] method) (Reddacliff et al., 2003). The visual counts were used to prepare the inoculation doses at 10^9 *M.ptb* organisms/mL of undiluted suspension. One millilitre aliquots of this stock suspension was diluted in 10 mL of PBS for each of the animals to be infected as shown in Table 1.

The remaining undiluted suspension (stock) was retained at 4°C in order to repeat the inoculation one week later. Another MPN was set up on the day of the second dose from the stock suspension stored at 4^{o}C to confirm the viable dose after storage. IS*900* and IS*1311* PCR assays conducted on the stock solution were used to confirm that the infectious material was *M.ptb* S strain.

A fresh suspension was prepared for further inoculation doses (typically one month later).

Preparation of gut homogenate inoculum.

Using the method of Begg et al (2005), gut tissue from animal 986 (sourced from a farm in the Southern Tablelands of NSW, Australia) with multibacillary lesions, shown to be infected by culture and *IS*900 PCR with the ovine strain confirmed by *IS*1311 PCR was stored at -80^{o}C until required. The tissue was defrosted and homogenized using a mortar and pestle in an equal volume of sterile distilled water. The homogenate was filtered through a funnel lined with 2 layers of sterile gauze followed by a 70um cell strainer. The sample was homogenized by vortexing for 30 minutes and passed through a 26 gauge needle 2 times. The number of *M.ptb* cells was enumerated to calculate the number of organisms/mL. This was done using direct visual counts using 4 uL of a 10^{-3} dilution of the homogenate smeared onto 5mm x 5mm square grid which was divided into equal quarters, the smears were then ZN stained and the acid fast bacilli were counted. A BACTEC MPN was also carried out on the sample. The sample was then frozen at -80^{o}C. The MPN showed the gut homogenate (total volume 54mL) to be at $2.3x10^8$ CFU/mL with direct visual count showing $3.67x10^8$ bacteria per mL. On the day prior to the first inoculation the homogenate was thawed diluted with 11mL of PBS giving a total volume of 65mL at $1.9x10^8$CFU/mL. One in ten dilutions of the homogenate were spread onto TSA plates to enumerate the amount of contaminating bacteria in the sample. The plates were incubated at 37^{o}C for 3 days. Fewer than 1000 CFU/mL of contaminating bacteria were observed.

Twenty two millilitres was then frozen at -80^{o}C to be held as the 3rd and final inoculation a further 22mLs was stored for one week at 4^{o}C for the second inoculation. The remaining 21 mLs of suspension were put into 1mL aliquots and were mixed with 9mL of PBS for the first challenge dose, the same proceedure was done with the stored doses either refrigerated and frozen stocks, when required.

Necropsy: All animals were euthanased using an intravenous injection of barbiturate into the jugular vein. The intestines from the duodenum to the rectum were removed from the animal and placed in a clean tray. The trays were cleaned with warm water and a virucidal disinfectant, Trigene 2 (Medichem International, UK). Samples were then taken from the following sections of the small intestine terminal ileum, posterior jejunum, mid distal jejunum, middle jejunum, mid proximal jejunum and anterior jejunum and ileocecal lymph node. The ileocaecal lymph node and jejunal lymph nodes corresponding to the sections of jejunum sampled were also collected

Table 1: Experimental infection trials used in OJD031 for the examination of IFN-γ ELISA, ELISPOT and Cell-ELISA assays

Experiment	Treatment	Sheep breed	Age of animals at challenge	No of animals	Strain of Mptb	First dose	Second dose	Third dose
031.3*	Telford	Merino X	4 months	23	Telford 9.2	2.3×10^5	2.3×10^5	2.3×10^5
031.4	Telford	Merino	3 months	18	Telford 9.2	9.3×10^6	9.3×10^6	2.4×10^8
031.5	Telford	Merino	3 months	12	Telford 9.2	9.3×10^7	4.3×10^7	9.3×10^6
031.6	Telford	Merino	4 months	20	Telford 9.2	9.3×10^7	9.3×10^7	1.5×10^8
031.6	Gut isolate	Merino	4 months	20	Gut isolate	1.9×10^8	9.3×10^7	9.3×10^7
031.6	Control	Merino	4 months	20	None given			

* The 031.3 animals received 2 extra doses of Mptb at 11 and 12 months post inoculation. The fourth dose at 11 months contained 2.4×10^8cfu while the fifth dose contained 9.3×10^7 CFU.

Isolation of *M. paratuberculosis* from faeces and tissue: Samples collected from animals were frozen at -80°C until they were processed. Faecal samples and tissue samples were processed for BACTEC culture as described previously (Whittington et al., 1999). Briefly after decontamination samples were inoculated into Bactec Vials and cultured for 12 weeks at 37°C. After culture any positive samples were confirmed by PCR and REA as previously described (Whittington et al., 1998a; Whittington et al., 1998b).

Purification of peripheral white blood cells for the ELISPOT and Cell-ELISA

Ficoll density gradient centrifugation

A ten millilitre heparinized vaccutainer of blood was centrifuged at 1,455 x *g* for 20 min. The buffy coat of white blood cells was removed and layered on to 2 mL of ficoll paque (GE Healthcare, Sweden δ = 1.077) and centrifuged at 754 x *g* for 30 minutes with no brake. The cloudy layer of white blood cells was removed and washed twice by centrifugation in 10 ml of phosphate buffered saline (PBS). The cells were resuspended in 5 mL of 10% fetal calf serum (Gibco BRL, Grand Island, NY) made up in RPMI 1640 (Gibco BRL) supplemented with L-glutamine and penicillin/streptomycin (Gibco BRL) (complete media). The cells were enumerated using trypan blue and suspended at 2.5×10^6 viable cells/mL

ELISPOT assay to detect IFN-γ

ELISPOT plates (Millipore) were coated with 50µL of 2 µg/mL of IFN6.19 (immunoglobulin G2a clone 6.19, supplied by Gregers Jungerson Denmark) or MCA2112 (Serotec) and incubated overnight at 4^{o}C. The plates were washed 6 times with phosphate buffered saline (PBS) to remove excess antibody. Purified white blood cells at a concentration of 2.5 x 10^6 cells per mL were diluted to concentrations of 1.25 x 10^6 cells per mL and 6.25 x 10^5 cells per mL with 100 µL of the three dilutions being placed into each well as required into the plate (Millipore). The cells were incubated with 50mL of either culture media (unstimulated), *M.ptb* 316v antigen 30µg/mL (EMAI Australia), Purified protein derivative from *Mycobacterium avium* (PPD-A) 30µg/mL (CSL) and Pokeweed Mitogen (PWM) 10µg/mL (Sigma). The plates were incubated for 18-24 hours at 37^{o}C with 5% CO_2.

The plates were washed 6 times using PBS to remove the cells and 50µL of the secondary antibody MCA1783b (Serotec) was added at a concentration of 0.5µg/mL diluted in PBS. The plate was then incubated at 37^{o}C for 1 hour. The plates were washed in PBS and 50uL of 1µg/mL of alkaline phosphatase streptavidin (Vector Laboratories) was added to the wells. The plate was then incubated at 37^{o}C for 1 hour.

The plate was washed 5 times in PBS and 100µL BCIP substrate (Vector Laboratories) was added for 1 hour at room temperature. The BCIP substrate was then removed and the plate was washed 6 times in water.

The plates are allowed to dry and read in a KS ELISPOT reader (Carl Zeiss).

Results were presented as the number of *M.ptb* antigen specific IFN-γ producing cells/ 10^5 white blood cells by taking the number of antigen reactive cells and subtracting the number of unstimulated IFN-γ producing cells/10^5 white blood cells.

Cell-ELISA to detect IFN-γ

ELISA plates (Nunc, Maxisorb plates) were coated with 50µL of 2 µg/mL anti IFN antibody (Serotec MCA2112) and incubated overnight at 4^{o}C

The plates are washed 6 times with phosphate buffered saline (PBS) to remove excess antibody. 100µL of purified white blood cells at a concentration of 2.5 x 10^6 cells per mL were added to the wells as required. The cells were incubated with 50 mL of either culture media (unstimulated), *M.ptb* 316v antigen 30µg/mL (EMAI Australia), Purified protein derivative from *Mycobacterium avium* (PPD-A) 30µg/mL (CSL) and Pokeweed Mitogen (PWM) 10µg/mL (Sigma). The plates were incubated for 44-48 hours at 37^{o}C with 5% CO_2. The plates were hand washed 6 times using wash buffer (PBS with 0.05% Tween 20) to remove the cells and 50 µL of the secondary antibody MCA1783b (Serotec) was added at a concentration of 0.5µg/mL diluted in PBS. The plates were incubated at 37^{o}C for 1 hour. The plates were washed 6 times using wash buffer and 50 uL of horse radish peroxidase streptavidin (Vector laboratories) at a concentration of 0.01µg/mL was added. The plates were incubated at 37^{o}C for 1 hour and washed 6 times using wash buffer. 100µL of TMB substrate (Pierce) was added to each well as required and the plate was incubated in the dark for 30minutes. The reaction was stopped with 100 uL of 2M Sulphuric acid. The optical density (OD) was measured in an ELISA reader at 450nm. Results are presented as OD of the *M.ptb* antigen stimulated sample – the OD of the media stimulated sample.

IFN-γ ELISA

Stimulation of the blood samples: Briefly 0.5 mL of heparinised blood was placed into wells and stimulated with 0.5 mL of *M.ptb* 316v antigen at 20µg/mL. A negative control consisted of the blood having 0.5 mL of media added while the positive control had 0.5 mL PWM added at 10ug/mL. After 48 hours of culture at 37^{o}C with 5% CO_2 the plasma supernatant was collected and stored at -20^{o}C.

Two ELISA assays were used to detect the IFN-γ, the most commonly used was the Ovigam assay an ELISA built in house to detect IFN-γ and the other was the commercial Bovigam (Pfizer) assay

Ovigam: ELISA plates (Nunc, Maxisorb plates) were coated with 50µL of 1.5 µg/mL anti IFN antibody (IFN 6.19) and incubated overnight at 4^{o}C. The frozen plasma supernatant samples were thawed and brought to room temperature. The plates were machine washed 5 times using wash buffer (PBS with 0.05% Tween 20). 50µL of PBS was added to all wells required followed by 50uL of plasma supernatant samples. The plates were incubated at room temperature for 1 hour and washed 5 times using wash buffer. 50µL of the secondary antibody MCA1783b (Serotec) was added at a concentration of 0.5µg/mL diluted in PBS. The plates were incubated at room temperature for 1 hour. The plates were machine washed 5 times using wash buffer and 50uL of horse radish peroxidase streptavidin (Vector laboratories) at a concentration of 0.01µg/mL was added. The plates were incubated at room temperature for 1 hour and machine washed 5 times using wash buffer. 100µL of TMB substrate (Pierce) was added to each well as required and the plate was incubated in the dark for 30minutes. The reaction was then stopped with 100 uL of 2M Sulphuric acid. The OD was measured in an ELISA reader at 450nm. Results are presented as OD of the *M.ptb* antigen stimulated sample – the OD of the media stimulated sample.

Bovigam: An analysis of IFN-γ was preformed using the standard protocol outlined for the Bovigam ELISA kit. Results are presented as OD of the *M.ptb* antigen stimulated sample – the OD of the negative control (media stimulated) sample.

Results

The three different assays for detecting IFN-γ from sheep showed different profiles of responses. This can be easily observed in the data from 031.4, (Figure 1) where the average IFN-γ ELISPOT responses from the sheep rose from 3-6 months then slowly declined over time. The average IFN-γ ELISA had a zig zag profile, while the Cell-ELISA results showed a steady response over the sampling period.

Unsurprisingly the different infection experiments also showed different IFN-γ responses over time periods sampled. Within an experiment differences could be seen in the IFN-γ responses of the sheep depending on the strain of *M.ptb* the animals were inoculated with (Figure 1: 031.6). In the experiment 031.6 animals infected with the Gut homogenate strain developed stronger IFN-γ responses than the sheep inoculated with the Telford 9.2 pure clonal strain of *M.ptb*. The animals inoculated with the Gut homogenate developed more severe disease at an earlier stage. The first clinical animal was observed at 8 months post infection compared to 13 months for the Telford 9.2 infected animals. The histological lesions recorded in the Gut homogenate inoculated sheep were also more severe than the Telford 9.2 inoculated animals (data not shown).

The animals found to be infected or apparently free of infection by tissue culture showed similar IFN-γ profiles within each of the three IFN-γ assays (Figure 2). Interestingly none of the assays can definitively distinguish between sheep that have been inoculated and developed an active infection from those that were exposed but are apparently free of infection as measured by tissue culture (Figure 2).

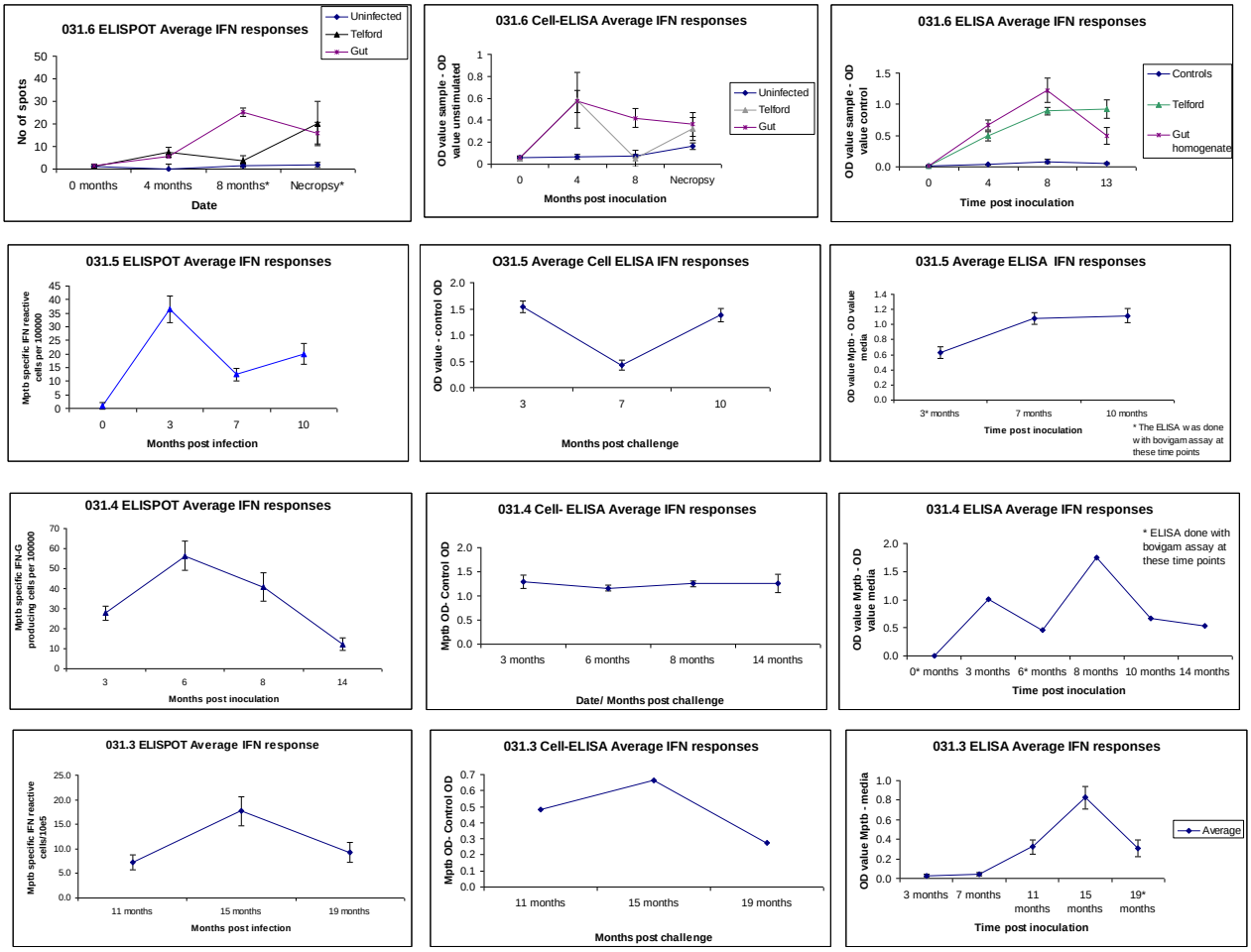

Figure 1: Average IFN-γ responses to *M.ptb* antigens recorded by the three detection assays, the ELISPOT, Cell-ELISA and traditional ELISA from four experimental infection trials 031.3, 4, 5 and 6. Error bars indicate standard error of the mean.

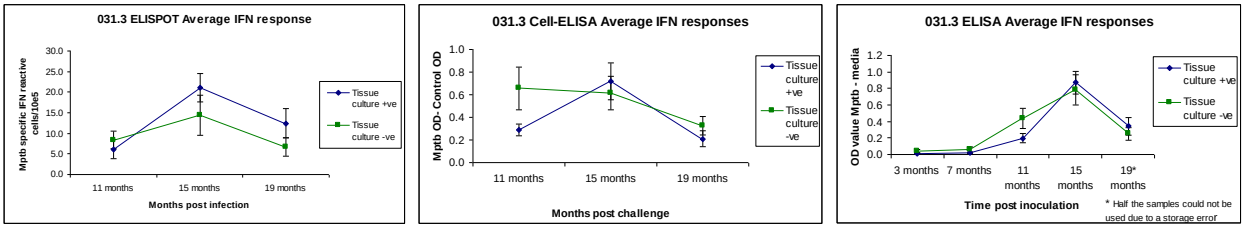

Figure 2: The average IFN-γ responses as recorded by the three different assays from 031.3 experimentally challenged animals identified as infected or uninfected by tissue culture. Error bars indicate standard error of the mean

Discussion

A difference was seen in the IFN-γ profiles of the three IFN-γ detection assays, as the ELISPOT, Cell-ELISA and ELISA record different aspects of cytokine production. The ELISPOT and Cell-ELISA assays showed the greatest degree of similarity in their IFN-γ profiles for the experimental infections. This similarity seen in the responses between the ELISPOT and Cell ELISA assays can be explained by the isolation of white blood cells which was done for both assays at the same time. After the white blood cells had been isolated the cells were then divided as required for the ELISPOT and Cell-ELISA. Any problems with the handling or processing of the cells would therefore affect both assays. Internal controls are used in these assays, by establishing the viability of the cells and using Pokeweed mitogen to stimulated non-specific IFN-γ production to check the function of the cells. Handling problems may explain the reduction of IFN-γ measured by the ELISPOT and Cell-ELISA assays at eight months post inoculation with the Telford 9.2 strain *M.ptb* in the 031.6 experimental challenges (Figure 1). The viability of these cells was normal but the Pokeweed mitogen responses were reduced and the *M.ptb* responses were severely retarded. The gut homogenate challenged and control animal blood samples were processed in separate batches and all the animals tested with the traditional ELISA (where the blood is processed in a different manor) had higher responses at this time point.

The ability of the different assays to detect infected sheep from those that had been exposed to *M.ptb* but were apparently uninfected at necropsy was disappointing as none of the assays could distinguish the difference.

Overall the Cell-ELISA appears to be the better of the two new assays in the detection of IFN-γ from inoculated animals, with detection of the cytokine as early as 3 months post inoculation. The ELISPOT seems to be somewhat more variable in the strength of the response at this time (Figure 1: 031.6 compared to 031.4). The advantage of the assays developed is that they all measure different aspects of the IFN-γ production from the white blood cells. These different readouts of IFN-γ assays in combination with improved antigens may enable better identification of animals with Johne's disease.

References

Bakhiet, M., Ozenci, V., Withagen, C., Mustafa, M., Fredrikson, S. and Link, H. 1999. A new cell enzyme-linked immunosorbent assay demonstrates gamma interferon suppression by beta interferon in multiple sclerosis. Clin Diagn Lab Immunol 6, 415-9.

Begg, D. J., O'Brien, R., Mackintosh, C. G. and Griffin, J. F. 2005. Experimental Infection Model for Johne's Disease in Sheep. Infection and Immunity 73, 5603-11.

Dolz, G., Araya, L. N., Suarez, J. and Jimenez, C. 1999. Prevalence of antibodies to bovine paratuberculosis detected by a LAM-ELISA in Costa Rica. Veterinary Record 144, 322-3.

Eda, S., Bannantine, J. P., Waters, W. R., Mori, Y., Whitlock, R. H., Scott, M. C. and Speer, C. A. 2006. A highly sensitive and subspecies-specific surface antigen enzyme- linked immunosorbent assay for diagnosis of Johne's disease. Clin Vaccine Immunol 13, 837-44.

Griffin, J. F., Chinn, D. N. and Rodgers, C. R. 2004. Diagnostic strategies and outcomes on three New Zealand deer farms with severe outbreaks of bovine tuberculosis. Tuberculosis (Edinb) 84, 293-302.

Griffin, J. F., Spittle, E., Rodgers, C. R., Liggett, S., Cooper, M., Bakker, D. and Bannantine, J. P. 2005. Immunoglobulin G1 enzyme-linked immunosorbent assay for diagnosis of Johne's Disease in red deer (*Cervus elaphus*). Clinical and Diagnostic Laboratory Immunology 12, 1401-9.

Gumber, S., Eamens, G. and Whittington, R. J. 2006. Evaluation of a Pourquier ELISA kit in relation to agar gel immunodiffusion (AGID) test for assessment of the humoral immune response in sheep and goats with and without Mycobacterium paratuberculosis infection. Veterinary Microbiology 115, 91-101.

Marsh, I. B., Bannantine, J. P., Paustian, M. L., Tizard, M. L., Kapur, V. and Whittington, R. J. 2006. Genomic comparison of Mycobacterium avium subsp. paratuberculosis sheep and cattle strains by microarray hybridization. J Bacteriol 188, 2290-3.

Marsh, I. B. and Whittington, R. J. 2007. Genomic diversity in Mycobacterium avium: single nucleotide polymorphisms between the S and C strains of M. avium subsp. paratuberculosis and with M. a. avium. Mol Cell Probes 21, 66-75.

McKenna, S. L., Keefe, G. P., Barkema, H. W. and Sockett, D. C. 2005a. Evaluation of three ELISAs for Mycobacterium avium subsp. paratuberculosis using tissue and fecal culture as comparison standards. Veterinary Microbiology 110, 105-11.

McKenna, S. L., Sockett, D. C., Keefe, G. P., McClure, J., VanLeeuwen, J. A. and Barkema, H. W. 2005b. Comparison of two enzyme-linked immunosorbent assays for diagnosis of Mycobacterium avium subsp. paratuberculosis. J Vet Diagn Invest 17, 463-6.

Miller, D. S., Collins, M. T., Smith, B. B., Anderson, P. R., Kramsky, J., Wilder, G. and Hope, A. 2000. Specificity of four serologic assays for Mycobacterium avium ss paratuberculosis in llamas and alpacas: a single herd study [In Process Citation]. J Vet Diagn Invest 12, 345-53.

Reddacliff, L. A., Nicholls, P. J., Vadali, A. and Whittington, R. J. 2003. Use of Growth Indices from Radiometric Culture for Quantification of Sheep Strains of *Mycobacterium avium* subsp. *paratuberculosis*. Applied and Environmental Microbiology 69, 3510-6.

Robbe-Austerman, S., Gardner, I. A., Thomsen, B. V., Morrical, D. G., Martin, B. M., Palmer, M. V., Thoen, C. O. and Ewing, C. 2006a. Sensitivity and specificity of the agar-gel-immunodiffusion test, ELISA and the skin test for detection of paratuberculosis in United States Midwest sheep populations. Vet Res 37, 553-64.

Robbe-Austerman, S., Stabel, J. R. and Palmer, M. V. 2006b. Evaluation of the gamma interferon ELISA in sheep subclinically infected with Mycobacterium avium subspecies paratuberculosis using a whole-cell sonicate or a johnin purified-protein derivative. J Vet Diagn Invest 18, 189-94.

Stewart, D. J., Stiles, P. L., Whittington, R. J., Lambeth, C., Windsor, P. A., Reddacliff, L., McGregor, H., Dhungyel, O. P., Cousins, D., Francis, B. R., Morcombe, P. W., Butler, R., Salmon, D. D., Roberts, C. F., Sergeant, E., Jasenko, I. and Jones, S. L. (2002). Validation of the interferon-γ for diagnosis of ovine Johne's disease: sensitivity and specificity field trials. Seventh International Colloquium on Paratuberculosis, Bilbao, Spain, International Association for Paratuberculosis.

Tanguay, S. and Killion, J. J. 1994. Direct comparison of ELISPOT and ELISA-based assays for detection of individual cytokine-secreting cells. Lymphokine Cytokine Res 13, 259-63.

Whitlock, R. H., Wells, S. J., Sweeney, R. W. and Van Tiem, J. 2000. ELISA and fecal culture for paratuberculosis (Johne's disease): sensitivity and specificity of each method. Veterinary Microbiology 77, 387-398.

Whittington, R., Marsh, I., Choy, E. and Cousins, D. 1998a. Polymorphisms in IS1311, an insertion sequence common to Mycobacterium avium and M. avium subsp. paratuberculosis, can be used to distinguish between and within these species. Mol Cell Probes 12, 349-58.

Whittington, R. J., Eamens, G. J. and Cousins, D. V. 2003. Specificity of absorbed ELISA and agar gel immuno-diffusion tests for paratuberculosis in goats with observations about use of these tests in infected goats. Australian Veterinary Journal 81, 71-5.

Whittington, R. J., Marsh, I., McAllister, S., Turner, M. J., Marshall, D. J. and Fraser, C. A. 1999. Evaluation of modified BACTEC 12B radiometric medium and solid media for culture of *Mycobacterium avium* subsp. *paratuberculosis* from sheep. Journal of Clinical Microbiology 37, 1077-83.

Whittington, R. J., Marsh, I., Turner, M. J., McAllister, S., Choy, E., Eamens, G. J., Marshall, D. J. and Ottaway, S. 1998b. Rapid detection of Mycobacterium paratuberculosis in clinical samples from ruminants and in spiked environmental samples by modified BACTEC 12B radiometric culture and direct confirmation by IS900 PCR. J Clin Microbiol 36, 701-7.

9.5 Appendix 1B-3 Subprogram 1 Mptb antigen-specific secretion of IL-10 by ovine mononuclear cells in ovine Johne's disease

Abbreviations

PBMC: peripheral blood mononuclear cells; IL: interleukin ILN: ileal lymph node; JLN: jejunal lymph node; PLN: prescapular lymph node; p.i.: post-inoculation; con A: concanavalin A; PWM; pokeweed mitogen; LPS: lipopolysaccharide

Introduction

IL-10 is a cytokine mainly secreted by monocytes which downregulates the expression of Th1-type cytokines and enhances B cell survival and antibody production (Mocellin, Marincola et al. 2004). There is accumulating evidence that IL-10 levels may be enhanced in Johne's disease. From among a multitude of cytokines studied (including IFNγ, TGFβ, TNFα, IL-1α, IL-4, IL-6, IL-8, and IL-12p35) only expression of the IL-10 gene is consistently increased when PBMC from subclinically infected cattle are stimulated with Mptb in vitro (Coussens, Verman et al. 2004). In ovine JD, while animals with paucibacillary disease are more likely to have elevated levels of IFNγ in ileal tissue, elevated levels of IL-10 are more likely in multibacillary animals (Smeed, Watkins et al. 2007)

An assay to determine secretion of IL-10 by stimulated ovine mononuclear cells was established based on Kwong et al (Kwong, Hope et al. 2002).

Methods

A 96-well microtitre plate was coated overnight with the anti-IL-10 antibody CC318 (Serotec) and washed 5 times with PBS/0.05% Tween20 (PBST). Samples were added to the plate, incubated for 1 hr, washed 5 times with PBST and incubated for 1 hr with a biotinylated anti-IL-10 antibody (CC320biotin, Serotec). The plate was washed 5 times with PBST prior to the addition of streptavidin HRP. The plate was incubated for another hour and washed 5 times with PBST. TMB substrate was then added and the plate incubated for 30 min prior to addition of 2M H_2SO_4. Absorbance was measured at 450 nm. Results are expressed as 'adjusted OD'.

Adjusted OD = Mptb antigen stimulated sample – medium alone sample

Stock negative and positive controls were generated using PBMC from Gudair® vaccinated sheep and included in all plates. The negative control was from culture supernatants in the presence of medium alone while the positive control was from cultures incubated in the presence of Mptb antigen.

The assay was optimised to minimise use of reagents and a Standard Operating Protocol was established.

Results

Initially, blood samples from vaccinated animals (OJD031.F) were used to develop tissue culture supernatants to develop this ELISA. Preliminary results showed that optimal results could be obtained by using tissue culture supernatants from PBMC stimulated with either Mptb antigen or concanavalin A for 6 days (Figure 1B.1).

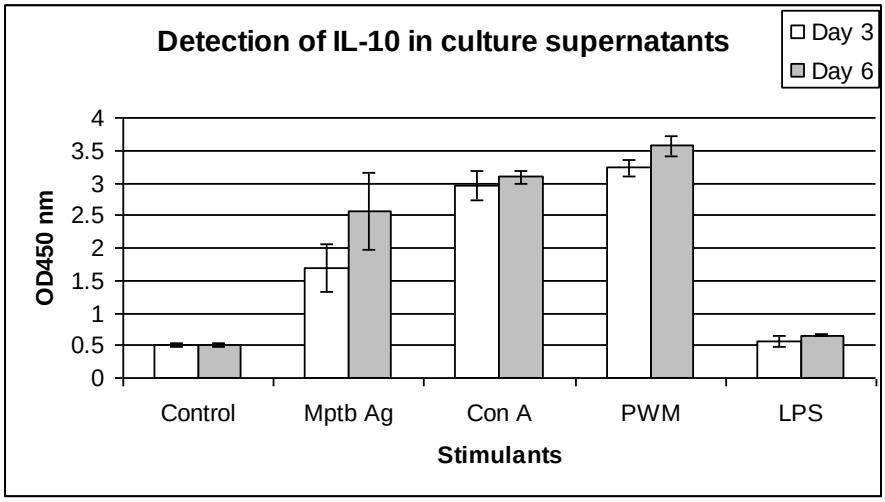

Figure 1B.1 Secretion of IL-10 by mononuclear cells in response to various stimulants
PBMC from Gudair® vaccinated animals (OJD031.F) were cultured in the presence of medium alone (control) or other stimulants. Cell culture supernatants were harvested on days 3 and 6 of culture and IL-10 secretion detected by the ovine IL-10 assay. Mean ± sem (n = 2) are shown. Con A: concanavalin A; PWM: Pokeweed mitogen; LPS: lipopolysaccharide

In a group of animals with no history of exposure to Mptb, secretion of IL-10 in response to Mptb antigen was extremely low (Fig. 1B.2, left panel). A 5-6 fold increase in IL-10 secretion (compared to Mptb antigen stimulation) was detected in response to con A in these animals. In animals exposed to Mptb (Fig 1B.2, right panel), IL-10 secretion was 5.9 fold higher than in animals that had not been exposed to Mptb. In the exposed group, infection status did not appear to play a part in the IL-10 response to Mptb antigen.

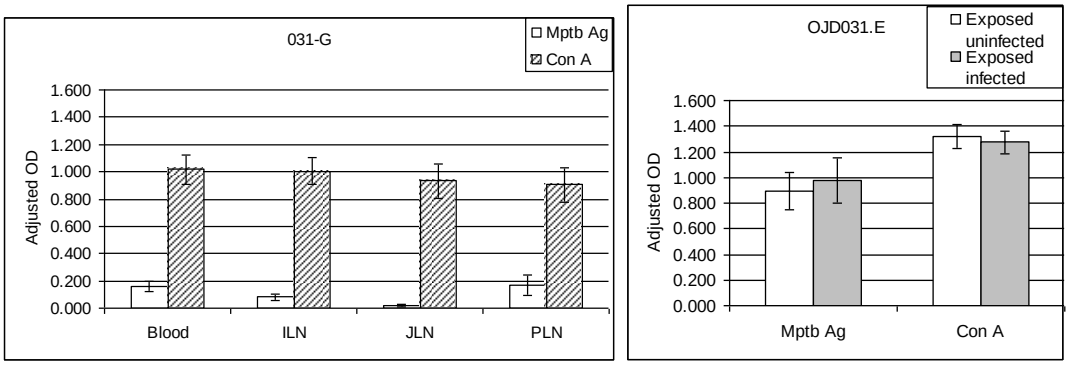

Figure 1B.2 Secretion of IL-10 in sheep not exposed or exposed to Mptb.
PBMC and lymph node cells from animals not exposed to Mptb and negative in tests for OJD (031.G, left panel) and PBMC from animals naturally exposed to Mptb (031.E, right panel) were tested in the IL-10 assay. Mean ± sem of adjusted OD are shown. For 031.G, n=10 and for 031.E n=13 for uninfected and n=17 for the infected group.

IL-10 secretion in response to recall antigen was also studied in experimentally challenged sheep in the OJD031.6 trial. PBMC were tested at 4, 8 and 11-13 months. The last blood samples were taken

within a week prior to necropsy. IL-10 secretion in PBMC from control sheep was low and remained low throughout the study period (Fig 1B.3, A). IL-10 secreted from lymph node cells taken from these animals at necropsy was also very low (Fig 1B.3, B). These animals remained free of disease throughout the study period.

Sheep experimentally challenged with Mptb had a higher IL-10 response to Mptb antigen in PBMC from as early as 4 months p.i. which remained elevated until the end of the trial at 11-13 months p.i. (Fig 1B.3, A). Ileal and jejunal lymph node cells of these animals also had an elevated IL-10 response when compared to control animals (Fig 1B.3, B). However, there was no difference in the response in cells from the prescapular lymph node between controls and experimentally challenged sheep.

When the experimentally challenged animals were separated into those that succumbed to infection (exposed infected) and those that did not (exposed uninfected) it was observed that the latter group had a higher IL-10 response in PBMC throughout the duration of the study (Fig 1B.3, C). The response in the lymph node cells was similar (Fig 1B.3, D).

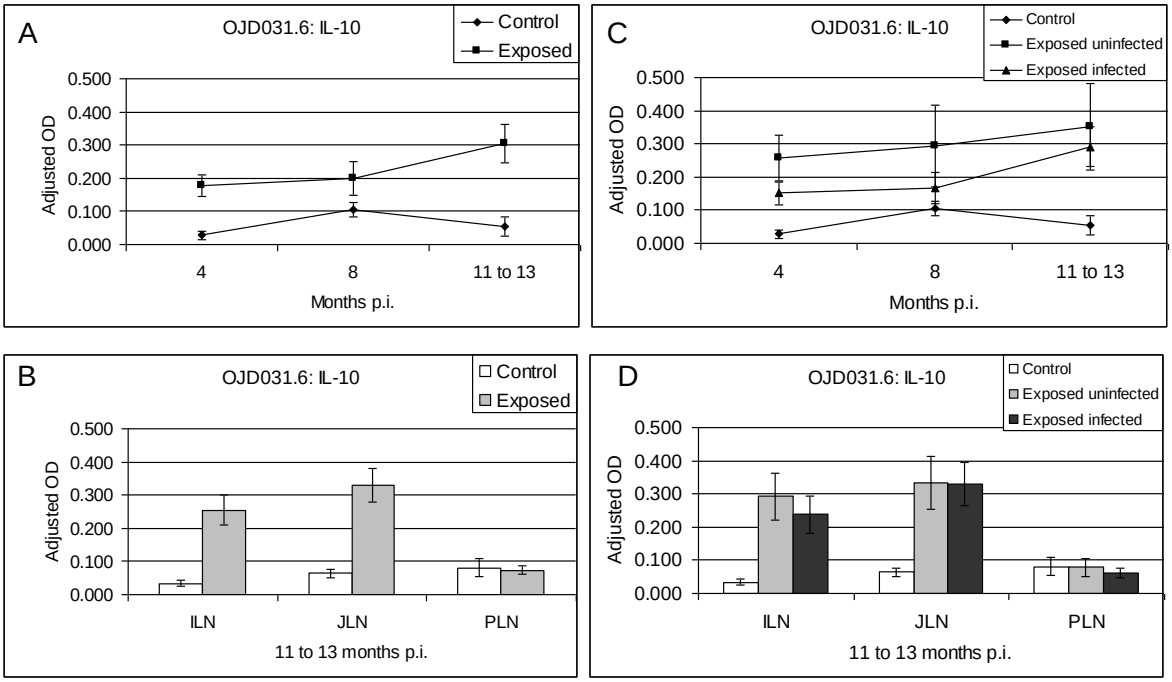

Figure 1B.3 Secretion of IL-10 in sheep experimentally challenged with Mptb
PBMC and lymph node cells from controls (unchallenged) and animals experimentally challenged with Mptb were tested in the IL-10 assay. Mean ± sem of adjusted OD are shown. Controls, n=20; Exposed, n = 37; Exposed uninfected, n=12; Exposed infected, n=26.

Discussion

The ovine IL-10 assay has been optimised and can be used routinely to test cells from blood and other tissues. Con A and pokeweed mitogen, but not LPS, can be used as a positive control in this assay to ensure that the cells are able to respond to the recall antigen. Unlike the IFNγ ELISA where the cells are stimulated for 1-2 days it is recommended that cells are cultured with the recall antigen for 6 days for the IL-10 assay.

There are several factors which make this IL-10 assay a potentially useful test in assisting diagnosis of OJD. An Mptb antigen-specific IL-10 response is not seen in the blood or lymph node cells in sheep that have not encountered the mycobacterium (Figs 1B.2 and 1B.3). An elevated IL-10

response is observed in blood and lymph node cells associated with sites of infection (ILN and JLN) of sheep that have been exposed to Mptb, but not in the PLN of these animals. The ability to detect an IL-10 response in blood cells makes it a potentially useful test in diagnosing disease. Further value is added to the test because a difference in the IL-10 response in control and experimentally challenged sheep can be detected as early as 4 months p.i. (Fig1B.3 A). More encouraging, is the finding that, early on in disease (4-8 months p.i.), the IL-10 response in PBMC tends to be higher in sheep that have been exposed to Mptb but do not succumb to disease (at least at 11-13 months p.i.) than animals that succumb to disease. Further investigation of this phenomenon is warranted.

References

Coussens, P. M., N. Verman, et al. (2004). "Cytokine gene expression in peripheral blood mononuclear cells and tissues of cattle infected with Mycobacterium avium subsp. paratuberculosis: evidence for an inherent proinflammatory gene expression pattern." Infect Immun **72**(3): 1409-22.

Kwong, L. S., J. C. Hope, et al. (2002). "Development of an ELISA for bovine IL-10." Vet Immunol Immunopathol **85**(3-4): 213-23.

Mocellin, S., F. Marincola, et al. (2004). "The multifaceted relationship between IL-10 and adaptive immunity: putting together the pieces of a puzzle." Cytokine & Growth Factor Reviews **15**(1): 61-76.

Smeed, J. A., C. A. Watkins, et al. (2007). "Differential cytokine gene expression profiles in the three pathological forms of sheep paratuberculosis." BMC Vet Res **3**(1): 18.

9.6 Appendix 1C-1 Subprogram 1 Development of apoptotic assays for sheep

Abbreviations

Mptb: Mycobacterium avium subsp paratuberculosis; PBS: phosphate buffered saline; PBMC: peripheral blood mononuclear cells; Q-PCR: quantitative polymerase chain reaction.

Introduction

Apoptosis is the active process of self-destruction by which cells no longer required are eliminated. It plays an important role in cell mediated immunity where it is responsible for the removal of pathogen-infected cells. In addition, lymphocytes which are produced by clonal expansion to mount an effective immune response are removed by apoptosis once they are no longer required. The apoptotic response to mycobacteria remains generally poorly understood with very limited knowledge of its role in ovine Johne's disease. Tools developed to monitor apoptosis in sheep are described in this study.

Methods

There are several characteristics of apoptosis which can be utilised to detect this process in cells and tissues. We used three different methods to detect three different aspects of apoptosis. Activation of caspase enzymes is central, and common, to apoptotic pathways. A flow cytometric method using a pan-caspase marker was established to detect apoptosis in ovine mononuclear cells. During apoptotic disassembly of cellular components, genomic DNA is cleaved into nucleosomal fragments. Nick end labelling of DNA using the TUNEL method was utilised for detection of apoptosis *in situ*. A balance between cellular pro- and anti-apoptotic proteins determines if cells survive or if they are destined for elimination. Real time quantitative PCR assays (Q-PCR) were developed for detection of pro- and anti-apoptosis gene expression in ovine intestinal tissue.

Detection of caspase activity in ovine mononuclear cells

CaspACE FITC-VAD-FMK (Cat No G7461/2, Promega) was used to detect apoptosis in ex vivo as well as in cultured ovine mononuclear cells by flow cytometry. CaspACE FITC-VAD-FMK (Cat No G7461/2, Promega) a fluoroisothiocyanate (FITC) conjugate of the cell permeable caspase inhibitor VAD-FMK was titrated to determine the optimal concentration for use with ovine cells.

Samples were tested in triplicate and a single unstained control was included for all animals. A positive control containing $2x10^5$ thymus cells was included in all experiments.

A total of $2x10^5$ cells at $1.25x10^6$ cells per mL were transferred into 96 well plates (round bottom) and pelleted by centrifuging at 1000 rpm for 3 minutes. Cell pellets were resuspended in either 200 µL of 5µM caspACE or PBS (unstained controls) and incubated for 20 minutes at 37°C/5% CO_2. Cells were then washed twice using FACS Buffer (PBS/1% newborn calf serum/0.1% azide) (1000 rpm for 3 minutes per wash) and resuspended in 200 µL of 1% paraformaldehyde. Plates were then sealed using parafilm and stored at 4°C for no more than 5 days prior to flow cytometric data collection.

Data acquisition

Flow cytometry data was acquired using a FACSCalibur (Becton Dickinson Immunocytometry Systems). Data was collected using BD™ PlateManager Software (BD Biosciences) in a 100 µL sample volume. During data acquisition mononuclear cell populations were visualized using forward and side scatter plots. Acquisition software was set to collect 10,000 events within the live lymphocyte population. All events were collected; no threshold was set. Single stained and unstained samples (FACS controls) were included.

Data analysis

Flow cytometric data was analysed using CellQuest software (Becton Dickinson, Oxford, UK) and WinList 5.0 (Verity Software House).

Caspase positive control

Thymus tissue was collected from lambs shortly after death (approx 1 to 2 hours) which had occurred during lambing. Tissue samples were collected into PBS and then diced to release the thymocytes. Homogenised tissue was then filtered and the suspension centrifuged at 1000 rpm for 10 minutes. The supernatant was discarded and the pellet resuspended in 10 mL PBS. The cells were washed in PBS again and the sample resuspended in culture medium (RPMI 1640/10% FBS/Pen/Strep). Cells were then frozen at $8x10^6$ cells/mL in culture medium with 20% newborn calf serum/20% DMSO at -80°C. Thawed thymus cells were included as a positive control for caspase labelling.

Optimising the caspACE assay

To determine the optimal concentration of caspACE to use with ovine mononuclear cells, isolated PBMCs were cultured for up to 2 days in RPMI 1640/10% FBS. The cell suspension was then heat treated for 15 minutes at 60°C using a Hybaid Shake 'n' Stack (Thermo Electron Corporation). The cell concentration was adjusted to $2x10^6$ cells/mL and 100µL per well was then transferred to a 96 well plate.

Heat-treated PBMCs were then stained with 0.5 µM to 25 µM caspACE prepared in PBS in a total volume of 200 µL. Excess caspACE was then removed by washing twice with PBS (200 µL volumes, centrifugation at 1000 rpm for 3 minutes).

The optimal period for mononuclear cell culture and antigen concentration were also assessed. PBMCs were cultured for up to 8 days with 0-20 µg/mL Mptb antigen and cellular apoptosis was monitored using the flow cytometric caspase assay.

Validating the caspACE assay

To validate that the caspase activity detected was due to apoptosis, ovine PBMCs were triple stained with caspase, annexin V and 7-AAD (7-amino actinomycin D). Annexin V is another marker of apoptosis. It binds to phosphatidylserine residues which are exposed on the surface as cells undergo apoptosis. 7-AAD is able to discriminate late apoptotic or necrotic cells from early apoptotic cells since the latter have intact membranes and are able to exclude the dye.

Ovine PBMCs were triple stained either soon after isolation or after 6 days of culture in the presence of medium alone.

Detection of apoptosis by the TUNEL method

A commercial kit was used to detect apoptotic bodies in ovine intestinal tissue. The ApopTag® Plus Peroxidase In situ Apoptosis Kit (Chemicon) was used following manufacturer's instructions. This kit

uses the TUNEL method where genomic DNA strand breaks due to apoptosis are detected by a specific enzyme (terminal uridine deoxynucleotidyl transferase) and are labelled with nucleotides. The presence of added nucleotides was visualised using peroxidase conjugated antibodies and peroxidase substrates.

Detection of apoptotic gene expression by real time quantitative PCR

Ovine primer design

The ovine nucleotide sequence was located using the NCBI website (http://www.ncbi.nlm.nih.gov). A selection of 4 ovine genes, two pro-apoptotic genes (Fas and Bax) and two anti-apoptotic genes (bcl-2 and Mcl-1), were chosen from a list of potential apoptosis genes of interest. Q-PCR primers (Table 1C.1) were designed using Beacon Designer 4.0 (Premier Biosoft) using the following parameters: primer length, 18-24bp; Tm 57°C +/- 3°C; product length 80-150 bp. Primers were synthesised by Sigma Genosys (http://www.sigmaaldrich.com) and reconstituted in nuclease-free water (Ambion) to a final concentration of 100 µM. Primers were stored at -20°C.

Preparation of tissue sections for RNA extraction

Samples stored at -80°C were transferred onto dry ice. While still on dry ice, a cross-section of tissue was cut using sterile forceps and a scalpel blade to approximately 3x3 mm (approximately 30 mg) and transferred into a new 1.5 mL Eppendorf tube. All samples were stored at -80°C prior to RNA extraction.

RNA Extraction

RNaseZAP (Sigma) was used to clean all equipment and benchtops prior to use.

RNA was extracted using the RNeasy mini kit (Qiagen) following manufacturer's instructions. Briefly, frozen prepared tissue sections were placed into sterile 5 mL yellow capped tubes (Interpath) containing 600 µL of RLT lysis buffer (to lyse the cells and tissues before RNA isolation). Samples were then homogenised using an Ultra Tarex (Janke and Kunkel, IKA-WERK) fitted with a small probe. The tissue lysate (approx 600 µL) was then placed into a QiaShredder column and centrifuged at 13,000 rpm for 2 minutes. The supernatant was transferred into a new microfuge tube containing 600 µL of 70% ethanol and mixed immediately. A 700 µL volume was then transferred into an RNeasy mini column fitted with a 2 mL collection tube and centrifuged at 13,000 rpm for 15 seconds. The flow- through was discarded and the remaining sample was added to an RNeasy column. Samples were then re-centrifuged and the flow-through discarded. The column was washed by adding 700 µL of buffer RW1 (provided in the RNeasy mini kit) and centrifugation (13,000rpm for 15 seconds). The collection tube and flow through were then discarded and the RNeasy column was transferred into a new 2 mL collection tube. Wash buffer RPE (500 µL, provided in the RNeasy mini kit) was added to the column, the sample was centrifuged (13,000 rpm for 15 seconds) and the flow-through discarded. Another 500 µL of RPE buffer was added to the column and the sample was centrifuged (13,000 rpm for 2 minutes) to dry the RNeasy silica membrane; flow-through was discarded. The RNeasy column was then placed into a new 1.5 mL collection tube and RNA eluted using 40 µL of Rnase-free water. The water was added directly to the RNeasy silica membrane and left to elute for 5 minutes. The sample was then centrifuged (13,000 rpm for 1 minute) to collect RNA. As a quality control measure RNA samples were then visualized using gel electrophoresis. All RNA samples were stored at -80°C.

DNase treatment of RNA samples

To every 40 µL of tissue RNA, 10µl of RQ1 DNAse buffer (Cat No. M198A, Promega, USA), 10 µl of RQ1 DNAse-free water (Cat No.M610A, Promega, USA) and 40 µL of RNase-free, Molecular

Biology Grade water (Eppendorf) were added. Samples were mixed and incubated at 37 °C for 2 hours. Samples were vortexed, spun down briefly and placed on ice. Quality of RNA (1 µL) was checked by electrophoresis on an RNAse-free 1% agarose gel (Agarose-LE powder, Ambion) and visualized by ethidium bromide and ultraviolet light. To check that the DNase-treated RNA was free from DNA contamination, 0.5 µL of RNA was used as template in a Q-PCR reaction using the MX3000P Real-time PCR machine (Stratagene). The following reagents were used per reaction:

- 10 µL 2x ABsolute-Q-PCR SYBR Green Master Mix (Cat No. AB1166, ABgene)
- 0.12 µL of 100 µM Ov B2M primers (Table 1)
- 0.25 µL of diluted ROX (1 µL/1999 µL using RNase free water) (AB gene)
- 9.13µL of RNase-free water

Table 1C.1: List of primer sequences for Q-PCR

Accession number	Gene	Primer name	PrimerSequence	Position	Length (bp)	Tm (°C)	Product Length (bp)
AY423861	Bcl-2	Q5 Ovis aries Bcl-2	TCGCCGAGATGTCCAGTC	2	18	55.2	92
		Q3 Ovis aries Bcl-2	CACCCCGTCCCTGAAGAG	93	18	55.4	
AY609317	Bax	Q5 Ovis aries Bax	ATGATCGCAGCCGTGGAC	21	18	56.6	90
		Q3 Ovis aries Bax	GCCCCAGTTGAAGTTGCC	110	18	55.3	
AB011671	Fas	Q5 Ovis aries Fas	GCCTATATCGTGAGCACCTG	158	20	54.9	132
		Q3 Ovis aries Fas	TCTTGTCTGTGTACTCGTTCC	289	21	54.6	
AF144097	Mcl-1	Q5 Ovis aries Mcl-1	CATCGAACCACTAGCAGAAAGC	121	22	57.2	100
		Q3 Ovis aries Mcl-1	GAAGAACTCCACAAACCCATCC	220	22	56.6	
		Q5 Ov B2M	CTGCTGTCGCTGTCTGGA		18		
		Q3 Ov B2M	CAGTTCAGGTAATTTGGCTTTCC		23		
		oligo dT15	TTTTTTTTTTTTTTTN		16		

Ovine cDNA (0.5 µL at 10-20ng/µL) was used as a positive control and 0.5 µL of RNase -free water was used as a non-template control (NTC). RNA (0.5 µL) was also used to run a Q-PCR check using 10 µL ABsolute-Q-PCR SYBR Green Master Mix. DNase-treated RNA was left for 15 minutes at -80°C to inactivate the DNase. RNA was then precipitated by the addition of acrlymide (Ambion), 10µL 3M sodium acetate (Sigma Aldrich) and 300 µL of absolute ethanol (Sigma Aldrich). Samples were incubated at -80°C for one hour and then centrifuged at 4°C for 30 minutes to harvest the RNA. The supernatant was removed and the pellet briefly air dried. Samples were then resuspended in 20 µL of RNase-free water. The RNA was then purified using a Micro Spin^{TM} G-50 column (Amersham

Biosciences). RNA concentration was determined using optical density (1/60 dilution) at 260 nm (Bio Photometer, Eppendorf). Readings were taken in triplicate and the mean value recorded. All RNA samples were stored at -80°C.

Note: During all the DNase Treatment procedure RNaseZAP was used to clean all equipment and benchtops (Cat No. R2020, Sigma, USA).

cDNA synthesis

For each cDNA synthesis, approximately 25 µg of DNase-treated RNA was used. RNA was made up to a total volume of 50 µL in RNase-free PCR tubes (Ambion) using 4 µg oligo dT15 (Table 4) and RNase-free water (Molecular Biology Grade, Eppendorf). Samples were heated at 70°C for 3 minutes in a PCR machine (Px2, Thermo Electron Corporation) to denature the RNA and then placed on ice for 2 minutes. The samples were then spun down and added to 40 µL of 5x M-MLV RT buffer (Promega), 8 µL 25 mM dNTP's (Promega), 1 µL RNasin RNase Inhibitor (Fermentas), 99 µL MQ water and 2 µL M-MLV Reverse Transcriptase (Cat No.M170A, Promega). The reaction mix was then divided into two, (100 µL per tube), mixed and the reaction allowed to proceed at 42 °C for 2 hours. The Reverse Transcriptase was then inactivated at 75°C for 10 minutes. PCR tubes were then pooled into 1.5 mL Eppendorf tubes and the cDNA was precipitated using 2 µL of linear acrylamide, 20µL 3M NaOH, pH 5.2 and 600 µL ethanol (Sigma). Samples were then left to precipitate at -80°C for one hour and then centrifuged for 30 minutes at 13000 rpm. The solution was removed and pellets were resuspended in 25 µL MQ water. cDNA was then purified using G50 columns (Amersham). The synthesis was determined by OD (1/60 dilution) at 260 nm. Readings were taken in triplicate and the mean value recorded. All cDNAs were stored at -80°C. Each sample was diluted to 1 ng/µL with MQ water prior to QPCR analysis. Some diluted samples (20 ng/µL in MQ water) were stored at -20°C.

Optimizing QPCR conditions

To select optimal concentration of template cDNA per reaction and to check that primers were quantitative and had 100% efficiencies, standard curves were generated for each primer set using diluted ileal gut cDNA (in MQ water) ranging from 100 ng to 0.01 ng. Q-PCR was run using 2x QuantiTect SYBR green Q-PCR Master Mix (QIAGEN) as per manufacturer's instructions.

Reference genes

An established reference gene, HK 5.1 (accession number 78369221), was provided by Dr Lyrissa Di Fiore (Faculty of Veterinary Science, University of Sydney) for use as a reference gene for ovine terminal ileum samples. HK5.1 has homology to a bovine gene called "splicing factor arginine/serine-rich 6".

Q-PCR protocol

An MX3000p real-time PCR machine (Stratagene) was used to quantify RNA transcripts using QuantiTect SYBR Green mix (QIAGEN) in 25 µL volumes containing 1-10 ng of cDNA. Primers were used at a final concentration of 300 nM. Cycle conditions were set at (95°C for 15 seconds, 56°C for 30 seconds and 70°C for 20 seconds) x 40, 95°C for 1 minute, 65°C for 30 seconds and then 95°C for 30 seconds. Ct values were exported to Excel (Microsoft) for further analysis. For quantitative, comparative analysis, transcript levels were normalised to the level of HK1.5 and fold changes were determined using the ($2^{-(deltadeltaCt)}$) method.

Results and Discussion

Caspase assay

Conversion of the method from a tube-based assay to a plate-based assay meant that flow cytometric data could be acquired rapidly by using the high throughput system. This made it suitable for use in large scale studies. Flow cytometry was chosen as the detection method as it has the added advantage of incorporating cell phenotype.

Optimisation studies indicated culture of ovine mononuclear cells for 6 days in the presence of 10 µg/mL Mptb antigen was best. Titration of the caspase inhibitor found that, in ovine mononuclear cells, this reagent could be used at 5 µM (Fig 1C.1) which is half the recommended concentration.

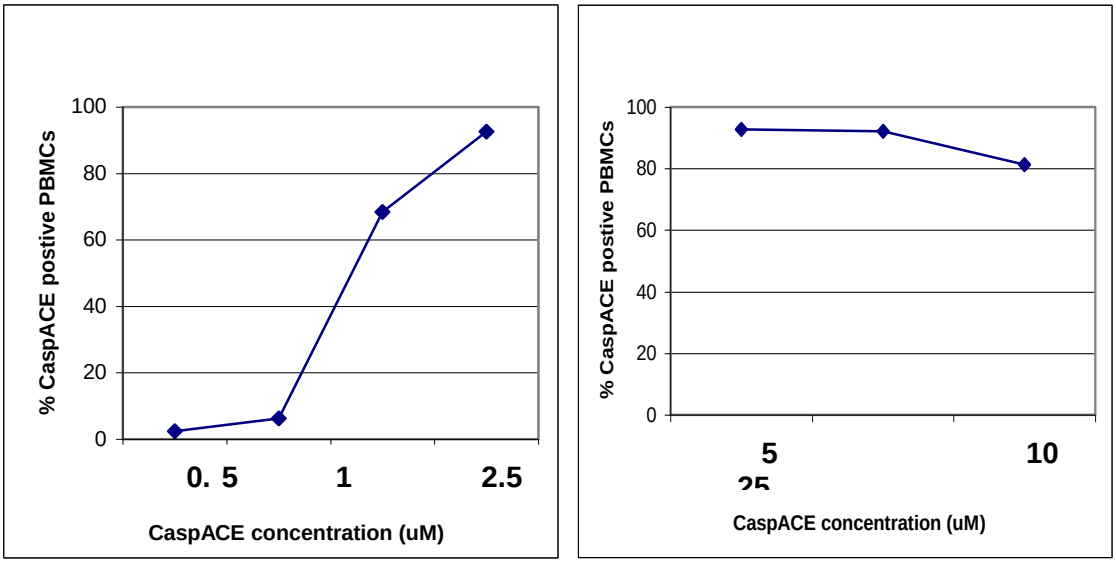

Check formatting of graph caption

Figure 1C.1 CaspACE titration for optimisation of assay

Heat-treated PBMC were stained with 0.5 µM to 25 µM caspACE. Caspase activity was detected by flow cytometry in heat treated PBMCs cultured for 2 days stained with 0.5 µM to 25 µM caspACE.

Positive control for caspACE assay

Thymic regression begins at birth and the thymus is an excellent source of apoptotic cells. Thymus cells from a neonatal lamb were used as a positive control for the caspase assay (Figure 1C.2).

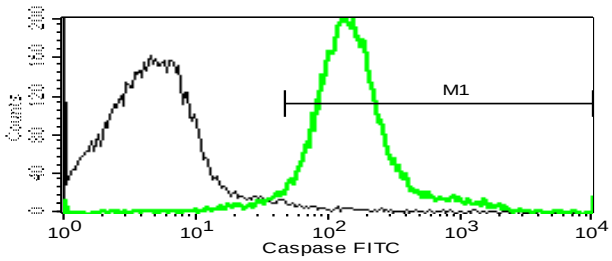

Figure 1C.2: Caspase activity in regressing ovine thymus cells.

Thymus cells from a neonatal lamb were stained with caspACE®. Fluorescence of unstained (black line) and caspACE® stained (green) thymus cells is shown on the x-axis and cell number on the y-axis. The M1 marker indicates cells with active caspases.

Validation of caspase assay

Caspase activation is not exclusive to apoptosis. Therefore, other markers of apoptosis were assessed to confirm the presence of active caspases was associated with apoptosis. Triple staining of PBMCs with caspase, annexin V and 7-AAD revealed that the caspase assay did detect apoptotic cells since most of the cells that had active caspases also labelled with annexin V. This is demonstrated in panels A to C in Figure 1C.3. A similar proportion of PBMCs labelled had active caspases (panel A, bottom right quadrant) or annexin V (panel B, bottom right quadrant). In addition, when cells positive for annexin V alone (panel B, bottom right quadrant) were analysed it was observed that the majority of these cells had active caspases (panel C, upper right quadrant. Less than 5% of cells were in the later stages of apoptosis as indicated by 7-AAD labelling (panels A and B, upper right quadrants).

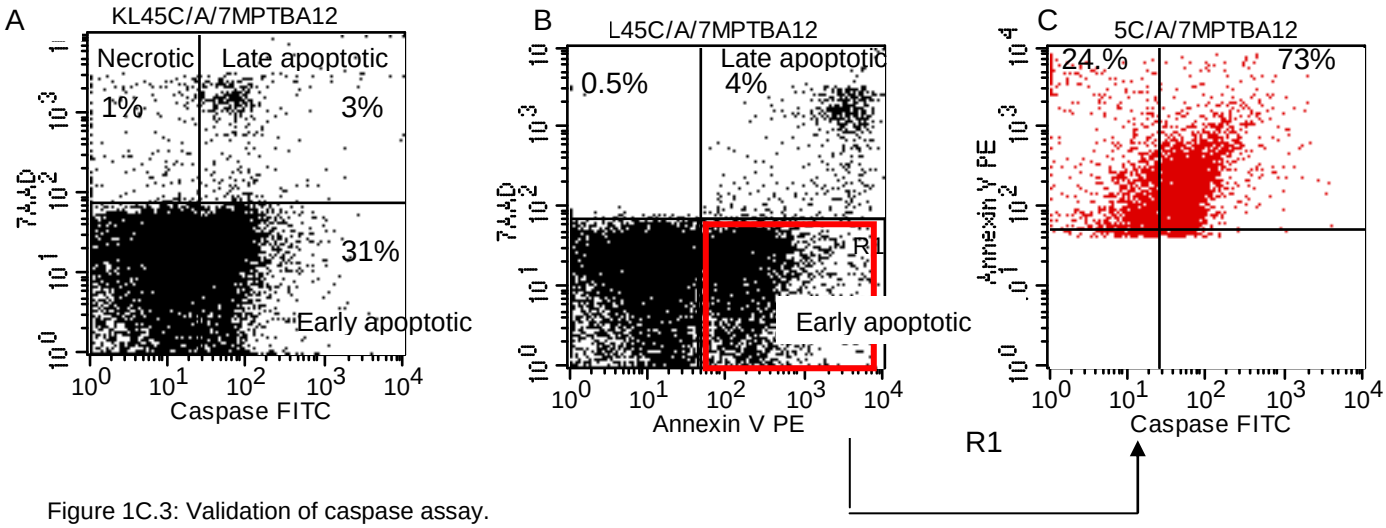

Figure 1C.3: Validation of caspase assay.

Ovine PBMCs were stained with either caspACE and 7-AAD (A) or caspACE, 7AA-D and annexin V (B). Early and late apoptotic cells as detected by caspase activity (A) or annexin V labelling (B) are shown. A gate was set around annexin V positive early apoptotic cells (B, lower right quadrant) and caspase activity and annexin V were evaluated within this gate (C). The majority of annexin V positive cells have active caspases (C, upper right).

9.7 Appendix 1C-2 Subprogram 1 Apoptotic response in ovine Johne's Disease

Abbreviations

Mptb: Mycobacterium avium subsp paratuberculosis; PBS: phosphate buffered saline; PBMC: peripheral blood mononuclear cells; Q-PCR: quantitative polymerase chain reaction; p.i.: post inoculation; ICLN: ileal lymph node; PJLN: posterior jejunal lymph node; PLN: prescapular lymph node; PPDA: M. avium purified protein derivative;

Introduction

Apoptosis is important in many different biological systems including embryonic development, cell turnover and the immune response. It is well recognised that the cell mediated immune response plays an important role in the host response to mycobacterial infection. While much attention has focused on lymphocyte proliferation and cytokine production in relation to the progress of mycobacterial disease in ruminants, the role of apoptosis remains relatively uncharted. This is especially true in relation to ovine Johne's disease.

The main objective of this study was to examine apoptosis in mononuclear cells *ex vivo* as well as apoptosis in response to recall of the Mptb antigen in sheep that have not been exposed to Mptb as well as animals that have been exposed to the mycobacterium either naturally or by experimental infection.

Methods

Three techniques were used to monitor apoptosis in ovine Johne's disease. A high throughput flow cytometric assay was utilised to detect the presence of active caspase enzymes, which are central to apoptosis pathways, in peripheral blood and lymph node mononuclear cells. Apoptosis in the terminal ileum, a site predisposed to the formation of lesions in Johne's disease, was determined in situ using a commercially available kit. This test detected DNA fragmentation in apoptotic cells. Specially designed real time quantitative PCR assays were used to assess expression of pro- and anti-apoptotic genes in ovine intestinal tissue. Methods are described in detail in Appendix 1C-1.

Animals

The apoptotic response was assessed in naturally infected as well as experimentally challenged sheep.

In the natural infection trials (OJD031.A, OJD031.E and OJD031.G) animals were sourced from farms from the Southern Highlands region of New South Wales. Infected animals as well as animals that had been exposed to Mptb yet remained free of disease were selected. Animals for the OJD031.G trial had never been exposed to Mptb. Extensive screening of animals was carried to ensure diseased or disease-free status.

In the experimental infection model animals were orally challenged with Mptb. Sheep from OJD031.3-OJD031.6 experimental infection trials (Table 1C.1) were assessed. All animals in the OJD031.3-5 trials were exposed to a clonal inoculum of Mptb (Telford). In OJD031.6, one group was left unexposed to Mptb and a second group was challenged with the same clonal inoculum of Mptb as in the previous trials or with a gut homogenate prepared from an animal with clinical disease. These experimental infection trials are described in detail in Subprogram 2B.

Table 1C.1 OJD trials

Experimental trial	Breed (n)	Inoculum	Months p.i. at necropsy
OJD031.3	Cross-bred (n=23)	Telford*	19
OJD031.4	Merino (32)	Telford	14
OJD031.5	Merino (12)	Telford	10
OJD031.6	Merino (58)	None (20), Telford (18), Gut homogenate (20)	11 to 13
OJD031.A	Merino	Natural exposure	#
OJD031.E	Merino	Natural exposure	#
OJD031.G	Merino	No exposure	#

*These animals received a 'booster' inoculum 12 months after the first challenge.
#All animals were 3-5 years of age at necropsy

Sampling

Blood samples were collected throughout the duration of each trial and also prior to necropsy. Faecal samples were collected bimonthly while tissue samples were collected at necropsy. At the termination of each experimental trial, Mptb antigen-driven proliferation was assessed in cells from the ileal (ILN), posterior jejunal (JLN) and prescapular (PLN) lymph nodes.

Classification of disease

Culture of Mptb from tissue samples (radiometric BACTEC culture) and IS900 PCR confirmation were used to identify animals with OJD. The presence of histological lesions was also recorded.

Results and Discussion

Apoptosis in ex vivo mononuclear cells

Apoptosis in *ex vivo* mononuclear cells was similar in animals that had no history of exposure to Mptb and were negative in tests for ovine JD (Fig 1C.1 A) and animals with clinical ovine JD (Fig. 1C.1B). Apoptosis was low (<20%) in isolated PBMCs, but was much higher (40-50%) in lymph node cells.

A. Animals not exposed to Mptb (OJD031.G)

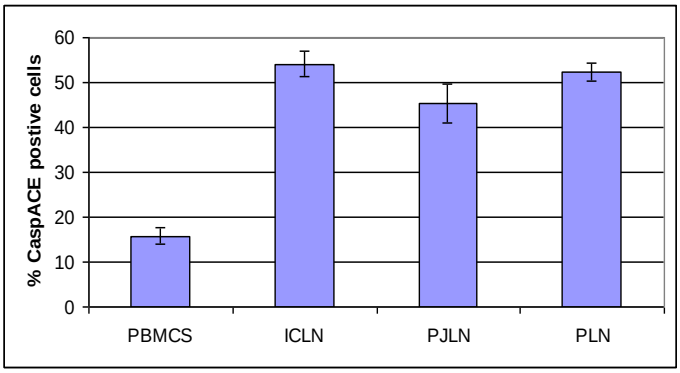

B. Animals with natural ovine JD (OJD031.E)

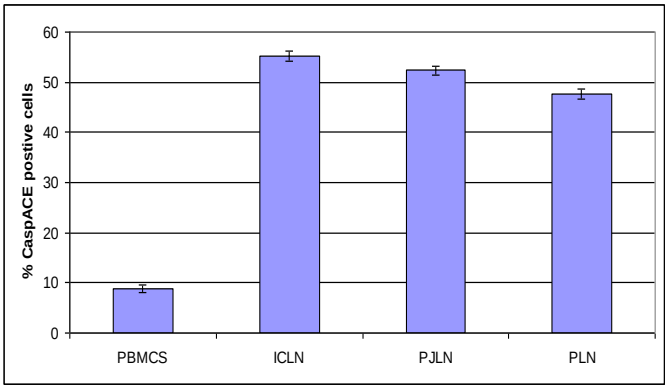

Figure 1C.1: Apoptosis in ex vivo blood and lymph node mononuclear cells.

Caspase activity was assessed in mononuclear cells derived from blood and gut lymph nodes of animals not exposed to Mptb (A) and those that had natural ovine JD (B). Apoptosis was detected by flow cytometry using a pan-caspase inhibitor (caspACE®).

OJD031.G, n=10; OJD031.E, n=32. ICLN=ileal lymph node; PJLN=posterior jejunal lymph node; PLN=prescapular lymph node.

In an experimental infection model (OJD031.6), all animals had a similar level of apoptotic mononuclear cells in PBMCs prior to inoculation with Mptb (Fig. 1C.2). In animals not exposed to Mptb (controls), this remained at a similar low level throughout the duration of the study. At 4 months p.i. apoptosis was significantly higher in animals that had been exposed to Mptb ($P > 0.05$) (Figure 1C.2, Telford and Gut Homogenate). At later time points, the level of apoptosis in *ex vivo* PBMCs declined in the exposed animals and was similar to the control group. At 12 months p.i., apoptosis in the Telford exposed group was significantly higher than in the Gut Homogenate exposed group ($P > 0.05$).

Thus it appears that while a difference in the level of apoptotic cells in PBMCs of exposed and unexposed sheep can been detected soon after exposure to Mptb, there is no difference between these two groups at later time points. This may account for the observation that the level of apoptosis was similar in PBMCs and lymph node cells from unexposed sheep and those with natural ovine JD infection.

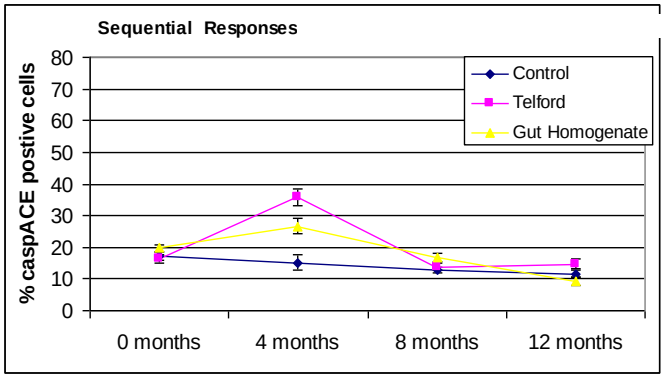

Figure 1C.2: Apoptotic responses in *ex vivo* PBMCs from OJD031.6.

Merino sheep were either exposed to Mptb (Telford and Gut Homogenate) or left unexposed (Control). Blood samples were taken over a 12 month period following inoculation. PBMCs were labelled to detect cells with active caspases and apoptosis is shown as the percentage of caspACE positive cells.

Apoptosis in cultured PBMC

Apoptosis in response to recall of Mptb antigen was followed in an experimental model of ovine JD from pre-inoculation to 12 months p.i. The presence of active caspases was detected by flow cytometry as a marker for apoptosis in PBMCs. Predicted means were used to determine significant differences.

Statistical analysis indicated that there was a significant three way interaction between all fixed effects tests. These fixed effects include time point examined (0-12 months), culture conditions tested (medium alone or Mptb antigen) and the treatment group (Control, Telford or Gut homogenate). Therefore all three effects were equally important in explaining the level of apoptosis observed. For this reason all three interactions were graphed together (Fig 1C.3).

Prior to Mptb exposure there were no significant differences been all three fixed effects (Fig 1C.3). Apoptosis was low in the peripheral blood, <25% for all animals tested. Importantly, Mptb antigen-induced apoptosis did not significantly differ from apoptosis in medium alone.

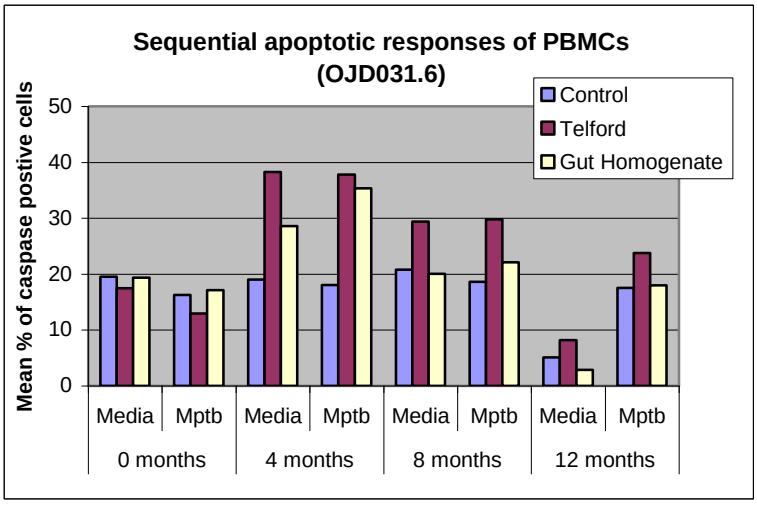

Figure 1C.3 Mptb antigen-specific apoptotic responses of cultured PBMCs (OJD031.6).

Animals were either exposed to Mptb (Telford, n=18 and Gut Homogenate, n=20) or left unexposed (control, n=20). Isolated PBMCs were cultured in the presence of either media alone or Mptb antigen for 6 days prior to detection of apoptotic cells by the flow cytometric caspase assay. Results are expressed as predicted mean values. Mean response ± SEM is shown.

Background apoptosis and Mptb antigen-specific apoptosis varied in all treatment groups during the study period. Background apoptosis of cultured PBMC from Control animals remained consistently similar to pre-inoculation levels at the 4 and 8 months p.i. sampling times (Fig 1C.3). There was no response to Mptb antigen at these times points. However, at 12 months p.i., apoptosis in medium alone was lower than usual (<10%) and apoptosis in the presence of Mptb antigen was elevated significantly ($P < 0.05$).

In the Telford-treated group, background apoptosis was elevated (compared to pre-inoculation) at 4 and 8 months p.i. (Fig 1C.3). However, apoptosis in response to Mptb antigen was not elevated above background levels. At 12 months p.i., like the Control animals, the Telford-treated animals also had lower than usual background apoptosis which was significantly elevated ($P < 0.05$) in the presence of Mptb antigen (Fig 1C.3).

The apoptotic response was different in Gut Homogenate treatment group. At 4 months p.i., background apoptosis was higher than in Control animals and was elevated further in the presence of Mptb antigen (Fig 1C.3). Four months later both background and Mptb antigen-specific apoptosis had declined to levels seen in the Control animals. At 12 months p.i., similar to the other two groups, background apoptosis was low and Mptb-specific apoptosis was significantly higher ($P < 0.05$) (Fig 1C.3).

The reason behind the unusually low level of background apoptosis at 12 months p.i. is not known. These results indicate that Mptb-specific apoptosis detected by cellular caspase activity is variable in cultured PBMCs and it will not be a useful tool in assessing ovine JD.

In another experimental trial, OJD031.3, cross-bred sheep were challenged with Mptb and monitored for 19 months. All sheep were given a second ‘booster’ dose 12 months after the first challenge. Blood samples were taken at 15 and 19 months after the first inoculation to assess Mptb antigen-specific apoptosis by detection of active caspases in cultured PBMCs (Fig. 1C.4). Predicted mean values were used to determine any significant apoptotic changes of PBMCs.

At the 15 month p.i. time point, Mptb antigen-specific apoptosis was significantly higher in all animals regardless of whether or not they succumbed to disease (Fig. 1C.4). It is interesting to note that this was 3 months after the animals had received the Mptb ‘booster’ dose. Similar results were seen in the OJD031.6 trial where at 4 months p.i. Mptb antigen-specific apoptosis was higher than background levels in animals exposed to Mptb in a gut homogenate (Fig. 1C.3).

At 19 months after initial exposure to Mptb, background apoptosis in cultured PBMC was significantly higher than at 15 months p.i. (Fig. 1C.4). The Mptb antigen-specific apoptosis was not significantly different at this time point.

Predicted means analysis indicated that there was no significant interaction between infection status of the animals and the level of apoptosis in PBMCs at both timepoints tested. Therefore Mptb antigen-specific apoptosis in PBMC detected by caspase activity does not appear to be beneficial in discriminating sheep that will remain free of disease and those that will succumb to ovine JD.

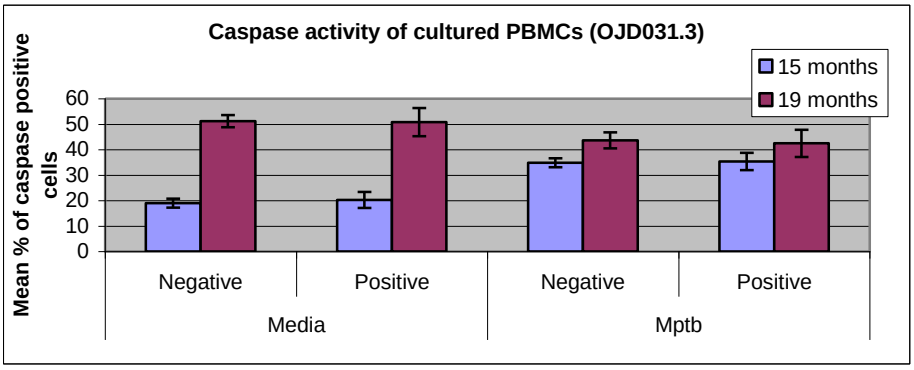

Figure 1C.4 Mptb antigen-specific apoptotic responses of cultured PBMCs (OJD031.3).

Cross-bred sheep were all exposed to Mptb and given a second 'booster' inoculation 12 months after the first dose. Isolated PBMCs were cultured in the presence of either media alone or Mptb antigen for 6 days prior to detection of apoptotic cells by the flow cytometric caspase assay. Animals are grouped into negative and positive status based on histology and tissue culture results. Results are expressed as predicted mean values. Mean response ± SEM is shown.

Comparison between Mptb antigen and PPDA induced apoptosis

Apoptosis in response to Mptb antigen and *M. avium* purified protein derivative (PPDA) was compared to determine the specificity of the Mptb antigen. Apoptosis was measured using the caspase assay and predicted means were used to determine any significant differences.

Generally, PPDA-induced apoptosis did not differ significantly from Mptb antigen-induced apoptosis at all time points and in all animals tested (Fig 1C.5). The exception was in the Telford group at 8 months, where there was significantly more PPDA-induced apoptosis.

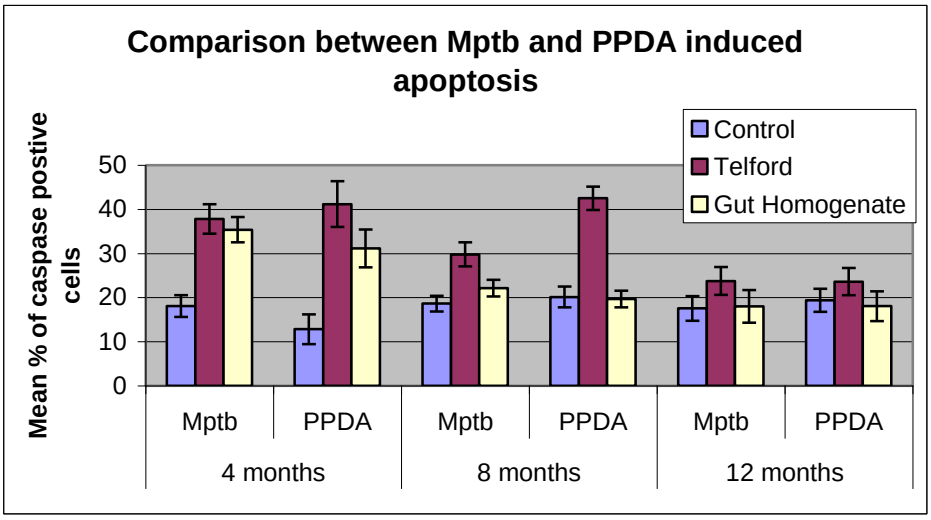

Figure 1C.5 Apoptosis in PBMC in response to Mptb antigen or PPDA.

Animals were either exposed to Mptb (Telford, n=18 and Gut Homogenate, n=20) or left unexposed (control, n=20). Isolated PBMCs were cultured in the presence of either Mptb antigen or PPDA for 6

days prior to detection of apoptotic cells by the flow cytometric caspase assay. Results are expressed as predicted mean values. Mean response ± SEM is shown.

Phenotype of apoptotic cells in ovine Johne's disease

At 12 months p.i. Mptb antigen-specific apoptosis was assessed in CD4, CD8 and γδ T cell subsets using caspase staining (Fig. 1C.6). Apoptosis of all three subpopulations in control animals remained low at <5%. Mptb-specific apoptosis in CD4 and γδ T cells was significantly higher in the gut homogenate group when compared to the control group.

Attempts to identify the phenotype of apoptotic cells at earlier time points were unsuccessful due to assay optimisation concerns. It was found that the order in which the cells were labelled was crucial to the success of the protocol. The cells have to be labelled for phenotype prior to labelling for caspase activity.

It may be beneficial to determine the phenotype of *ex vivo* apoptotic cells at earlier time points in experimental infection as it was observed that apoptosis was elevated in *ex vivo* PBMC at 4 months p.i (Fig 1C.2).

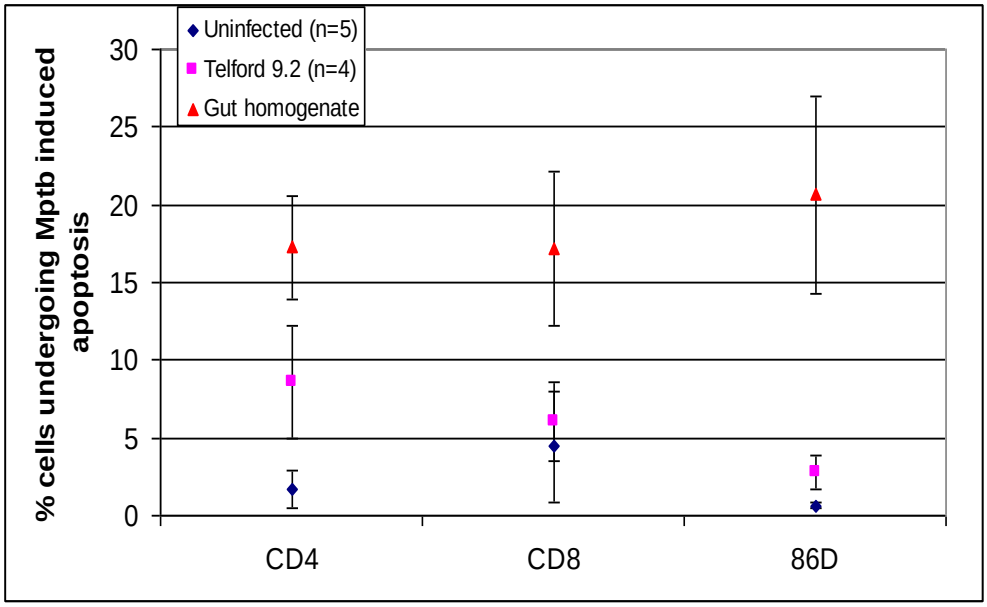

Figure 1C.6: Mptb Ag induced apoptosis in T cell subsets (OJD031.6)

PBMCs were isolated from OJD exposed animals 12 months p.i. and incubated for 6 days in the presence of media alone or Mptb antigen stimulation. Cell surface markers together with caspase staining were used to determine the relative proportions of apoptotic CD4 T cells, CD8 T cells and γδT cells (86D). Values are displayed as mean Mptb specific antigen induced responses minus non specific background apoptosis (media alone). Flow cytometric analysis was used to detect each subpopulation.

Apoptosis in cultured lymph node cells

Mononuclear cells were isolated from ileal (ILN), posterior jejunal (JLN) and prescapular (PLN) lymph nodes and cultured for 6 days in the presence of medium alone or Mptb antigen prior to detection of caspase activity. In animals with no history of exposure to Mptb and negative in tests for OJD (OJD031.G), apoptosis in response to Mptb antigen was significantly higher than in medium alone in ILN and PLN cells (Fig 1C.7A). This recall response to the antigen was not expected as this group of animals had no prior exposure to Mptb. A similar effect was seen in response to PPDA (Fig 1C.7A). When the response to Mptb and PPDA was compared in experimental OJD, while both antigens stimulated apoptosis in Mptb inoculated animals above unexposed controls, there was no significant difference in the level of apoptosis in response to these antigens (Fig 1C.5). In addition, there was no apoptosis in response to PPDA in the unexposed control animals. Therefore, it is possible that in the OJD031.G group the apoptotic response seen was due to exposure to environmental mycobacteria.

In a group of animals exposed to Mptb on farm (OJD031.E), lymph node cells from all animals responded significantly to Mptb antigen regardless of infection status (Fig. 1C.7B). Mptb antigen-specific apoptosis was significantly higher in ILN of animals with OJD when compared to animals free of disease ($P < 0.05$). This was similar in animals experimentally inoculated with Mptb (OJD031.1) at 19 months p.i. (Fig 1C.7C). In the same group, PLN cells of sheep with OJD also responded to Mptb antigen at a significantly higher level than sheep without disease ($P < 0.05$).

Thus it appears that ILN cells of Mptb exposed sheep with OJD are more likely to undergo apoptosis when in contact with Mptb antigens than ILN cells from Mptb exposed animals that remain disease-free.

Conclusions

The main objective of this study was to examine apoptosis in peripheral blood mononuclear cells (PBMCs) as well as apoptosis in response to recall of the Mptb antigen in sheep. A difference in the level of apoptotic cells in PBMCs of exposed and unexposed sheep was detected soon after exposure to Mptb, but there was no difference between these two groups at later time points: the level of apoptosis was similar in PBMCs from unexposed sheep and those with natural ovine JD infection. In a stimulation assay, Mptb-specific apoptosis detected by cellular caspase activity was variable in cultured PBMCs and it will not be a useful tool in assessing ovine JD. In another trial the analysis indicated that there was no significant relation between infection status of the animals and the level of apoptosis in PBMCs at two time points tested. Therefore Mptb antigen-specific apoptosis in PBMCs detected by caspase activity does not appear to be beneficial in discriminating sheep that will remain free of disease and those that will succumb to ovine JD. However, cells from the ileal lymph nodes (ILN) of Mptb exposed sheep with OJD are more likely to undergo apoptosis when in contact with Mptb antigens than ILN cells from Mptb exposed animals that remain disease-free. The observations of increased apoptosis in gut and lymph node tissues do not have practical diagnostic application as they were not mirrored in peripheral blood, which is more easily accessible in live animals.

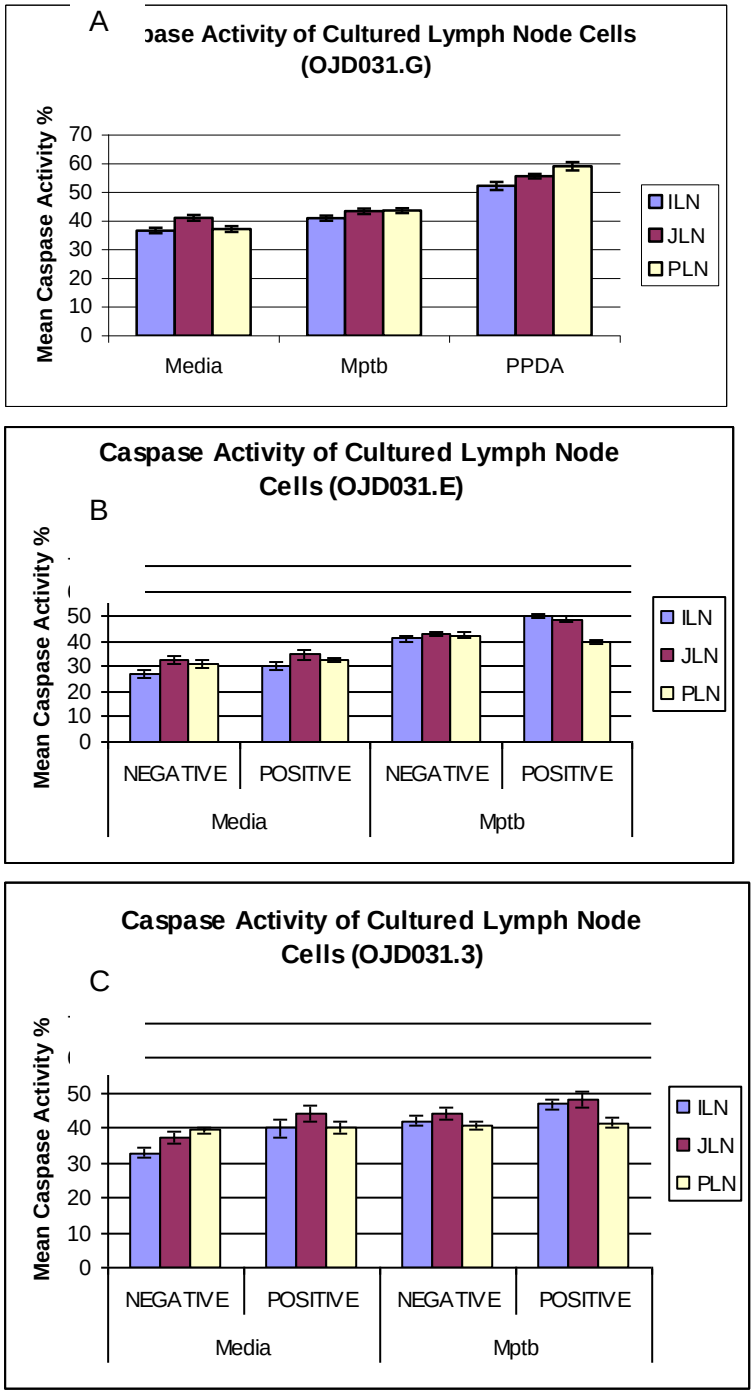

Figure 1C.7: Apoptotic responses of cultured lymph node cells in unexposed and Mptb exposed sheep
The caspase assay was used to detect apoptosis in mononuclear cells from ileal (ILN), jejunal (JLN) and prescapular (PLN) lymph nodes. Mononuclear cells were cultured for 6 days in the presence of media alone, Mptb antigen or PPDA. Unexposed control animals (A) were negative for histology and tissue culture. Sheep exposed to Mptb both naturally (B) and experimentally (C) were further sub-grouped according to tissue culture and histology results into positive and negative groups.

9.8 Appendix 1C-3 Subprogram 1 Apoptosis in the terminal ileum (gene expression and DNA degradation) in ovine Johne's Disease

Abbreviations

Mptb: Mycobacterium avium subsp paratuberculosis; TUNEL: terminal uridine deoxynucleotidyl transferase nick end labelling; PBS: phosphate buffered saline; PBMC: peripheral blood mononuclear cells; Q-PCR: quantitative polymerase chain reaction; p.i.: post inoculation; ICLN: ileocaecal lymph node; PJLN: posterior jejunal lymph node; PLN: prescapular lymph node; PPDA: M. avium purified protein derivative;

Introduction

Apoptotic cells undergo several notable morphological alterations including cell shrinkage, surface blebbing and condensation of chromatin (Van Cruchten and Van Den Broeck 2002). These occur as a result of molecular and biochemical events. Apoptosis can be initiated by external stimuli via the death receptors on the cell surface or by internal stimuli which lead to mitochondrial changes. Three families of proteins are fundamental to apoptotic death pathways: caspases, Bcl-2 family of proteins and inhibitor of apoptosis family of proteins.

The involvement of Fas (CD95)/FasL in the death receptor pathway has been well documented in macrophages undergoing mycobacteria-induced apoptosis (Li, Bassiri et al. 1998; Mustafa, Phyu et al. 1999; Zhang, Jiang et al. 2005). Fas (CD95) is expressed at significantly higher levels in PBMCs from Mptb infected cattle compared to uninfected controls (Coussens, Pudrith et al. 2005).

Mitochondrial pathways to apoptosis are regulated by members of the Bcl-2 family which include proteins involved in inducing apoptosis including Bax, Bad, Bak and Bid as well as proteins involved in inhibiting apoptosis including Bcl-2, Mcl-1 and Bcl-w (Adams 2003).

Mycobacteria have been shown to be capable of modulating the expression of several pro- and anti-apoptotic proteins and genes to evade macrophage apoptosis. Some examples include the up regulation of anti-apoptotic Mcl-1mRNA during TB infections (Sly, Hingley-Wilson et al. 2003), inactivation of pro-apoptotic Bad (Maiti, Bhattacharyya et al. 2001) and the down regulation of Bax together with increased expression of Bcl-2 (Mogga, Mustafa et al. 2002).

DNA fragmentation is generally associated with later stages of apoptosis and can be detected using a number of techniques including DNA electrophoresis which shows a typical ladder pattern associated with apoptosis and the nick-end labelling (TUNEL) assay. By the TUNEL method DNA cleavage and chromatin condensation associated with apoptosis are identified by labelling DNA strand breaks with modified nucleotides. This assay is widely used in many applications for the study of apoptosis. One advantage of this assay is that it can be adapted for use in a number of applications including both flow cytometry and immunohistochemical staining. In this way apoptotic cells can be visualised on a single cell level, making this assay more sensitive over alternative methods such an DNA electrophoresis. Using immunohistochemical labeling has further advantages in that it allows the location of apoptotic cells to be visualised *in situ* within tissues (Allen, Hunter et al. 1997).

The aims of this study were to firstly examine the relative expression of genes encoding for proteins involved in both promoting and inhibiting pathways central to apoptosis at active sites of infection. Secondly, to examine apoptosis *in situ* within active sites associated with Mptb lesions using the TUNEL technique. The terminal ileum and associated lymph node was chosen for examination in this study as other studies related to this subprogram have shown that the ileocaecal lymph node (ICLN) had the highest caspase activity. All the genes examined are involved in apoptotic pathways that activate caspases.

Materials and Methods

Gene expression studies

Animals

Twenty-six sheep were used to examine the relative expression of apoptosis related genes. Animals were grouped into six categories based on the level of disease progression. Category-1 included six individuals negative for OJD confirmed by histology and tissue culture and were obtained from a JD free farm (OJD031.G) (Table 1C-3.1.). Animals in categories 2-6 were all obtained from JD infected properties and were all positive for tissue culture and histology. Lesions were scored according the (Perez, Garcia Marin et al. 1996) identification method.

RNA extraction and processing for quantitative PCR

Primers were designed using Beacon Designer 4.0 (Premier Biosoft) and supplied commercially by Sigma Genosys. cDNA was synthesized from gut tissues, Q-PCR conditions were optimised and assays carried out. Relative fold changes in expression ($\Delta\Delta$Ct) were then analysed using a general analysis of variance (ANOVA). All methods are described in detail in Appendix 1C-1.

Three major genes involved in pathways central to apoptosis were examined: Fas and Bax (pro-apoptotic) and Bcl-2 (anti-apoptotic). Expression of these genes was examined in the terminal ileum and corresponding ilealocaecal lymph node (ICLN).

TUNEL analysis

Animals

Twenty-four animals were used to examine apoptosis within the terminal ileum by the TUNEL method. Animals were categorised according to lesion severity as described earlier (Table 1C-3.1). A smaller group of animals was selected from trial OJD031.A to examine responses within the ICLN. A total of twelve animals were examined; four animals from category 2, three animals from category 3 and 5 and two animals from category 6.

Preparation of tissue samples and TUNEL labeling

Sections of the terminal ileum and ICLN were prepared and embedded in paraffin. The TUNEL assay was carried out as described in Appendix 1C-1. TUNEL positive cells were then counted and analysed using a weighted analysis of variance (weight being the number of fields of view).

Table 1C-3.1: Sheep included in gene expression and TUNEL analysis studies

Disease Category (n)	Infection status
1 (6)	Unexposed negative
2 (6)	Exposed negatives
3 (6)	Lesion type 3a
4 (3)	Lesion type 3a-3c
5 (5)	Lesion type 3c
6 (6)	Lesion type 3b

Results

Animals used in the gene expression and TUNEL studies include sheep that had no history of exposure to Mptb (these animals were also negative in tests for OJD), animals that were naturally exposed to Mptb but were free of disease and animals with OJD. The latter were classified according to histological lesion type.

Expression of genes encoding proteins related to pro- and anti-apoptotic pathways

Expression of two genes which promote apoptosis (Fas and Bax) and one gene which inhibits apoptosis (Bcl-2) were studied. The relative expression of Fas in both the terminal ileum and ICLN did not differ significantly in the two control groups (Fig. 1C-3.1A and Fig. 1C-3.2A). Within the terminal ileum there was significant up regulation of Fas expression in infected animals from category 3, 5 and 6 (paucibacillary lesions) compared to unexposed uninfected controls (Fig. 1C-3.1A). In contrast, within the ICLN, Fas appeared to be down regulated compared to controls but was not significantly different between infected and Mptb exposed sheep (Fig. 1C-3.2A). There were no significant differences between animals infected with Mptb (category 3-6) and exposed control animals (category 2) in both tissues (Fig. 1C-3.1A and 1C-3.2A).

The relative expression of Bax increased significantly upon exposure to Mptb in all animals within the terminal ileum ($P < 0.05$) (Fig. 1C-3.1B). Similarly the ICLN showed an up regulation in infected animals compared to unexposed animals from category 1 and this was significant in animals from category 5 ($P < 0.05$) (Fig. 1C-3.2B). Similar to Fas expression, there was no significant difference between animals infected with Mptb (category 3-6) and exposed control animals from category 2 in both tissues (Fig. 1C-3.1B and 1C-3.2B).

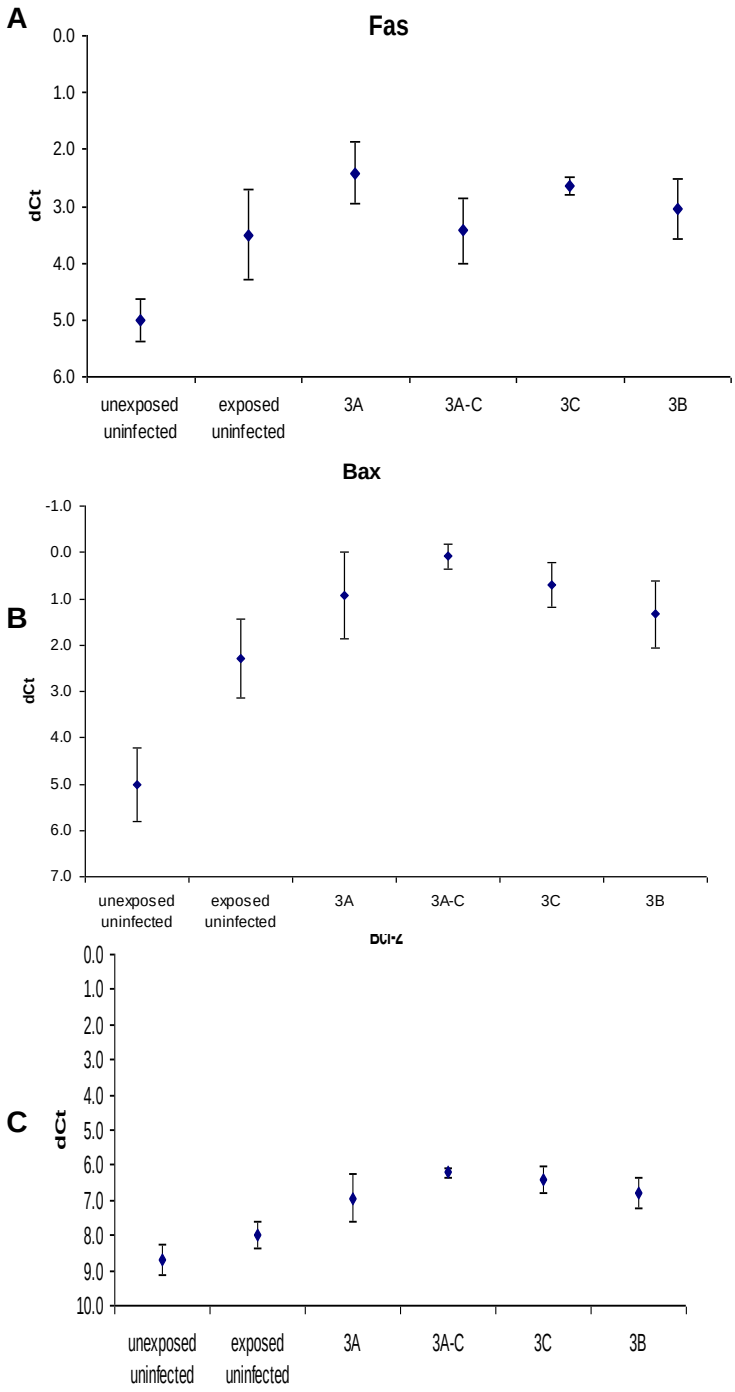

Figure 1C-3.1. Expression of apoptosis-related genes in ovine terminal ileum.
Expression of Fas (A), Bax (B) and Bcl-2 (C) genes within the terminal ileum of Mptb exposed and unexposed sheep was detected by real time Q-PCR. Animals were classified according to infection status which is shown on the x-axis.
Disease categories: Unexposed uninfected=1; Exposed uninfected=2; 3Alesions=3; 3A-C lesions=4; 3C lesions=5; 3B lesions=6

The expression of the anti-apoptotic survival gene Bcl-2 was also up regulated in animals exposed to Mptb (categories 2 to 6)compared to unexposed controls (category 1) in terminal ileum (Fig. 1C-3.1C) ($P < 0.05$). In addition, animals from categories 4 and 5 showed significantly higher expression of Bcl-2 than exposed but uninfected animals in category 2 ($P < 0.05$)."

Within the ICLN there was significantly more Bcl-2 expressed in animals from category 5 compared to all groups tested ($P < 0.05$) (Fig. 1C-3.2C). Animals from category 6 with the most severe lesion type showed a down regulation in Bcl-2 expression; this was significantly different from animals in category 5 ($P < 0.05$). Again, similar to Fas, there was no significant difference between the two control groups in either tissue (Fig. 1C-3.1C and 1C-3.2C).

Ratio of pro-apoptotic Bax and anti-apoptotic Bcl-2

The ratio of Bcl-2 to Bax is used to assess tendency for pro- or anti-apoptotic activities to exist. In the terminal ileum the ratio of Bcl-2/Bax in control animals (category 1 and 2) was 0.2, suggesting the predominance of pro-apoptotic activity in control animals. This ratio was similar in all animals infected with Mptb (categories 3-6). In the ICLN, both control groups also showed a predominance of pro-apoptotic activity with the Bcl-2/Bax at 0.2. In contrast to the terminal ileum, the Bcl-2 to Bax ration in Mptb infected animals from categories 4 and 5 was elevated at 1.3 and 1.5 respectively. This suggests that anti-apoptotic activity predominates in the ICLN of these animals. In animals with more severe disease (category 6) the ratio was similar to the controls at 0.4.

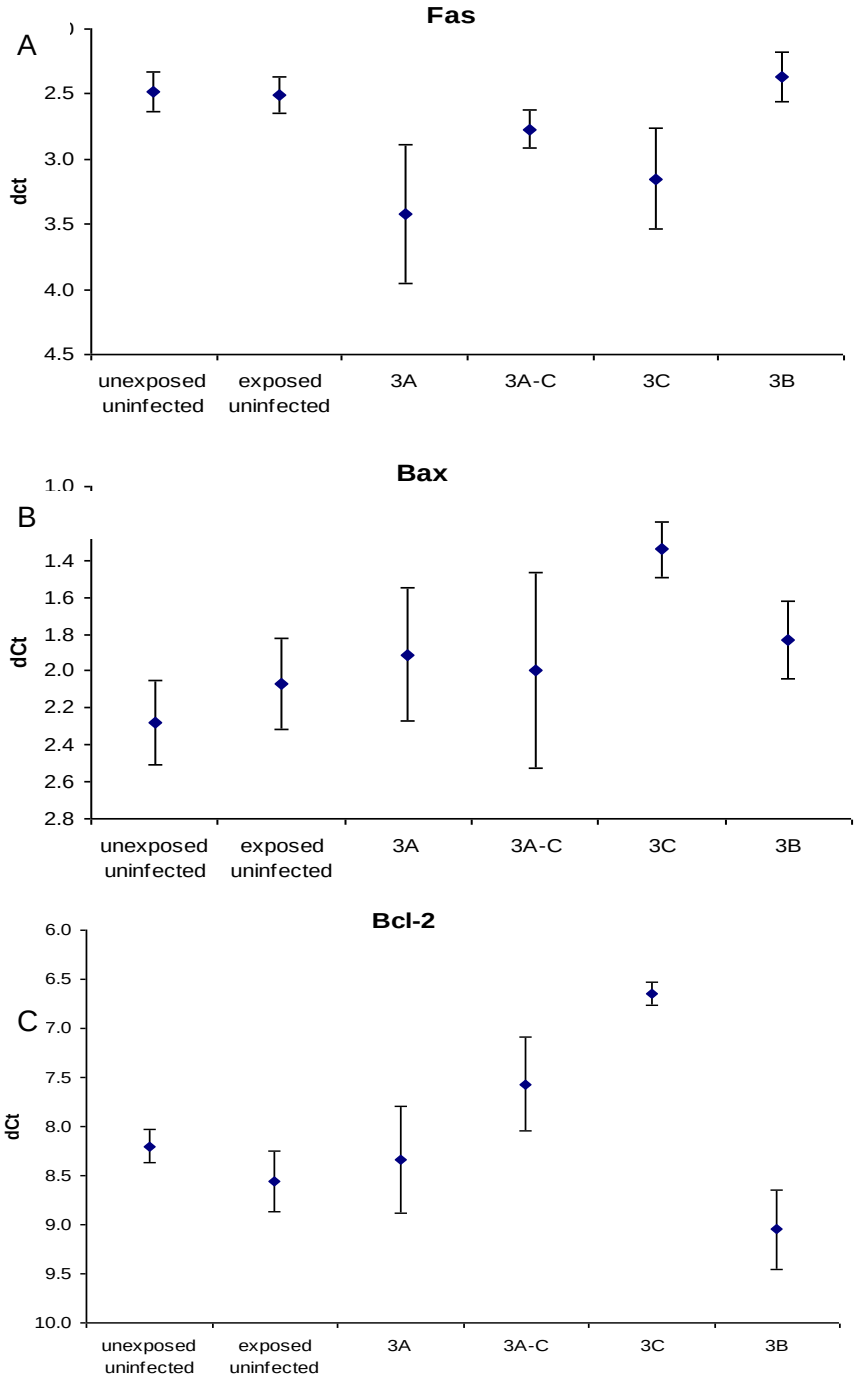

Figure 1C-3.2: Expression of apoptosis related gene expression in the ICLN Expression of Fas (A), Bax (B) and Bcl-2 (C) genes within the ICLN of Mptb exposed and unexposed sheep was detected by real time Q-PCR. Animals were classified according to infection status which is shown on the x-axis. Mean dCt of expression is shown on the y-axis. Error bars show standard error.

Disease categories: Unexposed uninfected=1; Exposed uninfected=2; 3A lesions=3; 3A-C lesions=4; 3C lesions=5; 3B lesions=6

TUNEL assay

Terminal ileum

TUNEL positive cells were sparsely distributed within the lamina propria of all animals (Fig. 1C-3.1A). Within the two control groups (category 1 and 2) there were higher numbers of TUNEL positive cells in category 1 controls but this was not significantly different (Fig. 1C-3.3B). Overall, animals with OJD in categories 3-6 had more TUNEL positive staining than control animals (Fig. 1C-3.3B). Animals from category 5 had the highest overall TUNEL counts. There was no significant difference between animals with early paucibacillary type lesions (category 3 and 4) when compared to category 2 Mptb exposed controls. In animals in the later stages of disease with late paucibacillary and multibacillary lesions (category 5 and 6) there were significantly higher TUNEL counts when compared to control animals from category 2.

When comparing animals with OJD to category 1 unexposed controls; there was no significant difference in TUNEL counts with animals from category 3, 4 (Fig. 1C-3.3B). Again, animals from category 5 showed significantly higher TUNEL staining compared to category 1 controls. There was no significant difference in TUNEL counts between animals from category 6 compared to category 1 controls.

A

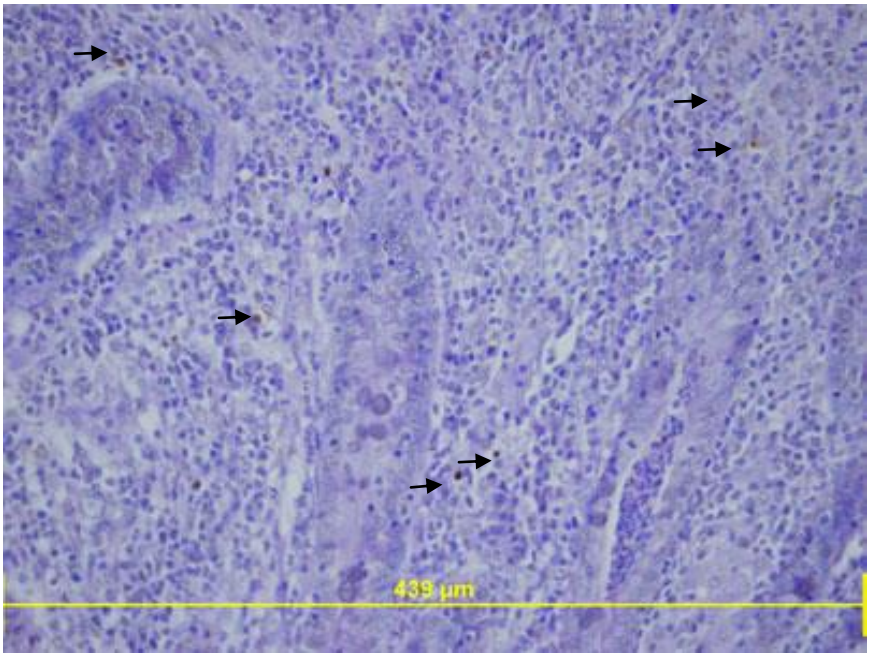

B

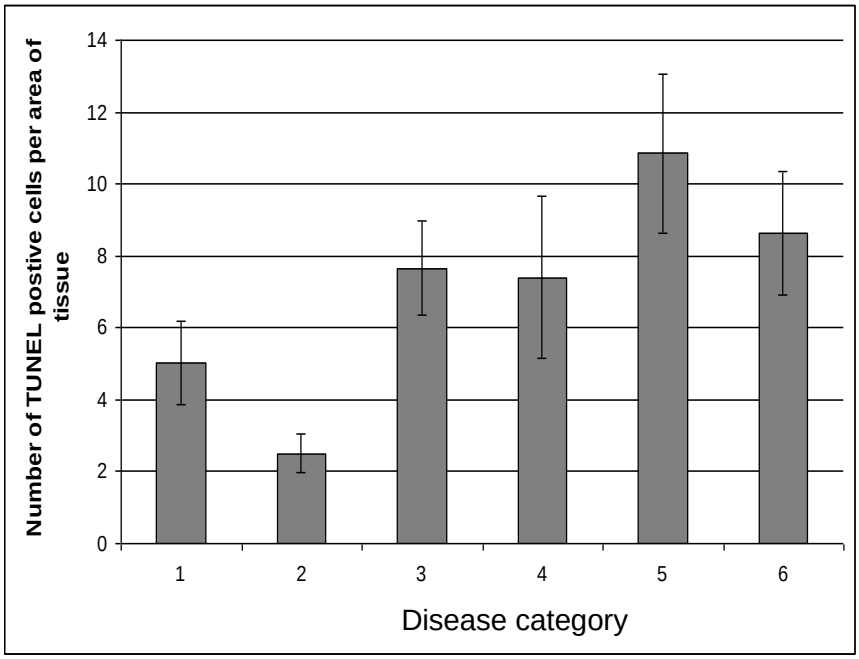

Figure 1C-3.3: TUNEL staining in the terminal ileum

TUNEL positive (apoptotic) cells within the lamina propria of an Mptb infected animal with late paucibacillary lesions (category 5) (A). Cells were counted under light microscopy at 40x magnification. TUNEL positive cells are indicated by the arrows. Number of TUNEL positive cells per field of view (mean ± sd) are show (B).

Disease categories: Unexposed uninfected=1; Exposed uninfected=2; 3a lesions=3; 3a-c lesions=4; 3c lesions=5; 3b lesions=6

ICLN

The distribution of TUNEL positive cells within the ICLN was assessed in a group of sheep from a farm with OJD. TUNEL positive cells were present in low numbers scattered throughout regions of the medulla including the cords, tracts, trabeculae and sinuses within the ICLN of all animals tested. Due to low frequencies of apoptotic cells no attempt was made to quantify TUNEL activity within sub-regions of the medulla. There was a trend towards higher numbers of TUNEL positive cells in infected animals within the medulla regions; cells were not detectable in some control animals (Fig. 1C-3.4).

Overall, control animals had lower frequencies of TUNEL positive cells in the parafollicular zones and primary and secondary follicles. Notably TUNEL positive cells were located at germinal centres within secondary follicles and on the outer edges of primary follicles. In the cortex, in contrast to the medulla, TUNEL positive cells were observed at higher frequencies in OJD infected animals (Fig. 1C-3.4). Interestingly animals that had type 3c lesions had noticeably higher frequencies of TUNEL activity within the primary follicles while infected animals with type 3a and 3b lesions remained similar to exposed control animals.

There were similar numbers of TUNEL positive cells within secondary follicles of animals with lesion type 3a and control animals, while animals with 3c and 3b lesions had higher numbers of TUNEL positive cells (Fig. 1C-3.4). In the parafollicular zones control animals again had low numbers of TUNEL positive cells while infected animals had increased numbers of apoptotic cells (Fig. 1C-3.4).

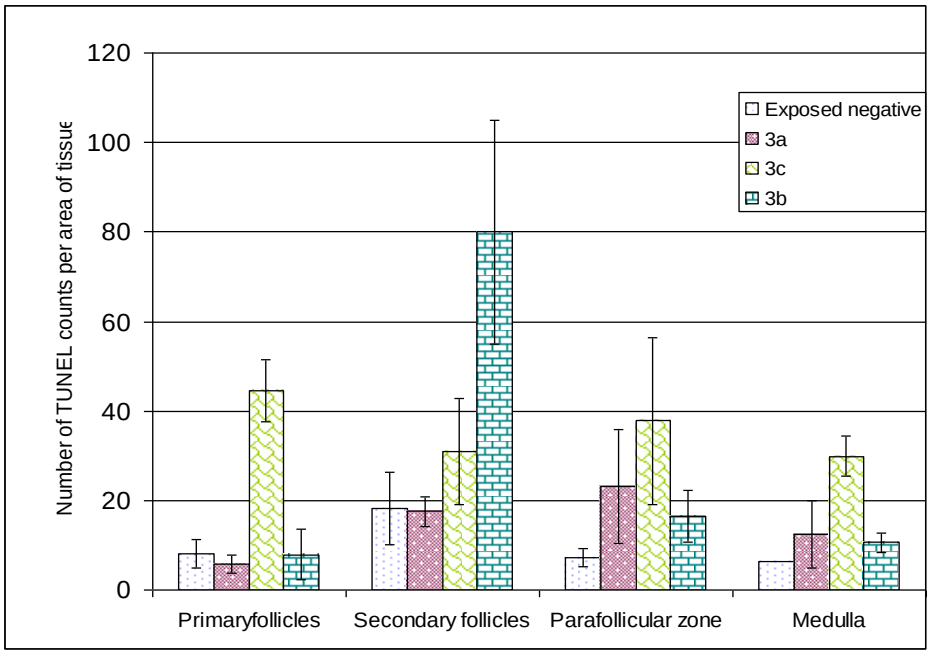

Figure 1C-3.4: TUNEL staining in the ICLN
TUNEL positive (apoptotic) cells within the secondary follicles of animals with late paucibacillary type lesions (type 3c lesions). Cells were counted under 40 x magnification. TUNEL positive cells are indicated by black arrowheads. (B) Mean counts (+/- sd) per field of view are shown. Each field of view was 439 mm^2.

Discussion

Apoptotic gene expression

This study presents novel results describing the expression of apoptotic genes in the tissues of Mptb infected sheep. Apoptotic genes related to inhibiting and promoting apoptosis were significantly up regulated ileal tissue of in infected animals above that of unexposed negative animals.

Little attention has been focused on examining apoptotic gene expression *in situ* in tissues at active sites during mycobacterial infections. In wild boars naturally exposed to M. bovis differentially expressed genes which may have anti-apoptotic activity were detected upon examination of the oropharyngeal tonsils and mandibular lymph nodes (Naranjo, Hofle et al. 2006).

There is evidence from numerous publications describing the regulation of apoptotic genes in the blood during mycobacterial disease progression (Klingler, Tchou-Wong et al. 1997; Hernandez, Neves et al. 2003). Similar to the present study (Coussens, Pudrith et al. 2005) described several differentially expressed genes encoding proteins involved in apoptosis within the blood of clinically infected cattle using microarray technology. Apoptotic genes identified in this study included the up regulation of the pro-apoptotic genes Bad, somatic cytochrome *c* and CD95 (Fas). Several anti apoptotic genes were shown to be down regulated including TNFR1 and MCL-1.

Several differentially expressed genes related to apoptosis have also been described during *in vitro* mycobacterial stimulation and infection models (McGarvey, Wagner et al. 2004); (Ragno, Estrada-Garcia et al. 1998; Danelishvili, McGarvey et al. 2003; Spira, Carroll et al. 2003; Hasan, Ashraf et al. 2006). Similar to the present study Grell et al, (8^{th} International colloquium on Paratuberculosis, 2005) described the up regulation of several cytokines and genes encoding proteins involved in apoptosis in the blood of Mptb infected cattle. This study identified the up regulation of several genes including Fas and Bcl-2 after *in vitro* Mptb PPD antigen specific stimulation.

Furthermore several studies have described differential expression of apoptotic genes in virulent mycobacterial strains and comparisons have been made to avirulent strains (Ragno, Estrada-Garcia et al. 1998; Sly, Hingley-Wilson et al. 2003; Spira, Carroll et al. 2003; Zhang, Jiang et al. 2005). Zhang, Jiang et al. in 2005 described the regulation of anti-apoptotic Bcl-2 and proapoptotic proteins Fas/FasL during an *in vitro* Mtb infection model using a J774 macrophage cell line. This study examined the relative responses of macrophages infected with virulent and attenuated strains compared to uninfected controls. They showed a significant up regulation of Bcl-2 in the virulent strain and a down regulation with the avirulent strain, compared to controls. Fas expression was significantly down regulated in both infection models compared to controls. Similarly (Spira, Carroll et al. 2003) described the down regulation of several pro-apoptotic genes by virulent Mtb strains using human alveolar macrophages infected *in vitro* with Mtb.

There are several limitations when comparing current responses with other studies.

1. It appears likely that apoptotic responses are a reflection of the precise stage of disease progression. There is evidence from longitudinal studies that suggest that apoptotic responses will vary as disease progresses (Mogga, Mustafa et al. 2002).
2. Virulence of the strain given in experimental infection models will influence apoptotic responses. The ability of virulent strains of mycobacteria to modulate macrophage apoptosis has been documented widely (Maiti, Bhattacharyya et al. 2001; Sly, Hingley-Wilson et al. 2003; Spira, Carroll et al. 2003; Zhang, Jiang et al. 2005). The current study used animals naturally exposed to OJD therefore virulence was undetermined in this study.
3. Due to the fact that there a limited studies describing apoptotic gene expression at sites of active infection comparisons are therefore made with the well studied responses of the blood. Responses of blood are likely to differ from responses at active sites of infection for

several reasons including distribution of cell phenotypes. In the blood unlike regions of gut tissue (which contain high numbers of mature macrophages) there are typically no macrophages, rather low numbers of monocytes. Apoptosis plays an important role in both macrophages/monocytes during responses to mycobacteria. Furthermore the number of bacteria within tissues is much higher compared to the blood. Detection of Mptb in the blood of subclinically infected sheep has been shown to be limited (Gwozdz, Reichel et al. 1997; Gwozdz, Thompson et al. 2000) in comparison to active infection sites such as lymph nodes (Gwozdz, Reichel et al. 1997). Limited bacterial circulation in the blood together with low numbers of monocytes will mean that there are fewer stimuli promoting apoptotic responses in the blood compared to the tissues.

4. One potential limitation in interpretation of the results from some studies is the use of the popular reference gene β-actin in apoptosis related gene expression studies (Coussens, Pudrith et al. 2005; Zhang, Jiang et al. 2005). Although these studies most probably validated this gene for use as a reference/housekeeping gene, β-actin is involved in the formation of microfilament in apoptotic bodies. In 1995 Naora et al described differential expression of β-actin mRNA in a HL-60 cell line after the addition of several apoptosis inducing agents. This could potentially have an influence over the results obtained from these studies.

In addition, the ratio of Bcl-2/Bax remained steady in the terminal ileum of infected and control animals. On the other hand in the ICLN this ratio increased in animals with type 3a-c and 3c lesions associated with late paucibacillary disease, while a significant decline was then seen in animals with more severe type 3b lesions associated with multibacillary lesions.

For the mitochondrial pathways to cell death to occur it is essential that the pro-apoptotic proteins Bax and Bad are activated together with the anti-apoptotic protein Bcl-2. Bcl-2 is known for its ability to facilitate resistance to apoptosis (Kroemer 1997). While there is some evidence to suggest that these two proteins are capable of functioning independently to either inhibit or induce apoptosis, numerous studies have shown that susceptibly to apoptosis, including in mycobacterial infections, is determined by the ratio of Bcl2/Bax (Oltvai, Milliman et al. 1993; Knudson and Korsmeyer 1997). It is well established that for Bcl-2 to function it must form a heterodimer with Bax to neutralize apoptosis induction signals, on the other hand Bax can induce apoptosis by inhibiting Bcl-2 (Oltvai, Milliman et al. 1993; Kroemer 1997). When excess amounts of pro-apoptotic proteins are present, cells are more susceptible to apoptosis. When the balance between these pro-and anti-apoptotic proteins is disrupted apoptosis will either be down regulated or up regulated. Increased levels of Bax accelerate apoptosis, on the other hand up regulation of Bcl-2 causes inhibition of apoptosis.

One theory that might explain the current findings is that during late paucibacillary infection the cells of the ICLN are promoting cell survival. In this way apoptosis of infected macrophages is prevented allowing the mycobacterium to persist. These long-lived professional phagocytes may then provide an ideal niche for persistent chronic infections. This has been suggested during longitudinal studies examining responses to Mtb using a murine model (Mogga, Mustafa et al. 2002). Anti-microbial activity against mycobacteria is a direct result of macrophage apoptosis not cell lysis and is also important in controlling the spread of infection (Molloy, Laochumroonvorapong et al. 1994; Fratazzi, Arbeit et al. 1997; Fratazzi, Arbeit et al. 1999). As discussed earlier, there are numerous publications describing the ability of virulent mycobacteria to modulate key proteins and genes encoding proteins involved in apoptosis, allowing them to persist within infected cells.

TUNEL

In this study unexposed control animals had relatively higher TUNEL counts than exposed control animals. It was also observed that caspase activity in these animals was also elevated. Mptb associated lesion types 3a, 3c and 3b (*paucibacillary* and *multibacillary* lesions) showed a significant

increase in TUNEL positive cells, compared to exposed uninfected animals. These findings are not in general agreement with several other studies which describe low frequencies of TUNEL positive cells in mycobacterial associated lesions such as TB and leprosy lesions (Watson, Hill et al. 2000; Turner, Basaraba et al. 2003; Walsh, Lane et al. 2004). Some of these studies do not compare infected individuals with uninfected controls (Walsh, Lane et al. 2004) and do not attempt to quantify the frequency of TUNEL positive cells (Valheim, Sigurdardottir et al. 2004).

Low frequency of TUNEL positive cells has been observed in TB granulomas of guinea pigs, a popular small animal model to test immunological responses in TB infections (Turner, Basaraba et al. 2003). Similarly (Valheim, Sigurdardottir et al. 2004) found few TUNEL positive cells in intestinal tissues from goats with subclinical Mptb infection. Tissue samples were taken from the goats 2 years after experimental inoculation with Mptb. All infected animals were tissue culture positive. Histological examination in this study revealed granulomatous lesions in both the lamina propria and submucosa, however most lesions were small and contained few acid fast bacteria. It is not known whether or not these animals were actually shedding the bacteria. Low TUNEL positive cells in this study could therefore be the result of sample site examined and infection status of the animals.

In contrast a study by (Walsh, Lane et al. 2004) demonstrated TUNEL staining in paucibacillary and multibacillary skin lesions of untreated leprosy patients. Results from this study showed a higher proportion of TUNEL positive staining in paucibacillary patients compared with more advanced mutibacillary lesions. However, skin samples from uninfected controls were not included. The authors hypothesized that this may be due to the strong TH1 type responses occurring involving high cell turnover. This explanation could also help explain the high levels of TUNEL staining in paucibacillary animals observed in the present study.

In this study there were higher levels of apoptosis in follicular zones of Mptb infected animals compared to exposed control animals. There are few studies examining apoptosis (using the TUNEL technique) in lymph nodes at active infection sites during mycobacterial infections. One study (Palmer, Gosch et al. 2002) examined medial retropharyngeal lymph nodes in white tailed deer experimentally challenged with *M.bovis* and found that the area of TUNEL staining per granuloma varied as disease progressed. Apoptosis was highest on day 28 but by day 328 TUNEL positive cells were not detected. This differs from the current study in which higher numbers of TUNEL positive cells were observed in late subclinical and clinically infected animals.

Within the ICLN, apoptosis was seen on the edges of primary follicles and at the centre of secondary follicles. This is not surprising as these are sites of antigen presentation where contact between macrophages or dendritic cells and lymphocytes occur. Apoptosis plays a key role regulating the responses of host immune cells to foreign invaders like Mptb.

Conclusions

In the current study TUNEL counts within the terminal ileum were significantly higher in infected animals compared to exposed negative controls. Similarly pro-apoptotic genes Fas and Bax were significantly up regulated in infected animals compared to controls. The ratio of Bcl2/Bax showed that in these tissues there was an excess of pro-apoptotic Bax, which might make the cells more sensitive to apoptosis. This may help explain high number of TUNEL positive cells in infected animals.

References

Adams, J. M. (2003). "Ways of dying: multiple pathways to apoptosis." Genes Dev **17**(20): 2481-95.

Allen, R. T., W. J. Hunter, 3rd, et al. (1997). "Morphological and biochemical characterization and analysis of apoptosis." J Pharmacol Toxicol Methods **37**(4): 215-28.

Coussens, P. M., C. B. Pudrith, et al. (2005). "Johne's disease in cattle is associated with enhanced expression of genes encoding IL-5, GATA-3, tissue inhibitors of matrix metalloproteinases 1 and 2, and factors promoting apoptosis in peripheral blood mononuclear cells." Vet Immunol Immunopathol **105**(3-4): 221-34.

Danelishvili, L., J. McGarvey, et al. (2003). "Mycobacterium tuberculosis infection causes different levels of apoptosis and necrosis in human macrophages and alveolar epithelial cells." Cell Microbiol **5**(9): 649-60.

Fratazzi, C., R. D. Arbeit, et al. (1999). "Macrophage apoptosis in mycobacterial infections." J Leukoc Biol **66**(5): 763-4.

Fratazzi, C., R. D. Arbeit, et al. (1997). "Programmed cell death of Mycobacterium avium serovar 4-infected human macrophages prevents the mycobacteria from spreading and induces mycobacterial growth inhibition by freshly added, uninfected macrophages." J Immunol **158**(9): 4320-7.

Gwozdz, J. M., M. P. Reichel, et al. (1997). "Detection of Mycobacterium avium subsp. paratuberculosis in ovine tissues and blood by the polymerase chain reaction." Vet Microbiol **57**(2-3): 233-44.

Gwozdz, J. M., K. G. Thompson, et al. (2000). "Use of the polymerase chain reaction assay for the detection of Mycobacterium avium subspecies paratuberculosis in blood and liver biopsies from experimentally infected sheep." Aust Vet J **78**(9): 622-4.

Hasan, Z., M. Ashraf, et al. (2006). "M. leprae inhibits apoptosis in THP-1 cells by downregulation of Bad and Bak and upregulation of Mcl-1 gene expression." BMC Microbiol **6**: 78.

Hernandez, M. O., I. Neves, et al. (2003). "Induction of apoptosis in monocytes by Mycobacterium leprae in vitro: a possible role for tumour necrosis factor-alpha." Immunology **109**(1): 156-64.

Klingler, K., K. M. Tchou-Wong, et al. (1997). "Effects of mycobacteria on regulation of apoptosis in mononuclear phagocytes." Infect Immun **65**(12): 5272-8.

Knudson, C. M. and S. J. Korsmeyer (1997). "Bcl-2 and Bax function independently to regulate cell death." Nat Genet **16**(4): 358-63.

Kroemer, G. (1997). "The proto-oncogene Bcl-2 and its role in regulating apoptosis." Nat Med **3**(6): 614-20.

Li, B., H. Bassiri, et al. (1998). "Involvement of the Fas/Fas ligand pathway in activation-induced cell death of mycobacteria-reactive human gamma delta T cells: a mechanism for the loss of gamma delta T cells in patients with pulmonary tuberculosis." J Immunol **161**(3): 1558-67.

Maiti, D., A. Bhattacharyya, et al. (2001). "Lipoarabinomannan from Mycobacterium tuberculosis promotes macrophage survival by phosphorylating Bad through a phosphatidylinositol 3-kinase/Akt pathway." J Biol Chem **276**(1): 329-33.

McGarvey, J. A., D. Wagner, et al. (2004). "Differential gene expression in mononuclear phagocytes infected with pathogenic and non-pathogenic mycobacteria." Clin Exp Immunol **136**(3): 490-500.

Mogga, S. J., T. Mustafa, et al. (2002). "Increased Bcl-2 and reduced Bax expression in infected macrophages in slowly progressive primary murine Mycobacterium tuberculosis infection." Scand J Immunol **56**(4): 383-91.

Molloy, A., P. Laochumroonvorapong, et al. (1994). "Apoptosis, but not necrosis, of infected monocytes is coupled with killing of intracellular bacillus Calmette-Guerin." J Exp Med **180**(4): 1499-509.

Mustafa, T., S. Phyu, et al. (1999). "Increased expression of Fas ligand on Mycobacterium tuberculosis infected macrophages: a potential novel mechanism of immune evasion by Mycobacterium tuberculosis?" Inflammation **23**(6): 507-21.

Naranjo, V., U. Hofle, et al. (2006). "Genes differentially expressed in oropharyngeal tonsils and mandibular lymph nodes of tuberculous and nontuberculous European wild boars naturally exposed to Mycobacterium bovis." FEMS Immunol Med Microbiol **46**(2): 298-312.

Oltvai, Z. N., C. L. Milliman, et al. (1993). "Bcl-2 heterodimerizes in vivo with a conserved homolog, Bax, that accelerates programmed cell death." Cell **74**(4): 609-19.

Palmer, M. V., G. Gosch, et al. (2002). "Apoptosis in lymph node granulomas from white-tailed deer (Odocoileus virginianus) experimentally infected with Mycobacterium bovis." J Comp Pathol **127**(1): 7-13.

Perez, V., J. F. Garcia Marin, et al. (1996). "Description and classification of different types of lesion associated with natural paratuberculosis infection in sheep." J Comp Pathol **114**(2): 107-122.

Ragno, S., I. Estrada-Garcia, et al. (1998). "Regulation of macrophage gene expression by Mycobacterium tuberculosis: down-regulation of mitochondrial cytochrome c oxidase." Infect Immun **66**(8): 3952-8.

Sly, L. M., S. M. Hingley-Wilson, et al. (2003). "Survival of Mycobacterium tuberculosis in host macrophages involves resistance to apoptosis dependent upon induction of antiapoptotic Bcl-2 family member Mcl-1." J Immunol **170**(1): 430-7.

Spira, A., J. D. Carroll, et al. (2003). "Apoptosis genes in human alveolar macrophages infected with virulent or attenuated Mycobacterium tuberculosis: a pivotal role for tumor necrosis factor." Am J Respir Cell Mol Biol **29**(5): 545-51.

Turner, O. C., R. J. Basaraba, et al. (2003). "Immunopathogenesis of pulmonary granulomas in the guinea pig after infection with Mycobacterium tuberculosis." Infect Immun **71**(2): 864-71.

Valheim, M., O. G. Sigurdardottir, et al. (2004). "Characterization of macrophages and occurrence of T cells in intestinal lesions of subclinical paratuberculosis in goats." J Comp Pathol **131**(2-3): 221-32.

Van Cruchten, S. and W. Van Den Broeck (2002). "Morphological and biochemical aspects of apoptosis, oncosis and necrosis." Anat Histol Embryol **31**(4): 214-23.

Walsh, D. S., J. E. Lane, et al. (2004). "TUNEL and limited immunophenotypic analyses of apoptosis in paucibacillary and multibacillary leprosy lesions." FEMS Immunol Med Microbiol **41**(3): 265-9.

Watson, V. E., L. L. Hill, et al. (2000). "Apoptosis in mycobacterium tuberculosis infection in mice exhibiting varied immunopathology." J Pathol **190**(2): 211-20.

Zhang, J., R. Jiang, et al. (2005). "Survival of virulent Mycobacterium tuberculosis involves preventing apoptosis induced by Bcl-2 upregulation and release resulting from necrosis in J774 macrophages." Microbiol Immunol **49**(9): 845-52.

9.9 Appendix 2A-1 Subprogram 2 Cell culture for M. paratuberculosis research

Abbreviations

Mptb: Mycobacterium avium subsp. paratuberculosis; PBMC: peripheral blood mononuclear cells; PBS: phosphate buffered saline; CFSE: carboxy fluorescein diacetate succinimidyl ester; APC (allophycocyanin); MOI: multiplicity of infection; ILN: ileal lymph node; JLN: posterior jejunal lymph node; PLN: prescapular lymph node

Establishment of immortal macrophage/monocyte, epithelial and hybridoma cell lines and determination of optimal conditions for Mptb research

Cell lines/Reagents

Introduction

The initial stage of the immunology section of the OJD031 project was dedicated to the establishment of stocks of cell lines, the establishment of an *in vitro* infection model and generation of reagents for future studies.

Methods

A variety of immortal cell lines were acquired to enable establishment of an *in vitro* infection model. The cell lines listed in Table 2A.1 were obtained and a stock supply created by expanding cell numbers by culture and cryopreserved for future use.

Table 2A.1: Cell lines for *in vitro* models

Cell line	Cell type
BoMac	Bovine macrophage
U937	Monocyte, human
THP-1	Monocyte, human
HL-60	Promyeloblast, human
RAW.267	Monocyte/macrophage, murine
K562	Lymphoblast, human
YAC-1	Lymphoblast, murine
L929	Fibroblast, murine
Caco-2	Colon colorectal adenocarcinoma, human

Several hybridoma cell lines were acquired to generate reagents for use in flow cytometric and immunohistochemical techniques. These cell lines (Table 2A.2) were adapted for culture in CD Hybridoma medium, expanded by culture and cryopreserved. These hybridoma cell lines secrete a specific antibody product into the growth medium (tissue culture supernatant). The growth medium is then concentrated and purified.

Results and Discussion

Seed stocks of all cell lines were established. A setback, midway through the project, was the loss of cryopreserved cell lines and hybridoma which are used for generating reagents to detect ovine cell surface markers and cytokines. Antibody reagents were still available for use during the duration of the project as sufficient stocks had been prepared and stored. An insurance claim was made against the supplier of liquid nitrogen, and stocks of cells were replaced.

Table 2A.2: Cell lines to generate reagents for flow cytometry/immunohistochemistry

Product	Clone number	Current status
Anti-CD1(b)	CC20	Purified antibody
Anti-CD1	20.27	Purified antibody
Anti-CD4	17D	Purified antibody
Anti-CD6	CC38	Purified antibody
Anti-CD5	CC17	Purified antibody
Anti-CD8αβ	CC58	Purified antibody
Anti-CD8αα	CC63	Purified antibody
Anti-CD11a	F10-150-39	Purified antibody
Anti-CD11c	IL-A16	Purified antibody
Anti-CD45R	CC76	Purified antibody
Anti-WC1 (T19)	CC15	Purified antibody
Anti-γδT	86D	Purified antibody
Anti-WC4	CC57	Purified antibody
Anti-TNFα (bovine)	BC9	Purified antibody
Anti-IFNγ (bovine)	6.22A8B5	Cells of incorrect isotype
Anti-IFNγ (bovine)	6.19A6B8	Purified antibody

Some antibodies (CD4, CD5, 86D and WC1) were directly conjugated to a flurochrome (FITC) for use in intracellular staining protocols required for subprogram 1A. Stocks of anti-CD6 antibody are low and may need to be generated for future work. Stocks or anti-WC4 antibody will have to be generated if necessary for future work. CD11c was found to be positive only against new born lamb thymocytes.

In vitro infection model

Introduction

In vitro infection models were established using immortal cell lines to ascertain optimal conditions for Mptb research. Initially, human (differentiated U937), murine (RAW264.7) and bovine macrophages (BoMac) were used.

In vitro experiments were carried out to follow the effects of exposing macrophages to Mptb. The putative bovine cell line BoMac was found not to be of macrophage phenotype while the human myeloid cell line (U937) requires pre-incubation with a differentiating agent (e.g. phorbol esters). Therefore, the murine macrophage cell line RAW264.7 was chosen to study macrophage responses to *in vitro* infection with Mptb.

Methods

Studies were carried out to determine engulfment of Mptb by macrophages and the intracellular survival of the mycobacterium during *in vitro* infection of macrophages. RAW264.7 cells were incubated with Mptb at 1:65 for 4 and 16 hours. The cell culture medium was removed for detection of extracellular bacteria. Macrophages were then lysed and intracellular bacteria collected. The number of viable extracellular and intracellular bacteria was detected by the radiometric Bactec® culture system.

The effect of engulfment of Mptb on macrophages was also studied. RAW264.7 cells were exposed to medium alone, Mptb or heat-killed Mptb (at 10 mycobacteria per macrophage) for up to one week. Macrophages were harvested at days 0, 1, 2, 3, 4 and 7 post-exposure and assessed for viability (by trypan blue exclusion), cell proliferation (by determining total cell number), apoptosis (by detecting caspase activity by flow cytometry) and intracellular presence of Mptb (by Ziehl Neelsen staining). Cells from these experiments were provided for genomic analysis (Taylor DL, Thomson PC, de Silva K, Whittington RJ. *Vet Immunol Immunopathol*. 2007;115(1-2):43-55).

Results and Discussion

Figure 2A.1 shows that most of the Mptb are not engulfed by macrophages after 4 hrs of incubation and that the number of viable Mptb remained unchanged throughout the study period. Essentially, at an MOI of 1:65 it takes longer than 4 hours for the macrophages to engulf most of the bacteria and at 16 hours the majority of the bacteria remain viable inside the cells.

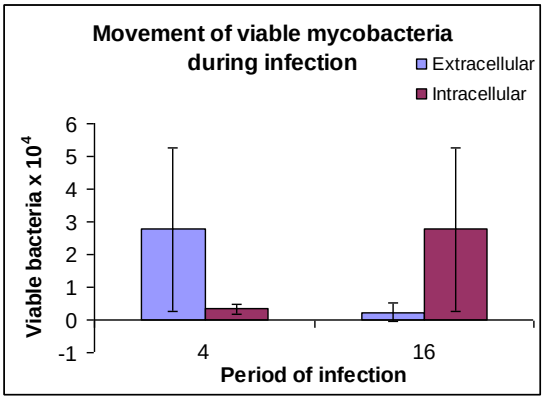

Figure 2A.1 Viability of Mptb during in vitro infection of macrophages

RAW264.7 cells were incubated with Mptb (Telford strain) at 65:1 for 4 and 16 hours. The cell culture medium was removed for detection of extracellular bacteria, cells were then lysed for detection of intracellular bacteria by the Bactec culture system. (n=2 for each time point)

Cell proliferation was not affected by the presence of Mptb (Figure 2A.2). Twenty-four hours after infection 20-50% of macrophages contained at least one mycobacterium but this value decreased to less than 20% at three or more days after infection. There were some differences in the responses of macrophages to live and heat-killed mycobacteria at day 2 post-infection. Macrophages cultured with live Mptb had a 1.7 fold higher number of infected cells (macrophages with one or more acid-fast bacilli) than macrophages cultured with heat-killed Mptb. Interestingly, apoptosis was also greatest in cells incubated with live Mptb at day 2 post-infection (Figure 2A.2). These results support other studies which have shown that mycobacteria actively promote apoptosis of infected macrophages {Keane, 1997 #721}.

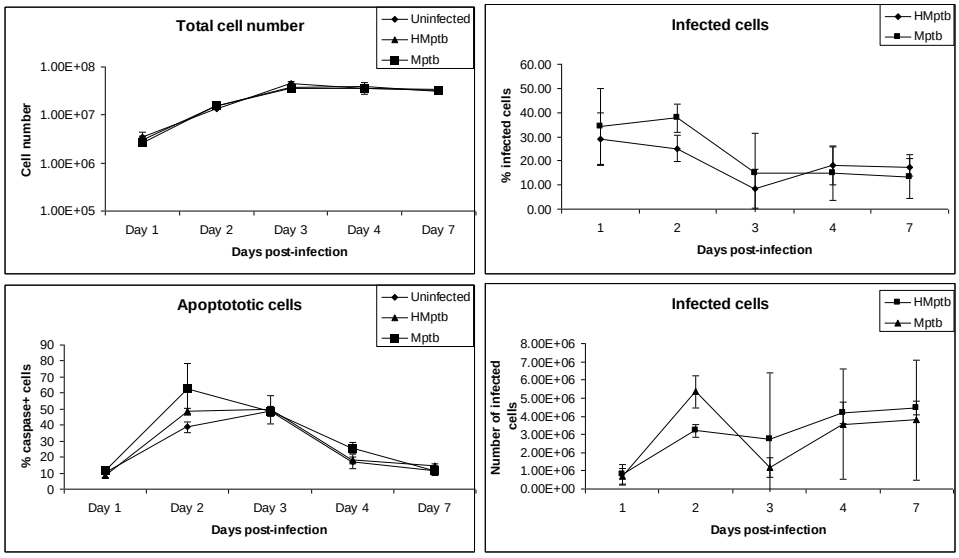

Figure 2A.2 Responses of macrophages to in vitro infection with Mptb.
RAW264.7 cells were cultured in the presence of 0 or 10:1 Mptb. Total cell number, presence of apoptotic cells and the number of infected macrophages were monitored for up to 7 days.

This experimental model can be used to study other aspects of macrophage-Mptb interactions.

Establishment of methods for primary culture of ovine blood leukocytes

Introduction

Methods have been established for isolating mononuclear cells from peripheral blood as well as lymph nodes and culture of these cells for studying cell proliferation as well as apoptosis. These methods can be adapted for studying other cellular responses. Methods for maintaining primary macrophage cultures from ovine blood have also been established.

Methods

Isolation and culture of ovine monocytes

A standard operating protocol was established for the isolation and culture of ovine peripheral blood monocyte-derived macrophages. Blood is collected into EDTA for cell isolation and into tubes without anticoagulant for preparation of autologous serum. Briefly, density gradient centrifugation, using Optiprep (Sigma), is used for isolation of monocytes. The harvested monocytes are incubated for 1 hr at $37^oC/5\%CO_2$ and the non-adherent cells are then washed off. Cells adherent to tissue culture plastic are then cultured in the presence of 12.5% autologous serum and recombinant human macrophage colony stimulating factor for at least 7 days.

In vitro infection of primary ovine monocytes

A preliminary study was carried out to assess the influence of OJD infection on the engulfment of Mptb by monocyte/macrophages. Animals from the OJD031.A trial were used for this study. Briefly, cultured ovine peripheral blood monocytes were incubated for 2 days with Mptb at an MOI of 10 mycobacteria per macrophage. Cells were transferred onto glass slides and the presence of acid-fast bacilli detected by Ziehl Neelsen staining.

Changes in proliferation of mononuclear cell subsets during ovine Johne's disease

In order to study proliferation of mononuclear cell subsets methods were optimised to isolate these cells from peripheral blood as well as lymph nodes. In addition a high throughput flow cytometric assay was designed for this purpose.

Isolation of peripheral blood mononuclear cells

A standard operating protocol has been established for isolating ovine mononuclear cells by density gradient centrifugation. Several parameters including dilution of blood, dilution of buffy coat and speed of centrifugation were assessed to determine the optimal method for isolating PBMC.

Briefly, blood collected into lithium heparin tubes are centrifuged at 2500 rpm for 20 min, buffy coats are harvested and diluted in 3 mL PBS. Buffy coats from up to 5 tubes from the same animal can be pooled. The diluted buffy coat is layered over 2 mL Ficoll-Paque Plus(Amersham) and tubes centrifuged at 1800 rpm for 30 min, brake off. The white cell layer is then harvested and washed twice in 30 mL PBS and counted microscopically prior to resuspension in culture medium (RPMI 1640/10% FBS/Pen/Strep).

Isolation of lymph node cells

A 1-2 cm^2 section of lymph node is collected into cold RPMI 1640/2%FBS and processed within 1 hour. The node, trimmed of excess fat and other tissue, is diced to release lymph node cells into the collection medium and the suspension is strained through a 70 µm filter. The cells are counted and the cell concentration adjusted as necessary.

Proliferation assay

For the proliferation assay, PBMC or lymph node cells are first labelled the fluorescent tracking dye CFSE (carboxy fluorescein diacetate succinimidyl ester). Up to $50x10^6$ cells can be labelled by this method. Cells are resuspended in 1 mL of PBS/5% FBS and 100 µL of 50 mM CFSE is added and mixed quickly. The suspension is then incubated for 5 min, protected from light. Labelling is stopped

by the addition of cold PBS/5%FBS and cells are washed 3 times in PBS/5%FBS prior to resuspending in culture medium (RPMI 1640/10% FBS/Pen/Strep). The mononuclear cells are then plated into a 96-well plate and cultured in medium alone, Mptb antigen (316v) or con A for 5 days. At the end of the culture period, data for some cells were acquired on a flow cytometer while others are labelled with various cell surface markers to determine the phenotype of proliferating cells.

To determine cell phenotype, cells were first labelled with antibodies to CD5, CD4, CD8αβ, 86D (a maker for γδ T cells), WC4 (a marker for B cells) and then with a secondary antibody conjugated to APC (allophycocyanin). Data were then acquired by flow cytometry.

Flow cytometric data was acquired on a High Throughput System on a FACSCalibur (BD Biosciences) and data were analysed using WinList 5.0 software (Verity Software House).

Investigation of methods for explant tissue culture

Prior to investigating methods for ovine explant culture, an *in vitro* model, using the human epithelial cell line Caco-2, was tested to study the invasion of epithelial cells by Mptb. Caco-2 cells are human epithelial cells which express characteristics of enterocytic differentiation upon reaching confluence.

Caco-2 cells were grown to confluence in DMEM (high glucose)/10% FBS and incubated with 10 Mptb per Caco-2 cell for up to 48 hrs. At the end of the incubation period the culture supernatant was removed, cells were heat-fixed and subjected to Ziehl Neelsen staining. The location of acid-fast bacilli (either intracellular or extracellular) was determined by microscopy

Results and Discussion

Isolation and culture of ovine monocytes

Monocytes can be separated from other mononuclear cells by their ability to adhere to surfaces. Several types of surfaces were tested and tissue culture-treated plastic was found to be as good as other specially treated surfaces. Approximately 1-2% of PBMC are recovered as monocytes by this method.

Cells isolated from ovine PBMC by adherence have been confirmed as monocyte/macrophages by their expression of CD14 on 94.5% of the cell population (Figure 2A.3). CD14 is a cell surface marker which is found on monocytes but not on lymphocytes. These cells have been maintained in culture for up to 6 weeks.

One recurrent problem with monocyte/macrophage culture is the contamination with fibroblasts. Several methods have been trialled to reduce or remove contaminating cells but none have been successful.

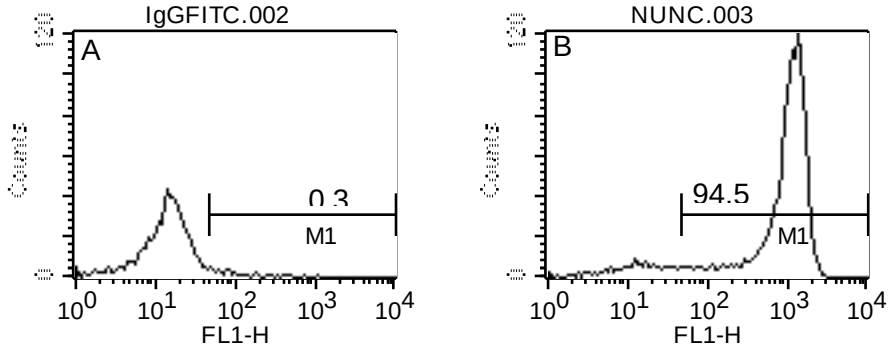

Figure 2A.3. Expression of CD14 on cultured ovine monocytes.

Cells were isolated by density gradient centrifugation and cultured for 6 weeks prior to labelling with an isotype control (A) or an anti-CD14 antibody (B).

Due to the recovery of low numbers of monocytes by the density gradient method, isolation of monocytes by magnetic cell sorting was also assessed. Direct and indirect methods were tested. In the direct method, monocytes were labelled with an antibody to a cell surface marker which is directly conjugated to a magnetic bead. In the indirect method, monocytes were first labelled with an antibody to a cell surface marker which is conjugated to a fluorochrome. The cells were then stained with an antibody to the fluorochrome which is conjugated to a magnetic bead. Purity of cells separated by this method was only 50% compared to 100% by adherence methods. Therefore, the magnetic cell sorting method was not pursued.

Cultured macrophages were provided for genomic analysis to determine optimal cell numbers required for an adequate yield of RNA. It was found that it would be difficult to isolate adequate numbers of cells to yield sufficient RNA for genomic work.

Protocols were tested and have been established for isolation of PBMC from larger volumes of blood (200 mL) than previously used in this laboratory. Approximately 1-2% of PBMC are recovered as monocytes by this method. This reflects the low numbers of monocytes in ovine peripheral blood as similar percentages were found when directly phenotyping blood (Results shown in subprogram 4).

Due to the low numbers of monocytes isolated from blood, and the inappropriateness of removing large volumes of blood from sheep, it was decided that it would not be possible to supply adequate numbers of ovine monocytes for Mptb research.

In vitro infection of primary ovine monocytes

Monocyte-derived macrophages isolated from peripheral blood from OJD031.A animals (uninfected and naturally infected) were infected with Mptb at 10 bacteria per macrophage. Infected cells were detected by Ziehl-Neelsen staining (Figure 2A.4A).

A.

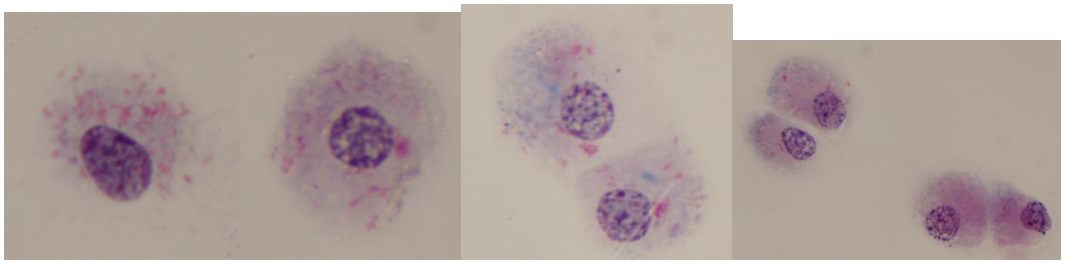

B.

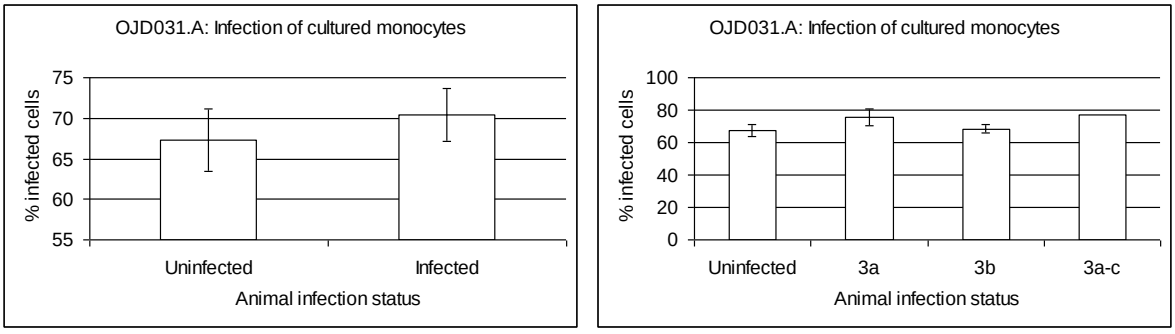

Figure 2A.4 Phagocytosis of Mptb by cultured ovine macrophages

Ovine monocyte-derived macrophages from infected and uninfected sheep were cultured in the presence of 10 Mptb per macrophage for 2 days. Acid-fast bacilli were detected by Ziehl Neelsen staining (A). Macrophages with one or more acid-fast bacilli were counted as an ‘infected’ cell (B). Uninfected, n=4; Infected, n=6; 3a, n=3; 3b, n=2; 3a-c, n=1.

There were no significant differences in the ability of cultured macrophages from animals of differing infection status to phagocytose Mptb (Figure 2A.4B). The major hindrance to the progress of this type of study was the inability to isolate large numbers of monocytes from ovine peripheral blood.

Investigation of methods for explant tissue culture

The ability of Mptb to cross an epithelial barrier was initially tested in an *in vitro* model. No acid-fast bacilli are seen when Caco-2 cells were incubated in the absence of Mptb (Fig 2A.5, left panel). In cells exposed to Mptb, the mycobacteria were mainly found extracellularly (Fig 2A.5, right panel). At an MOI of 10:1, less than 3% of Caco-2 cells were infected (contained more than one acid-fast bacilli per cell) with Mptb after 48 hr incubation. Cells that had detached from the monolayer into the culture supernatant were also assessed. Approximately 7% of cells that had detached during the incubation period were infected. Due to the low rate of infection of epithelial cells by Mptb it was decided not to progress with explant cultures.

A B

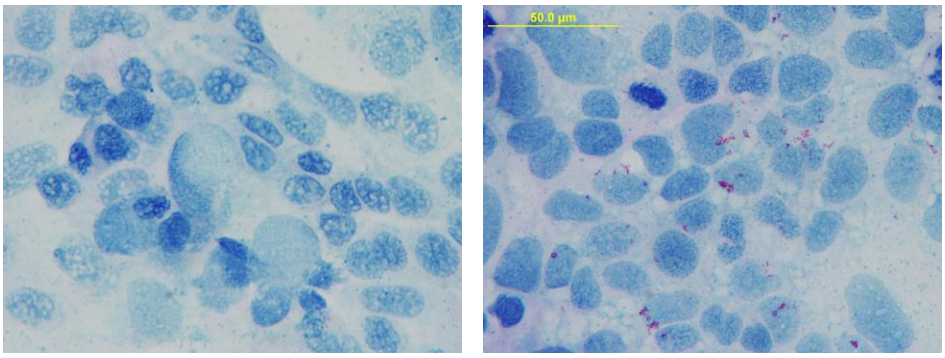

Figure 2A.5 Infection of Caco-2 cells

Confluent Caco-2 cells were cultured in the absence (A) or the presence of 10 Mptb per Caco-2 cell for 48 hrs and subjected to Ziehl Neelsen staining.

9.10 Appendix 2A-2 Subprogram 2 Mtb proliferation of ovine mononuclear cell subsets in early OJD

Abbreviations

Mptb: Mycobacterium avium subsp. paratuberculosis; PBMC: peripheral blood mononuclear cells; PBS: phosphate buffered saline; CFSE: carboxy fluorescein diacetate succinimidyl ester; APC (allophycocyanin); MOI: multiplicity of infection; ILN: ileal lymph node; JLN: posterior jejunal lymph node; PLN: prescapular lymph node; p.i.: post-inoculation; SI: stimulation index

Introduction

Protection against mycobacterial disease relies on T-cell dependent immune responses. In Johne's disease, cell-mediated immune responses predominate in subclinical disease. As disease progresses, these responses diminish and can be undetectable while there is a concurrent strong humoral response, demonstrated by elevated serum anti-Mptb antibodies. If the infection is not eliminated by the initial T-cell response then Mptb are able to persist and proliferate resulting in lesion formation and chronic infection. Much work has been published on cellular responses throughout the course of bovine Johne's disease but knowledge of similar responses in sheep is lacking.

A major undertaking in this subprogram was to study antigen-driven proliferation of lymphocyte subsets during the course of early ovine Johne's disease in animals that succumb to disease and those that remain free of disease.

Methods

Experimental infection

Sheep from OJD031.3-OJD031.6 experimental infection trials (Table 2A.3) were assessed. All animals in the OJD031.3-5 trials were exposed to a clonal inoculum of Mptb (Telford). In OJD031.6, one group was left unexposed to Mptb and a second group was challenged with the same clonal inoculum of Mptb as in the previous trials or with a gut homogenate prepared from an animal with clinical disease. These experimental infection trials are described in detail in Subprogram 2B.

Table 2A.3 OJD experimental trials

Experimental trial	Breed (n)	Inoculum	Months p.i. at necropsy
OJD031.3	Cross-bred (n=23)	Telford*	19
OJD031.4	Merino (32)	Telford	14
OJD031.5	Merino (12)	Telford	10
OJD031.6	Merino (58)	None (20), Telford (18), Gut homogenate (20)	11 to 13

*These animals received a 'booster' inoculum 12 months after the first challenge.

Sampling

Blood samples were collected throughout the duration of each trial and also prior to necropsy. Faecal samples were collected bimonthly while tissue samples were collected at necropsy. At the termination of each experimental trial, Mptb antigen-driven proliferation was assessed in cells from the ileal (ILN), posterior jejunal (JLN) and prescapular (PLN) lymph nodes.

Classification of disease

Culture of Mptb from tissue samples (radiometric BACTEC culture) and IS900 PCR confirmation were used to identify animals with OJD. The presence of histological lesions was also recorded.

Isolation of peripheral blood mononuclear cells

Blood collected into lithium heparin tubes were centrifuged at 2500 rpm for 20 min, buffy coats were harvested and diluted in 3 mL PBS. Buffy coats from up to 5 tubes from the same animal can be pooled into one tube. The diluted buffy coat was layered over 2 mL Ficoll-Paque Plus (Amersham) and tubes centrifuged at 1800 rpm for 30 min, brake off. The white cell layer was then harvested, washed twice in 30 mL PBS and counted microscopically prior to resuspension in culture medium (RPMI 1640/10% FBS/Pen/Strep).

Isolation of lymph node cells

A 1-2 cm^2 section of lymph node was collected into cold RPMI 1640/2%FBS and processed within 1 hour. The node, trimmed of excess fat and other tissue, was diced to release lymph node cells into the collection medium and the suspension strained through a 70 µm filter. The cells were counted and the cell concentration adjusted as necessary.

Proliferation assay

For the proliferation assay, PBMC or lymph node cells were first labelled with the fluorescent tracking dye CFSE (carboxy fluorescein diacetate succinimidyl ester). Up to $50x10^6$ cells can be labelled by this method. Cells were resuspended in 1 mL of PBS/5% FBS and 110 µL of 50 mM CFSE was added and mixed quickly. The suspension was then incubated for 5 min, protected from light. Labelling was stopped by the addition of cold PBS/5%FBS and cells were washed 3 times in PBS/5%FBS prior to resuspending in culture medium (RPMI 1640/10% FBS/Pen/Strep). The mononuclear cells were then plated into a 96-well plate and cultured in medium alone, 10 µg/mL Mptb antigen (316v) or 10 µg/mL Con A for 5 days. At the end of the culture period, data for some cells were acquired on a flow cytometer while others were labelled with various cell surface markers to determine the phenotype of proliferating cells.

To determine cell phenotype, cells were first labelled with antibodies to CD5 (CC17), CD4 (17D), CD8αβ (CC58), 86D (a marker for γδ T cells) or WC4 (a marker for B cells) (CC57) and then with a secondary antibody conjugated to APC (allophycocyanin). Data were then acquired by flow cytometry.

Flow cytometric data was acquired on a High Throughput System on a FACSCalibur (BD Biosciences) and analysed using WinList 5.0 software (Verity Software House).

Data are presented as Mptb antigen Stimulation Index (SI):

Mptb Ag SI = % $CFSE^{dim}$ cells in the presence of Mptb Ag

% $CFSE^{dim}$ cells in the presence of medium

Results and Discussion

Mptb antigen-driven proliferation of ovine PBMC was monitored at regular intervals in experimentally challenged animals. The total PBMC proliferative response as well as the proliferation of specific lymphocyte subsets was assessed. The high throughput flow cytometric proliferation assay developed for this purpose enabled rapid collection of data from a large number of samples. A major advantage of this method over radioactive and spectrophotometric methods is the ability to

simultaneously detect cell proliferation and phenotype. Using six replicates of each sample, the proliferation assay was found to be highly reproducible (Fig. 2A.6).

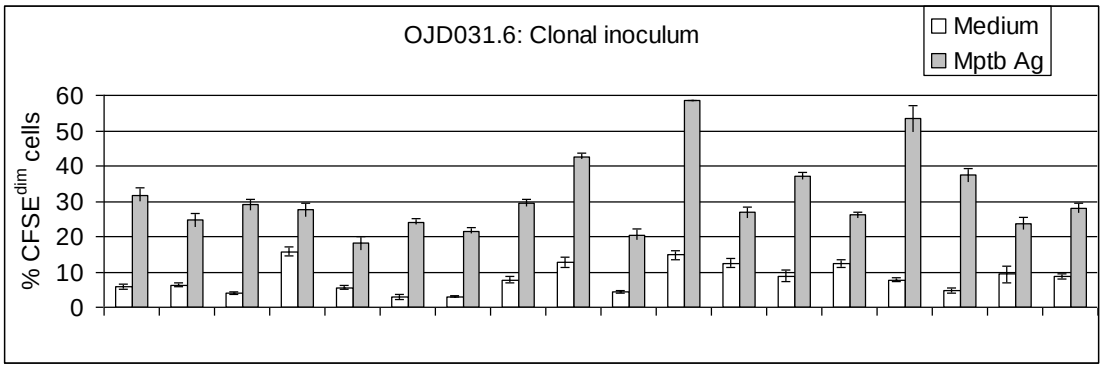

Figure 2A.6 Reproducibility of results of the proliferation assay

PBMC from sheep exposed to the Telford clonal inoculum were labelled with CFSE and cultured for 5 days in the absence (Medium) or presence of Mptb antigen (Mptb Ag) prior to data collection by flow cytometry. Proliferation is shown on the y-axis. The mean of six replicates (± sem) is shown for each animal.

The OJD031.6 trial consisted of 2 groups of animals: uninfected and exposed to either a clonal inoculum of Mptb or a gut homogenate from an animal with clinical OJD. Prior to inoculation, there was no Mptb antigen-specific proliferative response in any of the animals (Fig 2A.7). As expected, sheep exposed to Mptb mounted a strong cellular immune response. This could be detected in the blood as early as 4 months after challenge (Fig. 2A.7). Peak Mptb SI in PBMC was seen at around 8 months p.i. and it remained elevated in the exposed animals even at 11-13 months after challenge. In contrast, in animals not exposed to Mptb, the response was low throughout the duration of the study. The distinction between control and exposed animals was greatest at 8 months p.i. (Fig. 2A.7) and is reflected in the proliferation of cells that express the pan-lymphocyte marker CD5 (Fig. 2A.8).

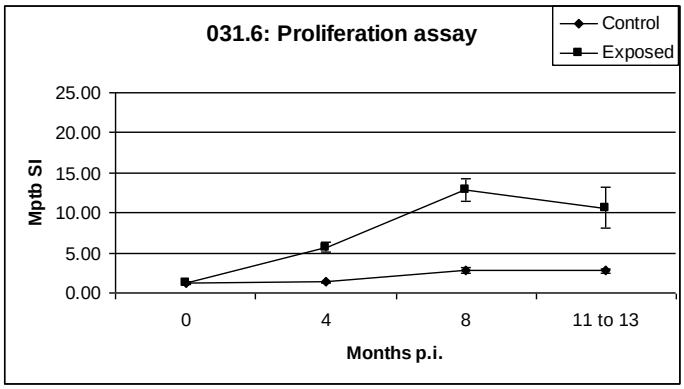

Figure 2A.7 Mptb antigen-driven proliferation of PBMC in OJD031.6 sheep.
PBMC from sheep exposed to Mptb (n=38) or left unchallenged (Control, n=20) were labelled with CFSE and cultured for 5 days in the absence or presence of Mptb antigen prior to data collection by flow cytometry. The mean of six replicates were used to determine the Mptb SI for each animal. The mean ± sem for each group is shown.

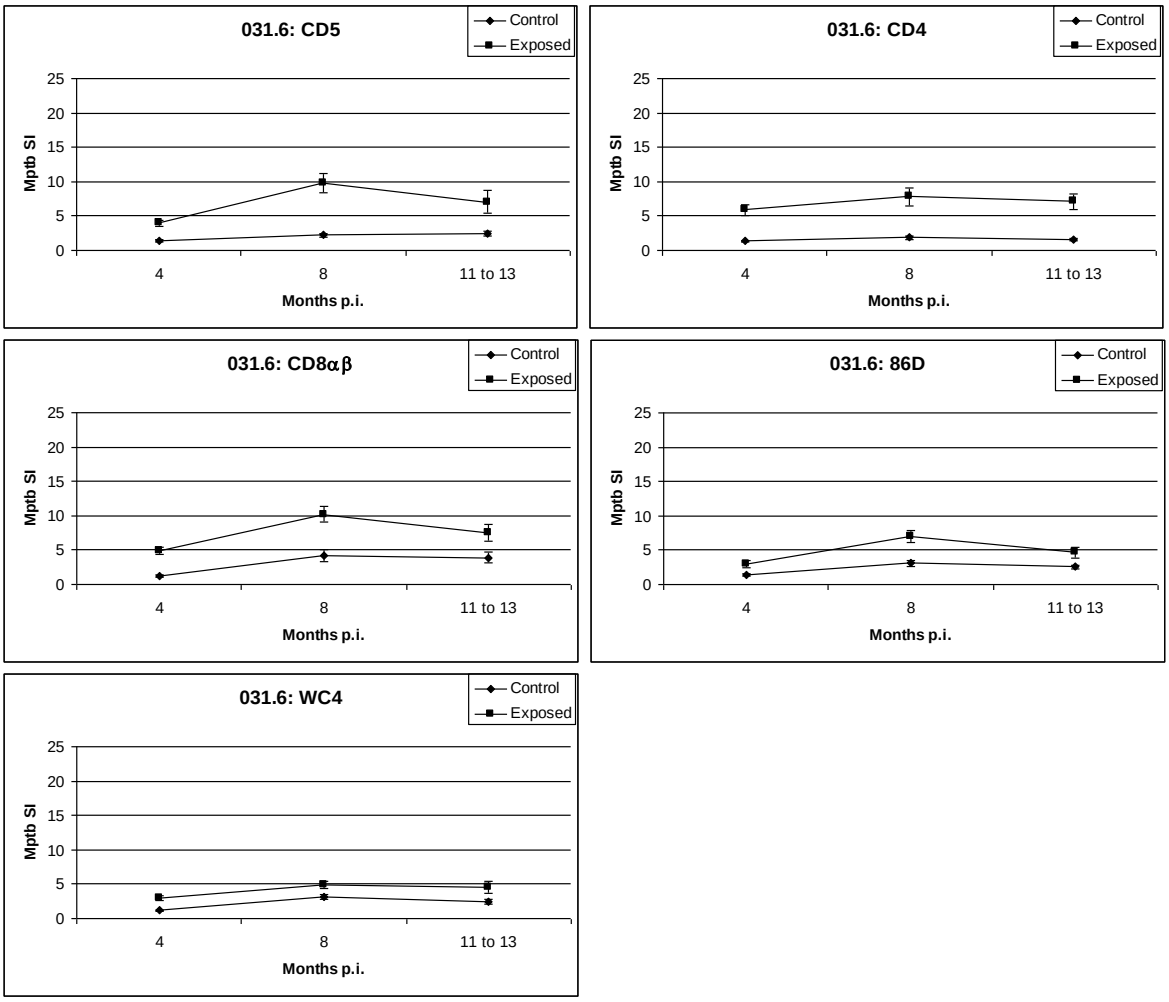

Figure 2A.8 Phenotype of proliferating PBMC in OJD031.6 sheep.

PBMC from sheep exposed to Mptb (n=38) or left unchallenged (Control, n=20) were labelled with CFSE and cultured for 5 days in the absence or presence of Mptb antigen. Cells were then labelled with a surface marker to determine phenotype prior to data collection by flow cytometry. The mean ± sem for each group is shown.

We studied the proliferation of 4 other lymphocyte subsets: $CD4^+$ T cells, $CD8\alpha\beta^+$ T cells, γδ ($86D^+$) cells and B ($WC4^+$) cells. At 8 months p.i., $CD8\alpha\beta^+$ and $CD4^+$ T cells were the major types of lymphocytes in the peripheral circulation responding to the recall antigen (Fig. 2A.8). This was similar at necropsy 11-13 months p.i. (Fig. 2A.8).

At necropsy, the lymph node cells of control sheep did not respond to Mptb antigen in the proliferation assay (Fig. 2A.9). In the exposed animals, proliferation was elevated in both ILN and JLN cells but remained low in PLN cells. Again, a similar response is seen in $CD5^+$ cells (Fig.2A.10). Proliferation of $CD4^+$ T cells was elevated in both ILN and JLN cells at necropsy (Fig. 2A.10). However, $CD8\alpha\beta^+$ cells from the ILN but not the JLN cell population was elevated compared to control animals.

Merino sheep were also used in the OJD031.4 and OJD031.5 trials. However, in these trials all animals were exposed to Mptb. Therefore an Mptb antigen-specific cell mediated immune response is seen in all animals (Fig 2A.11). Similar to the results seen in OJD031.6, peak Mptb SI is seen at

6-8 months p.i. in the OJD031.4 trial (Fig. 2A.11). The OJD031.5 trial was terminated at 10 months p.i. and Mptb SI was highest at that time point (Fig. 2A.11).

There were no differences in lymph node cell proliferation between uninfected and infected animals in both OJD031.4 and OJD031.5 trials at 14 and 10 months p.i. respectively.

Cross-bred sheep were used in the OJD031.3 trial. In addition, these animals were re-challenged with Mptb 12 months after the first inoculation. This is reflected in their proliferation assay results (Fig. 2A.12). At 11 months p.i. the Mptb antigen-driven proliferative response was low, but 3 months after the second inoculation (15 months after the initial inoculation) the response had increased. It is interesting that when the trial was terminated 19 months after the first inoculation, the Mptb-driven proliferative response was higher in animals that did not succumb to disease than in animals that did acquire OJD. The ability to mount a strong cell mediated immune response may have been important in the ability of these sheep to remain free of disease. $CD4^+$ T cells were the main proliferating cell type in the PBMCs of these animals at this time point (Fig. 2A.13). There was no difference in the proliferation of lymph node cells between infected and uninfected animals at the termination of this trial (Fig. 2A.14).

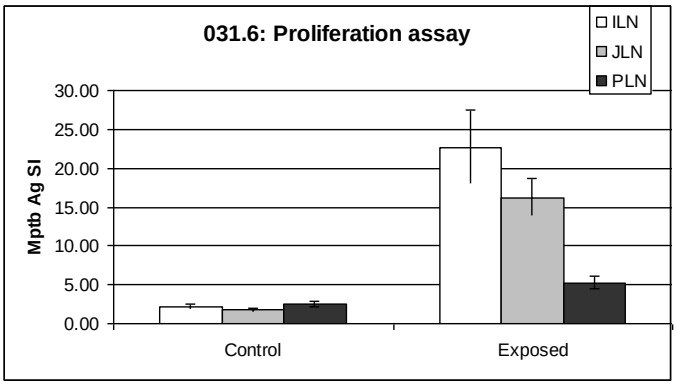

Figure 2A.9 Antigen-driven proliferation of lymph node cells in OJD031.6 sheep.

Lymph node mononuclear cells from sheep exposed to Mptb (n=38) or left unchallenged (Control, n=20) for 11-13 months were labelled with CFSE and cultured for 5 days in the absence or presence of Mptb antigen prior to data collection by flow cytometry. The mean ± sem for each group is shown. ILN = ileal lymph node; JLN = posterior jejunal lymph node; PLN = prescapular lymph node

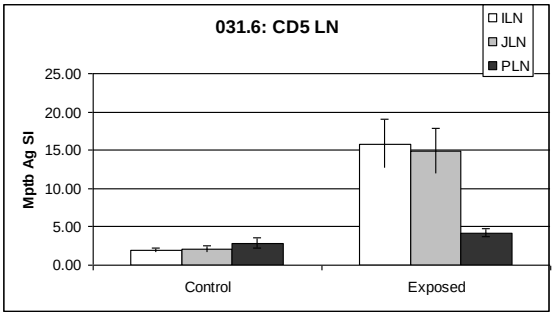

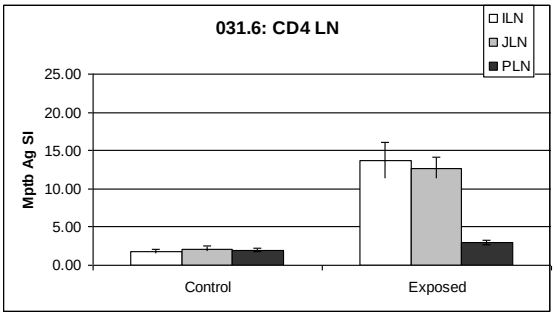

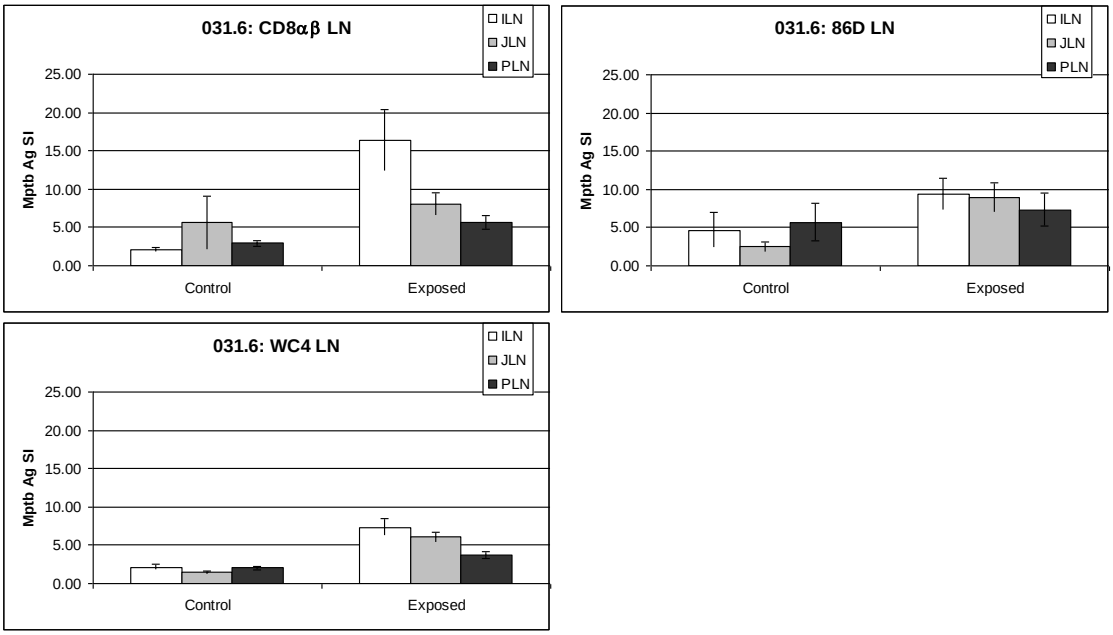

Figure 2A.10 Phenotype of proliferating lymph node cells in OJD031.6 sheep.

Lymph node mononuclear cells from sheep exposed to Mptb (n=38) or left unchallenged (control, n=20) for 11-13 months were labelled with CFSE and cultured for 5 days in the absence or presence of Mptb antigen. Cells were then labelled with a surface marker to determine phenotype prior to data collection by flow cytometry. The mean ± sem for each group is shown. ILN = ileal lymph node; JLN = posterior jejunal lymph node; PLN = prescapular lymph node.

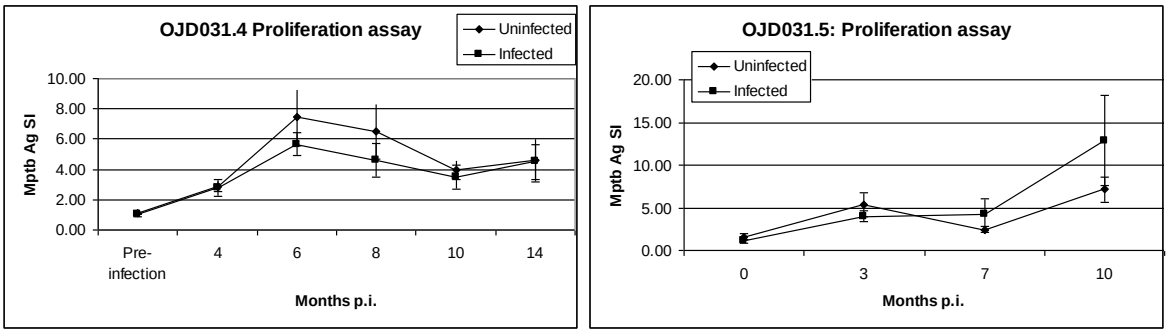

Figure 2A.11 Mptb antigen-driven proliferation of PBMC in OJD031.4 and OJD031.5 sheep.

PBMC from sheep exposed to Mptb were taken at various times during the trials, labelled with CFSE and cultured for 5 days in the absence or presence of Mptb antigen prior to data collection by flow cytometry. The mean ± sem for each group is shown. OJD031.4 uninfected, n= 9; infected n=9. OJD031.5, uninfected n=5; infected, n=7.

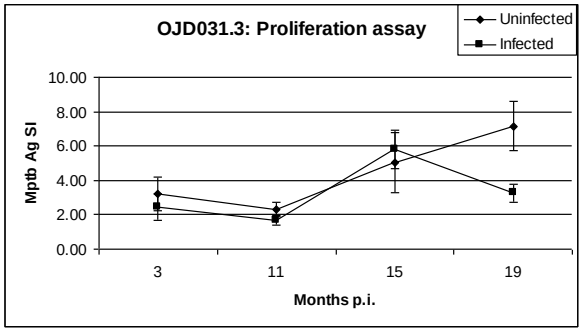

Figure 2A.12 Mptb antigen-driven proliferation of PBMC in OJD031.3 sheep.

PBMC from cross-bred sheep exposed to Mptb (uninfected, n=12; infected, n=11) were labelled with CFSE and cultured for 5 days in the absence or presence of Mptb antigen prior to data collection by flow cytometry. The mean ± sem for each group is shown.

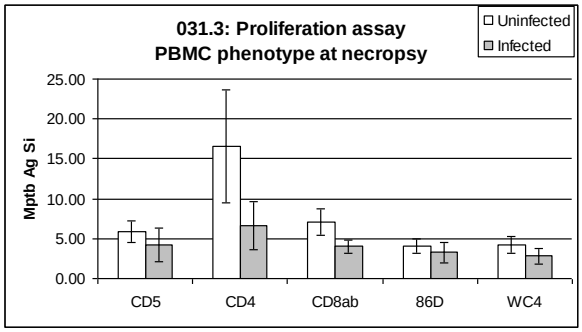

Figure 2A.13 Phenotype of proliferating PBMC in OJD031.3 sheep at necropsy.

PBMC from cross-bred sheep exposed to Mptb (uninfected, n=12; infected, n=11) for 15 months were labelled with CFSE and cultured for 5 days in the absence or presence of Mptb antigen. Cells were then labelled with a surface marker to determine phenotype prior to data collection by flow

cytometry. The mean ± sem for each group is shown. These animals received a second inoculation 12 months after the first challenge.

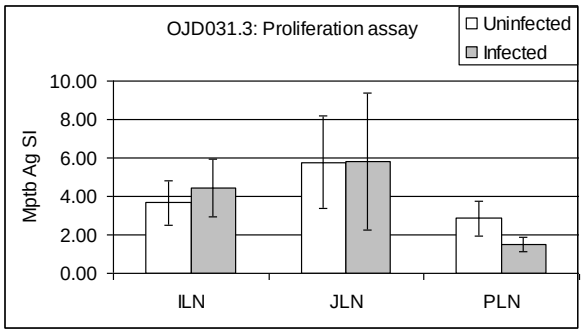

Figure 2A.14 Mptb antigen-driven proliferation of lymph node cells in OJD031.3 sheep at necropsy.

Lymph node mononuclear cells from cross-bred sheep exposed to Mptb (uninfected, n=12; infected, n=11) for 15 months were labelled with CFSE and cultured for 5 days in the absence or presence of Mptb antigen prior to data collection by flow cytometry. The mean ± sem for each group is shown. These animals received a second inoculation 12 months after the first challenge.

Conclusions

To the best of our knowledge these are the first studies to follow lymphocyte subset proliferation in ovine JD. The proliferation assay we developed is primarily a research tool as it requires special equipment and technical expertise. However, it is well-suited to large scale studies.

A strong cellular immune response can be detected in the peripheral circulation of sheep as early as 4 months following exposure to Mptb. Cell proliferation in response to Mptb antigen in exposed animals peaks at approximately 8 months p.i. $CD4^+$ and $CD8^+$ T cells produce the greatest proliferative response.

Within the groups of sheep exposed to Mptb, we were not able to detect differences in animals that remained free of disease and those that went on to develop OJD. Further analysis of these data sets is required to determine if differences in mononuclear cell proliferation phenotype can be distinguished based on lesion type.

9.11 Appendix 2B-1 Subprogram 2 Experimental animal infection models for Johne's disease, an infectious enteropathy caused by Mycobacterium avium subsp. Partuberculosis.

Introduction

Mycobacterium avium subspecies *paratuberculosis* (*Mptb*) is the causative agent of Johne's disease in ruminant species worldwide. The organism is usually transmitted from mother to offspring via the faecal-oral route. The resulting infection will either be cleared by the host or develop into subclinical and in some cases clinical disease. The infection causes granulomatous lymphadenitis and enteritis resulting in diarrhoea (more common in cattle and deer than sheep) and weight loss leading to the eventual death of the animal (Clarke, 1997). There are multiple strains of *Mptb* which have been divided into two broad categories called C (Type I, cattle or bovine) and S (Type II, sheep or ovine). The strains are easily distinguished by typing using the IS*1311* insertion sequence (Marsh et al., 1999), among other methods, and typically associate with their named host species, but this depends on the geographic region and probably also on the length of epidemiological association (Sevilla et al., 2005).

Due to the high economic costs of the disease (Chiodini et al., 1984; Brett, 1998) resulting from reduced production and earlier replacement of clinically affected animals, a considerable amount of research has been devoted to the elimination or control of Johne's disease in the past 100 years. One of the tools has been the use of experimental infection models. These are an essential part of Johne's disease research, allowing for guaranteed infection of animals and more control of the variables. Although all of the animals exposed to *Mptb* may not develop disease after experimental challenge a greater proportion will develop clinical signs than seen in natural infection. In natural infection it is not possible to regulate when or if the animals come in contact with *Mptb* and the number of bacteria ingested is always uncertain. Experimental models are beneficial for the examination of pathogenesis, vaccine efficacy, testing of diagnostic assays, changes in the production levels of the animals and immunological changes throughout the infection. When considering general principles of animal models (Davidson et al., 1987), using a normal ruminant as the model species provides benefits which include having a direct homologue of the disease, easy transfer of information and a large body of information regarding the background properties of the animals. In contrast, using laboratory animal models as an analogue has benefits with regard to genetic uniformity, lower costs and easy adaptability to experimental manipulation.

There has been a wide degree of variation in the types of experimental model used to study Johne's disease. Variables include the strain of *Mptb*, the animal species and breed, the route of infection and the number and size of the doses used to initiate the infection. In addition, the timing, extent and intensity of pathological and microbiological examination of subjects has varied widely, making comparisons of model applicability quite challenging. Consequently there is large variation in apparent or actual outcomes between experimental infection models. This critical review examines some of the published research identifying key points which may be of interest in model development and usage.

Electronic searches

Electronic literature searches were undertaken for the period 1938 - 2006 using key words “paratuberculosis”, or “Johnei” with the following words to limit the search “experimental infection”, “experimental inoculation” and “challenge” within the following databases: NCBI PubMed and ISI Web of Knowledge. Redundant references were eliminated. Manual literature search techniques were employed to access reports from 1938 to 1951. Criteria for inclusion of reports in this review were: any papers where experimental infection with *Mptb* was used; reports were excluded if there was evidence that the same experimental animals had been used as part of an earlier published experiment. Reports were then divided by host species and information was tabulated in a standard format.

Searches of the NCBI PubMed database identified 122 references, while searches of the ISI Web of Knowledge identified 142 references. After removing redundant references 97 eligible papers were identified and could be sourced. Seventy three references were admitted for the review after exclusion of papers where the animal data were duplicated among several papers.

Experimental infection of sheep

Experimental infections of sheep have been developed predominantly in countries where ovine Johne’s disease has been noted as a problem, typically Australasia and Europe. The infectious material used has been sourced from both sheep and cattle, suggesting use of both C and S strains of *Mptb* (Table 1). However, very few of the experiments have used verified infectious material typed as S or C strain. Of the experiments that used typed strains, variable results were seen. Infection rates from 0% (Begg et al., 2005) through to 100% (Brotherston et al., 1961; Reddacliff and Whittington, 2003) have been observed.

The rate of clinical disease was also variable between experimental protocols ranging from greater than 50% (Karpinski and Zorawski, 1975; Gwozdz et al., 2001) to none (Brotherston et al., 1961). Much of the variation seen in the outcomes of experimental models was likely due to strain differences between the *Mptb* isolates used, the dose of *Mptb* and the breed of sheep. While some of the experiments that used different strains were designed to test whether sheep could become infected with certain strains prevalent in the local area, other experiments were designed to look at the immunological responses of the sheep to infection. The results of some of this research using strains of *Mptb* that naturally do not infect sheep must be questioned as it has been shown different strains of *Mptb* result in different disease outcomes (Stewart et al., 2004; Begg et al., 2005). The breed of sheep also is an important consideration. Williams et al. (1983a) infected domestic and Bighorn sheep and had a higher rate of infection in the latter. The same strain of *Mptb* used by Williams et al. (1983a) was used to infect the Grivette breed of sheep and the animals were able to control and clear the infection (Thorel et al., 1992).

Various routes of infection have also been examined, the most usual being oral inoculation though other methods have been examined (Table 1). These include intratonsillar (Begg et al., 2005), intravenous (Brotherston et al., 1961; Kluge et al., 1968; Thorel et al., 1992) and intratracheal infection (Kluge et al., 1968). All of these routes of inoculation have resulted in infection of the gut and disease while some also led to altered immunological responses, development of fever, anorexia, diarrhoea and coughing in the early stages of the infection (Kluge et al., 1968). These are not natural features of Johne’s disease and the relevance of such routes of infection must be questioned.

Table 1: Experimental infection of sheep

Author	Year	Breed	Source strain of organism	Cultured/ tissue isolate	Age of host at challenge	Route of infection	Dose	No. of doses	No of animals inoculated	Necropsy post infection	Infected %[#]	Clinical disease %
Gwozdz et al.	2000	Crossbred	Sheep	Tissue isolate	4-6 weeks	Via stomach tube	4.4×10^8	1	14	8-12 months	64	50
Gwozdz et al.	2001	Not stated	Sheep	Tissue isolate	1-4 weeks	Via stomach tube	3.4×10^9	1	28	19-108 weeks	50	50
Brotherston et al.	1961	South Country Cheviots	mixed	Cultured	<7 days	oral	1×10^8	1-3	14	1-53 weeks	68	0
Brotherston et al.	1961	South Country Cheviots	mixed	Cultured	7-10 days	oral	1×10^8	8	10	10-53 weeks	100	11
Brotherston et al.	1961	South Country Cheviots	mixed	Cultured	3 weeks	oral	1×10^2	10	12	1-9 months	50	0
Brotherston et al.	1961	South Country Cheviots	mixed	Cultured	3 weeks	oral	1×10^5	10	12	1-9 months	50	0
Brotherston et al.	1961	South Country Cheviots	mixed	Cultured	3 weeks	oral	1×10^8	10	12	1-9 months	82	18
Gilmour and Brotherston	1962	South Country Cheviots	Sheep	Cultured	8 months	oral	1×10^9	1	12	12 h -56 days	75	0
Kluge et al.	1968	Corriedale	Cattle	Tissue isolate	3 weeks	oral	5×10^9	1	18	1 day - 16 months	Not stated	22
Karpinski and Zorawski	1975	Merion Cross	Cattle (760)	Cultured	10-12 weeks	oral	200 mg	1	7	7-24 months	100	71
Karpinski and Zorawski	1975	Merion Cross	Cattle (1305)	Cultured	10-12 weeks	oral	20 mg	10	6	7-24 months	83	33
Gilmour et al.	1977	Cheviot X Suffolk	Sheep	3rd sub culture	5 months	oral	1×10^9	10	30	5-27 months	63	3%
Willaims et al.	1983a	domesticated	Big horn sheep	Cultured	4-5 months	oral	50 mg wet weight	1	9	6 and 12 months	40	0
Willaims et al.	1983b	Bighorn	Big horn sheep	Cultured	4-5 months	oral	50 mg wet	1	9	6 and 12 months	100	0

							weight					
Dukes et al.	1992	domesticated	Saiga Antelope	Tissue isolate	1 day	oral	0.325g mucosa	2	2	18 months	100	50%
Thorel et al.	1992	Grivette	Big horn sheep	Cultured	< 1 month	oral	500 mg	1	6	2 years	0	0
Juste et al.	1994	Rasa	Cattle	Cultured	50 days	oral	1.36×10^6	2	5	15-220 days	Not stated	Not stated
Klausen et al.	1997	Not stated	Not stated	Not stated	1 month	oral	2×10^{12}	4	24	120-700 days	100	Not stated
Begara-McGorum et al.	1998	Dorset	Deer	Not stated	5 days	oral	1×10^9	3	8	3-41 days	38	0
Beard et al.	2000	Suffolk-Texel	Deer	Not stated	8-19 days	oral	1×10^9	3	Not stated	28 days	0	0
Reddacliff and Whittington	2003	Merino	Sheep *	Cultured	3-4 months	oral	1×10^7	3 or 10	12	7-14 weeks	100	0
Reddacliff and Whittington	2003	Merino	Sheep *	Cultured	3-4 months	oral	1×10^3	3 or 10	12	7-14 weeks	0	0
Reddacliff and Whittington	2003	Merino	Sheep *	Cultured	3-4 months	oral	1×10^1	3 or 10	6	7-14 weeks	0	0
Kurade et al.	2004	Crossbred	Sheep	Tissue isolate	8-12 weeks	oral	$9. \times 10^9$	8	20	10-330 days	35	15
Stewart et al.	2004	Merino	Sheep *	Cultured	10 months	oral	1-2E+10	4	5	35 months	Not stated	0
Stewart et al.	2004	Merino	Sheep *	Tissue isolate	10 months	oral	15-20 g mucosa	4	5	20-35 months	Not stated	20
Stewart et al.	2004	Merino	Cattle*	Cultured	6 months	oral	$1\text{-}2 \times 10^{10}$	4	5	54 months	Not stated	0
Stewart et al.	2004	Merino	Cattle*	Tissue isolate	6 months	oral	15-20 g mucosa	4	5	32-54 months	Not stated	20
Begg et al.	2005	Merino	Sheep *	Tissue isolate	3 months	oral	1×10^9	4	30	6-10 months	70	0
Begg et al.	2005	Merino	Sheep *	Tissue isolate	3 months	oral	5×10^8	3	30	11-22 months	53	33
Begg et al.	2005	Merino	Sheep *	Cultured	3 months	oral	5×10^8	3	30	11-22 months	0	0
Begg et al.	2005	Merino	Sheep *	Tissue	3 months	oral	5×10^7	2	12	7-16 months	66	0

				isolate								
Begg et al.	2005	Merino	Sheep *	Cultured	3 months	oral	1 x 10^9	2	12	7-16 months	25	0
Brotherston et al.	1961	South Country Cheviots	mixed	Cultured	10 weeks	intravenous	2 x 10^7	1	16	3-22 months	81	0
Kluge et al.	1968	Corriedale	Cattle	Tissue isolate	3 weeks	intravenous	5 x 10^9	1	9	1 day - 16 months	Not stated	0
Thorel et al.	1992	Grivette	Big horn sheep	Cultured	< 1 month	intravenous	50mg	1	6	2 years	0	0
Kluge et al.	1968	Corriedale	Cattle	Tissue isolate	3 weeks	intratracheal	5 x 10^9	1	18	1 day - 16 months	Not stated	0
Begg et al.	2005	Merino	Sheep *	Tissue isolate	3 months	Intratonsillar	5 x 10^7	2	12	7-16 months	66	0

* Strains of *Mptb* were typed using IS*900* and IS*1311*

Percentage infection was determined primarily by tissue culture at necropsy, if these data were not available other methods of detection were used such as histology and faecal culture

Experimental infection of cattle

Experimental infection has been examined in cattle more often than in sheep with the majority of studies being carried out in Europe or North America. Most of the studies have used strains of *Mptb* sourced from cattle, and little has been done to examine the infectivity of the S strain of *Mptb* in cattle (Table 2). Differences have been seen in the virulence of *Mptb* strains for cattle. Stabel et al., (2003) observed that beef calves were more susceptible to a strain of *Mptb* isolated from a bison whilst bison calves were more susceptible to a strain isolated from cattle. The age of inoculation has been discovered to be one of the limiting factors in creating an experimental infection model; older animals are more resistant to infection (Hagan, 1938; Payne and Rankin, 1961a; Larsen et al., 1975).

Generally infection rates of cattle with *Mptb* have been high but there were fewer cases of clinical disease compared to experimental infection in sheep (Table 2). An explanation for this could be the length of time animals are held before necropsy. Clinical disease in experimentally infected animals is typically observed two years after inoculation while most experimental protocols have run for approximately 1 year or less. Although most experimental infection models confirmed infection via tissue culture post necropsy, it is not possible to predict when or if animals would have developed clinical disease or resisted the infection, leading to questions about the validity of the data gathered.

Other than oral challenge various routes of inoculation have been found to cause infection in cattle, including intratonsillar (Waters et al., 2003), subcutaneous (Johnson et al., 1977; Larsen et al., 1977; Simutis et al., 2005), intravenous (Rankin, 1961; Stuart, 1965; Johnson et al., 1977) and intrauterine (Merkal et al., 1982). There were no immunological differences between subcutaneous, intravenous and oral routes of infection (Johnson et al., 1977). However, Larsen et al. (1977) noted that the intravenous route resulted in the highest level of infection between the three routes of inoculation used. This indicates different host pathogen interactions occur when animals are infected via alternative routes. Variation in genetic susceptibility has also been observed between different breeds and blood lines (Koets et al., 2000a), therefore careful selection and description of animals will be important to the eventual disease outcome and reproducibility of trials.

Experimental infection of laboratory animals

Numerous species of laboratory animals have been experimentally infected to test their suitability for studying Johne's disease. Species include mice (Francis, 1943; Lominski et al., 1956; Chandler, 1961a; Madge, 1971; Collins et al., 1985; Frelier et al., 1990; Hamilton et al., 1991; Mutwiri et al., 1992; Adams et al., 1993; Chiodini and Buergelt, 1993; Tanaka et al., 1994; Veazey et al., 1995a; Mutwiri et al., 2001), rabbits (Hirch, 1956; Rankin, 1958b; Mokresh et al., 1989; Mokresh and Butler, 1990; Vaughan et al., 2005), rats (Chandler, 1961b; Koets et al., 2000b), hamsters (Hirch, 1956; Gilmour et al., 1963; Larsen and Miller, 1978), guinea pigs (Francis, 1943; Merkal et al., 1982) and chickens (Larsen and Moon, 1972; Van Kruiningen et al., 1991) as seen in Table 3.

Table 2: Experimental infection of cattle

Author	Year	Breed	Source strain of organism	Cultured/tissue isolate	Age of host at challenge	Route of infection	Dose	No. of doses	No of animals inoculated	Necropsy post infection	Infected % [#]	Clinical disease %
Hagan	1938	Not stated	Cattle	Tissue isolate	< 1 year	oral	20 mg	3	9	4 months- 5 years	Not stated	55
Hagan	1938	Not stated	Cattle	Tissue isolate	1-2 years	oral	20 mg	3	3	Not stated	Not stated	100
Hagan	1938	Not stated	Cattle	Tissue isolate	>2 years	oral	20 mg	3	3	12 months or more	Not stated	0
Rankin	1958	Ayrshire	Cattle	Culture	1 month	intravenous	100 mg			4 years	100	66.6
Payne and Rankin	1961a	Ayrshire	Cattle	Cultured	3 months	oral	200 mg	1	21	1 day - 14 months	100	0
Payne and Rankin	1961b	Ayrshire	Cattle	Cultured	3 months	oral	200 mg	1	8	2-6 months	75	0
Payne and Rankin	1961b	Ayrshire	Cattle	Cultured	3 years	oral	200 mg	1	8	2-6 months	13	0
Rankin	1961	Ayrshire	Cattle	Culture	3 years	intravenous	100 mg	1	6	4 years	100	0
Stuart	1965	Various	Cattle	Culture	1 week	intravenous	100 mg	1	40	10 months	100	45
Gilmour et al.	1965	Ayrshire	Cattle	Cultured	3 weeks	oral	1×10^{8}	10	14	1-13 months	93	0
Gilmour et al.	1965	Ayrshire	Cattle	Cultured	3 weeks	oral	1×10^{10}	10	12	1-13 months	100	0
Gilmour et al.	1965	Various	Cattle	Cultured	2 months	oral	1×10^{9}	10	10	1- 6 months	100	0
Larsen et al.	1975	Holstein-Friesian X	Cattle	Cultured	1 month	oral	180 mg	1	2	150 days	100	0
Larsen et al.	1975	Holstein-Friesian X	Cattle	Cultured	9 months	oral	180 mg	1	4	150 days	33	0
Larsen et al.	1975	Holstein-Friesian X	Cattle	Cultured	5-11 years	oral	180 mg	1	4	150 days	66	0
Gilmour and Angus	1976	Various	Sheep	Cultured	6-8 weeks	oral	1×10^{9}	10	10	32-34 months	60	0
Johnson et al.	1977	Holstein-Friesian	Cattle	Cultured	21 days	oral	100 mg	1	3	153 days	100	Not

		X										stated
Johnson et al.	1977	Holstein-Friesian X	Cattle	Cultured	21days	intravenous	100 mg	1	4	153 days	100	Not stated
Johnson et al.	1977	Holstein-Friesian X	Cattle	Cultured	21 days	subcutaneous	33.3 mg	3	7	153 days	100	Not stated
Merkal et al.	1982	Holstein	Not stated	Not stated	3-4 years	intrauterine	5×10^8	1	13	1 day - 4 weeks	38	0
Krishnappa et al.	1989	Not stated	Cattle	Tissue isolate	Not stated	oral	50 g	10	6	Not stated	Not stated	Not stated
Lepper et al.	1989	Not stated	Not stated	Not stated	2 weeks	oral	50 mg	6	20	28-33 months	70	30
Beard et al.	2001	Holstein-Friesian X	Rabbit*	Cultured	1-5 days	oral	8×10^8 – 1×10^9	3	8	6 months	87.5	0
Beard et al.	2001	Holstein-Friesian X	Cattle*	Cultured	1-5 days	oral	$4\text{-}7 \times 10^8$	3	4	6 months	75	0
Waters et al.	2003	Holstein	Cattle	Cultured	2 weeks	intratonsillar	4×10^6	4	3	320 days	100	0
Uzonna et al.	2003	Holstein	Cattle	Cultured	2 days	oral	1×10^{10}	2	7	49 days	100	0
Uzonna et al.	2003	Holstein	Cattle	Cultured	28 days	oral	1×10^{10}	2	5	21 days	100	0
Stabel et al.	2003	Beef calves	Cattle	Cultured	2 weeks post weaning	stomach tube	6×10^9	5	6	6 months	≥83	0
Stabel et al.	2003	Beef calves	Bison	Cultured	2 weeks post weaning	stomach tube	6×10^9	5	6	6 months	100	0
Koo et al.	2004	Holstein	Not stated	Not stated	1 day	oral	1×10^7	7	5	Not stated	40%	Not stated
Simutis et al.	2005	Holstein	Cattle (ATTC 19698)	Cultured	4-5 weeks	subcutaneous	1×10^8	1	25	150 days	Not stated	0
Sweeny et al.	2006	Holstein	Cattle (ATCC700533)	Cultured	2 days	oral	2.5×10^{10}	2	6	42-44 days	100	0
Sweeny et al.	2006	Holstein	Cattle (ATCC700533)	Cultured	21 days	oral	5×10^9	2	8	21-23 days	100	0
Sweeny et al.	2006	Holstein	Cattle	Cultured	21 days	oral	5×10^8	2	6	21-23 days	100	0

			(ATCC700533)									
Sweeny et al.	2006	Holstein	Cattle (ATCC700533)	Cultured	21 days	oral	1.5 x10^6	2	6	21-23 days	100	0
Rosseels et al.	2006	Friesian-Holstein	Cattle (ATTC 19698)	Cultured	2-3 weeks	oral	1.0 x 10^8	10	5	Not stated	Not stated	Not stated

* Both rabbit and cattle strains are of the same genotype

Percentage infection was determined primarily by tissue culture at necropsy, if these data were not available other methods of detection were used such as histology and faecal culture

The reasons for using small animal models are numerous and include improved understanding of the immune response in both immunologically and microbiologically defined animals, faster development of infection and disease, ease in handling and reduced cost. Early experiments to infect laboratory animals resulted in a range of outcomes from little or no infection to high rates of infection (Francis, 1943; Chandler, 1961a). This was probably dependent on the strains of mice and *Mptb* used in the model. The more recent use of athymic or SCID (severe combined immunodeficiency) mice (Hamilton et al., 1989; Mutwiri et al., 1992) and mice identified as having genes conferring resistance or susceptibility to other mycobacteria such as BCG (Frelier et al., 1990) have been found to increase the levels of infection and disease.

The use of SCID or athymic mice allows for the adoptive transfer of specific immunologically identified cells from wild-type mice, such as regulatory T cells, as has been done in experimental models for inflammatory bowel disease (Martin et al., 2004; Kanai and Watanabe, 2005; Maloy et al., 2005). Rather than remove large portions of the immune system there are now moves towards using gene knock out mice where selected host genes are removed such as the gene for gamma delta T cells (Tanaka et al., 2000). This will help determine the importance of different parts of the immune system, pathways and individual genes involved in resisting *Mptb* infection.

There are also reasons not to use laboratory animals as models of infection. There has only been a small amount of transfer of knowledge from the use of small animal models to actual clinical application (Hein and Griebel, 2003). Specific reasons include the use of routes of infection other than the oral route normally applicable in ruminants, such as intravenous (Hirch, 1956; Larsen and Moon, 1972; Van Kruiningen et al., 1991), intraperitoneal (Francis, 1943; Frelier et al., 1990; Tanaka et al., 1994) and intrauterine inoculation (Merkal et al., 1982), all of which may result in altered immune reactions, and disease formation which would not be observed normally in a naturally infected host. This limits the relevance of data collected from these studies compared to infections in normal ruminant hosts.

When the oral route is used to infect mice they appear more resistant to *Mptb* infection than if intraperitoneal inoculation is used (Mutwiri et al., 1992). Mice may develop infection and accommodate bacterial replication but there may be no progression to disease, and in some cases regression may be observed (Hirch, 1956). The most common experimental infection route used in laboratory animals is intraperitoneal injection. Results are normally taken from enumerating the number of bacteria or histological lesions in the liver, spleen and in some cases intestinal tissues of the infected animal. Up to 10 weeks is required before *Mptb* can be recovered from the gut tissues (Francis, 1943; Tanaka et al., 1994). Finally the phenotypic response of laboratory animals cannot be correlated easily to that of a larger outbred ruminant with many of the host – bacterium interactions beyond the analytical sensitivity of currently available detection assays. Most of the signals of host-bacterium interactions (including immunological, physiological, pathological, gene and protein expression) that can be recorded in laboratory animals have been for single time points and do not reflect the temporal responses relevant during the course of infection and at the site of the infection in ruminant hosts.

The selection of the species and strain is crucial to the success of laboratory animal models. Lewis rats (Koets et al., 2000b), NZ white rabbit (Vaughan et al., 2005), CBA (Chandler, 1961c), Swiss white (Chandler, 1961c), BCG resistant or C3H (Frelier et al., 1990; Tanaka et al., 1994) mice have all been shown to be more resistant to *Mptb* infections than the BALB/c (Tanaka et al., 1994) and C57 (Chandler, 1961c; Frelier et al., 1990) strains. Species such as the chicken, hamster and guinea pig

have also been examined (Table 3) but little has been done to elucidate which strains are more susceptible to *Mptb* infection.

Importantly the strain of *Mptb* used to infect these animals appears to have a large influence on the outcome of infection and disease development (Hirch, 1956; Mokresh and Butler, 1990). Some strains result in florid infection while other strains may be cleared from the animal. Most models have only used strains sourced from cattle and not ovine strains of *Mptb* which may result in different infection profiles.

Table 3 Experimental infection of laboratory animals

Author	Year	Species/ Breed	Source strain of organism	Cultured/tissue isolate	Age of host at challenge	Route of infection	Dose	No of doses	No of animals inoculated	Necropsy post infection	Infected % [#]	Clinical disease %
Van Kruiningen et al.	1991	Chickens	Human (Linda)	Cultured	2 weeks	oral	1×10^7	1	6	2-9 weeks	33	0
Van Kruiningen et al.	1991	Chickens	Human (Linda)	Cultured	2 weeks	intraperitoneal	1×10^7	1	6	2-9 weeks	100	0
Van Kruiningen et al.	1991	Chickens	Human (Linda)	Cultured	2 weeks	intravenously	1×10^7	1	6	2-9 weeks	60	0
Larsen et al.	1972	Chickens (white leghorn)	Cattle	Culture	2 weeks	intravenously	5 mg	1	12	30-240 days	42	0
Larsen et al.	1972	Chickens (white leghorn)	Cattle	Culture	2 weeks	oral	30 mg	1	4	30 days	100	0
Valente et al.	1997	Chickens (white leghorn)	Cattle	Culture	1 week	oral	5 mg	2	10	1-4 months	40	0
Francis	1943	Guinea pigs	Cattle (passaged through a mouse)	Tissue isolate	2 days	intraperitoneal	0.2-0.4 ml	2	2	6 months	Not stated	Not stated
Merkal et al.	1982	Guinea pigs (English short hair)	Not stated	Not stated	Not stated	Intrauterine	1×10^{10}	1	18	1 day-15 weeks	89	0
Merkal et al.	1982	Guinea pigs (English short hair)	Not stated	Not stated	Not stated	Intrauterine	1×10^{10}	1	18	1 day-15 weeks	100	0
Merkal et al.	1982	Guinea pigs (English short hair)	Not stated	Not stated	Not stated	Intrauterine	1×10^{10}	1	18	1 day-15 weeks	72	0
Francis	1943	Hamster	Cattle	Cultured	23 days	intraperitoneal	2.5 mg	2	5	5- 32 weeks	80	Not stated
Francis	1943	Hamster	Cattle (passaged through a hamster)	Tissue isolate	10-12 days	intraperitoneal	0.1 mL	2	4	12-25 weeks	100	Not stated
Hirch	1956	Hamster	Various	Culture	Adults	oral	1.5-0.6 mg	6 or 11	14	4-40 weeks	71	Not stated
Hirch	1956	Hamster	Various	Culture	Adults	oral	0.6 mg	6 or 11	4	6-40 weeks	25	Not stated

Hirch	1956	Hamster	goat	Culture	Adults	intraperitoneal	0.3 mg	1	7	3-40 weeks	85	Not stated
Hirch	1956	Hamster	Hamster	Culture	Adults	intraperitoneal	0.8 mg	1	2	12-40 weeks	100	Not stated
Hirch	1956	Hamster	Hamster	Culture	Adults	intraperitoneal	0.2 mg	1	3	12-40 weeks	100	Not stated
Hirch	1956	Hamster	Rabbit	Culture	Adults	intraperitoneal	0.5 mg	1	2	12-13 weeks	100	Not stated
Hirch	1956	Hamster	goat	Culture	2-3 days	intraperitoneal	0.08 mg	1	4	6-35 weeks	100	Not stated
Hirch	1956	Hamster	Hamster	Culture	2-3 days	intraperitoneal	0.04 mg	1	4	7-35 weeks	100	Not stated
Hirch	1956	Hamster	Rabbit	Culture	2-3 days	intraperitoneal	0.08 mg	1	4	6-35 weeks	75	Not stated
Gilmour et al.	1963	Hamster	Cattle	Culture	8 weeks	oral	6×10^{7}	1	36	1 hour -11 months	55	14
Gilmour et al.	1963	Hamster	Cattle	Culture	8 weeks	oral	1×10^{5}	4	28	1 week- 8 months	21	Not stated
Larsen et al.	1978	Hamster	Cattle	Cultured	3 weeks	oral	15 mg	1	15	14 weeks	100	0
Francis	1943	Mice	Cattle	Cultured	15 days	intraperitoneal	2.5 mg	2	4	9-34 weeks	100	0
Francis	1943	Mice	Cattle (passaged through a mouse)	Cultured	13 days	intraperitoneal	1 mg	2	5	12- 20 weeks	75	Not stated
Francis	1943	Mice	Cattle (passaged through a mouse)	Cultured	13 days	intraperitoneal	0.5 mg	2	2	20-24 weeks	50	0
Francis	1943	Mice	Cattle (passaged through a mouse)	Tissue isolate	13 days	intraperitoneal	0.1 or 0.2mL	2	7	5-17 weeks	100	Not stated
Lominski et al.	1956	Mice Swiss white	Various Cattle	Culture	2-3 months	intraperitoneal or intravenously	1 mg	1	82	1-9 months	13	Not stated
Lominski et al.	1956	Mice Swiss white	Various Cattle	Culture	7-28 days	intraperitoneal or intravenously	2.64-0.2mg	1	65	7-27 months	72	Not stated
Lominski et al.	1956	Mice Swiss white	Various Cattle	Tissue isolate	not stated	intraperitoneal	0.2-0.4mL	1	54	12-15 months	87	Not stated
Chandler	1961	Swiss White mice	Cattle	Culture	3-4 weeks	intraperitoneal	24 mg	1	15	3 -12 months	100	Not stated
Chandler	1961	Swiss White mice	Cattle	Culture	3-4 weeks	intraperitoneal	8 mg	1	20	3 -12 months	100	Not stated

Chandler	1961	Swiss White mice	Cattle	Culture	3-4 weeks	intraperitoneal	2 mg	1	15	3 -12 months	100	Not stated
Chandler	1961C	Swiss White mice	Cattle	Culture	3-4 weeks	intraperitoneal	2 mg	1	50	3-15 months	90	4
Chandler	1961C	C57 mice	Cattle	Culture	3-4 weeks	intraperitoneal	2 mg	1	50	3-15 months	100	0
Chandler	1961C	CBA mice	Cattle	Culture	3-4 weeks	intraperitoneal	2 mg	1	50	3-15 months	92	6
Madge	1971	Mice C57	Not Stated	Culture	4 weeks	intraperitoneal then oral	1×10^{8}-1×10^{9}	2	120	12-15 months	Not stated	28
Hamilton et al.	1989	Athymic BALB/c mice	Human (Linda ATCC 43015)	Culture	Not stated	Stomach tube	1×10^{10}	1	Not stated	0-25 weeks	Not stated	Not stated
Frelier et al.	1990	Mice	Not stated	Cultured	Not stated	intraperitoneal	1×10^{9}	1	Not stated	50 days	Not stated	Not stated
Hamilton et al.	1989	Euthymic BALB/c mice nu/+	Human (Linda ATCC 43015)	Culture	Not stated	Stomach tube	1×10^{10}	1	Not stated	0-25 weeks	Not stated	Not stated
Hamilton et al.	1991	gnotobiotic athymic BALB/c mice	Human	Cultured	Not stated	Stomach tube	1×10^{10}	1	33	1 week-15 months	Not stated	18 (first at 5 months
Mutwiri et al.	1992	Mice (SCID bg)	Cattle	Tissue isolate	Not stated	intraperitoneal	1×10^{5}	1	58	2-26 weeks	Not stated	Not stated
Mutwiri et al.	1992	Mice (SCID bg)	Cattle	Tissue isolate	Not stated	oral	1×10^{5}	1	18	8-26 weeks	50	0
Adams et al.	1993	Euthymic mice (BALB/c)	Human (Linda)	Culture	not stated	intragastrically	1×10^{10}	1	Not stated	3-6 months	Not stated	Not stated
Adams et al.	1993	Athymic mice (BALB/c)	Human (Linda)	Culture	not stated	intragastrically	1×10^{10}	1	Not stated	3-6 months	Not stated	Not stated
Tanaka et al.	1994	BALB/c mice	ATCC19698	Culture	6 weeks	intraperitoneal	5×10^{8}	1	12	3-32 weeks	100	0
Tanaka et al.	1994	C3H/HeJ mice	ATCC19698	Culture	6 weeks	intraperitoneal	5×10^{8}	1	12	3-32 weeks	100	0
Veasey et al.	1995	Mice (C3H/HeN)	ATCC19698	Culture	4- 6 weeks	intraperitoneal	1×10^{9}	1	Not stated	3-269 days	Not stated	Not stated
Veasey et al.	1995	Mice (C57BL/6N)	ATCC19698	Culture	4- 6 weeks	intraperitoneal	1×10^{9}	1	Not stated	3-269 days	Not stated	Not stated
Stabel et al.	1998	Beige Mice	ATCC19698	Culture	8 weeks	intraperitoneal	1×10^{8}	1	10	1-6 months	Not stated	Not stated
Tanaka et al.	2000	GDT cell knockout BALB/c mice	ATCC19698	Cultured	10 weeks	intraperitoneal	4×10^{6}	1	10	6-18 weeks	Not stated	Not stated

Tanaka et al.	2000	GDT cell knockout BALB/c mice	ATCC19698	Cultured	10 weeks	intraperitoneal	4×10^{9}	1	10	6-18 weeks	Not stated	Not stated
Tanaka et al.	2000	BALB/c Mice	ATCC19698	Cultured	10 weeks	intraperitoneal	4×10^{6}	1	10	6-18 weeks	Not stated	Not stated
Tanaka et al.	2000	BALB/c Mice	ATCC19698	Cultured	10 weeks	intraperitoneal	4×10^{9}	1	10	6-18 weeks	Not stated	Not stated
Mutwiri et al.	2001	Beige SCID Mice	Cattle	Tissue isolate	6 weeks	intraperitoneal	1×10^{3}	1	8	32 weeks	Not stated	100
Mutwiri et al.	2001	Beige SCID Mice	Cattle	Tissue isolate	6 weeks	intraperitoneal	1×10^{2}	1	8	32 weeks	Not stated	Not stated
Mutwiri et al.	2001	Beige SCID Mice	Cattle	Tissue isolate	6 weeks	intraperitoneal	1×10^{1}	1	8	32 weeks	Not stated	Not stated
Thomsen et al.	2001	Euthymic mice (BALB/cAnCrlBR)	ATCC19698	Culture	3-7 days	intraperitoneal	3×10^{7}	1	8	5 months	100	Not stated
Thomsen et al.	2001	Athymic nude mice (BALB/cAnNCrl-nuBR)	ATCC19698	Culture	3-7 days	intraperitoneal	3×10^{7}	1	10	5 months	100	Not stated
Hirch	1956	Rabbit	Rabbit	Culture	4-5 weeks	oral	5.6-1.6mg	7	16	4-40 weeks	6	Not stated
Hirch	1956	Rabbit	Hamster	Culture	4-5 weeks	oral	2.8 mg	7	6	4-40 weeks	50	Not stated
Hirch	1956	Rabbit	Goat	Culture	4-6 weeks	intraperitoneal	0.2 mg	1	6	≤ 42 weeks	Not stated	Not stated
Hirch	1956	Rabbit	Rabbit	Culture	4-6 weeks	intraperitoneal	0.2 mg	1	4	≤ 42 weeks	≤ 50	Not stated
Hirch	1956	Rabbit	Goat	Culture	8-10 weeks	intravenously	0.5 mg	2	4	1-33 weeks	100	Not stated
Hirch	1956	Rabbit	Rabbit	Culture	8-10 weeks	intravenously	0.5 mg	2	6	1-33 weeks	100	Not stated
Francis	1943	Rabbit	Cattle	Cultured	10 days	intraperitoneal	8.9mg	2	4	12-27 weeks	100	Not stated
Vaughan et al.	2005	Rabbit (NZ white)	Cattle*	Cultured	3 months	oral	5×10^{8}	3	4	24-32 months	50	25 at 20 months
Vaughan et al.	2005	Rabbit (NZ white)	Cattle*	Cultured	2 weeks	oral	1×10^{8}	3	16	2-21 months	19	13
Mokresh et al.	1989	Rabbits NZ white	ATCC19698	Culture	1 day	oral	7×10^{6}	5 or 10	21	8-10 months	43	5
Mokresh et al.	1990	Rabbits NZ white	ATCC19698	Culture	1 day	oral	3.6×10^{8}	1	15	2 weeks- 9 months	38	0

Mokresh et al.	1990	Rabbits NZ white	Bovine (22206)	Culture	1 day	oral	2.6×10^8	1	5	2 weeks- 9 months	100	0
Chandler	1961b	White Wistar rats	Cattle	Culture	4 weeks	intraperitoneal	2 mg	1	24	3 -12 months	84	0
Chandler	1961b	White Wistar rats	Cattle	Culture	4 weeks	intraperitoneal	0.2 mg	1	24	3 -12 months	72	0
Koets et al.	2000	(SPF) Lewis Rats	B854	Cultured	26 days	oral	1×10^9	12	28	8-267 days	0	0

Percentage infection was determined primarily by tissue culture at necropsy, if these data were not available other methods of detection were used such as histology and faecal culture

Table 4: Experimental infections in other animal species

Author	Year	Species/ Breed	Source strain of organism	Cultured/tissue isolate	Age of host at challenge	Route of infection	Dose	No. of doses	No of animals inoculated	Necropsy post infection	Infected % #	Clinical disease %
Stabel et al.	2003	Bison	Cattle	Cultured	2 weeks post weaning	Stomach tube	6×10^9	5	6	6 months	≥83	0
Stabel et al.	2003	Bison	Bison	Cultured	2 weeks post weaning	Stomach tube	6×10^9	5	6	6 months	≥50	0
Stewart et al.	2006	Goat (Angora)	Sheep *	Cultured	10 months	oral	$1\text{-}2 \times 10^{10}$	4	5	35 months	100	0
Stewart et al.	2006	Goat (Angora)	Sheep *	Tissue isolate	10 months	oral	15-20 g mucosa	4	5	20-35	80	20
Stewart et al.	2006	Goat (Angora)	Cattle*	Cultured	5 months	oral	$1\text{-}2 \times 10^{10}$	4	5	54 months	100	40
Stewart et al.	2006	Goat (Angora)	Cattle*	Tissue isolate	5 months	oral	15-20 g mucosa	4	5	32-54 months	100	80
Munjal et al.	2005	Goat (crossbred)	Goat	Tissue isolate	7-10 weeks	oral	1×10^{10}	7	10	15-270 days	10	40
Sigurdardottir et al.	1999	Goat (Norwegian)	Goat	Cultured	7-26 days	oral	10 mg	10	8	3-49 weeks	25	0
Storset et al.	2001	Goat (Norwegian)	Goat (P173)	Cultured	5-8 weeks	oral	10 mg	25	7	106-117 weeks	71	14
Willaims et al.	1983b	White tail deer	Big horn sheep	Cultured	4-5 months	oral	50 mg wet weight	1	2	6 & 12 months	100	Not stated
Willaims et al.	1983b	Elk	Big horn sheep	Cultured	4-5 months	oral	50 mg wet weight	1	8	6 & 12 months	100	Not stated
Willaims et al.	1983b	Mule Deer	Big horn sheep	Cultured	4-5 months	oral	50 mg wet weight	1	8	6 & 12 months	100	Not stated
O'Brien et al.	2006	Red Deer	Sheep *	Tissue isolate	4 months	oral	1×10^7	4	16	44 weeks	69	Not stated
O'Brien et al.	2006	Red Deer	Cattle * (from a	Tissue isolate	4 months	oral	1×10^9	4	16	44 weeks	100	Not stated

			red deer)									
O'Brien et al.	2006	Red Deer	Cattle * (from a red deer)	Tissue isolate	5 months	oral	1 x 10^7	4	16	44 weeks	100	Not stated
O'Brien et al.	2006	Red Deer	Cattle * (from a red deer)	Tissue isolate	6 months	oral	1 x 10^3	4	16	44 weeks	50	Not stated
Larsen et al.	1971	Pig	Cattle	Cultured	10 days	Stomach tube	200 mg	1	5	7-8 months	100	0
Larsen et al.	1971	Pig	Cattle	Cultured	10 days	intravenously	60 mg	1	2	5-8 months	100	0
Larsen et al.	1972	Horse	Cattle	Cultured	10 days	Stomach tube	180 mg	1	2	120 days	100	0
Larsen et al.	1972	Horse	Cattle	Cultured	10 days	intravenously	100 mg	1	2	120 days	100	100

* Strains of *Mptb* were typed using IS900 and IS1311

Percentage infection was determined primarily by tissue culture at necropsy, if these data were not available other methods of detection were used such as histology and faecal culture

Experimental infection in other animals

Experimental infection has been carried out in a small list of other species including deer (Williams et al., 1983b; O'Brien et al., 2006), goats (Sigurdardottir et al., 1999; Storset et al., 2001; Munjal et al., 2005; Stewart et al., 2006), bison (Stabel et al., 2003), horses (Larsen et al., 1972) and pigs (Larsen et al., 1971) (Table 4). In deer, O'Brien et al. (2006) showed high levels of infection using the bovine strain of *Mptb* while the ovine strain created lower levels of infection and the subjects had lower immunological responses. Williams et al. (1983) showed that several species of deer could become infected with *Mptb* isolated from Bighorn sheep endemic to the area. Pigs intravenously challenged with *Mptb* can shed bacteria into the environment indicating these animals could become a reservoir host (Larsen et al., 1971).

Strains of M. paratuberculosis

The strain of *Mptb* used in the infection model appears to influence the disease outcomes observed. Several studies have noted a reduced infection rate or total failure of experimental infection due to the strain of *Mptb* used (Hirch, 1956; Mokresh and Butler, 1990; Begg et al., 2005; O'Brien et al., 2006; Stewart et al., 2006). Hirch (1956) noted a strain of *Mptb* isolated from an experimentally infected rabbit was less virulent than other strains examined in several host species. In the studies by Begg et al. (2005) using two ovine strains and Mokresh et al. (1990) using two bovine strains of *Mptb*, differences were observed between strains in experimental infection outcomes. Adding to the problem is that the ovine and bovine strains of *Mptb* have been shown to result in different immunological profiles in experimentally infected animals (O'Brien et al., 2006; Stewart et al., 2006).

While both bovine and ovine strains can cause infection in a wide range of species the strain of *Mptb* recovered from naturally infected animals is related to the host species and geographical region. In New Zealand and Australia it appears sheep are more susceptible to the ovine strain of *Mptb* while cattle and deer are more susceptible to the bovine strain (Cousins et al., 2000; Whittington et al., 2000; Whittington et al., 2001; O'Brien et al., 2006), although this may also reflect differences in opportunity for infection. In India *Mptb* isolated from sheep are more likely to be the bovine strain (Sevilla et al., 2005). This means experimental infection models will have to use strains of *Mptb* most relevant to the geographical region in relation to outcomes expected from the research, rather than one universal infectious strain.

Very few studies have used strains of *Mptb* that have been typed using genotypic criteria such as IS*900* and/or IS*1311* before inoculation (Reddacliff and Whittington, 2003; Stewart et al., 2004; Begg et al., 2005; O'Brien et al., 2006; Stewart et al., 2006). This is a key step that is required to understand what is being used to infect the animals and it may enable better comparisons between trials.

The method of preparation of the inoculum of *Mptb* may result in altered disease outcomes. There have been two main methods used, the first being a direct tissue harvest, where tissues from infected animals are homogenised and used for the inoculation. The second method is to culture *Mptb* from an infected animal and use *in vitro* grown organisms for inoculation. However, virulence may be lost *in vitro*. Stewart et al. 2004 showed that immunological differences could be observed between animals infected with cultured *Mptb* or tissue isolates of *Mptb.*

The use of direct tissue isolates of *Mptb* in replicated experiments is limited by the amount of homogenate material available from any given animal and uncertainty of the effect of storage on such material. Isolation of homogenate material from another animal may result in a different outcome due to it containing a different strain or viable count of *Mptb*. For this reason the use of tissue isolates for experimental *Mptb* infections has limited application. Laboratory cultures of *Mptb* have greater potential to provide a repeatable outcome. However, pure cultures seem seldom to

have been used, and the concept of a seed stock from a typed strain appears absent from the literature. Most experimental infections have been undertaken with non-clonal laboratory isolates of an unspecified passage level. Furthermore, some of the observations related to the strain of *Mptb* maybe confounded by the lack of standardisation of the dose used.

Infectious dose

There has been no consistent dose used to infect experimental animals. The lowest dose used to infect ruminants was recorded by Brotherston et al. (1961) where 10^3 bacteria caused infection. Typically, higher doses of bacteria of 10^9-10^{12} have been used (Gilmour et al., 1965; Klausen et al., 1997). The time it takes for lesions and or clinical disease to develop appears to be correlated to the dose given to the animals (Hirch, 1956) with larger doses resulting in earlier disease development. Therefore animals given lower doses of *Mptb* can become infected but may require several years before signs of infection and disease develop. Similarly, animals dosed with higher numbers of bacteria have earlier immunological responses than animals that receive lower doses of *Mptb.* That is, with lower doses a longer lag phase in the immunological response is observed (O'Brien et al., 2006).

A further complication is the lack of standardisation of enumeration methods, or omitting enumeration and administration of a dose measured in milligrams dry or wet weight. Enumerating viable bacteria in a challenge dose was first reported by Brotherston et al (1961), although doses measured by weight were still commonly used until the 1980s. Colony counts typically underestimate the viable count by several orders of magnitude compared to counts by limiting dilution in liquid media (Reddacliff et al., 2003). This means that most of the doses reported in the existing literature are underestimates. The tendency of *Mptb* to form clumps is another reason why actual doses are likely always to be higher than specified.

The number of doses used to create the infection has also varied from 1 - 25 doses, with the time between doses ranging from one day to monthly (Tables 1-4). The time between doses may also alter the effect of the infection. Where doses are separated by long intervals this may give the host time to mount an effective immune response especially if the doses are small or of a less virulent strain of *Mptb* (Mackintosh and Griffin, 2003, personal communication). Therefore the time between repeat dosing should be short.

The factors that have probably led to pragmatic use of high doses of freshly prepared inoculum are the lengthy periods required to obtain a viable count of *Mptb*, typically 8-12 weeks, the uncertain effects of storing an inoculum for this period prior to challenge of animals and the perceived risk to a research program of not establishing infection. Microscopic counts have sometimes been used, but no information is obtained about the viable count from a visual count.

The route of infection may influence the effective dose due to losses of inoculum or failure of the inoculum to come into close contact with the host. For a given effect the oral route likely will require more bacteria than the intravenous or intraperitoneal routes as a portion of the bacteria will be lost by spillage or regurgitation from the oral cavity and by passing straight through the gut. It has been shown by Sweeny et al., (1992) and Reddacliff and Whittington (2003) that the number of bacteria measured in the faeces in the first five days post inoculation was dependent on the oral dose given to the animal (Sweeney et al., 1992). It would be very hard to compare the losses of bacteria in faecal excretion to the systemic loss that would occur in intravenous and intraperitoneal inoculation.

Desired outcomes of the research

The desired outcome of a study will ultimately determine the final design of the experimental infection model. The broad categories of outcome that could be tested using infection models include vaccine efficacy, pathology of disease, genetic susceptibility, immunological changes and evaluation of diagnostic assays. All of these outcomes will require different approaches to infection

and involve choices of the species and breed of animal to be tested, the strain of *Mptb*, the dose given and the duration of the experiment. This means that no single experimental model will become accepted as the universal method.

Vaccine efficacy

The animal species and strain of *Mptb* used will need to be based on the region and may be determined by regulatory authorities that require objective efficacy or safety data in the target species. A vaccine developed for cattle against a C strain of *Mptb* may not provide protection against S strains of *Mptb* or be as efficacious in other animal species such as sheep. In the absence of specific information about cross protection obtained through generic research, local authorities may not accept data for a vaccine from a species or breed of animal not commonly seen in the region, infected with a strain of *Mptb* normally found in another region or country. An example is the extensive validation data required for the acceptance of a vaccine developed in Spain for use in Australia (Reddacliff et al., 2006).

Another important consideration when testing vaccines is the end point of the experimental model. It is possible to test vaccine efficacy by counting the number of clinically diseased animals, examining the grade of histopathological lesions (Gwozdz et al., 2000), enumerating bacteria recovered post mortem (hence infection only) (Gilmour et al., 1965), assessing faecal shedding rates or measuring immunological responses (Reddacliff et al., 2006). There still has not been a study that has conclusively shown that higher numbers of bacteria detected at an early stage of infection are correlated with worse disease outcome. Animals with paucibacillary lesions may develop clinical disease although they have few bacteria present. Animals with clinical disease can have a range of pathological lesions (Clarke and Little, 1996). Consequently very long time courses for vaccine efficacy studies are needed together with comprehensive examination of subjects (eg Reddacliff et al. 2006). Finally the dose and route of *Mptb* inoculation used in the model cannot be so different from natural infection as to impinge on reasonable vaccine efficacy.

Pathogenesis

Many experimental models of infection have been conducted to test pathological and bacteriological outcomes in various animal species/breeds and with various strains of *Mptb*. Although there have been large numbers of these experiments very few used the same time points for sampling or end point for necropsy. The question must be asked: does infection (microbiological presence/absence and intensity) and histological lesion (graded) at a single time point provide enough information to assess the disease outcome? Longitudinal studies and sequential biopsies may be required to elucidate pathogenesis along with greater standardisation of what constitutes the end point of this type of experiment.

Genetic susceptibility/immunological changes

Experimental challenge models may be used to test the susceptibility of species or breed lines to *Mptb* infection; they may also be used to examine immunological changes occurring in the animal as the disease develops. This type of work will require an experimental infection model where changes at early time points are highly predictive of disease outcomes. This will allow for short term experiments where the infected animal can be necropsied days or weeks after inoculation to examine changes in the host intestinal response to infection. It has been shown that not all inoculated animals develop infection or disease (Hirch, 1956; Begg et al., 2005).

Laboratory animal models will be an invaluable part of the discovery work in these areas helping to identify genes and immunological pathways that may be vital to the eventual outcome after infection. Following gene and pathway identification in laboratory animals, validation testing in ruminants will be required. In designing the infection model used, the route and dose of inoculation will be vital to the eventual outcome of the experimental work. Using an inappropriate route may result in altered pathways of protection being activated thus skewing the eventual results, while using excessively large doses may result in masking of any potential protective responses that may be present.

Evaluation of diagnostic assays

As natural infection in most species is characterised by considerable between-animal variation in pathology and immune responsiveness, and changes in these parameters over time, a suitable model is one in the same species, that produces variation between subjects in disease outcome. It is necessary to induce a range of pathology in subjects, including those with minimal pathology in the early stages of infection to others with severe and widespread lesions, and subcategories of each with and without large numbers of acid fast bacilli in macrophages. Test performance will vary with lesion stage and over time, and so it is important that the experimental cohort is sampled longitudinally or biased estimates of test validity will be obtained (Whittington and Sergeant, 2001).

Infection models will have to be developed to suit local conditions as has been observed in the New Zealand deer industry where natural infection can be particularly severe in young animals (Mackintosh et al., 2004). An ELISA with high sensitivity and specificity levels has been developed using experimentally and naturally infected deer herds (Griffin et al., 2005).

Other important considerations

In experimental animal research there is always a trade-off between what can be achieved with the resources available and what is ideal. This is especially true for Johne's disease where there is a long interval between inoculation and disease development. Unfortunately there is no ideal infection model for Johne's disease. The lengthy incubation period and the costs involved with maintaining subjects of any species for several years means that development and validation of an infection model is difficult. Validation of the model itself requires that it be shown to be repeatable.

Many of the studies shown in Tables 1-4 have never been replicated using the same parameters and so have little claim to designation as true models. Although the incubation period can be shortened by increasing the dose, this may result in the overwhelming of natural immunity. Generally researchers cannot afford an experimental infection to fail, as it would waste large amounts of money and time. This is why a large number of experiments have used tissue homogenates, high doses of inoculum and routes of inoculation guaranteed to bring the organism into close proximity to the host and cause infection.

Studies have been lacking in the use of a defined type strain of *Mptb* in pure culture prepared from an archived seed stock of *Mptb* that can be used again at the same passage level in a later trial. Replication of experimental groups has been very uncommon, temporal replication equally rare, as

have been sufficiently long time scales so as to be able to observe a full range of immunological and pathological changes at different stages of the disease process.

Finally the financial cost of doing the research is a key limiting factor. While it may be difficult to develop a satisfactory experimental infection model, there is room for improvement in the way models have been designed and carried out to date.

Acknowledgements

The authors would like to thank the following people for their help with editing this review, Lyrissa Di Fiore, Deborah Taylor, Kumudika de Silva and David Emery.

References

Adams, J., Follett, D., Hamilton, H. and Czuprynski, C. 1993. Effects of administration of anti-CD4 and anti-CD8 monoclonal antibodies on *Mycobacterium paratuberculosis* infection in intragastrically challenged mice. Immunology Letters 35, 183-9.

Beard, P. M., Rhind, S. M., Sinclair, M. C., Wildblood, L. A., Stevenson, K., McKendrick, I. J., Sharp, J. M. and Jones, D. G. 2000. Modulation of gammadelta T cells and CD1 in *Mycobacterium avium* subsp. *paratuberculosis* infection. Veterinary Immunology and Immunopathology 77, 311-319.

Beard, P. M., Stevenson, K., Pirie, A., Rudge, K., Buxton, D., Rhind, S. M., Sinclair, M. C., Wildblood, L. A., Jones, D. G. and Sharp, J. M. 2001. Experimental Paratuberculosis in Calves following Inoculation with a Rabbit Isolate of *Mycobacterium avium* subsp. *paratuberculosis*. Journal of Clinical Microbiology 39, 3080-4.

Begara-McGorum, I., Wildblood, L. A., Clarke, C. J., Connor, K. M., Stevenson, K., McInnes, C. J., Sharp, J. M. and Jones, D. G. 1998. Early immunopathological events in experimental ovine paratuberculosis. Veterinary Immunology and Immunopathology 63, 265-87.

Begg, D. J., O'Brien, R., Mackintosh, C. G. and Griffin, J. F. 2005. Experimental Infection Model for Johne's Disease in Sheep. Infection and Immunity 73, 5603-11.

Brett, E. (1998). Johne's disease an economic evaluation of control options for the New Zealand livestock industries, Agriculture New Zealand**:** 5.

Brotherston, J. G., Gilmour, N. J. and Samuel, J. 1961. Quantitative Studies of *Mycobacterium johnei* in the Tissues of Sheep. Journal of Comparative Pathology 71, 286 - 299.

Chandler, R. L. 1961a. Infection of laboratory animals with *Mycobacterium johnei*. I. Infection in Swiss white mice and its modification by suramin and cortisone. Journal of Comparative Pathology 71, 118-30.

Chandler, R. L. 1961b. Infection of laboratory animals with *Mycobacterium johnei*. II. Infection in white rats; effect of cortisone treatment. Journal of Comparative Pathology 71, 131-4.

Chandler, R. L. 1961c. Infection of laboratory animals with *Mycobacterium johnei*. IV. Comparative susceptibility to infection of C.57, C.B.A and Swiss white mice. Journal of Comparative Pathology 71, 233-42.

Chiodini, R. J. and Buergelt, C. D. 1993. Susceptibility of Balb/c, C57/B6 and C57/B10 mice to infection with *Mycobacterium paratuberculosis*. Journal of Comparative Pathology 109, 309-19.

Chiodini, R. J., Van Kruiningen, H. J. and Merkal, R. S. 1984. Ruminant paratuberculosis (Johne's disease): the current status and future prospects. Cornell Veterinarian 74, 218-62.

Clarke, C. J. 1997. The pathology and pathogenesis of paratuberculosis in ruminants and other species. Journal of Comparative Pathology 116, 217-61.

Clarke, C. J. and Little, D. 1996. The pathology of ovine paratuberculosis: gross and histological changes in the intestine and other tissues. Journal of Comparative Pathology 114, 419-37.

Collins, P., McDiarmid, A., Thomas, L. H. and Matthews, P. R. 1985. Comparison of the pathogenicity of *Mycobacterium paratuberculosis* and *Mycobacterium* spp isolated from the wood pigeon (*Columba palumbus-L*). Journal of Comparative Pathology 95, 591-7.

Cousins, D. V., Williams, S. N., Hope, A. and Eamens, G. J. 2000. DNA fingerprinting of Australian isolates of *Mycobacterium avium* subsp *paratuberculosis* using IS900 RFLP. Australian Veterinary Journal 78, 184-90.

Davidson, M. K., Lindsey, J. R. and Davis, J. K. 1987. Requirements and selection of an animal model. Israel Journal of Medical Sciences 23, 551-5.

Dukes, T. W., Glover, G. J., Brooks, B. W., Duncan, J. R. and Swendrowski, M. 1992. Paratuberculosis in saiga antelope (*Saiga tatarica*) and experimental transmission to domestic sheep. Journal of Wildlife Diseases 28, 161-70.

Francis, J. 1943. Infection of laboratory animals with *Mycobacterium johnei*. Journal of Comparative Pathology 53, 140-150.

Frelier, P. F., Templeton, J. W., Estes, M., Whitford, H. W. and Kienle, R. D. 1990. Genetic regulation of *Mycobacterium paratuberculosis* infection in recombinant inbred mice. Veterinary Pathology 27, 362-364.

Gilmour, N. J. and Brotherston, J. G. 1962. Quantitative studies of *Mycobacterium johnei* in the tissues of sheep. IV. The distribution of M. johnei shortly after oral dosing. Journal of Comparative Pathology 72, 165-9.

Gilmour, N. J., Campbell, J. and Brotherston, J. G. 1963. The pathogenesis of *Mycobacterium johnei* in orally dosed hamsters. Journal of Comparative Pathology 73, 98-106.

Gilmour, N. J., Nisbet, D. I. and Brotherston, J. G. 1965. Experimental oral infection of calves with *Mycobacterium johnei*. Journal of Comparative Pathology 75, 281-6.

Gilmour, N. J. L. and Angus, K. W. 1976. The specificity and sensitivity of the fluorescent antibody test in cattle experimentally infected with *Mycobacterium avium* and *Mycobacterium johnei*. Research in Veterinary Science 20, 6-9.

Gilmour, N. J. L., Angus, K. W. and Mitchell, B. 1977. Intestinal infection and host response to oral administration of *Mycobacterium Johnei* in sheep. Veterinary Microbiology 2, 223-235.

Griffin, J. F., Spittle, E., Rodgers, C. R., Liggett, S., Cooper, M., Bakker, D. and Bannantine, J. P. 2005. Immunoglobulin G1 enzyme-linked immunosorbent assay for diagnosis of Johne's Disease in red deer (*Cervus elaphus*). Clinical and Diagnostic Laboratory Immunology 12, 1401-9.

Gwozdz, J. M., Thompson, K. G. and Manktelow, B. W. 2001. Lymphocytic neuritis of the ileum in sheep with naturally acquired and experimental paratuberculosis. Journal of Comparative Pathology 124, 317-20.

Gwozdz, J. M., Thompson, K. G., Manktelow, B. W., Murray, A. and West, D. M. 2000. Vaccination against paratuberculosis of lambs already infected experimentally with *Mycobacterium avium* subspecies *paratuberculosis*. Australian Veterinary Journal 78, 560-6.

Hagan, W. A. 1938. Age as a factor in susceptibility to Johne's disease. Cornell Veterinarian 28, 34-40.

Hamilton, H. L., Cooley, A. J., Adams, J. L. and Czuprynski, C. J. 1991. *Mycobacterium paratuberculosis* monoassociated nude mice as a paratuberculosis model. Veterinary Pathology 28, 146-55.

Hamilton, H. L., Follett, D. M., Siegfried, L. M. and Czuprynski, C. J. 1989. Intestinal multiplication of *Mycobacterium paratuberculosis* in athymic nude gnotobiotic mice. Infection and Immunity 57, 225-30.

Hein, W. R. and Griebel, P. J. 2003. A road less travelled: large animal models in immunological research. Nature Reviews. Immunology 3, 79-84.

Hirch, A. 1956. Infection of hamsters and rabbits with *Mycobacterium johnei*. Journal of Comparative Pathology 66, 260-269.

Johnson, D. W., Muscoplat, C. C., Larsen, A. B. and Thoen, C. O. 1977. Skin testing, fecal culture, and lymphocyte immunostimulation in cattle inoculated with *Mycobacterium paratuberculosis*. American Journal of Veterinary Research 38, 2023-2025.

Juste, R. A., Garcia Marin, J. F., Peris, B., Saez de Ocariz, C. S. and Badiola, J. J. 1994. Experimental infection of vaccinated and non-vaccinated lambs with *Mycobacterium paratuberculosis*. Journal of Comparative Pathology 110, 185-94.

Kanai, T. and Watanabe, M. 2005. Clinical application of human CD4+ CD25+ regulatory T cells for the treatment of inflammatory bowel diseases. Expert Opinion on Biological Therapy. 5, 451-62.

Karpinski, T. and Zorawski, C. 1975. Experimental paratuberculosis of sheep. I. Clinical, allergical, bacteriological and post-mortem examinations. Bulletin of the Veterinary Institute in Pulawy 19, 59-63.

Klausen, J., Perez, V., Giese, S. B., Marin, J. F. G. and Ahrens, P. 1997. Immunological detection of sheep experimentally infected with strains of *Mycobacterium avium* subspecies containing insertion sequence IS901/IS902 and a 40 kDa protein. Veterinary Microbiology 57, 181-187.

Kluge, J. P., Merkal, R. S., Monlux, W. S., Larsen, A. B., Kopecky, K. E., Ramsey, F. K. and Lehmann, R. P. 1968. Experimental paratuberculosis in sheep after oral, intratracheal, or intravenous inoculation lesions and demonstration of etiologic agent. American Journal of Veterinary Research 29, 953-62.

Koets, A. P., Adugna, G., Janss, L. L., van Weering, H. J., Kalis, C. H., Wentink, G. H., Rutten, V. P. and Schukken, Y. H. 2000a. Genetic variation of susceptibility to *Mycobacterium avium* subsp. *paratuberculosis* infection in dairy cattle. Journal of Dairy Science 83, 2702-8.

Koets, A. P., Rutten, V. P., Bakker, D., van der Hage, M. H. and van Eden, W. 2000b. Lewis rats are not susceptible to oral infection with *Mycobacterium avium* subsp. *paratuberculosis*. Veterinary Microbiology 77, 487-495.

Koo, H. C., Park, Y. H., Ahn, J., Waters, W. R., Hamilton, M. J., Barrington, G., Mosaad, A. A., Palmer, M. V., Shin, S. and Davis, W. C. 2004. New latex bead agglutination assay for differential diagnosis of cattle infected with *Mycobacterium bovis* and *Mycobacterium avium* subsp. *paratuberculosis*. Clinical and Diagnostic Laboratory Immunology 11, 1070-4.

Krishnappa, G., Jagannath, C. and Rao, B. U. 1989. The specificity of antibody response in experimental and natural bovine paratuberculosis studied by crossed immunoelectrophoresis with intermediate gel. Veterinary Microbiology 21, 67-78.

Kurade, N. P., Tripathi, B. N., Rajukumar, K. and Parihar, N. S. 2004. Sequential development of histologic lesions and their relationship with bacterial isolation, fecal shedding, and immune responses during progressive stages of experimental infection of lambs with *Mycobacterium avium* subsp. *paratuberculosis*. Veterinary Pathology 41, 378-87.

Larsen, A. B., Merkal, R. S. and Cutlip, R. C. 1975. Age of cattle as related to resistance to infection with *Mycobacterium paratuberculosis*. American Journal of Veterinary Research 36, 255-7.

Larsen, A. B. and Miller, J. M. 1978. Effect of dexamethasone on *Mycobacterium paratuberculosis* infection in hamsters. American Journal of Veterinary Research 39, 1866-1867.

Larsen, A. B., Miller, J. M. and Merkal, R. S. 1977. Subcutaneous exposure of calves to *Mycobacterium paratuberculosis* compared with intravenous and oral exposures. American Journal of Veterinary Research 38, 1669-71.

Larsen, A. B. and Moon, H. W. 1972. Experimental *Mycobacterium paratuberculosis* infection in chickens. American Journal of Veterinary Research 33, 1231-5.

Larsen, A. B., Moon, H. W. and Merkal, R. S. 1971. Susceptibility of swine to *Mycobacterium paratuberculosis*. American Journal of Veterinary Research 32, 589-595.

Larsen, A. B., Moon, H. W. and Merkal, R. S. 1972. Susceptibility of horses to *Mycobacterium paratuberculosis*. American Journal of Veterinary Research 33, 2185-9.

Lepper, A. W., Wilks, C. R., Kotiw, M., Whitehead, J. T. and Swart, K. S. 1989. Sequential bacteriological observations in relation to cell-mediated and humoral antibody responses of cattle infected with *Mycobacterium paratuberculosis* and maintained on normal or high iron intake. Australian Veterinary Journal 66, 50-5.

Lominski, I., Cameron, J. and Roberts, G. B. S. 1956. Experimental Johne's disease in mice. Journal of Pathology and Bacteriology 71, 211-222.

Mackintosh, C. G., de Lisle, G. W., Collins, D. M. and Griffin, J. F. 2004. Mycobacterial diseases of deer. New Zealand Veterinary Journal 52, 163-74.

Madge, D. S. 1971. Malabsorption in C57 mice experimentally infected with Johne's disease. Comparative Biochemistry and Physiology 40A, 649-658.

Maloy, K. J., Antonelli, L. R., Lefevre, M. and Powrie, F. 2005. Cure of innate intestinal immune pathology by CD4+CD25+ regulatory T cells. Immunology Letters 97, 189-92.

Marsh, I., Whittington, R. and Cousins, D. 1999. PCR-restriction endonuclease analysis for identification and strain typing of *Mycobacterium avium* subsp. *paratuberculosis* and *Mycobacterium avium* subsp. *avium* based on polymorphisms in IS*1311*. Molecular and Cellular Probes 13, 115-26.

Martin, B., Banz, A., Bienvenu, B., Cordier, C., Dautigny, N., Becourt, C. and Lucas, B. 2004. Suppression of CD4+ T lymphocyte effector functions by CD4+CD25+ cells in vivo. Journal of Immunology 172, 3391-8.

Merkal, R. S., Miller, J. M., Hintz, A. M. and Bryner, J. H. 1982. Intrauterine inoculation of *Mycobacterium paratuberculosis* into guinea pigs and cattle. American Journal of Veterinary Research 43, 676-678.

Mokresh, A. H. and Butler, D. G. 1990. Granulomatous enteritis following oral inoculation of newborn rabbits with *Mycobacterium paratuberculosis* of bovine origin. Canadian Journal of Veterinary Research 54, 313-9.

Mokresh, A. H., Czuprynski, C. J. and Butler, D. G. 1989. A rabbit model for study of *Mycobacterium paratuberculosis* infection. Infection and Immunity 57, 3798-807.

Munjal, S. K., Tripathi, B. N. and Paliwal, O. P. 2005. Progressive immunopathological changes during early stages of experimental infection of goats with *Mycobacterium avium* subspecies *paratuberculosis*. Veterinary Pathology 42, 427-36.

Mutwiri, G. K., Butler, D. G., Rosendal, S. and Yager, J. 1992. Experimental infection of severe combined immunodeficient beige mice with *Mycobacterium paratuberculosis* of bovine origin. Infection and Immunity 60, 4074-9.

Mutwiri, G. K., Kosecka, U., Benjamin, M., Rosendal, S., Perdue, M. and Butler, D. G. 2001. *Mycobacterium avium* subspecies *paratuberculosis* triggers intestinal pathophysiologic changes in beige/scid mice. Comparative Medicine 51, 538-544.

O'Brien, R., Mackintosh, C. G., Bakker, D., Kopecna, M., Pavlik, I. and Griffin, J. F. 2006. Immunological and molecular characterization of susceptibility in relationship to bacterial strain differences in *Mycobacterium avium* subsp. *paratuberculosis* infection in the red deer (*Cervus elaphus*). Infection and Immunity 74, 3530-7.

Payne, J. M. and Rankin, J. D. 1961a. A comparison of the pathogenesis of experimental Johne's disease in calves and cows. Research in Veterinary Science 2, 175-179.

Payne, J. M. and Rankin, J. D. 1961b. The pathogenesis of experimental Johne's disease in calves. Research in Veterinary Science 2, 167-174.

Rankin, J. D. 1958a. The experimental infection of cattle with *Mycobacterium johnei*. I. Calves inoculated intravenously. Journal of Comparative Pathology 68, 331-7.

Rankin, J. D. 1958b. The experimental production of Johne's disease in laboratory rabbits. Journal of Pathology and Bacteriology 75, 363-6.

Rankin, J. D. 1961. The experimental infection of cattle with *Mycobacterium johnei*. II. Adult cattle inoculated intravenously. Journal of Comparative Pathology 71, 6-9.

Reddacliff, L., Eppleston, J., Windsor, P., Whittington, R. and Jones, S. 2006. Efficacy of a killed vaccine for the control of paratuberculosis in Australian sheep flocks. Veterinary Microbiology 115, 77-90.

Reddacliff, L. A., Nicholls, P. J., Vadali, A. and Whittington, R. J. 2003. Use of Growth Indices from Radiometric Culture for Quantification of Sheep Strains of *Mycobacterium avium* subsp. *paratuberculosis*. Applied and Environmental Microbiology 69, 3510-6.

Reddacliff, L. A. and Whittington, R. J. 2003. Experimental infection of weaner sheep with S strain *Mycobacterium avium* subsp. *paratuberculosis*. Veterinary Microbiology 96, 247-58.

Rosseels, V., Marche, S., Roupie, V., Govaerts, M., Godfroid, J., Walravens, K. and Huygen, K. 2006. Members of the 30- to 32-kilodalton mycolyl transferase family (Ag85) from culture filtrate of *Mycobacterium avium* subsp. *paratuberculosis* are immunodominant Th1-type antigens recognized early upon infection in mice and cattle. Infection and Immunity 74, 202-12.

Sevilla, I., Singh, S. V., Garrido, J. M., Aduriz, G., Rodriguez, S., Geijo, M. V., Whittington, R. J., Saunders, V., Whitlock, R. H. and Juste, R. A. 2005. Molecular typing of *Mycobacterium avium* subspecies *paratuberculosis* strains from different hosts and regions. Revue Scientifique et Technique 24, 1061-6.

Sigurdardottir, O. G., Press, C. M., Saxegaard, F. and Evensen, O. 1999. Bacterial isolation, immunological response, and histopathological lesions during the early subclinical phase of experimental infection of goat kids with *Mycobacterium avium* subsp. *paratuberculosis*. Veterinary Pathology 36, 542-50.

Simutis, F. J., Cheville, N. F. and Jones, D. E. 2005. Investigation of antigen-specific T-cell responses and subcutaneous granuloma development during experimental sensitization of calves with *Mycobacterium avium* subsp *paratuberculosis*. American Journal of Veterinary Research 66, 474-82.

Stabel, J. R., Goff, J. P. and Ackermann, M. R. 1998. Dietary calcium modulates *Mycobacterium paratuberculosis* infection in beige mice. Veterinary Immunology and Immunopathology 66, 377-90.

Stabel, J. R., Palmer, M. V. and Whitlock, R. H. 2003. Immune responses after oral inoculation of weanling bison or beef calves with a bison or cattle isolate of *Mycobacterium avium* subsp. *paratuberculosis*. Journal of Wildlife Diseases 39, 545-55.

Stewart, D. J., Vaughan, J. A., Stiles, P. L., Noske, P. J., Tizard, M. L., Prowse, S. J., Michalski, W. P., Butler, K. L. and Jones, S. L. 2004. A long-term study in Merino sheep experimentally infected with *Mycobacterium avium* subsp. *paratuberculosis*: clinical disease, faecal culture and immunological studies. Veterinary Microbiology 104, 165-78.

Stewart, D. J., Vaughan, J. A., Stiles, P. L., Noske, P. J., Tizard, M. L., Prowse, S. J., Michalski, W. P., Butler, K. L. and Jones, S. L. 2006. A long-term study in Angora goats experimentally infected with *Mycobacterium avium* subsp. *paratuberculosis*: clinical disease, faecal culture and immunological studies. Veterinary Microbiology 113, 13-24.

Storset, A. K., Hasvold, H. J., Valheim, M., Brun-Hansen, H., Berntsen, G., Whist, S. K., Djonne, B., Press, C. M., Holstad, G. and Larsen, H. J. 2001. Subclinical paratuberculosis in goats following experimental infection. An immunological and microbiological study. Veterinary Immunology and Immunopathology 80, 271-87.

Stuart, P. 1965. Vaccination against Johne's Disease in Cattle Exposed to Experimental Infection. The British Veterinary Journal 121, 289-318.

Sweeney, R. W., Uzonna, J., Whitlock, R. H., Habecker, P. L., Chilton, P. and Scott, P. 2006. Tissue predilection sites and effect of dose on *Mycobacterium avium* subs. *paratuberculosis* organism recovery in a short-term bovine experimental oral infection model. Research in Veterinary Science 80, 253-9.

Sweeney, R. W., Whitlock, R. H., Hamir, A. N., Rosenberger, A. E. and Herr, S. A. 1992. Isolation of *Mycobacterium paratuberculosis* after oral inoculation in uninfected cattle. American Journal of Veterinary Research 53, 1312 - 1314.

Tanaka, S., Itohara, S., Sato, M., Taniguchi, T. and Yokomizo, Y. 2000. Reduced formation of granulomata in gamma(delta) T cell knockout BALB/c mice inoculated with *Mycobacterium avium* subsp. *paratuberculosis*. Veterinary Pathology 37, 415-21.

Tanaka, S., Sato, M., Taniguchi, T. and Yokomizo, Y. 1994. Histopathological and morphometrical comparison of granulomatous lesions in BALB/c and C3H/HeJ mice inoculated with *Mycobacterium paratuberculosis*. Journal of Comparative Pathology 110, 381-388.

Thomsen, B. V., Steadham, E. M., Gallup, J. M., Ackermann, M. R., Brees, D. J. and Cheville, N. F. 2001. T Cell-dependent Inducible Nitric Oxide Synthase Production and Ultrastructural Morphology in BALB/c Mice Infected with Mycobacterium avium subspecies paratuberculosis. Journal of Comparative Pathology 125, 137-44.

Thorel, M. F., Vialard, J., Manfroni, F., Bernardot, J., Ostyn, A. and Vandevelde, J. 1992. [Experimental paratuberculosis in sheep after intravenous or oral inoculation: pathogenicity and biologic diagnosis]. Annales de Recherches Vétérinaires 23, 105-15.

Uzonna, J. E., Chilton, P., Whitlock, R. H., Habecker, P. L., Scott, P. and Sweeney, R. W. 2003. Efficacy of commercial and field-strain *Mycobacterium paratuberculosis* vaccinations with recombinant IL-12 in a bovine experimental infection model. Vaccine 21, 3101-9.

Valente, C., Cuteri, V., Giandomenico, R. Q., Gialletti, L. and Franciosini, M. P. 1997. Use of an experimental chicks model for paratuberculosis enteritis (Johne's disease). Veterinary Research 28, 239-246.

Van Kruiningen, H. J., Ruiz, B. and Gumprecht, L. 1991. Experimental disease in young chickens induced by a *Mycobacterium paratuberculosis* isolate from a patient with Crohn's disease. Canadian Journal of Veterinary Research 55, 199-202.

Vaughan, J. A., Lenghaus, C., Stewart, D. J., Tizard, M. L. and Michalski, W. P. 2005. Development of a Johne's disease infection model in laboratory rabbits following oral administration of *Mycobacterium avium* subspecies *paratuberculosis*. Veterinary Microbiology 105, 207-13.

Veazey, R. S., Horohov, D. W., Krahenbuhl, J. L., Taylor, H. W., Oliver, J. L., 3rd and Snider, T. G., 3rd 1995a. Comparison of the resistance of C57BL/6 and C3H/He mice to infection with *Mycobacterium paratuberculosis*. Veterinary Microbiology 47, 79-87.

Veazey, R. S., Taylor, H. W., Horohov, D. W., Krahenbuhl, J. L., Oliver, J. L., 3rd and Snider, T. G., 3rd 1995b. Histopathology of C57BL/6 mice inoculated orally with *Mycobacterium paratuberculosis*. Journal of Comparative Pathology 113, 75-80.

Waters, W. R., Miller, J. M., Palmer, M. V., Stabel, J. R., Jones, D. E., Koistinen, K. A., Steadham, E. M., Hamilton, M. J., Davis, W. C. and Bannantine, J. P. 2003. Early induction of humoral and cellular immune responses during experimental *Mycobacterium avium* subsp. *paratuberculosis* infection of calves. Infection and Immunity 71, 5130-8.

Whittington, R. J., Hope, A. F., Marshall, D. J., Taragel, C. A. and Marsh, I. 2000. Molecular epidemiology of *Mycobacterium avium* subsp. *paratuberculosis*: IS900 restriction fragment length polymorphism and IS1311 polymorphism analyses of isolates from animals and a human in Australia. Journal of Clinical Microbiology 38, 3240-8.

Whittington, R. J. and Sergeant, E. S. 2001. Progress towards understanding the spread, detection and control of *Mycobacterium avium* subsp *paratuberculosis* in animal populations. Australian Veterinary Journal 79, 267-78.

Whittington, R. J., Taragel, C. A., Ottaway, S., Marsh, I., Seaman, J. and Fridriksdottir, V. 2001. Molecular epidemiological confirmation and circumstances of occurrence of sheep (S) strains of *Mycobacterium avium* subsp. *paratuberculosis* in cases of paratuberculosis in cattle in Australia and sheep and cattle in Iceland. Veterinary Microbiology 79, 311-22.

Williams, E. S., Snyder, S. P. and Martin, K. L. 1983a. Experimental infection of some North American wild ruminants and domestic sheep with *Mycobacterium paratuberculosis*: clinical and bacteriological findings. Journal of Wildlife Diseases 19, 185-91.

Williams, E. S., Snyder, S. P. and Martin, K. L. 1983b. Pathology of spontaneous and experimental infection of North American wild ruminants with *Mycobacterium paratuberculosis*. Veterinary Pathology 20, 274-90.

9.12 Appendix 2B-2 Subprogram 2 Johnes disease in sheep: Development of an experimental infection model using a pure clonal strain of Mycobacterium avium subspecies paratuberculosis

Introduction

Johne's disease is a severe intestinal enteritis cause by *Mycobacterium avium* subspecies *paratuberculosis* (*M.ptb*) infection. It occurs predominantly in ruminants including sheep, cattle, deer, goats and camilids. The disease results in the wasting and the eventual death of the animal. This has a major economic impact on the agricultural industry with farms found to have the disease experience problems with reduced reproduction rates, milk production levels and increased turnover of production animals (Ott et al., 1999; Bush et al., 2006). The cost of ovine Johne's disease (OJD) on an average sheep farm in Australia is approximately 13,700 AU dollars per year (Bush et al., 2006).

A number of researchers have used experimentally infected sheep to examine a range of pathological, bacteriological and immunological aspects of Johne's disease in sheep (Karpinski and Zorawski, 1975; Williams et al., 1983; Juste et al., 1994; Begara-McGorum et al., 1998; Gwozdz et al., 2000; Gwozdz and Thompson, 2002; Reddacliff and Whittington, 2003; Kurade et al., 2004; Stewart et al., 2004; Begg et al., 2005). Very few of these studies have taken the time to develop a reproducible and defined experimental infection model which mimics natural *M.ptb* infection. The experimental infections are biased by the species of animal used, the strain of *M.ptb*, the route of inoculation and timing of the endpoint of the trial. These may lead to biases in the data generated from the experimental model.

Currently the experimental infection models used for sheep lack reproducible results and in some experiments there has been a failure to cause any infection (Brotherston et al., 1961; Thorel et al., 1992; Reddacliff and Whittington, 2003; Begg et al., 2005). The reasons for the failures or variable disease outcomes are multifactorial and include using a highly passaged laboratory adapted culture strain or conversely tissue homogenates (ground up intestinal tissue from a diseased animal) of *M.ptb*, the use of extremely high or low doses of bacteria and the animal breed used for the infection. Although the use of tissue homogenates generally results in the infection of animals the following problems have been noted; a limited amount of infective material, difficulties in enumerating the number of viable *M.ptb* and the possibility of infecting the sheep with other gut associated micro-organisms (Begg and Whittington, 2007). It has been identified (Begg and Whittington, 2007; Hines et al., 2007) that using a low passage culture strain of *M.ptb* (preferably a defined type strain) in groups of susceptible animals (preferably of the same species/ breed /sire) will hopefully ensure reproducible results. The use of low passage culture sheep strains of *M.ptb* has been rare with few experimental infections and limited success, although this was probably due to the animals being culled before the disease could manifest (Reddacliff and Whittington, 2003) (Stewart et al., 2004).

This experiment was designed to create an experimental model for Johne's disease in sheep for Australian conditions that will be repeatable, reliable and standardised using the above suggestions. Variable necropsy times have been used so as to include animals with subclinical disease through to animals in the early stages of clinical disease with a range of gut and extra intestinal tissues taken at necropsy for culture and histopathology.

Methods

All animal experiments carried out for this study were approved by The University of Sydney animal ethic committee

Experimental animals: One hundred and twenty eight Merino or Merino cross lambs aged 3- 7 months sourced from farms shown to be free of Johne's disease were used for these trials. All animals were shown to be free from *M.ptb* infection by faecal culture and other tests applied to the parent flock. The animals were managed under conventional Australian sheep farming conditions in open paddocks.

Challenge strains

Preparation of the Telford *Mycobacterium paratuberculosis* inoculum.

Myobacterium paratuberculosis strain Telford 9.2, a pure clonal culture at passage level 5 (including its primary isolation from sheep faeces) was reconstituted from lyophilised stock and inoculated into a BACTEC vial supplemented with egg yolk and mycobactin J (MJ) (Whittington et al., 1999). After culture in BACTEC to achieve maximal growth, the vial was subcultured to 7H10+MJ slopes and incubated for 4-6 weeks at 37^{o}C. Telford 9.2 is an IS1311 S strain, IS900 RFLP type S1 (Marsh et al., 2006; Marsh and Whittington, 2007).

The slopes were harvested into single cell suspensions prepared in PBS with 0.1% V/V Tween 80. Enumeration was conducted using a visual count in a Thoma-ruled counting chamber and by end point titration in BACTEC medium (using a standard three tube most probable number [MPN] method) (Reddacliff et al., 2003). The visual counts were used to prepare the inoculation doses at 10^9 *M.ptb* organisms/mL of suspension. One millilitre aliquots of this stock suspension was diluted in 10 ml of PBS for each of the animals to be infected.

The remaining undiluted suspension (stock) was retained at 4°C in order to repeat the inoculation one week later. Another BACTEC MPN was set up on the day of the second dose from the stock suspension stored at 4^{o}C, to confirm the viable dose after storage. IS900 and IS1311 PCR assays were conducted on the stock solution to confirm that the infectious material was *M.ptb* and of the ovine strain.

For further inoculation doses (typically one month later) with the Telford 9.2 strain of *M.ptb*, a fresh suspension was prepared as shown above to be given as required.

Preparation of gut homogenate inoculum.

Using the method of Begg et al (2005) (Begg et al., 2005), gut tissue from animal 986 (sourced from a farm in the Southern Tablelands of NSW, Australia) with multibacillary lesions, shown to be infected by culture and *IS*900 PCR with the ovine strain confirmed by *IS*1311 PCR was stored at -80^{o}C until required. The tissue was defrosted and homogenized using a mortar and pestle in an equal volume of sterile distilled water. The homogenate was filtered through a funnel lined with 2 layers of sterile gauze followed by a 70um cell strainer. The sample was homogenized by vortexing for 30 minutes and passed through a 26 gauge needle 2 times. The number of *M.ptb* cells was enumerated to calculate the number of organisms/mL. This was done using direct visual counts using 4 uL of a 10^{-3} dilution of the homogenate smeared onto 5mm x 5mm square grid which was divided into equal quarters, the smears were then ZN stained and the acid fast bacilli were counted. A BACTEC MPN was also carried out on the sample. The sample was then frozen at -80^{o}C. The MPN showed the gut homogenate (total volume 54mL) to be at $2.3x10^8$ CFU/mL with direct visual count showing $3.67x10^8$ bacteria per mL. On the day prior to the first inoculation the homogenate was thawed diluted with 11mL of PBS giving a total volume of 65mL at $1.9x10^8$CFU/mL. One in ten

dilutions of the homogenate were spread onto TSA plates to enumerate the amount of contaminating bacteria in the sample. The plates were incubated at 37^{o}C for 3 days. Fewer than 1000 CFU/mL of contaminating bacteria were observed

Twenty two millilitres was then frozen at -80^{o}C to be held as the 3rd and final inoculation a further 22mLs was stored for one week at 4^{o}C for the second inoculation. The remaining 21 mLs of suspension were put into 1mL aliquots and were mixed with 9mL of PBS for the first challenge dose, the same procedure was done with the stored doses either refrigerated and frozen stocks, when required.

Table 1: Experimental infection trials used in OJD031

Experiment	Treatment	Sheep breed	Age of animals at challenge	No. of animals	Strain of *M.ptb*	First dose	Second dose	Third dose
031.1	Telford	Merino	3 months	3	Telford 9.2	1.1×10^{10}	1.5×10^{9}	1.5×10^{9}
031.2	High dose Telford	Merino	7 months	3	Telford 9.2	4.3×10^{7}	4.3×10^{7}	4.3×10^{7}
031.2	Medium dose Telford	Merino	7 months	3	Telford 9.2	4.3×10^{5}	4.3×10^{5}	4.3×10^{5}
031.2	Low dose Telford	Merino	7 months	3	Telford 9.2	4.3×10^{4}	4.3×10^{4}	4.3×10^{4}
031.2	Controls	Merino	7 months	3	None given			
031.3*	Telford	Merino X	4 months	23	Telford 9.2	2.3×10^{5}	2.3×10^{5}	2.3×10^{5}
031.4	Telford	Merino	3 months	18	Telford 9.2	9.3×10^{6}	9.3×10^{6}	2.4×10^{8}
031.5	Telford	Merino	3 months	12	Telford 9.2	9.3×10^{7}	4.3×10^{7}	9.3×10^{6}
031.6	Telford	Merino	4 months	20	Telford 9.2	9.3×10^{7}	9.3×10^{7}	1.5×10^{8}
031.6	Gut homogenate	Merino	4 months	20	Gut homogenate	1.9×10^{8}	9.3×10^{7}	9.3×10^{7}
031.6	Control	Merino	4 months	20	None given			

* The 031.3 animals received 2 extra doses of *M.ptb* at 11 and 12 months post inoculation. The fourth dose at 11 months contained 2.4×10^{8}cfu while the fifth dose contained 9.3×10^{7} CFU.

Ante-mortem blood and faecal sampling: Samples were collected every 3- 4 months from all animals to monitor the progress of the infection (Figures 1 and 2).

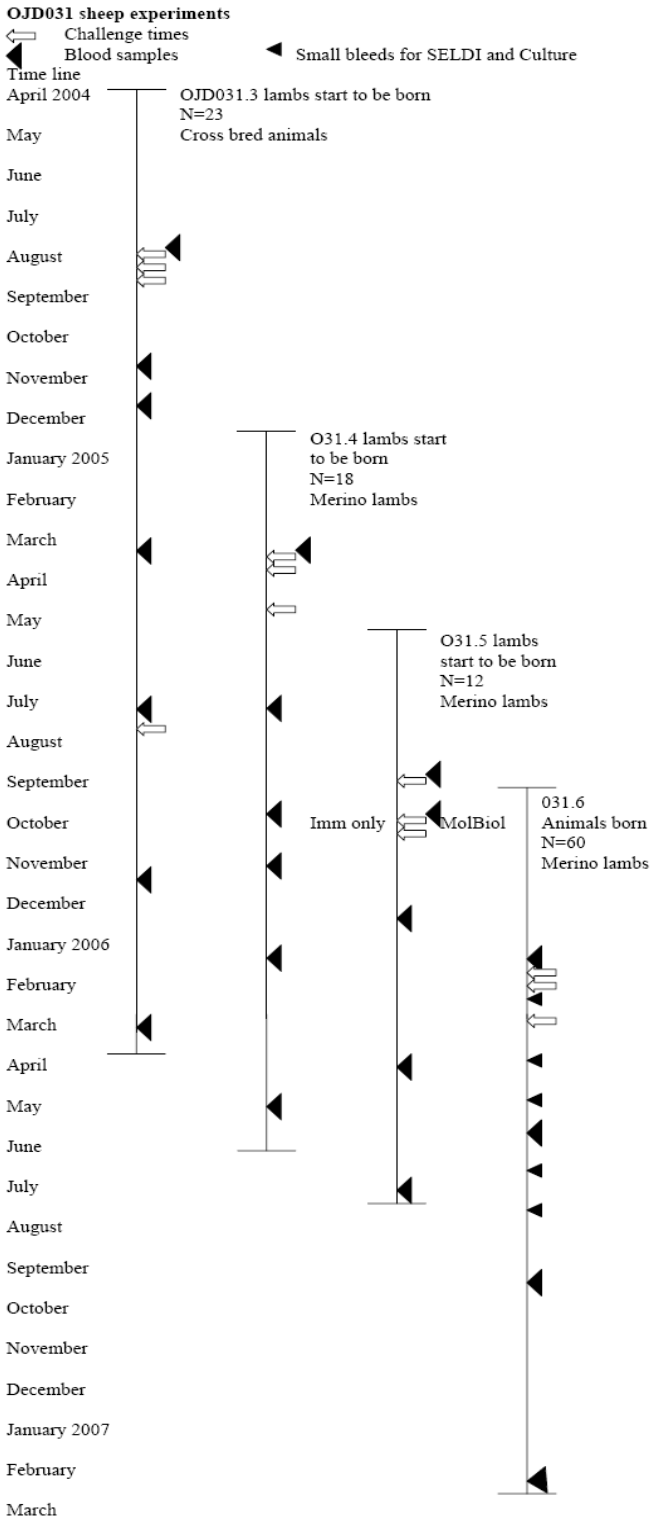

Figure 1: Time lines of the experimental infections 031.3-6, indicating inoculations with blood and faecal sampling times.

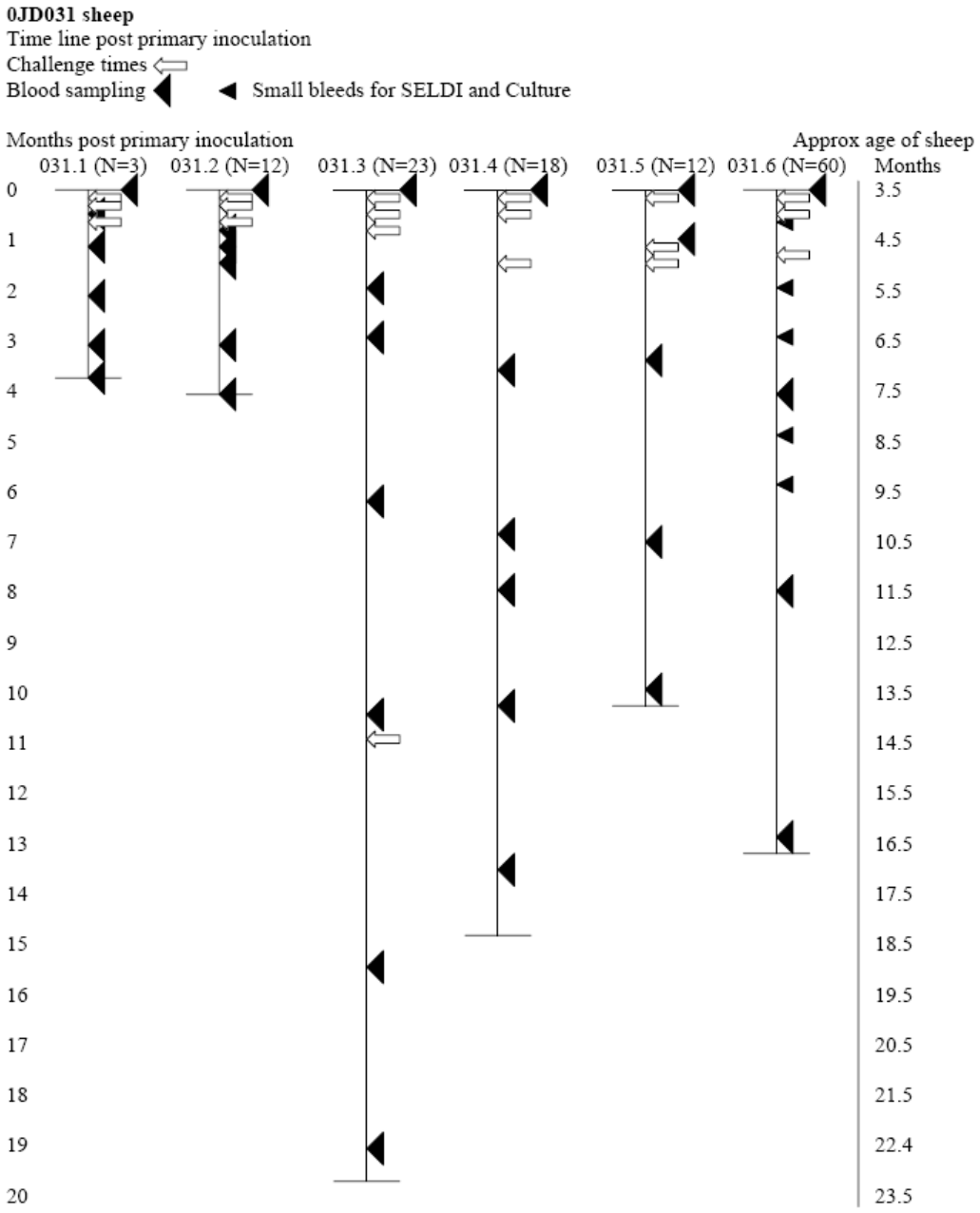

Figure 2: Experimental infection time lines set from the time of the first inoculation for all the 031 experimental infection trials. The left axis indicates the months post inoculation while the right axis indicates the approximate age of the animals.

Necropsy: All animals were euthanased using an intravenous injection of barbiturate into the jugular vein. The intestines from the duodenum to the rectum were removed from the animal and placed in a clean tray. The trays were cleaned with warm water and a virucidal disinfectant, Trigene 2 (Medichem International, UK). Samples were then taken from the following sections of the small intestine terminal ileum, posterior jejunum, mid distal jejunum, middle jejunum, mid proximal jejunum and anterior jejunum and ileocecal lymph node. The ileocaecal lymph node and jejunal lymph nodes corresponding to the sections of jejunum sampled were also collected.

Gross visible lesions: Gross macroscopic pathological changes were classified in one of three categories: *Minor lesions*: A small number of granulomas (<10) may be present in the jejunal lacteal ducts, with slight thickening of the jejunum or enlargement of the JJLN. *Moderate lesions*: Usually granulomas are present in the jejunal lacteal (lymphatic) ducts with enlarged JJLN, ICLN and or thickened ileum or jejunum. The mesentary may also be thickened with some cording apparent. *Severe lesions*: Granulomatous lesions in the lacteal ducts or gut lymph nodes and enlarged JJLN, ICLN and or thickening of the jejunum and ileum. Cording of the mesentery could occur with numerous lacteal granulomas.

Histology: Tissue samples were placed in 10% buffered formalin for 48- 72 hours, embedded in paraffin and sectioned at 8µm. Duplicate sections were stained with hematoxylin and eosin or the Ziehl-Neelsen stain. The sections were then graded using the criteria outline by Perez et al (1996) (Perez et al., 1996). Any section graded with a score of one or higher was considered to be positive.

Isolation of M. paratuberculosis: Samples were collected from animals were frozen at -80^{o}C until they were processed. Faecal samples and tissue samples were processed for Bactec culture as described previously. Briefly after decontamination (if required) samples were inoculated into Bactec Vials and cultured for 12 weeks at 37^{o}C. After culture any positive samples were confirmed by PCR and REA as previously described (Whittington et al., 1998a; Whittington et al., 1998b).

Identification of clinically affected animals: animals showing either visual signs of Johne's disease or showing weight loss of more than 10% over a one month period were deemed to have clinical disease.

Results

The experimental infection with the Telford 9.2 pure clonal strain resulted in disease outcomes resembling those of natural infection. In short term experiments (experiments 031.1, one of the three animals culture positive) and 031.2 very few animals were found to have culturable *M.ptb* from the gut tissues after 14-15 weeks of infection.

Longer term experimental infections produced typical Johne's disease pathology (Table 2), with similar percentages of the animals infected and developing clinical disease depending on the variables including the different necropsy times and challenge doses. The animals in experiment 031.3 had a low infection and clinical disease rate, although this was unsurprising as this group initially had a low challenge dose of 2.3 x 10^5 cfu, while the later trials had doses of 10^7-10^8 cfu. The experimental group that was held for the shortest time post inoculation, 031.5, had the lowest number of clinically diseased animals and the lowest percentage of animals with extra-intestinal infections.

Table 2: Outcomes from the experimental infection of sheep with the Telford 9.2 pure clonal strain of *M.ptb*

Experiment	Duration of the experiment	Clinically diseased %	Tissue culture positive %	Faecal culture positive %	Extra-intestinal infection %
031.1	14 weeks	0	33	33	NT*
031.2	15weeks	0	0	0	0
031.3	19 months	4	48	26	17
031.4	14.5 months	11	50	28	12
031.5	10 months	0	58	33	8
031.6	13 months	17	72	38	17

* NT: not examined

The histology from the sheep infected with the Telford 9.2 pure culture strain also showed a relationship between time to necropsy post inoculation and severity of disease (Figure 3). The 031.5 animals which where housed for 10 months post inoculation had no clinical disease and less severe lesions, made up primarily of 3a lesions compared to the higher proportion of 3b lesions seen in the 031.3, 4 and 5 experimental infection which were housed for longer periods, 13-19 months.

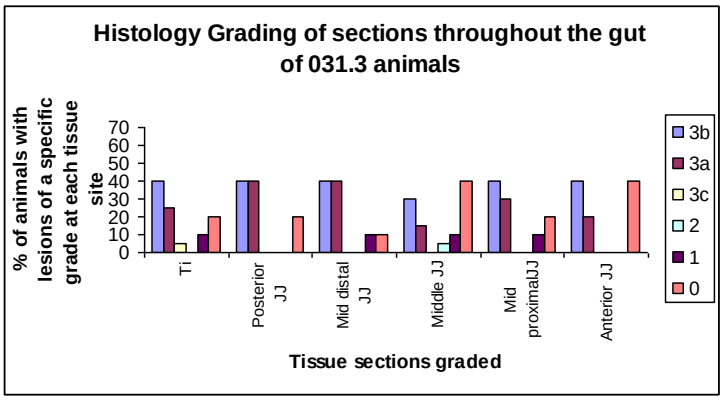

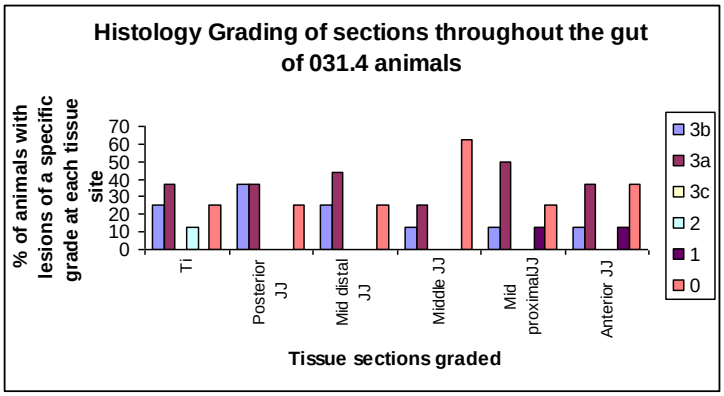

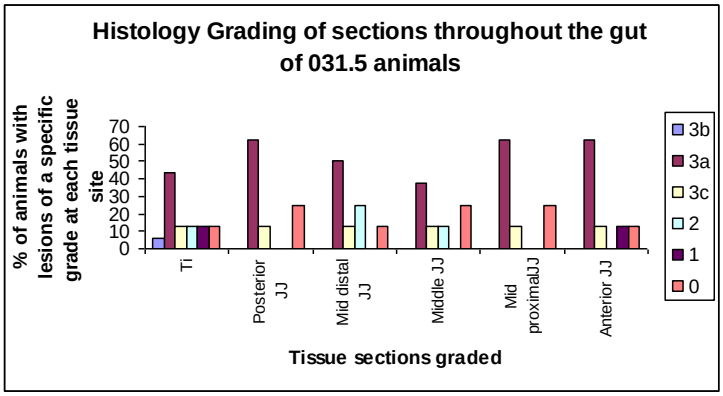

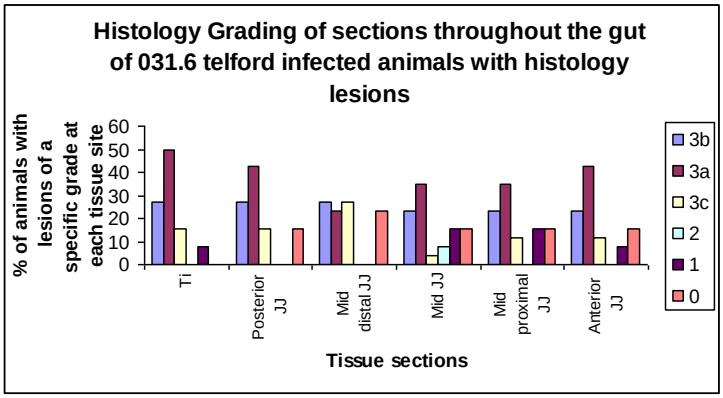

Figure 3: Histological lesions of sections of the small intestines recorded from experimental infection trials. Ti = Terminal ileum, JJ= jejunum

As part of 031.6 experiment, a comparison was made between infection with the Telford 9.2 pure clonal and gut homogenate strains of *M.ptb*. The rate of infection was similar for both of the experimental inoculation strains (72% compared to 68%). The animals infected with the gut homogenate developed more severe disease with clinical signs seen at 8 months compared to 13 months post inoculation for the Telford inoculated sheep. The percentage of animals with clinical disease was higher in the gut homogenate inoculated sheep, with higher rates of faecal and extra-intestinal infections (Table 3). The histological lesions recorded from the gut homogenate was similar to the above results with more 3b or severe lesions seen throughout the gut tissues sampled (Figure 4).

Table 3: Comparative disease and infection outcomes of sheep inoculated with either a pure culture strain or gut homogenate of *M. paratuberculosis*

Treatment group	Clinically diseased %	Tissue culture positive %	Faecal culture positive %	Extra-intestinal infection %
Unchallenged	0	0	0	0
Telford 9.2	17	72	38	17
Gut homogenate	37	65	47	37

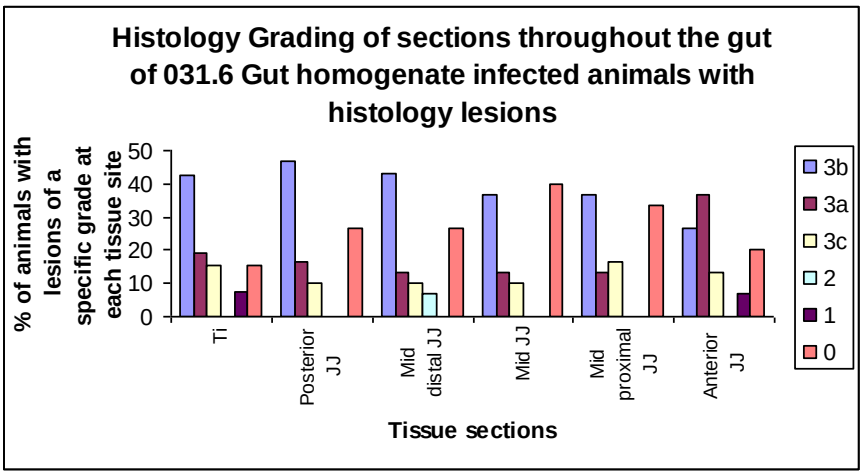

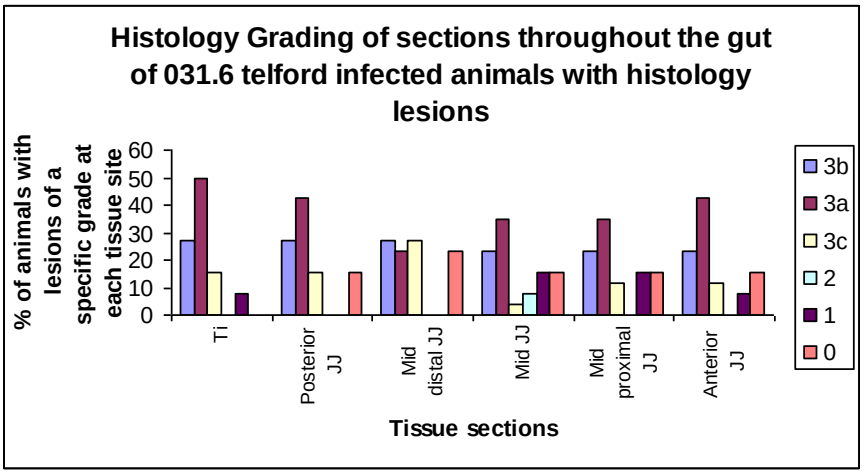

Figure 4: Histological lesions of sections of the small intestines recorded from the 031.6 experimental infection trial from animals infected with Telford 9.2 pure clonal and the gut homogenate strain. Ti = Terminal ileum, JJ= jejunum

Discussion

This series of experiments resulted in repeatable infection trial outcomes which have been obtained using a low passage, pure clonal culture of *M. paratuberculosis* which is archived as a seed stock as recommended in recent reviews on experimental infection models for Johne's disease (Begg and Whittington, 2007; Hines et al., 2007).

Unsurprisingly there were some differences in the numbers of animals developing clinical disease between the experimental infection trials but this can be explained by the interval of time post infection to necropsy and the dose of *M.ptb* given to the animals. An earlier study has shown that altering the time of necropsy post infection drastically altered the numbers of animals developing clinical disease, the severity of the histological lesions and the number of animals developing clinical disease (Begg et al., 2005). Therefore it was expected that the sheep experimentally infected in experiment 031.5 did not develop clinical disease and had lower grade histological lesions. The early necropsy time also explains why very few of the 031.1 and 031.2 challenged sheep were apparently infected. It was noted by Begg et al (2005) sheep killed at 6 month post inoculation, 20% of the animals were apparently infected, but by 9 months 100% were infected. Necropsy of the animals at 14-15 weeks as was done in experiments 031.1 and 2 may have been too early with low numbers of bacteria probably present below the level of detection for the culture method.

The 031.3 experimental sheep also had differing responses from the other experimental infection trials used in this study. The animals used in the trial were not pure bred Merinos and were given a significantly lower inoculation dose for the initial three challenges. Booster challenges were given at 11 and 12 months after the initial inoculations. Because of these issues this experimental inoculation trial cannot be directly compared to the other trials used in this project. The 031.4-6 Telford 9.2 pure clonal strain inoculated sheep had similar levels of infection (72-50%) and numbers of animals that were faecal culture positive (28-38%.

Historically many of the *M.ptb* experimental challenge models for sheep have used tissue/gut homogenates (ground up intestinal tissue) to inoculate the animals (Kluge et al., 1968; Dukes et al., 1992; Gwozdz et al., 2000; Gwozdz et al., 2001; Gwozdz and Thompson, 2002; Kurade et al., 2004; Begg et al., 2005). The reason for this is the fear cultured *M.ptb* may lose its virulence and therefore result in no animals developing disease (Begg et al., 2005; Begg and Whittington, 2007). As part of this experimental project a comparison was made between gut homogenate and the Telford 9.2 pure clone, both of which are of the ovine strain. The sheep were inoculated comparable amounts of *M.ptb* but as can be seen from the results (Table 3 and Figure 4) and the sheep inoculated with the gut homogenate developed more severe disease. This could have been caused by the culturing process reducing the virulence of the *M.ptb*. There could also have been minor differences in virulence between the two ovine strains as they were both isolated from different sheep in different areas.

The repeatable nature of the experimental infection model developed in this series of experiments for sheep will enable to study of numerous aspects Johne’s disease. These include studies on the pathogenesis of infection, vaccine efficacy, diagnostic test performance, immunological and genetic susceptibility.

References

Begara-McGorum, I., Wildblood, L. A., Clarke, C. J., Connor, K. M., Stevenson, K., McInnes, C. J., Sharp, J. M. and Jones, D. G. 1998. Early immunopathological events in experimental ovine paratuberculosis. Veterinary Immunology and Immunopathology 63, 265-87.

Begg, D. J., O'Brien, R., Mackintosh, C. G. and Griffin, J. F. 2005. Experimental Infection Model for Johne's Disease in Sheep. Infection and Immunity 73, 5603-11.

Begg, D. J. and Whittington, R. J. 2007. Experimental animal infection models for Johne's disease, an infectious enteropathy caused by Mycobacterium avium subsp. paratuberculosis. Vet J.

Brotherston, J. G., Gilmour, N. J. and Samuel, J. 1961. Quantitative Studies of *Mycobacterium johnei* in the Tissues of Sheep. Journal of Comparative Pathology 71, 286 - 299.

Bush, R. D., Windsor, P. A. and Toribio, J. A. 2006. Losses of adult sheep due to ovine Johne's disease in 12 infected flocks over a 3-year period. Aust Vet J 84, 246-53.

Dukes, T. W., Glover, G. J., Brooks, B. W., Duncan, J. R. and Swendrowski, M. 1992. Paratuberculosis in saiga antelope (*Saiga tatarica*) and experimental transmission to domestic sheep. Journal of Wildlife Diseases 28, 161-70.

Gwozdz, J. M. and Thompson, K. G. 2002. Antigen-induced production of interferon-gamma in samples of peripheral lymph nodes from sheep experimentally inoculated with *Mycobacterium avium* subsp. *paratuberculosis*. Veterinary Microbiology 84, 243-52.

Gwozdz, J. M., Thompson, K. G. and Manktelow, B. W. 2001. Lymphocytic neuritis of the ileum in sheep with naturally acquired and experimental paratuberculosis. Journal of Comparative Pathology 124, 317-20.

Gwozdz, J. M., Thompson, K. G., Manktelow, B. W., Murray, A. and West, D. M. 2000. Vaccination against paratuberculosis of lambs already infected experimentally with *Mycobacterium avium* subspecies *paratuberculosis*. Australian Veterinary Journal 78, 560-6.

Hines, M. E., 2nd, Stabel, J. R., Sweeney, R. W., Griffin, F., Talaat, A. M., Bakker, D., Benedictus, G., Davis, W. C., de Lisle, G. W., Gardner, I. A., Juste, R. A., Kapur, V., Koets, A., McNair, J., Pruitt, G. and Whitlock, R. H. 2007. Experimental challenge models for Johne's disease: A review and proposed international guidelines. Vet Microbiol 122, 197-222.

Juste, R. A., Garcia Marin, J. F., Peris, B., Saez de Ocariz, C. S. and Badiola, J. J. 1994. Experimental infection of vaccinated and non-vaccinated lambs with *Mycobacterium paratuberculosis*. Journal of Comparative Pathology 110, 185-94.

Karpinski, T. and Zorawski, C. 1975. Experimental paratuberculosis of sheep. I. Clinical, allergical, bacteriological and post-mortem examinations. Bulletin of the Veterinary Institute in Pulawy 19, 59-63.

Kluge, J. P., Merkal, R. S., Monlux, W. S., Larsen, A. B., Kopecky, K. E., Ramsey, F. K. and Lehmann, R. P. 1968. Experimental paratuberculosis in sheep after oral, intratracheal, or intravenous inoculation lesions and demonstration of etiologic agent. American Journal of Veterinary Research 29, 953-62.

Kurade, N. P., Tripathi, B. N., Rajukumar, K. and Parihar, N. S. 2004. Sequential development of histologic lesions and their relationship with bacterial isolation, fecal shedding, and immune responses during progressive stages of experimental infection of lambs with *Mycobacterium avium* subsp. *paratuberculosis*. Veterinary Pathology 41, 378-87.

Marsh, I. B., Bannantine, J. P., Paustian, M. L., Tizard, M. L., Kapur, V. and Whittington, R. J. 2006. Genomic comparison of Mycobacterium avium subsp. paratuberculosis sheep and cattle strains by microarray hybridization. J Bacteriol 188, 2290-3.

Marsh, I. B. and Whittington, R. J. 2007. Genomic diversity in Mycobacterium avium: single nucleotide polymorphisms between the S and C strains of M. avium subsp. paratuberculosis and with M. a. avium. Mol Cell Probes 21, 66-75.

Ott, S. L., Wells, S. J. and Wagner, B. A. 1999. Herd-level economic losses associated with Johne's disease on US dairy operations. Prev Vet Med 40, 179-92.

Perez, V., Garcia Marin, J. F. and Badiola, J. J. 1996. Description and classification of different types of lesion associated with natural paratuberculosis infection in sheep. Journal of Comparative Pathology 114, 107-122.

Reddacliff, L. A., Nicholls, P. J., Vadali, A. and Whittington, R. J. 2003. Use of Growth Indices from Radiometric Culture for Quantification of Sheep Strains of *Mycobacterium avium* subsp. *paratuberculosis*. Applied and Environmental Microbiology 69, 3510-6.

Reddacliff, L. A. and Whittington, R. J. 2003. Experimental infection of weaner sheep with S strain *Mycobacterium avium* subsp. *paratuberculosis*. Veterinary Microbiology 96, 247-58.

Stewart, D. J., Vaughan, J. A., Stiles, P. L., Noske, P. J., Tizard, M. L., Prowse, S. J., Michalski, W. P., Butler, K. L. and Jones, S. L. 2004. A long-term study in Merino sheep experimentally infected with *Mycobacterium avium* subsp. *paratuberculosis*: clinical disease, faecal culture and immunological studies. Veterinary Microbiology 104, 165-78.

Thorel, M. F., Vialard, J., Manfroni, F., Bernardot, J., Ostyn, A. and Vandevelde, J. 1992. [Experimental paratuberculosis in sheep after intravenous or oral inoculation: pathogenicity and biologic diagnosis]. Annales de Recherches Vétérinaires 23, 105-15.

Whittington, R., Marsh, I., Choy, E. and Cousins, D. 1998a. Polymorphisms in IS1311, an insertion sequence common to Mycobacterium avium and M. avium subsp. paratuberculosis, can be used to distinguish between and within these species. Mol Cell Probes 12, 349-58.

Whittington, R. J., Marsh, I., McAllister, S., Turner, M. J., Marshall, D. J. and Fraser, C. A. 1999. Evaluation of modified BACTEC 12B radiometric medium and solid media for culture of *Mycobacterium avium* subsp. *paratuberculosis* from sheep. Journal of Clinical Microbiology 37, 1077-83.

Whittington, R. J., Marsh, I., Turner, M. J., McAllister, S., Choy, E., Eamens, G. J., Marshall, D. J. and Ottaway, S. 1998b. Rapid detection of Mycobacterium paratuberculosis in clinical samples from ruminants and in spiked environmental samples by modified BACTEC 12B radiometric culture and direct confirmation by IS900 PCR. J Clin Microbiol 36, 701-7.

Williams, E. S., Snyder, S. P. and Martin, K. L. 1983. Experimental infection of some North American wild ruminants and domestic sheep with *Mycobacterium paratuberculosis*: clinical and bacteriological findings. Journal of Wildlife Diseases 19, 185-91.

9.13 Appendix 3A-1 Subprogram 3 Detection of Mycobacterium avium subsp. paratuberculosis in ovine faeces by direct quantitative PCR has similar sensitivity to radiometric culture

Introduction

Johne's disease (JD) caused by *Mycobacterium avium* subsp. *paratuberculosis* (MAP) is one of the most economically important diseases in livestock farming, and is prevalent worldwide in domestic animals including cattle, sheep and goats. Susceptible hosts become infected in the early stage in life primarily through ingestion of the pathogen in contaminated faeces, but other transmission routes such as via the placenta, and ingestion of contaminated colostrum, milk and pasture should not be ignored (33). Clinically diseased animals show chronic intermittent diarrhoea, decreased milk production and progressive weight loss. However, a prolonged incubation period and great individual variability in subclinical and clinical disease expression are characteristic of JD (37).

One of the gold standard tests to diagnose JD is isolation of the pathogen from shedding animals by culture. Infected animals shed varying numbers of MAP in faeces, depending on the stage of disease (21). As subclinically infected animals also shed variable amounts of the pathogen, MAP transmission to uninfected animals and contamination of the environment is likely to occur covertly. Therefore, detection and quantification of faecal shedding provides important information to estimate the risk of transmission from the animal, and counting the number of colonies on solid media is routinely performed for this purpose (36). For ovine strains of MAP, which tend not to grow on conventional solid media, a liquid modified BACTEC 12B radiometric culture method is used (38, 39). The number of viable organisms in a sample is determined approximately from the rate of development of growth index (GI) in BACTEC cultures (26). However, this organism grows very slowly and often takes several months (2 to 4) to form a visible colony on solid media. Growth in BACTEC culture is faster but remains time-consuming, as cultures should be checked for up to 12 weeks for confirmation of negative growth status (38, 39). Estimation of initial bacillary load by culturing systems is also influenced by other factors: contamination/overgrowth of culture media by other gut flora leading to potential false negative results (7), potential reduction in number of viable MAP by several orders of magnitude through decontamination procedures (27), and contribution to GI by irrelevant microbes that may have survived sample decontamination procedures.

The identification of the IS*900* element, an insertion sequence considered to be a MAP specific gene, allows rapid detection of MAP DNA by PCR (4, 15). As one genome of MAP has multiple copies of IS*900* (15 to 20 copies) (15), the element has been preferred by most workers as a target gene having potentially higher sensitivity for detection and identification of MAP than detection of single copy elements. However, IS*900*-like sequences exist in non-MAP mycobacteria (8, 13). To ensure analytical specificity of PCR for MAP, some alternative genes such as F57 (25), *hspX* (11), IS*Mav2* (32) and ISMap*02* (23) have been suggested and reinforced by examination of the whole genome sequence of MAP (19), although they might have a disadvantage of lower analytical sensitivity compared to the detection of IS*900*, because only a single copy of F57 and *hspX*, 3 copies of IS*Mav2* and 6 copies of ISMap*02* are present in the MAP genome (11, 23, 25, 32).

Compared to conventional competitive PCR, a real-time, quantitative PCR (QPCR) assay has been shown to be a rapid and simple method for quantification of target DNA from *M. tuberculosis* in a clinical sample (10). There are several reports that a QPCR assay might be useful to detect and quantify MAP DNA in bovine faeces, circumventing the dependence on culture (1, 3, 14, 16, 17, 31, 36) (Table 1). The apparent sensitivities of some QPCR assays based on the amplification of the IS*900* element were similar to or even higher than that of culture (1, 3, 14, 16, 17, 31), while a test for detection of IS*Mav2* (36) had lower sensitivity, nested PCR was needed to obtain sufficient sensitivity for an assay based on ISMap*02* (31), and additional replicates were needed in an F57-based test (16) (Table 1). However, most workers used solid media such as Herrold's egg yolk

medium (HEYM) or Loewenstein-Jensen slants (LJ) for isolation of MAP from faeces. These solid media have been shown to have lower analytical sensitivity compared to radiometric culture (6, 38, 39), suggesting that the high apparent sensitivity of QPCR assays compared to culture results might be because of comparison with insensitive culture methods. IS*900* is still useful as a target gene due to its multiplicity, but so far no direct faecal QPCR tests have concurrently acceptable simplicity and proven analytical sensitivity and specificity to be of practical benefit. Another point is that previous studies for detection of MAP DNA in faecal samples by using QPCR system focused on bovine faeces and cattle strains of MAP.

In this study, a new test based on a novel faecal nucleic acid extraction method and IS*900*-based QPCR method was developed for detection and quantification of MAP DNA in faecal samples, and validated for use on ovine faeces and sheep strains of MAP. Its performance was similar to that of radiometric culture.

Materials and Methods

Mycobacterial strains.

A total of 53 mycobacterial species/strains including defined Sheep (S) and Cattle (C) strains of MAP were used to evaluate the analytical sensitivity and specificity of the QPCR assay (Table 2).

Table 1. Summary of reported direct faecal QPCR assays. Only data from studies that included field validation are summarized.

Samples (No.)	DNA extraction method from faecal samples	Target gene	QPCR condition (annealing temperature)	Analytical sensitivity	QPCR results compared to culture results (sample size)		Faecal culture	Ref.
					Sensitivity %	Specificity %		
Bovine faeces (41)	Bead-beating	IS*900*	molecular beacon 3 step × 45 cycles (58°C)	7.7×10^{-4} pg of MAP DNA	93 (29)	92 (12)	HEYM	(14)
Bovine faeces (63)	1. HerdChek® Mycobacterium paratuberculosis DNA Test Kit (IDEXX Laboratories) 2. Bead-beating	IS*900*	molecular beacon 3 step × 45 cycles (58°C)	Not done	1. 93 (44) 2. 98 (44)	1. 100 (19) 2. 95 (19)	HEYM	(3)
Bovine faeces (23)	Immunomagnetic bead separation and bead-beating	IS*900*	TaqMan 2 step × 40 cycles (60°C)	Not done	100 (17)	100 (6)	HEYM	(17)
MAP #19698 spiked faeces Bovine faeces (310)	High Pure PCR Template Preparation Kit (Roche)	IS*900*	SYBR Green semi nested 1st: 3 step × 40 cycles (60°C) 2nd: 3 step × 50 cycles (65°C)	31 CFU/g of faeces	60 (20)	93 (290)	LJ	(1)
MAP K-10 spiked faeces Bovine faeces (81)	Boiled at 100 °C for 10 min	1. IS*900* 2. ISMap*02*	SYBR Green 1. 3 step × 35 cycles (50°C) 2. nested 1st: 3 step × 20 cycles (58°C) 2nd: 3 step × 30 cycles (60°C)	1. 10^2 CFU/g of faeces 2. 10^3 CFU/g of faeces	1. 100 (60) 2. 98 (60)	1. 100 (21) 2. 100 (21)	HEYM	(31)
Bovine faeces (2155)	QIAamp DNA Stool Mini Kit (QIAGEN)	IS*Mav2*	TaqMan 2 step × 50 cycles (57°C)	7.5×10^3 CFU/g of faeces	23 (395)	99.7 (347)	HEYM	(36)
Bovine faeces (56)	Bead-beating and QIAamp DNA Stool Mini Kit	1. IS*900* (3 sets)	Probe 2step × 45 cycles (60°C)	1. 0.1-0.3 MAP genomes/µl	1. 100 (56)	Not done	LJ HEYM	(16)

(QIAGEN)			2. 100 (56)
	2. F57	2. 1 MAP genomes/µl	(more replicates were needed)

Table 2. Mycobacterial taxa and strains used in this study

Taxon	Strain/Source	QPCR detection
M. avium subsp. *paratuberculosis*	316v (C-strain)	+
M. avium subsp. *paratuberculosis*	Telford (S-strain)	+
M. avium subsp. *avium* [a]	ST1	-
M. avium subsp. *avium* [a]	ST9	-
M. avium subsp. *avium* [a]	ST11	-
M. avium subsp. *avium* [a]	ST12	-
M. avium subsp. *avium* [a]	ST15	-
M. avium subsp. *avium* [a]	ST16	-
M. avium subsp. *avium* [a]	ST17	-
M. avium subsp. *avium* [a]	ST18	-
M. avium subsp. *avium* [a]	ST19	-
M. avium subsp. *avium* [a]	ST23	-
M. avium subsp. *avium* [a]	ST26	-
M. avium subsp. *avium* [a]	ST28	-
M. avium subsp. *avium* [a]	ST29	-
M. avium subsp. *avium* [a]	ST31	-
M. avium subsp. *avium* [a]	ST38	-
M. avium subsp. *avium* [a]	ST49	-
M. avium subsp. *avium* [a]	ST54	-
M. avium subsp. *avium* [a]	ST55	-
M. avium subsp. *avium* [a]	ST60	-
M. avium subsp. *avium* [a]	ST62	-
M. avium subsp. *avium*	TMC715	-
M. chitae	ATCC19627	-
M. flavescens	ATCC14474	-
M. gordonae	ATCC14470	-
M. intracellulare	ATCC13950	-
M. kansasii	ATCC12478	-
M. nonchromogenicum	ATCC19530	-
M. parafortuitum	ATCC19686	-
M. phlei	ATCC11758	-
M. scrofulaceum	ATCC19981	-
M. terrae	ATCC15755	-
M. thermoresistibile	ATCC19527	-
M. triviale	ATCC23292	-
M. vaccae	ATCC15483	-
M. xenopi	ATCC10042	-
M. tuberculosis [d]	Aoyama B	-

M. tuberculosis [d]	Tapir C-3		-
M. bovis BCG [d]	Tokyo		-
M. bovis [d]	B-10		-
Mycobacterium sp.	#2333	IS*900*-like [e]	-
Mycobacterium sp. [b]	AM1	IS*900*-like [f]	-
Mycobacterium sp. [b]	AM3	IS*900*-like [f]	-
Mycobacterium sp. [b]	AM4	IS*900*-like [f]	-
Mycobacterium sp. [b]	AM5	IS*900*-like [f]	-
Mycobacterium sp. [a]	IWGMT90236	IS*900*-like [f]	-
Mycobacterium sp. [c]		IS*900*-like [f]	-
Mycobacterium sp. [b]	P99-4609	IS*900*-like [f]	-
M. scrofulaceum-like [c]	Vic	IS*900*-like [f]	-
M. scrofulaceum-like [c]	Vic	IS*900*-like [f]	-

[a] Collection of Qld Department of Health, D Dawson

[b] Collection of Western Australian Department of Agriculture, D Cousins

[c] Collection of Victorian Institute of Animal Science

[d] Collection of National Institute of Animal Health, Japan

[e] Englund et al., 2002 (13)

[f] Cousins et al., 1999 (8)

Purification of genomic DNA from mycobacteria.

Genomic DNA was purified from each mycobacterial strain based on the method described previously (2). Briefly, bacterial pellets resuspended in TE buffer were heated at 80°C for 30 min. 120 µl of lysozyme (200 mg/ml) (Sigma Chemical Co.) and 200 units of mutanolysin (Sigma) was added, and the samples were incubated at 37°C overnight with gentle mixing. After the addition of 70 µl of proteinase K (10 mg/ml) (Sigma) and 120 µl of 10% SDS, the samples were incubated at 65°C for 20 min with gentle mixing every 5 min. The entire contents were transferred into a Phase Lock Gel Heavy, 15 ml column (Eppendorf), and an equal volume of 24:1 chloroform/isoamyl alcohol was added. Following centrifugation at 1,500 g for 5 min, the aqueous phase was transferred to a clean tube and 3× sample volume of 100% ethanol was added. The sample was centrifuged at 16,100 g for 15 min and the supernatant was removed. DNA pellets were washed with 1.0 ml of 70% ethanol and resuspended in 300 µl of TE buffer (pH 8.0). The purity and concentration of each purified DNA sample was determined by spectrophotometry at 260 nm (BioPhotometer, Eppendorf), and 10 pg of each was used as template DNA for evaluation of the specificity of the QPCR assay. Tenfold serial dilutions ranging from 10^{1} to 10^{-4} pg of genomic DNA from MAP strain 316v was prepared for determination of the sensitivity of the QPCR. The DNA from 316v was also used as standard DNA in each batch of samples tested by QPCR.

QPCR assay.

Primers for the detection of MAP IS*900* were designed referring to IS*900*-like sequences, particularly *Mycobacterium* sp. strain 2333 harbouring one copy of a sequence with 94% identity to IS*900* (13) (Table 3). The QPCR reaction mixture in a total volume of 25 µl contained 2.5 µl of template DNA, 12.5 µl of 2× QuantiTect SYBR Green PCR Master Mix (QIAGEN), and 0.125 µl of 100 pmol of each of the primers in nuclease free water. QPCR was performed on a MX3000*p* Multiplex Quantitative PCR system (Stratagene), and the reaction conditions were arranged as follows: initial activation step of 15 min at 95°C, and 45 cycles of PCR amplification at 95°C for 30 sec and 68°C for 60 sec. After PCR amplification, the dissociation curve data were collected and analysed. For quantitation, a standard curve was created by using genomic DNA extracted from MAP strain 316v.

Table 3. Primers for the detection of MAP IS*900* used in this study compared to other IS*900*-like sequences

Name	Sequence
Forward primer: MP10-1	5'- ATG CGC CAC GAC TTG CAG CCT -3'
M. sp. 2333 [a]	5'- ... ... .G. ... ...G -3'
WA-1 [b]	5'- ... ... .G. ... C.. ..A ..G -3'
WA-2 [b]	5'- ... ..T .G. ..T C.. ... ..A -3'
Reverse primer: MP11-1	5'- GGC ACG GCT CTT GTT GTA GTC G -3'
M. sp. 2333 [a]	5'- C.. ... ... .C. ... ... A -3'
WA-1 [b]	5'- ... CTT .T. T.. .C. ... A.. A -3'
WA-2 [b]	5'- ... CTT .T. GGC .C. ... A.. . -3'

[a] Englund et al., 2002 (13), [b] Cousins et al., 2001 (8)

Table 4. Analytical sensitivity of the QPCR assay

Plasmid DNA		Genomic DNA from 316v		MAP in spiked faeces	
Plasmid IS*900* DNA (copies)	Detection	Genomic DNA (pg)	Detection	Number of MAP per 1g of faeces	Detection (no. positive/ no. replicates)
1×10^6	+	1×10^0	+	1×10^6	3/3
1×10^5	+	1×10^{-1}	+	1×10^5	3/3
1×10^4	+	1×10^{-2}	+	1×10^4	3/3
1×10^3	+	1×10^{-3}	+	1×10^3	3/3
1×10^2	+	1×10^{-4}	-	1×10^2	3/3
1×10^1	+	0	-	1×10^1	3/3
1×10^0	+			1×10^0	0/3
1×10^{-1}	-			0	0/3
0	-				

Preparation of cloned IS*900* DNA.

IS*900* fragments obtained by the QPCR from MAP 316v were purified using a MinElute PCR Purification Kit (QIAGEN). The purified fragments were cloned into pCR2.1 using a TA cloning kit (Invitrogen), plasmid vectors were transformed into competent Top10 *Escherichia coli* cells (Invitrogen) and grown on LB/Amp/X-Gal/IPTG plates for screening. Colony PCR was conducted on bacterial colonies using M13 (-20) Forward (5'-TGT AAA ACG ACG GCC AGT-3') and M13 Reverse (5'-CAG GAA ACA GCT ATG ACC-3') primers to confirm the desired plasmid product. The transformant was grown in Luria Bertani broth supplemented with ampicillin (100 µg/ml), and the plasmid DNA was extracted using a QIAprep Spin Miniprep Kit (QIAGEN) and digested by *Eco*RI (NEB) to check the size of the insert. The plasmid was linearised by restriction with *Xho*I (NEB) and purified using a MinElute PCR Purification Kit (QIAGEN). Following quantification by electrophoresis in comparison with a standard (MassRuler DNA Ladder, Fermentas), tenfold serial dilutions of the plasmid DNA ranging from 10^6 to 10^{-1} copies were prepared for the QPCR assay to evaluate its analytical sensitivity with respect to IS*900*.

Preparation of MAP spiked faeces.

A faecal sample was collected from a known paratuberculosis-free sheep. A stock suspension of the Telford S strain of MAP was prepared and the most probable number (MPN) was determined according to previous reports (26, 27). The stock suspension was diluted tenfold in PBS to provide bacterial suspensions ranging from 10^6 to 10^0 viable cells/ml. 500 µl of each dilution and a PBS control was used to spike 0.5 g of the faeces to yield final concentrations ranging from 10^6 to nil viable cells/g. Three sets of spiked faeces were prepared to enable testing in triplicate.

Sheep and faecal samples.

A total of 506 individual faecal samples and 27 pooled faecal samples originated from sheep from several flocks with different levels of exposure to MAP. Faecal BACTEC culture was undertaken for all samples as described previously (38, 39). All faeces were stored at -20°C prior to testing in QPCR.

Individual faecal samples were allocated into 5 groups (Table 5). MAP were isolated in BACTEC culture only from faecal samples in Category-5, and all faeces in Categories-1 to 4 were faecal culture negative. Category-1 included 176 individual sheep faeces from a JD free farm. Category-2 included 208 faeces from previously unexposed sheep from a JD free farm, but the pasture to which the sheep were introduced 2 months before faecal sampling had a low level of contamination with MAP due to grazing 16 months previously with JD infected sheep. Faecal samples in Category-3 (n=13) were collected from sheep experimentally infected orally with MAP S strain (Telford), but no evidence of infection with MAP was obtained from histological examinations and culture of intestinal tissues and faeces. In 40 faecal samples in Category-4, the sheep were exposed to MAP and had histological evidence and/or were tissue culture positive, but faecal culture results for MAP were all negative. Category-5 included 69 faecal culture positive faeces which were obtained at various times from 40 sheep, and the time taken for cumulative growth index (CGI) to reach over 900 was obtained. Histological status of terminal ileum and associated lymph nodes was determined for 93 sheep exposed to MAP from Category-3, 4 and 5 (24).

Five of 27 pooled faecal samples were provided as control negative samples, and 22 pools were provided from sheep which originated on two JD affected farms in the Central Tablelands district of New South Wales. Each pool contained faeces from 50 sheep processed as described previously (40).

DNA extraction from faecal samples.

DNA extraction from faecal samples was performed by using a DNA preparation kit (JohnePrep^{TM}, Kyoritsu Seiyaku Co., Tokyo, Japan). Briefly, 0.5 g of faeces was placed in 10 ml of sterile saline and shaken well until the sample was evenly suspended. Following standing for 30 min at room temperature, 1 ml of the supernatant was transferred to a 2.0 ml screw cap tube containing about 0.3 ml of 0.1 mm zirconia/silica beads (BioSpec Products, Inc.). The suspension was centrifuged at 12,000 rpm for 5 min and the supernatant was carefully removed. After washing with 1ml of Washing Solution, 700 µl of Working Solution and 700 µl of organic solvent (equal volume of chloroform and isobutanol) were added to the pellet with microbeads. Samples were agitated on speed at 6.0 m/sec for 45 sec twice using a homogeniser (BIO 101 FastPrep, Qbiogene). Each homogenized sample was centrifuged at 12,000 rpm for 5 min and 350 µl of supernatant was transferred to a new 1.5 ml tube containing 350 µl of isopropanol, and then mixed by inverting. Following centrifugation at 15,000 rpm for 10 min, the supernatant was removed. DNA pellets were washed with 1.0 ml of ice-cold 70% ethyl alcohol and resuspended in 50 µl of nuclease free water, and then stored at -20°C until QPCR analyses were performed.

All DNA templates extracted from faecal samples were tested by the QPCR assay in duplicate, and in the case of contradiction (1 of 2 wells positive) the faecal sample was retested from the beginning of the DNA extraction. If either well was positive in the second test, the sample was defined as positive.

Statistical analysis.

Differences in $\log_{10}$ DNA quantities for QPCR positive samples between categories were evaluated by a Kruskal-Wallis test following Dunn procedure to generate *P* values for two-group comparisons. McNemar's test (two tailed) was used to compare the detection of MAP by QPCR and culture. The relationship between the DNA quantity detected in the QPCR test and the time for CGI to reach over 900 in BACTEC cultures was assessed by the linear regression among the 68 samples that were positive in both QPCR and culture.

Results

Analytical specificity of detection of MAP by the IS*900* based QPCR assay.

Approximately 10 pg of template DNA extracted from S and C strains of MAP were detected after 20 cycles of the QPCR (Fig. 1). On the other hand, no products were amplified among genomic DNA templates from 51 non-MAP mycobacterial strains including 10 IS*900*-like sequence containing strains (Table 2, Fig. 1).

Fig. 1 Specificity of the IS*900*-based QPCR test for MAP using 10 pg of each template DNA from mycobacterial strains

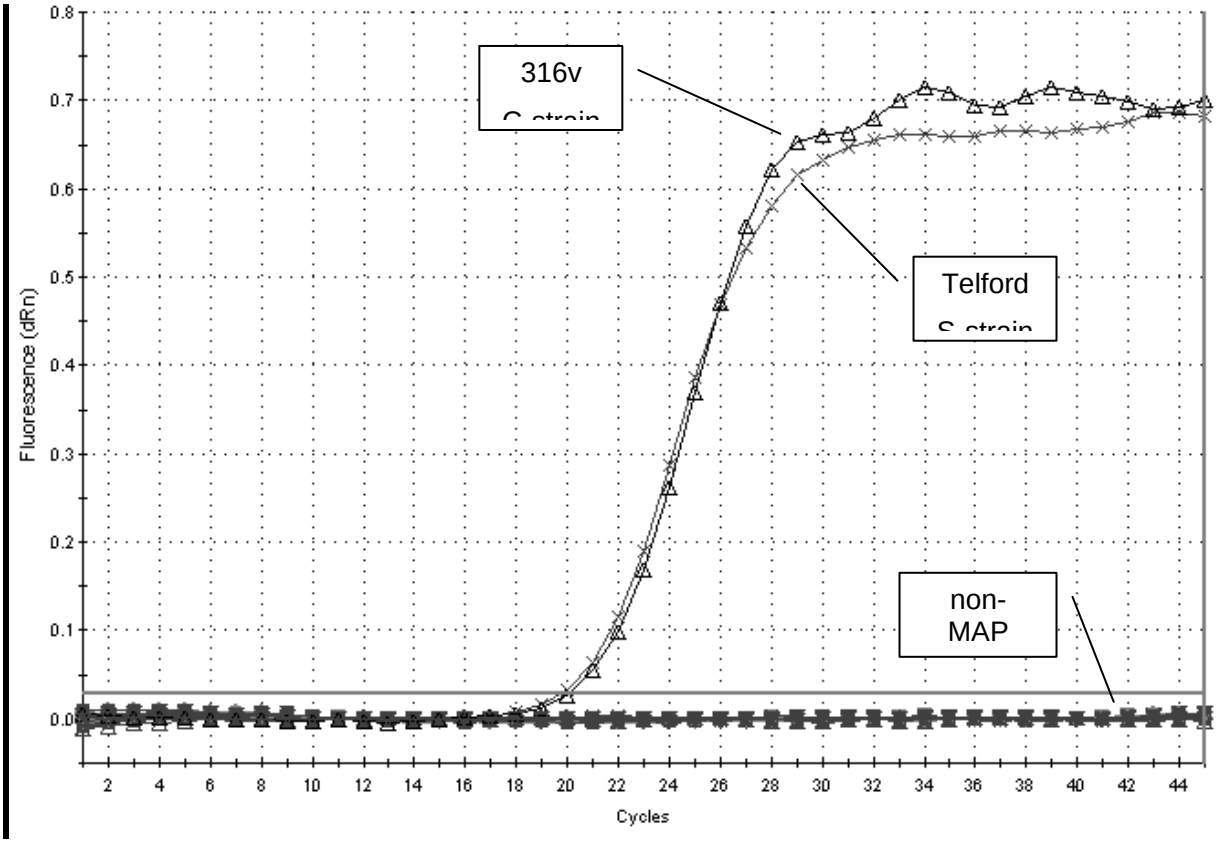

Analytical sensitivity of the QPCR assay.

The analytical sensitivity of the QPCR assay was evaluated in three different ways (Table 4, Fig 2).

(i) Detection of a fragment of IS*900* cloned into plasmid DNA.

Using IS*900* cloned plasmid DNA, the sensitivity of detection by the QPCR assay was evaluated (Table 4, Fig. 2a). One copy of IS*900* was amplified by 35 cycles of the assay (Fig. 2a).

(ii) Detection of IS*900* in genomic DNA from MAP strain 316v.

Ten-fold serial dilutions of genomic DNA from MAP 316v were tested to determine the sensitivity of detection by the QPCR method (Table 4, Fig. 2b). The minimum detectable limit was 1 fg, which was approximately equivalent to 0.2 MAP organisms according to an equation presented previously: one genome of MAP contains around 5 Mbp that represents 5.28 fg DNA (29).

(iii) Detection of IS*900* in MAP cells in spiked sheep faeces.

The sensitivity of detection of MAP DNA from sheep faeces spiked with dilutions of a suspension of S strain MAP (Telford) cells was examined in triplicate (Table 4, Fig. 2c). The reproducible experimental limit was ten viable MAP in 1 g of faecal material.

Fig. 2 Evaluation of analytical sensitivity of the QPCR assay in three different ways a. plasmid DNA (copies)

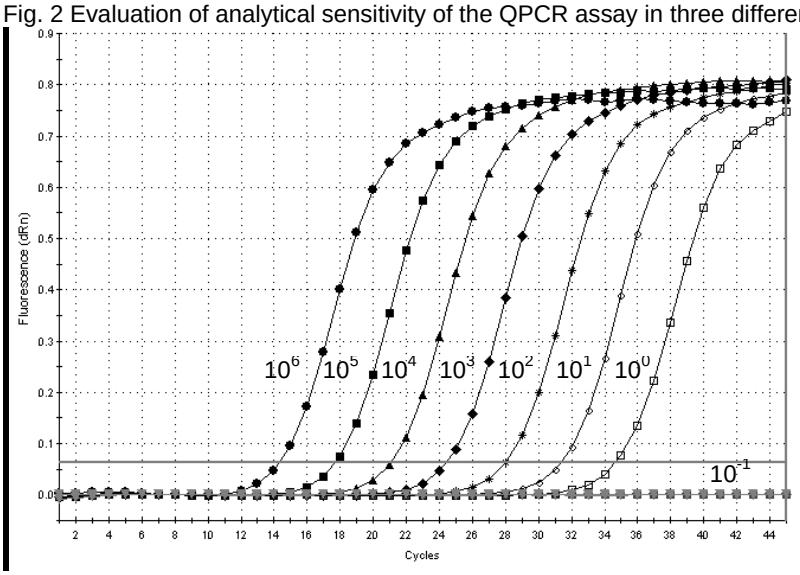

b. Genomic DNA from 316v (pg)

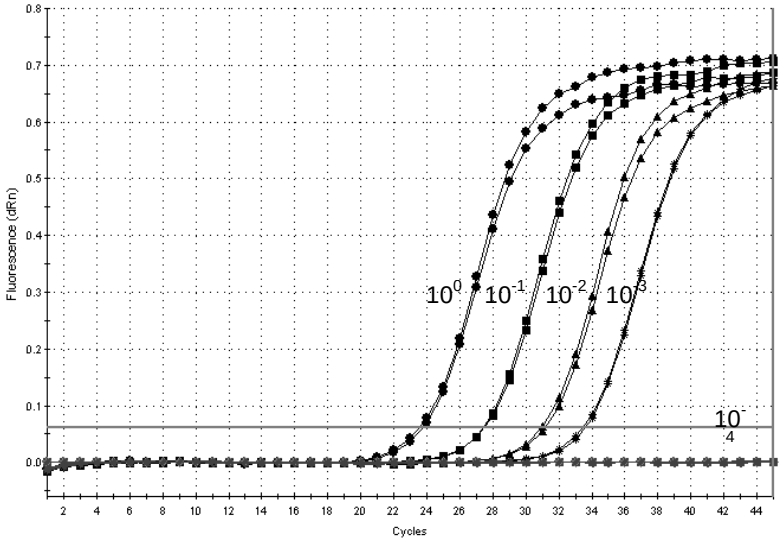

c. Spiked faeces (number of MAP per 1g of faeces)

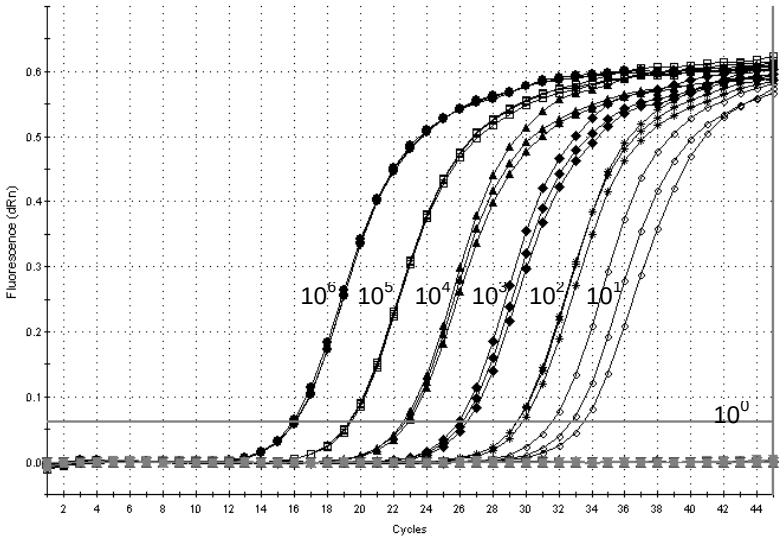

Fig. 3 The relationship between the DNA quantity detected by the QPCR assay and the time to detection of MAP by culture

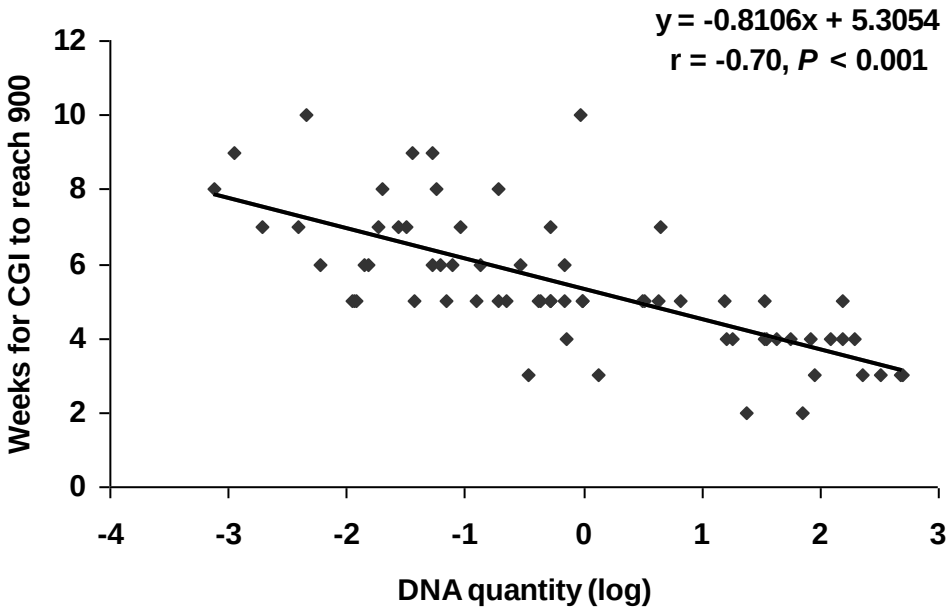

PCR assay on field samples.

(i) Individual faecal samples.

A total of 506 individual faecal samples with known culture results from sheep of known histological status were tested by the QPCR assay (Table 5). They were grouped into 5 categories according to the degree of exposure to MAP, assessed by the history of the sheep and the pasture on which they were grazed. Positive results in the QPCR were directly related to the likelihood of exposure of the sheep to MAP. Samples in Category-1 which included 176 culture negative faeces from sheep on a JD free farm were all negative in the QPCR. The samples in Categories-2, 3 and 4 were also faecal culture negative. Category-2 had 208 faeces from sheep from a JD free farm, but these sheep were kept on pasture with a low level of MAP contamination, and 14 of 208 (6.7 %) were positive in the QPCR test. Faecal samples in Category-3 were collected from sheep that had been experimentally inoculated with MAP, and 8 of 13 (61.5 %) were positive in the QPCR. In Category-4, 40 faecal samples were collected from faecal culture negative but histologically positive sheep, and 24 (60.0 %) were positive in the QPCR. All faecal samples in Category-5 were culture positive, and MAP DNA was detected from 68 of 69 (98.6 %).

DNA quantities for QPCR positive samples in Categories-2, 3 and 4 were significantly lower than those in Category-5 ($P < 0.001$), but there were no differences among Categories-2, 3 and 4 (Table 5).

(ii) Pooled faecal samples. A total of 22 pools of previously cultured faecal samples (50 sheep per pool) from sheep exposed to MAP were tested by the QPCR assay (Table 6). Culture detected 18 samples as positive while QPCR detected 17. A kappa value of 0.59 was obtained indicating moderate agreement between the results of the two tests. None of 5 control negative pooled faeces were positive in QPCR.

Table 6. Results of QPCR and culture for pooled faecal samples

		QPCR		
		Positive	Negative	Total
Culture	Positive	16	2	18
	Negative	1	3	4
Total		17	5	22

Kappa value = 0.59

Comparison of MAP detection in faecal samples by radiometric culture and QPCR on the basis of histological classification.

The results of faecal culture and QPCR were compared among 93 infected sheep stratified on histological classification (Table 7). All faecal samples representing sheep with multibacillary lesions were positive in both culture and QPCR, while for no lesion and paucibacillary samples QPCR had significantly higher sensitivity than culture (no lesion samples: McNemar $X^2 = 11.27$, $P < 0.001$, paucibacillary samples: McNemar $X^2 = 18$, $P < 0.001$) (Table 7). DNA quantities for QPCR positive samples in no lesion and paucibacillary samples were significantly lower than those in multibacillary samples ($P < 0.001$) (Table 7).

Table 5. Field validation of the QPCR assay for ovine faeces

Category	History and laboratory results	No. of samples	Positive		Negative		DNA quantity for positive samples	
			No.	%	No.	%	Range (pg)	Log Median *
1	JD free sheep grazing uncontaminated pasture	176	0	0.0	176	100.0	-	-
2	JD free sheep grazing contaminated pasture	208	14	6.7	194	93.3	7.63×10^{-2} - 2.12×10^{-4}	-2.709 [a]
3	Experimentally infected sheep, faecal culture –ve, tissue culture –ve, histopathology –ve	13	8	61.5	5	38.5	7.06×10^{-3} - 6.08×10^{-4}	-2.697 [a]
4	Infected sheep, faecal culture –ve, tissue culture +ve and/or histopathology +ve	40	24	60.0	16	40.0	3.67×10^{-2} - 5.34×10^{-5}	-2.545 [a]
5	Infected sheep, faecal culture +ve	69	68	98.6	1	1.4	4.89×10^{2} - 7.57×10^{-4}	-0.285 [b]

* Different letters indicate differences in a Kruskal-Wallis test following multiple comparison (P<0.001).

Table 7. MAP detection in faecal samples of sheep exposed to MAP by BACTEC culture and QPCR on the basis of histological classification

Category (Histopathology)	Histo grade*	No.	Faecal culture		QPCR		DNA quantity for QPCR positive samples	
			No. of positive	%	No. of positive	%	Range (pg)	Log Median**
No lesion	0	38	14	36.8	27	71.1	1.56×10^{1} - 6.08×10^{-4}	-2.335 [a]
Paucibacillary	1, 2, 3a, 3c	42	13	31.0	31	73.8	1.64×10^{1} - 2.58×10^{-4}	-1.921 [a]
Multibacillary	3b	13	13	100.0	13	100.0	4.89×10^{2} - 2.73×10^{-2}	1.920 [b]
Total		93	40	43.0	71	76.3		

* Perez et al., 1996 (24) ** Different letters indicate differences in a Kruskal-Wallis test following multiple comparison (P<0.001).

Comparison of MAP DNA quantity detected by QPCR and BACTEC culture results.

There was a significant relationship between the DNA quantity detected in the QPCR test and the time for CGI to reach over 900 in BACTEC cultures among 68 faecal samples that were both QPCR and culture positive from category-5 (Fig. 3).

Discussion

A real-time, quantitative PCR assay is a rapid and simple method for detection and quantification of target DNA in a sample. Several studies have already reported that QPCR tests might be useful to detect animals that are faecal shedders of MAP, circumventing the needs for time-consuming culturing systems (1, 3, 14, 16, 17, 31, 36) (Table 1). However, a protocol which has enough simplicity, sensitivity and specificity has not been established. Previous studies utilized relatively insensitive culture methods as the gold standard and arguably therefore overestimated diagnostic sensitivity of QPCR. These studies were focused on bovine faeces and cattle strains of MAP, and although the general principles and findings should be transferable between host animal species and strains of MAP, there have been no studies related to S strains of MAP or sheep. This study presents a new faecal extraction and IS*900*-based QPCR method for detection and quantification of MAP DNA in faecal samples, and evaluation of the sensitivity and specificity including field validation for sheep.

The QPCR assay showed high specificity for detection of MAP IS*900*. Both S and C strains of MAP were detected in this assay, while DNA templates from 51 non-MAP mycobacterial strains including IS*900*-like sequence containing strains were not amplified (Table 2, Fig. 1). The occurrence of clinical isolates of IS*900*-like sequence harbouring mycobacteria have discouraged use of IS*900* as a target gene in PCR (31, 34, 35, 36), but this novel IS*900*-based QPCR test was found to be highly specific for MAP. This might be explained by the novel primers which were designed specifically for MAP IS*900* and to avoid IS*900*-like sequences (Table 3) and employment of a 2-step thermocycling regime with high annealing temperature. In this reaction annealing and extension were concurrent at 68°C. Annealing temperatures greater than 60°C have been recommended for IS*900* PCR to assist specificity (9), and 62°C is used commonly in Australia for conventional PCR (20), but it appears that annealing temperature higher than this may be beneficial and can overcome problems with detection of IS*900*-like sequence containing strains such as 2333 (13).

The analytical sensitivity of the QPCR assay was evaluated in three different ways. One copy of IS*900* in a recombinant plasmid, 1 fg of MAP genomic DNA representing 0.2 organisms and 10 viable MAP in 1 g of ovine faeces were detected (Table 4, Fig. 2). The analytical sensitivity of this test was similar to or higher than previously published IS*900*-based QPCR protocols (14, 17, 22).

During our field validation, the QPCR test showed high sensitivity for the detection of sheep shedding MAP in faeces, as MAP DNA was detected from 98.6 % of faeces in Category-5 which were all culture positive (Table 5). In addition to individual faecal samples, results of the QPCR in pooled faecal samples also showed agreement with those of culture (Table 6). Pooled faecal culture is a sensitive and cost effective method, and it is commonly used for flock diagnosis of JD in sheep in Australia (40). With direct faecal PCR, it has been problematical to achieve an equal sensitivity to culture due to difficulties of recovering MAP DNA from low numbers of organisms in a complex matrix and removing amplification inhibitors (5, 20, 30). One of the reasons for the high

agreement between results of the QPCR assay and culture in Category-5 was assumed to be use of a commercial DNA preparation kit, JohnePrep ™ (Kyoritsu Seiyaku Co., Tokyo, Japan), for the DNA extraction from faecal samples. Kojima et al. suggested that a DNA preparation method using bead-beating in optimal lysis buffer, currently available as JohnePrep, effectively improved the sensitivity of PCR (18). Christopher-Hennings et al. pointed out that DNA extraction was the key for the detection of MAP in faeces, and indicated that a method of DNA extraction using bead-beating combined with real-time PCR had 98 % sensitivity compared to culture results (3). By using immunomagnetic bead separation coupled with bead-beating for isolation and extraction of MAP DNA from faeces, Khare et al. also showed that the results of QPCR exactly matched those of culture (17). However, these authors used a relatively insensitive culture method (6, 38, 39) which would have improved the apparent sensitivity of the PCR.

Another reason for the high sensitivity in the QPCR relative to culture was assumed to be the employment of the IS*900* element as a target DNA. Some direct faecal QPCR protocols based on alternative genes such as IS*Mav2*, ISMap*02* or F57 have already been published, but only 23.0 % of faecal shedders were detected by IS*Mav2*-based QPCR (36), nested PCR was needed for the ISMap*02*-based test (31) and additional replicates were needed for the F57-based test (16) to obtain similar sensitivity to culture. Putting aside the question of specificity, the IS*900* gene is still an ideal target to achieve higher sensitivity in PCR due to its multiplicity within the MAP genome.

In this study, MAP DNA was detected in many culture negative faecal samples from Categories-2, 3 and 4 (Table 5). Category-2 had 208 faeces from previously unexposed sheep that were recently introduced to a pasture with presumed low levels of contamination, and 6.7 % were positive in the QPCR test (Table 5). Although the pasture where the sheep were kept had not been grazed with JD infected sheep for 16 months, non-viable MAP likely remained. MAP can survive in the environment for a long period and its DNA remains even though the organism is dead or not cultivable (41). MAP DNA was demonstrated in culture negative sheep faecal pellets/soil 32 weeks after deposition (41). It is also established that MAP can be shed passively, or “pass through” the gut for some days after ingestion (7, 28). Thus the QPCR positive sheep in Category-2 possibly ingested non-viable MAP or MAP DNA from dead cells that remained on the pasture or in soil. Samples in Category-3 and 4 were collected from sheep exposed to MAP, and 61.5 % and 60.0 % of faeces were positive by the QPCR, respectively (Table 5). The sheep in Category-3 were experimentally infected, but no evidence of infection with viable organisms was obtained from histological examinations and culture of tissues and faeces, while in Category-4 the sheep were exposed to MAP and showed histological evidence and/or were tissue culture positive. The apparent discrepancy between the results of QPCR and faecal culture in those two categories might also be explained by the detection of “pass through” MAP cells in the QPCR and/or false-negative results in faecal culture. In addition to the low sensitivity of faecal culture because of contamination of other gut flora and/or decontamination processes (7, 27), it has been shown that MAP has a state of dormancy and is not always cultured even though the organisms are alive (41). Ellingson et al. also compared results of IS*900* based direct PCR and faecal culture, and attributed false-positive results on the PCR were attributed to cross-reaction with non-MAP mycobacteria or detection of MAP DNA actually contained in the sample (12). Since our QPCR assay showed high analytical specificity for the detection of MAP IS*900* and all QPCR positive but culture negative sheep had been exposed to MAP, it is more likely than not that it detected actual MAP DNA in faecal samples. Additionally, the prevalence of positive test results was related to the history of exposure of sheep in each category to MAP, and therefore can provided good information to assess the likely

potential for MAP contamination by the flock, although it is impossible to distinguish live infectious MAP from dead cells by the QPCR.

Stage of disease affected the results of QPCR and faecal culture among 93 sheep exposed to MAP and classified on histological status (Table 7). All faecal samples representing sheep with multibacillary lesions were positive in both tests, while for no lesion and paucibacillary samples the QPCR showed significantly higher sensitivity than culture.

QPCR systems have great advantage for rapid and simple determination of initial DNA quantity in a sample. Quantification of MAP DNA in faeces by QPCR tests provides immediate information to estimate the risk of transmission from shedding animals (14, 36). During our field study, there were no differences in DNA quantities in QPCR positive samples among Categories-2, 3 and 4, but significantly higher amounts of MAP DNA were present in Category-5 which comprised MAP shedders (Table 5). Furthermore, when DNA quantities detected by the QPCR were analysed on the basis of histological classification, faecal samples representing sheep with multibacillary lesions showed significantly higher levels of MAP DNA than no lesion and paucibacillary samples (Table 7). The present study also showed that the DNA quantity detected in the QPCR assay correlated well with the time for CGI to reach over 900 in BACTEC cultures among both QPCR and culture positive ovine faeces (Fig. 3). The number of viable organisms in an inoculated sample can be estimated from CGI in BACTEC cultures (26). Therefore, quantification of MAP DNA by the QPCR test is assumed to be a good method to measure the initial bacillary load in ovine faeces and to detect sheep with higher risk of transmission. However, it remains a challenge to develop a rapid assay that can differentiate live MAP from dead MAP.

In conclusion, the new IS*900* based QPCR assay was highly specific and sensitive for the detection and quantification of MAP DNA in ovine faeces. From the results of the field validation, the assay might be useful not only to detect and quantify faecal shedding but also to assess JD contamination level in the flock. Employment of the QPCR test for diagnosis would be an advance for JD control programs by reducing the time to reporting results from several months to several days.

References

Bögli-Stuber, K., C. Kohler, G. Seitert, B. Glanemann, M. C. Antognoli, M. D. Salman, M. M. Wittenbrink, M. Wittwer, T. Wassenaar, T. Jemmi, and B. Bissig-Choisat. 2005. Detection of *Mycobacterium avium* subspecies *paratuberculosis* in Swiss dairy cattle by real-time PCR and culture: a comparison of the two assays. J. Appl. Microbiol. 99:587-597.

Choy, E., R. J. Whittington, I. Marsh, J. Marshall, and M. T. Campbell. 1998. A method for purification and characterisation of *Mycobacterium avium* subsp. *paratuberculosis* from the intestinal mucosa of sheep with Johne's disease. Vet. Microbiol. 64:51-60.

Christopher-Hennings, J., M. A. Dammen, S. R. Weeks, W. B. Epperson, S. N. Singh, G. L. Steinlicht, Y. Fang, J. L. Skaare, J. L. Larsen, J. B. Payeur, and E. A. Nelson. 2003. Comparison of two DNA extractions and nested PCR, real-time PCR, a new commercial PCR assay, and bacterial culture for detection of *Mycobacterium avium* subsp. *paratuberculosis* in bovine feces. J. Vet. Diagn. Invest. 15:87-93.

Collins, D. M., D. M. Gabric, and G. W. de Lisle. 1989. Identification of a repetitive DNA sequence specific to *Mycobacterium paratuberculosis*. FEMS Microbiol. Lett. 51:175-178.

Collins, D. M., D. M. Stephens, and G. W. de Lisle. 1993. Comparison of polymerase chain reaction tests and faecal culture for detecting *Mycobacterium paratuberculosis* in bovine faeces. Vet. Microbiol. 36:289-299.

Collins, M. T., K. B. Kenefick, D. C. Sockett, R. S. Lambrecht, J. McDonald, and J. B. Jorgensen. 1990. Enhanced radiometric detection of *Mycobacterium paratuberculosis* by using filter-concentrated bovine fecal specimens. J. Clin. Microbiol. 28:2514-2519.

Collins, M. T. 1996. Diagnosis of paratuberculosis. Vet. Clin. North Am. Food Anim. Pract. 12:357-371.

Cousins, D. V., R. Whittington, I. Marsh, A. Masters, R. J. Evans, and P. Kluver. 1999. Mycobacteria distenct from *Mycobacterium avium* subsp. *paratuberculosis* isolated from the faeces of ruminants possess IS*900*-like sequences detectable IS*900* polymerase chain reaction: implications for diagnosis. Mol. Cell. Probes 13:431-442.

Cousins, D. V., R. J. Condron, G. J. Eamens, R. J. Whittington, and G. W. de Lisle. 2001. Paratuberculosis (Johne's Disease). Australian and New Zealand Standard Diagnostic Procedures. Sub-Committee on Animal Health Laboratory Standards, Veterinary Committee, Canberra. pp. 1-21.

Desjardin, L. E., Y. Chen, M. D. Perkins, L. Teixeira, M. D. Cave, and K. D. Eisenach. 1998. Comparison of the ABI 7700 system (TaqMan) and competitive PCR for quantification of IS*6110* DNA in sputum during treatment of tuberculosis. J. Clin. Microbiol. 36:1964-1968.

Ellingson, J. L., C. A. Bolin, and J. R. Stabel. 1998. Identification of a gene unique to *Mycobacterium avium* subspecies *paratuberculosis* and application to diagnosis of paratuberculosis. Mol. Cell. Probes 12:133-142.

Ellingson, J. L., J. J. Koziczkowski, and J. L. Anderson. 2004. Comparison of PCR prescreening to two cultivation procedures with PCR confirmation for detection of *Mycobacterium avium* subsp. *paratuberculosis* in U.S. Department of Agriculture fecal check test samples. J. Food Prot. 67:2310-2314.

Englund, S., G. Bolske, and K. E. Johansson. 2002. An IS*900*-like sequence found in a *Mycobacterium* sp. other than *Mycobacterium avium* subsp. *paratuberculosis*. FEMS Microbiol. Lett. 209:267-271.

Fang, Y., W. H. Wu, J. L. Pepper, J. L. Larsen, S. A. Marras, E. A. Nelson, W. B. Epperson, and J. Christopher-Hennings. 2002. Comparison of real-time, quantitative PCR with molecular beacons to nested PCR and culture methods for detection of *Mycobacterium avium* subsp. *paratuberculosis* in bovine fecal samples. J. Clin. Microbiol. 40:287-291.

Green, E. P., M. L. Tizard, M. T. Moss, J. Thompson, D. J. Winterbourne, J. J. McFadden, and J. Hermon-Taylor. 1989. Sequence and characteristics of IS*900*, an insertion element identified in a human Crohn's disease isolate of *Mycobacterium paratuberculosis*. Nucleic Acids Res. 17:9063-9073.

Herthnek, D., and G. Bölske. 2006. New PCR systems to confirm real-time PCR detection of *Mycobacterium avium* subsp. *paratuberculosis*. BMC Microbiol. 6:87. doi:10.1186/1471-2180-6-87.

Khare, S., T. A. Ficht, R. L. Santos, J. Romano, A. R. Ficht, S. Zhang, I. R. Grant, M. Libal, D. Hunter, and L. G. Adams. 2004. Rapid and sensitive detection of *Mycobacterium avium* subsp. *paratuberculosis* in bovine milk and feces by a combination of immunomagnetic bead separation-conventional PCR and real-time PCR. J. Clin. Microbiol. 42:1075-1081.

Kojima, K., N. Nishimura, Y. Mori, and Y. Yokomizo. 2002. Efficiency of polymerase chain reaction using a novel method of DNA preparation and amplification for detection of *Mycobacterium avium* subsp. *paratuberculosis* in bovine fecal samples. Proceedings of the Seventh International Colloquium on Paratuberculosis. Bilbao, Spain, pp. 267-269.

Li, L., J. P. Bannantine, Q. Zhang, A. Amonsin, B. J. May, D. Alt, N. Banerji, S. Kanjilal, and V. Kapur. 2005. The complete genome sequence of *Mycobacterium avium* subspecies *paratuberculosis*. Proc. Natl. Acad. Sci. U S A 102:12344-12349.

Marsh, I. B., and R. J. Whittington. 2001. Progress towards a rapid polymerase chain reaction diagnostic test for the identification of *Mycobacterium avium* subsp. *paratuberculosis* in faeces. Mol. Cell. Probes 15:105-118.

Nielsen, S. S., and N. Toft. 2006. Age-specific characteristics of ELISA and fecal culture for purpose-specific testing for paratuberculosis. J. Dairy Sci. 89:569-579.

O'Mahony, J., and C. Hill. 2004. Rapid real-time PCR assay for detection and quantitation of *Mycobacterium avium* subsp. *paratuberculosis* DNA in artificially contaminated milk. Appl. Environ. Microbiol. 70:4561-4568.

Paustian, M. L., A. Amonsin, V. Kapur, and J. P. Bannantine. 2004. Characterization of novel coding sequences specific to *Mycobacterium avium* subsp. *paratuberculosis*: implications for diagnosis of Johne's Disease. J. Clin. Microbiol. 42:2675-2681.

Perez, V., J. F. G. Marin, and J. J. Badiola. 1996. Description and classification of different types of lesion associated with natural paratuberculosis infection in sheep. J. Comp. Pathol. 114:107-122.

Poupart, P., M. Coene, H. Van Heuverswyn, and C. Cocito. 1993. Preparation of a specific RNA probe for detection of *Mycobacterium paratuberculosis* and diagnosis of Johne's disease. J. Clin. Microbiol. 31:1601-1605.

Reddacliff, L. A., P. J. Nicholls, A. Vadali, and R. J. Whittington. 2003. Use of growth indices from radiometric culture for quantification of sheep strains of *Mycobacterium avium* subsp. *paratuberculosis*. Appl. Environ. Microbiol. 69:3510-3516.

Reddacliff, L. A., A. Vadali, and R. J. Whittington. 2003. The effect of decontamination protocols on the numbers of sheep strain *Mycobacterium avium* subsp. *paratuberculosis* isolated from tissues and faeces. Vet. Microbiol. 95:271-282.

Reddacliff, L. A., H. McGregor, K. Abbott, and R. J. Whittington. 2004. Field evaluation of tracer sheep for the detection of early natural infection with *Mycobacterium avium* subsp *paratuberculosis*. Aust. Vet. J. 82:426-433.

Rodríguez-Lázaro, D., M. D'Agostino, A. Herrewegh, M. Pla, N. Cook, and J. Ikonomopoulos. 2005. Real-time PCR-based methods for detection of *Mycobacterium avium* subsp. *paratuberculosis* in water and milk. Int. J. Food Microbiol. 101:93-104.

Stabel, J. R., T. L. Bosworth, T. A. Kirkbride, R. L. Forde, and R. H. Whitlock. 2004. A simple, rapid, and effective method for the extraction of *Mycobacterium paratuberculosis* DNA from fecal samples for polymerase chain reaction. J. Vet. Diagn. Invest. 16:22-30.

Stabel, J. R., and J. P. Bannantine. 2005. Development of a nested PCR method targeting a unique multicopy element, ISMap*02*, for detection of *Mycobacterium avium* subsp. *paratuberculosis* in fecal samples. J. Clin. Microbiol. 43:4744-4750.

Strommenger, B., K. Stevenson, and G. F. Gerlach. 2001. Isolation and diagnostic potential of IS*Mav2*, a novel insertion sequence-like element from *Mycobacterium avium* subspecies *paratuberculosis*. FEMS Microbiol. Lett. 196:31-37.

Sweeney, R. W. 1996. Transmission of paratuberculosis. Vet. Clin. North Am. Food Anim. Pract. 12:305-312.

Tasara, T., and R. Stephan. 2005. Development of an F57 sequence-based real-time PCR assay for detection of *Mycobacterium avium* subsp. *paratuberculosis* in milk. Appl. Environ. Microbiol. 71:5957-5968.

Vansnick, E., P. De Rijk, F. Vercammen, D. Geysen, L. Rigouts, and F. Portaels. 2004. Newly developed primers for the detection of Mycobacterium avium subspecies paratuberculosis. Vet. Microbiol. 100:197-204.

Wells, S. J., M. T. Collins, K. S. Faaberg, C. Wees, S. Tavornpanich, K. R. Petrini, J. E. Collins, N. Cernicchiaro, and R. H. Whitlock. 2006. Evaluation of a rapid fecal PCR test for detection of *Mycobacterium avium* subsp. *paratuberculosis* in dairy cattle. Clin. Vaccine Immunol. 13:1125-1130.

Whitlock, R. H., and C. Buergelt. 1996. Preclinical and clinical manifestations of paratuberculosis (including pathology). Vet. Clin. North Am. Food Anim. Pract. 12:345-356.

Whittington, R. J., I. Marsh, M. J. Turner, S. McAllister, E. Choy, G. J. Eamens, D. J. Marshall, and S. Ottaway. 1998. Rapid detection of *Mycobacterium paratuberculosis* in clinical samples from ruminants and in spiked environmental samples by modified BACTEC 12B radiometric culture and direct confirmation by IS900 PCR. J. Clin. Microbiol. 36:701-707.

Whittington, R. J., I. Marsh, S. McAllister, M. J. Turner, D. J. Marshall, and C. A. Fraser. 1999. Evaluation of modified BACTEC 12B radiometric medium and solid media for culture of *Mycobacterium avium* subsp. *paratuberculosis* from sheep. J. Clin. Microbiol. 37:1077-1083.

Whittington, R. J., S. Fell, D. Walker, S. McAllister, I. Marsh, E. Sergeant, C. A. Taragel, D. J. Marshall, and I. J. Links. 2000. Use of pooled fecal culture for sensitive and economic detection of *Mycobacterium avium* subsp. *paratuberculosis* infection in flocks of sheep. J. Clin. Microbiol. 38:2550-2556.

Whittington, R. J., D. J. Marshall, P. J. Nicholls, I. B. Marsh, and L. A. Reddacliff. 2004. Survival and dormancy of *Mycobacterium avium* subsp. *paratuberculosis* in the environment. Appl. Environ. Microbiol. 70:2989-3004.

9.14 Appendix 3A-2 Subprogram 3 Protein extraction from *Mycobacterium avium* subsp. *paratuberculosis*: comparison of methods for analysis by sodium dodecyl sulphate polyacrylamide gel electrophoresis, native PAGE and surface enhanced laser desorption/ionization time of flight mass spectrometry

Introduction

Johne's disease is a chronic inflammatory disease of ruminants caused by *Mycobacterium paratuberculosis* that is associated with economic losses worldwide. *M*. *paratuberculosis* is a very robust organism and can survive in the environment for a very long period, presenting a challenge to the control of paratuberculosis [1]. Currently, existing diagnostic assays for the detection of infected animals are inadequate due to the slow-growing nature of the organism and the lack of appropriate molecular resources for *M*. *paratuberculosis* that may enable the development of specific and sensitive assays [2]. A unique feature of all mycobacteria is their thick waxy outer cell wall, consisting of mycolic acids and arabinogalactans linked to the peptidoglycan envelope [3, 4]. Mycolic acids are strongly hydrophobic molecules that form a lipid shell around the organism, affecting permeability properties at the cell surface. They are considered to be a significant virulence factor of mycobacteria [3]. The cell envelope not only helps in intracellular survival and immune modulation, but also plays a role in drug resistance [4] and renders mycobacteria highly resistant to common lysis techniques, so that relatively harsh disruption techniques are required [5]. Cells can be lysed by several techniques, though the most common ones involve removing the cell wall by mechanical shearing or enzymatic treatment [6]. The mechanical method of bead beating has been shown to be a rapid and efficient method for extracting the proteins from *M*. *paratuberculosis* [5]. In addition, various lysis/solubilisation buffers have been used to release proteins from cells, but one buffer is not sufficient for all purposes. Therefore, a thorough study of a number of extraction buffers to identify the conditions that cause efficient extraction of proteins must be employed in each experiment [6]. Also, it is probably unwise to assume that all mycobacterial species will be susceptible to the same extraction procedures, because there are significant differences in cell wall composition between species and even between strains within species [7].

Methods used for investigation of protein profiles of *M*. *paratuberculosis* include SDS-PAGE and 2-dimensional gel electrophoresis (2-D-GE) [5, 8, 9]. 2-D gels have certain disadvantages as they are time consuming, unsuitable for low molecular weight proteins, require a large amount of sample and lack reproducibility [10, 11]. The development of matrix assisted laser desorption/ionization time of flight mass spectrometry (MALDI-TOF) has widened the application of mass spectrometry to study proteins from complex biological materials [12]. A further development in mass spectrometry, SELDI-TOF-MS, was introduced by Hutchens and Yip [13], and simplified sample extraction and on-probe investigation of proteins. SELDI-TOF-MS, also known as ProteinChip® array technology (Ciphergen Biosystems, CA, USA), is based on selective protein extraction and retention on a chromatographic chip surface and successive analysis by simple laser desorption/ionization mass spectrometry [14, 15]. The spectrum of protein peaks obtained with SELDI analysis can distinguish small differences between samples of interest [14]. SELDI-TOF-MS ProteinChip® arrays enable the detection of proteins at femtomole levels directly from their "native" state.

Recently, the complete genome sequence of *M*. *paratuberculosis* K-10 strain has been published [16]. However, it has been suggested that a complete genome sequence is not sufficient for the elucidation of the biological function of the organism, as the cell is dependant on different metabolic and regulatory pathways for its survival. Moreover, there is no strict linear relationship between the genes and the proteins of the cell [17] and the central dogma of molecular biology states that proteins are closer to the actual biological functions of cells than mRNA or DNA [18]. Therefore, optimization of a powerful tool such as SELDI-TOF-MS for the identification of protein profiles of *M*. *paratuberculosis* would be useful for future investigation of novel proteins, predominantly in the low molecular weight range as these are currently difficult to detect by SDS-PAGE and 2-D gel electrophoresis. Identification of novel proteins from *M*. *paratuberculosis* may be helpful in development of better diagnostic tests and vaccine targets for the control of paratuberculosis. The present study was designed with the following aims: to assess the efficacy of various lysis buffers on the extraction of proteins from *M*. *paratuberculosis* cells by SDS-PAGE, native PAGE and SELDI-TOF-MS, to compare two energy absorbing molecules (EAMs) or matrices on different SELDI-TOF-MS ProteinChip surfaces, and to evaluate the reproducibility of these assays.

Experimental section

Bacterial suspension

M. paratuberculosis strain CM00416, which appears identical to strain K-10 in whole genome microarray analysis [19], was reconstituted from a freeze dried seed stock by adding 0.1 ml of sterile water, inoculating this into a radiometric culture medium (modified BACTEC 12B, BD) and incubating at 37°C for 3 weeks until the Growth Index (GI) read 999. The BACTEC vial was subcultured onto Middlebrook's modified 7H10+MJ slopes and incubated at 37°C for 6 wks when colonies were abundant [20, 21]. Bacteria were harvested into 200 µl of PBS plus 0.1% v/v Tween80 (PBST), vortexed for 1 minute, diluted 1:10 in sterile PBST, passed through a 26g needle, filtered through an 8 µm filter and examined by light microscopy at 400 × magnification to confirm that the majority of cells were single. Viable cells were enumerated using an end point titration method [22] and found to have a concentration of $4.3x10^7$ viable cells/ml. Suspensions were stored at - 80°C until required with no loss of viability (data not shown). Prior to the experiment, the suspension was thawed at room temperature followed by thorough mixing by vortexing.

Lysis buffers

Six different lysis buffers; 0.4% v/v Triton X-100, 0.4% v/v Tween20, 8M Urea with 1% w/v CHAPS, 0.1% v/v Decon90, 0.5% v/v Decon90 and 0.8M potassium thiocyanate (KSCN) in 80mM sodium chloride (NaCl) were used for extraction of proteins followed by resolution by SDS-PAGE. Of these, 0.4% v/v Triton X-100, 0.4% v/v Tween20, 0.1% v/v Decon90 and 0.5% v/v Decon90 extracts were suspended in 500mM Tris-HCl (pH 7.0) and 150mM β-mercaptoethanol. For native PAGE and SELDI-TOF-MS four buffers; 0.4% v/v Triton X-100, 0.4% v/v Tween20, 0.8M KSCN/80mM NaCl and 8M Urea with 1% w/v CHAPS were used. 0.4% v/v Triton X-100 and 0.4% v/v Tween20 extracts were suspended in PBS (pH 7.0) and 150mM β-mercaptoethanol.

Sample preparation

For each lysis treatment, 1ml of mycobacterial suspension was centrifuged at 16,060 × *g* (Biofuge® pico, Heraeus) for 1min. The supernatants were discarded and weights of cell pellets (~10mg each) were recorded. Cell pellets were washed three times with 1ml of ice-cold PBS. The cell lysis buffers (250µl), 0.5µl of protease inhibitor cocktail (Sigma-Aldrich, product number P8849) and 0.5g of 0.1mm zirconium beads (BioSpec Products Inc., catalog number 11079101z) were added to the respective cell pellets in 2ml screw cap polypropylene tubes (Scientific Specialties Inc, catalog number 233000). Cell pellets were resuspended thoroughly by vortexing for 15s to 30s and cells were disrupted in a cell homogenizer (FastPrep® FP120, Thermo Electron Corporation) using 7 × 20s pulses at maximum speed (6.5) with 2min rest on ice between pulses.

The beads were allowed to settle for 2min, small outlets were created at the bottom of each Fastprep tube with a tuberculin syringe and each tube was secured in another microfuge tube. These secured tubes were placed in 50ml plastic tubes and centrifuged at 360 × *g* for 5min (Beckman coulter, Allegra™-X12R centrifuge) to obtain the whole lysed cell suspension without zirconium beads. The lysed cell suspension was centrifuged at 16,060 × *g* to pellet the cellular debris and aliquots of the supernatant were stored at -80°C for SDS-PAGE, native PAGE and SELDI-TOF-MS. The mycobacterial extracts prepared in 0.8M KSCN/80mM NaCl and Decon90 buffers were dialyzed through 3kDa dialysis membrane using a microdiaylzer (Pierce Biotechnology) to remove salts that may interfere with protein determination. Ziehl Neelsen stained smears were prepared to test the efficacy of lysis as a positive result requires an intact cell wall. Ziehl Neelsen staining was performed as described by Cruickshank *et al* [23]. A Bradford assay for the estimation of protein concentration was performed as previously described [24].

SDS-PAGE and Native PAGE

Discontinuous electrophoresis buffer conditions as described previously by Laemmli were used [25]. The separating gel was prepared to give a final polyacrylamide concentration of 12% from a stock solution containing 30% Acrylamide:Bis solution, 29:1(Bio-Rad Laboratories, catalog number 1610156) and the final concentration of stacking gel was 4%. The sample reducing buffer comprised 0.0625M Tris-HCl pH 6.8, 10% glycerol, 2% SDS, 5% β-mercaptoethanol in purified water. The samples were boiled for 5min after addition of sample reducing buffer and wells were loaded with ~7.5 µg of sample protein in sample reducing buffer. Electrophoresis was carried out in a Hoeffer™ SE260 electrophoresis system (Amersham Biosciences) at a constant current of 30mA for 2h. Fermentas PageRuler prestained protein ladder was used to determine the molecular weight of proteins in SDS-PAGE and native PAGE.

The protocol for native PAGE was a modification of Hames non-denaturing PAGE [26-28]. The main differences from the Laemmli protocol were the absence of SDS in electrophoresis and sample buffers, samples were not boiled and resolving gel was overlaid with purified water. Acrylamide gels were rinsed in MQW and stained with colloidal coomassie stain as described by Neuhoff *et al* [29].

SELDI-TOF-MS

Three ProteinChip® arrays (Ciphergen Biosystems, CA, USA) with different surface chemistries were used; cation exchange (CM10), anion exchange (Q10) and immobilized metal affinity chromatography (IMAC30) charged with $CuSO_4$ according to the manufacturer's instruction. Each reaction surface (spot) on the CM10 and Q10

arrays was equilibrated three times with 5µl of 50mM Tris-HCl pH 7.0 binding buffer (5min each) and the IMAC30 array with 5µl PBS binding buffer. ProteinChip® array spots were loaded in duplicate with 5µl containing 1.7µg of *M. paratuberculosis* protein extract and incubated for 1h with orbital agitation in a humidity chamber. The protein samples were removed by capillary action using a paper wick and surfaces were washed three times with 5µl of the appropriate equilibration buffer (5min each). The arrays were then washed twice with 1mM HEPES buffer for 1min. The surfaces were allowed to dry for 15min at room temperature, followed by two additions of a freshly made 1µl volume of 50% saturated solution of EAM-1 proprietary formulation or SPA (Ciphergen) in 50% acetonitrile and 0.5% trifluoroacetic acid.

ProteinChip® arrays were analysed on a Ciphergen PBS IIC instrument using ProteinChip® software version 3.1.2. The mass scale was externally calibrated with the All-in-one peptide standard (Ciphergen Biosystems, CA, USA). Baseline subtraction was performed, and traces were normalized to total ion current with a minimum mass to charge of 2000Da. Mass spectra were collected over the low molecular weight range (2-20kDa) and medium molecular weight range (20-60kDa) at various sensitivities and intensities of detector and laser, respectively. The spectra with mass/charge values <2000 were not considered for analysis, as the EAM signal can interfere with peak detection in this region. The data were analyzed as described by Cordingley *et al* [30]. Briefly, the numbers of peaks were identified and mass range was calculated. Peak Cleanness 1 (PC1), which was a measure of the shape of peaks i.e. average broadness of peaks relative to their mass, was calculated as $PC1 = 1/NP\ \Sigma M/W^{1/2}$, where NP was the number of peaks, M was the mass of a peak, $W^{1/2}$ was the width of peak at its half height and summation was carried out over all the peaks in the trace. Peak Cleanness 2 (PC2) was defined as a measure of the minimum peak resolution from a trace. It was calculated between each consecutive pair of peaks as $PC2 = 2(M_2 - M_1) / W_1^{1/2} + W_2^{1/2}$, where M was the mass of peak and $W^{1/2}$ is the width of peak at its half height. Higher PC1 and PC2 values were considered advantageous.

Reproducibility of assays

The reproducibility of extraction methods for SDS-PAGE was tested by using protein samples prepared from aliquots of the same batch of suspension on two different days. The reproducibility of SELDI-TOF-MS was evaluated by calculating the coefficient of variation (CV) of intensity and mass/charge for each of four different protein peaks, three in the low molecular weight range and one in the medium molecular weight range. Tween20 and Urea CHAPS protein extracts were analysed on CM10 ProteinChip® arrays. Protein extract was applied on each chip in 4 replicates. A single batch of sinapinic acid EAM was used throughout the reproducibility study. The chips were read on a Ciphergen PBS IIC reader with laser intensity 230; detector sensitivity 2 for low molecular weight proteins. For medium molecular weight proteins, laser intensity and detector sensitivity were changed to 230 and 8 for Tween20 and 235 and 8 for Urea CHAPS, respectively. Interchip variation was calculated as the CV of the means of the replicates from the 2 chips. To assess the relationship between CV and peak intensity, low peak intensity was defined to be < 30.0, and low CV to be < 15.0%. A two sample *t*-test was used (Minitab 14, Minitab Inc., Pennsylvania State University) to compare the differences in masses of 4 peaks among the two chips. Least squares regression analyses were conducted (Minitab 14) to estimate the relation between mass/charge and CV of mass/charge, intensity and CV of intensity and mass and CV of intensity.

Results

Efficacy of lysis buffers for protein extraction

Once it has been absorbed, intact mycobacteria do not release carbol fuchsin stain on acid treatment, and acid-fast bacilli appear pink. The efficacy of buffers on cell disruption and protein solubilisation from *M*. *paratuberculosis* was assessed on the basis of presence or absence of intact acid fast bacilli following Ziehl Neelsen staining and on the amount of protein extracted, respectively. Although all treatments effectively lysed the cells, Tween20 was the most effective solubilisation buffer and only a few intact bacilli were observed in Ziehl Neelsen stained smears (Fig 1). Additionally, it yielded the highest amount of protein from *M*. *paratuberculosis* cells compared to the other lysis buffers (Table 1). 0.1% Decon90 and 0.8M KSCN/80mM NaCl were the least efficient lysis buffers. Experiments were repeated temporally with similar outcomes (Table 1).

Resolution of proteins by SDS-PAGE and Native PAGE

No qualitative difference between the different lysis buffers was observed. All buffers irrespective of protein yield produced a similar and well resolved banding pattern on SDS-PAGE, both for low and high molecular weight proteins (Fig 2). In contrast, on native PAGE, Tween20 extraction appeared to result in a more complex protein profile than was obtained from other buffers (Fig 3).

Generation of protein profiles by SELDI using SPA matrix CM10 chip surface

Of the lysis buffers used, Triton X-100 generated the maximum number of protein peaks in the low molecular weight range. Tween20 was comparable to Triton X-100 but produced sharper peaks (PC1) with slightly decreased resolution (PC2). The mass range of peaks detected for both Tween20 and Triton X-100 was 5-18kDa (Table 2). However, Tween20 was the most efficient lysis buffer for the identification of medium molecular weight proteins (Table 3). Other lysis buffers also led to identification of proteins in the low and medium molecular weight ranges, but 0.8M KSCN/80mM NaCl detected only one protein peak in the medium molecular weight range.

IMAC chip surface

The best PC1 values were obtained with 0.8M KSCN/80mM NaCl lysis buffer. The mass range for low molecular weight proteins varied from 2-19kDa (Table 2). In contrast, Tween20 and Triton X-100 were less efficient at detection of low molecular weight proteins and no proteins were detected in the medium molecular weight range (Table 3). Urea CHAPS was able to identify peaks for both low and medium molecular weight proteins but more proteins were identified in the medium molecular weight range (20-41kDa).

Q10 chip surface

All the buffers were efficient for detecting the proteins on Q10 surface. Urea CHAPS proved best buffer for low molecular weight range by identifying proteins peaks between 5-18kDa (Table 2). However, Triton X-100 was more efficient than Urea CHAPS for the detection of medium molecular weight proteins on the basis of PC1 and PC2 criteria and the mass range varied from 20-41kDa (Table 3).

Generation of protein profiles by SELDI with EAM-1 matrix

CM10 chip surface

All buffers resulted in detection of proteins on the CM10 surface, though Urea CHAPS was the most efficient, producing additional peaks for low and medium molecular weight proteins. The peaks were of higher intensity, sharper but of lower resolution than for other buffers. The mass range for low molecular weight proteins varied from 5-14kDa, while that for medium molecular weight proteins ranged from 20-34kDa (Table 4-5). 0.8M KSCN/80mM NaCl proved to be the least efficient lysis buffer (Table 4-5).

IMAC chip surface

0.8M KSCN/80mM NaCl and Urea CHAPS were efficient buffers for the detection of proteins in both molecular weight ranges (Table 4-5). Tween20 and Triton X-100 were the least efficient buffers. The mass ranges for 0.8M KSCN/80mM NaCl were 2-18kDa and 22-41kDa for low and medium molecular weight proteins, respectively (Table 4-5).

Q10 chip surface

Protein peaks were detected using all the lysis buffers. However, 0.8M KSCN/80mM NaCl detected protein peaks of low molecular weight that were not identified with the use of other lysis buffers. The mass range varied from 5-11kDa. Urea CHAPS detected fewer lower intensity peaks than 0.8M KSCN/80mM NaCl, but the mass range varied from 2-18kDa (Table 4). In contrast, 0.8M KSCN/80mM NaCl did not identify any medium molecular weight protein peaks. Tween20 produced more protein peaks for the medium molecular weight range and their mass varied from 20-55kDa (Table 5).

Overall, 0.8M KSCN/80mM NaCl generated greatest number of protein peaks in low molecular weight range on IMAC ProteinChip®array. Sinapinic acid produced additional and sharper peaks compared to EAM-1 proprietary formulation. Triton X-100, which generated maximum number of protein peaks for medium molecular weight range on Q10 chip surface was compared with SDS-PAGE. A total of 10 protein peaks were identified by SELDI-TOF-MS in the mass range of 20-41kDa and no peaks were detected for proteins >60kDa, even after adjusting the laser intensity and detector

sensitivity (data not shown). In contrast, SDS-PAGE detected ~25 intense protein bands in this region (Fig 2).

Reproducibility of assays

Identical banding patterns were observed on SDS-PAGE analysis of protein samples prepared at two different times (data not shown). For SELDI-TOF-MS, intra-chip CV for mass/charge values for 4 protein peaks varied from 0.01% to 0.07% among two chips (Table 6). The CV for peak intensity ranged from 3.1% to 17.3% for Tween20 and 5.6% to 26.8% for Urea CHAPS on chip 1. Higher CV for peak intensity was observed for Tween20 (18.9% to 33.0%) and Urea CHAPS (9.0% to 31.5%) on chip 2 (Table 6). Inter-chip CV for mass/charge ranged from 0.00% to 0.08% for 4 peaks among both lysis buffers and the CV for intensity of peaks varied from 1.2% to 35.6% (Table 7). The estimate of the masses of some peaks were significantly different between the two chips: there was significant difference in masses for peak 1 and peak 4 for Tween20 and peak 1 and 2 for Urea CHAPS (Table 7). The differences in mean mass/charge between chip 1 and chip 2 accounted to 2-3Da for the two peaks < 8kDa and 25Da for the peak of about 23kDa. There was significant effect of mass/charge on the CV with larger proteins to have a more variable mass/charge (p<0.01) (Fig 4a, 4b). The variability in intensity tended to be greater for low intensity peaks, but this was statistically significant only in the case of Urea CHAPS (Fig 5a, 5b). Pooling the data in Table 6, 8 of 9 low intensity peaks had high CV while 6 of 7 high intensity peaks had low CV. The degree of variability in intensity was not related to the mass of the peak.

Discussion

SDS-PAGE and Native PAGE

SDS-PAGE is a rapid, low cost and reproducible method for quantifying, comparing and characterizing proteins. It separates proteins primarily on the basis of mass. SDS binds to hydrophobic portions of a protein and causes disruption of its folded structure, allowing its existence in solution in an extended conformation with uniform charge [25, 31]. Nevertheless, this method cannot be used for analysis of intact protein complexes where biological activity needs to be retained for functional testing and different proteins with the same mass cannot be resolved [28]. Thus, non-denaturing (native) PAGE was used also in the present study for the analysis of native proteins. A further aim was to optimize SELDI-TOF-MS with native protein samples, as use of SDS can interfere with ProteinChip® arrays by causing ion suppression (Ciphergen Biosystems, CA, USA). Decon90 which is a strong detergent was not used because it can also interfere with ProteinChip® arrays. The complexity of the protein profile, number of bands and their resolution were considered. Tween20 buffer, which showed a similar banding pattern in SDS-PAGE to other lysis buffers revealed different proteins on native PAGE than Triton X-100, Urea CHAPS and 0.8M KSCN/80mM NaCl (Fig 2 and 3). This could be explained because native PAGE separates proteins on the basis of both mass and charge [28].

SELDI vs. PAGE

SELDI-TOF-MS mostly detected protein peaks in the range 2-19kDa (Table 2), while fewer proteins resolved on native PAGE and SDS-PAGE in this range. However, in the medium molecular weight range (20-60kDa) many protein bands appeared on the SDS-PAGE, while few protein peaks were identified by SELDI-TOF-MS. It has been reported that the higher the detector sensitivity and laser intensity, the better would be detection

of high mass proteins, but low intensity peaks then cannot be detected [32]. However, in the present study SELDI-TOF-MS did not detect higher molecular weight proteins regardless of sensitivity and intensity settings. Perhaps after application of sample to ProteinChip® arrays, proteins of lower molecular weight migrate towards the chip surface more quickly than higher molecular weight proteins and exclude binding of the latter if the chip is saturated.

Efficacy of lysis buffers

This is the first study in which different lysis buffers for the extraction of proteins from *M. paratuberculosis* were compared in three protein analysis systems. A similar pattern of bands was obtained in SDS-PAGE and also in native PAGE analysis regardless of buffer. However, lysis buffer was a significant determinant of the spectrum obtained using SELDI-TOF-MS. For SELDI-TOF-MS, it has been reported that different ProteinChip® arrays can be used for a given sample, but choice of chip array requires some prior knowledge so that proteins of interest can be detected [33]. Therefore different chip surfaces were included in the present study and the goal was to find the best chip array and lysis buffer combination to detect the maximum number of proteins in low and medium molecular weight ranges. The two non-ionic detergents, Tween20 and Triton X-100, were included along with the chaotropic agents Urea CHAPS and 0.8M KSCN/80mM NaCl, as they were considered useful for isolation of functional protein complexes [34]. However, non-ionic detergents cannot disrupt protein-protein interactions and zwitterionic detergents were considered to be more efficient for disrupting these [34]. Consequently, the zwitterionic detergent CHAPS was used along with Urea.

Results from different lysis buffers on different chip surfaces were quite different. Tween20 and Triton X-100 buffers were most efficient when used in conjunction with the CM10 surface, while Urea CHAPS was the most appropriate buffer on the Q10 surface. The manufacturer suggested that the active spots on the CM10 surface contains weak anionic carboxylate groups that interact with the positive charged surface of proteins or with proteins having a high isoelectric point (pI). The Q10 surface contains cationic quaternary ammonium groups, which interact with the negative charges on the surface of proteins or proteins with low pI. These claims suggest that the non-ionic detergents were more efficient in extraction of proteins with high pI and Urea CHAPS extracted more proteins with low pI. Conversely, 0.8M KSCN/80mM NaCl was the most efficient lysis buffer on the IMAC chip surface and proteins were not detected on this chip by non-ionic detergents. The manufacturer suggests that the IMAC surface contains active spots having nitrilotriacetic acid (NTA) groups with ability to chelate the metal ion and the proteins bound to the chelated metal ions. The results suggested that 0.8M KSCN/80mM NaCl extracted more metal binding proteins than the non-ionic detergents.

In contrast, Urea CHAPS was efficient for the detection of proteins on all the chip surfaces. Urea CHAPS is recommended by the manufacturer (Ciphergen Biosystems, CA, USA) for sample preparation for ProteinChip® arrays, but a unique finding in the present study was that 0.8M KSCN/80mM NaCl, another chaotropic agent, performed better than Urea CHAPS on the IMAC surface by detecting a greater number of protein peaks, although the amount of protein extracted from *M. paratuberculosis* cells was lower than with non-ionic detergents (Table 1). The diversity of protein species resolved may be more important than total protein yield in biodiscovery projects.

Chaotropic agents are specific anions which dissociate aggregated proteins by increasing the solubility of hydrophobic regions in an aqueous environment [35]. Recently,

it was found that these agents could disrupt the hydrogen bonding between water molecules and reduce the native state of proteins. A high concentration can lead to denatuaration of proteins [36]. These harsh buffers proved efficient for the disruption of *M*. *paratuberculosis*, perhaps by disrupting the complex nature of the mycobacterial cell wall through a number of mechanisms. 0.8M KSCN/80mM NaCl was the most efficient lysis buffer overall on the ProteinChip® arrays as it led to detection of the highest number of protein peaks. This observation would be useful for the identification of protein profiles of *M*. *paratuberculosis* that cannot be detected by the use of other lysis buffers.

Energy absorbing molecules

Two EAMs were compared in this study because the EAM is considered to be important for determination of spectra [30]. Moreover, it has been reported that one EAM may not be effective for all proteins. The EAM is selected on the basis of the molecular weight and the chemical nature of the analyte. EAM-1 proprietary formulation is recommended for proteins of 10-50kDa and for determination of glycosylated proteins, while SPA is recommended for all larger proteins and peptides (Ciphergen Biosystems, CA, USA). In biodiscovery research, the nature of the targets is unknown, requiring evaluation of both EAM. Interestingly, in this study SPA performed better than EAM-1 proprietary formulation by detecting additional protein peaks in both the low and the medium molecular weight ranges. Further, peaks of higher intensity were generated with SPA compared to EAM-1.

Reproducibility of SELDI

In a previous study it was observed that important extrinsic factors which can influence the reproducibility of peak detection include matrix composition and instrument settings [32]. Consequently, identical matrix composition and instrument settings were used throughout this study. The reproducibility of the assay was calculated for both non-ionic and chaotropic agents. Extremely low CV values for mass/charge indicate high reproducibility of mass/charge estimation. However, the estimated masses of peaks can be significantly different between chips. Further, there was substantial variation in peak intensity for some peaks. Higher CV for intensity was recorded in general for peaks with lower intensity. This finding was in agreement with earlier studies [32, 37, 38]. The potential sources of variability that arise during SELDI-TOF-MS profiling include spot to spot variation of chip surface, variation in laser intensity and detector sensitivity over time, pipetting and operator variability and the crystallization process of the matrix [30, 38]. Variability may be reduced by using automated robotic during sample transfer and processing [39].

Conclusion

SELDI-TOF-MS was an efficient tool for study of the proteome of *M*. *paratuberculosis*, particularly for low molecular weight proteins. A range of different lysis buffers can be used for the extraction of proteins from *M*. *paratuberculosis* for SDS-PAGE and native PAGE analysis. However, for SELDI-TOF-MS ProteinChip® array surface analysis, energy absorbing molecule and lysis buffer should be selected carefully. Chaotropic agents, particularly 0.8M KSCN/80mM NaCl proved to be efficient and was compatible with ProteinChip® arrays. The IMAC surface chemistry revealed a greater proteome complexity than other surfaces. Estimation of mass using SELDI-TOF-MS was straightforward and highly reproducible.

Table 1 Protein released from 10mg *M. paratuberculosis* cells using six different lysis buffers in two independent experiments

Lysis buffer	Protein content (mg/ml)
0.4% Tween20	0.62-0.67
0.4% Triton X-100	0.57-0.58
8M Urea, 1% CHAPS	0.51-0.56
0.5% Decon90	0.52-0.58
0.1% Decon90	0.35-0.38
0.8M KSCN/80mM NaCl	0.36-0.40

Table 2 Low molecular weight proteins identified in *M. paratuberculosis* according to lysis buffer on three ProteinChip® arrays by using SPA matrix

Chip Array	Lysis Buffer	Chip Protocol[a]	No. of Peaks[b]	Mass Range (kDa)	PC1[b]	PC2[b]	Peaks with Intensity >10	>5	>3
CM10	Tween20	7-220	17	5-18	226	59	2	2	5
	Triton X-100	7-220	18	5-18	175	67	2	2	7
	Urea CHAPS	7-220	13	5-18	262	58	2	3	4
	KSCN NaCl	7-220	13	5-12	309	30	1	4	3
IMAC	Tween20	8-225	3	7-11	266	127		1	1
	Triton X-100	8-225	1	7	461			1	
	Urea CHAPS	8-225	16	4-18	297	31	3	6	5
	KSCN NaCl	8-225	23	2-19	336	18	9	8	3
Q10	Tween20	8-225	11	5-18	256	33	2	4	3
	Triton X-100	8-225	18	5-18	315	32	4	13	
	Urea CHAPS	8-225	21	5-18	377	25		9	9
	KSCN NaCl	8-225	18	5-16	203	16	1	9	6

[a] Detector sensitivity- Laser intensity

[b] High values beneficial

Table 3 Medium molecular weight proteins identified in *M. paratuberculosis* according to lysis buffer on three ProteinChip® arrays by using SPA matrix

Chip Array	Lysis Buffer	Chip Protocol[a]	No. of Peaks[b]	Mass Range (kDa)	PC1[b]	PC2[b]	Peaks with Intensity >10	>5	>3
CM10	Tween20	7-230	7	20-33	49	256	1	1	2
	Triton X-100	7-230	5	22-34	107	143		1	1
	Urea CHAPS	7-230	7	20-44	54	201		1	1
	KSCN NaCl	7-230	1	22	47				
IMAC	Tween20	7-235	1	28	161				
	Triton X-100	7-235	0						
	Urea CHAPS	7-235	8	20-41	143	94			2
	KSCN NaCl	7-235	4	22-24	182	131			1
Q10	Tween20	7-235	6	20-41	35	512			4
	Triton X-100	7-235	10	20-41	73	99		3	4
	Urea CHAPS	7-235	6	20-55	45	525			3
	KSCN NaCl	7-235	5	23-66	86	176			

[a] Detector sensitivity- Laser intensity
[b] High values beneficial

Table 4 Low molecular weight proteins identified in *M. paratuberculosis* according to lysis buffer on three ProteinChip® arrays by using EAM-1 matrix

Chip Array	Lysis Buffer	Chip Protocol[a]	No. of Peaks[b]	Mass Range (kDa)	PC1[b]	PC2[b]	Peaks with Intensity >10	>5	>3
CM10	Tween20	7-225	6	5-14	74	140	1	1	1
	Triton X-100	7-225	7	5-11	75	74	1	2	1
	Urea CHAPS	7-225	10	5-14	104	51	1	2	3
	KSCN NaCl	7-225	4	5-11	33	243			2
IMAC	Tween20	8-230	1	7	996				
	Triton X-100	8-230	1	7	294				1
	Urea CHAPS	8-230	4	7-11	93	63		3	1
	KSCN NaCl	8-230	7	2-18	175	76	2	3	1
Q10	Tween20	8-220	7	5-11	98	43		1	5
	Triton X-100	8-220	6	5-11	207	57	1	1	3
	Urea CHAPS	8-220	6	2-18	238	117		2	3
	KSCN NaCl	8-220	13	5-11	191	33		2	4

[a] Detector sensitivity- Laser intensity
[b] High values beneficial

Table 5 Medium molecular weight proteins identified in *M. paratuberculosis* according to lysis buffer on three ProteinChip® arrays by using EAM-1 matrix

Chip Array	Lysis Buffer	Chip Protocol[a]	No. of Peaks[b]	Mass Range (kDa)	PC1[b]	PC2[b]	Peaks with Intensity >10	>5	>3
CM10	Tween20	8-235	3	22-34	51	450			1
	Triton X-100	8-235	3	20-24	17	1403			1
	Urea CHAPS	8-235	4	20-34	29	729	1		
	KSCN NaCl	8-235	1	22	28				
IMAC	Tween20	7-235	0						
	Triton X-100	7-235	0						
	Urea CHAPS	7-235	3	22-41	45	705			
	KSCN NaCl	7-235	5	22-41	63	258		1	
Q10	Tween20	7-225	9	20-55	32	534			1
	Triton X-100	7-225	5	20-41	50	289			
	Urea CHAPS	7-225	5	23-44	77	312			
	KSCN NaCl	7-225	0						

[a] Detector sensitivity- Laser intensity
[b] High values beneficial

Table 6 Intra - chip variation on two CM10 ProteinChip® arrays using two different lysis buffers

	Peak	Mass/charge	CV[a]	Intensity	CV[a]
Chip 1					
Tween20	Peak 1	5672.41	0.01	35.02	6.8
	Peak 2	7650.24	0.01	12.12	3.1
	Peak 3	11330.16	0.02	65.19	8.8
	Peak 4	22704.73	0.04	10.19	17.3
Urea CHAPS	Peak 1	5654.87	0.01	39.07	13.4
	Peak 2	7647.21	0.02	11.27	26.8
	Peak 3	11311.40	0.02	73.05	5.6
	Peak 4	22671.62	0.03	12.83	20.2
Chip 2					
Tween20	Peak 1	5669.13	0.04	20.93	20.7
	Peak 2	7653.98	0.03	9 .00	31.2
	Peak 3	11329.50	0.03	64.73	18.9
	Peak 4	22679.37	0.07	8.72	33.0
Urea CHAPS	Peak 1	5657.53	0.02	36.10	14.5
	Peak 2	7649.43	0.01	11.74	31.5
	Peak 3	11314.19	0.02	71.81	9.0
	Peak 4	22670.98	0.03	9.82	31.4

[a] CV in percent

Table 7 Inter - chip variation on two CM10 ProteinChip® arrays using two different lysis buffers

	Peak	Mean mass/charge	CV[a]	*P* value[b]	Mean intensity	CV[a]
Tween20	Peak 1	5670.78	0.04	0.05	27.97	35.61
	Peak 2	7652.11	0.03	0.07	10.56	20.88
	Peak 3	11329.83	0.00	0.74	64.96	0.50
	Peak 4	22692.05	0.08	0.04	9.46	11.00
Urea CHAPS	Peak 1	5656.20	0.03	0.00	37.59	5.60
	Peak 2	7648.32	0.02	0.02	11.50	2.84
	Peak 3	11312.80	0.02	0.11	72.43	1.20
	Peak 4	22671.30	0.00	0.88	11.32	18.79

[a] CV in percent
[b] Two sample *t*- test, mean chip 1 vs. mean chip 2. Individual means are shown in table 6

References

Whittington, R. J.; Marshall, D. J.; Nicholls, P.; Marsh, I. B.; Reddacliff, L. A., Survival and dormancy of *Mycobacterium avium* subsp. *paratuberculosis* in the environment. *Appl Environ Microbiol* 2004, 70, (5), 2989-3004.

Bannantine, J. P.; Barletta, R. G.; Stabel, J. R.; Paustian, M. L.; Kapur, V., Application of the genome sequence to address concerns that Mycobacterium avium subspecies paratuberculosis might be a foodborne pathogen. *Foodborne Pathog Dis* 2004, 1, (1), 3-15.

Brennan, P. J., The envelope of mycobacteria. *Annu Rev Biochem* 1995, 64, 29-63.

Rastogi, N.; Legrand, E.; Sola, C., The mycobacteria: an introduction to nomenclature and pathogenesis. *Rev Sci Tech* 2001, 20, (1), 21-54.

Lanigan, M. D.; Vaughan, J. A.; Shiell, B. J.; Beddome, G. J.; Michalski, W. P., Mycobacterial proteome extraction: comparison of disruption methods. *Proteomics* 2004, 4, (4), 1094-100.

Edward, H., Immunoprecipitation. In *Using antibodies : a laboratory manual.*, Cold Spring Harbor Laboratory Press: 1999; pp 230-31.

Laurent, J. P.; Hauge, K.; Burnside, K.; Cangelosi, G., Mutational analysis of cell wall biosynthesis in Mycobacterium avium. *J Bacteriol* 2003, 185, (16), 5003-6.

White, W. B.; Whipple, D. L.; Stabel, J. R.; Bolin, C. A., Comparison of cellular and extracellular proteins expressed by various isolates of Mycobacterium paratuberculosis and other mycobacterial species. *Am J Vet Res* 1994, 55, (10), 1399-1405.

Sung, N.; Takayama, K.; Collins, M. T., Possible association of GroES and antigen 85 proteins with heat resistance of Mycobacterium paratuberculosis. *Appl Environ Microbiol* 2004, 70, (3), 1688-97.

Talapatra, A.; Rouse, R.; Hardiman, G., Protein microarrays: challenges and promises. *Pharmacogenomics* 2002, 3, (4), 527-36.

Seibert, V.; Wiesner, A.; Buschmann, T.; Meuer, J., Surface-enhanced laser desorption ionization time-of-flight mass spectrometry (SELDI TOF-MS) and ProteinChip technology in proteomics research. *Pathol Res Pract* 2004, 200, (2), 83-94.

Karas, M.; Hillenkamp, F., Laser desorption ionization of proteins with molecular masses exceeding 10,000 daltons. *Anal Chem* 1988, 60, (20), 2299-301.

Hutchens, T. W.; Yip, T. T., New desorption strategies for the mass spectrometric analysis of macromolecules. *Rapid Commun Mass Spectrom* 1993, 7, (7), 576-580.

Issaq, H. J.; Veenstra, T. D.; Conrads, T. P.; Felschow, D., The SELDI-TOF MS approach to proteomics: protein profiling and biomarker identification. *Biochem Biophys Res Commun* 2002, 292, (3), 587-92.

Merchant, M.; Weinberger, S. R., Recent advancements in surface-enhanced laser desorption/ionization-time of flight-mass spectrometry. *Electrophoresis* 2000, 21, (6), 1164-77.

Li, L.; Bannantine, J. P.; Zhang, Q.; Amonsin, A.; May, B. J.; Alt, D.; Banerji, N.; Kanjilal, S.; Kapur, V., The complete genome sequence of Mycobacterium avium subspecies paratuberculosis. *Proc Natl Acad Sci U S A* 2005, 102, (35), 12344-9.

Pandey, A.; Mann, M., Proteomics to study genes and genomes. *Nature* 2000, 405, (6788), 837-46.

Alberts, B.; Bray, D.; Lewis, J.; Ra, M.; Roberts, K.; Watson, J. D., *Molecular biology of the cell*. New York : Garland: 1994.

Marsh, I. B.; Bannantine, J. P.; Paustian, M. L.; Tizard, M.; Kapur, V.; Whittington, R., Genomic comparison of *Mycobacterium avium* subsp. *paratuberculosis* sheep and cattle strains by microarray hybridization. *Mol Cell Probes* 2006, (*In press*).

Whittington, R. J.; Marsh, I.; McAllister, S.; Turner, M. J.; Marshall, D. J.; Fraser, C. A., Evaluation of modified BACTEC 12B radiometric medium and solid media for culture of *Mycobacterium avium* subsp. *paratuberculosis* from sheep. *J Clin Microbiol* 1999, 37, (4), 1077-83.

Whittington, R. J.; Marsh, I.; Turner, M. J.; McAllister, S.; Choy, E.; Eamens, G. J.; Marshall, D. J.; Ottaway, S., Rapid detection of *Mycobacterium paratuberculosis* in clinical samples from ruminants and in spiked environmental samples by modified BACTEC 12B radiometric culture and direct confirmation by IS900 PCR. *J Clin Microbiol* 1998, 36, (3), 701-7.

Whittington, R. J.; Reddacliff, L. A.; Marsh, I.; McAllister, S.; Saunders, V., Temporal patterns and quantification of excretion of Mycobacterium avium subsp paratuberculosis in sheep with Johne's disease. *Aust Vet J* 2000, 78, (1), 34-7.

Cruickshank, R.; Duguid, J. P.; Marmion, B. P.; Swain, R. H. A., *Medical microbiology; a guide to the laboratory diagnosis and control of infection*. 12th ed.; Edinburgh, Churchill Livingstone: 1973.

Bradford, M. M., A rapid and sensitive method for the quantitation of microgram quantities of protein utilizing the principle of protein-dye binding. *Anal Biochem* 1976, 72, 248-54.

Laemmli, U. K., Cleavage of structural proteins during the assembly of the head of bacteriophage T4. *Nature* 1970, 227, (5259), 680-5.

Bollag, D. M.; Edelstein, S. J.; Rozycki, M. D., Gel electrophoresis under non-denaturating conditions. In *Protein methods*, Wiley-Liss: New York, 1996; pp 155-172.

Simpson, R. J., Nondenaturating PAGE of proteins. In *Proteins and proteomics*, Cold Spring Harbor Laboratory Press: New York, 2003; pp 85-86.

Hames, B. D., Non denaturating polyacrylamide gel electrophoresis. In *Gel electrophoresis of proteins : a practical approach*, Oxford University Press: New York, 1998; pp 35-40.

Neuhoff, V.; Arold, N.; Taube, D.; Ehrhardt, W., Improved staining of proteins in polyacrylamide gels including isoelectric focusing gels with clear background at nanogram sensitivity using Coomassie Brilliant Blue G-250 and R-250. *Electrophoresis* 1988, 9, (6), 255-62.

Cordingley, H. C.; Roberts, S. L.; Tooke, P.; Armitage, J. R.; Lane, P. W.; Wu, W.; Wildsmith, S. E., Multifactorial screening design and analysis of SELDI-TOF ProteinChip array optimization experiments. *Biotechniques* 2003, 34, (2), 364-5, 368-73.

Bollag, D. M.; Edelstein, S. J.; Rozycki, M. D., Gel electrophoresis under denaturating conditions. In *Protein methods*, Wiley-Liss: New York, 1996; pp 107-54.

Schaub, S.; Wilkins, J.; Weiler, T.; Sangster, K.; Rush, D.; Nickerson, P., Urine protein profiling with surface-enhanced laser-desorption/ionization time-of-flight mass spectrometry. *Kidney Int* 2004, 65, (1), 323-32.

Aldred, S.; Grant, M. M.; Griffiths, H. R., The use of proteomics for the assessment of clinical samples in research. *Clin Biochem* 2004, 37, (11), 943-52.

Bollag, D. M.; Edelstein, S. J.; Rozycki, M. D., Preparation for protein isolation. In *Protein methods*, Wiley-Liss: New York, 1996; pp 1-27.

Hatefi, Y.; Hanstein, W. G., Solubilization of particulate proteins and nonelectrolytes by chaotropic agents. *Proc Natl Acad Sci U S A* 1969, 62, (4), 1129-36.

Salvi, G.; De Los Rios, P.; Vendruscolo, M., Effective interactions between chaotropic agents and proteins. *Proteins* 2005, 61, (3), 492-499.

Semmes, O. J.; Feng, Z.; Adam, B. L.; Banez, L. L.; Bigbee, W. L.; Campos, D.; Cazares, L. H.; Chan, D. W.; Grizzle, W. E.; Izbicka, E.; Kagan, J.; Malik, G.; McLerran, D.; Moul, J. W.; Partin, A.; Prasanna, P.; Rosenzweig, J.; Sokoll, L. J.; Srivastava, S.; Thompson, I.; Welsh, M. J.; White, N.; Winget, M.; Yasui, Y.; Zhang, Z.; Zhu, L., Evaluation of serum protein profiling by surface-enhanced laser desorption/ionization time-of-flight mass spectrometry for the detection of prostate cancer: I. Assessment of platform reproducibility. *Clin Chem* 2005, 51, (1), 102-12.

Koopmann, J.; Zhang, Z.; White, N.; Rosenzweig, J.; Fedarko, N.; Jagannath, S.; Canto, M. I.; Yeo, C. J.; Chan, D. W.; Goggins, M., Serum diagnosis of pancreatic adenocarcinoma using surface-enhanced laser desorption and ionization mass spectrometry. *Clin Cancer Res* 2004, 10, (3), 860-8.

White, C. N.; Chan, D. W.; Zhang, Z., Bioinformatics strategies for proteomic profiling. *Clin Biochem* 2004, 37, (7), 636-41.

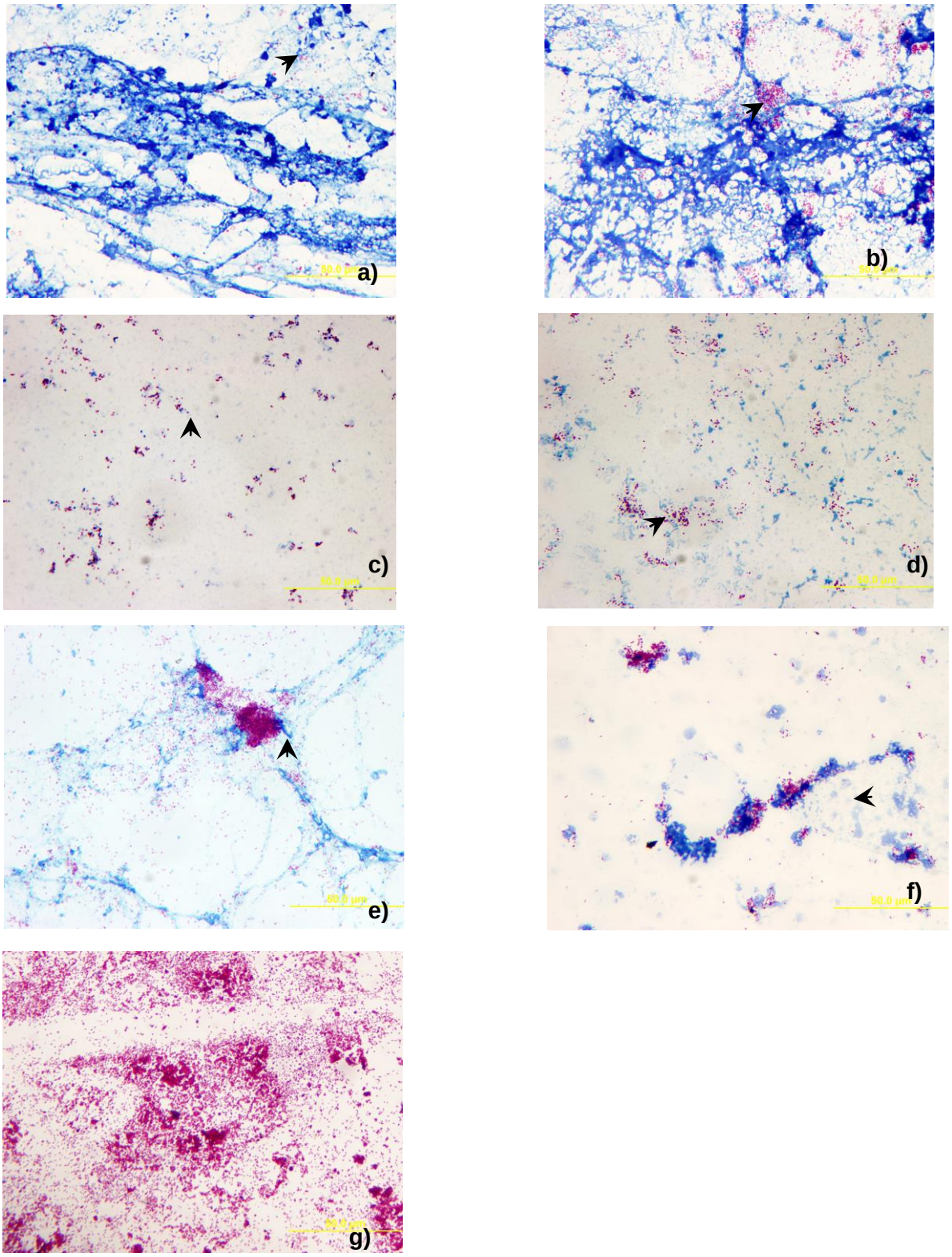

Figure 1 Ziehl Neelsen stained smears (100 ×) of *M. paratuberculosis* with different lysis buffers; a) 0.4% Tween20 b) 0.4% Triton X-100 c) 0.1% Decon 90 d) 0.5% Decon 90 e) 0.8M KSCN/80mM NaCl f) 8M Urea and 1% CHAPS g) positive control *M. paratuberculosis* Fig 1 a) to g) Arrow bars indicate pink intact bacilli, blue color indicates staining of intracellular contents after cell lysis.

1 2 3 4 5 6 7

kDa

170

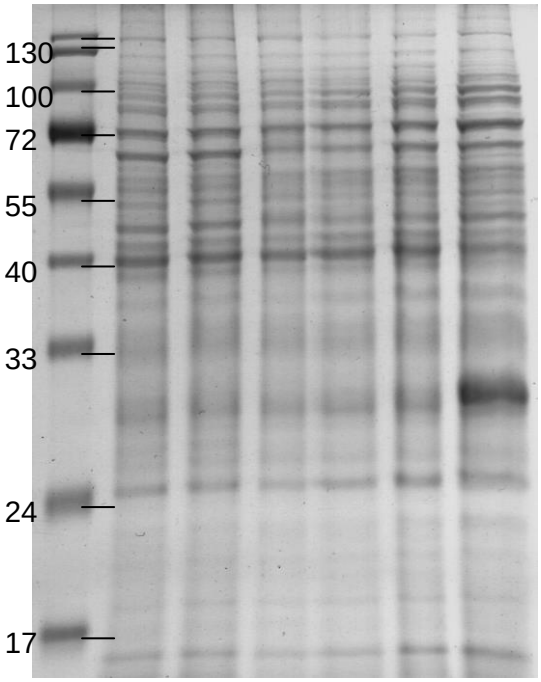

Figure 2 SDS-PAGE analysis of protein samples extracted from *M. paratuberculosis* by different lysis buffers; Lane 1- Molecular weight standard, Lane 2 - 0.4% Tween20, Lane 3 - 0.4% Triton X-100, Lane 4 - 8M Urea with 1% CHAPS, Lane 5 - 0.1% Decon90, Lane 6 - 0.5% Decon90, Lane 7 - 0.8M KSCN/80mM NaCl

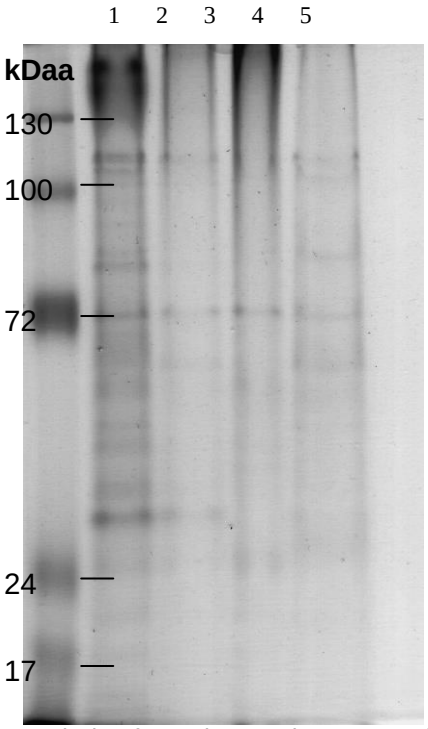

Figure 3 Native PAGE analysis of protein samples extracted from *M. paratuberculosis* by different lysis buffers; Lane 1 – Molecular weight standard, Lane 2 - 0.4% Tween20, Lane 3 - 0.4% Triton X-100, Lane 4 - 8M Urea, 1% CHAPS, Lane 5 - 0.8M KSCN/ 80mM NaCl

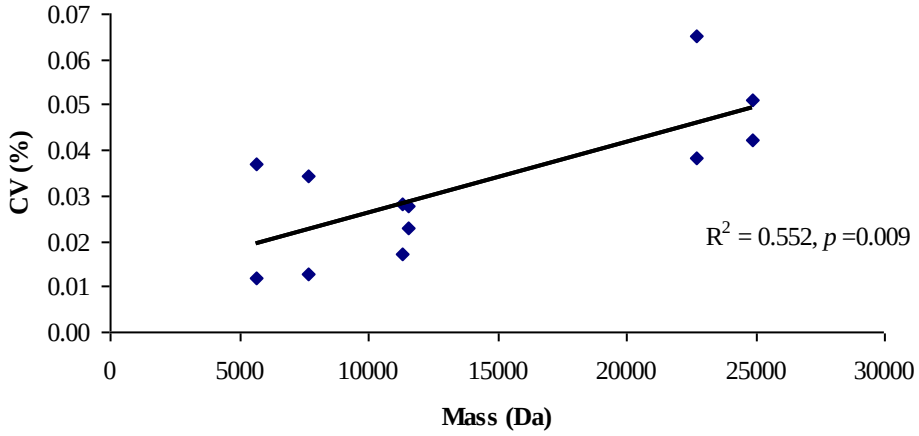

a

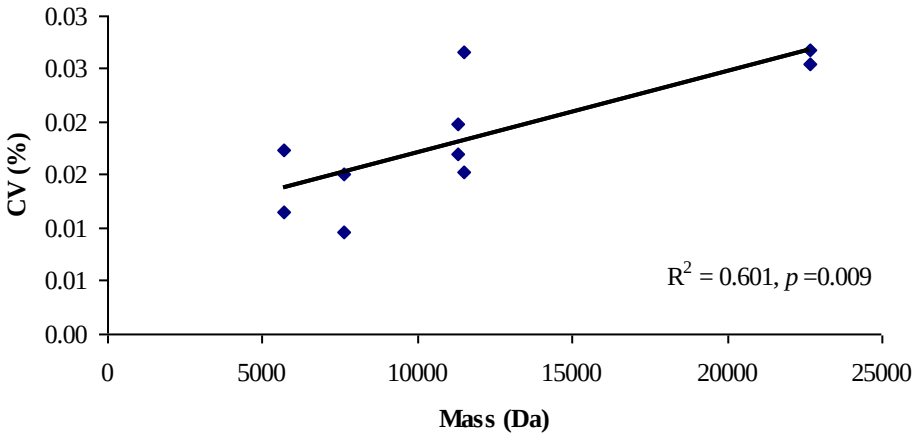

b

Figure 4 Relation between mass/charge and CV of mass/charge for two buffers a) Tween20 b) Urea CHAPS

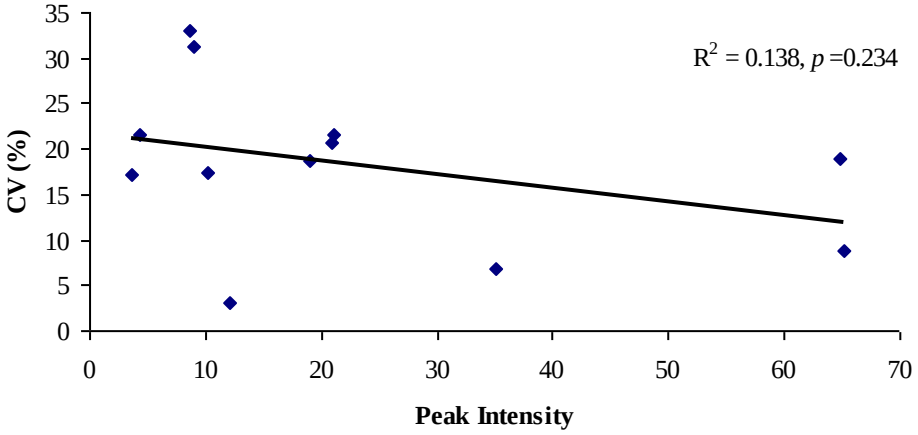

a

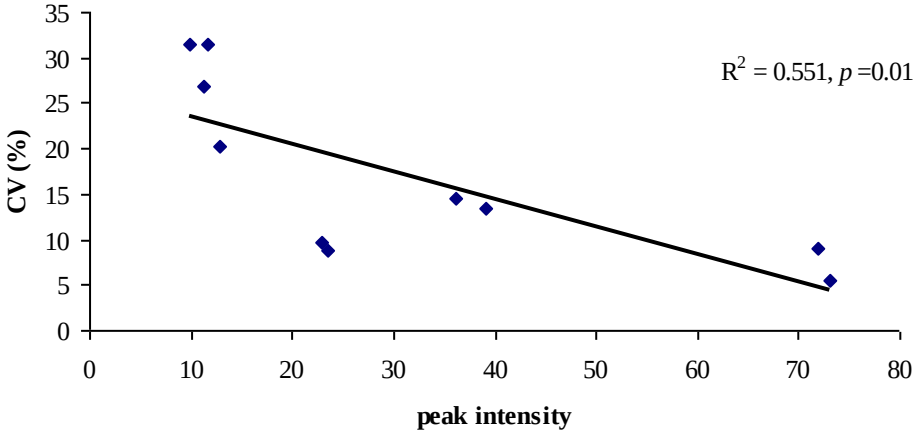

b

Figure 5 Relation between peak intensity and CV of peak intensity for two buffers a) Tween20 b) Urea CHAPS

Synopsis

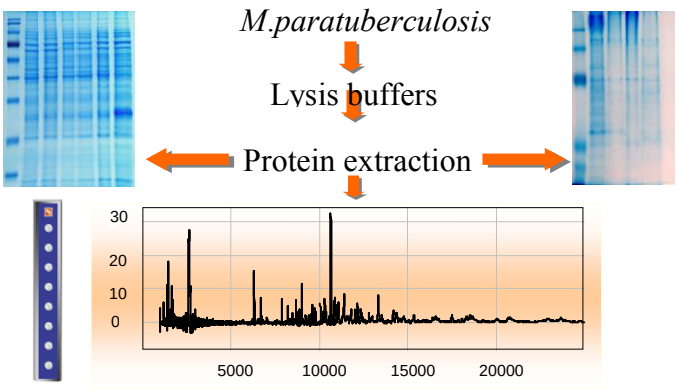
M.paratuberculosis
Lysis buffers
Protein extraction
30
20
10
0
5000
10000
15000
20000

9.15 Appendix 3A-3 Subprogram 3 Growth pattern and proteome of Mycobacterium avium subsp. paratuberculosis in a temperature flux-induced dormancy model

Introduction

Johne's disease is a chronic inflammatory disease of ruminants caused by *Mycobacterium avium* subsp. *paratuberculosis* (MAP) associated with economic losses worldwide (10, 51). In addition there is speculation that MAP is the etiological agent of Crohn's disease in humans, a potential source being the milk of infected cattle (27, 68). Consequently, there are disease control programs for MAP in most developed countries and data on the biological behavior of this organism are needed in human and veterinary medicine. MAP exists in two distinct major genotypic groups, S and C which are partially defined by a point mutation in IS*1311* and a major genomic deletion in S compared to C strain (45). Little is known of the physiological adaptability of either strain in the host or the environment.

MAP is a very robust organism. Although an obligate parasite and pathogen of animals, in the Australian environment it survives in feces/soil for about a year if fully shaded. In contrast it lives for only a few weeks in an exposed unshaded location; diurnal temperature flux was proposed to explain this difference (78). MAP may also survive high temperature, short time pasteurization of bovine milk when the initial concentration is greater than 10^1 cells/ml (69). The organism also survived heat treatment at 63°C for 30 min and 71.7°C for 15 s, if present in numbers 10^4 to 10^7 viable cells/ml (14, 25).

Adaptation to stress is crucial for the survival of microbes in nature. Analysis of cell physiology in natural ecosystems and identification of proteins expressed is an important step in investigation of bacterial adaptational networks (30). Bacterial pathogens also regulate gene expression in response to stimuli within the host (71). As adaptational networks include common pathways that may be activated by different types of stress (13, 30), data on responses to environmental stress may have relevance for understanding responses *in vivo*.

M. *tuberculosis* may enter a dormant or latent state in which it remains viable for many years, without the patient showing clinical signs of the disease. *M*. *tuberculosis* has potential to survive in the host without being recognized by the immune system and these latent forms resuscitate later to cause the disease (52). Most cases of clinical tuberculosis are believed to arise by reactivation of such dormant bacteria (7). Genes with homology to mycobacterial dormancy genes have been identified in MAP: homologues of the Dps protein of *M*. *smegmatis* and the *RelA* gene product of *M*. *tuberculosis*. Moreover, the *in vitro* growth pattern of MAP recovered from the environment was suggestive of dormancy (77, 78). Therefore, it is possible that MAP can enter a dormant state similar to other pathogenic mycobacteria, both in the environment and in the host.

The aim of the present study was to develop an *in vitro* model of dormancy to study the proteome of MAP during dormancy. Growth and proteomic data were obtained for both S and C strains, and compared to responses recently measured following hypoxia and starvation, suggesting both common and unique pathways in the response of this pathogen to different types of stress.

Materials and Methods

Preparation of bacterial suspensions. Suspensions of MAP with a concentration of 4.3×10^7 viable cells/ml (stock suspensions) were used: a clonal S strain (Telford 9.2), with an S1 IS*900* RFLP pattern (74) and an IS*1311* S pattern (44) and a C strain field isolate (CM00/416) with a C3 IS*900* RFLP pattern (74) and IS*1311* C pattern (44) that appeared identical to strain K-10 in whole genome microarray analysis (45). Each strain was reconstituted from a freeze dried seed stock by adding 0.1 ml of sterile water, inoculating this into radiometric culture medium and incubating at 37°C for 3 weeks until the Growth Index (GI) read 999. The radiometric medium consisted of 4 ml enriched Middlebrook 7H9 medium (BACTEC 12B; Becton Dickinson, Sparks, MD, USA) with 200 µl PANTA PLUS (Becton Dickinson), 1 ml egg yolk, 5 µg of mycobactin J (Allied Monitor Inc., Fayette, MO, USA) and 0.7 ml of water (75). GI were measured with an automatic ion chamber (BACTEC 460; Johnston Laboratories, Towson, MD, USA). The liquid medium was subcultured onto Middlebrook's modified 7H10+MJ slopes and incubated at 37°C for 6 weeks when colonies were abundant (75, 76). Bacteria were harvested into 200 µl of phosphate buffered saline (PBS) plus 0.1% v/v Tween80 (PBST), vortexed for 1 min, diluted 1:10 in sterile PBST, passed through a 26 g needle, filtered through an 8 µm filter and examined by light microscopy at 400 × magnification to confirm that the majority of cells were single. Viable cells were enumerated using an end point titration method (79). Suspensions were stored at -80°C until required, with no loss of viability (data not shown). At the start of the experiment, suspensions were thawed at room temperature followed by thorough mixing by vortexing and dilution in PBS with Tween 80 (0.1%v/v), to prepare the required viable cells/ml. Suspensions were passed through a 26 g needle to remove the clumps.

Thermal tolerance experiments. A series of experiments were conducted in which MAP suspensions were exposed to either constant temperature or to cycles of heating and cooling. All experiments were conducted in 200 uL thin walled PCR tubes (Scientific Specialties Inc., CA, USA) in a 96 well PCR thermocycler (Corbett Research, Sydney, Australia). A thermal cycling pattern was designed to mimic diurnal temperature patterns but on a compressed time scale. Temperature records from shaded and unshaded terrestrial locations (78) revealed a diurnal pattern with phases in the ratio 8.5 (temperature trough = minimum + 10%), 3 (ascending), 4.5 (peak = maximum – 10%) and 8 (descending) units duration (1 cycle) where 1 unit = 1 hour. This pattern was programmed into the thermocycler with 1 unit = 1 minute. Due to programming limitations a pattern of 4:8:4:8 units duration (1 cycle) was used in some experiments. The temperature regimes studied are summarized in Table 1. All experiments were replicated at least once.

In each experiment, 100 µl of bacterial suspension ($4.3\times10^{5\text{-}7}$ viable cells/ml) was placed in each PCR tube. One or two tubes were removed from the thermocycler at appropriate times during the experiment and the contents were inoculated into BACTEC media. Control tubes were not subjected to heat treatment. BACTEC vials were incubated for 12 weeks at 37°C. Growth was measured weekly with an automated BACTEC 460 ion chamber machine. MAP was confirmed by IS*900* PCR in serially diluted template DNA samples and by subculture onto modified Middlebrook 7H10 slopes with and without mycobactin J (75).

Assessment of dormancy. During the lag phase of the bacterial growth cycle there is no increase in cell number. However, the length of lag phase can vary considerably depending on inoculum size (53). To determine the inoculum size for MAP, cumulative

growth indices were calculated and plotted against days of incubation as described by Reddacliff *et al* (56). The linear relationship was calculated as Log_{10} inoculum size = 8.59-0.185 × number of days taken for the cumulative growth index to reach 1000. Based on Reddacliff *et al* (56) an inoculum size of approximately 1 viable MAP in a BACTEC culture medium will result in peak growth index within 6 weeks. As the time required to reach peak GI following commencement of growth is about 1-2 weeks, an inoculum was deemed to consist predominantly of dormant cells where it had a lag phase of **≥** 4 weeks followed by rapid growth

Identification of proteins expressed by dormant C and S strains of MAP after temperature flux treatment. Fresh suspensions of MAP (4.3×10^7 cells/ml) were subjected to temperature flux treatment to induce stress proteins. A temperature range of 10-50°C with a 7.5: 4: 4.5: 8 unit pattern was maintained for 420 cycles (168 h) and samples were collected at 322 and 420 cycles. The contents of 10 PCR tubes per strain per time point were pooled (total 1 ml) into 2 ml screw cap polypropylene tubes. 0.9 ml of the suspension was centrifuged at 21,910 ×*g* and the pellet was stored at -80°C until processing for protein extraction and 100 µl was inoculated into BACTEC culture media to determine the growth pattern. The control gels were produced from the control suspension that was not exposed to temperature flux treatment. The entire experiment was replicated.

Protein extraction from MAP. Protein samples were prepared using an homogenizer with 160 µl of cell lysis buffer (8 M Urea, 100 mM Dithiothreitol, 4% w/v CHAPS, 0.8% v/v carrier ampholytes, 40 mM Tris) as described previously (28). The lysed cell suspension was centrifuged at 16,060 ×*g* for 1 h at 4°C to pellet the cellular debris and the supernatant was collected. The aliquots of supernatant were stored at -80°C for 2-D PAGE. Protein concentration was performed (Bio-Rad protein assay) and 60 µg of protein sample was purified with a 2-D clean up kit (Amersham Biosciences) as described by the manufacturer.

2-D PAGE. For each strain of MAP, 60 µl (~ 60 µg) of the purified protein sample (as described above) was diluted in 90 µl of protein sample extraction buffer and used to re-hydrate a 7 cm IPG strip (pH 4-7) (ReadyStrip, Bio-Rad) passively, according to the manufacturer's instructions. Isoelectric focusing was undertaken in a Bio-Rad Protean IEF at 15000 Vh and IPG strips were equilibrated in a two-step equilibration procedure as described by the manufacturer. Briefly, IPG strips were washed for 10 min in equilibration buffer 1 (6 M Urea, 375 mM Tris-HCl pH 8.8, 2% w/v SDS, 20% v/v glycerol and 2% w/v DTT) followed by a second 10 min wash in equilibration buffer 2 (6 M Urea, 375 mM Tris-HCl pH 8.8, 2% w/v SDS, 20% v/v glycerol and 2.5% w/v iodoacetimide). IPG strips were rinsed in SDS-PAGE tank buffer and run in the 2nd dimension on 12% vertical SDS-PAGE gels (10 x 10.5 cm) as described by Laemmli (39). Gels were rinsed in deionized water and proteins were visualized with silver stain as described previously (8). Duplicate gels were run for each sample. The 2-D gels were scanned with ImageScanner™ II via LabScan™ software (Amersham Biosciences) and differences in protein expression level between control and treatment were determined initially by ImageMaster 2D Platinum v5.0 software (Amersham Biosciences) using the following parameters for spot detection: smooth = 4, minimal area = 10 and saliency =15. Spots were verified by visual examination. Briefly, the patterns of each sample were overlaid and aligned using six landmarks selected from all regions of the gel; they were spots clearly present in all gels. After automatic spot matching, manual matching was required for several spots that had been selected visually. Spot normalization was based on relative volume (%Vol), the volume of each spot divided by the total volume of all spots

in the gel. The normalized volumes of an identified protein spot in control and treatment gels were compared to calculate the expression ratio.

In gel digestion and mass spectrometry. The spots of interest were excised from stained gels and digested as follows. Briefly, excised gel spots were incubated with DTT (20 mM) in NH_4HCO_3 (30 µl, 25 mM) for 30 min at 37°C; after removal of the liquid the spot was incubated with iodoacetamide (30 µl, 40 mM) in NH_4HCO_3 (30 µl, 25 mM) for 30 min at 37°C. The spot was washed with CH_3CN (2 x 50 µl, 10 min). Trypsin (~100 ng) in NH_4HCO_3 (10 mM, 25 µl) was added and the solution was left at 37°C for 14 h. The gel pieces were washed with H_2O (0.1% formic acid, 50 µl) and H_2O:CH_3CN (1:1) (0.1% formic acid, 50 µl) for 15 min and the combined extracts were dried and peptides dissolved in H_2O with 0.05% heptafluorobutyric acid and 0.1% formic acid, 10 µl. Digested peptides were separated by nano-Liquid Chromatography (LC) using a Cap-LC autosampler system (Waters, Milford MA). Samples (5 µl) were concentrated and desalted onto a micro C18 precolumn (500 µm x 2 mm, Michrom Bioresources, Auburn, CA) with H_2O:CH_3CN (98:2, 0.05 % HFBA) at 15 µl/min. After a 4 min wash the pre-column was automatically switched (Valco 10 port valve, Houston, TX) into line with a fritless nano column as described previously (23). Peptides were eluted using a linear gradient of H_2O:CH_3CN (98:2, 0.1 % formic acid) to H_2O:CH_3CN (50:50, 0.1 % formic acid) at ~200 nl/min over 30 min. The precolumn was connected via a fused silica capillary (10 cm, 25 µ) to a low volume tee (Upchurch Scientific), where high voltage (2600 V) was applied and the column tip positioned ~ 1 cm from the Z-spray inlet of an Ultima API hybrid Quadrupole Time-of-Flight (Q-TOF) tandem mass spectrometer (Micromass, Manchester, UK). Positive ions were generated by electrospray and the Q-TOF operated in data dependent acquisition mode (DDA). A TOF-MS survey scan was acquired (m/z 350-1700, 1 s) and the 2 largest multiply charged ions (counts > 20) were sequentially selected by Q1 for tandem mass spectrometry or MS-MS analysis. Argon was used as collision gas and an optimum collision energy chosen (based on charge state and mass). Tandem mass spectra were accumulated for up to 8 s (m/z 50-2000). Peak lists were generated by MassLynx (Micromass) using the Mass Measure program and submitted to the database search program Mascot (version 2.1, Matrix Science, London, England). Search parameters were: Precursor and product ion tolerances ± 0.25 and 0.2 Da, respectively; Met (O) and Cys-carboxyamidomethylation specified as variable modification; enzyme specificity was trypsin; 1 missed cleavage was possible. The matches with Mascot probability scores greater than 50 (p<0.05) were used to query the NCBI nr database using the BLASTp algorithm. The matches were further subjected to searches of the *M*. *tuberculosis* H37Rv genome sequence database (Tuberculist, Institute Pasteur, Paris, http://genolist.pasteur.fr/Tuberculist/). The complete amino acid sequence for each of the *M*. *paratuberculosis* proteins identified was obtained from the *M*. *paratuberculosis* K-10 genome (GenBank accession, AE016958). The theoretical pI of proteins was calculated using Biomanager, Australian National Genomic Information Service (ANGIS) (http://www.angis.org.au/). The expressed protein sequences were further analyzed to identify the pattern or profiles of proteins using the Interpro Scan algorithm of the ExPASy (Expert Protein Analysis System) proteomics server of the Swiss Institute of Bioinformatics (SIB) (http://us.expasy.org/tools/). Peptides matching trypsin and human keratin were excluded.

RESULTS

Growth patterns following thermal stress. The non-heated controls achieved peak Growth Index (GI) after 2-3 weeks of incubation in each experiment. In general, growth was delayed progressively with increasing number of thermal cycles or duration of

heating at a constant temperature and survival was brief at peak temperatures greater than 60°C. The results of all experiments are summarized in table 1. Temperature flux experiments with a peak temperature of 50°C resulted in lag phases greater than 4 weeks after 140 to 161 cycles, but a slightly shorter lag phase was observed with a ten fold greater inoculum (Figs. 1 and 2). The lag phase was followed by rapid growth and peak GI within 2-3 weeks. Lag phases greater than 4 weeks (and hence dormancy) were not observed following fewer cycles, with a peak temperature of 60°C or after heating to a constant temperature.

In each experiment the C strain appeared to have greater thermotolerance than the S strain (Table 1, Fig. 3). It survived 18 h at 50°C but the S strain did not survive at this temperature for more than 16 h. At 60°C, S and C strains were inactivated after 20 and 30 min, respectively. Samples of culture media inoculated with suspension that failed to grow after thermal stress had either negative or trace results in IS*900* PCR, suggestive of residual inoculum. In contrast, samples with evidence of growth (GI>10) were positive in PCR at a dilution of 10^{-3} of higher and mycobactin-dependent growth was observed on solid medium (data not shown).

Proteome changes in MAP following thermal stress. Protein expression was investigated in both strains after 322 and 420 cycles of temperature flux in the range 10-50°C (Fig. 2). Both strains achieved peak GI in 7 weeks after 420 cycles, with a lag phase of 4-5 weeks, consistent with dormancy. Dormancy did not appear to be present in suspensions at 322 cycles because the lag phase was about 3 weeks, indicating that >1 viable cell was present in the inoculum (Fig. 2). Duplicate 2-D gels were run from each sample, yielding identical and reproducible protein spot patterns. A summary of the number of spots resolved and their expression levels relative to controls is provided in table 2. Twenty one spots unique to treatment gels were identified across strains. A total of 37 up-regulated spots were selected for identification (Table 2). Only one spot was down-regulated following temperature flux. The patterns of spots were almost identical in bacteria examined after 322 and 420 cycles (Fig. 4).

The software identified 1165 protein spots in the C strain following temperature flux treatment with a matching rate of about 84% with the control gel; 27 differentially expressed spots were selected for identification, 12 being unique to this treatment (Table 2, Fig. 4). For the S strain 1613 protein spots were detected with a matching rate of about 79%; 11 differentially expressed spots were selected for identification, 9 being unique to this treatment (Table 2, Fig. 4).

Identification and functional classification of differentially expressed proteins. The differentially expressed spots of interest were excised from stained gels and prepared for identification by tandem mass spectrometry. Of the 38 differentially expressed protein spots selected for identification, 37 were proteins of novel or up-regulated expression in the treatment samples. Four proteins, spots 25, 26 (C strain) and spots 10, 11 (S strain) returned erroneous identification or artifact results (Tables 4a and 4b addendum). The 34 remaining spots comprised 29 unique proteins (Table 3, Tables 4a and 4b addendum). Only one protein, FadB4, in one strain (S) was down-regulated following temperature flux. The expression levels of proteins representing a range of constitutive and adaptive biochemical pathways were altered by temperature flux (Table 3 and Fig. 5). Differentially expressed proteins were classified based on biological functions and 12 categories were identified including antioxidant enzymes, fatty acid metabolism, energy production and conversion, ATP and purine biosynthesis, proteolysis, protein synthesis, heat shock protein chaperone, iron storage, cyanate hydrolysis, hypothetical proteins with putative function, hypothetical proteins with unknown function, and phosphate

metabolism. The greatest numbers of differentially expressed proteins were categorized under fatty acid metabolism (23%) and hypothetical proteins with putative function (23%). Although some of the latter could possibly be classified into functional categories mentioned above, they were listed separately into tumor suppressors and cellular processes to create a total of 13 categories (Fig. 5). Characteristics of the differentially expressed proteins are briefly discussed below within their functional category.

Antioxidant enzymes. The Tpx protein was differentially expressed in the C strain after temperature flux. Thiol peroxidase is considered to be the most abundant and effective antioxidant enzyme of *M*. *tuberculosis* that protects mycobacteria within host phagocytes (72).

Fatty acid metabolism. These comprised 23% of the spots identified in the C strain. The acyl-ACP desaturases are a major functional class of soluble di-iron enzymes (22) that insert double bonds into fatty acyl chains after their biosynthesis (65).They are also involved in fatty acid and mycolic acid biosynthesis in *M*. *tuberculosis* and act as a major B cell antigen (33). Mycolic acids are a significant component of the mycobacterial cell wall and form an effective barrier to the penetration of chemotherapeutic agents. Therefore, the fatty acid biosynthesis pathway is believed to be a potential target for developing antimycobacterial drugs (81). EchA20 catalyzes the second step in the beta-oxidation pathway of fatty acid metabolism. It contains a short chain acyl-CoA dehydrogenase (SCAD) domain which is involved in beta oxidation of fatty acids (2). The upregulation of these following temperature flux suggests increased energy demands and possible alteration to the cell wall.

Energy production and conversion. MAP1164 had homology to GAPDH from *Coturnix coturnix,* part of the the glycolysis and gluconeogenesis pathways (42). However, it was not a perfect match based on molecular weight and pI of the protein expressed by the S strain. The genome sequence of the S strain is not available and it is possible that the protein is specific for the S strain. Another protein the same functional category was FadB4 which contains three conserved domains: (i) Qor; NADPH:quinone reductase and related Zn-dependent oxidoreductases; (ii) ADH_N; Alcohol dehydrogenase GroES-like domain; (iii) ADH_zinc_N; Zinc-binding dehydrogenase (42).

ATP and purine biosynthesis. The upregulation of PurE and AtpC in MAP suggests altered demand for ATP for survival under heat stress. PurE (Aminoimidazole carboxylase) catalyses the conversion of aminoimidazole ribonuceotide (AIR) to carboxy aminoimidazole ribonuceotide (CAIR), the sixth step of *de novo* purine biosynthesis (43). In *E*. *coli*, PurE favorably influences metabolic consumption of ATP (20). In contrast, *atpC* encodes ATP synthases of bacteria which perform two functions. Firstly, the catalysis of ATP synthesis from ADP and Pi using energy from the electrochemical ion gradient, and secondly, as an ATPase, generating a transmembrane ion gradient by ATP hydrolysis (17).

Proteolysis. Bacteria respond to stress by increasing the synthesis of molecular chaperones that assist proper folding of proteins, and increasing the expression of proteases which degrade proteins that cannot be refolded (24). ClpP is an ATP dependent protease responsible for the turnover of short-lived regulatory proteins and the removal of abnormal polypeptides, functions which are vital for processes such as cell cycle control, signal transduction and antigen presentation (41).

Protein synthesis. 50s ribosomal protein L10 contains RplJ conserved domain that binds the two ribosomal protein L7/L12 dimers and anchors them to the large ribosomal

subunit. A more than two fold upregulation in the C strain suggests its significance during survival under stress.

Heat Shock protein chaperone. These proteins constituted 12% of differentially expressed spots. They belong to the α-crystallin (Acr) family of molecular chaperons which are widespread in prokaryotic and eukaryotic organisms and prevent the irreversible aggregation of proteins during various forms of stress (31). *M*. *tuberculosis* has two members of the Acr family, Acr1 and Acr2 (67) which have a conserved region of ~90 amino acids called the α-crystallin domain (35). Both are involved in the response to oxidative stress and persistence in the host macrophage in *M. tuberculosis* (82) (66). Acr2 has also been shown to be a major target for humoral and T cell immunity during the early phase of *M. tuberculosis* infection in humans (80). Thus expression of these in MAP has a plausible role in resistance to environmental stress and pathogenesis.

Iron storage. A greater than two fold increase in expression of the bacterioferritin subunit was found in the C strain. Iron is important for the growth of all living cells; it is required for the transport and storage of oxygen and acts as a catalyst in electron transport (54). Iron metabolism is considered to play a key role in microbial pathogenicity. However, iron is toxic when present in excess of that needed for cellular homeostasis (63). There are different mechanisms which involve detoxification of ferrous ions such as oxidation or by storage of excess iron in ferritin-like proteins. In *M*. *tuberculosis*, bacterioferritin is synthesized only when iron is in excess and there is need to store iron in a form other than mycobactin. Bacterioferritin was also identified as differentially expressed under hypoxic conditions in *M*. *tuberculosis* (57). MAP may upregulate bacterioferritin synthesis to increase iron stores for use during dormancy.

Cyanate hydrolysis. The MAP4098 protein was uniquely identified in the C strain, and protein family analysis revealed this as a putative member of the cyanate hydratase family. Organisms that possess cyanase may overcome the toxicity of environmental cyanate (43). In *E*. *coli*, these enzymes catalyze the reaction of cyanate with bicarbonate to produce ammonia and carbon dioxide (37). Strains of *E*. *coli* with inducible cyanase can grow on cyanate as the sole source of nitrogen (3). Cyanate may be recruited as a source of nitrogen for MAP survival during temperature flux.

Hypothetical proteins with putative function (i) Tumor suppressors. MAP0593c showed increased expression after temperature fluctuations in the C strain. A search of the Interpro database revealed that MAP0593c displayed homology to Histidine triad protein (HIT). Members of this family are found in prokaryotes as well as in lower and higher eukaryotes (62). HIT proteins can be classified into the histidine triad nucleotide binding (Hint) proteins, fragile histidine triad (Fhit) proteins, and the GalT branch. Fhit homologues are involved in regulation of DNA replication and signaling during stress responses (48), and in humans have been demonstrated to function as tumor suppressors (9).

(ii) Cellular processes. MAP2487c displayed homology to carbonic anhydrase (CA), an enzyme that catalyses the reversible hydration of carbon dioxide to form bicarbonate. This conversion is important for many biological functions including fatty acid biosynthesis, production of a number of small molecules, pH and homeostasis (15). In *M*. *tuberculosis*, its homologue Rv1284, is essential in strain H37Rv (59), and was highly up-regulated following nutrient starvation in an *in vitro* model (6). In *E*. *coli*, the most important conditions which influenced the expression of CA were growth rate and growth phase (49). A higher level of expression of CA was observed in slow growing cultures compared to cultures growing rapidly. It may be possible that elevated level of CA is also

needed during slow growth of MAP within the host. MAP0540 has homology to the siderophore binding protein (Rv3525c) of *M*. *tuberculosis*. Siderophores are small metabolites induced in response to iron limitation. In the host, iron is mainly stored in the form of transferrin, lactoferrin and ferritin, and free iron is not available to invading bacteria (4). To overcome iron deficiency during growth in human macrophages and lungs, *M*. *tuberculosis* synthesizes the cell-associated siderophore, mycobactin (60) which can acquire intracellular iron through lipid trafficking (38). MAP1168c belongs to a family of luciferase like monooxygenases (42) which catalyse the oxidation of long chain aldehydes and releases energy in the form of visible light using flavin as a substrate (21). MAP 3567 contains two conserved domains (i) FabG; dehydrogenases (related to short-chain alcohol dehydrogenases); (ii) adh_short; short chain dehydrogenase (43). MAP3538 displayed homology to nodulation factor N of *M*. *tuberculosis* (42) which is involved in producing signal molecules (Nod factors) for *Rhizobium* and related species to convert atmospheric nitrogen to ammonia on the roots of legume hosts. (11). The differential expression of NodN under temperature flux suggests a putative source of nitrogen for MAP under stress. MAP1923c has homology to TB16.3 of *M. tuberculosis* a potent seroantigen, detecting 48 to 55% of Danish TB patients and 88 to 98% of African TB patients (73).

Hypothetical proteins with unknown function. Searches of relevant databases revealed no putative functions for MAP 3555 and MAP4107. They may be important for stress and dormancy responses in MAP and warrant further investigation.

Phosphate metabolism. Inorganic pyrophosphatase was uniquely identified in the S strain. A basal level of expression is essential for growth of *E*. *coli* (12). *ppa* was also induced during intracellular infection of U937 macrophage-like cells with *Legionella pneumophila* (1). Inorganic pyrophosphate (PPi) is produced in phosphorylation, oxidative phosphorylation and glycolysis. PPi serves as a source of energy and regulates many enzymes indirectly (40).

Discussion

A rapid increase in environmental temperature results in physical and chemical changes in bacterial proteins. Changes such as protein unfolding induce a number of heat shock proteins essential for survival (83). Two genomically distinct strains of MAP were examined in this study and there was differential thermotolerance. Environmental temperature fluctuations were simulated in a thermocycler; a specific cyclical pattern led to induction of a dormant state and expression of many proteins that were not detected in controls.

Factors influencing the thermotolerance of MAP. There are few data on the thermotolerance of MAP at temperatures that it might be exposed to in temperate terrestrial or aquatic locations. At 50°C, the C strain of MAP was viable after 18 h (initial concentration 10^6 cells/ml). This agreed with a study in which *M*. *avium* (10^5organisms/ml) was viable after 16.8 h of heating in glass beakers lying in a water bath (61). There are no prior thermotolerance data for the S strain, but the C strain has been studied extensively in relation to pasteurization of milk, which typically is undertaken at about 70°C. In the present study 10^6 cells/ml of the C strain were inactivated after 35 s at 70°C and 30 s at 80°C. The estimated 100% inactivation times at 71°C for various clinical C strain isolates (10^5/ml) in milk and lactate were 59 s and 62 s, respectively and for 10^6 /ml were 70 s and 73 s (69). Heating of MAP (10^{6-7} organisms/ml) at 63°C for 30 min resulted in > 6 log reduction in viable count, but some bacteria survived after heating for 30 min (25, 36). In contrast, in the present study, MAP

were inactivated after 28 min to 30 min at 60°C. These findings suggest that the C strain used in the present study was either less thermotolerant than those used in the other studies or that procedural factors accounted for the difference. The first technical reason might be use of sealed test tubes suspended in a water bath in the milk product studies. Secondly, the thermocycler used in the present study probably provided more efficient heat conduction and convection through the PCR tubes than a water bath with glass tubes. Thirdly, the milk or lactate media may have had some protective effect on the MAP suspension. Two other procedural factors would have had the opposite impact on assessment of thermotolerance, and suggest that C strain is less thermotolerant than previously thought. Radiometric medium was used in the present study for the recovery of MAP from heat-treated suspensions; sublethally injured cells are more readily isolated in radiometric liquid media than on solid media (64, 69). Secondly, most mycobacteria have a tendency to form clumps in liquid media because of the hydrophobic nature of their cell walls (47). Bacteria inside the clump may be protected because of slow heat penetration or some other protective mechanism (58). In the present experiments steps were taken to minimize clumping, but it is difficult to prevent entirely.

The C strain appeared consistently to be more thermotolerant than the S strain in the temperature flux and constant heating experiments (Table 1). This finding is of potential public health significance, since Crohn's disease in humans is suspected by some authors to be caused by MAP (27). However, there are no known S strain MAP isolates from humans. MAP has been reported in Britain and the USA in 2-3% of bovine retail pasteurized milk samples (19, 26), in which C strain would be most likely. Thus, there is potential for human exposure to C strain through consumption of milk and other dairy products. There are no data on pasteurization of milk containing s strain but this study suggests that the S strain is likely to be more easily inactivated than C strain. The genome of the S strain of MAP does not contain *mmpL5* (46). *MmpL* genes are required for synthesis or transport across membranes of several components of the mycobacterial cell wall including sulfolipid-1 (SL-1) (*mmpL8*) (18) and phthiocerol dimycocerosate (PDIM) (*mmpL7*) (16). Inactivation of *mmpL* genes typically leads to a change in surface characteristics such as altered colony morphology and reduced sliding motility (55). Observed differences in the genome of the S and C strains reflected in cell wall composition may explain the difference in thermotolerance (45, 46).

Temperature flux was more detrimental to the viability of MAP than holding at the same peak temperature. This supports an hypothesis derived from observations in pasture plot experiments (78). Using a starting concentration of 10^6 cells/ml and a temperature cycle in the range 10-50°C, both strains lost viability after 11 hours (aggregate time at 50°C). However, both survived constant heating at 50°C for up to 16 hours (Table 1). This pattern was confirmed using a temperature cycle of 12-60°C. The magnitude of the temperature differential also influenced survival: 168 cycles at 18-50°C compared to 147 cycles at 10-50°C. These findings have potential practical application in assessing likely environmental persistence of the organism, which is important for animal disease control. In microclimates with moderate diurnal fluctuations in temperature, persistence would be greater than in more extreme locations.

Induction of dormancy in MAP. Dormancy is defined as a reversible state of low metabolic activity in which cells can persist for extended periods without division (34), a survival strategy. During stress, bacteria may appear to be non-culturable in media in which they are known to be able to grow. Dormant cells are differentiated from dead cells on the basis of reversibility i.e. dormant cells can resuscitate and multiply under suitable conditions (50, 78). The lag phase of bacterial growth is the interval between

inoculation of the organism and the onset of detectable growth in culture media (5) and varies considerably with inoculum size (53, 56). The growth pattern of MAP in the present study after certain treatments was suggestive of a dormant state. When MAP cells were treated cyclically at 10-50°C, the lag phase increased progressively with the number of cycles and a lag phase of >4 weeks was followed quickly by an exponential growth phase suggesting synchronous resuscitation of many dormant cells (Fig. 1). At earlier time points the population would consist mainly of viable growing cells with some dormant cells and dead cells. Constant heating did not lead to dormancy, and with more extreme treatments all cells died. The growth index measured radiometrically is the sum of metabolism of the entire bacterial population and provides little information about individual cells.

Common and unique metabolic pathways during cellular stress. Proteins differentially expressed during dormancy induced by temperature flux were compared with those induced by hypoxia and starvation (S. Gumber, D. L. Taylor, I. B. Marsh and R. J. Whittington, submitted for publication) to reveal the activation of common and/or unique metabolic pathways during these stresses (Table 5). Ten common metabolic pathways appear to provide overlapping control during these stresses in MAP creating a multidefense strategy that may be relevant for survival in the environment and within the host. However, several unique metabolic pathways were identified following either temperature flux or hypoxia/starvation stresses. These represent responses specific for a limited range of stress conditions.

The number of proteins identified in this study represented a small part of the pool of differentially expressed proteins. Only protein spots with marked changes in expression detectable visually in the low to medium molecular weight range were selected for mass spectrometry in order to obtain well-resolved spots to increase the accuracy of protein identification. Further, the selection criteria were based on the presence of dormancy-associated proteins in these regions in other mycobacteria (29, 70). Further work is required to fully elucidate the proteome of MAP under these stresses including use of different pH range gels, other protein purification methods and multiplexed proteomics technology. It was noteworthy that the patterns of spots were almost identical in bacteria examined after 322 and 420 cycles. This suggests that the population of viable bacteria included many dormant individuals at time points earlier than 420 cycles, which was the point at which the growth phenotype of dormancy was recognizable in this model. Alternatively, the proteins detected during the dormant state are expressed prior to entry to this state, as a result of heat stress per se.

Overall, a single *in vitro* model may reveal only part of the suite of proteins regulated in MAP within an infected host. Although little is known about metabolic pathways in MAP, these differentially expressed proteins may mediate important biological functions by interacting with host cells, especially macrophages, and may be important for virulence and pathogenesis of MAP. It is hoped that these *in vitro* results can be extrapolated to the *in vivo* situation to complement results presented by other groups from MAP cells extracted from the intestinal wall of severely affected animals (32). A problem with such studies is the requirement for considerable amounts of mycobacterial protein which can only be obtained from multibacillary cases, that is from animals with advanced lesions. The important early stages of the disease process, which likely involve dormant MAP, are difficult to access other than through *in vitro* study and inference, as too few bacilli are present in lesions to provide useful protein yields. Thus further research is required to identify the proteome of the organism within the host during different stages of the disease. The changes in the protein levels that were detected in this *in vitro* study

contribute significantly to an understanding of how the proteome and the metabolic state of MAP varies in response to different environments.

References

Abu Kwaik, Y. 1998. Induced expression of the Legionella pneumophila gene encoding a 20-kilodalton protein during intracellular infection. Infect. Immun. 66:203-12.

Agnihotri, G., and H. W. Liu. 2003. Enoyl-CoA hydratase reaction, mechanism, and inhibition. Bioorg Med Chem 11:9-20.

Anderson, P. M., Y. C. Sung, and J. A. Fuchs. 1990. The cyanase operon and cyanate metabolism. FEMS. Microbiol. Rev. 7:247-52.

Andrews, S. C., A. K. Robinson, and F. Rodriguez-Quinones. 2003. Bacterial iron homeostasis. FEMS Microbiol Rev 27:215-37.

Barer, M. R. 2003. Physiological and molecular aspects of growth, non-growth, culturability and viability in bacteria, p. 1-37. In A. R. Coates (ed.), Dormancy and Low-Growth States in Microbial Disease. Cambridge University Press.

Betts, J. C., P. T. Lukey, L. C. Robb, R. A. McAdam, and K. Duncan. 2002. Evaluation of a nutrient starvation model of Mycobacterium tuberculosis persistence by gene and protein expression profiling. Mol. Microbiol. 43:717-31.

Bloom, B. R., and C. J. Murray. 1992. Tuberculosis: commentary on a reemergent killer. Science 257:1055-64.

Blum, H., H. Beier, and H. Gross. 1987. Improved silver staining of plant proteins, RNA and DNA in polyacrylamide gels. Electrophoresis 8:93-99.

Brenner, C. 2002. Hint, Fhit, and GalT: function, structure, evolution, and mechanism of three branches of the histidine triad superfamily of nucleotide hydrolases and transferases. Biochemistry 41:9003-14.

Bush, R. D., J. A. Toribio, and P. Windsor. 2006. Losses of adult sheep due to ovine Johne's disease in 12 infected flocks over a 3-year period. Aust. Vet. J. 84:246-53.

Carlson, R. W., N. P. Price, and G. Stacey. 1994. The biosynthesis of rhizobial lipo-oligosaccharide nodulation signal molecules. Mol Plant Microbe Interact 7:684-95.

Chen, J., A. Brevet, M. Fromant, F. Leveque, J. M. Schmitter, S. Blanquet, and P. Plateau. 1990. Pyrophosphatase is essential for growth of Escherichia coli. J Bacteriol 172:5686-9.

Cheng Vollmer, A., and T. K. Van Dyk. 2004. Stress responsive bacteria: biosensors as environmental monitors. Adv Microb Physiol 49:131-74.

Chiodini, R. J., and J. Hermon-Taylor. 1993. The thermal resistance of Mycobacterium paratuberculosis in raw milk under conditions simulating pasteurization. J Vet Diagn Invest 5:629-31.

Covarrubias, A. S., T. Bergfors, T. A. Jones, and M. Hogbom. 2006. Structural mechanics of the pH-dependent activity of beta-carbonic anhydrase from Mycobacterium tuberculosis. J Biol Chem 281:4993-9.

Cox, J. S., B. Chen, M. McNeil, and W. R. Jacobs, Jr. 1999. Complex lipid determines tissue-specific replication of Mycobacterium tuberculosis in mice. Nature 402:79-83.

Deckers-Hebestreit, G., and K. Altendorf. 1996. The F0F1-type ATP synthases of bacteria: structure and function of the F0 complex. Annu. Rev. Microbiol. 50:791-824.

Domenech, P., M. B. Reed, C. S. Dowd, C. Manca, G. Kaplan, and C. E. Barry, 3rd. 2004. The role of MmpL8 in sulfatide biogenesis and virulence of Mycobacterium tuberculosis. J Biol Chem 279:21257-65.

Ellingson, J. L., J. L. Anderson, J. J. Koziczkowski, R. P. Radcliff, S. J. Sloan, S. E. Allen, and N. M. Sullivan. 2005. Detection of viable Mycobacterium avium subsp. paratuberculosis in retail pasteurized whole milk by two culture methods and PCR. J Food Prot 68:966-72.

Firestine, S. M., S. W. Poon, E. J. Mueller, J. Stubbe, and V. J. Davisson. 1994. Reactions catalyzed by 5-aminoimidazole ribonucleotide carboxylases from Escherichia coli and Gallus gallus: a case for divergent catalytic mechanisms. Biochemistry 33:11927-34.

Fisher, A. J., T. B. Thompson, J. B. Thoden, T. O. Baldwin, and I. Rayment. 1996. The 1.5-A resolution crystal structure of bacterial luciferase in low salt conditions. J Biol Chem 271:21956-68.

Fox, B. G., K. S. Lyle, and C. E. Rogge. 2004. Reactions of the diiron enzyme stearoyl-acyl carrier protein desaturase. Acc Chem Res 37:421-9.

Gatlin, C. L., G. R. Kleemann, L. G. Hays, A. J. Link, and J. R. Yates, 3rd. 1998. Protein identification at the low femtomole level from silver-stained gels using a new fritless electrospray interface for liquid chromatography-microspray and nanospray mass spectrometry. Anal. Biochem. 263:93-101.

Goff, S. A., and A. L. Goldberg. 1985. Production of abnormal proteins in E. coli stimulates transcription of lon and other heat shock genes. Cell 41:587-95.

Grant, I. R., H. J. Ball, S. D. Neill, and M. T. Rowe. 1996. Inactivation of Mycobacterium paratuberculosis in cows' milk at pasteurization temperatures. Appl Environ Microbiol 62:631-6.

Grant, I. R., H. J. Ball, and M. T. Rowe. 2002. Incidence of Mycobacterium paratuberculosis in bulk raw and commercially pasteurized cows' milk from approved dairy processing establishments in the United Kingdom. Appl Environ Microbiol 68:2428-35.

Greenstein, R. J. 2003. Is Crohn's disease caused by a mycobacterium? Comparisons with leprosy, tuberculosis, and Johne's disease. Lancet Infect Dis 3:507-14.

Gumber, S., D. L. Taylor, and R. J. Whittington. 2007. Protein extraction from Mycobacterium avium subsp. paratuberculosis: Comparison of methods for analysis by sodium dodecyl sulphate polyacrylamide gel electrophoresis, native PAGE and surface enhanced laser desorption/ionization time of flight mass spectrometry. J. Microbiol. Methods 68:115-127.

Gupta, S., S. B. Pandit, N. Srinivasan, and D. Chatterji. 2002. Proteomics analysis of carbon-starved Mycobacterium smegmatis: induction of Dps-like protein. Protein Eng 15:503-12.

Hecker, M., and U. Volker. 2001. General stress response of Bacillus subtilis and other bacteria. Adv Microb Physiol 44:35-91.

Horwitz, J. 1992. Alpha-crystallin can function as a molecular chaperone. Proc Natl Acad Sci USA 89:10449-53.

Hughes, V., S. Smith, A. Garcia-Sanchez, J. Sales, and K. Stevenson. 2007. Proteomic comparison of Mycobacterium avium subspecies paratuberculosis grown in vitro and isolated from clinical cases of ovine paratuberculosis. Microbiology 153:196-205.

Jackson, M., D. Portnoi, D. Catheline, L. Dumail, J. Rauzier, P. Legrand, and B. Gicquel. 1997. Mycobacterium tuberculosis Des protein: an immunodominant target for the humoral response of tuberculous patients. Infect Immun 65:2883-9.

Kaprelyants, A. S., J. C. Gottschal, and D. B. Kell. 1993. Dormancy in non-sporulating bacteria. FEMS. Microbiol. Rev. 10:271-85.

Kennaway, C. K., J. L. Benesch, U. Gohlke, L. Wang, C. V. Robinson, E. V. Orlova, H. R. Saibil, and N. H. Keep. 2005. Dodecameric structure of the small heat shock protein Acr1 from Mycobacterium tuberculosis. J Biol Chem 280:33419-25.

Keswani, J., and J. F. Frank. 1998. Thermal inactivation of Mycobacterium paratuberculosis in milk. J Food Prot 61:974-8.

Kozliak, E. I., J. A. Fuchs, M. B. Guilloton, and P. M. Anderson. 1995. Role of bicarbonate/CO2 in the inhibition of Escherichia coli growth by cyanate. J. Bacteriol. 177:3213-9.

Krithika, R., U. Marathe, P. Saxena, M. Z. Ansari, D. Mohanty, and R. S. Gokhale. 2006. A genetic locus required for iron acquisition in Mycobacterium tuberculosis. Proc Natl Acad Sci USA 103:2069-74.

Laemmli, U. K. 1970. Cleavage of structural proteins during the assembly of the head of bacteriophage T4. Nature 227:680-5.

Lahti, R. 1983. Microbial inorganic pyrophosphatases. Microbiol. Rev. 47:169-78.

Lee, C., M. P. Schwartz, S. Prakash, M. Iwakura, and A. Matouschek. 2001. ATP-dependent proteases degrade their substrates by processively unraveling them from the degradation signal. Mol. Cell 7:627-37.

Marchler-Bauer, A., J. B. Anderson, P. F. Cherukuri, C. DeWeese-Scott, L. Y. Geer, M. Gwadz, S. He, D. I. Hurwitz, J. D. Jackson, Z. Ke, C. J. Lanczycki, C. A. Liebert, C. Liu, F. Lu, G. H. Marchler, M. Mullokandov, B. A. Shoemaker, V. Simonyan, J. S. Song, P. A. Thiessen, R. A. Yamashita, J. J. Yin, D. Zhang, and S. H. Bryant. 2005. CDD: a Conserved Domain Database for protein classification. Nucleic Acids Res 33:D192-6.

Marchler-Bauer, A., J. B. Anderson, P. F. Cherukuri, C. DeWeese-Scott, L. Y. Geer, M. Gwadz, S. He, D. I. Hurwitz, J. D. Jackson, Z. Ke, C. J. Lanczycki, C. A. Liebert, C. Liu, F. Lu, G. H. Marchler, M. Mullokandov, B. A. Shoemaker, V. Simonyan, J. S. Song, P. A. Thiessen, R. A. Yamashita, J. J. Yin, D. Zhang, and S. H. Bryant. 2005. CDD: a Conserved Domain Database for protein classification. Nucleic Acids Res. 33:D192-6.

Marsh, I., R. Whittington, and D. Cousins. 1999. PCR-restriction endonuclease analysis for identification and strain typing of Mycobacterium avium subsp. paratuberculosis and Mycobacterium avium subsp. avium based on polymorphisms in IS1311. Mol Cell Probes 13:115-26.

Marsh, I. B., J. P. Bannantine, M. L. Paustian, M. L. Tizard, V. Kapur, and R. J. Whittington. 2006. Genomic Comparison of Mycobacterium avium subsp.

paratuberculosis Sheep and Cattle Strains by Microarray Hybridization. J. Bacteriol. 188:2290-3.

Marsh, I. B., and R. J. Whittington. 2005. Deletion of an mmpL gene and multiple associated genes from the genome of the S strain of Mycobacterium avium subsp. paratuberculosis identified by representational difference analysis and in silico analysis. Mol Cell Probes 19:371-84.

McFadden, J. 1992. Mycobacteria., p. 203-215, Encyclopedia of Microbiology, vol. 3rd. San Diego, Academic press.

McLennan, A. G. 2000. Dinucleoside polyphosphates-friend or foe? Pharmacol. Ther. 87:73-89.

Merlin, C., M. Masters, S. McAteer, and A. Coulson. 2003. Why is carbonic anhydrase essential to Escherichia coli? J Bacteriol 185:6415-24.

Mukamolova, G. V., A. S. Kaprelyants, D. B. Kell, and M. Young. 2003. Adoption of the transiently non-culturable state-a bacterial survival strategy? Adv. Microb. Physiol. 47:65-129.

Ott, S. L., S. J. Wells, and B. A. Wagner. 1999. Herd-level economic losses associated with Johne's disease on US dairy operations. Prev. Vet. Med. 40:179-92.

Parrish, N. M., J. D. Dick, and W. R. Bishai. 1998. Mechanisms of latency in Mycobacterium tuberculosis. Trends Microbiol. 6:107-12.

Perry, J. M., J. T. Staley, and S. Lory. 2002. Microbial growth, p. 127-45. In A. D. Sinauer (ed.), Microbial life. Sinauer Associates.

Pessolani, M. C., D. R. Smith, B. Rivoire, J. McCormick, S. A. Hefta, S. T. Cole, and P. J. Brennan. 1994. Purification, characterization, gene sequence, and significance of a bacterioferritin from Mycobacterium leprae. J Exp Med 180:319-27.

Recht, J., A. Martinez, S. Torello, and R. Kolter. 2000. Genetic analysis of sliding motility in Mycobacterium smegmatis. J Bacteriol 182:4348-51.

Reddacliff, L. A., P. J. Nicholls, A. Vadali, and R. J. Whittington. 2003. Use of growth indices from radiometric culture for quantification of sheep strains of Mycobacterium avium subsp. paratuberculosis. Appl. Environ. Microbiol. 69:3510-6.

Rosenkrands, I., P. B. Rasmussen, M. Carnio, S. Jacobsen, M. Theisen, and P. Andersen. 1998. Identification and characterization of a 29-kilodalton protein from Mycobacterium tuberculosis culture filtrate recognized by mouse memory effector cells. Infect Immun 66:2728-35.

Rowe, M. T., I. R. Grant, L. Dundee, and H. J. Ball. 2000. Heat resistance of Mycobacterium avium subsp. paratuberculosis in milk. Irish J Agric Food Res 39:203-208.

Sassetti, C. M., and E. J. Rubin. 2003. Genetic requirements for mycobacterial survival during infection. Proc Natl Acad Sci USA 100:12989-94.

Schaible, U. E., and S. H. Kaufmann. 2004. Iron and microbial infection. Nat Rev Microbiol 2:946-53.

Schulze-Robbecke, R., and K. Buchholtz. 1992. Heat susceptibility of aquatic mycobacteria. Appl Environ Microbiol 58:1869-73.

Seraphin, B. 1992. The HIT protein family: a new family of proteins present in prokaryotes, yeast and mammals. DNA Seq. 3:177-9.

Smith, J. L. 2004. The physiological role of ferritin-like compounds in bacteria. Crit Rev Microbiol 30:173-85.

Sockett, D. C., D. J. Carr, and M. T. Collins. 1992. Evaluation of conventional and radiometric fecal culture and a commercial DNA probe for diagnosis of Mycobacterium paratuberculosis infections in cattle. Can. J. Vet. Res. 56:148-53.

Sperling, P., P. Ternes, T. K. Zank, and E. Heinz. 2003. The evolution of desaturases. Prostaglandins Leukot Essent Fatty Acids 68:73-95.

Stewart, G. R., S. M. Newton, K. A. Wilkinson, I. R. Humphreys, H. N. Murphy, B. D. Robertson, R. J. Wilkinson, and D. B. Young. 2005. The stress-responsive chaperone alpha-crystallin 2 is required for pathogenesis of Mycobacterium tuberculosis. Mol Microbiol 55:1127-37.

Stewart, G. R., L. Wernisch, R. Stabler, J. A. Mangan, J. Hinds, K. G. Laing, D. B. Young, and P. D. Butcher. 2002. Dissection of the heat-shock response in Mycobacterium tuberculosis using mutants and microarrays. Microbiology 148:3129-38.

Streeter, R. N., G. F. Hoffsis, S. M. Bech-Nielsen, W. P. Shulaw, and D. M. Rings. 1995. Isolation of Mycobacterium paratuberculosis from colostrum and milk of subclinically infected cows. Am J Vet Res 56:1322-24.

Sung, N., and M. T. Collins. 1998. Thermal tolerance of Mycobacterium paratuberculosis. Appl Environ Microbiol 64:999-1005.

Tabira, Y., N. Ohara, N. Ohara, H. Kitaura, S. Matsumoto, M. Naito, and T. Yamada. 1998. The 16-kDa alpha-crystallin-like protein of Mycobacterium bovis BCG is produced under conditions of oxygen deficiency and is associated with ribosomes. Res. Microbiol. 149:255-64.

Triccas, J. A., and B. Gicquel. 2000. Life on the inside: probing Mycobacterium tuberculosis gene expression during infection. Immunol Cell Biol 78:311-7.

Trujillo, M., P. Mauri, L. Benazzi, M. Comini, A. De Palma, L. Flohe, R. Radi, M. Stehr, M. Singh, F. Ursini, and T. Jaeger. 2006. The mycobacterial thioredoxin peroxidase can act as a one-cysteine-peroxiredoxin. J. Biol. Chem. 281:20555-66.

Weldingh, K., I. Rosenkrands, L. M. Okkels, T. M. Doherty, and P. Andersen. 2005. Assessing the serodiagnostic potential of 35 Mycobacterium tuberculosis proteins and identification of four novel serological antigens. J. Clin. Microbiol. 43:57-65.

Whittington, R. J., A. F. Hope, D. J. Marshall, C. A. Taragel, and I. Marsh. 2000. Molecular epidemiology of Mycobacterium avium subsp. paratuberculosis: IS900 restriction fragment length polymorphism and IS1311 polymorphism analyses of isolates from animals and a human in Australia. J. Clin. Microbiol. 38:3240-8.

Whittington, R. J., I. Marsh, S. McAllister, M. J. Turner, D. J. Marshall, and C. A. Fraser. 1999. Evaluation of modified BACTEC 12B radiometric medium and solid media for culture of Mycobacterium avium subsp. paratuberculosis from sheep. J. Clin. Microbiol. 37:1077-83.

Whittington, R. J., I. Marsh, M. J. Turner, S. McAllister, E. Choy, G. J. Eamens, D. J. Marshall, and S. Ottaway. 1998. Rapid detection of Mycobacterium paratuberculosis in clinical samples from ruminants and in spiked environmental samples by modified

BACTEC 12B radiometric culture and direct confirmation by IS900 PCR. J. Clin. Microbiol. 36:701-7.

Whittington, R. J., I. B. Marsh, and L. A. Reddacliff. 2005. Survival of Mycobacterium avium subsp. paratuberculosis in Dam Water and Sediment. Appl. Environ. Microbiol. 71:5304-8.

Whittington, R. J., D. J. Marshall, P. Nicholls, I. B. Marsh, and L. A. Reddacliff. 2004. Survival and dormancy of Mycobacterium avium subsp. paratuberculosis in the environment. Appl. Environ. Microbiol. 70:2989-3004.

Whittington, R. J., L. A. Reddacliff, I. Marsh, S. McAllister, and V. Saunders. 2000. Temporal patterns and quantification of excretion of Mycobacterium avium subsp. paratuberculosis in sheep with Johne's disease. Aust. Vet. J. 78:34-7.

Wilkinson, K. A., G. R. Stewart, S. M. Newton, H. M. Vordermeier, J. R. Wain, H. N. Murphy, K. Horner, D. B. Young, and R. J. Wilkinson. 2005. Infection biology of a novel alpha-crystallin of Mycobacterium tuberculosis: Acr2. J Immunol 174:4237-43.

Yang, J. K., H. J. Yoon, H. J. Ahn, B. I. Lee, S. H. Cho, G. S. Waldo, M. S. Park, and S. W. Suh. 2002. Crystallization and preliminary X-ray crystallographic analysis of the Rv2002 gene product from Mycobacterium tuberculosis, a beta-ketoacyl carrier protein reductase homologue. Acta Crystallogr D Biol Crystallogr 58:303-5.

Yuan, Y., D. D. Crane, R. M. Simpson, Y. Q. Zhu, M. J. Hickey, D. R. Sherman, and C. E. Barry, 3rd. 1998. The 16-kDa alpha-crystallin (Acr) protein of Mycobacterium tuberculosis is required for growth in macrophages. Proc Natl Acad Sci USA 95:9578-83.

Zugel, U., and S. H. Kaufmann. 1999. Role of heat shock proteins in protection from and pathogenesis of infectious diseases. Clin Microbiol Rev 12:19-39.

Table 1 Thermotolerance of *M. paratuberculosis.* Dormancy was defined as a lag phase > 4 weeks followed by rapid growth

Temperature (°C)	Viable cells/ml	Maximum duration of survival at peak temperature [a]		Dormancy after nth cycle	
		S strain	C strain	S strain	C strain
Constant temperature					
50	4.3×10^6	16 h or 213 CE [b]	18 h or 240 CE	-	-
60	4.3×10^6	28 m or 6 CE	30 m or 6.5 CE	-	-
70	4.3×10^6	30 s	35 s	-	-
80	4.3×10^6	25 s	30 s	-	-
Temperature flux					
10-50	4.3×10^6	11 h [c]	11 h [c]	140	140
18-50	4.3×10^6	11 h 12 m [c]	11 h 12 m [c]	161	161
10-50	4.3×10^7	31 h 30 m [c]	31 h 30 m [c]	420	420
12-60	4.3×10^6	9 m [c]	13.5 m [c]	-	-

[a] h = hour; m = minute; s = seconds
[b] Cycle equivalents
[c] Total duration for which the organism was exposed to peak period in temperature flux experiments

Table 2 Summary of the proteome of C and S strains of *M. paratuberculosis* according to protein expression levels after thermal stress

Category of expression change	Temperature flux		Total
	C	S	
Spots present only in treatment	12[c]	9[c]	21
Spots present in control but up-regulated in treatment	15	1	16
[a] Total spots up-regulated in treatment	27	10	37
[b] Spots present in control but down-regulated in treatment	0	1	1
Total protein spots resolved	1155	1613	

Total number of differentially expressed protein spots *a*+*b* = 38
[c]2 spots in each strain were erroneously identified or artifact

Table 3 Differentially expressed proteins of *M. paratuberculosis* following thermal stress

Protein Category	Figure	Spot No.	Gene/Locus tag [a]	Protein description [a]	Interpro Scan Family/Function	Temperature flux [c] CS
Antioxidant enzymes						
	4 B,C	13	*tpx*, MAP1653	Putative thiol peroxidase	Antioxidant enzymes and defense against sulphur containing radicals	*
Fatty acid metabolism						
	4 B,C	1	*desA2*, MAP2698c	Acyl-Acyl Carrier Protein desaturase	Fatty acid metabolism, dodecameric ferritin homologue that binds and protects DNA	*
	4 B,C	3, 4	*fabG3_2*, MAP3577	FabG3_2	Oxidoreductase activity	3.368, 1.595
	4 B,C	7	*fabG*, MAP2872c	3-ketoacyl-reductase	-ditto-	1.982
	4 B,C	8	*echA20*, MAP0516c	Enoyl-CoA hydratase	Fatty acid metabolism	1.930
	4 B,C	9	MAP0508	Short chain dehydrogenase	Oxidoreductase activity	1.184
	4 B,C	10	*echA8_1*, MAP1017c	Enoyl-CoA hydratase	Fatty acid metabolism	1.962
	4 B,C	27	*fadE3_2*, MAP3651c	FadE3_2	Oxidoreductase activity, lipid metabolism	1.623
Energy production and conversion						
	4 E	1	*fadB4*, MAP3190	FadB4	Zinc ion binding, Oxidoreductase activity. Similar to GroES family which helps in protein folding and intercellular signaling.	↓
	4 E, F	9	*GAPDH*	Glyceraldehyde phosphate dehydrogenase (*Coturnix coturnix*)	Glycolysis and gluconeogenesis	*
ATP and Purine biosynthesis						
	4 B,C	14	*purE*, MAP3393c	Phosphoribosyl aminoimidazole carboxylase catalytic subunit	'de novo' IMP biosynthesis	*
	4 E, F	8	*atpC*, MAP2450c	ATP synthase subunit epsilon	membrane bound enzyme complexes involved in ATP synthesis coupled proton transport	1.691
Proteolysis						
	4 E, F	2, 3	*clpP*,	ATP dependant Clp protease	Proteolysis	*

Protein Category	Figure	Spot No.	Gene/Locus tag [a]	Protein description [a]	Interpro Scan Family/Function	Temperature flux [c] CS
			MAP2281c	proteolytic subunit		
Protein synthesis						
	4 B,C	2	*rplJ*, MAP4125	50s ribosomal protein L10	protein synthesis	2.351
Heat Shock protein chaperone						
	4 B,C	17, 18-19, 21	*hsp18_3* (MAP3268), *hsp18_2* (MAP1698c), *hsp* (MAP3701c)	Hsp18_3, Hsp18_2, Hsp	Alpha crystallin family protein. Respond to heat shock or other environmental stress and act as chaperons	*, 6.009-*, 55.067
Iron storage						
	4 B,C	12	*bfrA*, MAP1595	Bacterioferritin subunit	Iron ion transport and storage	2.479
Cyanate hydrolysis						
	4 B,C	23	MAP4098	Cyanate hydratase	Bacteria can overcome the toxicity of environmental cyanate by hydrolysis of cyanate	*
Hypothetical proteins with putative function						
Tumor suppressors						
	4 B,C	20	MAP0593c	Hypothetical protein MAP0593c	Histidine triad protein, diadenosine polyphospahte hydrolases and function as tumor suppressors in human and mice	*
Cellular processes						
	4 B,C	15	MAP2487c	Hypothetical protein MAP2487c	Carbonic anhydrase, Carbon utilization and prevents depletion of cellular bicarbonate	1.519
	4 B,C	16	MAP0540	Hypothetical protein MAP0540	Tranferases composed of hexapeptide, LpxA-like	*
	4 B,C	5	MAP1168c	Hypothetical protein MAP1168c	Oxidation of long chain aldehydes and releases energy in the form of visible light	2.907
	4 B,C	6, 11	MAP3567	Hypothetical protein MAP3567	Oxidoreductase activity	1.700, 3.500
	4 B,C	22	MAP3538	Hypothetical protein	Oxidoreductase activity, synthesis of monoamine	*

Protein Category	Figure	Spot No.	Gene/Locus tag [a]	Protein description [a]	Interpro Scan Family/Function	Temperature flux [c] S	C
				MAP3538	oxidase		
	4 B,C	24	MAP1923c	Hypothetical protein MAP1923c	Antioxidant enzymes and defense against sulphur containing radicals,	*	
Hypothetical proteins with unknown function							
	4 E, F	6	MAP3555	Hypothetical protein	Unknown		*
	4 E, F	7	MAP4107	Hypothetical protein	Unknown		*
Phosphate metabolism							
	4 E, F	4, 5	*ppa*, MAP0435c [b]	Inorganic pyrophosphatase	Phosphate metabolism, magnesium ion binding		*

[a] Locus tags are from NCBInr database (http://www.ncbi.nlm.nih.gov/entrez/query.fcgi?db=Protein&itool=toolbar) except where shown [b] in which case homologues in *M. paratuberculosis* were identified when significant hits belonged to other *Mycobacterium* spp.

[c] Columns show pattern or ratios which represent relative protein abundance between treatment and control. Asterisks (*) represent unique proteins that were not identified in control samples, ↓ indicates down-regulation and were not identified in the S and C strains after temperature flux

Addendum

Table 4a Differentially expressed protein profiles of C strain using a temperature flux cycle of 10-50°C for 322-420 cycles

Spot No.[a]	Accession No.[b]	Gene/Locus tag[b]	Mass (kDa)	pI[d]	Tuberculist Synonym[e]	M.S.D[f]	Ratio[g]
1	41408796	*desA2*, MAP2698c	31.4	4.7	Rv1094	-	*
2	41410223	*rplJ*, MAP4125	20.1	5.08	Rv0651	0.054	2.351
3	41409675	*fabG3_2*, MAP3577	25.9	5.62	Rv2002	0.075	3.368
4	41409675	*fabG3_2*, MAP3577	25.9	5.62	Rv2002	0.022	1.595
5	41407266	MAP1168c	31.9	5.92	-	0.063	2.907
6	41409665	MAP3567	30.1	5.98	Rv0148	0.151	1.700
7	41408970	*fabG*, MAP2872c	26.7	5.94	Rv2766c	0.075	1.982
8	41406614	*echA20*, MAP0516c	26.8	5.91	Rv3550, *echA20*	0.056	1.930
9	41406606	MAP0508	27.5	5.82	Rv3559c	0.008	1.184
10	41407115	*echA8_1*, MAP1017c	27.8	5.51	Rv1070c	0.068	1.962
11	41409665	MAP3567	30.1	5.98	Rv0148	0.120	3.500
12	41407693	*bfrA*, MAP1595	18.4	4.41	*bfr*, Rv1876	0.034	2.479
13	41407751	*tpx*, MAP1653	16.4	4.24	*tpx, cfp20*, Rv1932	-	*
14	41409491	*purE*, MAP3393c	17.5	5.68	Rv3275c, *pure*	-	*
15	41408585	MAP2487c	17.8	5.61	Rv1284	0.032	1.519
16	41406638	MAP0540	17.6	6.13	Rv3525c	-	*
17	41409366	*hsp18_3*, MAP3268	16.4	4.88	-	-	*
18	41407796	*hsp18_2*, MAP1698c	16.3	5.06	-	0.093	6.009
19	41407796	*hsp18_2*, MAP1698c	16.3	5.06	-	-	*
20	41406691	MAP0593c	14.8	5.25	-	-	*
21	41409799	*hsp*, MAP3701c	16.2	5.32	Rv0251c, *acr2*	0.045	55.067
22	41409636	MAP3538	15.9	6.1	Rv0130	-	*
23	41410196	MAP4098	18.7	5.8	-	-	*
24	41408021	MAP1923c	16.4	5.15	Rv2185c, TB16.3	-	*
25,26	136429	Trypsin precursor	-	-	-	-	*
27	41409749	*fadE3_2*, MAP3651c	43.9	6.15	Rv0215c, *fadE3*	0.047	1.623

Table 4b Differentially expressed protein profiles of S strain using a temperature flux cycle of 10-50°C for 322-420 cycles

Spot No. [a]	Accession No. [b]	Gene/Locus tag [b]	Mass (kDa)	pI [d]	Tuberculist Synonym [e]	M.S.D [f]	Ratio [g]
1	41409288	*fadB4*, MAP3190	33.3	5.27	Rv3141	-	↓
2	41408379	*clpP*, MAP2281c	21.6	4.62	Rv2460c	-	*
3	41408379	*clpP*, MAP2281c	24.5	6.36	*clp*, Rv2461c	-	*
4,5	13883596	*ppa*, MAP0435c MT3730 [c]	18.3	4.58	-	-	*
6	41409653	MAP3555	18.8	4.76	Rv0138	-	*
7	41410205	MAP4107	17.7	4.56	-	-	*
8	41408548	*atpC*,MAP2450c	13.1	4.23	Rv1311	0.039	1.691
9	62616	*GAPDH*, MAP1164 [c]	35.6	8.81	Rv1436, *gap*		*
10	7331218	Keratin	-	-	-	-	*
11	136429	Trypsin precursor	-	-	-	-	*

[a] Spot numbers in Table 4a and 4b are identical to those in Fig. 4
[b] Accession number and locus tags are from NCBInr database (http://www.ncbi.nlm.nih.gov/entrez/query.fcgi?db=Protein&itool=toolbar)) except where shown [c] in which case homologues in *M. paratuberculosis* were identified after finding the homologue in another *Mycobacterium* spp.
[d] Theoretical isoelectric point (pI) of matching protein was calculated by Biomanager (http://www.angis.org.au/)
[e] Homologues in *M. tuberculosis* were identified from the H37Rv genome sequence database (http://genolist.pasteur.fr/Tuberculist/)
[f] Mean squared deviation was calculated by ImageMaster 2D Platinum software
[g] Ratios represent relative protein abundance between treatment and control. Asterisks (*) represent unique proteins that were not identified in control samples, ↓ indicates downregulation

Table 5 Summary of the metabolic pathways activated in *M. paratuberculosis* as a result of different stresses

Common metabolic pathways [a]	**Hypoxia/Starvation** [b]	**Temperature flux** [c]
Antioxidant enzymes	Amino acid metabolism	Energy production and conversion
Fatty acid metabolism	Cell wall synthesis	Heat Shock protein chaperone
ATP and purine biosynthesis	Signal recognition	Iron storage
Proteolysis	Universal stress proteins	
Protein synthesis	Two component response regulators	
Tumor suppressors	Cell division	
Cellular processes		
Hypothetical proteins with unknown function		
Cyanate hydrolysis		
Phosphate metabolism		

[a] Common metabolic pathways identified during hypoxia/starvation and temperature flux treatments
[b] Metabolic pathways activated uniquely during hypoxia and starvation treatment
[c] Metabolic pathways activated uniquely during temperature flux treatment

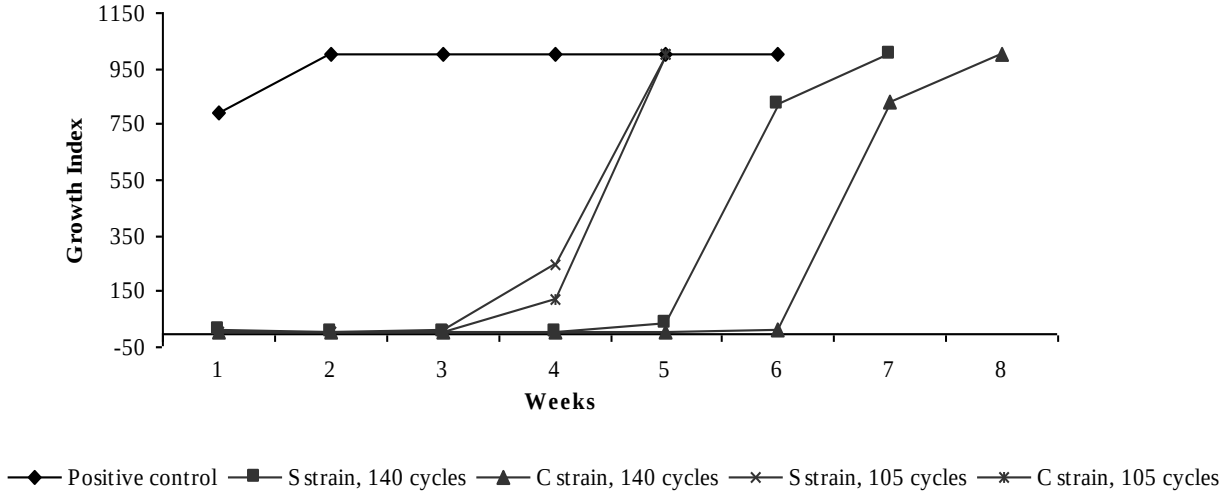

Fig. 1 Growth pattern of *M. paratuberculosis* following a temperature cycle range of 10-50°C; starting concentration 4.3 x 10^{6} cells/ml. Growth was delayed by 5-6 weeks after 140 cycles

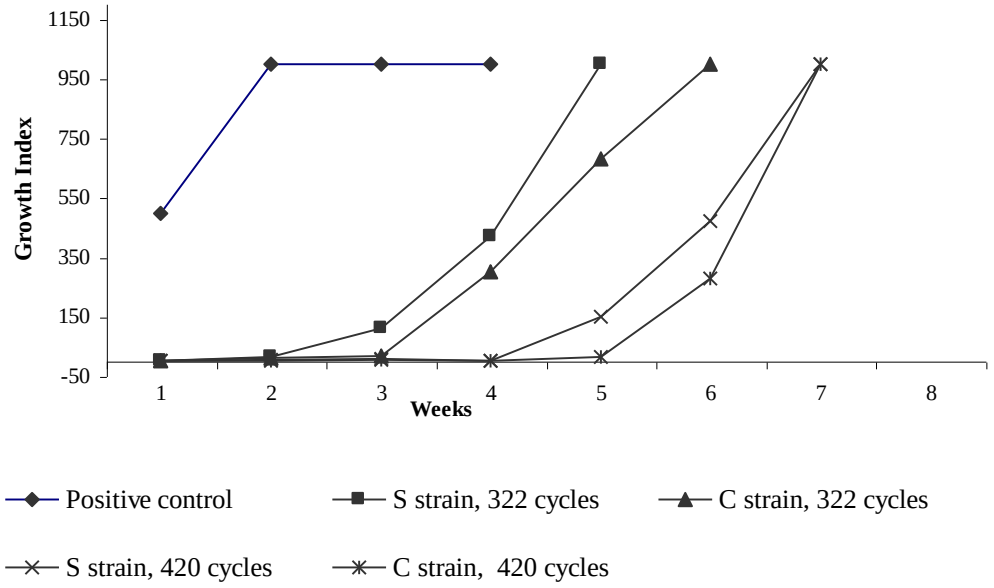

Fig. 2 Growth pattern of *M. paratuberculosis* following a temperature cycle range of 10-50°C; starting concentration 4.3 x 10^{7} cells/ml. Growth was delayed by 4-5 weeks after 420 cycles

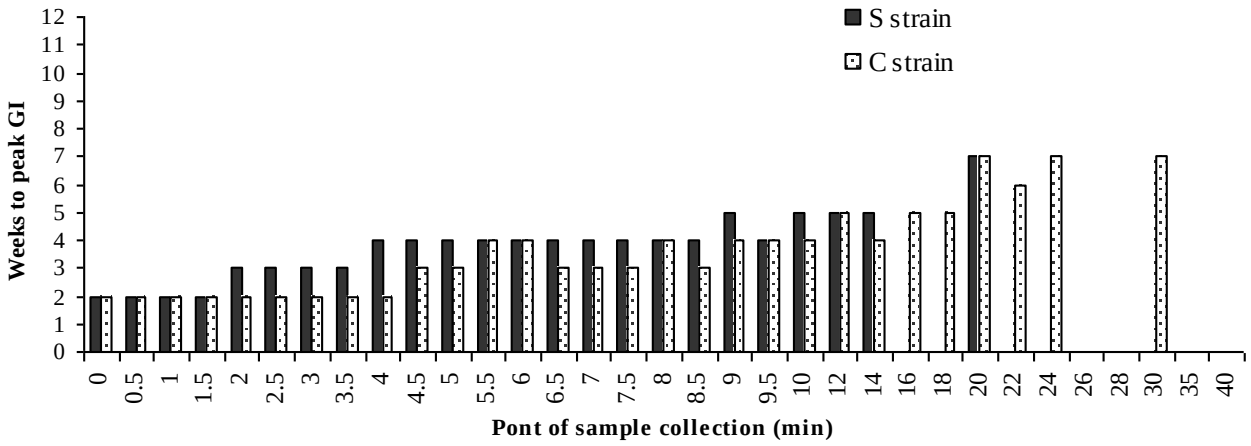

Fig. 3 Effect of constant heating on survival of *M. paratuberculosis* at 60°C; starting concentration 4.3×10^{6}cells/ml

Fig. 4 Two dimensional gel electrophoresis analysis of proteins of *M. paratuberculosis*. (panels A and D) controls; (panels B and C) C strain and (panels E and F) S strain after temperature flux using a temperature cycle of 10-50°C; (panels B and E) 322 cycles and (panels C and F) 420 cycles. Protein spots 6-7 and 10-11 are located in the same circle (panels D-F). Open circles represent protein spots with altered protein expression (refer to addendum tables 4a and 4b). The figures on the left indicate molecular mass markers in kDa. Proteins were separated by isoelectric focusing on pH 4-7 IPG strips in the first dimension and 12% SDS-PAGE in the second dimension. Proteins were visualized by silver staining.

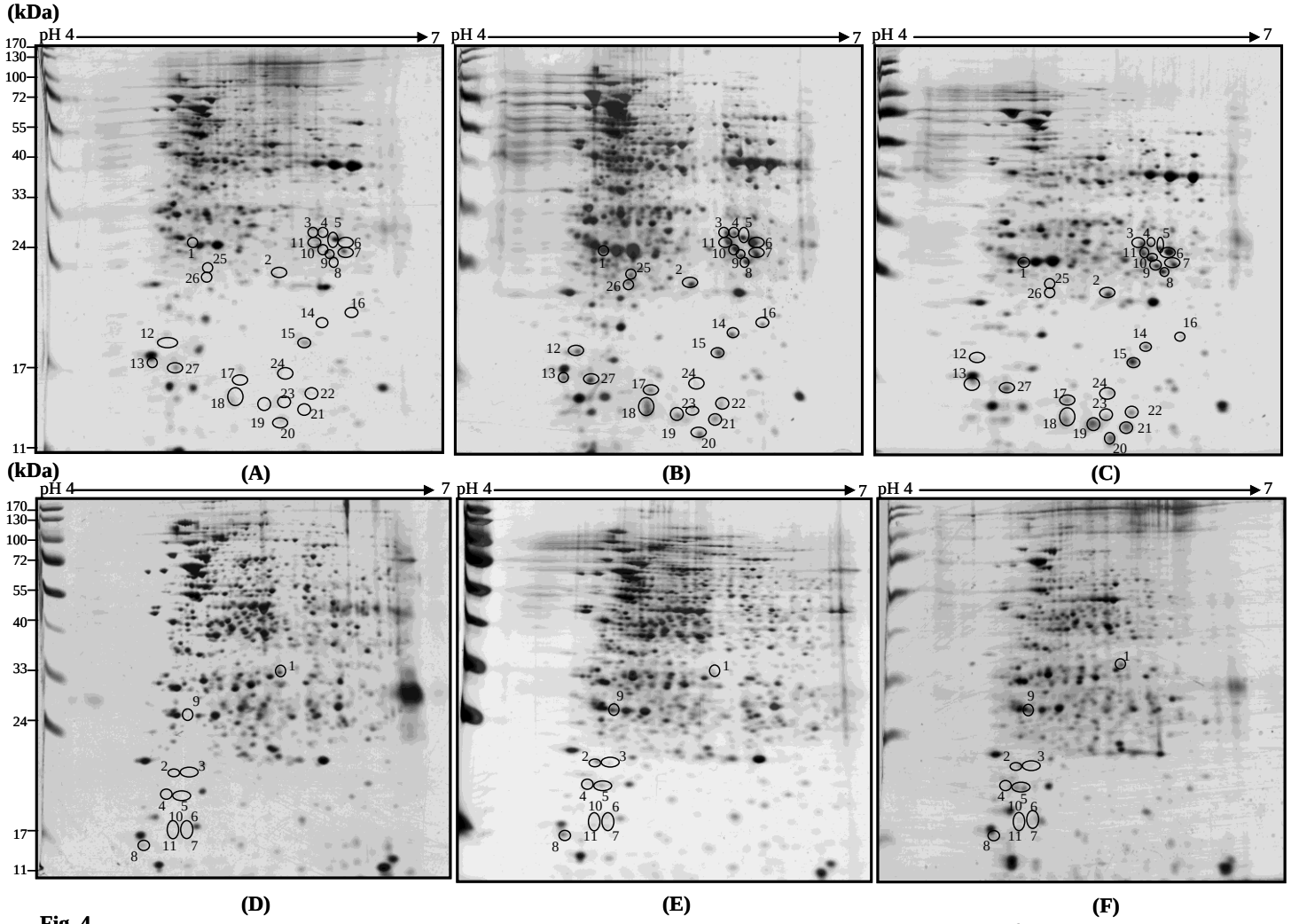

Fig. 4

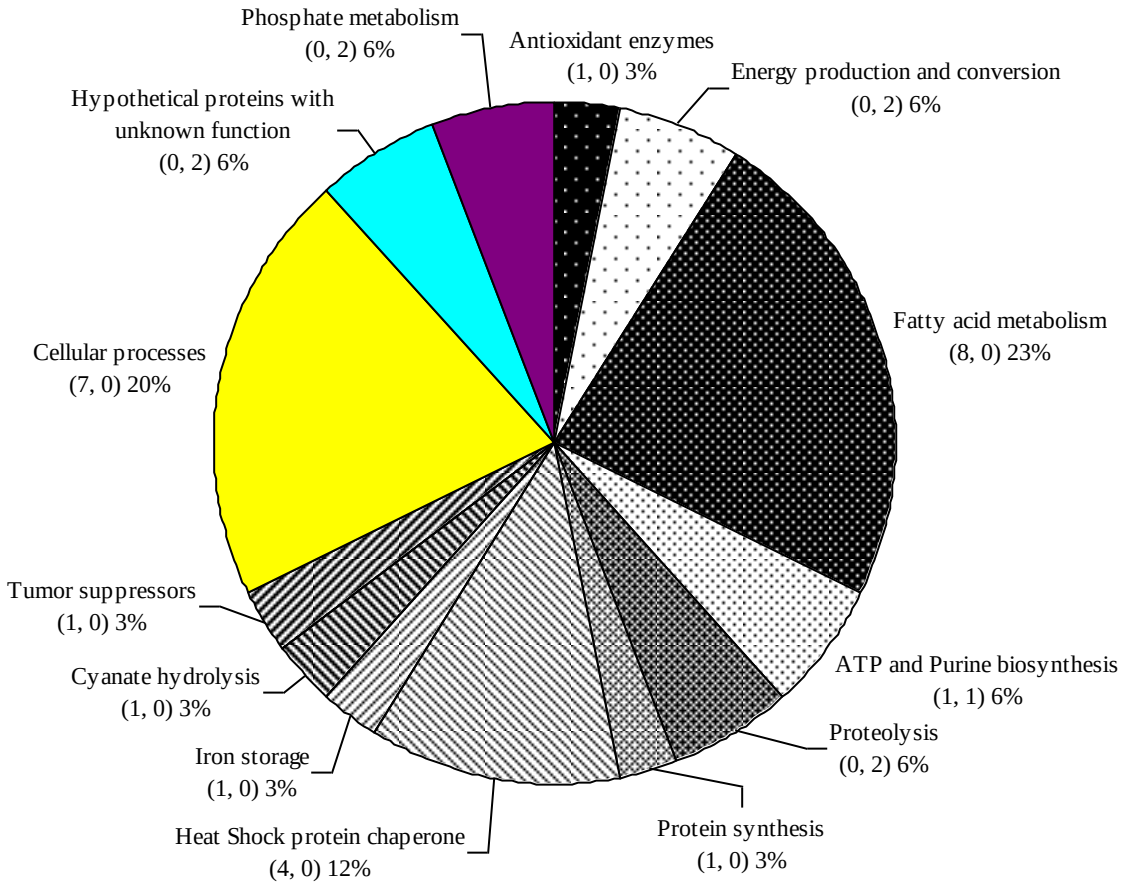

Fig. 5 The distribution of functional classes based on global protein profiling of S and C strains of *M. paratuberculosis* during temperature flux. Figures in parentheses indicate number of protein spots for C and S strain, respectively. The relative abundance (%) of each class was calculated from a total of 34 protein spots (refer table 3).

9.16 Appendix 3A-4 subprogram 3 Survival, dormancy and the proteome of Mycobacterium avium subsp. paratuberculosis during the stress response to hypoxia and nutrient starvation

Introduction

Pathogens within the *Mycobacterium avium* complex (MAC) and the *Mycobacterium tuberculosis* complex share common pathogenic mechanisms, particularly their propensity to survive in the hostile environment of the phagolysosome within host macrophages. *M*. *tuberculosis* trapped within macrophages in a pulmonary granuloma face stresses including hypoxia, starvation, extreme pH, reactive oxygen and nitrogen intermediates and toxic fatty acids. Under these conditions, *M*. *tuberculosis* is assumed to enter a dormant or latent state in which it remains viable for many years, without the patient showing clinical signs of tuberculosis [1]. Similarly in the natural environment mycobacteria may be exposed to a wide variety of stressful conditions such as nutrient deprivation, temperature extremes, pH extremes, hypoxia, the presence of toxic compounds and UV radiation [2]. Bacteria have developed different strategies to survive under such adversity and most stress-evading mechanisms require the altered expression of specific genes [3] leading to a lowering or 'shut-down' of metabolic activity. In bacteria that produce spores, metabolism is undetectable [3, 4]. In non-sporulating bacteria, metabolism is very low and causes loss of culturability or dormancy, which is also known as the Viable But Non Culturable (VBNC) state. The process by which cells restore their culturability is called resuscitation [3, 4].

When aerobically growing *M*. *tuberculosis* cultures are shifted to anaerobic conditions, the cultures survive and adapt to anaerobiosis by slowing metabolism to achieve a state of non-replicating persistence [5, 6]. Cultures of *M*. *bovis* kept under anaerobic conditions for 6 months reveal a marked thickening of the cell wall [7]. Many morphological and physiological similarities between latent bacilli *in vivo* and starved cultures *in vitro* suggested that mycobacteria in granulomas might be nutritionally starved [8]. Adaptation of mycobacteria to the deprivation of amino acids, carbon, nitrogen, phosphorus or fatty acids occurs through a mechanism called the stringent response. During starvation, many bacteria accumulate hyperphosphorylated guanine (ppGpp), alter gene expression to suppress the synthesis of stable RNA, induce degradative pathways, activate certain stationary phase genes and induce genes that regulate DNA replication and growth rate [9]. The hallmark of the stringent response is the activation of idle RelA and SpoT which leads to the accumulation of ppGpp [10]. Clearly these and other stresses have resulted in the development of adaptational networks in bacteria that balance gene expression with environmental conditions [11].

The MAC includes pathogens affecting both humans and animals. *Mycobacterium avium* subsp. *paratuberculosis* causes Johne's disease (JD), a chronic enteric disorder of ruminants and may also be involved in Crohn's disease in man. JD is distributed worldwide. In Australia, JD in sheep is reported to cause an average of $64,100 economic loss per infected farm per year [12] while JD costs the US dairy industry $ 200 - 250 million annually [13]. Despite many decades of research there is still need to develop improved early diagnostic tests for JD and other significant mycobacterial diseases of animals and man. There are two distinct major genotypic groups of *M*. *paratuberculosis*, sheep (S) and cattle (C). The S strains are more difficult to culture *in vitro* and are defined by a point mutation in IS*1311* and an 11.5 Kbp genomic deletion compared to C strain [14-16]. In addition there are other genomic differences including several large sequence polymorphisms [17, 18]. There have been few studies of the behavior of *M*. *paratuberculosis* strains in natural environments or hosts although dormancy of the S strain was observed in dam water and faeces/soil [19, 20]. The phenomenon of dormancy in *M*. *paratuberculosis* has not yet been induced *in vitro* or proven to occur *in vivo*. Studies of adaptive responses to stress are of fundamental importance because the lack of understanding of the metabolism of *M*. *paratuberculosis* during the lengthy incubation period of JD, which is measured in years, has hampered the development of

efficient diagnostic tests. Proteins which are differentially expressed during hypoxia or starvation conditions might be important for the survival of latent bacilli *in vivo* and in the environment and may be the target for diagnosis. The aim of the present study was to determine the effect of hypoxia and nutrient starvation on the growth pattern, viability and proteome of the S and C strains of *M*. *paratuberculosis*.

Materials and Methods

Preparation of bacterial suspensions

Suspensions of *M*. *paratuberculosis* with a concentration of 4.3×10^7 viable cells/ml (stock suspensions) were used: a clonal S strain (Telford 9.2), with an S1 IS*900* RFLP pattern [15] and an IS*1311* S pattern [21] and a C strain field isolate (CM00/416) with a C3 IS*900* RFLP pattern [15] and IS*1311* C pattern [21] that appeared identical to strain K-10 in whole genome microarray analysis [18]. Each strain was reconstituted from a freeze dried seed stock by adding 0.1 ml of sterile water, inoculating this into radiometric culture medium and incubating at 37°C for 3 weeks until the Growth Index (GI) read 999. The radiometric medium consisted of 4 ml enriched Middlebrook 7H9 medium (BACTEC 12B; Becton Dickinson, Sparks, MD, USA) with 200 µl PANTA PLUS (Becton Dickinson), 1 ml egg yolk, 5 µg of mycobactin J (Allied Monitor Inc., Fayette, MO, USA) and 0.7 ml of water [22]. Growth indices were measured with an automatic ion chamber (BACTEC 460; Johnston Laboratories, Towson, MD, USA). The liquid medium was subcultured onto Middlebrook's modified 7H10+MJ slopes and incubated at 37°C for 6 weeks when colonies were abundant [22, 23]. Bacteria were harvested into 200 µl of phosphate buffered saline (PBS) plus 0.1% v/v Tween80 (PBST), vortexed for 1 min, diluted 1:10 in sterile PBST, passed through a 26 g needle, filtered through an 8 µm filter and examined by light microscopy at 400 × magnification to confirm that the majority of cells were single. Viable cells were enumerated using an end point titration method [24]. Suspensions were stored at -80°C until required, with no loss of viability (data not shown). Suspensions were thawed at room temperature followed by thorough mixing by vortexing. Where further culture was required, egg yolk was omitted from the BACTEC medium.

Experimental design for an in vitro hypoxia model

A modified Wayne's dormancy model was used in this study. In Wayne's dormancy model, hypoxic responses were assessed by culturing *M*. *tuberculosis* H37Rv strain in Dubos Tween-albumin broth using screw cap test tubes and conical flasks [5]. However, *M*. *paratuberculosis* is historically difficult to isolate and static BACTEC12B radiometric media, which is routinely used for culture of *M*. *paratuberculosis* was applied in this study [23]. Firstly, bacteria were initially exposed to aerobic conditions to allow entry into the exponential growth phase then switched to anaerobic conditions. Secondly, bacteria were provided only an anaerobic environment. This is described in more detail below.

Aerobic growth then anaerobic shock

Two BACTEC vials were used for each of 8 time points for each strain of *M*. *paratuberculosis*. Vials were pre-equilibrated once with aerobic gases (78.084 % N_2, 20.947 % O_2, 0.033% CO_2, 0.934 % Argon) (BOC, Australia) by exchanging the gas phase of the culture vials using a BACTEC 460 ion chamber and then incubated at 37°C for 1 week. Thawed *M*. *paratuberculosis* suspension (1 ml) containing 4.3×10^7 viable cells/ml was pelleted by centrifugation (21, 910 ×*g*), resuspended in 100 µl of distilled water and inoculated into each BACTEC vial. After 1 week of incubation at 37°C, the atmosphere in each vial was replaced with anaerobic gas (10% CO_2, 90% N_2) each day while GI was read using the BACTEC 460 ion chamber. This was achieved by connecting the air valve of the machine to an anaerobic gas cylinder with a gas pressure of 800 psi. Samples were collected at weekly intervals for 4 weeks: the medium from one culture vial was centrifuged (21,910 ×*g*) and the pellet was stored at -80°C for protein extraction. The gas in the remaining culture vial in the pair was replaced with air and the vial was incubated for a further 8 weeks at 37°C to investigate the resuscitation capacity of *M*. *paratuberculosis* following hypoxic shock; GI was recorded every week. A control culture vial incubated aerobically was included for each time point. Proteome analysis was conducted for the samples collected after 1 week and 4 weeks of hypoxic stress and compared with the aerobic control.

Anaerobic conditions only

The experimental conditions were the same those described above in the first experiment except that the gas in the culture vials was replaced with anaerobic gas immediately before and after inoculation of *M*. *paratuberculosis* and so the bacteria were not exposed to an initial period of aerobic conditions, although there may have been residual dissolved oxygen in the broth.

Experimental design for an *in vitro* nutrient starvation model

Freshly thawed *M*. *paratuberculosis* suspension (1 ml) was added to each of 16 polypropylene tubes (Becton Dickinson) which contained 9 ml of deionized water and these were incubated at 37°C for 16 weeks. One tube was collected every 2 weeks to analyze growth capacity: 100 µl of the starved suspension was inoculated into a BACTEC vial. At 8 and 14 weeks the remaining suspension was pelleted by centrifugation (21,910 ×*g*) and stored at - 80°C for proteome analysis. To assess the loss in viability of *M*. *paratuberculosis* subsequent to starvation, viable cells were enumerated from the 14 week starved samples by the most probable number (MPN) method as described previously [24].

Protein extraction from *M. paratuberculosis*

Protein samples were prepared using an homogenizer with 160 µl of cell lysis buffer (8 M Urea, 100 mM Dithiothreitol, 4% w/v CHAPS, 0.8% v/v carrier ampholytes, 40 mM Tris) as described previously [25]. The lysed cell suspension was centrifuged at 16,060 ×*g* for 1 h at 4°C to pellet the cellular debris and the supernatant was collected. The aliquots of supernatant were stored at -80°C for 2-D PAGE. Protein concentration was performed (Bio-Rad protein assay) and 60 µg of protein sample was purified with a 2-D clean up kit (Amersham Biosciences) as described by the manufacturer.

2-D PAGE

For each strain of *M. paratuberculosis*, 60 µl (~ 60 µg) of the purified protein sample (as described above) was diluted in 90 µl of protein sample extraction buffer and used to re-hydrate a 7 cm IPG strip (pH 4-7) (ReadyStrip, Bio-Rad) passively, according to the manufacturer's instructions. Isoelectric focusing was undertaken in a Bio-Rad Protean IEF at 15000 Vh and IPG strips were equilibrated in a two-step equilibration procedure as described by the manufacturer. Briefly, IPG strips were washed for 10 min in equilibration buffer 1 (6 M Urea, 375 mM Tris-HCl pH 8.8, 2% w/v SDS, 20% v/v glycerol and 2% w/v DTT) followed by a second 10 min wash in equilibration buffer 2 (6 M Urea, 375 mM Tris-HCl pH 8.8, 2% w/v SDS, 20% v/v glycerol and 2.5% w/v iodoacetimide). IPG strips were rinsed in SDS-PAGE tank buffer and run in the 2nd dimension on 12% vertical SDS-PAGE gels (10 x 10.5 cm) as described by Laemmli [26]. Gels were rinsed in deionized water and stained with silver stain as described previously [27]. The experiment was repeated and duplicate gels were run for each sample. The 2-D gels were scanned with ImageScanner™ II via LabScan™ software (Amersham Biosciences) and differences in protein expression level between control and hypoxic or starvation 2D gels were determined initially by ImageMaster 2D Platinum v5.0 software (Amersham Biosciences) using the following parameters for spot detection: smooth = 4, minimal area = 10 and saliency =15. All analyses were performed twice by conducting independent experiment to overcome technical variation. Spots were verified by visual examination. Briefly, the patterns of each sample were overlaid and aligned using six landmarks selected from all regions of the gel; they were spots clearly present in all gels. After automatic spot matching, manual matching was required for several spots that had been selected visually. Spot normalization was based on relative volume (%Vol), the volume of each spot divided by the total volume of all the spots in the gel. The normalized volumes of an identified protein spot in control and treatment gels were compared to calculate the expression ratio.

In gel digestion and mass spectrometry

The spots of interest were excised from stained gels and were digested as follows. Briefly, excised gel spots were incubated with DTT (20 mM) in NH_4HCO_3 (30 µl, 25 mM) for 30 min at 37°C; after removal of the liquid the spot was incubated with iodoacetamide (30 µl, 40 mM) in NH_4HCO_3 (30 µl, 25 mM) for 30 min at 37°C. The spot was washed with CH_3CN (2 x 50 µl, 10 min). Trypsin (~100 ng) in NH_4HCO_3 (10 mM, 25 µl) was added and the solution was left at 37°C for 14 h. The gel pieces were washed with H_2O (0.1% formic acid, 50 µl) and H_2O:CH_3CN (1:1) (0.1% formic acid, 50 µl) for 15 min and the combined extracts were dried and peptides dissolved in H_2O with 0.05% heptafluorobutyric acid and 0.1% formic acid, 10 µl. Digested peptides were separated by nano-Liquid Chromatography (LC) using a Cap-LC autosampler system (Waters, Milford MA). Samples (5 µl) were concentrated and desalted onto a micro C18 precolumn (500 µm x 2 mm, Michrom Bioresources, Auburn, CA) with H_2O:CH_3CN (98:2, 0.05 % HFBA) at 15 µl/min. After a 4 min wash the pre-column was automatically switched (Valco 10 port valve, Houston, TX) into line with a fritless nano column as described previously [28]. Peptides were eluted using a linear gradient of H_2O:CH_3CN (98:2, 0.1 % formic acid) to H_2O:CH_3CN (50:50, 0.1 % formic acid) at ~200 nl/min over 30 min. The precolumn was connected via a fused silica capillary (10 cm, 25 µ) to a low volume tee (Upchurch Scientific), where high voltage (2600 V) was applied and the column tip positioned ~ 1 cm from the Z-spray inlet of an Ultima API hybrid Quadrupole Time-of-Flight (Q-TOF) tandem mass spectrometer (Micromass, Manchester, UK). Positive ions were generated by electrospray and the Q-TOF operated in data dependent acquisition mode (DDA). A TOF-MS survey scan was acquired (m/z 350-1700, 1 s) and the 2 largest multiply charged ions (counts > 20) were sequentially selected by Q1 for tandem mass spectrometry or MS-MS analysis. Argon was used as collision gas and an optimum collision energy chosen (based on charge state and mass). Tandem mass spectra were accumulated for up to 8 s (m/z 50-2000). Peak lists were generated by MassLynx (Micromass) using the Mass Measure program and submitted to the database search program Mascot (version 2.1, Matrix Science, London, England). Search parameters were comprised of trypsin digestion, MS/MS

ion search, monoisotropic mass values, unrestricted protein mass range, precursor and product ion tolerances ± 0.25 and 0.2 Da, respectively, Met (O) and Cys-carboxyamidomethylation specified as variable modification and 1 missed cleavage was possible. The matches with Mascot probability scores greater than 50 (p<0.05) were used to query the NCBI nr database using the BLASTp algorithm. The matches were further subjected to searches of the *M*. *tuberculosis* H37Rv genome sequence database (Tuberculist, Institute Pasteur, Paris, http://genolist.pasteur.fr/Tuberculist/). The complete amino acid sequence for each of the *M*. *paratuberculosis* proteins identified was obtained from the *M*. *paratuberculosis* K-10 genome (GenBank accession, AE016958). The theoretical pI of proteins was calculated using Biomanager, Australian National Genomic Information Service (ANGIS) (http://www.angis.org.au/). The expressed protein sequences were further analysed to identify the pattern or profiles of proteins using the Interpro Scan algorithm of the ExPASy (Expert Protein Analysis System) proteomics server of the Swiss Institute of Bioinformatics (SIB) (http://us.expasy.org/tools/). Peptides matching trypsin and human keratin were excluded. Sequence coverage (%) was calculated as the number of amino acids contained within the set of matched peptides divided by the total number of amino acids making up the sequence of the identified protein.

Results and discussion

Viability and growth pattern of *M. paratuberculosis* following hypoxia

Firstly, culture vials with *M*. *paratuberculosis* were incubated aerobically for a week before exchange of the atmosphere with anaerobic gases. There was no difference in growth pattern between control and treatment vials during the initial aerobic phase and for several days after the switch to anaerobic conditions (Fig. 1). After that, the GI of control cultures incubated aerobically was slightly higher than the GI of cultures incubated anaerobically, but GI for both declined after 3 days and was <100 by day 7 suggesting entry to stationery phase due to gradual depletion of nutrients or C^{14} -labelled palmitate during the initial log phase, or accumulation of wastes to which the organism had not adapted. After day 7 there was negligible GI until restoration of an aerobic atmosphere whereupon it increased within 1 week to between 100 and 300 then slowly declined over the next 7 weeks (Fig. 1). Patterns of growth were similar for 7, 14, 21 and 28 days of anaerobic exposure (data for 14 and 21 days not shown). This pattern of growth suggests minimal metabolic activity and probable dormancy during the extended anaerobic phase. The growth pattern of both S and C strains was similar.

In the second experiment in which there was no initial aerobic phase, the GI of anaerobic treatment vials were restricted compared to controls (Fig. 2). In contrast to the previous experiment, a rapid increase in GI to 999 followed the provision of an aerobic atmosphere to treatment vials; the lag phase was less than 1 week. Patterns of growth were similar for 7, 14, 21 and 28 days of anaerobic exposure (data for 14 and 21 days not shown). During the anaerobic phase in this experiment the GI of the S strain did not exceed 600 (Fig. 2) whereas the C strain did not exceed 300 (Fig. 2) and was consistently lower than that for S strain until aerobic conditions were provided. Despite possible greater adaptation to hypoxic conditions by the S strain, both strains appeared to remain viable and metabolically active throughout the period of anaerobic incubation, albeit at a low level. However, a proportion of the cells may have been dormant. The methods used provided an aggregated assessment of the entire culture without any information about the status of metabolic sub-groups of bacteria within the population. Further, in these models several sampling time points were selected to verify changes consistent with a long lasting stress response with an assumption that *M*. *paratuberculosis* might behave in a similar way *in vivo*.

In Wayne's dormancy model it was observed that an abrupt shift from aerobic to anaerobic conditions caused death of *M*. *tuberculosis* cells. However, a gradual shift from an aerobic to an anaerobic state resulted in adaptation of *M*. *tuberculosis* to the stress by entering a non-replicating persistent state [5] and on resuspension and aeration, hypoxic *M*. *tuberculosis* cells showed

synchronized replication [29]. Findings consistent with this were observed in this study because *M*. *paratuberculosis* resumed synchronized growth after exposure to aerobic conditions (Fig. 2). These findings reinforce observations that *M*. *paratuberculosis* can exhibit a dormant state in nature [19, 20].

Viability and growth pattern of *M*. *paratuberculosis* following nutrient starvation

The viable count after 12 weeks of starvation was 4 logs lower than at the start (2.6×10^3 for C strain; 9.2×10^3 for S strain) representing >99.9% loss in viability for both strains. The S strain did not grow at all after 14 weeks of starvation while only 9.3×10^1 viable C strain cells remained. The C strain survived for at least 16 weeks without nutrients, suggesting that it may have greater capacity to withstand deprivation of nutrients than S strain. The entire experiment was repeated with similar outcomes. The viability and growth patterns of *M*. *paratuberculosis* following starvation were entirely consistent with its obligatory parasitic existence and in this respect it is similar to *M*. *tuberculosis* H37Rv, which was shown to lose 99% viability in tris buffered saline over 3 months [9]. In contrast, *M*. *avium intracellulare*, which is an environmental organism and opportunistic pathogen of animals, lost less than 90% viability following more than 2 years in deionized water [30].

During starvation stress, the transient loss of culturability or lag phase depended on the period of starvation, suggesting slowing of metabolism of all cells and/or death of a proportion. The lag phase is generally considered to be the adaptation phase of the organism to the new environment. Lag phases of <1 week duration were observed for controls, 2-3 weeks duration after starvation for 12 weeks and 3-4 weeks duration after starvation for 16 weeks. Examples of growth curves are shown in Fig. 3. As 10^0 viable *M*. *paratuberculosis* cells will result in a GI of 999 within 6 weeks [31], lag phases as short as 4 weeks indicate that viable and culturable cells are still present in an inoculum. Similarly the time taken to reach peak GI progressively increased with period of starvation (Fig. 3). As in the anaerobiosis experiments, a proportion of the starved cells may have been dormant. The proteome data (see below) including synthesis of molecular chaperones, dormancy-associated proteins and activation of various metabolic pathways during starvation justifies the conclusion that *M*. *paratuberculosis* can enter into the dormant state.

Proteome of *M*. *paratuberculosis* during hypoxia and nutrient starvation

Protein expression was investigated after both 1 and 4 weeks of hypoxic stress and after 8 weeks of nutrient starvation and compared to controls. Duplicate 2-D gels were run from each sample collected from two independent experiments, yielding identical and reproducible protein spot patterns. Up to 1650 spots were observed in gels. A summary of the number of spots/proteins resolved and their expression levels relative to controls is provided in table 1. Twenty eight protein spots unique to treatment gels were identified across strains (C and S) and treatments (hypoxia and starvation) from a total of 66 differentially expressed protein spots, as shown in table 2 and tables 3-4 (Addendum). There were 44 up-regulated protein spots selected for identification, and these represented 29 proteins (Tables 1 and 2). Seven of these were up-regulated by both hypoxia and starvation, 4 for S strain (atpC, ClpP, MAP4107 and Ppa) and 3 for C strain (MAP1653, MAP0593c and MAP1339) (Addendum tables 3-4). The expression of only 1 protein was down-regulated during hypoxia but during nutrient starvation 7 were down-regulated in S strain and 3 in the C strain. One protein (MAP1586 for S strain) was down-regulated by both kinds of stress (addendum tables 3-4).

The software identified 1650 protein spots in the S strain following hypoxia treatment with a matching rate of about 81% with the control gel; 15 differentially expressed spots were selected for identification, 12 being unique to this treatment (Table 2 and addendum table 3a, Fig. 4). For the C strain 1185 protein spots were detected with a matching rate of about 85%; 10 differentially expressed spots were selected for identification, 5 being unique to this treatment (Table 2 and addendum table 3b, Fig. 5). The protein expression pattern was similar after short (1 week) or long

(4 weeks) exposure to hypoxic stress (Figs. 4 and 5), regardless of strain. Furthermore, the protein expression patterns were identical irrespective of whether an aerobic log phase preceded the hypoxic treatment. This suggests a general response of *M*. *paratuberculosis* to hypoxic stress which can be manifested at least as early as 1 week after exposure to hypoxic conditions.

The protein profiles of *M*. *paratuberculosis* were studied after 8 weeks of starvation on the basis that this would be sufficient to induce a response, as differential expression of proteins was observed after 6 weeks of starvation in *M*. *tuberculosis* [32] which grows more slowly. The software identified 1623 spots in the starved cells of S strain with a matching rate of about 79% with control gels; 25 differentially expressed spots were selected for identification, 4 being unique to the starved samples (Table 2 and addendum table 4a, Fig. 6). For the C strain 1095 spots were detected with a matching rate of 76%; 16 differentially expressed spots were selected for identification, 6 being unique to this treatment (Table 2 and Table 4b (Addendum), Fig. 6).

The number of proteins identified in this study represented a small part of the pool of differentially expressed proteins. Only protein spots with marked changes in expression detectable visually in the low to medium molecular weight range were selected for mass spectrometry in order to obtain well resolved spots to increase the accuracy of protein identification. Further, the selection criterion were based on the presence of dormancy-associated proteins in these regions in other mycobacteria [33, 34]. Further work is required to fully elucidate the proteome of *M*. *paratuberculosis* under these stresses including use of different pH range gels, other protein purification methods and multiplexed proteomics technology.

Functional classification of differentially expressed proteins

The expression levels of proteins representing a range of constitutive and adaptive biochemical pathways were altered by hypoxia and or nutrient starvation. Differentially expressed proteins were classified based on biological functions and 13 categories were identified (Table 2 and Fig. 7). The greatest number of differentially expressed proteins (25%) were categorized under hypothetical proteins with putative function. Although some could possibly be classified into functional categories mentioned above, they were listed separately into tumor suppressors, universal stress proteins, cellular processes and two component response regulators (Fig. 7). The proteins identified as differentially expressed are briefly discussed below within their functional category.

Antioxidant enzymes

These proteins comprised 9% of the spots identified and were identified following both hypoxia and nutrient starvation but only in C strain. Pathogenic mycobacteria produce enzymes such as peroxyredoxins, catalase, peroxidase, superoxidase dismutase and nitrosothiol reductase to neutralize reactive oxygen species and enable persistence in the host [35]. Thiol peroxidase is considered to be the most effective peroxidase of *M*. *tuberculosis*. It reduced a broad spectrum of hydroperoxides including hydrogen peroxide, is more abundant than other antioxidant enzymes and is considered to be the dominant antioxidant that protects mycobacteria within host phagocytes [36]. AhpD catalyzes the reduction of peroxides to their corresponding alcohols via oxidation of cysteine residues. It assists the survival of pathogens in the oxidative environment of host phagocytes [37]. AhpC and AhpD provide protection against reactive nitric and oxidative metabolites also induce a strong IFN-γ response in goats with experimental subclinical paratuberculosis [38]. Four fold increases in expression of TrxC was observed after starvation; it regulates the functions of at least 30 target proteins, some of which are enzymes and transcription factors. It also plays an important role in the defense against oxidative stress by directly reducing hydrogen peroxide and certain radicals, and by serving as a reductant for peroxiredoxins [39].

Amino acid metabolism

Five (9%) of the differentially expressed spots were proteins that influence amino acid metabolism, but were differentially expressed only in the S strain. ArgC, DapA and HisI were down-regulated under the influence of starvation, suggesting conservation of energy resources for survival. ArgC regulates arginine biosynthesis and interconnects several other metabolic pathways such as pyrimidine and polyamine biosynthesis as well as diverse degradative pathways [40]. DapA (Dihydrodipicolinate synthase) is a key enzyme in lysine biosynthesis and produces Diaminopimelate as the metabolic byproduct in bacteria. It is involved in peptidoglycan formation in mycobacteria [41] and was down-regulated in this study. HisI (Phosphoribosyl-AMP cyclohydrolase), which catalyses the third step in the histidine biosynthetic pathway [39], was also down-regulated in starvation. In contrast, HisA and HisG, which also control histidine biosynthesis, were up-regulated during hypoxia and starvation stress, respectively, suggesting a complex role for the histidine biosynthetic pathway in survival of *M*. *paratuberculosis* during these stresses in the S strain. While genomic differences between the S and C strains of *M*. *paratuberculosis* are being progressively recorded, this is one of the first functional differences to be identified.

Fatty acid metabolism

EchA20 (Enoyl-CoA hydratase) catalyzes the second step in the physiologically important beta-oxidation pathway of fatty acid metabolism. This enzyme facilitates the syn-addition of a water molecule across the double bond of a trans-2-enoyl-CoA thioester, resulting in the formation of a β-hydroxyacyl-CoA thioester [42]. FabG plays a role in fatty acid biosynthesis which is considered to be important for the survival of bacteria [43]. In *M*. *tuberculosis*, the protein encoded by *fabG3* has similarity to β-ketoacyl-carrier protein (ACP) reductase [44]. ACP reductase catalyzes the NADPH-dependent reduction of β-ketoacyl-carrier protein to generate (3*S*)-β-hydroxyacyl-ACP during the chain elongation of bacterial fatty acids [45]. Mycolic acids produced by all mycobacteria are homologues to α-alkyl β-hydroxy fatty acid. These are a significant component of the mycobacterial cell wall and form an effective barrier to the penetration of chemotherapeutic agents. Therefore, the fatty acid biosynthesis pathway is believed to be a potential target for developing antimycobacterial drugs [44]. MAP0508 also contains a domain which plays a role in fatty acid biosynthesis [39] . The downregulation of these three proteins in the C strain following starvation suggests conservation of energy resources and possible alteration to the cell wall.

ATP and Purine biosynthesis

Two proteins in this category were up-regulated following hypoxia and starvation in the S strain and after hypoxia in the C strain. *atpC* encodes ATP synthases of bacteria which perform two important physiological functions. Firstly, the enzyme catalyzes the synthesis of ATP from ADP and Pi by using energy derived from the electrochemical ion gradient, and secondly, it functions as an ATPase, generating a transmembrane ion gradient by ATP hydrolysis [46]. PurE (Aminoimidazole carboxylase) catalyses the conversion of aminoimidazole ribonuceotide (AIR) to carboxy aminoimidazole ribonuceotide (CAIR), the sixth step of *de novo* purine biosynthesis [39]. In *E*. *coli*, PurE favorably influences metabolic consumption of ATP [47]. The upregulation of AtpC and PurE in *M*. *paratuberculosis* after hypoxia and starvation suggests altered demand for ATP for survival under stress.

Proteolysis

The necessity for bacterial adaptation to starvation and other physical stresses has forced the evolution of complex regulatory networks which respond to changes in the environment. During adverse conditions, bacteria respond by increasing the synthesis of molecular chaperones that assist proper folding of proteins, and increasing the expression of proteases which degrade proteins

that cannot be refolded [48]. Nine percent of the differentially expressed spots identified were proteases. ClpP is an ATP dependent protease and was up-regulated in both strains of *M*. *paratuberculosis*. ATP-dependent proteases are responsible for the turnover of short-lived regulatory proteins and the removal of abnormal polypeptides, functions which are vital for processes such as cell cycle control, signal transduction and antigen presentation [49]. Proteasomes are large multimeric self-compartmentalizing proteases, involved in the clearance of misfolded proteins, the breakdown of regulatory proteins, and the processing of proteins such as the preparation of peptides for immune presentation [39]. There was over 30 fold upregulation of the proteosome subunit PrcA in the S strain under nutrient starvation.

Cell wall synthesis

Differentially expressed CysQ_2 has homology to a bacterial member of the inositol monophosphatase family and has 3'-Phosphoadenosine-5'-phosphosulfate (PAPS) 3'-phosphatase activity [39]. Inositol monophosphatase is an enzyme in the biosynthesis of myo-inositol, a crucial substrate for the synthesis of phosphatidylinositol. Phosphatidyl-myo-inositol (PI) and its metabolically derived products such as phosphatidyl-myo-inositol-mannosides (PIMs), lipomannan (LM) and lipoarabinomannan (LAM) are important phospholipids in the mycobacterial cell wall. PI and PIMs are believed to play essential roles in membrane stability and cell viability [50]. The upregulation of CysQ_2 in *M*. *paratuberculosis* after starvation suggests that changes in the cell wall of *M*. *paratuberculosis* are required for its survival under adverse conditions.

Protein synthesis

GreA was identified via the homology of *M*. *paratuberculosis* locus tag MAP1027c to *M*. *avium*. Bacterial proteins GreA and GreB are necessary for efficient transcription elongation by RNA polymerase beyond template-encoded arresting sites [51]. The differential expression of this protein indicates an increased transcription requirement for *M*. *paratuberculosis* during hypoxia. However, most ribosomal protein genes have been reported to be repressed during stationary phase and dormancy due to inefficient and error prone translation that is likely due to the low concentration of charged tRNAs [52]. RplJ was repressed in S strain during starvation in this study.

Signal recognition

Heparin binding haemagglutinin adhesin like protein (HBHA) identified during hypoxia is required for extra pulmonary dissemination of *M*. *tuberculosis*. A strong T cell response to HBHA was recorded for latently infected humans, but no response was observed for patients with active disease, suggesting it to be a good marker for the immunodiagnosis of latent tuberculosis [53]. Recently, recombinant HBHA was found to be immunogenic and induced antibody responses in cattle against *M*. *paratuberculosis* [54]. The role of HBHA in *M*. *paratuberculosis* infection and persistence is not known. However, the upregulation of HBHA in *M*. *paratuberculosis* under hypoxia reveals its possible role in persistence in the host.

Hypothetical proteins with putative function

Tumor suppressors

MAP0593c showed increased expression after hypoxia and starvation in C strain and after starvation in S strain. A search of the Interpro Scan database revealed that MAP0593c displayed homology to Histidine triad protein (HIT). Members of this family are found in prokaryotes as well as in lower and higher eukaryotes [55]. HIT proteins can be classified into the histidine triad nucleotide binding proteins (Hint) branch, which consist of adenosine 5′-monophosphoramide hydrolases; the fragile histidine triad (Fhit) branch, consisting of diadenosine polyphosphate hydrolases, and; the GalT branch consisting of nucleoside monophosphate transfereases. Fhit homologues have

substrate specificity for diadenosine triphosphate (ApppA) and diadenosine tetraphosphate (AppppA). ApppA and AppppA are involved in cellular functions including regulation of DNA replication and signaling during stress responses [56]. In humans, Fhit proteins have been demonstrated to function as tumor suppressors [57].

Cellular processes

Hypothetical proteins MAP0711c and MAP3007 probably act as oxidoreductase enzymes and were down-regulated following starvation in S strain. MAP1560 which was found after hypoxia in C strain has homology to region PaaI_thioesterase. It is a tetrameric acyl-CoA thioesterase with a hot dog fold and is responsible for phenylacetic acid (PA) degradation in bacteria [39]. MAP2411 which was overexpressed following starvation displayed homology to Pyridoxamine 5'-phosphate oxidase [39], an FMN flavoprotein that catalyses the oxidation of pyridoxamine-5-phosphate (PMP) and pyridoxine-5-phosphate (PNP) to pyridoxal-5-phosphate (PLP). PLP is a cofactor required by cellular enzymes involved in amino acid metabolism and is also involved in the synthesis of neurotransmitters, modulation of steroid-receptor interaction and regulation of immune function [58]. The >5 fold increased protein expression in *M*. *paratuberculosis* reveals the significance of this protein during starvation stress. A two fold increase in expression of MAP2705 was observed in S strain following hypoxia. This protein displayed homology to Ketosteroid isomerases, which plays a crucial role in the biosynthesis of all classes of hormonal steroids. These enzymes are widely distributed in bacteria. MAP1885c which was identified only after starvation of S strain displayed homology to Phosphatidyl-Ethanolamine-Binding Protein (PEBP) and its eukaryotic homologue Raf Kinase Inhibitor Protein (RKIP). A number of biological roles for the members of the PEBP/RKIP family include serine protease inhibition, membrane biogenesis, and Raf-1 kinase inhibition [39]. The protein has homology to TB18.6 of *M*. *tuberculosis* which was identified in culture filtrate [59]. TB18.6 induced delayed type hypersensitivity responses in guinea pigs and released IFN-γ from splenic lymphocytes isolated from mice infected with *M*. *tuberculosis* [59].

Universal stress proteins

MAP1339 was differentially expressed in C strain following starvation and hypoxia and belongs to the Universal stress protein (Usp) family. These novel proteins were identified in oxygen starved *M*. *tuberculosis*, *M*. *bovis* and *M*. *smegmatis*. Usp may play a role in adaptation of mycobacteria to oxygen deprivation and might be important in latent tuberculosis. *M*. *tuberculosis* encodes eight Usp proteins and it is possible that these may be expressed under conditions other than oxygen limitation [60]. In *E*.*coli*, *uspA* was up-regulated in response to growth arrest [61]. All the Usps were expressed during starvation and heat shock, while cold shock suppressed the production of *Usp* proteins. Expression of *uspC*, *uspD* and *uspE* in *E*.*coli* was shown to be dependant on the stringent response and they appeared to provide protection against DNA damaging agents [62]. The deletion of *RelA* and *SpoT* stopped the production of ppGpp, thereby reducing the induction of all *usp* genes. Overproduction of ppGpp during growth triggered the increased expression of *usp* genes [63, 64]. Recently, *uspA* appeared to be involved in regulating the capacity of *E*.*coli* to withstand oxidative stress [65]. The hypothetical protein Rv2623 which was induced during the adaptive dormant response in *M*. *tuberculosis* also belongs to the universal stress protein family [6].

Two component response regulators

MAP0834 and MAP3200 were expressed in both strains following hypoxia, but not in controls. MAP0834 was identified in S strain and contains three conserved domains: trans_reg_C, REC and OmpR [39]. MAP3200 was identified in the C strain contains a REC signal receiver domain similar to MAP0834c which receives the signal from the sensor partner in a two-component system [39]. Trans_reg_C is the effector domain of a response regulator. Bacteria and certain eukaryotes like

protozoa and higher plants use two-component signal transduction systems to detect and respond to changes in the environment. Response regulators also regulate important physiological and metabolic processes such as stress responses, nutrient utilization, quorum sensing, cell division and play a critical role in virulence by coordinating expression of genes involved in pathogenesis [66]. Oxygen starvation triggers an adaptive dormancy response in aerobic tubercle bacilli. The hallmark of the dormant response in *M*. *tuberculosis* is considered to be survival during hypoxia and upregulation of dormancy survival regulator (DosR or Rv3133c) which contains a REC receiver domain similar to that in *M*. *paratuberculosis* [6].

Hypothetical proteins with unknown function

MAP1586, MAP3864, MAP1076, MAP0643c, and MAP4107 which constituted the second major category (13%) of differentially expressed spots following hypoxia and starvation. However, searches of relevant databases revealed no putative functions for these proteins. It is possible that they may be important for stress and dormancy responses in *M*. *paratuberculosis* and warrant further investigation.

Cyanate hydrolysis

A greater than three fold increase in expression of Cyanate hydratase was found following starvation in C strain. Organisms that possess cyanase may overcome the toxicity of environmental cyanate [39]. In *E*. *coli*, these enzymes catalyze the reaction of cyanate with bicarbonate to produce ammonia and carbon dioxide [67]. Strains of *E*. *coli* with inducible cyanase can grow on cyanate as the sole source of nitrogen [68]. It may be that cyanate is recruited as a source of nitrogen for *M*. *paratuberculosis* survival during nutrient starvation as nitrogen is required as an essential component of proteins, nucleic acids and other cellular constituents.

Phosphate metabolism

Inorganic pyrophosphatase was up-regulated in *M*. *paratuberculosis* after both starvation and hypoxic stresses. A basal level of pyrophosphatase expression was essential for the growth of *E*. *coli* [69]. *ppa* was also induced during intracellular infection of U937 macrophage-like cells with *Legionella pneumophila* [70]. Inorganic pyrophosphate (PPi) is produced in phosphorylation, oxidative phosphorylation and glycolysis. PPi serves as a source of energy and regulates many enzymes indirectly for several metabolic reactions [71].

Cell division

Single strand DNA binding protein (SSB) was up-regulated following hypoxic stress in C strain. During DNA replication, repair and recombination, double stranded DNA is converted to single stranded DNA (ssDNA). SSB protects the transiently formed ssDNA from nucleases, chemical attacks and prevents the formation of aberrant secondary structures and is one of the minimal gene products required for life [72]. Wag31 which was up-regulated after starvation in S strain was originally identified as an antigenic protein of pathogenic mycobacteria by studying the serum of patients with leprosy and tuberculosis [73]. The mechanism by which *M*. *tuberculosis* shifts between an active state of replication and the latent state is unclear. However, regulation of cell wall synthesis and cell division in response to stimuli encountered in the host is considered to be a likely factor. The *M*. *tuberculosis* genome contains 11 serine/threonine kinase genes including *pknA* and *pknB* which are involved in cell shape control and cell wall synthesis [74]. Wag31 is the preferred substrate for these genes and moderate overexpression of this protein can alter mycobacterial cell morphology [74] suggesting that there may be an altered cell wall in *M*. *paratuberculosis* following starvation.

Concluding remarks

Although the growth patterns of *M*. *paratuberculosis* during hypoxia and starvation stresses were suggestive of dormancy, this phenotype in mycobacteria is difficult to define and prove conclusively [75]. The cultures contain a mixed population of cells and GI is a measure of aggregate metabolic response of the population. GI may be generated by replicating cells or resting cells, the only requirement being conversion of palmitate to carbon dioxide through respiration. However, demonstration of the differential expression of proteins from known homologues of mycobacterial dormancy-associated domains (DosR and USP) (MAP1339 during starvation and MAP3200 and MAP0834c during hypoxia) is further evidence for a dormancy response in *M*. *paratuberculosis*. The regulator DosR has been implicated in control of 47 dormancy-associated genes in *M*. *tuberculosis* [76, 77] and nearly all the genes regulated by hypoxia require DosR for their induction [76]. DosR was also essential for *M*. *bovis* BCG survival under hypoxia [6].

A feature of the stringent response to starvation in bacteria is the accumulation of ppGpp as a result of the activation of RelA and SpoT [10]. These were not identified in *M*. *paratuberculosis* in the present study which could be due to spot selection or the masking effect of trypsin precursors and

further investigation is warranted. During starvation of bacteria there is a phase of adaptation i.e. a change from growth and replication to a survival state. During this phase in *M*. *tuberculosis* and *M*. *avium intracellulare* there is slower transcription, growth arrest, differential gene regulation and metabolic pathway rearrangement [30, 32]. The results of this study show that the patterns of growth and metabolism and differential expression of proteins in response to hypoxia and starvation is conserved in *M*. *paratuberculosis*. The induction of certain proteins in *M*. *paratuberculosis* may play a key regulatory role during dormancy, survival and hence virulence. It is likely that *M*. *paratuberculosis* cells express these proteins for protection against the stresses of the *in vivo* environment, and so they may have a significant role in the generation of an immune response against *M*. *paratuberculosis*. Further analysis of the role of these induced proteins by constructing mutants and characterizing their phenotypes would reveal proteins essential for survival during the persistent state.

The S and C strains of *M*. *paratuberculosis* are phenotypically and genotypically distinct. Studies based on representational difference and microarray analyses have identified small and large genomic polymorphisms between representatives of C and S strains [16, 18, 78]. Recently, 11 single nucleotide polymorphisms (SNPs) were identified between the S and C strains of *M*. *paratuberculosis* in eight genes [79] and SNPs have been shown to be responsible for altered phenotypes in *M*. *tuberculosis* [80]. It was therefore not unexpected that protein expression patterns in these two strains as a result of exposure to hypoxia and starvation were similar but distinct.

This study can be regarded as one step towards the description of the proteome of *M*. *paratuberculosis*. The *in vitro* models dissected many metabolic pathways active during hypoxia and starvation in and added evidence for the existence of a dormant state in *M*. *paratuberculosis*. These findings can be extrapolated to study microbial ecology. A better understanding of the ability of bacterial pathogens to withstand stress will enable the identification of more effective intervention strategies to limit their survival in these environments. The differentially expressed proteins and may serve as targets for better diagnosis, treatment and prevention of Johne's disease in sheep and cattle. Several of the proteins found in this study (HBHA, AhpC and AhpD) have already been evaluated and are immunogenic in animals with Johne's disease [38, 54].

References

Wayne, L. G., Dormancy of Mycobacterium tuberculosis and latency of disease. Eur. J. Clin. Microbiol. Infect. Dis. 1994, 13, 908-914.

Edwards, C., Problems posed by natural environments for monitoring microorganisms. Mol. Biotechnol. 2000, 15, 211-223.

Mukamolova, G. V., Kaprelyants, A. S., Kell, D. B., Young, M., Adoption of the transiently non-culturable state-a bacterial survival strategy? Adv. Microb. Physiol. 2003, 47, 65-129.

Kaprelyants, A. S., Gottschal, J. C., Kell, D. B., Dormancy in non-sporulating bacteria. FEMS Microbiol. Rev. 1993, 10, 271-285.

Wayne, L. G., Hayes, L. G., An in vitro model for sequential study of shiftdown of Mycobacterium tuberculosis through two stages of nonreplicating persistence. Infect. Immun. 1996, 64, 2062-2069.

[Boon, C., Dick, T., Mycobacterium bovis BCG response regulator essential for hypoxic dormancy. J. Bacteriol. 2002, 184, 6760-6767.

Cunningham, A. F., Spreadbury, C. L., Mycobacterial stationary phase induced by low oxygen tension: cell wall thickening and localization of the 16-kilodalton alpha-crystallin homolog. J. Bacteriol. 1998, 180, 801-808.

Nyka, W., Studies on the effect of starvation on mycobacteria. Infect. Immun. 1974, 9, 843-850.

Primm, T. P., Andersen, S. J., Mizrahi, V., Avarbock, D., et al., The stringent response of Mycobacterium tuberculosis is required for long-term survival. J. Bacteriol. 2000, 182, 4889-4898.

Chatterji, D., Ojha, A. K., Revisiting the stringent response, ppGpp and starvation signaling. Curr. Opin. Microbiol. 2001, 4, 160-165.

Volker, U., Hecker, M., From genomics via proteomics to cellular physiology of the Gram-positive model organism Bacillus subtilis. Cell. Microbiol. 2005, 7, 1077-1085.

Bush, R. D., Toribio, J. A., Windsor, P., Losses of adult sheep due to ovine Johne's disease in 12 infected flocks over a 3-year period. Aust. Vet. J. 2006, 84, 246-253.

Ott, S. L., Wells, S. J., Wagner, B. A., Herd-level economic losses associated with Johne's disease on US dairy operations. Prev. Vet. Med. 1999, 40, 179-192.

Whittington, R., Marsh, I., Choy, E., Cousins, D., Polymorphisms in IS1311, an insertion sequence common to Mycobacterium avium and M. avium subsp. paratuberculosis, can be used to distinguish between and within these species. Mol. Cell Probes 1998, 12, 349-358.

Whittington, R. J., Hope, A. F., Marshall, D. J., Taragel, C. A., Marsh, I., Molecular epidemiology of Mycobacterium avium subsp. paratuberculosis: IS900 restriction fragment length polymorphism and IS1311 polymorphism analyses of isolates from animals and a human in Australia. J. Clin. Microbiol. 2000, 38, 3240-3248.

Marsh, I. B., Whittington, R. J., Deletion of an mmpL gene and multiple associated genes from the genome of the S strain of Mycobacterium avium subsp. paratuberculosis identified by representational difference analysis and in silico analysis. Mol. Cell. Probes 2005, 19, 371-384.

Semret, M., Turenne, C. Y., de Haas, P., Collins, D. M., Behr, M. A., Differentiating host-associated variants of Mycobacterium avium by PCR for detection of large sequence polymorphisms. J. Clin. Microbiol. 2006, 44, 881-887.

Marsh, I. B., Bannantine, J. P., Paustian, M. L., Tizard, M. L., et al., Genomic Comparison of Mycobacterium avium subsp. paratuberculosis Sheep and Cattle Strains by Microarray Hybridization. J. Bacteriol. 2006, 188, 2290-2293.

Whittington, R. J., Marsh, I. B., Reddacliff, L. A., Survival of Mycobacterium avium subsp. paratuberculosis in Dam Water and Sediment. Appl. Environ. Microbiol. 2005, 71, 5304-5308.

Whittington, R. J., Marshall, D. J., Nicholls, P., Marsh, I. B., Reddacliff, L. A., Survival and dormancy of Mycobacterium avium subsp. paratuberculosis in the environment. Appl. Environ. Microbiol. 2004, 70, 2989-3004.

Marsh, I., Whittington, R., Cousins, D., PCR-restriction endonuclease analysis for identification and strain typing of Mycobacterium avium subsp. paratuberculosis and Mycobacterium avium subsp. avium based on polymorphisms in IS1311. Mol. Cell Probes 1999, 13, 115-126.

Whittington, R. J., Marsh, I., McAllister, S., Turner, M. J., et al., Evaluation of modified BACTEC 12B radiometric medium and solid media for culture of Mycobacterium avium subsp. paratuberculosis from sheep. J. Clin. Microbiol. 1999, 37, 1077-1083.

Whittington, R. J., Marsh, I., Turner, M. J., McAllister, S., et al., Rapid detection of Mycobacterium paratuberculosis in clinical samples from ruminants and in spiked environmental samples by modified BACTEC 12B radiometric culture and direct confirmation by IS900 PCR. J. Clin. Microbiol. 1998, 36, 701-707.

Whittington, R. J., Reddacliff, L. A., Marsh, I., McAllister, S., Saunders, V., Temporal patterns and quantification of excretion of Mycobacterium avium subsp. paratuberculosis in sheep with Johne's disease. Aust. Vet. J. 2000, 78, 34-37.

Gumber, S., Taylor, D. L., Whittington, R. J., Protein extraction from Mycobacterium avium subsp. paratuberculosis: Comparison of methods for analysis by sodium dodecyl sulphate polyacrylamide gel electrophoresis, native PAGE and surface enhanced laser desorption/ionization time of flight mass spectrometry. J. Microbiol. Methods 2007, 68, 115-127.

Laemmli, U. K., Cleavage of structural proteins during the assembly of the head of bacteriophage T4. Nature 1970, 227, 680-685.

Blum, H., Beier, H., Gross, H., Improved silver staining of plant proteins, RNA and DNA in polyacrylamide gels. Electrophoresis 1987, 8, 93-99.

Gatlin, C. L., Kleemann, G. R., Hays, L. G., Link, A. J., Yates, J. R., 3rd, Protein identification at the low femtomole level from silver-stained gels using a new fritless electrospray interface for liquid chromatography-microspray and nanospray mass spectrometry. Anal. Biochem. 1998, 263, 93-101.

Wayne, L. G., Synchronized replication of Mycobacterium tuberculosis. Infect. Immun. 1977, 17, 528-530.

Archuleta, R. J., Yvonne Hoppes, P., Primm, T. P., Mycobacterium avium enters a state of metabolic dormancy in response to starvation. Tuberculosis (Edinb) 2005, 85, 147-158.

Reddacliff, L. A., Nicholls, P. J., Vadali, A., Whittington, R. J., Use of growth indices from radiometric culture for quantification of sheep strains of Mycobacterium avium subsp. paratuberculosis. Appl. Environ. Microbiol. 2003, 69, 3510-3516.

Betts, J. C., Lukey, P. T., Robb, L. C., McAdam, R. A., Duncan, K., Evaluation of a nutrient starvation model of Mycobacterium tuberculosis persistence by gene and protein expression profiling. Mol. Microbiol. 2002, 43, 717-731.

Tabira, Y., Ohara, N., Ohara, N., Kitaura, H., et al., The 16-kDa alpha-crystallin-like protein of Mycobacterium bovis BCG is produced under conditions of oxygen deficiency and is associated with ribosomes. Res. Microbiol. 1998, 149, 255-264.

Gupta, S., Pandit, S. B., Srinivasan, N., Chatterji, D., Proteomics analysis of carbon-starved Mycobacterium smegmatis: induction of Dps-like protein. Protein Eng. 2002, 15, 503-512.

Dosanjh, N. S., Rawat, M., Chung, J. H., Av-Gay, Y., Thiol specific oxidative stress response in Mycobacteria. FEMS Microbiol. Lett. 2005, 249, 87-94.

Trujillo, M., Mauri, P., Benazzi, L., Comini, M., et al., The mycobacterial thioredoxin peroxidase can act as a one-cysteine-peroxiredoxin. J. Biol. Chem. 2006, 281, 20555-20566.

Tartaglia, L. A., Storz, G., Ames, B. N., Identification and molecular analysis of oxyR-regulated promoters important for the bacterial adaptation to oxidative stress. J. Mol. Biol. 1989, 210, 709-719.

Olsen, I., Reitan, L. J., Holstad, G., Wiker, H. G., Alkyl hydroperoxide reductases C and D are major antigens constitutively expressed by Mycobacterium avium subsp. paratuberculosis. Infect. Immun. 2000, 68, 801-808.

Marchler-Bauer, A., Anderson, J. B., Cherukuri, P. F., DeWeese-Scott, C., et al., CDD: a Conserved Domain Database for protein classification. Nucleic Acids Res. 2005, 33, D192-196.

Cunin, R., Glansdorff, N., Pierard, A., Stalon, V., Biosynthesis and metabolism of arginine in bacteria. Microbiol. Rev. 1986, 50, 314-352.

Pavelka, M. S., Jr., Jacobs, W. R., Jr., Biosynthesis of diaminopimelate, the precursor of lysine and a component of peptidoglycan, is an essential function of Mycobacterium smegmatis. J. Bacteriol. 1996, 178, 6496-6507.

Agnihotri, G., Liu, H. W., Enoyl-CoA hydratase reaction, mechanism, and inhibition. Bioorg. Med. Chem. 2003, 11, 9-20.

Campbell, J. W., Cronan, J. E., Jr., Bacterial fatty acid biosynthesis: targets for antibacterial drug discovery. Annu. Rev. Microbiol. 2001, 55, 305-332.

Yang, J. K., Yoon, H. J., Ahn, H. J., Lee, B. I., et al., Crystallization and preliminary X-ray crystallographic analysis of the Rv2002 gene product from Mycobacterium tuberculosis, a beta-ketoacyl carrier protein reductase homologue. Acta Crystallogr. D. Biol. Crystallogr. 2002, 58, 303-305.

Patel, M. P., Liu, W. S., West, J., Tew, D., et al., Kinetic and chemical mechanisms of the fabG-encoded Streptococcus pneumoniae beta-ketoacyl-ACP reductase. Biochemistry 2005, 44, 16753-16765.

Deckers-Hebestreit, G., Altendorf, K., The F0F1-type ATP synthases of bacteria: structure and function of the F0 complex. Annu. Rev. Microbiol. 1996, 50, 791-824.

Firestine, S. M., Poon, S. W., Mueller, E. J., Stubbe, J., Davisson, V. J., Reactions catalyzed by 5-aminoimidazole ribonucleotide carboxylases from Escherichia coli and Gallus gallus: a case for divergent catalytic mechanisms. Biochemistry 1994, 33, 11927-11934.

Goff, S. A., Goldberg, A. L., Production of abnormal proteins in E. coli stimulates transcription of lon and other heat shock genes. Cell 1985, 41, 587-595.

Lee, C., Schwartz, M. P., Prakash, S., Iwakura, M., Matouschek, A., ATP-dependent proteases degrade their substrates by processively unraveling them from the degradation signal. Mol. Cell. 2001, 7, 627-637.

Jackson, M., Crick, D. C., Brennan, P. J., Phosphatidylinositol is an essential phospholipid of mycobacteria. J. Biol. Chem. 2000, 275, 30092-30099.

Borukhov, S., Sagitov, V., Goldfarb, A., Transcript cleavage factors from E. coli. Cell 1993, 72, 459-466.

Voskuil, M. I., Visconti, K. C., Schoolnik, G. K., Mycobacterium tuberculosis gene expression during adaptation to stationary phase and low-oxygen dormancy. Tuberculosis (Edinb) 2004, 84, 218-227.

Locht, C., Hougardy, J. M., Rouanet, C., Place, S., Mascart, F., Heparin-binding hemagglutinin, from an extrapulmonary dissemination factor to a powerful diagnostic and protective antigen against tuberculosis. Tuberculosis (Edinb) 2006, 86, 303-309.

Sechi, L. A., Ahmed, N., Felis, G. E., Dupre, I., et al., Immunogenicity and cytoadherence of recombinant heparin binding haemagglutinin (HBHA) of Mycobacterium avium subsp. paratuberculosis: functional promiscuity or a role in virulence? Vaccine 2006, 24, 236-243.

Seraphin, B., The HIT protein family: a new family of proteins present in prokaryotes, yeast and mammals. DNA Seq. 1992, 3, 177-179.

McLennan, A. G., Dinucleoside polyphosphates-friend or foe? Pharmacol. Ther. 2000, 87, 73-89.

Brenner, C., Hint, Fhit, and GalT: function, structure, evolution, and mechanism of three branches of the histidine triad superfamily of nucleotide hydrolases and transferases. Biochemistry 2002, 41, 9003-9014.

Allgood, V. E., Oakley, R. H., Cidlowski, J. A., Modulation by vitamin B6 of glucocorticoid receptor-mediated gene expression requires transcription factors in addition to the glucocorticoid receptor. J. Biol. Chem. 1993, 268, 20870-20876.

Weldingh, K., Hansen, A., Jacobsen, S., Andersen, P., High resolution electroelution of polyacrylamide gels for the purification of single proteins from Mycobacterium tuberculosis culture filtrate. Scand. J. Immunol. 2000, 51, 79-86.

O'Toole, R., Williams, H. D., Universal stress proteins and Mycobacterium tuberculosis. Res. Microbiol. 2003, 154, 387-392.

Freestone, P., Nystrom, T., Trinei, M., Norris, V., The universal stress protein, UspA, of Escherichia coli is phosphorylated in response to stasis. J. Mol. Biol. 1997, 274, 318-324.

Diez, A., Gustavsson, N., Nystrom, T., The universal stress protein A of Escherichia coli is required for resistance to DNA damaging agents and is regulated by a RecA/FtsK-dependent regulatory pathway. Mol. Microbiol. 2000, 36, 1494-1503.

Kvint, K., Hosbond, C., Farewell, A., Nybroe, O., Nystrom, T., Emergency derepression: stringency allows RNA polymerase to override negative control by an active repressor. Mol. Microbiol. 2000, 35, 435-443.

Gustavsson, N., Diez, A., Nystrom, T., The universal stress protein paralogues of Escherichia coli are co-ordinately regulated and co-operate in the defence against DNA damage. Mol. Microbiol. 2002, 43, 107-117.

Nachin, L., Nannmark, U., Nystrom, T., Differential roles of the universal stress proteins of Escherichia coli in oxidative stress resistance, adhesion, and motility. J. Bacteriol. 2005, 187, 6265-6272.

Dziejman, M., Mekalanos, J. J., in: Hoch, J. A., Silhavy, T. J. (Eds.), Two-component signal transduction, American Society for Microbiology, Washington DC 1995, pp. 305-317.

Kozliak, E. I., Fuchs, J. A., Guilloton, M. B., Anderson, P. M., Role of bicarbonate/CO2 in the inhibition of Escherichia coli growth by cyanate. J. Bacteriol. 1995, 177, 3213-3219.

Anderson, P. M., Sung, Y. C., Fuchs, J. A., The cyanase operon and cyanate metabolism. FEMS Microbiol. Rev. 1990, 7, 247-252.

Chen, J., Brevet, A., Fromant, M., Leveque, F., et al., Pyrophosphatase is essential for growth of Escherichia coli. J. Bacteriol. 1990, 172, 5686-5689.

Abu Kwaik, Y., Induced expression of the Legionella pneumophila gene encoding a 20-kilodalton protein during intracellular infection. Infect. Immun. 1998, 66, 203-212.

Lahti, R., Microbial inorganic pyrophosphatases. Microbiol. Rev. 1983, 47, 169-178.

Mushegian, A. R., Koonin, E. V., A minimal gene set for cellular life derived by comparison of complete bacterial genomes. Proc. Natl. Acad. Sci. USA 1996, 93, 10268-10273.

Hermans, P. W., Abebe, F., Kuteyi, V. I., Kolk, A. H., et al., Molecular and immunological characterization of the highly conserved antigen 84 from Mycobacterium tuberculosis and Mycobacterium leprae. Infect. Immun. 1995, 63, 954-960.

Kang, C. M., Abbott, D. W., Park, S. T., Dascher, C. C., et al., The Mycobacterium tuberculosis serine/threonine kinases PknA and PknB: substrate identification and regulation of cell shape. Genes Dev. 2005, 19, 1692-1704.

Starck, J., Kallenius, G., Marklund, B. I., Andersson, D. I., Akerlund, T., Comparative proteome analysis of Mycobacterium tuberculosis grown under aerobic and anaerobic conditions. Microbiology 2004, 150, 3821-3829.

Park, H. D., Guinn, K. M., Harrell, M. I., Liao, R., et al., Rv3133c/dosR is a transcription factor that mediates the hypoxic response of Mycobacterium tuberculosis. Mol. Microbiol. 2003, 48, 833-843.

Sherman, D. R., Voskuil, M., Schnappinger, D., Liao, R., et al., Regulation of the Mycobacterium tuberculosis hypoxic response gene encoding alpha-crystallin. Proc. Natl. Acad. Sci. USA 2001, 98, 7534-7539.

Dohmann, K., Strommenger, B., Stevenson, K., De Juan, L., et al., Characterization of Genetic Differences between Mycobacterium avium subsp. paratuberculosis Type I and Type II Isolates. J. Clin. Microbiol. 2003, 41, 5215-5223.

Marsh, I. B., Whittington, R. J., Genomic diversity in Mycobacterium avium: Single nucleotide polymorphisms between the S and C strains of M. avium subsp. paratuberculosis and with M. a. avium. Mol. Cell. Probes 2007, 21, 66-75.

Behr, M. A., Schroeder, B. G., Brinkman, J. N., Slayden, R. A., Barry, C. E., 3rd, A point mutation in the mma3 gene is responsible for impaired methoxymycolic acid production in Mycobacterium bovis BCG strains obtained after 1927. J. Bacteriol. 2000, 182, 3394-3399.

Table 1 Summary of the proteome of *M. paratuberculosis* according to expression level in hypoxia and nutrient starvation treatment groups and their controls

Treatment	**Strain**	**N_1** [a]	**N_2** [b]	**N** [c]	**P_1** [d]	**P_2** [e]	**C** [f]	**E** [g]	**T** [h]	**Total proteins resolved**
Hypoxia	S	12	1	13	7		1	1		1650
	C	5	5	10	5		0	0		1185
Starvation	S	4	7	11	5		7	7		1623
	C	7	3	10	5		3	3		1095
Total		28	16	44	22	7	11	11	66	

[a] Number of spots present only in treatment
[b] Number of spots present in control but up-regulated in treatment
[c] Total number of spots up-regulated in treatment
[d] Number of proteins upregulated in only one treatment; refer table 2
[e] Number of proteins upregulated in both treatments refer table 2
[f] Number of spots present in control but down-regulated in treatment
[g] Spots with erroneous identification or artifact
[h] Total number of differentially expressed protein spots (N+C+E)

Table 2 Clustering of *M. paratuberculosis* differentially expressed proteins based on their biological functional categories following hypoxia and starvation stress

Protein Category	Figure	Spot No.	Gene/Locus tag [a]	Protein description	Interpro Scan Family/Function	Hypoxia S [c]	Starvation S [c]	Hypoxia C [c]	Starvation C [c]
Antioxidant enzymes									
	6	5	*ahpC*, MAP1589c	AhpC	Antioxidant enzymes and defense against sulphur containing radicals				*
	6	9	*trxC*, MAP4340	TrxC	Electron carrier activity and protein disulphide oxidoreductase activity				4.353
	5, 6	3, 8	*tpx*, MAP1653	Putative thiol peroxidase	-ditto-			*	*
	5	4	*ahpD*, MAP1588c	AhpD	Aromatic compound metabolism, AhpD for peroxidase activity			*	
Amino acid metabolism									
	6	5	*argC*, MAP1361	N-acetyl gamma glutamyl phosphate reductase	Arginine metabolism		↓		
	6	6	*dapA*,MAP2864c	Dihydrodipicolinate synthase	Key enzyme in lysine biosynthesis		↓		
	4	1	*hisA* ,MAP1297	1-(5-phosphoribosyl)-5-[(5-phosphoribosylamino) methylideneamino] imidazole-4-carboxamide isomerase	Enzymes that use FMN as a cofactor, Histidine biosynthesis	*			
	6	4	*hisG*, MAP1846c	ATP phosphoribosyl transferase	Histidine biosynthesis		3.807		
	6	17	*hisI*, MAP1300 MT1641.1 [b]	Phosphoribosyl AMP cyclohydrolase *M. tuberculosis*	-ditto-		↓		

Protein Category	Figure	Spot No.	Gene/Locus tag [a]	Protein description	Interpro Scan Family/Function	Hypoxia S [c]	Starvation S [c]	Hypoxia C [c]	Starvation C [c]
Fatty acid metabolism									
	6	3	*echA20*, MAP0516c	Enoyl-CoA hydratase	Fatty acid metabolism				- 2.482
	6	2	*fabG*, MAP2872c	3-ketoacyl- reductase	Oxidoreductase activity fatty acid biosynthesis				- 1.289
	6	4	MAP0508	Short chain dehydrogenase	-ditto-				↓
ATP and Purine biosynthesis									
	4, 6	8, 14	*atpC*, MAP2450c	ATP synthase subunit epsilon	membrane bound enzyme complexes involved in ATP synthesis coupled proton transport	*	3.652		
	5	6	*purE*, MAP3393c	Phosphoribosyl aminoimidazole carboxylase catalytic subunit	'de novo' IMP biosynthesis			3.488	
Proteolysis									
	4, 6, 6	4-5, 9, 6	*clpP*, MAP2281c, MAP2280c	ATP dependant Clp protease proteolytic subunit	Proteolysis	*	*		*
	6	3	*prcA,* MAP1834c	PrcA	Proteasome subunits, protein degradation		30.986		
Cell wall synthesis									
	6	1	*cysQ_2*, MAP2058c	CysQ_2	Enhance the synthesis or degradation of phosphorylated				*

Protein Category	Figure	Spot No.	Gene/Locus tag [a]	Protein description	Interpro Scan Family/Function	Hypoxia S [c]	Starvation S [c]	Hypoxia C [c]	Starvation C [c]
					messenger molecules				
Protein synthesis									
	4	10	*greA* [b]	Probable transcription elongation factor G *(M avium*)	Necessary for efficient RNA polymerase transcription past template encoded arresting sites	*			
	6	8	*rplJ*, MAP4125	50s ribosomal protein L10	Protein synthesis		↓		
Signal recognition									
	4	9	*Hbha,* MAP3968	Heparin binding haemagglutinin adhesin like protein	Signal recognistion particle protein, RNA binding and GTP binding	*			
Hypothetical proteins with putative function									
Tumor suppressors									
	6, 5, 6	16, 9, 11	MAP0593c	Hypothetical protein MAP0593c	Histidine triad protein, diadenosine polyphospahte hydrolases and function as tumor suppressors in human and mice		*****	3.328	*
Cellular processes									
	6	7	MAP0711c	Hypothetical protein MAP0711	Oxidoreductase activity		↓		
	6	1	MAP3007	Hypothetical protein MAP3007	-ditto-		↓		
	5	7	MAP1560	Hypothetical protein MAP1560	Catalytic activity with thioesterases			*	
	6	15	MAP2411	Hypothetical protein MAP2411	Electron transfer pathway at low redox potential		5.727		

Protein Category	Figure	Spot No.	Gene/Locus tag [a]	Protein description	Interpro Scan Family/Function	Hypoxia S [c]	Starvation S [c]	Hypoxia C [c]	Starvation C [c]
	4	12	MAP2705c	Hypothetical protein MAP2705c	Nuclear tansport of cargo protein, Steroid delata isomerase catlyzes isomerisation of unsaturated ketosteroids	2.89			
	6	12	MAP1885c	Hypothetical protein MAP1885c	Regulation of protein phosphorylation by kinases, lipid binding		*		
Universal stress proteins									
	5, 6	10, 12-13	MAP1339	Hypothetical protein MAP1339	Universal stress protein, Response to stress, Trancriptional induction of UspA gene of *E coli* occurs during growth arrest conditions.			*	*
Two component response regulators									
	4	2	MAP0834c	Hypothetical protein MAP0834c	Two component response regulator activity and respond to environmental changes	*			
	5	8	MAP3200	Hypothetical protein MAP3200	-ditto-			*	
Hypothetical proteins with unknown function									
	4, 6	14, 18	MAP1586	Hypothetical protein MAP1586	Unknown	↓	↓		
	5	7	MAP3864	hypothetical protein MAP3864	-ditto-				4.125
	4	13	MAP1076	Hypothetical protein MAP1076	-ditto-	*			

Protein Category	Figure	Spot No.	Gene/Locus tag [a]	Protein description	Interpro Scan Family/Function	Hypoxia S [c]	Starvation S [c]	Hypoxia C [c]	Starvation C [c]
	4	3	MAP0643c	Hypothetical protein MAP0643c	-ditto-	*			
	4, 6	11, 13	MAP4107	Hypothetical protein MAP4107	-ditto-	*	*		
Cyanate hydrolysis									
	6	10	MAP4098	Cyanate hydratase	Bacteria can overcome the toxicity of environmental cyanate by hydrolysis of cyanate				3.589
Phosphate metabolism									
	4, 6, 5	6-7, 10-11, 1-2	*ppa*, MAP0435c, MT3730 [b]	Inorganic pyrophosphatase	Phosphate metabolism, magnesium ion binding	*	8.272-18.441	1.762-2.388	
Cell division									
	5	5	*ssb*, MAP0068	Single strand DNA binding protein	DNA replication, recombination and repair			2.388	
	6	2	*wag31*, MAP1889c	Wag31	DivIVA		4.579		

[a] Locus tags are from the NCBInr database (http://www.ncbi.nlm.nih.gov/entrez/query.fcgi?db=Protein&itool=toolbar) except where shown [b] in which case homologues in *M. paratuberculosis* were identified after finding the homologue in another *Mycobacterium* spp.
[c] Columns show pattern or ratios which represent relative protein abundance between treatment and control. Asterisks (*) represent unique proteins that were not identified in control samples, ↓ indicates downregulation where the spot was not identified in treatment.

Addendum

Table 3a Differentially expressed protein profiles of the S strain after 1- 4 weeks of hypoxic stress

Spot No. [a]	Accession No. [b]	Gene/Locus tag [b]	Mass (kDa)	pI [d]	M.S.D [e]	Ratio [f]	No. of matched Peptides	Score [g]	Sequence coverage (%)	Tuberculist Synonym [h]
1	41407395	*hisA*, MAP1297	25.3	4.53	-	*	1	51	4.1	*hisA,* Rv1603
2	41406932	MAP0834c	24.9	4.81	-	*	1	57	4.3	Rv0903c, *prrA*
3	41406741	MAP0643c	25.3	5.21	-	*	1	72	5.1	-
4,5	41408379	*clpP*, MAP2281c	21.6	4.62	-	*	4	224	25.1	Rv2460c
6,7	41406533	*ppa*, MAP0435c	18.6	4.59	-	*	5	188	39.5	Rv3628
8	41408548	*atpC*, MAP2450c	13.1	4.23	-	*	7	327	69.4	Rv1311
9	33327135	*Hbha*, MAP3968	20.7	7.11	-	*	1	51	7.9	Rv0475, *hbhA*
10	48928144	*greA*, MAP1027c [c]	17.8	4.66	-	*	3	110	24.4	Rv1080c, *greA*
11	41410205	MAP4107	17.7	4.56	-	*	4	130	31.1	-
12	41408803	MAP2705c	13.9	4.59	0.050	2.89	3	116	31.5	-
13	41407174	MAP1076	14.4	5.17	-	*	1	51	9.8	-
14	41407684	MAP1586	16.9	7.1	-	↓	2	117	15.2	-
15	136429	Trypsin precursor	-	-	-	-	2	104	10.0	-

[a] Spot numbers are identical to those in Figs. 4.
[b] Accession number and locus tags are from NCBInr database (http://www.ncbi.nlm.nih.gov/entrez/query.fcgi?db=Protein&itool=toolbar)) except where shown [c] in which case homologues in *M. paratuberculosis* were identified after finding the homologue in another *Mycobacterium* spp.
[d] Theoretical isoelectric point (pI) of matching protein was calculated by Biomanager (http://www.angis.org.au/)
[e] Mean squared deviation was calculated by ImageMaster 2D Platinum software
[f] Ratios represent relative protein abundance between treatment and control. Asterisks (*) represent unique proteins that were not identified in control samples, ↓ indicates downregulation where the spot was not identified in the treatment
[g] Protein score assigned by the MASCOT program, protein score > 50 are significant (p<0.05). All the identified peptides carry 2+ charge state
[h] Homologues in *M. tuberculosis* were identified by H37Rv genome sequence database (http://genolist.pasteur.fr/Tuberculist/)

Table 3b Differentially expressed protein profiles of the C strain after 1- 4 weeks of hypoxic stress

Spot No. [a]	Accession No. [b]	Gene/Locus tag [b]	Mass (kDa)	pI [d]	M.S.D [e]	Ratio [f]	No. of matched Peptides	Score [g]	Sequence coverage (%)	Tuberculist Synonym [h]
1	41406533	*ppa*, MAP0435c	18.6	4.59	0.018	1.762	3	122	32.1	Rv3628
2	41406533	*ppa*, MAP0435c	18.6	4.59	0.028	2.388	3	110	32.1	Rv3628
3	73698151	*tpx*, MAP1653	16.4	4.24	-	*	1	52	9.4	*Tpx, cfp20*, Rv1932
4	41407686	*ahpD*, MAP1588c	18.8	4.79	-	*	1	51	5.6	Rv2429
5	41406166	*ssb*, MAP0068	17.5	4.94	0.028	2.388	3	186	23.2	Rv0054
6	41409491	*purE*, MAP3393c	17.5	5.68	0.029	3.488	3	93	30.1	Rv3275c
7	41407658	MAP1560	15.2	4.94	-	*	2	59	14.3	-
8	41409298	MAP3200	14.7	5.67	-	*	1	54	10.2	Rv3143
9	41406691	MAP0593c	14.8	5.25	0.088	3.328	3	64	39.6	Rv0759c
10	41407437	MAP1339	15.4	6.12	-	*	4	132	34.0	-

[a] Spot numbers are identical to those in Figs. 5
[b] Accession number and locus tags are from NCBInr database (http://www.ncbi.nlm.nih.gov/entrez/query.fcgi?db=Protein&itool=toolbar)) except where shown [c] in which case homologues in *M. paratuberculosis* were identified after finding the homologue in another *Mycobacterium* spp.
[d] Theoretical isoelectric point (pI) of matching protein was calculated by Biomanager (http://www.angis.org.au/)
[e] Mean squared deviation was calculated by ImageMaster 2D Platinum software
[f] Ratios represent relative protein abundance between treatment and control. Asterisks (*) represent unique proteins that were not identified in control samples, ↓ indicates downregulation where the spot was not identified in the treatment
[g] Protein score assigned by the MASCOT program, protein score > 50 are significant (p<0.05). All the identified peptides carry 2+ charge state
[h] Homologues in *M. tuberculosis* were identified by H37Rv genome sequence database (http://genolist.pasteur.fr/Tuberculist/)

Table 4a Differentially expressed protein profiles of the S strain after 8 weeks of starvation

Spot No. [a]	Accession No. [b]	Gene/Locus tag [b]	Mass (kDa)	pI [d]	M.S.D [e]	Ratio [f]	No. of Peptides matched	Score [g]	Sequence coverage (%)	Tuberculist Synonym [h]
1	41409105	MAP3007	29.9	4.37	-	↓	8	372	40.9	Rv2971
2	41407987	*wag31*, MAP1889c	28	4.45	0.190	4.579	11	625	67.3	Rv2145c, *ag84*
3	41407932	*prcA,* MAP1834c	27.9	5.16	0.050	30.986	2	69	9.8	Rv2109c, *prcA*
4	41407944	*hisG*, MAP1846c	30.5	4.67	0.038	3.807	3	140	14.1	Rv2121c, *hisG*
5	41407459	*argC*, MAP1361	35.2	6.28	-	↓	5	235	20.7	Rv1652, *argC*
6	41408962	*dapA*,MAP2864c	30.9	5.62	-	↓	5	249	25.0	Rv2753c, *dapA*
7	41406809	MAP0711c	29.8	5.74	-	↓	4	206	20.6	-
8	41410223	*rplJ*, MAP4125	20.1	5.08	-	↓	6	278	42.3	Rv0651, *rplJ*
9	41408379	*clpP*, MAP2281c	21.6	4.62	-	*	2	82	13.6	Rv2460c
10	13883596	*ppa*, MAP0435c MT3730 [c]	18.3	4.58	0.005	8.272	3	116	25.3	-
11	13883596	*ppa*, MAP0435c MT3730 [c]	18.3	4.58	0.067	18.441	3	165	25.3	-
12	41407983	MAP1885c	18.4	4.73	-	*	2	55	15.9	Rv2140c, *TB18.6*
13	41410205	MAP4107	17.7	4.56	-	*	3	119	28.3	-
14	41408548	*atpC*, MAP2450c	13.1	4.23	0.068	3.652	4	145	45.5	Rv1311
15	41408509	MAP2411	15.5	4.63	0.021	5.727	5	172	40.8	-
16	41406691	MAP0593c	14.8	5.25	-	*	2	58	29.9	Rv0759c
17	13881271	*hisI*, MAP1300, MT1641.1[c]	12.4	5.15	-	↓	2	62	21.7	Rv1606
18	41407684	MAP1586	16.9	7.1	-	↓	2	117	15.2	-
19-25	136429	Trypsin precursor	-	-	-	-	2	102	10.0	-

[a] Spot numbers are identical to those in Fig 6
[b] Accession number and locus tags are from NCBInr database (http://www.ncbi.nlm.nih.gov/entrez/query.fcgi?db=Protein&itool=toolbar)) except where shown [c] in which case homologues in M. paratuberculosis were identified after finding the homologue in another Mycobacterium spp.
[d] Theoretical isoelectric point (pI) of matching protein was calculated by Biomanager (http://www.angis.org.au/)
[e] Mean squared deviation was calculated by ImageMaster 2D Platinum software
[f] Ratios represent relative protein abundance between treatment and control. Asterisks (*) represent unique proteins that were not identified in control samples, ↓ indicates downregulation where the spot was not identified in the treatment
[g] Protein score assigned by the MASCOT program, protein score > 50 are significant (p<0.05). All the identified peptides carry 2+ charge state
[h] Homologues in M. tuberculosis were identified by H37Rv genome sequence database (http://genolist.pasteur.fr/Tuberculist/)

Table 4b Differentially expressed protein profiles of C strain after 8 weeks of starvation

Spot No. [a]	Accession No. [b]	Gene/Locus tag [b]	Mass (kDa)	pI [d]	M.S.D [e]	Ratio [f]	No. of Peptides matched	Score [g]	Sequence coverage (%)	Tuberculist Synonym [h]
1	41408156	*cysQ_2*, MAP2058c	25.4	4.64	-	*	2	106	13.6	Rv2131c, *cysQ*
2	41408970	*fabG*, MAP2872c	26.7	5.94	0.018	- 1.289	6	290	29.7	Rv2766c
3	41406614	*echA20*, MAP0516c	26.8	5.91	0.038	- 2.482	13	527	96.0	Rv3550
4	41406606	MAP0508	27.5	5.82	-	↓	7	432	39.3	Rv3559c
5	41407687	*ahpC*, MAP1589c	21.6	4.32	-	*	7	406	54.9	Rv2428, *ahpC*
6	41408378	*clpP2*, MAP2280c	23.2	4.84	-	*	3	83	20.1	Rv2460c, *clpP2*
7	41409962	MAP3864	16.4	4.47	0.168	4.125	1	84	10.4	Rv0360c
8	73698151	*tpx*, MAP1653	16.4	4.24	-	*	3	171	29.9	-
9	41410438	*trxC*, MAP4340	12.4	4.56	0.179	4.353	2	60	19.7	*mpt46*, Rv3914, *trx*, *trxA*
10	41410196	MAP4098	18.7	5.8	0.147	3.589	1	53	8.8	-
11	41406691	MAP0593c	14.8	5.25	-	*	3	90	33.6	Rv0759c
12,13	41407437	MAP1339	15.4	6.12	-	*	3	83	31.3	-
14-16	136429	Trypsin precursor	-	-	-	-	2	120	10.0	-

[a] Spot numbers are identical to those in Fig 6
[b] Accession number and locus tags are from NCBInr database (http://www.ncbi.nlm.nih.gov/entrez/query.fcgi?db=Protein&itool=toolbar)) except where shown [c] in which case homologues in *M. paratuberculosis* were identified after finding the homologue in another *Mycobacterium* spp.
[d] Theoretical isoelectric point (pI) of matching protein was calculated by Biomanager (http://www.angis.org.au/)
[e] Mean squared deviation was calculated by ImageMaster 2D Platinum software
[f] Ratios represent relative protein abundance between treatment and control. Asterisks (*) represent unique proteins that were not identified in control samples, ↓ indicates downregulation where the spot was not identified in the treatment
[g] Protein score assigned by the MASCOT program, protein score > 50 are significant (p<0.05). All the identified peptides carry 2+ charge state
[h] Homologues in *M. tuberculosis* were identified by H37Rv genome sequence database (http://genolist.pasteur.fr/Tuberculist/)

Fig. 1 Daily Growth Index of the S (panels A and B) and C (panels C and D) strains in BACTEC culture vials following hypoxic stress for: (panels A, C) 7 days; (panels B, D) 28 days before return to an aerobic atmosphere. Culture vials were initially incubated for 1 week in air. The data for days 12-24 are not shown but were similar to day 11. The arrow indicates the time when samples were taken for proteomic analysis.
Fig. 2 Daily Growth Index of the S (panels A and B) and C (panels C and D) strains in BACTEC culture vials following hypoxic stress for: (panels A, C) 7 days; (panels B, D) 28 days before return to an aerobic atmosphere. The data for days 12-24 are not shown but were similar to day 11. The arrow indicates the time when samples were taken for proteomic analysis.

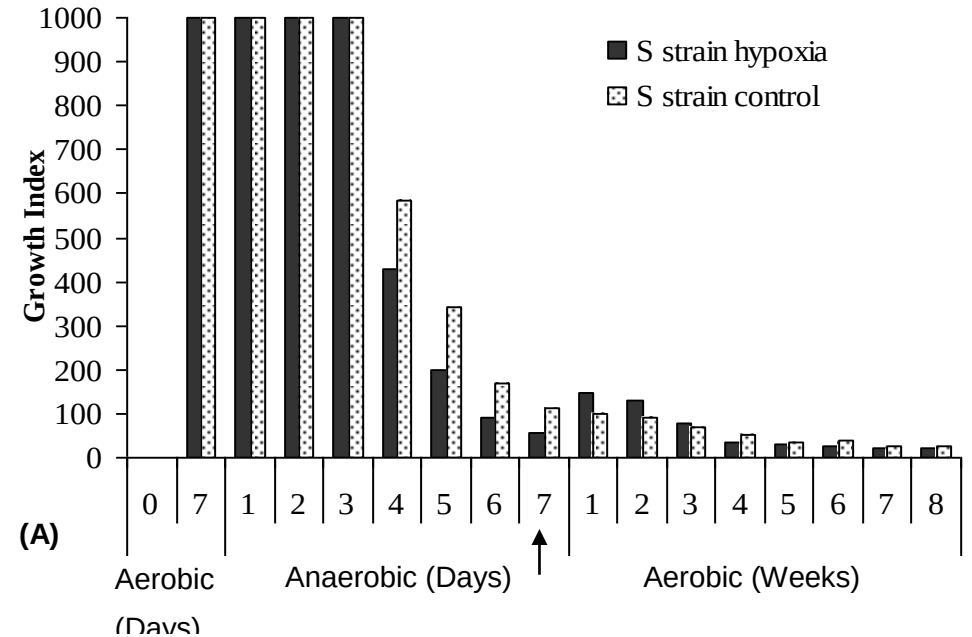
Growth Index
1000
900
800
700
600
500
400
300
200
100
0
S strain hypoxia
S strain control
0 7 1 2 3 4 5 6 7 1 2 3 4 5 6 7 8
(A)
Aerobic (Days)
Anaerobic (Days)
Aerobic (Weeks)

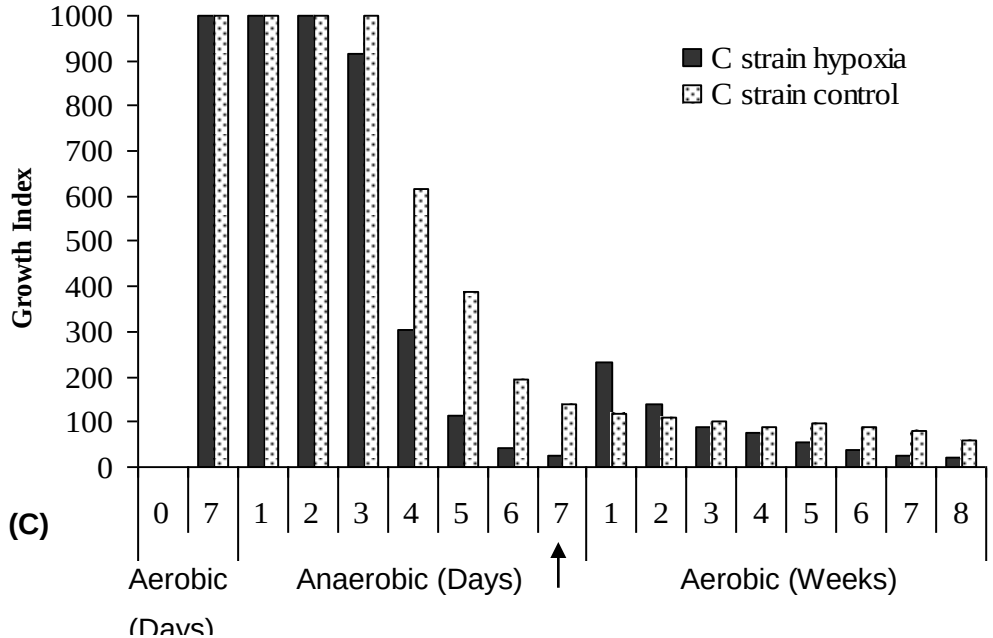
Growth Index
1000
900
800
700
600
500
400
300
200
100
0
C strain hypoxia
C strain control
0 7 1 2 3 4 5 6 7 1 2 3 4 5 6 7 8
(C)
Aerobic (Days)
Anaerobic (Days)
Aerobic (Weeks)

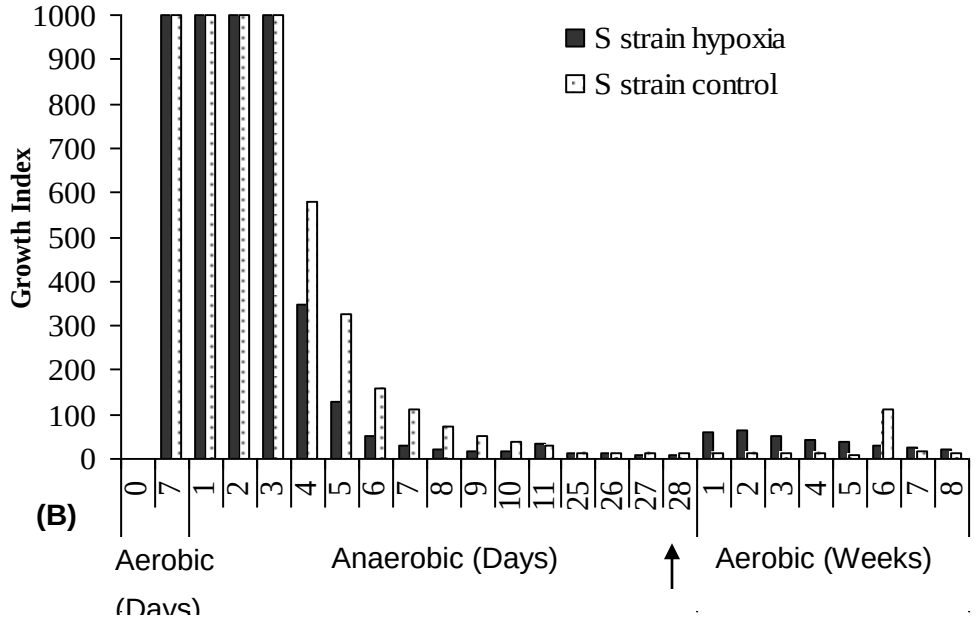
Growth Index
1000
900
800
700
600
500
400
300
200
100
0
S strain hypoxia
S strain control
0 7 1 2 3 4 5 6 7 8 9 10 11 25 26 27 28 1 2 3 4 5 6 7 8
(B)
Aerobic (Days)
Anaerobic (Days)
Aerobic (Weeks)

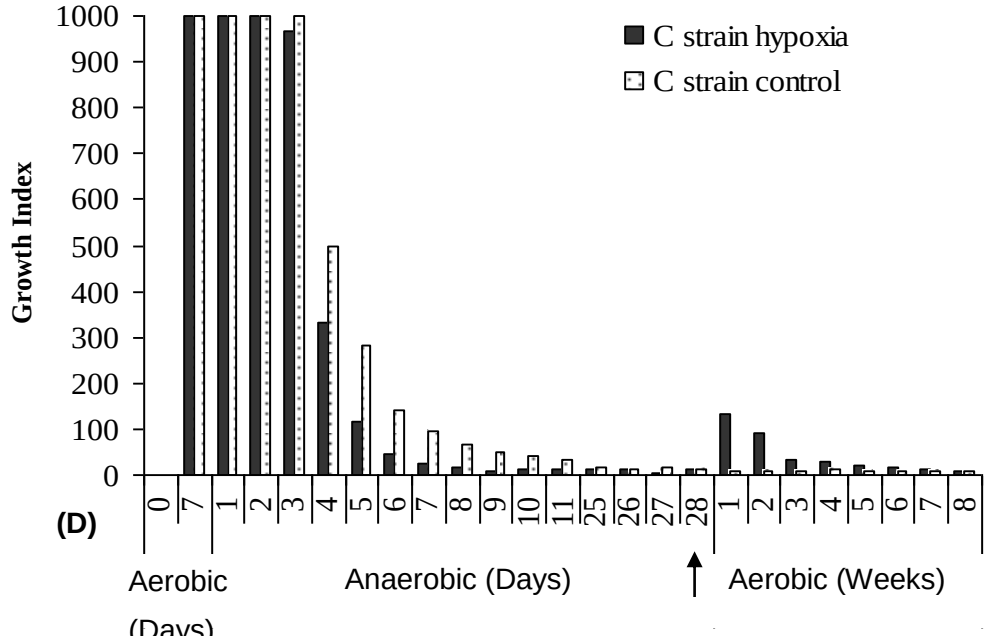
Growth Index
1000
900
800
700
600
500
400
300
200
100
0
C strain hypoxia
C strain control
0 7 1 2 3 4 5 6 7 8 9 10 11 25 26 27 28 1 2 3 4 5 6 7 8
(D)
Aerobic (Days)
Anaerobic (Days)
Aerobic (Weeks)

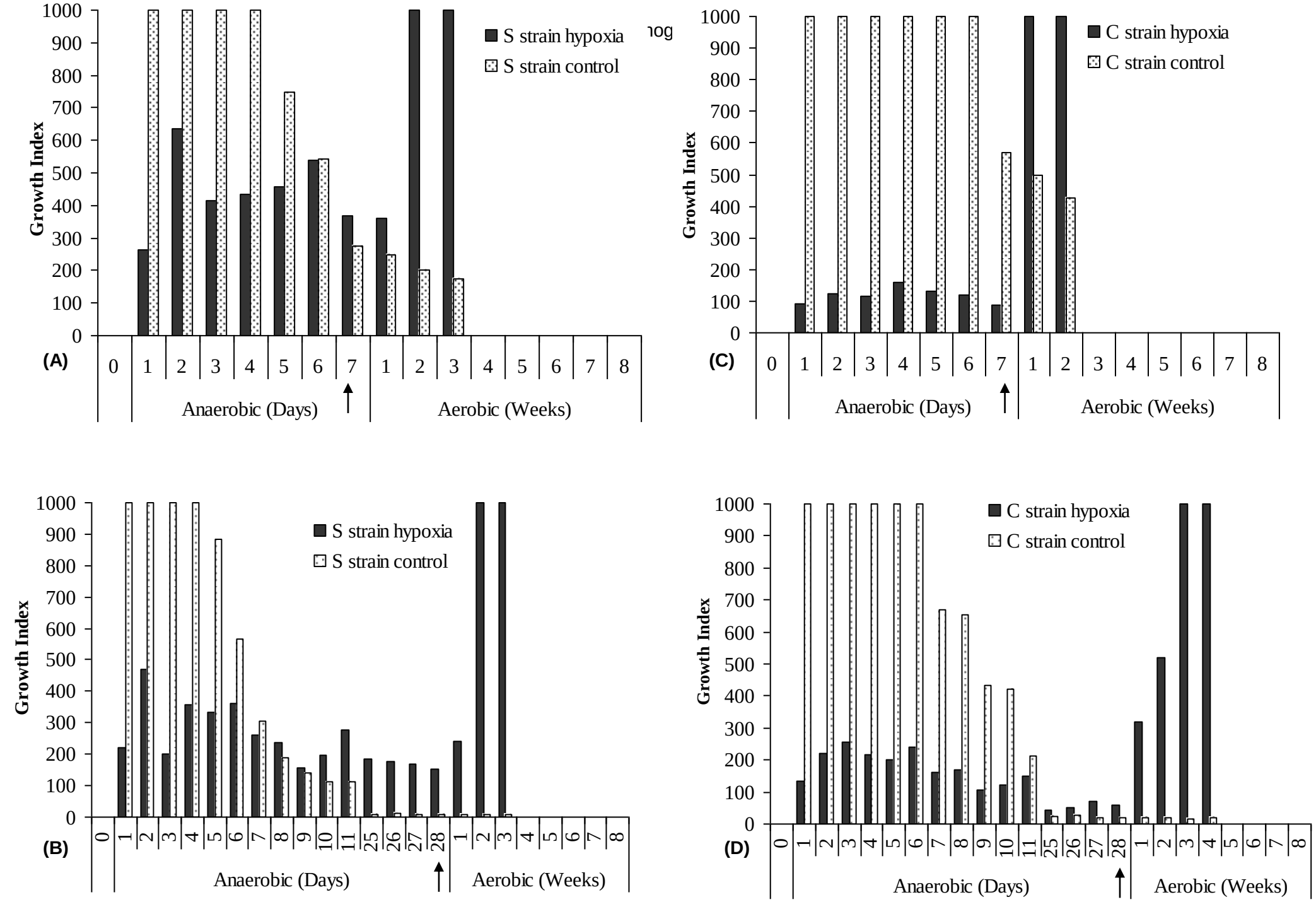
(A)
Growth Index
S strain hypoxia
S strain control
Anaerobic (Days)
Aerobic (Weeks)
(C)
C strain hypoxia
C strain control
(B)
(D)

Fig. 2

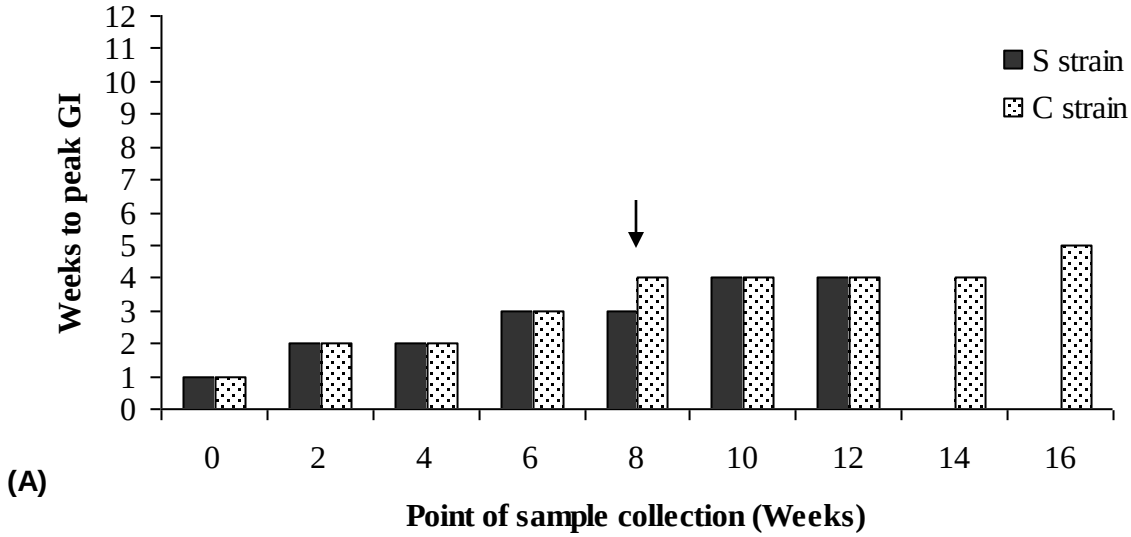

(A)

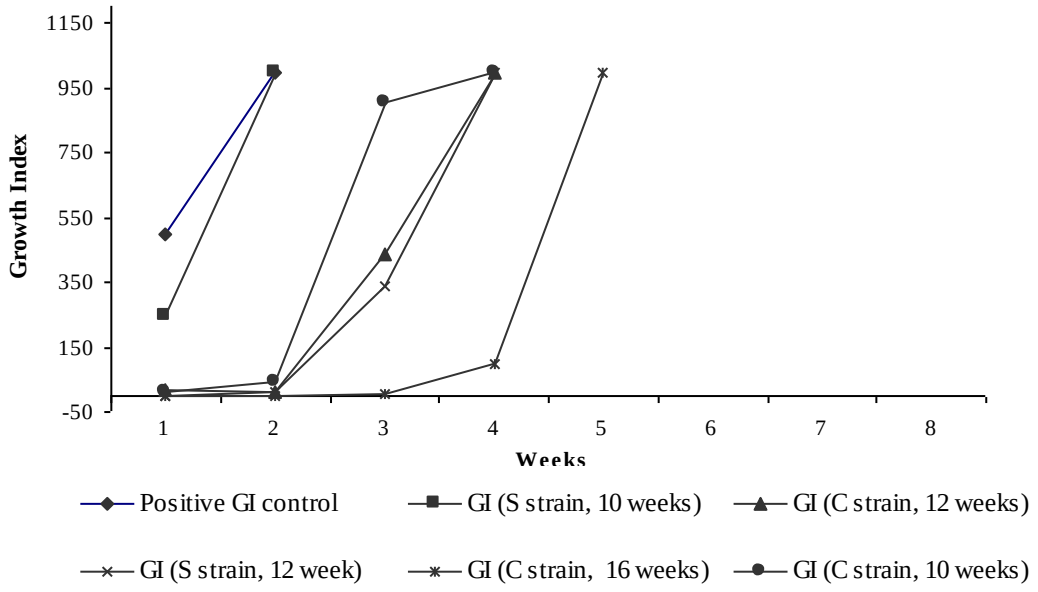

(B)

Fig. 3 (A) Rate of growth of *M. paratuberculosis* following inoculation of BACTEC culture media after nutrient starvation for up to 16 weeks. The arrow indicates the time when samples were taken for proteomic analysis. (B) Examples of growth curves following inoculation of BACTEC culture media after nutrient starvation for 0 weeks (control), 10, 12 or 16 weeks.

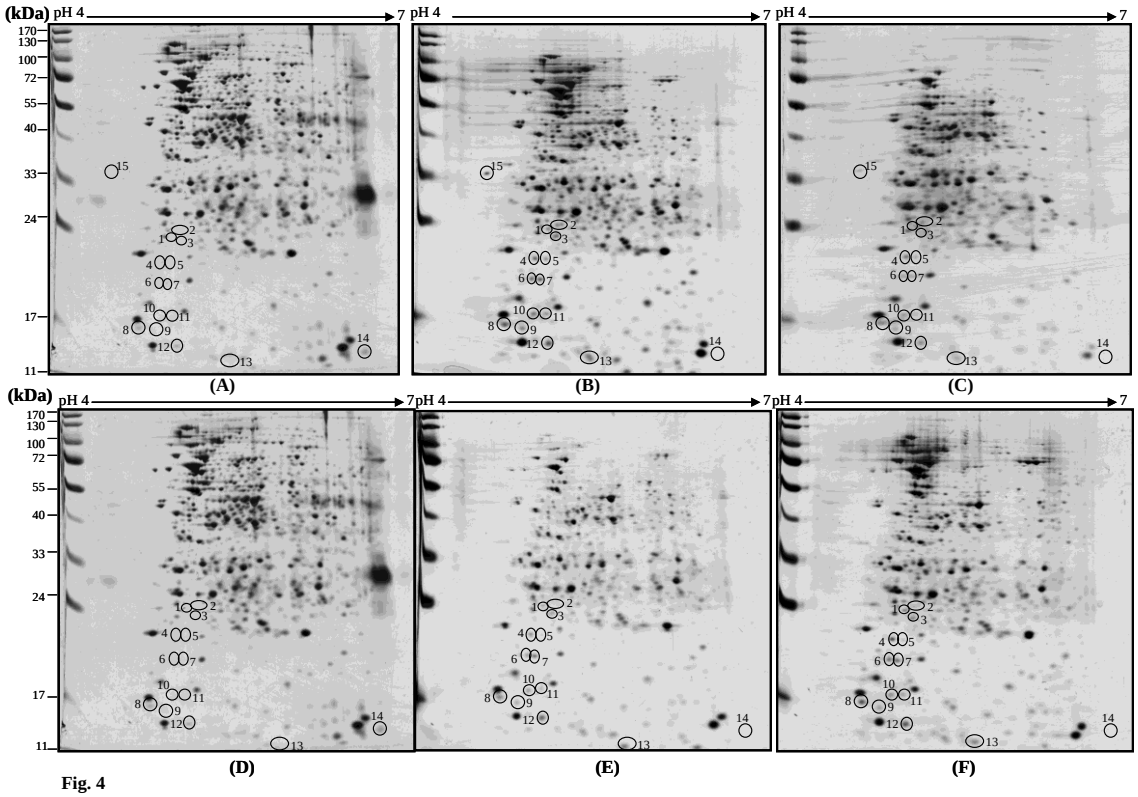

Fig. 4 Two dimension gel electrophoresis analysis of proteins of the S strain of *M. paratuberculosis* in two hypoxia experiments; (panels A-C) only anaerobic conditions; (panels D-F) anaerobic conditions after 1 week exposure to aerobic conditions. (panels A, D) control; (panels B, E) 1 week of hypoxic stress; (panels C, F) 4 weeks of hypoxic stress. Open circles represent protein spots with altered protein expression relative to the control (refer addendum table 3a and table 2). The figures on the left indicate molecular mass markers in kDa. Proteins were separated by isoelectric focusing on pH 4-7 IPG strips in the first dimension and 12% SDS-PAGE in the second dimension. Proteins were visualized by silver staining.

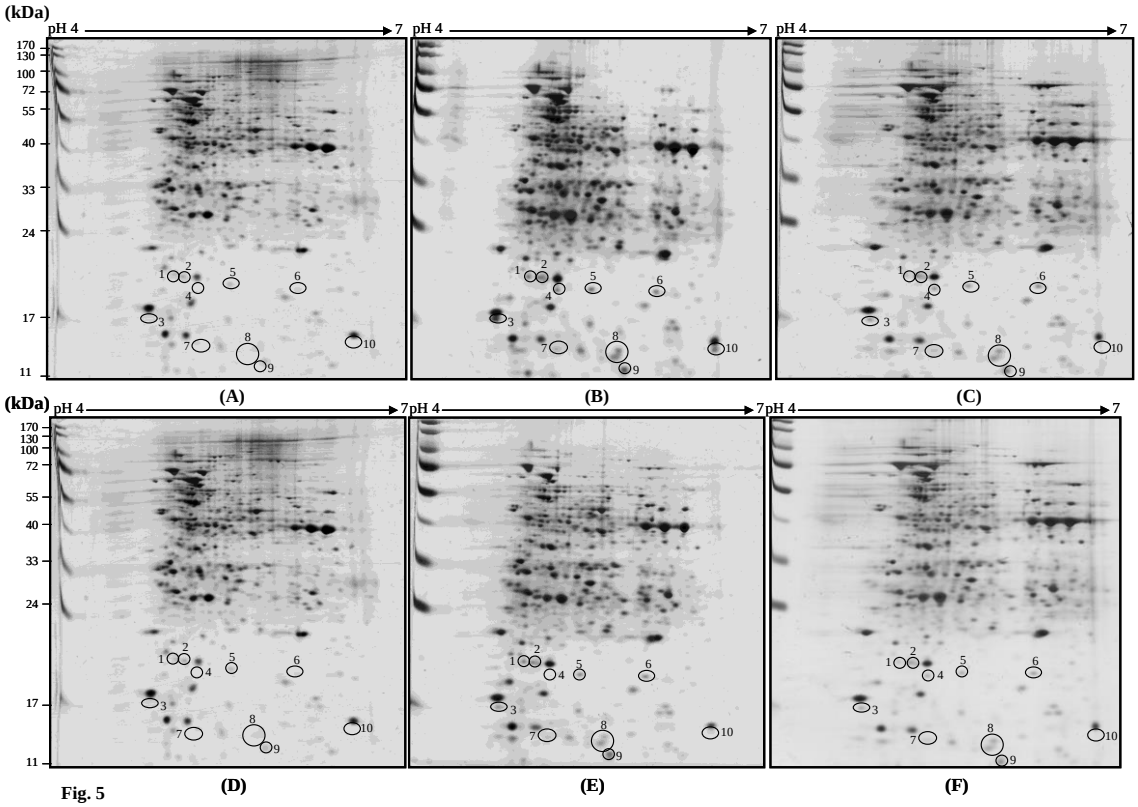

Fig. 5 Two dimension gel electrophoresis analysis of proteins of the C strain of *M. paratuberculosis* in two hypoxia experiments; (panels A-C) only anaerobic conditions; (panels D-F) anaerobic conditions after 1 week exposure to aerobic conditions. (panels A, D) control; (panels B, E) 1 week of hypoxic stress; (panels C, F) 4 weeks of hypoxic stress. Open circles represent protein spots with altered protein expression relative to the control (refer addendum table 3a and table 2). The figures on the left indicate molecular mass markers in kDa. Proteins were separated by isoelectric focusing on pH 4-7 IPG strips in the first dimension and 12% SDS-PAGE in the second dimension. Proteins were visualized by silver staining.

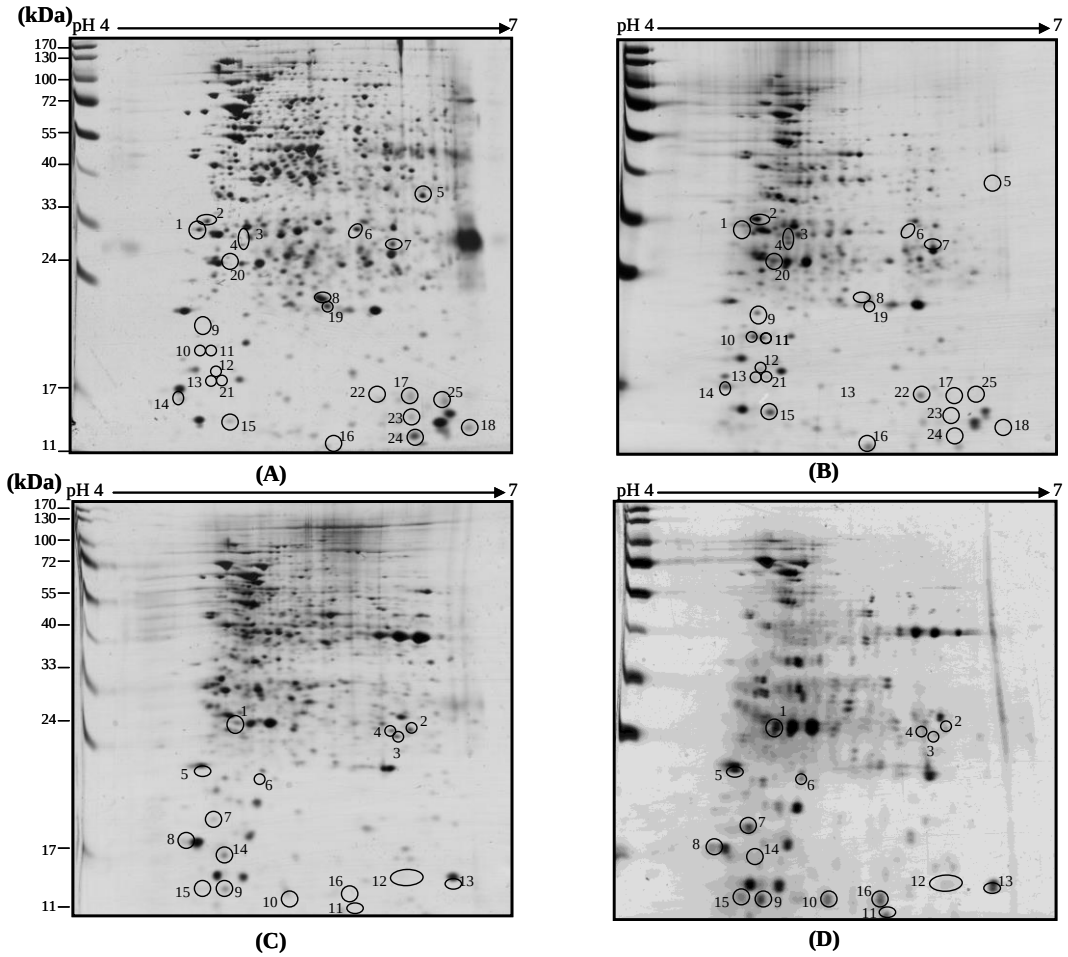

Fig. 6

Fig. 6 Two dimension gel electrophoresis analysis of proteins of the S and C strains of *M*. *paratuberculosis*. (panels A and C) S and C strain control; (panels B and D) S and C strain after 8 weeks of starvation. Open circles represent protein spots with altered protein expression (refer to addendum). The figures on the left indicate molecular mass markers in kDa. Proteins were separated by isoelectric focusing on pH 4-7 IPG strips in the first dimension and 12% SDS-PAGE in the second dimension. Proteins were visualized by silver staining.

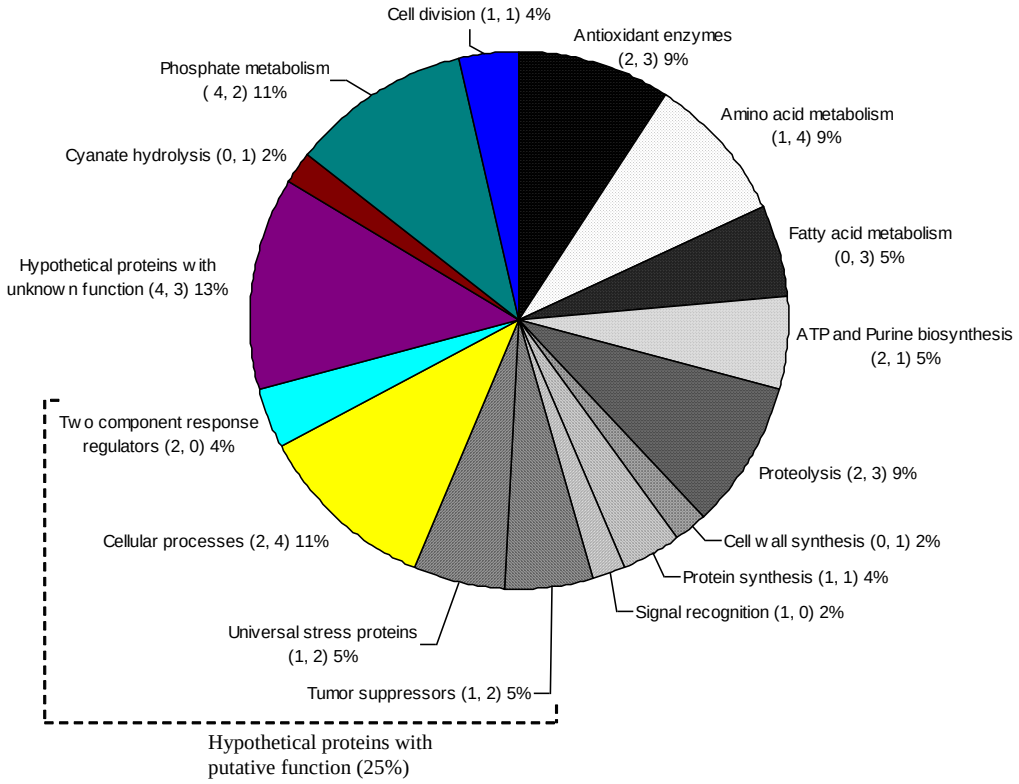

Fig. 7

Fig. 7 The distribution of functional classes based on global protein profiling of S and C strains of *M. paratuberculosis* during hypoxia and starvation. Figures in parentheses indicate number of protein spots for hypoxia and starvation, respectively. The relative abundance (%) of each class was calculated from a total of 55 protein spots (refer table 2).

9.17 Appendix 3A-5 Subprogram 3 Evaluation of the immunogenicity of recombinant dormancy-associated proteins during Mycobacterium paratuberculosis infection: implications for pathogenesis and diagnosis

Introduction

Johne's disease is a chronic inflammatory disease of the bowel of ruminants caused by *Mycobacterium avium* subsp*. paratuberculosis* that is associated with economic losses worldwide. The incidence of Johne's disease can be reduced by good management but eradication is dependant on detection and culling of infected animals. Eradication programmes for Johne's disease are not successful because of the lack of simple and specific diagnostic tests for the early detection of disease (1, 4, 36). Early diagnosis is important to identify potential faecal shedders of *Mptb* to prevent the spread of Johne's disease, and requires the development of sensitive and specific serological tests. The advantage of using an antibody-based assay instead of a cell mediated immune response is that a serological test can be developed into a simple and robust kit (43). Current immuno-diagnostic tests for *M*. *paratuberculosis* are based on crude antigen mixtures and warrant use of new antigens for the development of an improved diagnostic test. A number of antigens have been previously characterized including cell wall derived glycolipid lipoarabinomannan (16), 35 kDa antigen (11), 34 kDa protein of A36 complex (7), 65kDa protein of GroEL family (10), eighty five complex (85A, 85B and 85C) and superoxide dismutase (SOD) (35), 22kDa exported protein (9), 70kDa (Hsp70)(38), MAP2609 (44), MAP2492c (44) and MAP0210c (44).

Recently, dormancy-associated proteins have been a focus of research for diagnosis and vaccine development against tuberculosis (8, 18). A strong cellular and humoral immune response to the 16-kDa α-crystallin protein was observed in latently infected individuals (6, 8). This protein is the hallmark of the dormancy response in *M*. *tuberculosis* (2). However, there is no published information on the immunogenicity of these proteins in animals with *M*. *paratuberculosis* infection and standardized sources of antigen are not available to conduct immunologic studies. During *M*. *paratuberculosis* infection, host defenses either clear the infection or drive the host into different stages of disease (37). In *M*. *tuberculosis*, latent or asymptomatic disease has been reported in many studies (12, 41, 42, 45). Likewise the findings under stress conditions confirm that *M*. *paratuberculosis* has the ability to enter into a dormant state of metabolism *in vitro*. (S. Gumber, D. L. Taylor, I. B. Marsh and R. J. Whittington, unpublished data) It is possible that *M*. *paratuberculosis* can also enter into a dormant state in the host. We hypothesized that early stage or latently infected animals might have antibodies specific for *M*. *paratuberculosis*, which can be detected by a serological test. In this novel study, we performed serological screening of dormancy-associated recombinant proteins to identify potential immunogenic proteins for the development of a diagnostic test for Johne's disease, and confirmed that dormancy associated proteins elicit an immune response in naturally infected animals relatively early in the infection.

Materials and Methods

Bacterial strains used during this study. *E*. *coli* TOP 10 cells (Invitrogen) F´ *mcr*A, Δ (*mrr-hsd*RMS-*mcr*BC), φ80*lac*ZΔM15, Δ*lac*X74, *rec*A1, *ara*D139, Δ (*araleu*) 7697, galU, galK, *rps*L (StrR), *end*A1, *nup*G were used in cloning experiments. *E*. *coli* BL21(DE3)pLysS cells (Novagen) F´ *ompT*, *hsdSB* (r_B^- m_B^-), *gal dcm* (DE3)pLysS (CamR) were used as the host strain for the pET-15b expression vector.

Nucleic acid extraction and PCR amplification. DNA from an S strain (Telford 9.2) of *M*. *paratuberculosis* was extracted and purified using a modified chloroform/isoamyl alcohol technique as previously described (5). To amplify 5 genes which were expressed during various stressful conditions *in vitro* (S. Gumber, D. L. Taylor, I. B. Marsh and R. J. Whittington, unpublished data), primers (Table 1), containing *Nde*I and *Bam*HI restriction endonuclease sites were designed on the basis of DNA sequence available for the *M*. *paratuberculosis* K-10 genome. DNA amplification was carried out in a 50 µl reaction containing 10 ng *M*. *paratuberculosis* DNA (S strain, Telford 9.2), 200 µM dNTPs, 0.5 µM each primer and 2U Taq polymerase (Expand High Fidelity PCR System, Roche). Each reaction was subjected to the following conditions: 1 cycle of denaturation at 95°C for 3 min followed by 30 cycles of denaturation at 95°C for 30 s, annealing at 57°C for 1 min and extension at 72°C for 30 s. After 30 cycles of amplification, final extension was carried at 72°C for 10 min. PCR products were visualized by 2% agarose gel electrophoresis using ethidium bromide.

Transformation of chemically competent *E. coli*. Briefly, a tube of TOP 10 competent cells was removed from -80°C and placed on ice for 10 min to thaw. 50 µl was dispensed into a tube containing ligated product and incubated on ice for 30 min. The cells were then heat shocked at 37°C for 1 min, placed on ice for 2 min and 500 µl of Luria Bertani (LB) broth was added. The tubes were further incubated at 37°C for 45 min. The cells were pelleted by centrifugation at 16,100 × *g* for 30 s and a small amount of supernatant was decanted and resuspended in the residual liquid and plated on LB agar plates containing the selection agent 100 µg/ml ampicillin, 1 mM IPTG and 20 µg/ml X-gal. The plates were incubated for 16-18 h at 37°C. White colonies were selected and grown overnight in LB broth with 100 µg/ml ampicillin and inserts were confirmed by restriction digestion. Plasmids were recovered with a QIAprep® Miniprep (Qiagen) kit as described by the manufacturer.

DNA ligations and Restriction Digestion of DNA plasmids. Amplified PCR products were purified using the Mini? Elute PCR purification kit (Qiagen) and were cloned into the pCR2.1 vector (TA cloning kit, Invitrogen) according to the manufacturer's instructions. The cloning reaction was transformed into chemically competent TOP10 *E*. *coli* cells. The isolated plasmids were digested with restriction endonucleases *Nde*I and *Bam*HI (NEB). The reaction was carried out as a double digest. Briefly, 1 µg of DNA, 1 µl of each enzyme (*Nde*I, *Bam*HI), 2 µl of reaction buffer (NEB 2) and 0.2 µl of bovine serum albumin (100X) were made up to 20 µl with nuclease free water. The reaction was mixed gently and incubated at 37°C for 2 h. The digest was verified by electrophoresis on a 0.8% agarose gel. Plasmids containing an insert were sent for DNA sequencing using M13 Forward (5'-TGTAAAACGACGGCCAGT-3') and M13 Reverse (5'-CAGGAAACAGCTATGACC-3') primers. DNA sequencing was performed at the Australian Genome Research Facility Ltd (AGRF, Australia). Nucleotide sequences were translated to amino acid sequences using the Emboss Transeq database (European Bioinformatics Institute, http://www.ebi.ac.uk/emboss/transeq/) and were aligned with the nucleotide and amino acid sequences of the K-10 strain of *M*. *paratuberculosis* using the

CLUSTALW alignment tool of the Genome Net database (Bioinformatics Center Institute for Chemical Research Kyoto University, http://align.genome.jp/).

Subcloning into expression vector pET-15b. The DNA inserts were excised from the agarose gel and purified using a Qiagen Gel Purification kit. Purified insert DNA was ligated to the digested pET-15b vector. An insert to vector ratio of 3:1 was determined by comparing the staining intensity in agarose gel after electrophoresis. The reaction was carried out overnight at 4°C. Transformations were performed in TOP10 *E*. *coli* cells and plated on to LB plates containing the selection agent. The plasmids were isolated and verified by restriction digestion and sequencing using the T7 promotor primer (5'-TAATACGACTCACTATAGG-3').

Expression of recombinant protein. Properly oriented pET-15b constructs were transformed into a chemically competent BL21(DE3)pLysS strain of *E*. *coli*. A single colony was inoculated into 20 ml of LB broth containing ampicillin (100 µg/ml) and chloramphenicol (34 µg/ml) and grown at 37°C on an orbital shaker incubator overnight. The following day 15 ml of cell culture was diluted into 150 ml of LB broth with ampicillin (100 µg/ml) and chloramphenicol (34 µg/ml). The culture was grown to a cell density value 0.5-0.6 and recombinant protein expression was induced by addition of 1 mM (IPTG). After three hours of induction, cultures were harvested by centrifugation (1 min, 16,100 × *g*) in 2 ml screw cap polypropylene tubes (Scientific Specialties Inc.). The supernatant was discarded and the cell pellet was stored at -20°C for analysis. Unless stated otherwise, discontinuous electrophoresis buffer conditions as described previously by Laemmli were used (21). The separating gel was prepared to give a final polyacrylamide concentration of 12% from a stock solution containing 30% Acrylamide:Bis solution, 29:1(Bio-Rad Laboratories) and the final concentration of stacking gel was 4%. The gels were stained with colloidal Coomassie stain as described by Neuhoff *et al* (28). For Western blot, monoclonal antipolyhistidine (mouse, Sigma) was used as primary antibody and antimouse IgG peroxidase (Sigma) was used as a secondary antibody. Electrophoresis was carried out in a Hoeffer™ SE260 electrophoresis system (Amersham Biosciences) at a constant current of 30 mA for 2 h. Fermentas PageRuler prestained protein ladder was used to determine the molecular weight of proteins in SDS-PAGE and Western blot analyses.

Protein purification. The pET-15b vector encodes an N-terminal polyhistidine tag which is fused to the proteins expressed in this study. Therefore, the expressed proteins were purified using TALON metal affinity resin (Clontech) or Ni-NTA agarose resin (Invitrogen). TALON resin was used for purification of proteins MAP2411, Ppa, GreA under native conditions. The cell pellets were resuspended in 1 ml of binding buffer pH 7.8 (50 mM sodium phosphate, 500 mM NaCl, 0.1% Triton-X-100, 20 mM PMSF, 1 µl of Protease inhibitor cocktail, Sigma) and 0.5 g of 0.1 mm zirconium beads were added to the respective cell pellets. The pellets were lysed using a cell homogenizer (FastPrep® FP120, Thermo Electron Corporation) using 7 × 15 s pulses at maximum speed (6.5) with 2 min rest on ice between pulses. The beads were allowed to settle for 2 min, small outlets were created at the bottom of each Fastprep tube with a tuberculin syringe and each tube was secured in another microfuge tube. These secured tubes were placed in 50 ml plastic tubes and centrifuged at 360 × *g* for 5 min to obtain the whole lysed cell suspension without zirconium beads. Cell debris (insoluble fraction) was pelleted at 16,100 × *g* for 10 min at 4°C, the supernatant (soluble fraction) was collected and both were stored at -20°C for SDS-PAGE analysis. The lysate prepared above was passed through a 0.45-µm filter to prevent clogging of the column. Native purification of proteins was performed at 4°C. Briefly, the cleared lysate was mixed with 2 ml pre-washed

TALON resin in a column and suspended on a suspension mixer (Ratek) for 40 min and then resin was allowed to settle for 30 min. The settled resin in the column was washed with 6 bed volumes of binding buffer (pH 7.8) which was followed by 4 washes with wash buffer (pH 6.0) (50 mM sodium phosphate, 500 mM NaCl, 10 mM imidazole, 20 mM PMSF). The flow through of each wash was collected and stored for SDS-PAGE analysis. Protein was eluted with 8 ml of elution buffer (pH 6.0) (50 mM sodium phosphate, 500 mM NaCl, and 150 mM imidazole). Protein concentrations of fractions were measured by spectrophotometry (Bio-Rad Protein assay). The fractions were initially analyzed by SDS-PAGE and subsequently pooled and dialyzed through a 3 kDa membrane with PBS using a microdialyzer (Pierce) and stored at -80°C.

Nickel based resin was used for purification of ClpP and MAP0593c proteins under denaturing conditions. Denaturing purification was performed at room temperature. Briefly, the lysate was prepared in denaturing binding buffer (DBB) (8 M Urea, 20 mM sodium phosphate, 500 mM NaCl) pH 7.8 and was allowed to bind to nickel resin for 1.5 h at room temperature on a suspension mixer as described above. The resin was then washed once with DBB pH 7.8 followed by two washes with DBB pH 6.0 and finally two washes with DBB pH 5.3. The bound protein was eluted with 6 ml of DBB pH 4.0. The protein concentration of eluted fractions was determined as above. Following SDS-PAGE analysis, the pooled fractions were dialyzed with PBS and 0.05% Tween20 using a SnakeSkin pleated dialysis tubing, 3.5 kDa cut-off (Pierce) to refold the protein for use in ELISA and then stored at -80°C.

Preparation of *E. coli* proteins for serum preadsorption. Overnight grown cultures of *E. coli* BL21(DE3)pLysS in LB broth (150 ml) were centrifuged at 3000 × *g* for 30 min to obtain bacterial pellets. The bacterial pellets were heat killed at 90°C for 10 min, followed by resuspension in lysis buffer (PBS, 1% Tween20) and were sonicated for 7 × 30 s. Cell debris was pelleted at 16,100 × *g* for 5 min, the supernatant was collected and stored at -20°C. Protein concentration was determined using the Bio-Rad Protein assay.

ELISA. The recombinant proteins were diluted in carbonate buffer pH 9.6 to a final concentration of 5 µg/ml (GreA), 10 µg/ml (Ppa), 30 µg/ml (MAP 2411), 10 µg/ml (MAP0593c), 5 µg/ml (ClpP), a cocktail of 2.5 µg/ml GreA and 5 µg/ml Ppa, a cocktail of 2.5 µg/ml MAP0593c and 5 µg/ml ClpP and another cocktail of 2.5 µg/ml GreA, 2.5 µg/ml Ppa, 2.5 µg/ml ClpP and 2.5 µg/ml MAP0593c. 100 µl of each antigen solution was coated onto a 96 well plate (Maxisorp, Nunc International) at 4°C overnight. After washing in PBS and 0.05% v/v Tween20 wash buffer, the wells were blocked with 3% w/v skim milk powder in PBS and 0.05% v/v Tween20 at room temperature for 1.5 h. The serum samples were absorbed with 500 µg/ml proteins extracted from *E. coli* BL21(DE3)pLysS cells (described above) in *M. phlei* buffer (Institut Pourquier) for 30 min and remaining steps in the ELISA were performed as described previously (13). However, for the ClpP ELISA, sera were diluted 1:10 in *M. phlei* buffer with specify concentration *E. coli* soluble proteins.

Serum samples from sheep. To assess the immunogenicity of recombinant proteins, serum samples collected from sheep known to be at different stages of development of Johne's disease and control sheep were tested. A total of 41 known negative (control) sheep sera from Western Australia and 41 Johne's disease positive sera from New South Wales were included in this study. The infection status of positive animals was confirmed by histopathology and both positive and negative sera were previously tested using a commercial Johne's disease ELISA (Institut Pourquier) (13). An arbitrary cut off value was selected for each recombinant protein ELISA to differentiate between positive and negative serum samples.

Results

Cloning, expression and purification of *M. paratuberculosis* dormancy-associated genes. The expected band size of the dormancy-associated genes is given in Table 1. Following amplification, the products were analyzed by agarose gel electrophoresis to confirm the amplification of expected genes. The gel revealed that PCR amplified bands of the expected size, confirming that the reaction was successful (Fig 1). The amplified DNA was purified and ligated into the pCR2.1 vector. After transformation, white colonies were screened by colony PCR and restriction digestion analysis and contained inserts of desired size and appropriate DNA sequence. The translated amino acid sequences were homologous to *M. paratuberculosis* K-10 proteins (NCBI) with the exception of a single amino acid substitution in the ClpP and Ppa proteins. Digested expression vector and purified inserts were ligated, and the orientation and size of inserts in the expression vector were determined by restriction digestion and sequence analysis.

SDS-PAGE analysis of recombinant clones indicated high levels of production of recombinant proteins. Four recombinant proteins, MAP2411, Ppa, GreA and ClpP, were soluble (Fig 2) while MAP0593c was insoluble in nature (Fig 3). The findings were also confirmed by Western blot analysis (Figs 2 and 3). It is clear from Table 1 that the expected molecular mass of ClpP was 14.8 kDa. However, SDS-PAGE revealed a band size of ~ 23 kDa.

Recombinant proteins (MAP2411, GreA, Ppa, ClpP, MAP0593c) were purified using nickel and cobalt based resins. After purification, His-tag proteins with the appropriate predicted molecular masses became the major protein bands in each eluent (Table 1). However, there were still many other bands present in the purified preparations. Dialysis of the samples resulted in reduction of multiple bands (Fig 4). In each case the recombinant protein remained the predominant protein in the sample (Fig 4). The total yield of each purified protein was estimated to be 1.2-1.4 mg/150 ml of induced *E. coli* culture.

Immunogenicity of recombinant proteins. The relationship between the humoral immune responses of sheep to dormancy-associated proteins of *M. paratuberculosis* and the stage of development of Johne's disease was investigated by measuring serum antibody levels to the five recombinant antigens that were suitable for ELISA. The serum samples used in this study were previously screened by a commercially available Johne's disease ELISA kit (Institut Porquier) and comparative data were collected (Table 2). An arbitrary mean OD value was selected for each recombinant protein to differentiate seropositive and seronegative samples. Depending on antigen, between 9 and 19 samples from sheep with early stage lesions of paratuberculosis (paucibacillary) had antibody responses. In contrast, there were detectable antibody responses against a crude mixture of antigens in the commercial kit in only 15 samples from animals from the same group. Interestingly, all the recombinant antigens detected animals in early stages of disease and more multibacillary cases were identified by the MAP0593c, ClpP and Ppa antigens than by the Pourquier ELISA.

However, some samples from sheep without paratuberculosis also contained antibodies reactive with one or more recombinant antigens. Preadsorption of sera with proteins from *E. coli* BL21(DE3)pLysS cells in *M. phlei* buffer resulted in a decrease in OD values of known negative samples without affecting the OD values of positive samples. This

suggests that some of the ELISA reactivity detected in samples was non-specific or directed against *E. coli* antigens.

MAP2411 antigen proved to be non-immunogenic in this study (Fig 9).

An arbitrary mean OD value was selected for each recombinant protein to differentiate the disease positive and negative sera. When plotted, immune responses against the recombinant dormancy-associated antigens can be used to differentiate animals with and without *M. paratuberculosis* with degrees of overlap ranging from minor to moderate (Figs 5-12).

Discussion

The identification of antigenic proteins is vital for understanding the pathogenic mechanisms of *M*. *paratuberculosis* and the immune responses against this organism. In addition, these proteins help us complement existing panels of antigens for diagnosis and/or vaccine development. This is a novel study in which recombinant dormancy-associated proteins were used to assess the humoral immune responses in sheep infected with *M*. *paratuberculosis*. A total of 5 dormancy-associated genes (S. Gumber, D. L. Taylor, I. B. Marsh and R. J. Whittington, unpublished data) were selected for cloning and protein purification. The selection criterion for genes was their consistent expression during three different stresses: hypoxia, nutrient starvation and temperature flux (Gumber et al unpublished data). Therefore it is reasonable to assume that they may be part of a general response of the organism to unfavourable environments. This may include that within the host macrophage and as such these proteins may be expressed throughout the infection including the early stages, where current diagnostic tests have very limited application. However, hypothetical proteins were also included in the study because nothing is known currently about the function or potential utility of such proteins.

The pET expression system (Novagen) was used to express the recombinant proteins because of its versatility (27, 30, 39). Sequence analysis of each gene and its predicted amino acid sequence revealed an alteration of a single amino acid for the ClpP and Ppa recombinant proteins compared to *M. paratuberculosis* K-10. Furthermore the molecular mass of ClpP on SDS-PAGE was not as predicted (14.8kDa). Such discrepancies have been reported previously (for example see (26), (3)) and there are several possible reasons including non-uniform binding of negatively charged SDS to the protein (reference), hydrophobicity, charge, glycosylation and phosphorylation differences (14), single amino acid substitutions and differences in genome sequence of the S and C strains of *M*. *paratuberculosis* (24, 25). The last reason may in fact be the most likely one. The sequence of the S strain is not yet available. .

Polyhistidine tagged proteins have affinity for Cu^{2+}, Ni^{2+}, Co^{2+} and Zn^{2+} which allows the His-tagged protein to be quickly separated from the bulk of other bacterial proteins with 95% purity using metal chelate affinity chromatography (15). In this study, both cobalt and nickel affinity resins were used. The cobalt based TALON resin binds 6 x His-tag proteins with higher selectivity than do nickel-based IMAC resins. It utilizes Sepharose CL-6B beads with a chelated cobalt adsorptive center, consisting of a small adsorption ligand and cobalt ion, to bind histidine clusters present on the surface of a protein of interest (Clontech). In contrast Ni-NTA Agarose uses nitrilotriacetic acid (NTA), a tetradentate chelating ligand, in a highly cross-linked 6% agarose matrix. NTA binds Ni^{2+} ions by four coordination sites (Invitrogen). Although the manufacturer's claims suggest that TALON resin has higher selectivity for the polyhistidine proteins, it was unable to bind the ClpP protein under native and denaturing conditions. In contrast, nickel resin

bound to ClpP protein using denaturing conditions, suggesting more affinity of ClpP proteins for Ni^{2+} than for Co^{2+}. MAP0593c was also purified under denaturing conditions using nickel resin.

During the purification of recombinant proteins, some other protein bands were observed with the desired protein possibly due to non-specific binding of *E*. *coli* proteins to the resin. Although a number of attempts were made to purify the recombinant proteins on a small scale, the undesired bands were routinely observed. It seemed unlikely that all of these were degraded proteins because the bacterial cell lysates had been prepared in buffer containing a protease inhibitor cocktail and PMSF. It seems most likely that these bands were contaminating proteins from the host *E. coli* although this was not proven. The alternative is that they were shortened forms or multimers of the fusion product (His-tag protein) formed through disulfide bridges between cysteine residues, or co-aggregates of *E*. *coli* proteins attached to the fusion product through disulfide bonds (22). Nevertheless, SDS-PAGE of the dialyzed recombinant proteins revealed them to be the predominant proteins and therefore suitable for the assessment of humoral immune responses using ELISA. It has been observed previously that preadsorption of sera with *E*. *coli* lysates can reduce the effect of cross reactive antibodies without affecting the detection of antibodies against antigens/epitopes that are specific to mycobacteria (20, 31, 32). Therefore, assuming that the unwanted proteins were from the *E. coli* host cells, serum samples from sheep were preadsorbed with *E*. *coli* proteins in this study.

In the ELISA, reagents were used from the Pourquier ELISA kit (13) but preliminary trials were conducted to optimize new assay formats that incorporated the recombinant antigens and titrate reagents. When serum samples were adsorbed with *M*. *phlei* buffer only, an increase in the OD values of negative serum samples was observed. In contrast, adsorption with *M. phlei* along with *E*. *coli* proteins reduced the background dramatically in negative samples. Further, there was no negative effect of this absorption step on OD values of samples from sheep with paratuberculosis, which was in agreement with earlier studies (20, 31, 32). However, despite adsorption of sera with *E*. *coli* proteins some of the known negative samples showed a signal in the ELISA test. Prolonged adsorption of sera with *E*. *coli* proteins in *M*. *phlei* buffer was not tried in this study but may be worthwhile. Nevertheless, the strong reactivity of sera from known positive samples with some of these antigens suggests that dormancy-associated recombinant proteins possess specific immunoreactive epitopes which are expressed *in vivo* during the development of Johne's disease in sheep.

Surprisingly, sera from paucibacillary animals in the early stages of disease reacted to GreA, Ppa, MAP0593c, ClpP, a cocktail of GreA and Ppa, a cocktail of MAP0593c and ClpP and a cocktail of GreA, Ppa, MAP0593c and ClpP antigens. These animals are considered to be the most problematic cases in terms of diagnosis. The same serum samples failed to show a signal in the Pourquier ELISA test which is based on non-defined native antigens; typically the current commercial ELISA kits for Johne's disease utilize crude extracts of homogenized or mechanically disrupted *M. paratuberculosis* cells where dormancy-associated proteins may be absent or a minor component.

The immunological evidence suggests that GreA, Ppa, ClpP and MAP0593c proteins were expressed *in vivo* during early paratuberculosis infection. Ppa, ClpP, and MAP0593c were also expressed *in vitro* during hypoxia, nutrient starvation and thermal flux (S. Gumber, D. L. Taylor, I. B. Marsh and R. J. Whittington, unpublished data) and may be essential for survival of *M*. *paratuberculosis* during a wide range of stresses. MAP0593c and ClpP were more immunogenic than GreA and Ppa. This could be mainly

due to the presence of more epitopes exposed on the MAP0593c and ClpP than on Ppa and GreA or the epitopes exposed on the MAP0593c and ClpP may be more antigenic than Ppa and GreA. Antigen-specific immune responses can provide indirect evidence of bacterial metabolic activity during different stages of disease. It is clear from Table 2 that host immune responses to Ppa, ClpP, and MAP0593c were present in both paucibacillary and multibacillary cases suggesting that expression of these proteins may continue throughout the infection. In contrast, GreA reactivity with sera suggests that it may be the serodominant antigen during the early stages of disease. Clearly antibody responses may differ during different stages of the disease, and may be predictive of lesion stage. Further research is required to confirm this.

It has been reported that *M*. *paratuberculosis* purified protein derivative PPD (PPDP) specific IgG1 responses can differentiate asymptomatic shedders and clinically infected cattle (19). Recently, antigen recognition patterns of the early antibody response and contribution of IgM to the early response was evaluated for the rapid detection of cattle with *M*. *bovis* infection (40). It was found that IgM responses were detected prior to IgG responses but they also waned quickly, suggesting tests based on detection of both IgM and IgG antibodies have potential for early detection of infection (40). In the present study, only total IgG responses were measured in sera from sheep infected with *M*. *paratuberculosis*. It may be possible that these dormancy-associated antigens also stimulate an IgM or IgG1 response. This warrants further investigation.

Several studies in *M*. *tuberculosis* have suggested that antigen cocktails can be useful for the development of an efficient serodiagnostic test (17, 23). The three different cocktails of antigens (Table 2) used in this study resulted in an increase in specificity of ELISA in comparison to recombinant antigens used alone and higher sensitivity than GreA and Ppa antigens. However, the cocktail of antigens resulted in a decreased detection rate compared to MAP0593c and ClpP antigens alone (Table 2). The lower amount of respective antigen in the cocktail could be the reason. Further, MAP0593c was most immunogenic in this study. However, in combination with ClpP, a decrease in sensitivity was observed. The optimal results for the ClpP ELISA were observed at 1:10 serum dilution. However, in combination with MAP0593c, serum was used at 1:20 dilution, suggesting ClpP antigen required more antibodies to produce a given signal. The fusion of different antigens into a hybrid may simplify the production of a good ELISA test. Further, antigens that are expressed by bacteria during the dormant phase of the disease are perhaps more representative markers of recent acquisition of disease. Recently, dormancy-associated antigens Acr and DevR were used for immunostaining in guinea pigs infected with *M*. *tuberculosis* (34). Surprisingly, immunostaining with these antigens was observed after 4 weeks of infection and maximum expression was observed at 20 weeks of infection. It was suggested that dormancy-associated proteins are expressed during early infection (34).

It is becoming increasingly clear that the immunogenicity of many proteins is affected by post-translational modifications, especially glycosylation and acylation (29, 33). Moreover, transcription and translation of *M*. *tuberculosis* genes in mycobacterial hosts allows more accurate processing of gene products, including folding and post-translational modifications than in *E*. *coli*. It has also been observed that recombinant protein expressed in *M*. *smegmatis* was more immunogenic than the *E*. *coli* counterpart (29). Although some of the proteins expressed in *E*. *coli* in this study were immunogenic, it may be possible that the immunogenicity of dormancy-associated recombinant proteins can be increased by expressing the recombinant proteins in *M*. *smegmatis*. This requires further investigation.

These results clearly show the immunogenic nature of dormancy-associated recombinant proteins. Although the specificity of recombinant antigens was not 100% in this study, alternative expression and purification conditions such as through use of a mycobacterial host may help increase the sensitivity and specificity of ELISA based on dormancy-associated recombinant antigens. However, this study has established a framework on which further studies can be conducted. The data in this study also show that the immunogenicity of dormancy-associated antigens varies with stages of the disease and an immunodiagnostic test based on these dormancy-associated proteins could be useful to distinguish different states of the disease. It is likely that multiple early and late stage antigens will be helpful in the development of a better immunodiagnostic test for *M*. *paratuberculosis*. In this study, the cell-mediated immune responses against these recombinant proteins were not investigated and this requires further research. Although only 5 of the dormancy-associated antigens were tested in this study, it can be assumed that other antigens identified during the dormant or stress response state (S. Gumber, D. L. Taylor, I. B. Marsh and R. J. Whittington, unpublished data) will mimic the immunogenic pattern seen here, when applied alone or in combination.

Conclusion

The antigenicity of dormancy-associated recombinant proteins against sera from infected sheep suggests that these proteins are expressed *in vivo* and participate in the pathogenesis of paratuberculosis in sheep. Furthermore their immunogenicity indicates that they have potential for the development of a better diagnostic test for the detection of *M*. *paratuberculosis*. Research directed at elucidating the function of the dormancy-associated proteins will provide a better understanding of their use for the diagnosis of *M*. *paratuberculosis* and potentially, in prophylaxis through vaccination. This study has contributed to the enhancement of our knowledge of the diagnosis of *M*. *paratuberculosis* infection. Subsequent studies on the development of serodiagnostic tests and vaccines for *M*. *paratuberculosis* should take into account these proteins.

References

Bech-Nielsen, S., J. B. Jorgensen, P. Ahrens, and N. C. Feld. 1992. Diagnostic accuracy of a Mycobacterium phlei-absorbed serum enzyme-linked immunosorbent assay for diagnosis of bovine paratuberculosis in dairy cows. J Clin Microbiol 30:613-618.

Boon, C., and T. Dick. 2002. Mycobacterium bovis BCG response regulator essential for hypoxic dormancy. J Bacteriol 184:6760-6767.

Casaregola, S., A. Jacq, D. Laoudj, G. McGurk, S. Margarson, M. Tempete, V. Norris, and I. B. Holland. 1992. Cloning and analysis of the entire Escherichia coli ams gene. ams is identical to hmp1 and encodes a 114 kDa protein that migrates as a 180 kDa protein. J Mol Biol 228:30-40.

Chiodini, R. J. 1989. The genetic relationship between Mycobacterium paratuberculosis and the M. avium complex. Acta Leprol 7:249-251.

Choy, E., R. J. Whittington, I. Marsh, J. Marshall, and M. T. Campbell. 1998. A method for purification and characterisation of Mycobacterium avium subsp. paratuberculosis from the intestinal mucosa of sheep with Johne's disease. Vet Microbiol 64:51-60.

Davidow, A., G. V. Kanaujia, L. Shi, J. Kaviar, X. Guo, N. Sung, G. Kaplan, D. Menzies, and M. L. Gennaro. 2005. Antibody profiles characteristic of Mycobacterium tuberculosis infection state. Infect Immun 73:6846-6851.

De Kesel, M., P. Gilot, M. Coene, and C. Cocito. 1992. Composition and immunological properties of the protein fraction of A36, a major antigen complex of Mycobacterium paratuberculosis. Scand J Immunol 36:201-212.

Demissie, A., E. M. Leyten, M. Abebe, L. Wassie, A. Aseffa, G. Abate, H. Fletcher, P. Owiafe, P. C. Hill, R. Brookes, G. Rook, A. Zumla, S. M. Arend, M. Klein, T. H. Ottenhoff, P. Andersen, and T. M. Doherty. 2006. Recognition of stage-specific mycobacterial antigens differentiates between acute and latent infections with Mycobacterium tuberculosis. Clin Vaccine Immunol 13:179-186.

Dupont, C., K. Thompson, C. Heuer, B. Gicquel, and A. Murray. 2005. Identification and characterization of an immunogenic 22 kDa exported protein of Mycobacterium avium subspecies paratuberculosis. J Med Microbiol 54:1083-1092.

el-Zaatari, F. A., S. A. Naser, L. Engstrand, P. E. Burch, C. Y. Hachem, D. L. Whipple, and D. Y. Graham. 1995. Nucleotide sequence analysis and seroreactivities of the 65K heat shock protein from Mycobacterium paratuberculosis. Clin Diagn Lab Immunol 2:657-664.

el-Zaatari, F. A., S. A. Naser, and D. Y. Graham. 1997. Characterization of a specific Mycobacterium paratuberculosis recombinant clone expressing 35,000-molecular-weight antigen and reactivity with sera from animals with clinical and subclinical Johne's disease. J Clin Microbiol 35:1794-1799.

Fenhalls, G., L. Stevens, L. Moses, J. Bezuidenhout, J. C. Betts, P. Helden Pv, P. T. Lukey, and K. Duncan. 2002. In situ detection of Mycobacterium tuberculosis transcripts in human lung granulomas reveals differential gene expression in necrotic lesions. Infect Immun 70:6330-6338.

Gumber, S., G. Eamens, and R. J. Whittington. 2006. Evaluation of a Pourquier ELISA kit in relation to agar gel immunodiffusion (AGID) test for assessment of the humoral immune response in sheep and goats with and without Mycobacterium paratuberculosis infection. Vet Microbiol 115:91-101.

Hames, B. D. 1998. One dimesional PAGE. Gel electrophoresis of proteins : a practical approach. Oxford University Press, New York.

Hochuli, E., W. Bannwarth, H. Döbeli, R. Gentz, and D. Stüber. 1988. Genetic approach to facilitate purification of novel recombinant proteins with a novel metal chelate adsorbent. Biotechnology 6:1321-1325.

Jark, U., I. Ringena, B. Franz, G. F. Gerlach, and M. Beyerbach. 1997. Development of an ELISA technique for serodiagnosis of bovine paratuberculosis. Vet Microbiol 57:189-198.

Julian, E., L. Matas, J. Alcaide, and M. Luquin. 2004. Comparison of antibody responses to a potential combination of specific glycolipids and proteins for test sensitivity improvement in tuberculosis serodiagnosis. Clin Diagn Lab Immunol 11:70-76.

Khera, A., R. Singh, H. Shakila, V. Rao, N. Dhar, P. R. Narayanan, C. N. Parmasivan, V. D. Ramanathan, and A. K. Tyagi. 2005. Elicitation of efficient, protective immune responses by using DNA vaccines against tuberculosis. Vaccine 23:5655-5665.

Koets, A. P., V. P. Rutten, M. de Boer, D. Bakker, P. Valentin-Weigand, and W. van Eden. 2001. Differential changes in heat shock protein-, lipoarabinomannan-, and purified protein derivative-specific immunoglobulin G1 and G2 isotype responses during

bovine Mycobacterium avium subsp. paratuberculosis infection. Infect Immun 69:1492-1498.

Laal, S., K. M. Samanich, M. G. Sonnenberg, S. Zolla-Pazner, J. M. Phadtare, and J. T. Belisle. 1997. Human humoral responses to antigens of Mycobacterium tuberculosis: immunodominance of high-molecular-mass antigens. Clin Diagn Lab Immunol 4:49-56.

Laemmli, U. K. 1970. Cleavage of structural proteins during the assembly of the head of bacteriophage T4. Nature 227:680-685.

Lefkovits, I., and B. Pernis. 1990. Immunological methods. Academic Press, New York.

Lyashchenko, K. P., M. Singh, R. Colangeli, and M. L. Gennaro. 2000. A multi-antigen print immunoassay for the development of serological diagnosis of infectious diseases. J Immunol Methods 242:91-100.

Marsh, I. B., J. P. Bannantine, M. L. Paustian, M. L. Tizard, V. Kapur, and R. J. Whittington. 2006. Genomic Comparison of Mycobacterium avium subsp. paratuberculosis Sheep and Cattle Strains by Microarray Hybridization. J Bacteriol 188:2290-2293.

Marsh, I. B., and R. J. Whittington. 2007. Genomic diversity in Mycobacterium avium: Single nucleotide polymorphisms between the S and C strains of M. avium subsp. paratuberculosis and with M. a. avium. Mol Cell Probes 21:66-75.

Matagne, A., B. Joris, and J. M. Frere. 1991. Anomalous behaviour of a protein during SDS/PAGE corrected by chemical modification of carboxylic groups. Biochem J 280 (Pt 2):553-556.

Moffatt, B. A., and F. W. Studier. 1988. Entry of bacteriophage T7 DNA into the cell and escape from host restriction. J Bacteriol 170:2095-2105.

Neuhoff, V., N. Arold, D. Taube, and W. Ehrhardt. 1988. Improved staining of proteins in polyacrylamide gels including isoelectric focusing gels with clear background at nanogram sensitivity using Coomassie Brilliant Blue G-250 and R-250. Electrophoresis 9:255-262.

Roche, P. W., N. Winter, J. A. Triccas, C. G. Feng, and W. J. Britton. 1996. Expression of Mycobacterium tuberculosis MPT64 in recombinant Myco. smegmatis: purification, immunogenicity and application to skin tests for tuberculosis. Clin Exp Immunol 103:226-232.

Rosenberg, A. H., B. N. Lade, D. S. Chui, S. W. Lin, J. J. Dunn, and F. W. Studier. 1987. Vectors for selective expression of cloned DNAs by T7 RNA polymerase. Gene 56:125-135.

Samanich, K., J. T. Belisle, and S. Laal. 2001. Homogeneity of antibody responses in tuberculosis patients. Infect Immun 69:4600-4609.

Samanich, K. M., J. T. Belisle, M. G. Sonnenberg, M. A. Keen, S. Zolla-Pazner, and S. Laal. 1998. Delineation of human antibody responses to culture filtrate antigens of Mycobacterium tuberculosis. J Infect Dis 178:1534-1538.

Samanich, K. M., M. A. Keen, V. D. Vissa, J. D. Harder, J. S. Spencer, J. T. Belisle, S. Zolla-Pazner, and S. Laal. 2000. Serodiagnostic potential of culture filtrate antigens of Mycobacterium tuberculosis. Clin Diagn Lab Immunol 7:662-668.

Sharma, D., A. Bose, H. Shakila, T. K. Das, J. S. Tyagi, and V. D. Ramanathan. 2006. Expression of mycobacterial cell division protein, FtsZ, and dormancy proteins, DevR

and Acr, within lung granulomas throughout guinea pig infection. FEMS Immunol Med Microbiol 48:329-336.

Shin, S. J., H. S. Yoo, S. P. McDonough, and Y. F. Chang. 2004. Comparative antibody response of five recombinant antigens in related to bacterial shedding levels and development of serological diagnosis based on 35 kDa antigen for Mycobacterium avium subsp. paratuberculosis. J Vet Sci 5:111-117.

Sockett, D. C., D. J. Carr, and M. T. Collins. 1992. Evaluation of conventional and radiometric fecal culture and a commercial DNA probe for diagnosis of Mycobacterium paratuberculosis infections in cattle. Can J Vet Res 56:148-153.

Stabel, J. R. 2000. Transitions in immune responses to Mycobacterium paratuberculosis. Vet Microbiol 77:465-473.

Stevenson, K., N. F. Inglis, B. Rae, W. Donachie, and J. M. Sharp. 1991. Complete nucleotide sequence of a gene encoding the 70 kd heat shock protein of Mycobacterium paratuberculosis. Nucleic Acids Res 19:4552.

Studier, F. W., A. H. Rosenberg, J. J. Dunn, and J. W. Dubendorff. 1990. Use of T7 RNA polymerase to direct expression of cloned genes. Methods Enzymol 185:60-89.

Waters, W. R., M. V. Palmer, T. C. Thacker, J. P. Bannantine, H. M. Vordermeier, R. G. Hewinson, R. Greenwald, J. Esfandiari, J. McNair, J. M. Pollock, P. Andersen, and K. P. Lyashchenko. 2006. Early antibody responses to experimental Mycobacterium bovis infection of cattle. Clin Vaccine Immunol 13:648-654.

Wayne, L. G. 1994. Dormancy of Mycobacterium tuberculosis and latency of disease. Eur J Clin Microbiol Infect Dis 13:908-914.

Wayne, L. G., and C. D. Sohaskey. 2001. Nonreplicating persistence of Mycobacterium tuberculosis. Annu Rev Microbiol 55:139-163.

Weldingh, K., I. Rosenkrands, L. M. Okkels, T. M. Doherty, and P. Andersen. 2005. Assessing the serodiagnostic potential of 35 Mycobacterium tuberculosis proteins and identification of four novel serological antigens. J Clin Microbiol 43:57-65.

Willemsen, P. T., J. Westerveen, A. Dinkla, D. Bakker, F. G. van Zijderveld, and J. E. Thole. 2006. Secreted antigens of Mycobacterium avium subspecies paratuberculosis as prominent immune targets. Vet Microbiol 114:337-344.

Zahrt, T. C. 2003. Molecular mechanisms regulating persistent Mycobacterium tuberculosis infection. Microbes Infect 5:159-167.

Table 1 Primers used for PCR amplification and cloning

Protein/ Gene	Accession No.	Forward primer sequence (5´ 3´)[a] →	Reverse primer sequence (3´ 5´)[a] →	Size (base pairs)[b]	Molecular mass (kDa)[b]
MAP2411	41408509	CATATGAAACCCTTCAGCGAATCCG	GGATCCGACATGGTGCTCACCATGC	509	15.5
MAP0593c	41406691	CATATGGCGTCGATCTTCACCAAG	GGATCCAGGGTTGCTGCTTCCG	459	14.7
clpP	41408379	CATATGTCTGACATGCGTTCGCC	GGATCCTGGAGTGCTCGATGAACG	657	14.8
ppa	41406533	CATATGGAATTCGACGTGACCATCG	GGATCCGGTGTTCTTCATCGGAACGGC	553	18.5
greA	41407125	CATATGACGGATACTTCCGTGACC	GGATCCAGTTGATACGCCGAGCGC	520	17.8

[a] Restriction sites used for cloning are underlined. NdeI, CATATG; BamHI, GGATCC
[b] Expected sizes of PCR amplified products and expressed recombinant proteins

Table 2 Comparison of immunoreactivity of dormancy-associated recombinant proteins and a non-defined mixture of M. paratuberculosis antigens in the Pourquier ELISA kit. Data are the number of animals

Histopathology		Immunoreactivity of different *M. paratuberculosis* antigens							
Category	n[a]	GreA	Ppa	ClpP	MAP0593c	GreA+Ppa	ClpP+MAP0593c	GreA+Ppa+ClpP+MAP0593c	Pourquier
Paucibacillary									
Type 1	9	1	3	4	5	1	3	4	0
Type 2	2	1	0	0	0	1	0	0	0
Type 3a	20	5	5	8	12	6	8	8	11
Type 3c	3	2	1	1	2	1	0	1	4
Multibacillary (Type 3b)	7	1	5	6	5	3	3	4	3
Total	41	10	14	19	24	12	14	17	18

n^a = number of animals tested

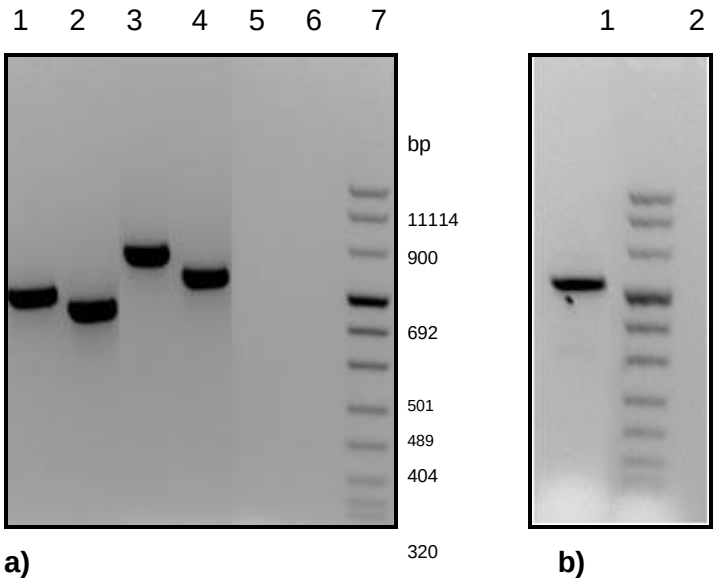

Fig 1 Agarose gel electrophoresis showing the PCR amplicons of dormancy- associated genes from Mptb. a) Lane 1 - MAP2411, Lane 2 - MAP0593c, Lane 3 - *clpP*, Lane 4 - *ppa*, Lane 5 - Negative control (MQW), Lane 6 - Quality control (PCR cocktail), Lane 7 - DNA molecular mass marker; b) Lane 1 - *greA*, Lane 2 - DNA molecular mass marker.

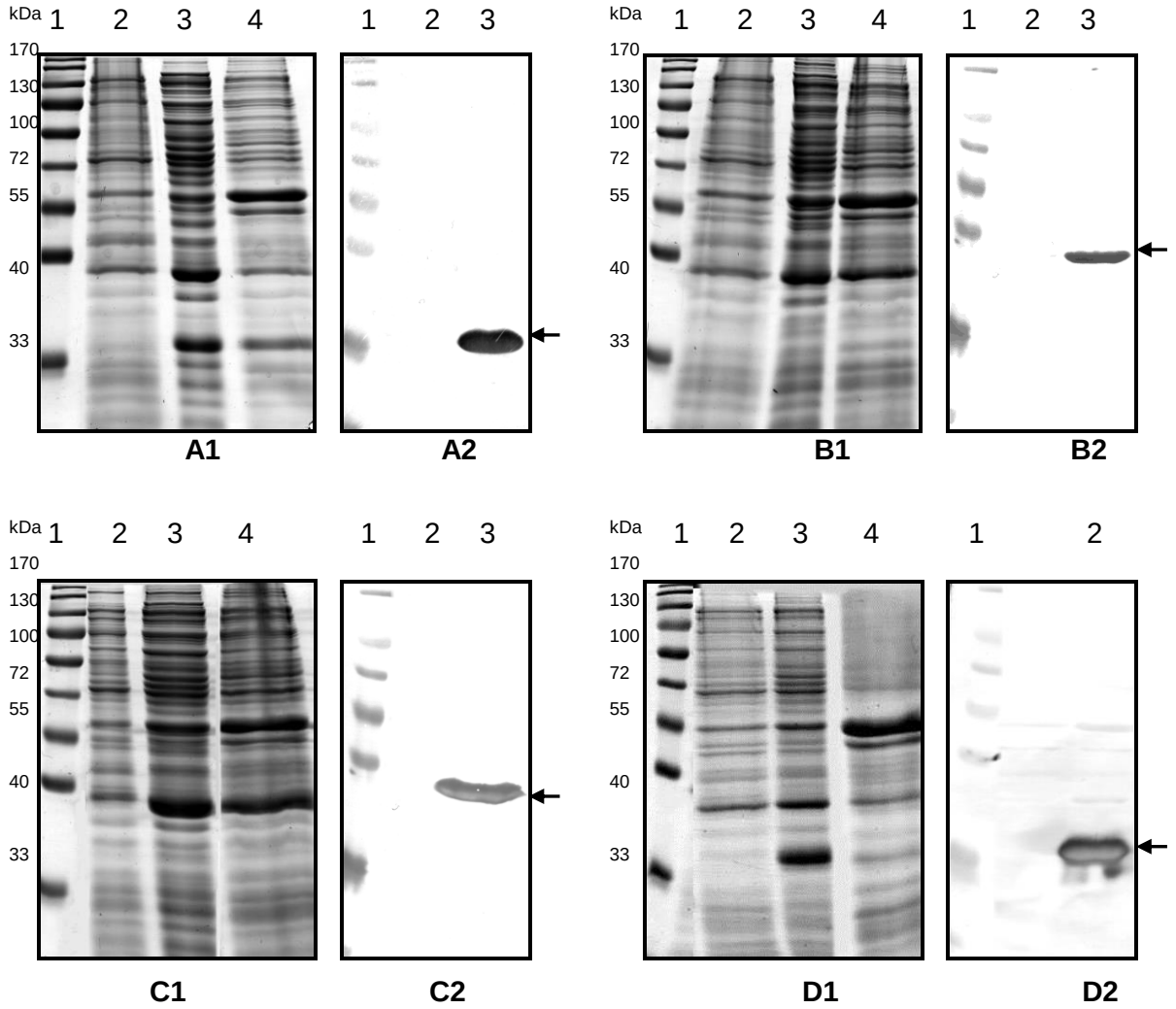

Fig 2 SDS-PAGE (1) and Western blot (2) analysis showing induction of the expressed soluble recombinant proteins in *E. coli* BL21 cells. The cells were induced with 1mM IPTG for 3 h. A1, A2 - MAP2411, B1, B2 - ClpP, C1, C2 - Ppa, D1, D2 - GreA. A1-D1 SDS-PAGE, Lane 1 - Molecular weight standard, Lane 2 -

Uninduced culture, Lane 3 - Soluble induced culture, Lane 4 Insoluble induced culture; A2-D2 Western blot, Lane 1 - Molecular weight standard, Lane 2 - Uninduced culture, Lane 3 - Induced culture. Arrows indicate induced recombinant proteins.

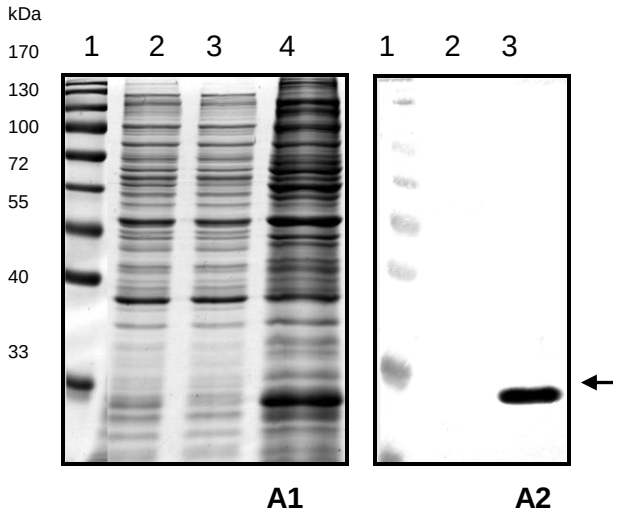

Fig 3 SDS-PAGE (1) and Western blot (2) analysis showing induction of the expressed insoluble MAP0593c recombinant protein in *E. coli* BL21 cells. The cells were induced with 1mM IPTG for 3 h. A1 SDS-PAGE, Lane 1 - Molecular weight standard, Lane 2 - Uninduced culture, Lane 3 - Soluble induced culture, Lane 4 Insoluble induced culture; A2 Western blot, Lane 1 - Molecular weight standard, Lane 2 - Uninduced culture, Lane 3 - Induced culture. Arrows indicate induced recombinant protein.

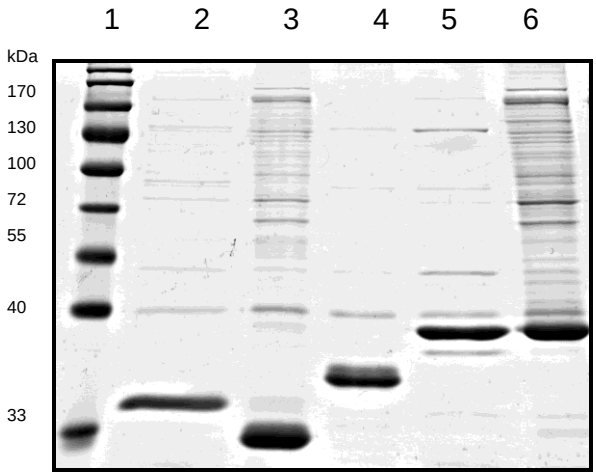

Fig 4 Dialyzed purified recombinant His-tag proteins were analyzed by SDS-PAGE by loading 5 µg on to a 12% gel, and were visualized by Coomassie blue staining; Lane 1 - Molecular weight standard, Lane 2 - MAP2411, Lane 3 - MAP 0593c, Lane 4 - GreA, Lane 5 - Ppa, Lane 6 - ClpP.

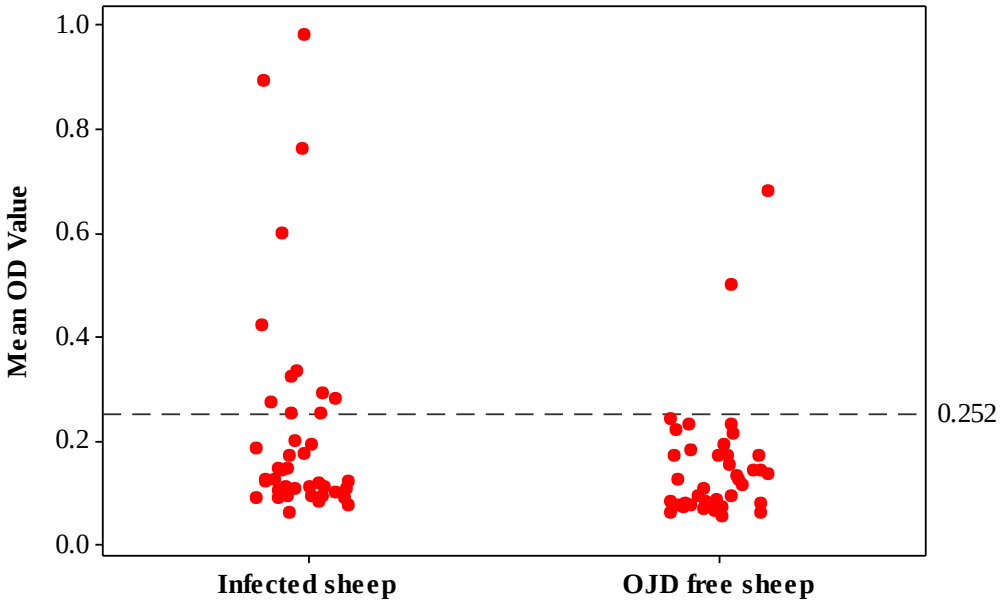

Fig 5 Immunoreactivity of GreA antigen to *M. paratuberculosis* infected and free sheep. The value 0.252 indicates an arbitrary cut off to distinguish positive and negative samples.

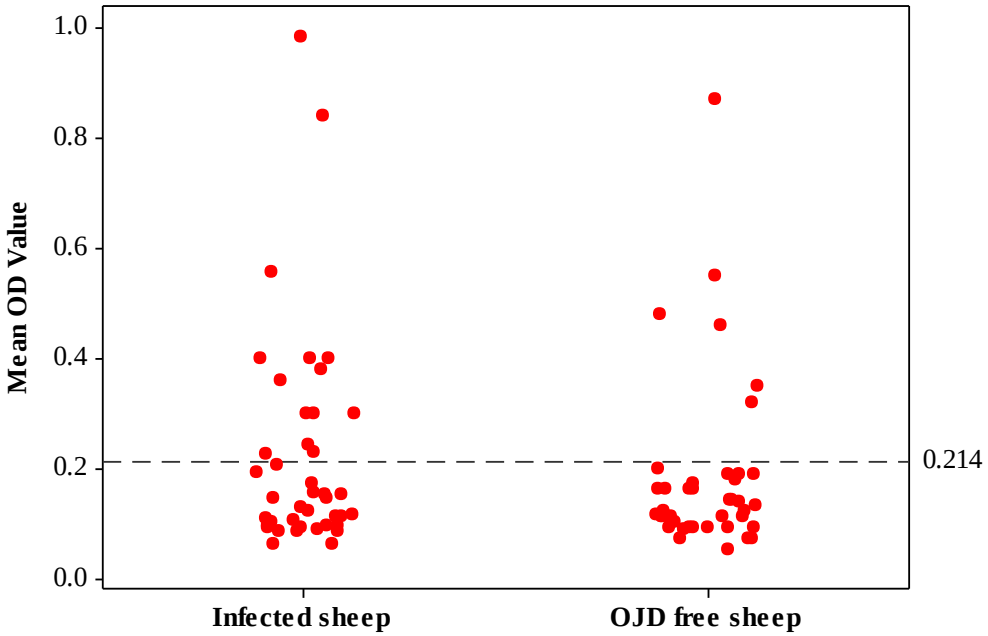

Fig 6 Immunoreactivity of Ppa antigen to *M. paratuberculosis* infected and free sheep. The value 0.214 indicates an arbitrary cut off to distinguish positive and negative samples.

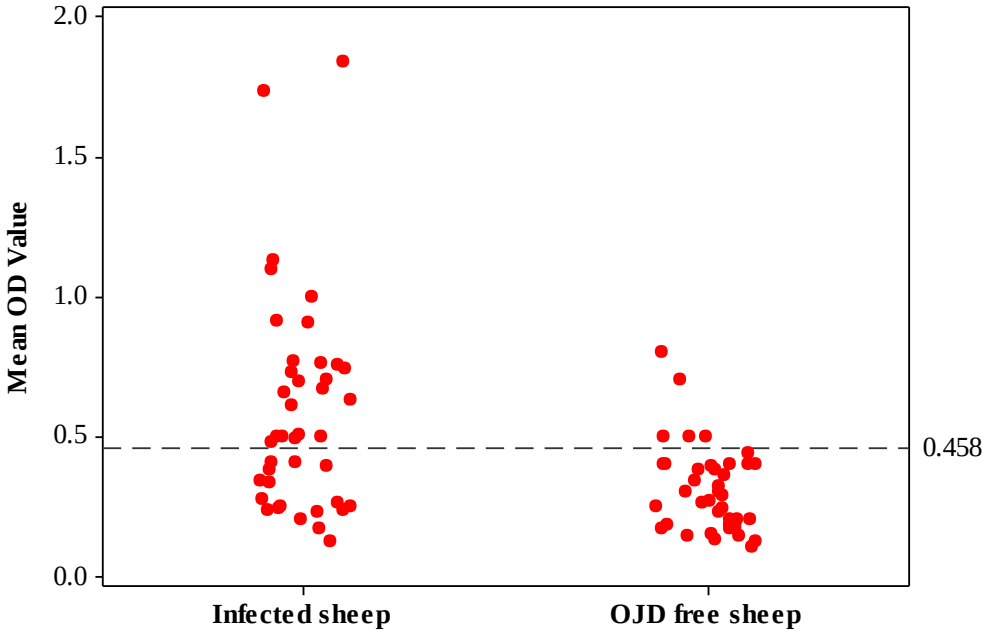

Fig 7 Immunoreactivity of MAP0593c antigen to *M. paratuberculosis* infected and free sheep. The value 0.458 indicates an arbitrary cut off to distinguish positive and negative samples.

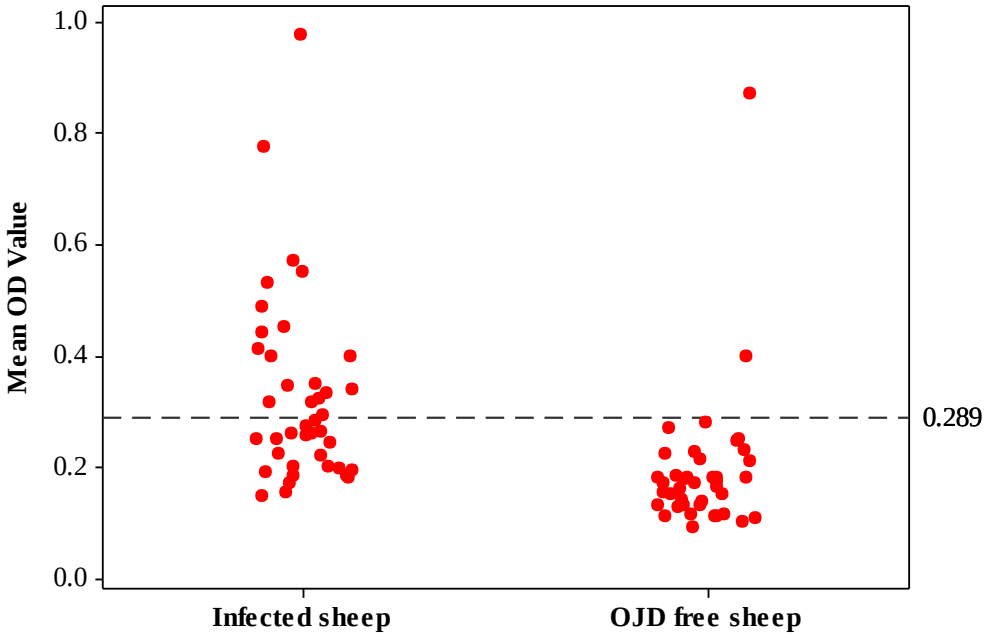

Fig 8 Immunoreactivity of ClpP antigen to *M. paratuberculosis* infected and free sheep. The value 0.289 indicates an arbitrary cut off to distinguish positive and negative samples.

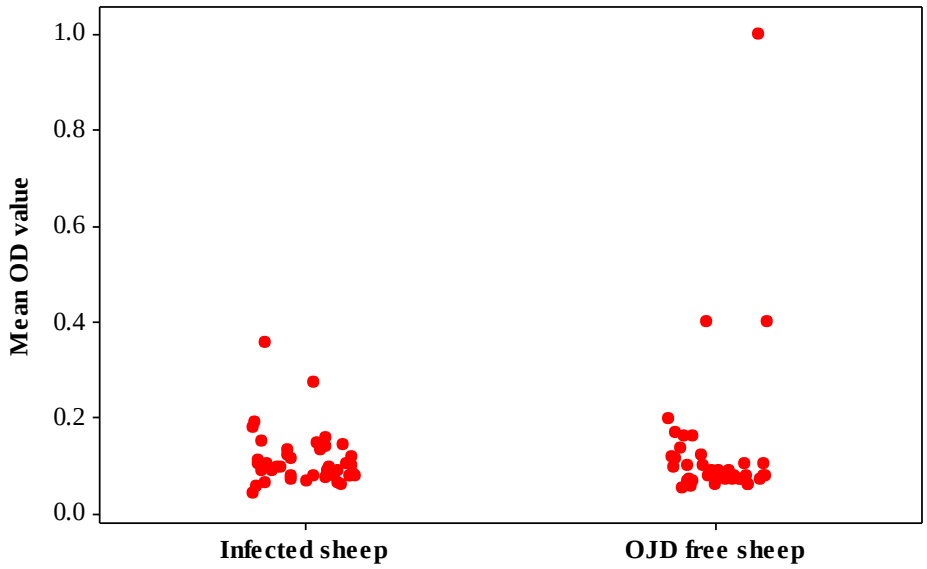

Fig 9 Immunoreactivity of MAP2411 antigen to *M. paratuberculosis* infected and free sheep. No difference was observed between positive and negative samples.

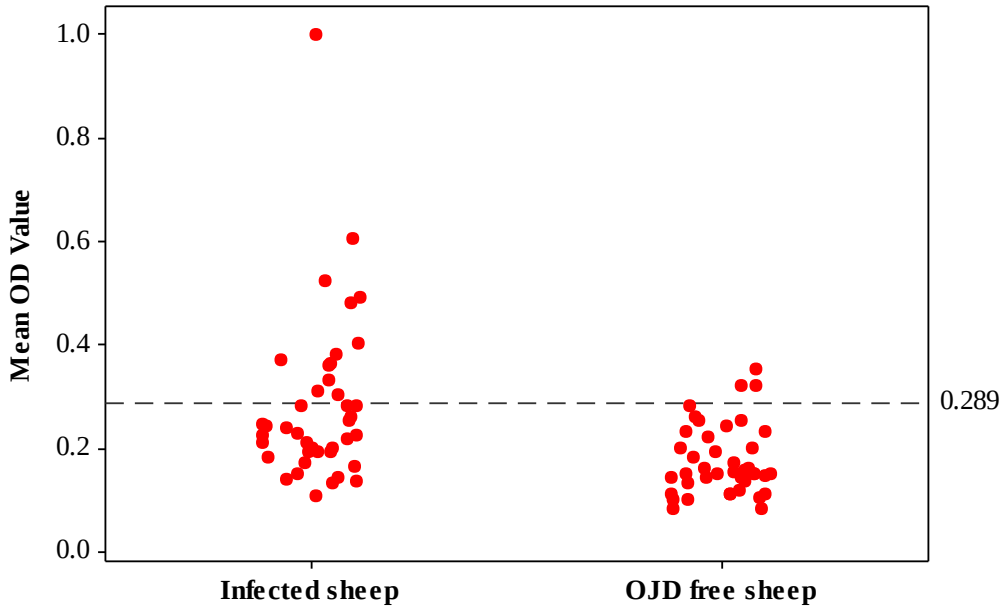

Fig 10 Immunoreactivity of a cocktail of GreA and Ppa antigens to *M. paratuberculosis* infected and free sheep. The value 0.289 indicates an arbitrary cut off to distinguish positive and negative samples.

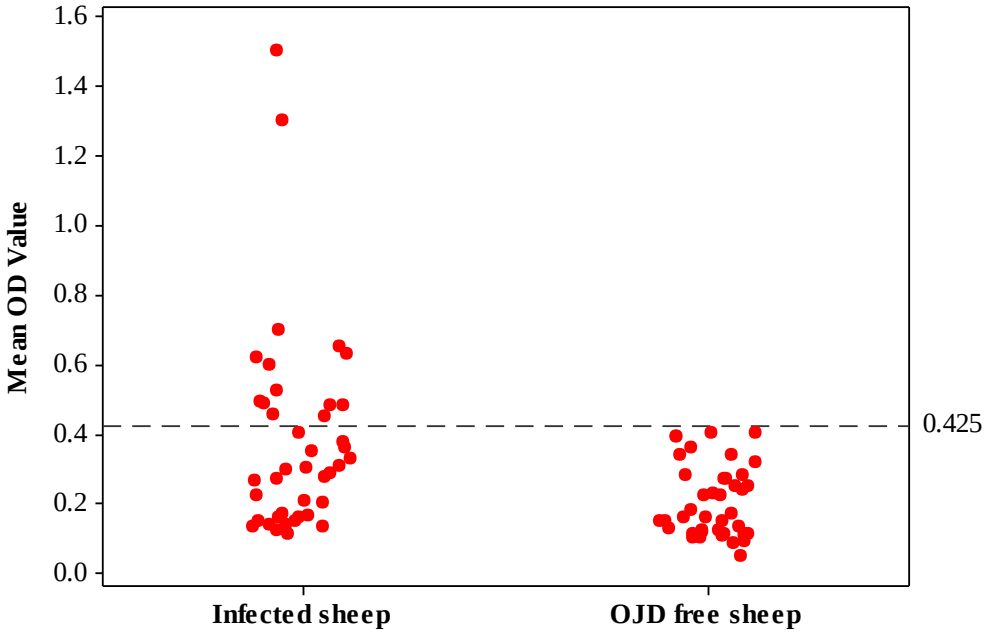

Fig 11 Immunoreactivity of a cocktail of ClpP and MAP0593c antigens to *M. paratuberculosis* infected and free sheep. The value 0.425 indicates an arbitrary cut off to distinguish positive and negative samples.

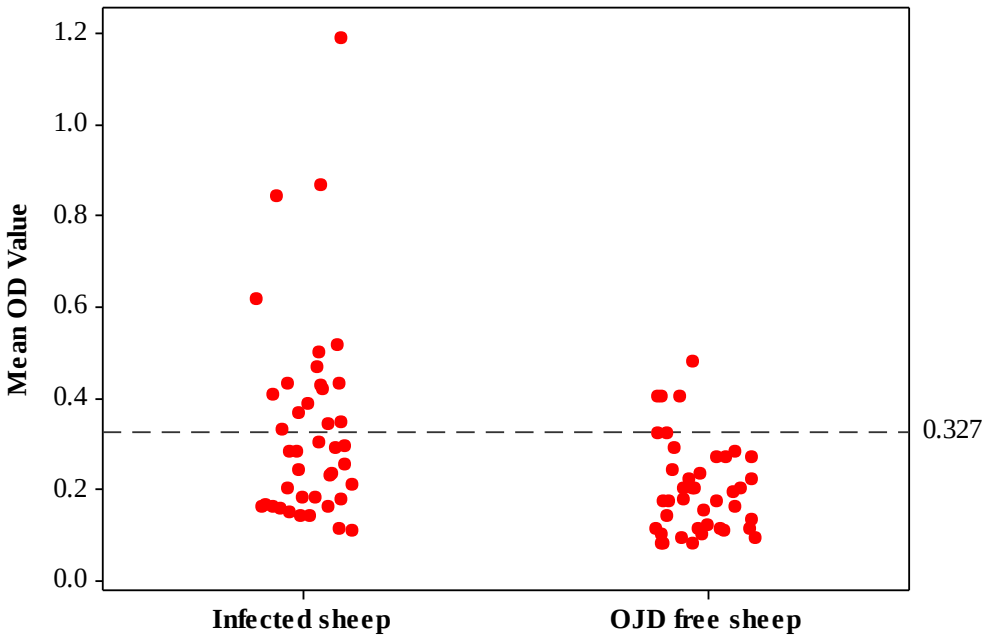

Fig 12 Immunoreactivity of a cocktail of ClpP, MAP0593c, Ppa and GreA antigens to *M. paratuberculosis* infected and free sheep. The value 0.327 indicates an arbitrary cut off to distinguish positive and negative samples.

9.18 Appendix 3B-1 Subprogram 3 Validation of endogenous reference3 genes for expression profiling of RAW 264.7 cells infected with *Mycobacterium avium* subsp. *paratuberculosis* by quantitative PCR

Introduction

The diseases resulting from infections with *Mycobacterium* species contribute a significant burden of global morbidity and mortality in man and animals. Current estimates suggest that in excess of 2 billion people are infected with *Mycobacterium tuberculosis*, the causative agent of tuberculosis, and approximately 3 million people die annually from this disease(Dye et al., 1999). Infections with *M. avium* increasingly are recognized as a cause of morbidity and mortality in humans with acquired immunodeficiency, while *Mycobacterium avium* subsp *paratuberculosis* (*M. ptb*), which is another member of the *Mycobacterium avium* complex (MAC) is responsible for a global epizootic in farmed ruminants (Horsburgh et al., 2001; Kemper et al., 1994; Manning et al., 1998; Petrini et al., 1991; Roos et al., 2001; Stehman, 1996). The pathogenic mycobacteria establish chronic infections and produce broadly similar pathologic changes in a variety of hosts, with granulomatous inflammation being the most common lesion. This pathogenesis is due to their ability to invade and replicate within macrophages, one of the first lines of host defence against invading pathogens(Aderem et al., 1999; Armstrong et al., 1975; Bermudez et al., 1997; Clemens et al., 1995; Russell et al., 1996; Sturgill-Koszycki et al., 1994). In contrast, non-pathogenic mycobacteria are rapidly killed by macrophages.

The identification of genetic elements in pathogen and host that encode virulence-associated factors and genes that are differentially expressed in response to pathogen invasion, respectively, is a major objective of molecular microbiology, as it allows a better understanding of how these factors contribute to pathogenesis in the susceptible host. This is central to developing improved approaches to control, treatment and immunoprophylaxis of these important diseases.

The advent of high-density microarray analysis has allowed researchers to attribute biological significance to differential gene expression patterns between tissue types, disease states, or following biological treatments and this method is being widely used to dissect the host-*Mycobacterium* interaction. However, measurement and validation of changes in expression level of individual genes remains problematic. Quantitative polymerase chain reaction (qPCR) has become the most sensitive technique for the detection of mRNA expression, particularly if present in low copy number, and it is now widely used to validate microarray data and quantify differential gene expression. However, for the latter task, normalization of data is a crucial step that requires critical consideration if data are to be reported in a biologically relevant context and subtle differences in gene expression are to be identified.

A widely used method is to quantify relative changes in gene expression using the $2^{-\Delta\Delta Ct}$ method (Fig. 1), where $\Delta\Delta Ct = (Ct_{\text{Gene of interest}} - Ct_{\text{reference}})_{\text{treated sample}} - (Ct_{\text{Gene of interest}} - Ct_{\text{reference}})_{\text{untreated sample}}$.

This requires normalization of mRNA levels to an internal “housekeeping” or reference gene, and that the amplification efficiencies of the target and reference to be approximately equal (Livak et al., 2001). The expression level of an ideal reference gene should remain constant between the treated and untreated populations under different experimental conditions(Thellin et al., 1999). If the expression of the reference gene is affected by one of the treatments, then normalization to this internal reference gene will lead to inaccurate quantitative results and small differences between genes of interest may be overlooked(Bustin, 2002). Recently, it has become clear that routinely used reference genes like β-actin and *GAPDH* may be inappropriate because their expression levels vary between tissue types and following various biological treatments(Radonic et al., 2004). In one study, following infection of human monocyte-derived macrophages with *Mycobacterium tuberculosis*, β-actin was found by microarray analysis to be up to 2-fold down-regulated 4 hours post-

infection(Wang et al., 2003). A two-fold change is a magnitude considered by many researchers to be indicative of biologically significant alteration in the expression of genes. Such a large change in β-actin would mask changes in genes of interest. Despite this and other accumulating evidence that β-actin and *GAPDH* are regulated in numerous tissue types and following experimental infection of cell lines with viruses (Bustin, 2000; Radonic et al., 2005; Radonic et al., 2004), both continue to be used as reference genes following experimentally induced infection of monocyte-derived macrophages with mycobacteria(McGarvey et al., 2004; Weiss et al., 2002).

There is increasing application of qPCR to the study of mycobacterial pathogenesis, but an evaluation of reference genes for gene expression studies in *Mycobacterium*-infected macrophages has not been performed so far. Therefore we have taken nine commonly used reference genes; *GAPDH*, β-actin, hexose-6-phosphate dehydrogenase (H6pd), TATA Box binding protein (TBP), β2-microglobulin (β2M), RNA polymerase II (RPII), cancer susceptibility candidate 3 (*casc3*), histone H3A, β–glucuronidase (β-glu) and evaluated their suitability as reference genes in the murine monocyte-derived macrophage cell line RAW264.7 following infection with *M. ptb*. We have used the following methods of evaluation for this purpose: BestKeeper – an Excel-based pair-wise correlation tool(Pfaffl et al., 2004); standard deviation (SD) analysis, and; a generalized least squares approach together with a generalized linear model that accounts for all the postulated sources of variation (GLS-GLM). A further aim of this study was to determine whether qPCR-based gene expression evaluation should be performed with samples in triplicate or duplicate with respect to cost and minimization of variability.

Materials and Methods

Bacterial culture

Mycobacterium avium subsp. *paratuberculosis* strain Telford 9.2 (*M. ptb*) was reconstituted from a freeze dried seed stock by adding 0.1 ml of sterile water, inoculating the resulting suspension into a radiometric culture vial (BACTEC 12B, BD) containing egg yolk and mycobactin J and incubating at 37°C for 3 weeks until the Growth Index (GI) reading was 999. The BACTEC vial was subcultured onto modified 7H10 agar slopes supplemented with mycobactin J and incubated at 37°C for 6 weeks until colonies were visible. Bacteria were harvested into 200 µl of PBS plus 0.1% V/V Tween 80 (PBST), vortexed for 1 minute, diluted 1:10 in sterile PBST, passed through a 26 g needle, filtered through an 8 µm filter and examined by light microscopy at x400 magnification to confirm that the majority of cells were single. Viable cells were enumerated using an end point titration method described previously (Whittington et al., 2000). Culture media were described previously(Whittington et al., 2000). *M. ptb* were heat-killed by incubation at 80^{o}C for 1 hour.

Cell Infection

Murine macrophage cells, RAW264.7 (ATCC TIB71), were maintained at 37°C/5% CO_2 in supplemented RPMI 1640 medium (10% fetal calf serum, 0.2 mM L-glutamine). RAW264.7 cells were plated (1 x 10^7 cells/175-cm^2 flask) 2 hours prior to infection and incubated for various times with or without *M. ptb*, heat-killed *M.ptb* or medium alone. The multiplicity of infection (MOI) and time of harvest are shown in Table 1. Cells were harvested by gentle scraping, transferred to a 50 ml tube and centrifuged at 375 xg in a Beckman Coulter Allegra X-12R using a swing out rotor SX4750 for 10 min.

Extraction of RNA from cultured RAW264.7 cells

Total RNA was extracted from 10^7 RAW264.7 cells using 1 ml of Trireagent (Sigma) according to the manufacturer's instructions. RNA quality assessment and quantification were done by visual examination on a 1% non-denaturing agarose gel in Tris-borate-EDTA buffer stained with ethidium bromide and by spectophotometry at 260 nm using an Eppendorf BioPhotometer. After extraction, traces of Trireagent were removed from the total RNA using a G50 sepharose buffer exchange column (Amersham) prior to DNA digestion.

Removal of DNA from total RNA preparations

Contaminating genomic DNA was removed by digestion with 10 µl of RQ1 DNAse (1 U/µl, Promega) at 37^{o}C for 2 hours. Following digestion, nucleotides were removed from the RNA using a G50 sepharose buffer exchange column (Amersham). RNA quality was checked by agarose gel electrophoresis, and removal of DNA was confirmed by qPCR using β-actin primers (Sigma-Genosys) as described below.

cDNA synthesis

25 µg of total RNA and 4 µg of oligo dT (Promega) was made up to a total volume of 50 µl with RNase free water. Samples were heated at 70^{o}C for 5 min and then placed at room temperature for 5 min to anneal the oligo dT. 40 µl of 5x reverse transcriptase buffer (Promega), 8 µl of 25 mM dNTPs (Promega), 1 µl RNaseIn RNAse inhibitor (MBI Fermentas) and 98 µl of H_2O were added and mixed before adding 2 µl of M-MLV reverse transcriptase (RNAse H-point mutant; Promega). The reaction was mixed and placed at 42^{o}C for 1 hour. A further 1 µl of reverse transcriptase was added, and the reaction was incubated for another hour at 42^{o}C. After synthesis, the cDNA was purified using a QIAquick PCR purification kit (Qiagen) to remove free nucleotides. cDNA was eluted in 50 µl QIAquick elution buffer.

Quantitative PCR

Gene-specific oligonucleotide PCR primers (Table 2) were designed using Beacon Designer 4 (Premier Biosoft International) and obtained from a commercial supplier (Sigma-Genosys). Quantitative PCR was performed in an MX3000p Multiplex Quantitative PCR system (Stratagene) using QuantiTect SYBR Green PCR kits (Qiagen). Quantitative PCR reactions were carried out in triplicate in 25 µl reaction volumes containing 300 nM forward and reverse primers and 5 ng template using the following program: 95°C for 15 min, and 40 cycles of 95°C for 20 s, 56°C for 30 s, and 72°C for 30 s with fluorescence acquisition at the end of the 56°C primer annealing step. Sequence-specific standard curves were generated by using serial dilutions of cDNA and the threshold values were noted. The built in amplification-based proprietary algorithm (Stratagene) was used to set the fluorescence threshold value for each primer pair reaction based on the efficiency as determined by standard curve generation. This algorithm determines the portion of the amplification plots where all of the data curves display an exponential increase in fluorescence, and calculates the

threshold value that minimizes the standard deviation in *Ct* values for each replicate set at a point which falls within 5-60% of the fluorescence shift for all the curves. The value of the fluorescence threshold for each primer pair was used to analyze data from experimental reactions. The number of cycles (*Ct*) at which the amplification-corrected normalized fluorescence (dRn) for each reaction crossed the threshold value was exported to Excel (Microsoft), PRISM (GraphPad) and BestKeeper (Pfaffl et al., 2004) and R (http://www.r-project.org/) for further analysis. The specificity of the reaction was checked post-amplification by melt curve analysis.

Variability of technical replicates

24 cDNA samples derived from RAW264.7 cells incubated for 4, 8 or 16 hours with *M. ptb* or medium alone were evaluated using qPCR as described above. Pairs of primers were used to amplify seven genes. The *Ct* values ranged from 17.06 to 29.28. 162 assays were conducted in 96-well plates over several days and each sample was tested in triplicate in each reaction. Decision limits for upper and lower cut off values of the standard deviations of *Ct* values were based on the distribution of the logarithm of the standard deviation values (x = log SD), due to the extreme positive skewed distribution of these values. Values (x) that were further than 3 standard deviations from the mean log-standard deviation were rejected (i.e. if $x > \bar{x} + 3SD_x$ or if $x < \bar{x} - 3SD_x$) for each of the 162 assays. Data for each of the three possible pairs of duplicates were then analysed to determine variability of the replicates and the number of rejected assays based on decision-limit quality control criteria.

Comparison of reference genes

Standard deviation method

Standard deviation (SD) of *Ct* was determined from triplicate reactions (Table 3). Genes producing a SD of greater than 1.0 at any time point were considered to be inappropriate for use as reference genes as this reflects a 2-fold change in expression level.

Bestkeeper method

BestKeeper is an Excel-based pair-wise correlation tool that analyzes variability in the expression of individual genes (SD and coefficient of variation) and generates a weighted expression index in the form of a geometric mean of *Ct* values from several candidate reference genes (Pfaffl et al., 2004) It also determines the Pearson correlation coefficient between expression levels of reference genes.

Evaluation of sources of variation amongst reference genes using a generalized least squares – generalized linear model (GLS-GLM) approach

To determine how the mean reference gene expression level differs we used an alternative approach to analyse all the reference data simultaneously, using a linear model that accounts for all the postulated sources of variation. Namely,

$$y_{ijkl} = \mu + G_i + T_j + H_k + GT_{ij} + GH_{ik} + TH_{jk} + GTH_{ijk} + \varepsilon_{ijkl}$$

where y_{ijkl} = observed *Ct* expression level; μ = overall mean expression level; G_i = effect of reference gene i; T_j = effect of treatment j; H_k = effect of hour k; GT_{ij}, GH_{ik}, TH_{jk}, and GTH_{ijk} are the two- and three-way interaction terms; and ε_{ijkl} = the random error, assumed to be $N(0,\sigma^2_{ijk})$. Allowance is made for different levels of variation across the reference gene - treatment - time combinations (σ^2_{ijk}) by using a generalized least squares (GLS) approach, implemented in R. The statistical

significance of terms in the above model can be evaluated by dropping terms, and calculating the significance using an *F* statistic.

Before considering selection of optimal reference genes, we also need to evaluate patterns in variation of *Ct* values. A more powerful method than standard deviation analysis is to look at the residuals from the model, and investigate systematic changes in the variation of the residuals. Note that in the above model, we allowed the variation in the random errors to change systematically, i.e. $\varepsilon_{ijkl} \sim N(0,\sigma^2_{ijk})$. Since the residuals are a proxy measure of the random errors, then the squared residuals, $res^2_{ijkl} = (y_{ijkl} - \hat{y}_{ijkl})^2$ will on average equal the variance σ^2_{ijk} for the particular gene - treatment - time combination. So we can set up a predictive model relating the res^2_{ijkl} to these terms. This is done by fitting the following generalized linear model (GLM) (Dobson, 2001) using R to these squared residuals, res^2_{ijkl}:

$$\sigma^{-2}_{ijk} = \nu + G_i + T_j + H_k + GT_{ij} + GH_{ik} + TH_{jk} + GTH_{ijk}$$

where σ^{-2}_{ijk} = inverse of the variance for the combination of reference gene *i*, treatment *j* at hour *k*; ν = overall constant (inverse of average variance); with the other terms as defined in the previous model for the raw reference gene data.

Selection of optimal reference genes

Step 1. If each reference gene has a different treatment × time profile, each of these would give a different normalized value to the target genes, when applying the $\Delta\Delta Ct$ method. So how do we select the best one or more reference genes that would minimize these differences? We also need to consider the variation in *Ct* values. Arguably, suitable reference genes would be those where there are no gene × treatment, gene × time, nor gene × treatment × time interactions, so the only effects would be gene, and possibly treatment × time interactions. So the ideal reference genes would be one where the following model fits:

$$y_{ijkl} = \mu + G_i + T_j + H_k + TH_{jk} + \varepsilon_{ijkl}.$$

To assess this model, and more importantly, to assess which reference genes comply with this model, a search over possible subsets of the reference genes can be performed, and the Residual MS used to evaluate the fit.

Note that when applying the $\Delta\Delta Ct$ method, we need to calculate

$\Delta\Delta Ct = (Ct_{\text{Gene of interest}} - Ct_{\text{reference}})_{\text{treated sample}} - (Ct_{\text{Gene of interest}} - Ct_{\text{reference}})_{\text{untreated sample}}$,

And so for the reference HK gene *i*, we need to calculate the difference

$$\Delta Ct_{ikl} = Ct_{\text{reference } i\text{, treated sample, time } k} - Ct_{\text{reference } i\text{, untreated sample, time } k} = y_{i1kl} - y_{i2kl}$$

We would like the variance of this to be as small as possible, for an appropriate choice of the HK gene, and it can be shown that the variance of this can be estimated as $\text{var}(\Delta Ct_{ikl}) = 2 \times \text{Residual MS}$, where the Residual MS is as obtained above.

Step 2. However, if we would like to improve the normalization process by including more than one reference gene, we simply calculate the average over all *g* reference genes,

$$\overline{\Delta Ct}_{kl} = \overline{Ct}_{\text{all } g \text{ reference, treated sample, time } k} - \overline{Ct}_{\text{all } g \text{ reference, untreated sample, time } k} = \bar{y}_{1kl} - \bar{y}_{2kl}.$$

It can be shown that the variance of this is estimated as $\text{var}\left(\overline{\Delta Ct}_{kl}\right) = \frac{2}{g} \times \text{Residual MS}$. The denominator *g* will tend to make the correction more precise as more genes are included, however this may be offset by increases in the Residual MS numerator, due to the inclusion of heterogeneous reference genes. So this measure can provide a basis for optimal selection of reference genes, allowing a resolution of two conflicting influences. Initially, all subsets of size $g = 2$ are assessed calculating $\text{var}\left(\overline{\Delta Ct}_{kl}\right)$ for each, selecting the subset with the smallest value. This step is repeated for larger values of *g* and the optimal subset is obtained when the inclusion of an any additional housekeeper gene leads to an increase in $\text{var}\left(\overline{\Delta Ct}_{kl}\right)$.

Results

To determine the effect of infection with *M. ptb* on the expression of putative reference genes, RAW264.7 cells were infected with *M. ptb* (MOI = 50, *n* = 4, *t* = 4, 8 or 16 hours; MOI = 10, *n* = 3, *t* = 1, 2, 3, 4, 7 days; heat killed *M. ptb* MOI = 10, *n* = 3, *t* = 1, 2, 3, 4, 7 days) or mock infected with medium alone (*n* = 4; *n* = 3; *n* = 3 respectively) and the expression levels of nine commonly used reference genes were determined by qPCR. To evaluate the different transcription levels, the *Ct* values were compared directly using the following three methods: standard deviation of *Ct* analysis; a pair-wise correlation tool called BestKeeper, and; we also developed a GLS-GLM procedure to account for all postulated sources of variation. *Ct*'s were observed directly to ensure that ordering of infected/non-infected samples was not occurring (i.e. uninfected samples having closely matched *Ct*'s, and infected samples having closely matched *Ct*'s distinct from the uninfected *Ct*'s). No ordering was observed during the course of these experiments and therefore expression of the genes tested was not influenced by cell viability.

Evaluating reference genes by standard deviation and raw Ct

An ideal reference gene would have constant expression levels over time and between treatments. At each time point the standard deviation (SD) of *Ct* was determined (Table 3). β-actin, β-2-microglobulin, *GAPDH*, H6PDH and RNA polymerase II (RPII) all had SD greater than 1.0 for at least one time point, indicating a greater than 2 fold change in expression level.

casc3 gave the smallest SD at 4, 8 and 16 hours post-infection, and also over the course of the experiment when measured collectively (Table 3). This reflects its stability over the course of infection with *M. ptb* and is represented graphically in Fig. 2. It was noted that β-actin had a much lower *Ct* value when infected with 50 bacteria per macrophage than with 10 bacteria, reflecting an increased level of transcription under this condition and suggesting that MOI affects the transcription level of some of the reference genes. β-actin transcription varied the most with *Ct*'s ranging from 16.62- 23.45 reflecting almost a 16 fold change in transcription level (Fig. 2). The transcription levels of β2-microglobulin, *GAPDH* and TBP also varied widely and suggest that they are not suitable reference genes in this cell infection model. However the levels of *casc3* transcription remain most unaffected by MOI. Analysis of SD over all periods of infection regardless of multiplicity of infection showed that all the genes except *casc3* had SD of greater than 1, and consequently are not suitable as reference genes. In addition to varied expression over time, H6PDH and RPII also had relatively low expression levels with a Ct of 30 or higher, and were therefore considered to be inappropriate for use as reference genes and were excluded from analysis by BestKeeper and GLS-GLM. Most genes in the cell infection model had *Ct*'s between 20 and 30.

Evaluating reference genes using BestKeeper

In addition to analyzing raw *Ct* data and standard deviation alone as a means to measure variability of reference gene expression, we evaluated genes using an Excel-based variation and pair-wise correlation tool called BestKeeper. The output is given in Table 4.

BestKeeper highlighted *casc3* as the reference gene with least overall variation from the list of seven genes, with an SD of 0.65, which represents a 1.57 fold change in expression (Table 4). Values for standard deviations were slightly different to those generated in Excel or Prism.

The variation in expression of the other reference genes was greater than 2-fold in each case (SD greater than 1.0), and when all 7 genes are used to generate an index it results in a BestKeeper SD [± x-fold] of 2.16 which is of lesser value than using *casc3* alone. The Pearson correlation coefficient generated by BestKeeper for each gene combination is shown in Table 5. These values suggest that the expression of all the reference genes appears to increase or decrease in parallel, although *casc3*, beta-glucuronidase, tbp and hisH3A appear most closely linked (Table 5).

If we use the three most stably expressed genes (*casc3*, *GAPDH* and beta-glucuronidase) to generate a BestKeeper index, the standard deviation of the BestKeeper index is reduced to 0.89 resulting in a fold change of 1.85 over all time points (Table 6). This is an improvement on using all seven reference genes, and the correlation between each gene and the BestKeeper index is increased to 0.93, 0.899 and 0.925 respectively. However, normalizing to the geometric mean of three genes in this case would lead to greater variability of the fold-change of the sample than if normalizing to *casc3* alone.

Evaluating reference genes using a generalized linear model

The generalized linear model enabled an evaluation of the sources of variation amongst reference genes to take account of all the experimental data on genes and treatments over time. There were overall significant differences in mean *Ct* levels across the gene - treatment - time combinations (F = 370, $P < 0.0001$). More importantly, no simplification of the three factor model was possible, as the three way interaction was significant (F = 11.98, $P < 0.0001$), implying that the *Ct* expression level pattern depends on the combination of gene, treatment and time effects.

As in the case of the actual reference gene expression values, there were significant differences in the variation in reference gene levels across the gene - treatment - time combinations (F = 9.86, $P <$ 0.001), and again there were significant three-way interactions (F = 4.29, $P < 0.001$) indicating no reduction in model complexity could be achieved. That is, the pattern of variation about the mean depended on the particular combination of gene, treatment and time.

The significant interactions of treatment and time with the reference gene indicated that a different normalization would result from different choices of reference genes. Using the approach outlined in the Methods for deciding on the optimal reference gene(s), the following results were obtained (Table 7). Step 1 reveals the model for *casc3* would be expected to produce the best normalization, in terms of the smallest variance of the ΔCt values. Step 2 shows the effect of adding a second reference gene (i.e. including *casc3* in each average). However, the variance for any of these 2-reference gene average models was higher, indicating a poorer normalization would be expected. This is in agreement with the data generated using BestKeeper

The effects of using an unsuitable reference gene

To determine how detrimental the effects of normalization to an unsuitable reference gene can be, we used relative quantitation to analyze the expression of two genes known to be induced in RAW264.7 cells following phagocytosis of *Brucella abortus*: *gadd45b* and *fas* (Eskra et al., 2003). RAW264.7 cells were incubated with *M. ptb* for 8 hours or with medium alone and the levels of *gadd45b* and fas analyzed by qPCR. Each gene was normalized individually to either *casc3*, β-actin

or *GAPDH*. fas expression was moderately induced in RAW264.7 cells following infection with *M. ptb* and the value generated depended on which reference gene was used for normalization. fas was up-regulated by 2.37-fold ($P < 0.0001$ (unpaired *t*-test)) when normalized to *casc3*, 2.18-fold when normalized to β-actin ($P = 0.001$) and 1.98-fold when normalized to *GAPDH* ($P = 0.006$) (Fig. 3a). Due to the moderate induction of fas, each normalization produced a significant change. However when the change in expression is less than 2-fold, as in the case of *gadd45b* (Fig. 3b) (1.39-fold when *casc3* normalized ($P = 0.002$), 1.27-fold when β-actin normalized ($P = 0.145$) and 1.13 when *GAPDH* normalized ($P = 0.400$)) the significance of the fold-change when normalized to casc3 is lost if normalized to the other genes. This would result in the data being interpreted as "no change in expression", when in fact there has been a significant induction that may have biological relevance. This example of normalization to inappropriate reference genes substantiates recent data from other researchers working on alternative immortal cell lines who have also found that normalization to un-verified reference genes results in non-significant data (Dheda et al., 2005). The SD of *casc 3 Ct* over 8 hours was 0.38, and consequentially a fold change of greater than 1.3-fold (i.e. $2^{0.38}$) would be the minimum change one could reliably measure using this reference gene at this given time point. However, given the greater variability of *casc3* over all periods of infection (SD=0.84), a more conservative estimate of greater than 1.8-fold ($2^{0.84}$) may be the minimum change one could reliably measure using this reference gene. The fold change one is prepared to endorse as potentially biologically significant would depend on how confident one needs to be in the outcome, and perhaps whether confirmatory analyses are possible. Selecting a 1.8 fold cut-off when using casc3 acknowledges that 30% of the time the normal variation in casc3 (i.e. > 1.8-fold) would potentially mask changes in genes of interest. A more stringent cut-off might be set at a 3.2-fold ($2^{2\times0.84}$) change, which would only include about 5% false positives.

Variability of technical replicates

A further aim of this study was to determine whether qPCR-based gene expression evaluation should be performed with samples in triplicate or duplicate to determine the benefits from minimization of cost versus maximization of precision of the assay. We wanted to know what the cut off for rejection of an assay should be and how this would affect the cost to our laboratory. All assays were performed in triplicate, consisting of three wells of technical replicates per template/primer combination. Using the data from 162 assays generated from 24 cDNA samples derived from RAW264.7 cells incubated for 4, 8 or 16 hours with *M. ptb* or medium and seven primer sets (*GAPDH*, β-actin, TBP, β-2M, *casc3*, hisH3A and β-glu) we formed decision limits for upper and lower cut off values of the standard deviations of *Ct* for replicates based on the convention of 3 standard deviations (SD_x) from the mean log SD of the *Ct* values, $\bar{x} \pm 3SD_x$. Log SD values (x) were approximately normally distributed. Using this formula, we determined an upper decision limit of 0.513 and a lower decision limit of 0.005 for log SD of *Ct* (Table 8). We then analyzed each of our triplicates (1, 2 and 3) as duplicates of (1, 2), (2, 3) and (1, 3), respectively. The precision of the estimate was slightly higher for triplicate data ($SD_x = 0.78$) compared to duplicate data (0.90 to 0.95). We then looked at how many of these tests would have been rejected from analysis based on the decision –limit criteria. We found that none of the triplicate assays and 11, 10 and 2 of the duplicate assays would have been rejected and thus require retesting due to having an SD of less than 0.005. None of the assays had an SD of greater than 0.516, in fact, only 6, 2 and 3 assays of duplicates had an SD of greater than 0.2 (data not shown). Therefore if the 162 assays had been performed in duplicate, a maximum of 11 would have required repeating. The conduct of 162 assays in duplicate requires the use of 324 wells, as opposed to 486 in triplicate, a 'saving' of 162 wells. If were added the 11 assays that needed to be repeated an extra 22 wells would be required, leading to an overall saving of 140 wells. Our current reagent costs are AU$1.40 per 25 µl assay, leading to a saving of AU$196 in reagents in this example, not including the cost of preparing template cDNA from experimental samples, and with little cost to precision of the assay.

Discussion

In this study we used several analytical methods to determine the most appropriate candidate to use as a single normalization gene in quantitative PCR using the murine macrophage cell line RAW264.7 infected with *Mycobacterium avium* subsp*. paratuberculosis*. We evaluated various multiplicities and periods of infection by direct SD analysis of *Ct*, a spreadsheet calculator "Bestkeeper" and a GLS-GLM procedure.

We found that all approaches generated the same outcome from this data set; that *casc3* showed the greatest stability in expression over the course of cell infection with various multiplicities and periods of infection, and was most suitable for normalization of quantitative PCR data when using a single gene. All the other commonly used reference genes analysed here showed variability in expression of greater than 1 SD in *Ct* when all the treatments and time points were considered, reflecting a >2-fold change in expression, suggesting unsuitability as reference genes in this cell infection model.

The simplest method for comparing and selecting reference genes was the evaluation of the SD and plotting of *Ct*'s, allowing gross differences in expression by treatment to be easily seen. It also allowed a visual determination of correlation in expression between the different genes. However this approach may be applicable mainly for simple data sets such as the one presented here. The GLS-GLM method would have greater application for complex data where simple trends are less apparent and interactions between experimental parameters likely. Using this method we found significant differences in both the means levels and variation about the means in reference gene levels across the gene - treatment - time combinations, where the pattern of variation depended on the particular combination of the three factors.

There is some discussion in the literature that normalization to multiple reference genes may be preferable to single gene normalization (Vandesompele et al., 2002). The use of BestKeeper allowed us to conveniently determine correlations between the expression levels of genes to select those that we may use in combination as an index for normalization, and generate the weighted expression index (the Bestkeeper index) to use in the normalization. However, the most closely correlated genes in our model were also some of the most variable, and so a decision has to be made on how to select genes for use in multi-gene normalization. Removing the most variable genes from the BestKeeper index and normalizing to the geometric mean of the three most stable genes, *casc3*, *GAPDH* and b-glu, reduced variation but still led to greater variability of the fold-change of the sample than if normalizing to *casc3* alone, as *GAPDH* and b-glu had expression levels that varied to 2-fold. Thus, using the geometric mean of three or more reference genes may generate spuriously normalized data generated from fluctuations in expression of single genes. Therefore it is preferable to normalize to one gene that shows minimum variation in expression. We suggest that high correlation is not a good reason to maintain highly variable genes in the normalization calculation. Minimum variability should be chosen over correlation. It has been suggested that three genes are the minimal necessary number for a good performance of qPCR analysis (Vandesompele et al., 2002), however normalization to multiple reference genes requires additional resources and depending on the experimental system, may not be necessary.

The copious amount of gene expression data that is being generated by microarray studies is widening the opportunity to select and validate multiple reference genes in particular systems before proceeding to qPCR analysis. However, it is important to validate and select a suitable reference gene for each experimental model, system or tissue under investigation, to begin reliable experiments with hypothesis driven questions, and not to select a reference gene solely on its historical use or frequency of reporting in the literature. For example, *GAPDH* has been cited at least 17 times since 2005 as a reference gene, compared to only twice for *casc3* (PubMed search conducted 8/5/06), when the latter is far superior in the experimental cell infection model used in the

present study. Several genes have been well documented in the literature as reference genes for expression analysis, however work has recently been published on the unsuitability of some of these genes in some models and tissues (Aerts et al., 2004; Dheda et al., 2004; Dheda et al., 2005; Hamalainen et al., 2001; Radonic et al., 2005; Radonic et al., 2004; Rodriguez-Mulero et al., 2005; Schmittgen et al., 2000).

The purpose of normalization using a reference gene/s is to minimize the error associated with any given experiment. The importance of selecting an appropriate reference gene was highlighted when we deliberately used inappropriate reference genes, *β-actin* and *GAPDH*, to analyze the expression of two genes, *fas* and *gadd45b,* known to be induced in RAW264.7 cells following phagocytosis of *Brucella abortus*. This demonstrated that a test for significance of the fold-change in expression when using variable reference genes may result in data being interpreted as 'no change in expression', when even a slight, but biologically significant induction may have relevance.

Dheda *et al.* (Dheda et al., 2005) raised the important question of whether a given fold change, although statistically significant, is meaningful if the variability of the reference gene is itself similar to that given fold change. This is an important issue that needs to be taken into consideration when choosing a reference gene for comparative quantitation, and should influence the decision on what constitutes a genuine alteration in expression.

A further aim of our study was to determine whether qPCR-based gene expression evaluation should be performed with samples in triplicate or duplicate with respect to cost and minimization of variability. We chose the decision-limit using 3 standard deviations (SD_x) from the mean of x = log SD to set our upper and lower decision limits for SD of replicates, based on the approximate normality of log SD.. This would accommodate > 99% of observations and highlight true outliers; the decision–limit is an arbitrary value and is user dependent. Using this method we found that performing assays in duplicate resulted in adequate precision. Based on the objective decision-limit criterion, less than 7% of assays performed in duplicate would have needed to be repeated leading to significant savings on resources compared to triplicate tests.

In conclusion, *casc3* is appropriate for use as a reference gene in RAW264.7 cells during infection with *Mycobacterium avium* subsp. *paratuberculosis,* when measuring fold-changes of greater than 1.8-fold. GAPDH, β-actin, hexose-6-phosphate dehydrogenase, TATA Box binding protein, β2-microglobulin, RNA polymerase II (RPII), histone H3A and β –glucuronidase were unsuitable for this purpose. Based on the results of this study we suggest the following approach. To select a reference gene we recommend performing a pilot experiment with all time and treatment combinations represented and determine the level of expression of at least six putative reference genes, with all samples tested in duplicate (technical replicates). Select the reference gene displaying least variation among experimental groups/time points using a graphical display (such as Figure 2) or based on lowest overall SD (calculated for each gene over all treatment-time combinations). The use of coefficient of variation is not required as variation is not generally dependent on the magnitude of *Ct.* for complex data sets we recommend use of the GLS-GLM procedure, where all sources of variation can be assessed and allowed for. Next, define decision-limits for quality control of replicate assays: log transform the data for the chosen reference gene(s), calculate the mean and SD of the x = log SD of the replicates, calculate $\bar{x} \pm 3SD_x$ and back transform these limits. When an actual assay is conducted, reject an assay where the SD of the technical replicates exceeds the decision-limit, and retest. To assess the significance of fold changers in gene expression using $\Delta\Delta Ct$, ensure that the fold change exceeds a pre-defined value chosen based on knowledge of variation i9n the reference gene(s). For example, where overall SD of the reference gene is 1.8 fold, changes smaller than this in a gene of interest would be unlikely to be indicative of differential expression.

References

Aderem, A., Underhill, D.M., 1999, Mechanisms of phagocytosis in macrophages. Annu Rev Immunol 17, 593-623.

Aerts, J.L., Gonzales, M.I., Topalian, S.L., 2004, Selection of appropriate control genes to assess expression of tumor antigens using real-time RT-PCR. Biotechniques 36, 84-86, 88, 90-81.

Armstrong, J.A., Hart, P.D., 1975, Phagosome-lysosome interactions in cultured macrophages infected with virulent tubercle bacilli. Reversal of the usual nonfusion pattern and observations on bacterial survival. J Exp Med 142, 1-16.

Bermudez, L.E., Parker, A., Goodman, J.R., 1997, Growth within macrophages increases the efficiency of Mycobacterium avium in invading other macrophages by a complement receptor-independent pathway. Infect Immun 65, 1916-1925.

Bustin, S.A., 2000, Absolute quantification of mRNA using real-time reverse transcription polymerase chain reaction assays. J Mol Endocrinol 25, 169-193.

Bustin, S.A., 2002, Quantification of mRNA using real-time reverse transcription PCR (RT-PCR): trends and problems. J Mol Endocrinol 29, 23-39.

Clemens, D.L., Horwitz, M.A., 1995, Characterization of the Mycobacterium tuberculosis phagosome and evidence that phagosomal maturation is inhibited. J Exp Med 181, 257-270.

Dheda, K., Huggett, J.F., Bustin, S.A., Johnson, M.A., Rook, G., Zumla, A., 2004, Validation of housekeeping genes for normalizing RNA expression in real-time PCR. Biotechniques 37, 112-114, 116, 118-119.

Dheda, K., Huggett, J.F., Chang, J.S., Kim, L.U., Bustin, S.A., Johnson, M.A., Rook, G.A., Zumla, A., 2005, The implications of using an inappropriate reference gene for real-time reverse transcription PCR data normalization. Anal Biochem 344, 141-143.

Dobson, A.J., 2001, An Introduction to Generalised Linear Models, 2 EditionLondon.

Dye, C., Scheele, S., Dolin, P., Pathania, V., Raviglione, M.C., 1999, Consensus statement. Global burden of tuberculosis: estimated incidence, prevalence, and mortality by country. WHO Global Surveillance and Monitoring Project. Jama 282, 677-686.

Eskra, L., Mathison, A., Splitter, G., 2003, Microarray analysis of mRNA levels from RAW264.7 macrophages infected with Brucella abortus. Infect Immun 71, 1125-1133.

Hamalainen, H.K., Tubman, J.C., Vikman, S., Kyrola, T., Ylikoski, E., Warrington, J.A., Lahesmaa, R., 2001, Identification and validation of endogenous reference genes for expression profiling of T helper cell differentiation by quantitative real-time RT-PCR. Anal Biochem 299, 63-70.

Horsburgh, C.R., Jr., Gettings, J., Alexander, L.N., Lennox, J.L., 2001, Disseminated Mycobacterium avium complex disease among patients infected with human immunodeficiency virus, 1985-2000. Clin Infect Dis 33, 1938-1943.

Kemper, C.A., Havlir, D., Bartok, A.E., Kane, C., Camp, B., Lane, N., Deresinski, S.C., 1994, Transient bacteremia due to Mycobacterium avium complex in patients with AIDS. J Infect Dis 170, 488-493.

Livak, K.J., Schmittgen, T.D., 2001, Analysis of relative gene expression data using real-time quantitative PCR and the 2(-Delta Delta C(T)) Method. Methods 25, 402-408.

Manning, E.J., Steinberg, H., Rossow, K., Ruth, G.R., Collins, M.T., 1998, Epizootic of paratuberculosis in farmed elk. J Am Vet Med Assoc 213, 1320-1322, 1280-1321.

McGarvey, J.A., Wagner, D., Bermudez, L.E., 2004, Differential gene expression in mononuclear phagocytes infected with pathogenic and non-pathogenic mycobacteria. Clin Exp Immunol 136, 490-500.

Petrini, B., Svahn, A., Julander, I., Kallenius, G., Ostlund, L., 1991, Prevalence of mycobacterium avium complex infection in AIDS patients. Scand J Infect Dis 23, 511-512.

Pfaffl, M.W., Tichopad, A., Prgomet, C., Neuvians, T.P., 2004, Determination of stable housekeeping genes, differentially regulated target genes and sample integrity: BestKeeper--Excel-based tool using pair-wise correlations. Biotechnol Lett 26, 509-515.

Radonic, A., Thulke, S., Bae, H.G., Muller, M.A., Siegert, W., Nitsche, A., 2005, Reference gene selection for quantitative real-time PCR analysis in virus infected cells: SARS corona virus, Yellow fever virus, Human Herpesvirus-6, Camelpox virus and Cytomegalovirus infections. Virol J 2, 7.

Radonic, A., Thulke, S., Mackay, I.M., Landt, O., Siegert, W., Nitsche, A., 2004, Guideline to reference gene selection for quantitative real-time PCR. Biochem Biophys Res Commun 313, 856-862.

Rodriguez-Mulero, S., Montanya, E., 2005, Selection of a suitable internal control gene for expression studies in pancreatic islet grafts. Transplantation 80, 650-652.

Roos, F., Flepp, M., Figueras, G., Bodmer, T., Furrer, H., 2001, Clinical manifestations and predictors of survival in AIDS patients with disseminated Mycobacterium avium infection. Eur J Clin Microbiol Infect Dis 20, 428-430.

Rulten, S.L., Ripley, T.L., Hunt, C.L., Stephens, D.N., Mayne, L.V., 2006, Sp1 and NFkappaB pathways are regulated in brain in response to acute and chronic ethanol. Genes Brain Behav 5, 257-273.

Russell, D.G., Dant, J., Sturgill-Koszycki, S., 1996, Mycobacterium avium- and Mycobacterium tuberculosis-containing vacuoles are dynamic, fusion-competent vesicles that are accessible to glycosphingolipids from the host cell plasmalemma. J Immunol 156, 4764-4773.

Schmittgen, T.D., Zakrajsek, B.A., 2000, Effect of experimental treatment on housekeeping gene expression: validation by real-time, quantitative RT-PCR. J Biochem Biophys Methods 46, 69-81.

Stehman, S.M., 1996, Paratuberculosis in small ruminants, deer, and South American camelids. Vet Clin North Am Food Anim Pract 12, 441-455.

Sturgill-Koszycki, S., Schlesinger, P.H., Chakraborty, P., Haddix, P.L., Collins, H.L., Fok, A.K., Allen, R.D., Gluck, S.L., Heuser, J., Russell, D.G., 1994, Lack of acidification in Mycobacterium phagosomes produced by exclusion of the vesicular proton-ATPase. Science 263, 678-681.

Thellin, O., Zorzi, W., Lakaye, B., De Borman, B., Coumans, B., Hennen, G., Grisar, T., Igout, A., Heinen, E., 1999, Housekeeping genes as internal standards: use and limits. J Biotechnol 75, 291-295.

Vandesompele, J., De Preter, K., Pattyn, F., Poppe, B., Van Roy, N., De Paepe, A., Speleman, F., 2002, Accurate normalization of real-time quantitative RT-PCR data by geometric averaging of multiple internal control genes. Genome Biol 3, RESEARCH0034.

Wang, J.P., Rought, S.E., Corbeil, J., Guiney, D.G., 2003, Gene expression profiling detects patterns of human macrophage responses following Mycobacterium tuberculosis infection. FEMS Immunol Med Microbiol 39, 163-172.

Weiss, D.J., Evanson, O.A., Moritz, A., Deng, M.Q., Abrahamsen, M.S., 2002, Differential responses of bovine macrophages to Mycobacterium avium subsp. paratuberculosis and Mycobacterium avium subsp. avium. Infect Immun 70, 5556-5561.

Whittington, R.J., Reddacliff, L.A., Marsh, I., McAllister, S., Saunders, V., 2000, Temporal patterns and quantification of excretion of Mycobacterium avium subsp paratuberculosis in sheep with Johne's disease. Aust Vet J 78, 34-37.

Table 1: Cell infection kinetics

	Medium alone	*M. ptb*	*Medium alone*	*M. ptb*	***H-K M. ptb***
Number of flasks	4	4	3	3	3
Multiplicity of Infection	-	50	-	10	10
%infected cells[a]	□	>80	0	>40	>40
Measuring point	4h, 8h,16h	4h, 8h,16h	1d, 2d, 3d, 4d, 7d	1d, 2d, 3d, 4d, 7d	1d, 2d, 3d, 4d, 7d

[a] Determined as cells containing >1 acid-fast bacilli per macrophage following Ziehl Neelsen staining; 1d=24h, 2d=48h, 3d=72h, 4d =96h, 7d=168h; H-K = heat killed.

Table 2: Primers used in this study

Primer name	*Gene*	*Sequence (5'-3')*	**Amplification efficiency %**
Q5Bglu	β-glucuronidase	TAGAGGTGATGGAGGAGCTG	104.9
Q3Bglu		GGTTTCAGAGCAGAGGAAGG	
Q5B2M	β2-microglobulin	GGAAGCCGAACATACTGAACTG	100.9
Q3B2M		TTTCCCGTTCTTCAGCATTTGG	
Q5h6pdh	hexose-6-phosphate dehydrogenase	GCCAGAGGAGCTGATCTCTAAG	95.4
Q3h6pdh		GACAGTGCCAGGTGGAACTT	
Q hisH3	H3 histone, family 3A	CGTGAAATCAGACGCTATCAGA	104.6
Q3hisH3		AGCAATTTCTCGCACCAGAC	
Q5TBP	TATA box binding protein	CCCTTCACCAATGACTCCTAT	101
Q3TBP		CCAAGATTCACGGTAGATACAATA	
Q5RPII	RNA polymerase II	GACTCACAAACTGGCTGACAT	101.3
Q3RPII		TACATCTTCTGCTATGACATGGG	
Q5mln51[a]	cancer susceptibility candidate 3/metastatic lymph node 51	CTGCCTTGTCTTTTGCAGTA	100.8
Q3mln51[a]		TGCAAGTACAGGAGCAGAAT	
Q5gapdh	glyceraldehyde-3-phosphate dehydrogenase	CAATGTGTCCGTCGTGGATC	99.7
Q3gapdh		AGCCCAAGATGCCCTTCAG	
Q5b-actin	β-actin	GGCTATGCTCTCCCTCACG	99.2
Q3b-actin		CACGCTCGGTCAGGATCTT	

Q5 denotes forward primer, Q3 denotes reverse primer.
[a] (Rulten et al., 2006). All other primers designed during this study.

Table 3: Standard deviation of reference gene expression levels during *M. ptb* infection of RAW 264.7 cells

Time	*n*	*β-act*	*β-glu*	*β-2M*	*Casc3*	*GAPDH*	*H6PDH*	*hisH3A*	*RPII*	*TBP*
4 h	8	1.35	0.63	1.13	0.54	1.45	1.58	0.91	1.81	0.89
8 h	8	0.46	0.29	0.51	0.38	0.43	0.70	0.45	0.65	0.35
16 h	8	0.73	0.66	0.67	0.54	0.57	1.04	0.75	0.76	1.35
1 d	9	0.29	0.47	1.13	0.73	0.49	[c]	0.66	[c]	0.52
2 d	7[a]	0.54	0.61	1.35	0.69	0.46	[c]	0.82	[c]	0.73
3 d	9	0.42	0.53	0.51	0.44	0.48	[c]	0.52	[c]	0.66
4 d	9	0.70	0.58	0.59	0.41	0.51	[c]	0.67	[c]	0.75
7 d	9	0.39	0.62	0.56	0.43	0.47	[c]	1.96	[c]	1.50
Combined times	67	1.64	1.35	1.56	0.84	1.23	2.70[b]	2.13	2.62[b]	2.49

Table shows SD of Ct values during various periods of infection with *M. ptb*.
[a] 2 samples were excluded from analysis due to RNA degradation; [b] *n*=24. [c] not available: expression was too low (*Ct*=40-45) to be reproducibly measured in these samples. Time shown in hours except: 1d=24h, 2d=48h, 3d=72h, 4d =96h, 7d=168h

Table 4: Output from BestKeeper: Seven gene analysis

	β-act	*β-glu*	*β-2M*	*Casc3*	*gap*	*his*	*tbp*	**BestKeeper index**
n	67	67	67	67	67	67	67	67
GM [CP]	22.42	24.37	21.80	26.43	20.32	22.58	27.29	23.49
AM [CP]	22.48	24.41	21.86	26.45	20.36	22.67	27.40	23.53
min [CP]	18.80	22.13	19.23	24.71	17.72	19.05	22.90	20.77
max [CP]	25.80	27.25	26.61	28.86	23.12	29.82	32.18	26.15
SD [± CP]	1.30	1.11	1.33	0.65	1.01	1.69	2.00	1.11
CV [% CP]	5.76	4.53	6.08	2.47	4.97	7.47	7.29	4.72
min [x-fold]	-12.27	-4.73	-5.94	-3.30	-6.07	-11.53	-20.90	6.58
max [x-fold]	10.43	7.36	28.02	5.37	6.96	151.46	29.74	6.33
SD [± x-fold]	±2.45	±2.15	±2.51	±1.57	±2.02	±3.23	±3.99	±2.16

Abbreviations: GM [CP], geometric mean of *Ct*; AM [CP], arithmetic mean of Ct; min [CP] and max [CP], upper and lower *Ct* values; SD [CP], standard deviation of *Ct*; CV, coefficient of variance expressed as percentage; min and max [x-fold], upper and lower values of expression levels expressed as absolute x-fold over or under coefficient; SD [± x-fold], standard deviation of the absolute regulation coefficients ((Pfaffl et al., 2004))

Table 5: Pearson correlation coefficients from BestKeeper: seven gene analysis

vs.	*β-act*	*β-glu*	*β2m*	*casc3*	*GAPDH*	*hisH3A*	**TBP**
β-glu	0.831	-	-	-	-	-	-
β2m	0.494	0.44	-	-	-	-	-
casc3	0.715	0.81	0.518	-	-	-	-
GAPDH	0.879	0.749	0.483	0.753	-	-	-
hisH3A	0.794	0.749	0.704	0.834	0.784	-	-
TBP	0.77	0.871	0.663	0.847	0.719	0.876	-
BestKeeper Index vs.coeff. of corr. [r]	0.893	0.876	0.722	0.875	0.865	0.946	0.942

Table shows repeated pair-wise correlation analysis and correlation analysis of candidate reference genes. Genes are pair-wise correlated one with another and then with the BestKeeper index (n = 7).

Table 6: Output from BestKeeper: Three gene analysis

	β-glu	*casc*	*GAPDH*	**BestKeeper**
n	67	67	67	67
geo Mean [CP]	24.37	26.43	20.32	23.57
ar Mean [CP]	24.41	26.45	20.36	23.59
min [CP]	22.13	24.71	17.72	21.39
max [CP]	27.25	28.86	23.12	25.58
std dev [± CP]	1.11	0.65	1.01	0.89
CV [% CP]	4.53	2.47	4.97	3.75
min [x-fold]	-4.73	-3.30	-6.07	4.54
max [x-fold]	7.36	5.37	6.96	4.02
std dev [± x-fold]	2.15	1.57	2.02	1.85

GM [CP], geometric mean of *Ct*; AM [CP], arithmetic mean of *Ct*; min [CP] and max [CP], upper and lower *Ct* values; SD [CP], standard deviation of *Ct*; CV, coefficient of variance expressed as percentage; min and max [x-fold], upper and lower values of expression levels expressed as absolute x-fold over or under coefficient; SD [± x-fold], standard deviation of the absolute regulation coefficients.

Table 7: The effect of adding a second reference gene

	$2/g \times$ Residual MS	
Gene	Step 1	Step 2
β-actin	412.5	285.6
β-glu	725.5	304.7
β2M	149.6	157.5
casc3	87.2	Included
GAPDH	1073.6	521.7
hisH3A	678.2	414.2
TBP	164.3	203.3
Action	Include casc3	Stop

Step 1 reveals *casc3* produces the best normalization, in terms of the smallest variance of the ΔCt values. Step 2 shows the effect of adding a second reference gene, including *casc3* in each average. The variation measure ($2/g \times$ Residual MS) for any of these 2- reference gene average models is higher, indicating a poorer normalization.

Table 8: Selection of decision limits for technical replicates

Technical replicates	**x = *log* SD**		x_U	x_L	**S D_U**	**S D_L**	***analysed***	***rejected***
	$\bar{x}$	***S D_x***						
1, 2, 3	**-3.002**	**0.778**	**-0.668**	**-5.336**	**0.513**	**0.005**	**162**	**0**
1, 2	**-3.172**	**0.944**	**-0.339**	**-6.005**	**0.713**	**0.002**	**151**	**11**
2, 3	**-3.287**	**0.902**	**-0.579**	**-5.994**	**0.560**	**0.002**	**152**	**10**
1, 3	**-3.093**	**0.950**	**-0.243**	**-5.943**	**0.784**	**0.003**	**160**	**2**

Decision limits for upper and lower cut off values of the standard deviations of *Ct* based on the standard use of 3 standard deviations (SD_x) from the mean log SD of the *Ct* values, $\bar{x} \pm 3SD_x$.

Abbreviations: $x_U = \bar{x} + 3 \times SD_x$; $x_L = \bar{x} - 3 \times SD_x$; $SD_U = e^{x_U}$ = upper decision limit for SD of *Ct*; $SD_L = e^{x_L}$ = lower decision limit for SD of *Ct*.

Fig. 1. Example of relative quantitation by ΔΔCt analysis. Example of qPCR data showing amplification curves of an invariant reference gene and a test gene in untreated and treated samples. The reference gene amplification in untreated and treated samples have the same *Ct*, demonstrating its invariant expression under these conditions. The difference in expression between the reference genes in each sample are known as Δ*Ct* (dotted arrows). The difference between the Δ*Ct*'s gives the ΔΔ*Ct* (solid arrows). The ΔΔ*Ct* in this example is 1*Ct*, indicating a 2-fold change in expression of this gene after treatment.

Key: *Ct* = point at which curve crosses the fluorescence threshold; Δ*Ct* = difference in *Ct* between test gene and reference gene for each sample; ΔΔ*Ct* = difference in Δ*Ct* between experimental samples (treated) and calibrator samples (untreated).

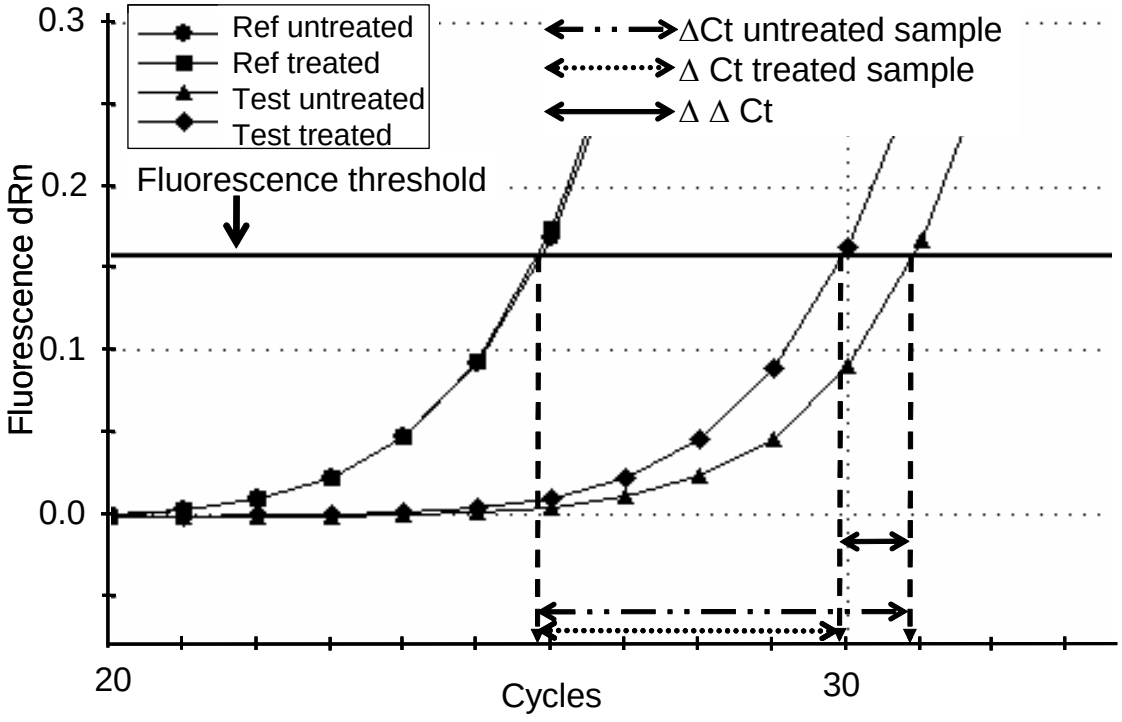

Fig 2: Expression of casc3 in RAW264.7 cells is most stable over various multiplicities of infection and infection times. Plots show the RNA transcription of the tested reference genes in absolute Ct values over a 7 day infection of RAW264.7 cells with M. ptb. Infected and un-infected data are shown. Bars indicate mean Ct.

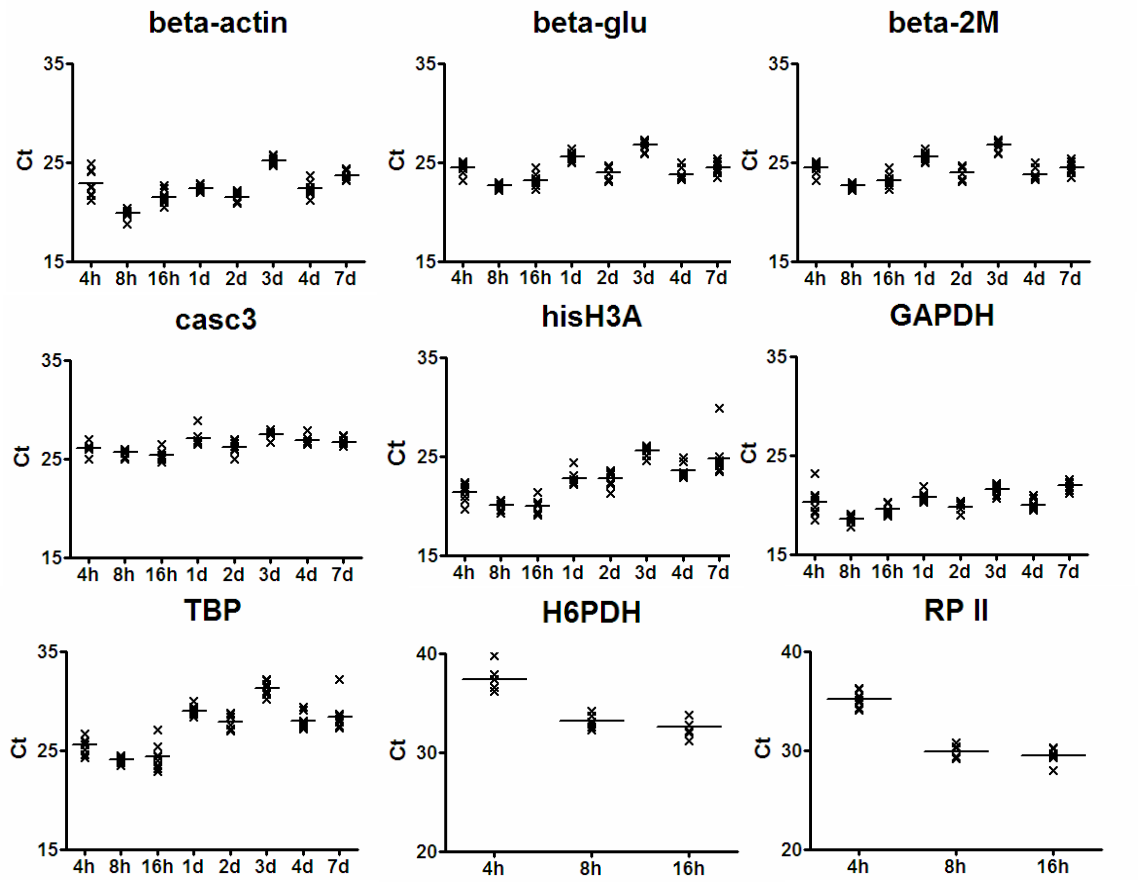

Fig 3: Expression of phagocytosis-inducible genes in RAW264.7 cells following infection with *M. ptb* normalized to inappropriate reference genes.

A. Expression of *fas* in RAW264.7 cells following incubation with *M. ptb* for 8 hours normalized either to a stable reference gene, *casc3*, or the less stable genes, β-actin and *GAPDH* (n=4); *P* values (unpaired t-test): casc3 *P*=1.89E-06; β-actin *P*=0.001; GAPDH *P*=0.006. B. Expression of *gadd45b* in RAW264.7 cells following incubation with *M. ptb* for 8 hours normalized either to a stable reference gene, *casc3*, or the less stable genes, β-actin and *GAPDH* (n=4). *P* values (unpaired t-test): casc3 *P*=0.002; β-actin *P*= 0.145; GAPDH *P*=0.400. Error bars show SD.

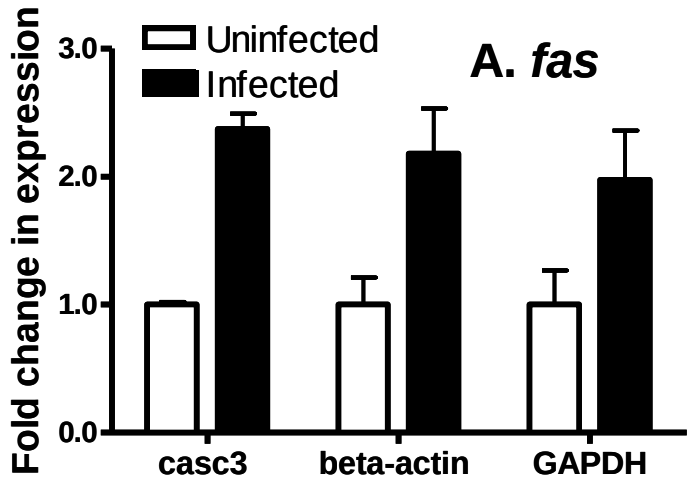

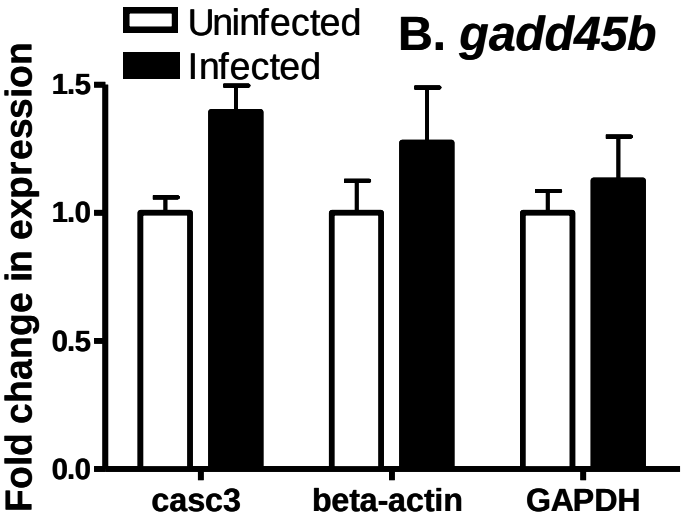

9.19 Appendix 3B-2 Subprogram 3 Identification of differentially expressed genes in the gut of Mptb infected sheep and the identification of a suitable ovine reference gene for gene expression analysis.

Introduction

Mycobacterium paratuberculosis (*Mptb*) causes a chronic progressive wasting disease in sheep known as ovine Johne's disease (OJD). A large number of organisms are typically found within the gut in chronically infected animals. Lesions develop in the gut wall and these contain epitheloid macrophages and giant cells and there is a general thickening of the mucosa (24, 38). The changes occurring following infection at the molecular level have not been well characterised in sheep. Most of the data on the molecular pathogenesis of the disease has come from studies in other species such as cattle (1-3, 5), or from macrophage infection models (12, 13, 17, 29-31).

There have been an increasing number of cytokines, cell markers and other molecules identified that have made a significant impact on our understanding of the host response to infection. New technologies that allow analysis of genes that alter in response to infection will no doubt provide a more complete view of the disease and allow the analysis of pathways that are regulating host responses. Given that the sheep genome has not been fully annotated it is difficult to perform large scale studies which require the use of known genes. Techniques that do not require previous knowledge of gene sequences are thus advantageous. There are needs for effective ways of identifying all genes that are differentially expressed in different cell types or under altered or diseased conditions. Differential display PCR (DD-PCR) (20), representational difference analysis (RDA) (15, 16, 36), serial analysis of gene expression (SAGE) (35) and cDNA microarray analysis (9, 27) are well established tools for studying differentially expressed genes under normal and altered/diseased conditions. These approaches all stem from the same origin; differential screening and differential hybridisation.

Additionally, there are currently few "reference" genes available for use in gene expression studies in ovine infection models. Reference genes are needed for meaningful study using QPCR to verify gene expression data acquired by other methods, for example microarray analysis and DD-PCR. GAPDH is one of the most common reference genes used, however it has been shown to be variable in different models of infection suggesting that it is not the best gene to use. Ideally researchers should be using genes known to be consistently expressed in their infection model and the tissue/sample they are examining. As a result, DD-PCR has been applied to discover more suitable reference genes in the ovine ileum, and in this case for gene expression studies in *Mptb* infected sheep.

Aims

Section 1 - To find a suitable reference gene for gene expression analysis in the ovine terminal ileum.

Section 2 - To identify differentially expressed genes in the ileum of naturally infected sheep.

Materials and Methods

Animals

Sheep were obtained from two separate properties in NSW, Australia. On the first, OJD.028, previously unexposed female Merino sheep were co-grazed with sheep infected with *M. paratuberculosis* for 14.5 weeks. After 2.5 years, animals were euthanized and sampled. Sheep from the second property, OJD.031A, were naturally exposed and 3 years of age. Tissue from the terminal ileum and associated lymph node was collected at the time of slaughter for all animals and stored at -80C until required. The Johne's disease status of the animals was determined by histopathology (Perez lesion grade) and culture of intestinal tissues (Table 1) (26, 37).

Table 1. Infection status of animals analysed by DD-PCR and QPCR

OJD 028 animal #	Infection status	OJD 031A animal #	Infection status
E22	Control	981	Control
A41	Control	982	Control
F31	Control	983	Control
A47	Control	991	Control
C33	Control	988	infected (pauci, 3a)
C3	infected (pauci, 3a)	989	infected (pauci, 3a)
B9-2	infected (pauci, 3a)	985	infected (pauci, 3d)
A14	infected (pauci, 3a)	992	infected (pauci, 3d)
H53	infected (pauci, 3a)	986	infected (multi, 3b)
H61	infected (pauci, 3a)	990	infected (multi, 3b)
I5	infected (pauci, 3a)		
A3	infected (multi, 3b)		
I34	infected (multi, 3b)		
J55	infected (multi, 3b)		
D68	infected (multi, 3b)		

RNA extraction

Total RNA was extracted using the Mini RNeasy extraction kit (Qiagen) according to the manufacturer's instructions from 30mg of homogenized, frozen tissue (Ultra Turrax, IKA). RNA was eluted in 40µl of RNase free water and stored at -80^{o}C until required. Quality assessment and quantification of the RNA was done by visual examination on a 1% non-denaturing agarose gel in Tris-borate-EDTA buffer stained with ethidium bromide, and spectrophotometry at 260 nm using an Eppendorf BioPhotometer.

DNA removal

The RNA sample (40 µl) was treated with 10 units RQ1 DNAase (Promega) at 37ºC for 2 hours in a total volume of 100 µl to remove any contaminating DNA. The RNA was precipitated by the addition of 0.5 µg linear acrylamide (Ambion), 10µl 3M sodium acetate, pH 5.3 (Sigma) and 300 µl of 100% ethanol and incubation for 30 minutes at -80ºC. RNA was harvested by centrifugation (16,000 xg, 30 min, 4ºC). The RNA was air dried and resuspended in 25µl RNase free water (Ambion) with RNase

Inhibitor (25U MBI Fermentas). Free nucleotides and sodium acetate were removed using a G50 sepharose buffer exchange column (Amersham) according to the manufacturer's instructions. RNA was quantified by spectrophotometry at A_{260} using an Eppendorf BioPhotometer and quality determined by visualization following gel electrophoresis as described above. The RNA samples were tested for residual DNA contamination by QPCR (Stratagene MX3000*p*) with ovine ß2-microglobulin primers using the following conditions: 2x ABgene PCR master mix (12.5µl), 100pmol/µl (0.5µl) of each primer, template (0.5µl), Rnase free water (11µl) in a total volume of 25µl. Cycling conditions were: 95^0C 15 mins ; 95^0C 30 sec, 56^0 C 30 sec, 72^0C 30 sec for 40 cycles; and 1 cycle at 72^0 for 5 mins. A positive control of ovine intestinal cDNA was included. A negative result confirmed that the RNA sample was free of DNA contamination.

cDNA synthesis

Up to 25 µg total RNA and 4µg oligo dT (Sigma-Genosys) was made up to a total volume of 50µl with RNase Free water (Ambion). Samples were heated at 70ºC for 3 minutes, placed on ice for 2 minutes and centrifuged briefly to collect the sample. cDNA was synthesised by the addition of 40 µl 5x MMLV buffer (Promega), 8 µl 25mM dNTP's (Promega), 1 µl RNAse inhibitor (40U, MBI Fermentas), 99 µl water and 1µl MMLV (200U/µl, Promega). Samples were mixed and incubated at 42ºC for 1 hour. Another 1 µl of MMLV was added and incubated at 42ºC for a further 1 hour. The reverse transcriptase was inactivated by heating to 75^oC for 10 minutes. The cDNA was precipitated with 0.5 µg linear acrylamide, 20 µl 3M sodium acetate, pH 5.3 (Sigma) and 600 µl of 100% ethanol and incubation for 30 minutes at -80ºC. cDNA was harvested by and centrifugation (16,000 xg, 30 min, 4ºC). The supernatant was removed and the RNA air dried and resuspended in 25µl RNase free water (Ambion) with RNaseIN (25U MBI Fermentas). Free nucleotides, oligo dT and sodium acetate were removed using a G50 sepharose buffer exchange column (Amersham) according to manufacturers instruction. cDNA was quantified at A_{260} using an Eppendorf BioPhotometer.

Long distance DD-PCR

DD-PCR was performed according to the Delta Differential Display kit (Clontech) using KlenTaq LA Taq polymerase (0.4 µl, Clontech) and 10ng cDNA labelled with α35S-dATP (0.12MBq/reaction, Amersham) and cycled in a PXE-2 thermal cycler (Thermo Hybaid) with arbitrary and anchor DDPCR primers listed in Table 2. In each experiment cycling conditions were as follows: 1 cycle of 94^0C 5 min, 40^0C 5 min, 68^0C 5 min; 2 cycles of 94^0C 30 sec, 40^0C 30 sec, 68^0C 5 mins; 23 cycles of 94^0C 20sec, 60^0C 30 sec, 68^0C 2 min; 1 cycle of 68^0C 7 min. 5 µl of the PCR product was combined with 5 µl of loading buffer, denatured by heating to 94°C for 2 min and 4 µl resolved by electrophoresis (Sequencing System S3S T-Rex Vertical Gel Running Apparatus, Medos) on a 5% polyacrylamide/8 M urea gel in 0.5x TBE buffer.

Electrophoresis was performed at 2300V (~60W) for 3hr or until the xylene cyanol dye migrated through the entire gel. The gel was removed from the electrophoresis apparatus by transfer onto Whatman paper and dried under vacuum (SG210D Integrated SpeedGel Slab Gel dryer, Thermo Electron) at 74°C for 35–40 min. DD-PCR products were visualised by exposure to BMR X-ray film (Kodak) at –70°C overnight in a Kodak film cassette.

Table 2. Primers used in long distance PCR reactions for differential display analysis

Primer name	Direction	Primer Sequence 5'-3'
T1	anchor	CATTATGCTGAGTGATATCTTTTTTTTTAA
T2	anchor	CATTATGCTGAGTGATATCTTTTTTTTTAC
T4	anchor	CATTATGCTGAGTGATATCTTTTTTTTTCA
T5	anchor	CATTATGCTGAGTGATATCTTTTTTTTTCC
T6	anchor	CATTATGCTGAGTGATATCTTTTTTTTTCG
T7	anchor	CATTATGCTGAGTGATATCTTTTTTTTTGA
T9	anchor	CATTATGCTGAGTGATATCTTTTTTTTTGG
P1	arbitrary	ATTAACCCTCACTAAATGCTGGGGA
P2	arbitrary	ATTAACCCTCACTAAATCGGTCATAG
P3	arbitrary	ATTAACCCTCACTAAATGCTGGTGG
P4	arbitrary	ATTAACCCTCACTAAATGCTGGTAG
P5	arbitrary	ATTAACCCTCACTAAAGATCTGACTG
P6	arbitrary	ATTAACCCTCACTAAATGCTGGGTG
P8	arbitrary	ATTAACCCTCACTAAATGGAGCTGG
P10	arbitrary	ATTAACCCTCACTAAAGCACCGTCC

Cloning and sequencing of putative reference and differentially expressed amplified gene products

Differentially expressed products were identified by visual examination of autoradiograms. Bands were located and excised by overlaying the x-ray film onto the dried gel using radioactive markings for alignment. Bands were excised from the dried acrylamide gel and DNA extracted by boiling in 40 µl of TE for 5 minutes. Products were re-amplified from 7 µl of extracted DNA using the appropriate primer combination and cycled as described above but without the addition of α35S-dATP. PCR products were resolved by electrophoresis on a 0.5% non-denaturing agarose gel in Tris-borate-EDTA buffer stained with ethidium bromide to confirm amplification, excised, and purified using a PCR extraction kit (Qiagen). The TOPO TA Cloning Kit (Invitrogen) was used to clone products into the pCR2.1 vector. Five to ten clones were selected from each ligation reaction and analyzed for the presence of an insert using restriction enzyme digestion with *Eco*RI (MBI Fermentas). Restriction analysis of the inserts was performed with *Mse*I (MBI Fermentas). If more than one digestion profile was obtained for a group of clones, each clone representing a different digestion profile was selected for sequencing and QPCR. Plasmid DNA was purified from bacterial cultures using the Qiagen mini-prep plasmid kit (according to manufactures instructions) and quantified at A_{260} using an Eppendorf BioPhotometer**.** Approximately 500ng of plasmid DNA from each positive DD-PCR clone and 6.4pmol of the sequencing primer (M13 forward or M13 reverse) were submitted to the Australian Genome Research Facility (AGRF) Brisbane, Australia for sequencing. Sequencing results were submitted to the NCBI nucleotide database (GenBank) for identification using various BLAST algorithms (Altschul *et al*, 1990).

QPCR Primer design

Primers were designed using Beacon Designer 4 (Premier Biosoft) and synthesized commercially (Sigma-Genosys) (Tables 3 and 4). Sequences for genes previously identified as putative reference genes; GAPDH, PPIA, β2M and β-actin (Radonic *et al*, 2004), were obtained from the NCBI Genbank database. QPCR primers were optimised using 300 or 600 nM final concentration using the Quantitect SYBR green assay (Qiagen) generating standard curves over a range of 0.1ng to 100 ng of template and generated efficiencies in the range of 95-109%.

Table 3 QPCR primer sequences designed for putative reference genes

Gene	5' primer	3' primer
Identified through differential display		
HK 1.4	GCCGCCAGTGTGCTG	CTCAGTAAACTCTGTTTTCTTGG
	*AGCTCGGATCACTAGTACGG	*ATCCATCCACCCAGCATTTAG
HK 2.1	CGGAGCGGTGTTGTAGC	CCCCACTTACAGCACTGC
	*TCCTACTTCTGTGCCCATCTG	*ACAACACCGCTCCGTCTG
HK 3.1	AAACACATAGAATATCTAACATGAAAC	CAGAACTAGGACTTTATCAGAAAC
HK 4.5	TGAAGAGAGACAGGCAGATG	ATGTTTTGGCTATGTTTAGTCATAG
HK 4.6	ACAGGAGGGTGGCATGG	TGGTGATTGTGGTCAAGGG
HK 5.1	TTAACAAAGTGGGAGAAAGATACC	TAACATGCCATAGTGCCTTTATG
HK 5.5	ATGAGTGTGGCGGAACC	CAGACTAGATTCCATGACAATTAC
	*AGACCCTCTTTATTATTTATAATACGC	*GTAAGGTAGCATCGACAATTAATAC
HK 6.3	AATTAGTTTTGTGTGGTCTGTCC	ACTAAATGCTGGTAGGAAATGAC
HK 7.2	CTTCTGTAGCCTTCAAAACTG	GGCTTATTAACCCTCACTAAAGC
HK 8.4	GAGCAGATTCACAGAATAGACC	GCATGTGGGCCTCATCC
	*TGCTGCTGCCGGAAGG	*GGCTTATTAACCCTCACTAAAGC
HK 10.1	TCCGCTATGGGTTAATCATCC	ATTCCATAAATTATACAGGGTAATGTG
	*ATGGCTGTATCAACTATGAAGAG	*ACAATCTCCCACAAGGAAGG
Previously used as a reference gene		
GAPDH	TTCCAGTATGATTCCACCCATG	GCCTTTCCATTGATGACGAG
B-Actin	CAT CCT GAC CCT CAA GTA CC	TCG TTG TAG AAG GTG TGG TG
PPIA	TGAGCACTGGAGAGAAAGGATTTG	AGTCACCACCCTGGCACATAA
B2M	CTGCTGTCGCTGTCTGGA	CAGTTCAGGTAATTTGGCTTTCC

* second set of primers designed if first set failed to amplify product or produced inefficient reactions.

Table 4. QPCR primer sequences for putative differentially expressed genes

Gene	5' Primer Sequence	3' Primer Sequence
Derived from lymph node 028 animals		
B1.2/2.3	GTTAGTAATCAAGTTGCCAGACC	CCCAAAGTTCACAAAGCAGTAC
B2.2	GCCATGCTGCCTGTGTC	TAAATGGAGCTGGGCTTGC
Derived from terminal ileum 028 animals		
B3.1	GCTTGGAGCCTGGAATCTC	CAACTATGTGGAAGAGGACTATTC
B3.3	GATCTGCTGCCTTCTGAGG	CGGGGCGGTGAGTCC
B4.1	AATGGCACTCTGATTAAACTGC	TTCTGGGTGGGACGACAG
B4.2*	GGGCACAACAGACAATCG	CGGACAGGTCGGTCTTG
B4.4	AACATATAGGAAAGCAAGTAGGAC	CACAAAATCCAGATCCACGAC
B5.1*	ATTGATTCTTTGAACCTTGATGAG	AGACGCTTGAGCCAGTTG
B7.1	CCTGGAAGATAGAGAGGTAAAC	CTAGTTAGCTTTAACCACTTGAG
B8.1*	GTACTCCTCTTGGTGTTCTGG	CCGTCCGCCCCAAAGG
B8.2*	AGTCTGGGAAGGCTTGGAG	GCGAACAACGTGAAATGGG
B8.3*	TTCTCTATGACAATCTCCGACTG	ACAAAGGATGCCCTCTAATGG
B9.1	CGTTATGAAGGAAAGGAGAACC	TTTGGTAGTAGCTTTTGAGGATG
B9.4	GTACCATAACCAAGGATTGAACC	AATTCCCATGTGGTCCAGTG
B10.1*	CCACAAAACAATCGCTCCTTC	GGGACAAGAACAAGAACAATACC
B10.2*	CTGTTCACTAAGTACCAGAAGG	ACGCCAAGTCTGACAGTG
B10.3	CTGTTCGCAGAATTACATCTTC	TGACATAAAGGAAGTGGTGAC
B11.1	ATTGTGTATTTTGAAGGTGTTATG	GGTGTTAAACAAAGAGGTAGC
B11.4	AGTCCCTGTGAATGAGAATTTAG	TAGGCTAAGAGATGTGACCAG
Derived from terminal ileum 031 animals		
PB1.1	TCCCCTAACACAGCACATAG	GCACAGCAGGAAGAAGTTAC
PB1.2	TTATTAAATTGGCTGCTTCAAAAG	CTTAGCTCCCCGACCAG
PB2.2	CGCAGACCTCGGATGATG	ACTGGGAGCCTGAGATTCC
PB3.1	TGACTACCTAGAGCAAAACCC	GCAGGCTGTGTGTGTCC
	[1]ACCGTTCCCAGTGTCAAGG	GCGGCGTGCTCGTAGG
PB3.2	ATTATCATTTCCTTCCTTTACTTCTG	TCGCAACATACAACAGAGTAAC
PB4.3/5.4	CTCCATTCCATTAACAGTCAGG	GATCTCACTATTCCGTTGCC
PB5.1	CTATGCCTCAGAGTAACTAAGC	GCAGTGGCTTCTCTTGTTG
	[1]AGAGTCTGCCTGCCAATGC	GCTCAGTAGTTGTGGTGCTTG
PB6.4	GGAGAACTCGGTTGGGAAAG	CCCTCAGACCCACACTGG
PB6.5	GTGAATGGGTCTAAAAGAGAAGG	GAGTGGGGAGGGTCTACG
PB7.4*	CTTATTAACCCTCACTAAAGCAC	TTTCAACCACCCTGAGAGC
PB7.6*	ACAGTAATGACATTCAAGATTTCTC	TCACTAAAGCACCGTCCAG

*primers did not amplify product therefore not examined by QPCR [1]Primers were redesigned in an attempt to overcome difficulties in low expression.

Determination of reference genes by standard deviation analysis

Standard deviation (SD) of Ct was determined from duplicate reactions using 1ng of cDNA generated from 6 infected and 4 exposed culture negative animals. Genes producing a SD of greater than 1.0 were considered to be inappropriate for use as reference genes, reflecting a 2-fold change in expression level.

Gene expression analysis by QPCR

QPCR reactions were performed in 25µl volumes using Quantitect SYBR green kit (Qiagen) according to the manufacturer's instructions. Forward and reverse primers were used at a final concentration of 300nM or 600nM. All reactions were run in duplicate. Real Time QPCR data was collected using the Mx3000*p* software version 3.0 (Stratagene). The efficiency of the amplification reactions was verified by generating standard curves over a range of 0.1 ng to 100 ng of cDNA template. An efficient reaction, which is one that exactly doubles the number of DNA molecules per cycle, would have an efficiency of 100%. All QPCR assays that generated efficiencies in the range of 95-109% were considered acceptable for this study.

Comparative quantification of transcripts between groups of sheep was undertaken using the 2^{-ddCt} method (Livak et al, 2001) following normalization to the reference gene HK 5.1 (similar to *B. taurus* splicing factor arginine/serine-rich 6) isolated during this study (see results). The level of expression of a gene of interest expressed as Ct was estimated by subtracting from it the Ct value for the reference gene to yield Delta Ct. The differences in levels of expression for a given gene between groups of sheep based on Delta CT were examined using restricted maximum likelihood (REML) in a linear mixed model (GenStat Release 10.1 2007, Lawes Agricultural Trust, Rothamsted Experimental Station). Sheep were grouped according to one of four histopathological outcomes following exposure: unaffected, early paucibacillary, late paucibacillary or multibacillary; group was included as a fixed effect while property of origin was included as a random factor in the model. Significance was assessed at the 99% level. The significance of differences between predicted means of groups were calculated in Excel (Microsoft) using a t test, applying the standard error of the difference for each pair of predicted means from the REML analysis, at the 95% level. The DeltaDeltaC(t) ($2^{-\Delta\Delta Ct}$) method was used to determine relative gene expression fold changes of each treatment group relative to the unaffected group (22) using the predicted means, and these data were illustrated graphically with the 95% confidence interval calculated for the difference between the predicted means.

Results

Identification of an ovine reference gene

Long distance DD-PCR was used to identify putative ovine ileal reference genes by selecting bands that remained unchanged in autoradiograms between the control and *Mptb* infected animals in the OJD.031A group, according to the density of bands. Nine bands, designated HK1-HK8 and HK10, were identified that remained apparently unchanged between uninfected and infected animals (Fig 1). The bands were re-amplified by PCR and cloned as described (Fig 2, Table 5). 5-10 clones from each ligation reaction were selected for restriction analysis with *Mse*I (NEB) to determine if more than one digestion profile was present as DD-PCR can generate heterogeneous sequences within apparently individual bands. Two restriction profiles appeared to be present for HK4 and HK5, and a single clone representing each unique insert was selected for sequencing and QPCR (designated HK4.5, HK4.6, HK5.1 and HK5.5 respectively). A single digestion profile was obtained for the other seven HK clones, and one clone from each ligation was selected for sequencing and QPCR.

Following sequencing, the putative identity of the 11 clones was determined by discontiguous megablast searches of the non redundant nucleotide database, GenBank (Table 6). Most of the

sequences isolated had homology with known bovine or human sequences; however one sequence, HK 7.2, had no homology to any sequence in the GenBank database. QPCR primers were designed for the 11 ovine sequences, optimized and gene expression analysis was performed using tissue samples from the ten OJD.031A sheep to determine the most stably expressed gene in ovine ileum. No expression of HK1, HK2, HK3.4, HK5.5 or HK7 could be detected in ovine ileum using 10ng of cDNA template. Additional primer sets to some of these sequences were designed in an attempt to overcome this (Table 3). However gene expression failed to be detected again suggesting these genes are expressed at levels too low to be detected by QPCR in ovine terminal ileum. Expression of HK4.5 could be detected at low levels, however the QPCR reaction was of low efficiency therefore not quantifiable by QPCR and was not progressed further. The remaining seven assays were analysed in addition to four previously reported reference genes. These genes included GAPDH, beta-actin, PPIA (peptidylprolyl isomerase A) and beta2-Microglobulin (Radonic et al, 2004). Tissue samples from eight OJD.028 sheep were used to analyse the expression of the previously reported reference genes in ovine ileum. QPCR analysis indicated that the seven putative reference genes identified by DDPCR and the previously reported reference genes were abundantly expressed in the ileum (Table 6).

The genes which were considered to be the most appropriate reference genes were those whose expression varied least between-animal, that is had the lowest standard deviation of cycle threshold (Ct). HK 5.1 (SD 0.43), HK 10.1 (SD 0.52) and PPIA (SD 0.6) had the lowest variation among the genes tested. Overall HK 5.1, which has homology with the bovine splicing factor (arginine/serine-rich 6), was the least variable, had a mid-range mean Ct value of 24 and was deemed most suitable for use as a reference gene (Table 6). GAPDH and ß-actin showed the highest variation in expression across the samples, followed by ß2-microglobulin and HK4.6. It is clear from the high variation amongst the previously reported reference genes that routinely used reference genes like β-actin and GAPDH may be inappropriate because their expression levels can vary between tissue types and following various biological treatments. If gene expression data are to be reported in a biologically relevant context and subtle differences in gene expression are to be identified, the use of a suitable stably expressed reference gene is a critical consideration.

Figure 1. Long Distance DD-PCR gels showing ovine reference gene bands selected for isolation from the ileum of control and infected animals

Lanes 1-4 represent control animals, lanes 5-10 represent infected animals, lane 11 is the negative control and lane 12 is the positive control (ovine ileum tissue (028)).

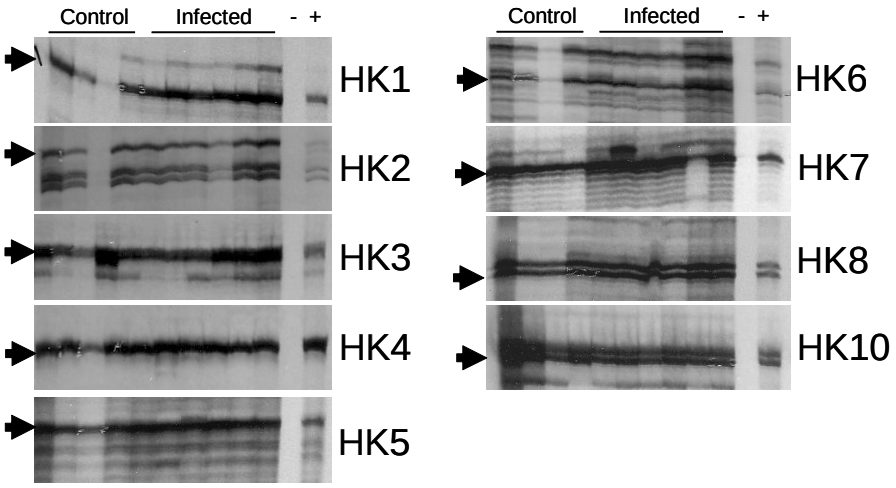

Figure 2. Re-amplification of potential reference genes from DD-PCR bands
Lane M contains GeneRuler 1kb DNA ladder (MBI fermentas).

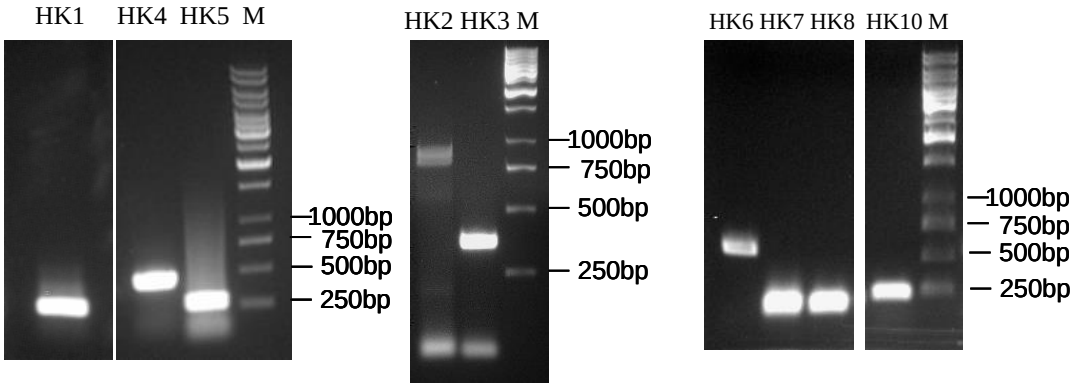

Table 5. Bands isolated from differential display gels of terminal ileum

Band	5' primer	3' primer	PCR Product size (kb)
HK1	P6	T1	250
HK2	P2	T7	850
HK3	P2	T1	350
HK4	P4	T6	480
HK5	P4	T5	300
HK6	P4	T9	600
HK7	P10	T4	200
HK8	P10	T5	200
HK10	P3	T6	250

Table 6. Identification of putative reference genes in terminal ileum of 031 animals by nearest homology

Clone	GenBank homologue	Species	Identities	GenBank #	QPCR results		
					Av Ct	St dev	N=
DD-PCR band							
HK 1.4	Similar to 30kDa protein	Bovine	172/183 (93%)	NM_001035056	No expression		
HK 2.1	PREDICTED: Bos taurus similar to SM-20(egl nine homolog 1)	Bovine	131/135 (97%)	XM_613709	No expression		
HK 3.1	Similar to homeobox protein Meis2	Bovine	308/308(100%)	NM_001076175	25.7	0.85	10
HK 4.5	Jagged 1	Human	382/397 (96%)	BC098393	Not determined		
HK 4.6	Predicted: Similar to synapse associated protein 102	Bovine	380/397 (95%)	XM_586942	29.6	1.2	10
HK 5.1	Splicing factor arginine/serine-rich 6	Bovine	207/216 (95%)	NM_001035272	23.7	0.43	10
HK 5.5	PREDICTED: Pan troglodytes titin (TTN) mRNA[a]	Chimp	12/31 (38%)[a]	XR_025598	No expression		
HK 6.3	catenin (cadherin-associated protein), alpha 1,	Human	440/555 (79%)	NM_001903	25.3	0.98	10
HK 7.2	no homology				No expression		
HK 8.4	ATPase H+ transporting lysosomal 31kDa, V1 subunit E isoform 1	Bovine	129/134 (96%)	BT021530	23.2	0.67	10
HK 10.1	Myosin, light peptide 6, alkali smooth muscle and non-muscle,	Bovine	177/188 (94%)	BC103428	20.4	0.52	10
Previously reported							
GAPDH	Glyceraldehyde-3-phosphate dehydrogenase	Ovine		AF035421	30.0	1.23	8
B-Actin	B-Actin	Ovine		U39357	26.7	1.68	8
PPIA	Peptidylprolyl isomerase A	Ovine		AY251270	24.1	0.60	8
B2M	B2-microglobulin	Ovine		AY549962	23.6	1.04	8

Identified by discontiguous megablast search of non-redundant nucleotide database
Predicted sequences refer to homology predicted by automated computational annotation of the genome
[a] Identified by blastx search of non-redundant nucleotide database
10 animals in 031 and / or 8 animals in 028 were tested

Identification of differentially expressed genes by Long distance DD-PCR in the ileum and lymph nodes of M. ptb infected animals

Long distance DD-PCR

Long distance DD-PCR was used to identify potentially differentially regulated genes in ovine ileum by selecting bands in autoradiograms that appeared to be either present/absent or more/less abundant between control and *Mptb* infected animals, according to the density of the bands. Using multiple combinations of arbitrary and anchor DDPCR primers, eleven differentially regulated bands appeared to be discernable when comparing control and infected animals from group OJD.028 (Figure 3a). Five exposed, but uninfected culture negative animals were used as control animals, and ten animals with a confirmed *M. ptb* infection comprised the infected population. The infected animals were further sub-classified into two groups on the basis of histological lesions according to the Perez classification, into multibacilliary or 3b (4 animals), and early paucibacilliary or 3a (6 animals) infection. Bands 1 and 2 were isolated from lymph node using primers P8 and T5, and Bands 3 to 11 were identified in ileum tissue using five primer combinations (Table 7). In this study, only genes isolated from the ileum were validated by QPCR due to the lack of a suitable reference gene for lymph node at this time.

A further 7 bands from potentially differentially regulated genes were found when comparing the ileum tissue from of a second group of animals, Trial OJD 031A, with additional combinations of arbitrary and anchor DDPCR primers (Table 7, Figure 3b). This population of animals comprised 4 exposed, uninfected animals and 6 animals with confirmed *M. ptb* infection. Again, the infected group was further sub-classified according to histopathology into multibacilliary or 3b animals (2 animals), early paucibacilliary or 3a (2 animals) and late paucibacilliary or 3d animals (2 animals). The primers and the sizes of the amplicons obtained when DNA purified from these 18 differentially regulated bands was reamplified are listed in Table 7.

Figure 3 Differential Display gels showing bands identified as differentially expressed between uninfected and infected animals

a) Bands isolated from the OJD.028 animals. B1 and B2 are lymph node samples, B3-11 are ileum samples b) bands isolated from the ileum of OJD.031A animals. Arrow heads indicate the differentially expressed bands isolated for identification.

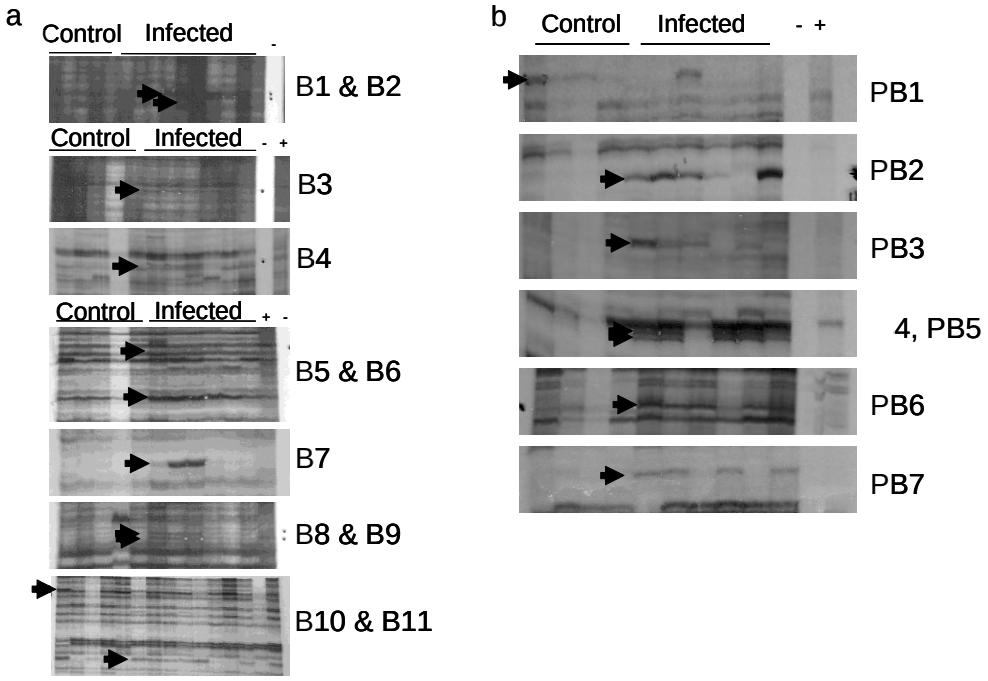

Table 7. Bands isolated by Long Distance DD-PCR from the lymph node or terminal ileum

Band Name	5' primer	3' primer	Tissue source	PCR Product (~kb)	Gel Number
B1	P8	T5	Lymph node	630	12
B2	P8	T5	Lymph node	635	12
B3	P8	T5	Terminal ileum	700	12
B4	P6	T4	Terminal ileum	1200	11
B5	P5	T2	Terminal ileum	750	8
B6	P5	T2	Terminal ileum	700	8
B7	P5	T2	Terminal ileum	400	8
B8	P3	T2	Terminal ileum	700	7
B9	P3	T2	Terminal ileum	650	7
B10	P1	T2	Terminal ileum	1400	6
B11	P1	T2	Terminal ileum	800	6
PB1	P4	T7	Terminal ileum	350	23
PB2	P2	T7	Terminal ileum	550	25
PB3	P6	T1	Terminal ileum	550	26
PB4	P6	T1	Terminal ileum	395	26
PB5	P6	T1	Terminal ileum	400	26
PB6	P6	T5	Terminal ileum	1100	26
PB7	P10	T2	Terminal ileum	250	28

Following excision, bands were re-amplified by PCR and cloned into pCR2.1 for analysis as described. Re-amplification of the bands by PCR is shown in Figure 4. 5. The B6 gene was unable to be cloned into pCR2.1 despite multiple attempts. Ten clones from each ligation reaction were selected for restriction analysis with *Mse*I (NEB) to determine if more than one digestion profile was present. Where more than one profile was present a single clone representing that profile was submitted for sequencing. Three restriction profiles were present for B8 and B10, designated B8.1-B8.3, and B10.1-B10.3 respectively. Two restriction profiles appeared to be present for B2 (2.2, 2.3), B3 (3.1, 3.3), B4 (4.1, 4.4), B9 (9.1, 9.4), B11 (11.1, 11.4), PB1 (1.1, 1.2), PB3 (3.1, 3.2), PB5 (5.1, 5.4), PB6 (6.4, 6.5) and PB7 (7.4,7.6). A single digestion profile was obtained for the five other clones, and one clone from each ligation was selected for sequencing and QPCR.

Figure 4. PCR amplification of long distance DDPCR bands from the lymph node or terminal ileum. a) Bands isolated from the OJD.028 animals. B1 and B2 are lymph node derived, B3-11 are ileum derived. b) Bands isolated from the ileum of OJD.031A animals. Lanes M contain GeneRuler 1kb DNA ladder (MBI fermentas).

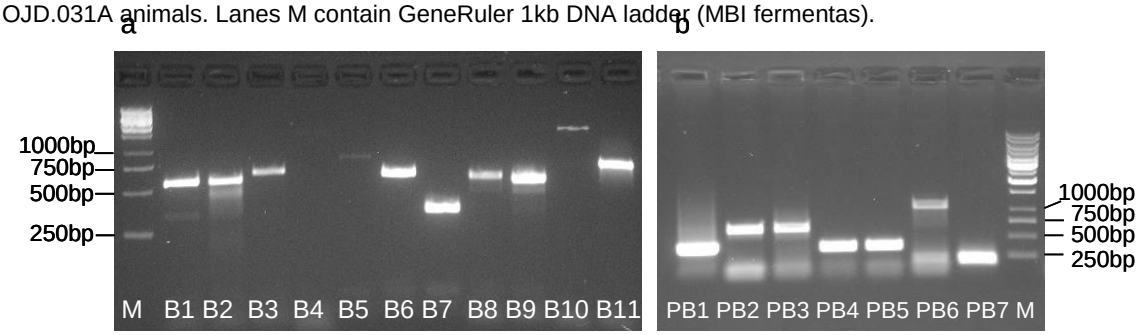

Identification of putative differentially expressed genes in the ileum and lymph nodes of M. ptb infected animals

Following sequencing, the putative identity of the 31 clones was determined by homology searches of the non redundant nucleotide database, GenBank (Table 6).

Most of the sequences isolated were found to have homology with known bovine genes (Table 8). Interestingly, only one sequence, PB2.2, matched with a gene from the ovine genomic database, having 95% homology over 629 nucleotides with the ovine MHC-DQA1 gene.

Of the three genes isolated from lymph node samples, 2 unique genes were identified. Clones B1.2 and B2.3 were found to both contain identical fragments of a gene with homology to a human gene encoding a protein from the Family with sequence similarity 46, member C family of proteins. The remaining lymph node clone was identified as having 91% homology to the bovine Bardet Biedel syndrome 4 gene. Genes isolated from lymph node samples were not validated by QPCR at this time due to the lack of an appropriate reference gene for comparative quantitation.

Of the 28 sequenced ileum genes, 26 unique clones were identified. The homologies of the cloned genes are shown in Table 8.

Clones PB4.3 and PB5.4 contained identical inserts with homology to the bovine mitochondrial import receptor Tom22 and sequence analysis revealed that B7.1 and B11.4 contained overlapping but different sized inserts of a gene with homology to Cathepsin K. Although each encoded unique sequences, B6.4 and B6.5 appeared to be non-overlapping segments of a gene with homology to the human RAB11 coupling protein.

Four clones, B8.2, B8.3, B9.1 and B10.3, could not be definitively identified by nucleotide searches due to lack of functional homologues in the database. B10.3 contained homology to a Bovine IMAGE clone. A translated nucleotide search against the protein database (tblastx) using B10.3 revealed some homology to an ATP binding cassette containing protein. B8.2 contained a fragment of DNA with homology to a human chromosome 19 segment that contains families of repetitive elements (LINE and SINE elements). B8.3 had homology to a bovine open reading frame located on chromosome 20. A protein family search of this bovine ORF using the Pfam database reveals it is an unintegrated protein with no identified function. Finally, B9.1 contained homology to a human chromosome 5 open reading frame (C5orf22). A Pfam search using this human protein reveals it belongs to a family of proteins containing a Misexpression of ras 6 protein. As the clones generated during DDPCR contain predominantly 3' untranslated regions of mRNA transcripts, large sections of open reading frames were not available in these clones for a more functional search of protein family databases (Pfam). The 26 unique clones isolated here were taken for verification as differentially expressed gene products by quantitative PCR.

PB1.1 and PB1.2 had homology to bovine sequences that encode hypothetical proteins. Pfam homology searches of these hypothetical proteins reveal that the PB1.1 homologue encodes a death domain/CARD motif similar to those encoded by caspases and proteins involved in apoptotic processes. The PB1.2 homologue, *B. taurus* LOC782049, belongs to a family of nucleic acid binding proteins that have Krab box and zinc finger c2h2 type domains.

Table 8. Identification of differentially expressed genes by Long DD-PCR in the ileum and lymph nodes of M. ptb infected animals

Clone	*Tissue*	*GenBank homologue*	*BLAST algorithm*	*Species*	*Identities*	*GenBank #*
028 animals						
B1.2	LN	Family with sequence similarity 46, member C (FAM46C)	Discontiguous megablast	Human	370/513 (72%)	NM_017709
B2.2	LN	Bardet Biedel syndrome 4	megablast	Bovine	465/506 (91%)	NM_001075956
B2.3	LN	Family with sequence similarity 46, member C (FAM46C)	discontiguous megablast	Human	370/513 (72%)	NM_017709
B3.1	Ileum	PREDICTED: Bos taurus similar to Vav 1 oncogene (LOC789767), partial mRNA	megablast	Bovine	531/561 (94%)	XM_001256421
B3.3	Ileum	Capra hircus serum amyloid A3 mRNA	megablast	Caprine	140/158 (88%)	EF564270
B4.1	Ileum	Bos taurus thymosin, beta 4, X-linked, mRNA	megablast	Bovine	152/157 (96%)	BC133478
B4.4	Ileum	calcium/calmodulin-dependent protein kinase (CaM kinase) II delta (CAMK2D), transcript variant 2, mRNA	megablast	Human	662/740 (89%)	NM_172128
B5.1*	Ileum	Homo sapiens calcium-sensing receptor (hypocalciuric hypercalcemia 1, severe neonatal hyperparathyroidism) (CASR) gene	megablast	Human	314/331 (94%)	DQ088967
B6**	Ileum	Never cloned				
B7.1	Ileum	Bos taurus cathepsin K, mRNA	megablast	Bovine	291/302 (96%)	BC109853
B8.1*	Ileum	Bos taurus similar to NYREN18 protein (LOC511298), mRNA (NEDD8 ultimate buster-1)	megablast	Bovine	165/187 (88%)	NM_001080906
B8.2*	Ileum	Homo sapiens chromosome 19, cosmid F14319, contains families of repetitive elements	blastn	Human	169/213 (79%),	AC006134
B8.3*	Ileum	Bos taurus chromosome 20 open reading frame 29 (unintegrated protein)	blastn	Bovine	140/183 (76%),	BC103476
B9.1	Ileum	Homo sapiens chromosome 5 open reading frame 22 (similar to Misexpression suppressor of ras 6)	blastn	Human	291/421 (69%),	BC032845
B9.4	Ileum	PREDICTED: Bos taurus similar to 19A protein (SLAM family member 7)	megablast	Bovine	411/466 (88%)	XM_001256711
B10.1*	Ileum	Borrelia turicatae P-209 (Tetratricopeptide repeat containing protein)	tblastx	Borrelia	16/43 (37%)	AY692272
B10.2*	Ileum	Stomatin (STOM), transcript variant 1	discontiguous megablast	Human	510/699 (72%)	NM_004099
B10.3	Ileum	Bos taurus cDNA clone IMAGE:8181414	discontiguous megablast	Bovine	568/722 (78%)	BC149298
		PREDICTED: Bos taurus similar to ATP-binding cassette transporter C4 (LOC521568)	tblastx	Bovine	16/20 (80%),	XM_599833
B11.1	Ileum	Bos taurus nicotinamide nucleotide transhydrogenase, mRNA	megablast	Bovine	274/293 (93%),	BC114660
B11.4	Ileum	Bos taurus cathepsin K, mRNA A	megablast	Bovine	625/650 (96%)	BC109853
031 animals						
PB1.1	Ileum	PREDICTED: Bos taurus hypothetical LOC539314 (LOC539314 Death domain/ card motif)	megablast	Bovine	206/244 (84%)	XM_586393
PB1.2	Ileum	Bos taurus hypothetical protein LOC782049 Krab box zinc finger c2h2 type nucleic acid binding	discontiguous megablast	Bovine	136/161 (84%)	XM_001250195
PB2.2	Ileum	MHC OVAR-DQ-ALPHA1 (MHC OVAR-DQA1)	megablast	Ovine	602/629 (95%)	M93430
PB3.1	Ileum	COX19 cytochrome c oxidase	discontiguous megablast	Human	93/116 (80%)	AY957566
PB3.2	Ileum	SATB homeobox 1 (SATB1	megablast	Human	617/669 (92%)	NM_002971

Clone	*Tissue*	*GenBank homologue*	*BLAST algorithm*	*Species*	*Identities*	*GenBank #*
PB4.3	Ileum	PREDICTED: Bos taurus similar to mitochondrial import receptor Tom22, transcript variant 1	megablast	Bovine	322/331 (97%)	XM_587978
PB5.1*	Ileum	ATP-binding cassette, sub-family D (ALD member 4	megablast	Bovine	208/268 (77%)	NM_001015636
	Ileum	Partial stat3 gene for signal transducer and activator of transcription 3	megablast	Bovine	95/108 (87%)	AJ620661
	Ileum	Potassium channel regulator (KCNRG / CLLD4-like	megablast	Bovine	116/134 (86%)	|NM_205808
PB5.4	Ileum	PREDICTED: Bos taurus similar to mitochondrial import receptor Tom22, transcript variant 1	megablast	Bovine	322/331 (97%)	XM_587978
PB6.4	Ileum	RAB11 family interacting protein 1 (class I), (Rab coupling protein)	discontiguous megablast	Human	137/186 (73%)	BC001314
PB6.5	Ileum	RAB11 family interacting protein 1 (class I), (Rab coupling protein)	discontiguous megablast	Human	180/258 (69%)	BC001314
PB7.4*	Ileum	KIAA0350 protein (C-type lectin domain family 16, member A (Hypothetical Gram-positive cocci surface protein 'anchoring' hexapeptide)	megablast	Human	119/127 (93%)	BC112897
PB7.6*	Ileum	Microfibrillar-associated protein 1(MFAP10)	megablast	Bovine	140/142 (98%)	NM_001034397

Predicted sequences refer to homology predicted by automated computational annotation of the genome

* Expression too low to be determined by QPCR0

Validation of putative differentially expressed genes in the ileum and lymph nodes of M. ptb infected animals by quantitative PCR

QPCR assays were designed for the 26 unique clones isolated as potentially differentially expressed gene products, and the efficiency of the amplification reactions was verified. A summary of the QPCR analysis of these genes is shown in Table 9. Not all QPCR primers generated an amplified PCR product despite numerous attempts to optimize experimental conditions or re-design primer sequences. Expression of 8 genes, B5.1, B8.2, B8.3, B10.1, B10.2, B10.3, PB7.4 and PB7.6 could not be detected in ileum by QPCR using 10ng of template cDNA. This could possibly be due synthesis failure of the primers, higher sensitivity of autoradiography than fluorescent QPCR or low abundance of these transcripts in ovine tissues.

Within genes discovered in the OJD028 group of sheep, expression of B3.1, B9.1, B10.3 and B11.1 were not significantly altered in the affected animals compared to the reference group and were likely to be false positives from the DDPCR process. However, six of the nine genes analysed showed significant changes in gene expression among affected and unaffected sheep. Within the OJD.031A group, two of the eight genes analyzed, PB4.3 and PB3.2 corresponding to putative homologues of TOM22 and DNA binding SATB1 respectively, were significantly regulated (Table 9).

The greatest changes in gene expression were seen for genes SAA3 (up to 22 fold change), cathepsin K (up to 48 fold change), SLAM F7 (up to 13.5 fold change) and tom22 (about 4 fold change) (upregulated) in animals with multibacillary disease. Animals with paucibacillary disease tended to have lower levels of increase in gene expression. Changes in calmodulin dependent PK, although significant, were less marked (about 2 fold change).

Table 9. QPCR validation summary of putative differentially expressed genes discovered in the ileum of animals with histological lesions of Johne's disease relative to uninfected animals. Samples were normalised to the reference gene HK 5.1. Sheep without histological lesions were compared to affected sheep with different histological grades of lesion using restricted maximum likelihood analysis.

Band	Gene identification	P
Genes discovered in OJD028 tissues		
B3.1	similar to vav proto-oncogene	0.145
B3.3	serum amyloid A3	<0.001
B4.1	Thymosin beta 4	0.048
B4.4	ca2+ calmodulin dependent protein kinase	0.007
B7.1 and 11.4	cathepsin k	<0.001
B9.1	C22orf5 homologue	0.261
B9.4	Similar to SLAMF7	<0.001
B10.3	Contains OFR with homology to ABC transporter	0.757
B11.1	Nicotinamide nucleotide transhydrogenase	0.576
Genes discovered in OJD031A tissues		
PB1.1	Contains death domain/Card motif	0.473
PB1.2	contains Krab box zinc finger c2h2 nucleic acid binding	0.377
PB2.2	MHC ovar-dqa1*	0.263
PB3.1	COX19 cytochrome oxidase	0.462
PB3.2	similar to satb1	0.019
PB4.3 and PB5.4	similar to tom22	<0.001
PB5.1	ATP binding cassette containing protein	0.934
PB6.4 and PB6.5	RAB11 interacting protein	0.870

Figure 5 QPCR validation summary of putative differentially expressed genes in the ileum of M. ptb infected animals. Data are dCt predicted means with standard errors; mean fold change relative to the uninfected group expressed as ddCt is shown as numerals above the bars; dCt values with different superscripts are significantly different. Provisional patent covers all these genes except B4.4.

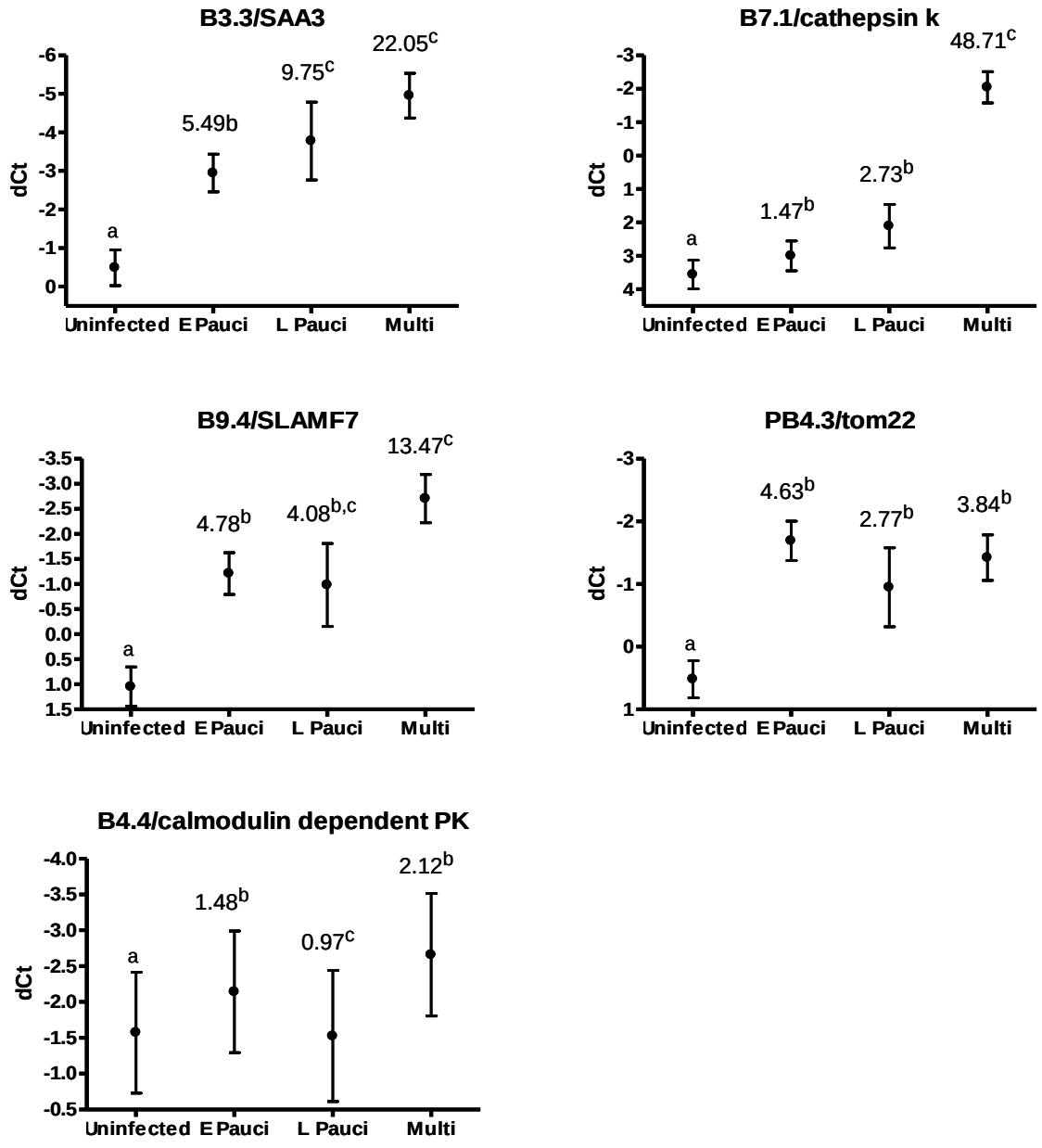

Discussion

Unlike study of human disease using human tissues or murine models, sheep disease research is hampered by lack of host genome data. The ovine genome is probably one of the least developed genomes, albeit slowly expanding through collaborative efforts between N.Z, U.S.A, U.K and Australia. With limited sheep genome available for gene expression studies, technologies such as microarray analysis may not be ideal. Technologies that do not require prior knowledge of a gene sequence, for example RDA, SAGE, DD-PCR or MPSS, may therefore be more suitable. DD-PCR is a powerful tool for studying changes in gene expression specific to any biological event. The advantages of this technique include the ability to look at up or down regulated transcripts using small amounts of starting material and to identify known or novel transcripts that are specific to *Mptb* infection in sheep. Another advantage is the capacity to include many sheep in a single experiment, which enables statistically robust comparisons of groups and therefore leads to greater confidence in outcomes. DD-PCR was successful in identifying genes whose expression was altered during the clinical stage of *Mptb* infection.

Genes discovered using DD-PCR were mostly confirmed to be differentially regulated by QPCR in the animals in which they were discovered. However, when examined in another group of animals, changes in gene expression levels for some genes were not significant. This cross validation suggested that some of the changes in gene expression measured were associated with trial/property/environment/age/diet of the animals and were not true differences associated with Johne's disease. However, four genes were confirmed to be differentially expressed in Johne's disease.

Band 3.3 was found to be similar to the bovine serum amyloid 3(SAA3) protein. It has been found that expression of SAA3 is associated with presence of inflammatory cells and tissue parasitism in certain infection models (Chagas disease). Additionally SAA3 has been shown to be associated with the intestinal mucin gene MUC3 whereby it provides a means of increasing MUC3 in intestinal cells for the prevention of GI diseases including infectious diarrhea and necrotizing enterocolitis (14, 18). A pathological change consistent with amyloidosis has previously been reported in a sheep with paratuberculosis (28) while serum amlyoid 3 has also been reported to be over expressed in serum during tuberculosis in man (4).

Band 9.4 identified as having homology to the predicted bovine 19A protein. 19A is a member of the SLAM family member 7 group of proteins. Members of the signaling lymphocyte activation molecule (SLAM) family of receptors are expressed in multiple cells of the immune system, including natural killer cells, T cells, and B cells (34). SLAM receptors interact with SH2 domain-containing, cytosolic adaptor proteins such as SAP, EAT-2, and SH2D1A, and mediate tyrosine phosphorylation events that contribute to immune cell activation. The finding that mutations in SAP are associated with an X-linked lymphoproliferative disorder suggests that signalling through SLAM receptors can influence the development and effector functions of immune cells (6). The receptors are single-pass type I membrane proteins, and 3 isoforms have been proposed to occur from alternative splicing. Isoform 1 mediates NK cell activation through a SAP-independent extracellular signal-regulated ERK-mediated pathway and may play a role in lymphocyte adhesion. Isoform 3 does not mediate any activation. The isoform 3 is expressed at much lower level than isoform 1. SAP can bind the cytoplasmic tail of isoform 1 when phosphorylated in the presence of Fyn (*in vitro*) (10, 19). SLAMF7 proteins are expressed in spleen, lymph node, peripheral blood leukocytes, bone marrow, small intestine, stomach, appendix, lung and trachea. Expression has been detected in NK cells, activated B-cells, NK-cell line but not in promyelocytic, B-, or T-cell lines. SLAMF7 proteins contain an Ig-like C2-type (immunoglobulin-like) domain and may be involved in natural killer cell activation and natural killer cell mediated cytotoxicity (7, 8).

Bands 7.1 and 11.4 were identified as having homology with the bovine Cathepsin K preprotein. At least some of cathepsin family is involved in specific cellular processes. Gene knock-out experiments have shown that cathepsins play an essential role in processes, such as wound

healing, antigen processing and presentation (immune disorders), prohormone processing and bone remodelling. Cathepsin K has been has been identified as a target for some therapies and compounds targeting cathepsin K (amongst other cathepsins) are being clinically evaluated. Cathepsin K in particular is found to be important for normal bone resorption (32, 33).

PB 4.3 and PB 5.4 were found to be homologous with the bovine form of a protein similar to the translocase of the mitochondrial outer membrane 22 (TOM22). Specifically, TOM22 is a preprotein receptor/organizer of the mitochondrial outer membrane translocase complex that, with other TOM's, control the activity of the complex during the transfer of precursor substrates (21, 25).

Band 2B4.2 was found to have homology with Macaca calcium/calmodulin-dependent protein kinase II. This protein has a wide distribution and plays an important role in the calcium signaling pathway. It is suggested that the protein kinase is associated with the enterocyte cytoskeleton and plays a role in regulating intestinal epithelial cytoskeleton (23).

The ileal cell brush border Na+/H+ exchange is also regulated by calcium/calmodulin dependent protein kinase II whereby it inhibits the brush border exchange which takes part in the regulation of Na+ absorption (11).

It is feasible that these particular genes may have important roles during the clinical stage of ovine Johne's disease, particularly when concerned with the immune response, apoptosis, cell signalling and absorption. Uncovering the mechanisms involved in regulating responses to infection may help identify molecules that could be used therapeutically or aid in identifying infected animals during earlier stages of the disease, before clinical symptoms are visible. Potentially these genes could be used to assess gene expression at different stages of the disease. If gene expression profiles are unique then there is potential to use them as diagnostic markers of the disease.

References

Adams, J. L., M. T. Collins, and C. J. Czuprynski. 1996. Polymerase chain reaction analysis of TNF-alpha and IL-6 mRNA levels in whole blood from cattle naturally or experimentally infected with Mycobacterium paratuberculosis. Can J Vet Res 60:257-262.

Adams, J. L., and C. J. Czuprynski. 1995. Ex vivo induction of TNF-alpha and IL-6 mRNA in bovine whole blood by Mycobacterium paratuberculosis and mycobacterial cell wall components. Microb Pathog 19:19-29.

Adams, J. L., and C. J. Czuprynski. 1994. Mycobacterial cell wall components induce the production of TNF-alpha, IL-1, and IL-6 by bovine monocytes and the murine macrophage cell line RAW 264.7. Microb Pathog 16:401-411.

Agranoff, D., D. Fernandez-Reyes, M. C. Papadopoulos, S. A. Rojas, M. Herbster, A. Loosemore, E. Tarelli, J. Sheldon, A. Schwenk, R. Pollok, C. F. Rayner, and S. Krishna. 2006. Identification of diagnostic markers for tuberculosis by proteomic fingerprinting of serum. Lancet 368:1012-1021.

Aldwell, F. E., D. N. Wedlock, and B. M. Buddle. 1996. Bacterial metabolism, cytokine mRNA transcription and viability of bovine alveolar macrophages infected with Mycobacterium bovis BCG or virulent M. bovis. Immunol Cell Biol 74:45-51.

Benoit, L., X. Wang, H. F. Pabst, J. Dutz, and R. Tan. 2000. Defective NK cell activation in X-linked lymphoproliferative disease. J Immunol 165:3549-3553.

Boles, K. S., and P. A. Mathew. 2001. Molecular cloning of CS1, a novel human natural killer cell receptor belonging to the CD2 subset of the immunoglobulin superfamily. Immunogenetics 52:302-307.

Bouchon, A., M. Cella, H. L. Grierson, J. I. Cohen, and M. Colonna. 2001. Activation of NK cell-mediated cytotoxicity by a SAP-independent receptor of the CD2 family. J Immunol 167:5517-5521.

Butte, A. 2002. The use and analysis of microarray data. Nat.Rev.Drug Discov. 1:951-960.

Chan, B., A. Lanyi, H. K. Song, J. Griesbach, M. Simarro-Grande, F. Poy, D. Howie, J. Sumegi, C. Terhorst, and M. J. Eck. 2003. SAP couples Fyn to SLAM immune receptors. Nat Cell Biol 5:155-160.

Cohen, M. E., L. Reinlib, A. J. Watson, F. Gorelick, K. Rys-Sikora, M. Tse, R. P. Rood, A. J. Czernik, G. W. Sharp, and M. Donowitz. 1990. Rabbit ileal villus cell brush border Na+/H+ exchange is regulated by Ca2+/calmodulin-dependent protein kinase II, a brush border membrane protein. Proc Natl Acad Sci U S A 87:8990-8994.

Coussens, P. M., C. J. Colvin, K. Wiersma, A. Abouzied, and S. Sipkovsky. 2002. Gene expression profiling of peripheral blood mononuclear cells from cattle infected with Mycobacterium paratuberculosis. Infect Immun 70:5494-5502.

Coussens, P. M., N. Verman, M. A. Coussens, M. D. Elftman, and A. M. McNulty. 2004. Cytokine gene expression in peripheral blood mononuclear cells and tissues of cattle infected with Mycobacterium avium subsp. paratuberculosis: evidence for an inherent proinflammatory gene expression pattern. Infect Immun 72:1409-1422.

Ferreira, L. R., A. M. Silva, V. Michailowsky, L. F. Reis, and R. T. Gazzinelli. 1999. Expression of serum amyloid A3 mRNA by inflammatory macrophages exposed to membrane glycoconjugates from Trypanosoma cruzi. J Leukoc Biol 66:593-600.

Hubank, M., and D. G. Schatz. 1999. cDNA representational difference analysis: a sensitive and flexible method for identification of differentially expressed genes. Methods Enzymol. 303:325-49.:325-349.

Hubank, M., and D. G. Schatz. 1994. Identifying differences in mRNA expression by representational difference analysis of cDNA. Nucleic Acids Res. 22:5640-5648.

Khalifeh, M. S., and J. R. Stabel. 2004. Upregulation of transforming growth factor-beta and interleukin-10 in cows with clinical Johne's disease. Vet Immunol Immunopathol 99:39-46.

Larson, M. A., S. H. Wei, A. Weber, D. R. Mack, and T. L. McDonald. 2003. Human serum amyloid A3 peptide enhances intestinal MUC3 expression and inhibits EPEC adherence. Biochem Biophys Res Commun 300:531-540.

Latour, S., R. Roncagalli, R. Chen, M. Bakinowski, X. Shi, P. L. Schwartzberg, D. Davidson, and A. Veillette. 2003. Binding of SAP SH2 domain to FynT SH3 domain reveals a novel mechanism of receptor signalling in immune regulation. Nat Cell Biol 5:149-154.

Liang, P., and A. B. Pardee. 1992. Differential display of eukaryotic messenger RNA by means of the polymerase chain reaction [see comments]. Science 257:967-971.

Lister, R., J. M. Hulett, T. Lithgow, and J. Whelan. 2005. Protein import into mitochondria: origins and functions today (review). Mol Membr Biol 22:87-100.

Livak, K. J., and T. D. Schmittgen. 2001. Analysis of relative gene expression data using real-time quantitative PCR and the 2(-Delta Delta C(T)) Method. Methods 25:402-408.

Matovcik, L. M., B. Haimowitz, J. R. Goldenring, A. J. Czernik, and F. S. Gorelick. 1993. Distribution of calcium/calmodulin-dependent protein kinase II in rat ileal enterocytes. Am J Physiol 264:C1029-1036.

Momotani, E., D. L. Whipple, A. B. Thiermann, and N. F. Cheville. 1988. Role of M cells and macrophages in the entrance of Mycobacterium paratuberculosis into domes of ileal Peyer's patches in calves. Vet Pathol 25:131-137.

Nakamura, Y., H. Suzuki, M. Sakaguchi, and K. Mihara. 2004. Targeting and assembly of rat mitochondrial translocase of outer membrane 22 (TOM22) into the TOM complex. J Biol Chem 279:21223-21232.

Perez, V., J. F. Garcia Marin, and J. J. Badiola. 1996. Description and classification of different types of lesion associated with natural paratuberculosis infection in sheep. J. Comp. Pathol. 114:107-122.

Pollock, J. D. 2002. Gene expression profiling: methodological challenges, results, and prospects for addiction research. Chem.Phys.Lipids 121:241-256.

Rings, D. M., and F. B. Garry. 1988. Amyloidosis associated with paratuberculosis in a sheep. Compendium on Continuing Education for the Practicing Veterinarian 10:381-382,384-385.

Sweeney, R. W., D. E. Jones, P. Habecker, and P. Scott. 1998. Interferon-gamma and interleukin 4 gene expression in cows infected with Mycobacterium paratuberculosis. Am J Vet Res 59:842-847.

Tooker, B. C., J. L. Burton, and P. M. Coussens. 2002. Survival tactics of M. paratuberculosis in bovine macrophage cells. Vet Immunol Immunopathol 87:429-437.

Tooker, B. C., and P. M. Coussens. 2004. Phagocytosis of M. paratuberculosis fails to activate expression of NADH dehydrogenase and nucleolin-related protein in bovine macrophages. Immunol Lett 93:137-142.

Troen, B. R. 2006. The regulation of cathepsin K gene expression. Ann N Y Acad Sci 1068:165-172.

Vasiljeva, O., T. Reinheckel, C. Peters, D. Turk, V. Turk, and B. Turk. 2007. Emerging roles of cysteine cathepsins in disease and their potential as drug targets. Curr Pharm Des 13:385-401.

Veillette, A. 2006. Immune regulation by SLAM family receptors and SAP-related adaptors. Nat Rev Immunol 6:56-66.

Velculescu, V. E., L. Zhang, B. Vogelstein, and K. W. Kinzler. 1995. Serial analysis of gene expression. Science 270:484-487.

Wallrapp, C., and T. M. Gress. 2001. Isolation of differentially expressed genes by representational difference analysis. Methods Mol.Biol. 175:279-94.:279-294.

Whittington, R. J., I. Marsh, S. McAllister, M. J. Turner, D. J. Marshall, and C. A. Fraser. 1999. Evaluation of modified BACTEC 12B radiometric medium and solid media for the culture of Mycobacterium avium subsp. paratuberculosis from sheep. Journal of Clinical Microbiology 37:1077-1083.

Whittington, R. J., and E. S. Sergeant. 2001. Progress towards understanding the spread, detection and control of Mycobacterium avium subsp paratuberculosis in animal populations. Aust Vet J 79:267-278.

9.20 Appendix 3B-3 Subprogram 3 Toll-like receptor genes are differentially expressed at the sites of infection during the progression of Johne's disease in outbred sheep

Introduction

Mycobacterium avium subsp. *paratuberculosis* (*M. ptb*) is the causative agent of Johne's disease, a chronic granulomatous enteritis in ruminants, characterized by thickening of the intestinal wall and progressive wasting leading to death of the animal [21]. Current estimates indicate that Johne's disease is one of the most costly infectious diseases of livestock in Australia, with about 2000 sheep flocks and more than 1000 dairy herds infected. Herd level prevalence in most countries exceeds 20% but is usually underestimated. Most Johne's disease cases remain sub-clinical, thereby maintaining infection in a population. Initially, sub-clinical cases shed low numbers of bacteria in faeces, 10^4/g, rising to 10^6-10^8/g in clinical cases [93]. Recent evidence of resistance to infection in some individuals suggests that genetic makeup of the host may be an important factor in the pathogenesis of Johne's disease [45]. Innate immune responses may play a role in resistance.

Following ingestion, the pathogenic mycobacteria translocate through the mucosal epithelium, via M-cells overlaying the ileal Peyers patches, where they are internalized and persist in the underlying epithelial macrophages. The bacteria are able to survive and replicate within macrophages, by preventing lysosome fusion, the production of reactive oxygen and nitrogen species and phago-lysosome maturation [19] as is also the case with *Mycobacterium tuberculosis (M. tb)* [1, 4, 12, 22, 75, 81]. The eradication of mycobacteria is mediated by the activation of infected macrophages within the granulomas. Interleukin-12 (IL-12) activated $CD4^+$ T lymphocytes play an important role in enhancing the microbicidal activity of macrophages via secretion of interferon-gamma (IFN-γ) [11, 13, 23, 60, 74, 78]. The bacteria appear able to resist acquired T-cell mediated immunity, and are subsequently shed from the intestinal mucosa. This shedding is usually coincident with a switch from Th1 dominated cell-mediated immunity to a Th2 dominated humoural immune response and has been demonstrated in both experimentally and naturally infected sheep and cattle with paratuberculosis [8, 18, 65, 79, 80, 88, 92]. Lesion formation is predominantly in the distal ileum, though can extend to the colon and jejunum. The lesions begin as small focal granulomas, rich in lymphocytes and macrophages but without visible bacilli, which extend to the adjacent lamina propria and become locally extensive, then generalized. At this stage, extensive multibacillary lesions containing large numbers of macrophages densely packed with *M. ptb* can often be detected in the ileum, and clinical signs can become apparent [24, 34, 64-66, 91]. Up to 30% of clinical cases may not have visible mycobacteria within the granulomas. These are known as paucibacillary lesions [20].

Our current understanding of the biology of *M. ptb* infection has been hindered by limited knowledge of the host factors involved in the immune response to the organism and the lack of appropriate molecular tools to dissect the host-pathogen interaction. Recognition by the host of molecular patterns displayed by microbes is essential to development of an effective immune response. Current models propose that Pattern Recognition Receptors (PRR) such as Toll-like receptors (TLR) play a central role, by responding rapidly to induce production of cytokines and reactive oxygen and nitrogen intermediates (Reviewed in [44]. Activation of TLRs has also been shown to coordinate the adaptive immune response to micro-organisms [77].

Thirteen mammalian TLRs have been identified that respond individually or in hetero-dimers to distinct pathogen associated molecular patterns (PAMPs), cooperatively recognizing lipid, carbohydrate, peptide and nucleic-acid moieties that are absent in the host, leading to the activation of specific anti-microbial pathways [44, 62]. Structurally, the TLRs are well conserved, being composed of an extra-cellular leucine-rich repeat region (LRR) involved in ligand binding and a

conserved cytoplasmic domain known as the Toll/IL-1 receptor (TIR) that directs intracellular signaling via interaction with TIR-domain-containing adaptor molecules, predominantly the myeloid differentiation response gene 88 (MyD88 [71]. The cellular localization of TLRs is diverse, with some found on the cell surface (TLR1, TLR2, TLR4, TLR5 and TLR6) and others on the membranes of intracellular vesicles such as endosomes (TLR3, TLR7, TLR8, and TLR9) [44].

Whole mycobacteria and many mycobacterial components have been shown to act as ligands for TLRs both *in vitro* and *in vivo* [5, 54, 61, 67]. Mycobacterial lipoproteins, lipomannan, arabinose-capped lipoarabinomannan (ara-LAM) and phosphatidyl-myo-inositol mannoside (PIM) can all activate TLR2 in association with TLR1 and/or TLR6 leading to the synthesis of the pro-inflammatory cytokines TNFα and IL-12, and also nitric oxide, which has potent anti-mycobacterial activity in mice [3, 14, 28, 30, 70, 87]. In addition, DNA from mycobacteria contains stimulatory CpG motifs that activate TLR9 [37]. The virulence of the mycobacterial strain has also affects the degree of TLR signalling [54, 57], and evidence suggests that this has a significant role in the pathophysiological processes during human *M. tb* infection. In some cases, mycobacteria may actually take advantage of the TLR-induced immune responses (reviewed in [48]).

Much of the work on TLR signalling pathways has focused on the identification of ligands, elucidation of individual signalling pathways, and *in vivo* studies of their involvement in resistance to infection using knock-out mice. Little is known of their role in Johne's disease, but it is likely they play a crucial part in the innate and adaptive response to *M. ptb* infection. The pathogenesis of *M. ptb* infection is understood to be similar in many ruminant species [21] with both paucibacillary and multibacillary disease forms occurring in both cattle and sheep. However, the sheep model is convenient experimentally due to shorter pathogenesis, availability and reduced cost compared to cattle.

Ten ovine TLR genes have recently been described [55]. In this study we analyzed the expression levels of TLR genes at intestinal predilection sites, associated lymph nodes and in peripheral blood mononuclear cells by comparative qPCR to determine if TLR expression is modulated by infection with *M. ptb*. Furthermore we tested the hypothesis that differences in TLR expression may be associated with the different pathologies observed in the sub-clinical forms of Johne's disease and may be predictive of exposure to, and infection with, *M. ptb*.

Methods

Experimental animals and sample collection

36 Merino sheep aged 2-3 years were obtained from 5 properties in New South Wales (Table I) and housed in pens at Camden for two weeks prior to collection of samples. They were fed a mixture of lucern chaff and lupins, and had *ad libitum* access to water. The Johne's disease status of the animals was determined by histopathology [64] and mycobacterial culture [93] and is shown in Table I. None of the animals from properties A and B had been exposed to *M. ptb*, while all of the animals from properties C, D and E were exposed.

Sample Collection

Faeces, intestinal tissues and corresponding draining lymph nodes were taken from the terminal ileum (adjacent to the ileo-caecal junction) and terminal jejunum (3m proximal to the ileo-caecal junction) at necropsy. Tissue samples (~200mg) for RNA preparation were snap frozen immediately after collection on dry ice and stored at -80^{o}C until required. Sections for histological analysis were fixed in 10% neutral buffered formalin, embedded in paraffin, sectioned at 5 µm and stained with haematoxylin and eosin and by the Ziehl-Neelsen method. Tissue and faecal samples for *M. ptb* culture were taken at the time of necropsy and processed as previously described [93].

Peripheral blood mononuclear cells (PBMCs) were extracted from whole blood collected 1 week prior to necropsy. 24 mL of blood was taken from the jugular vein into EDTA vacutainers (BD) and buffy coats were isolated by centrifugation (750 xg, 10 min, 19^{o}C). Buffy coats were aspirated with Pasteur pipettes, mixed with 2ml PBS and layered carefully onto 3 mL of Ficoll-Paque PLUS (Amersham Biosciences) before centrifugation to harvest the PBMCs (750 xg, 30 min, 19^{o}C). The PBMCs were carefully aspirated with a Pasteur pipette and washed by the addition of 10 mL of PBS, harvested by centrifugation (230 xg, 10 min, 19^{o}C), the supernatant removed and the cells taken within one hour of collection for RNA extraction as described below.

Animal disease status classification

Animals were classified into four subgroups on the basis of exposure to *M. ptb* and their disease status as determined by histopathology and mycobacterial culture. 1) Unexposed animals were sourced from properties with no history of JD and returned negative results in histopathology and mycobacterial culture of tissues and faeces; 2) Exposed, uninfected animals were from properties with a history of JD, had been run with shedding animals and returned negative results in mycobacterial culture of tissues and faeces and had no histopathology; 3) Infected animals with early paucibacillary lesions were from properties with a history of JD, showed histopathology in the terminal ileum consistent with 3a type lesions [64] and with a single exception, were positive for mycobacterial culture of tissues; 4) Infected animals with multibacillary lesions showed histopathology in the terminal ileum consistent with 3b type lesions [64], and were positive for mycobacterial culture of tissues. Granulomatous lesions were observed in the mesenteric lymph nodes of all infected animals (Table I) and were graded as 1 (mild focal), 2 (mild multi-focal) or 3 (severe).

Extraction of RNA

Total RNA was extracted from 30mg frozen intestinal tissue or PBMC samples using the Mini RNeasy extraction kit (Qiagen) according to the manufacturer's instructions. RNA quality assessment and quantification were done by visual examination on a 1% non-denaturing agarose gel in Tris-borate-EDTA buffer stained with ethidium bromide and spectrophotometry at 260 nm (Eppendorf BioPhotometer).

Removal of DNA from total RNA preparations

Contaminating genomic DNA was removed by digestion with 10U of RQ1 DNAse (1 U/ µL, Promega) at 37^{o}C for 2 hours. Following digestion, RNA was precipitated by the addition of 0.5 µL linear acrylamide (1µg/ µL, Ambion), 0.1 volume of 3M sodium acetate pH5.3 (Sigma), 3 volumes of ethanol (Sigma) and incubation on dry ice for 60 minutes. RNA was harvested by centrifugation (16,000 xg, 45 min, 4^{o}C), re-suspended in 25 µL of RNase free water (Ambion), and free nucleotides and sodium acetate removed using a G50 sepharose buffer exchange column (Amersham). RNA quality was checked by agarose gel electrophoresis. Removal of DNA was confirmed by qPCR using β-2 microglobulin primers (Sigma-Genosys) as described below.

cDNA synthesis

25 µg of total RNA and 4 µg of oligo dT (Sigma-Genosys) was made up to a total volume of 50 µL with RNase free water (Ambion). Samples were heated at 70^{o}C for 5 min and then placed at room temperature for 5 min to anneal the oligo dT. 40 µL of 5x reverse transcriptase buffer (Promega), 8 µL of 25 mM dNTPs (Promega), 1 µL RNaseIn RNAse inhibitor (40U/ µL MBI Fermentas) and 98 µL of RNase free water were added and mixed before adding 1 µL of M-MLV reverse transcriptase (RNAse H-point mutant, 200U/ µL; Promega). The reaction was mixed and placed at 42^{o}C for 1 hour. A further 1 µL of reverse transcriptase was added, and the reaction was incubated for another hour at 42^{o}C. After synthesis, the cDNA was precipitated by the addition of 0.5 µL of linear acrylamide (1µg/ µL, Ambion), 0.1 volumes of 3M sodium acetate pH 5.3 (Sigma) and 3 volumes of ethanol (Sigma) and incubation on dry ice for 60 minutes. The cDNA was harvested by centrifugation (16,000 xg, 45 min, 4^{o}C), re-suspended in 25 µL of RNase free water (Ambion) and free nucleotides and sodium acetate removed using a G50 sepharose buffer exchange column (Amersham).

Quantitative PCR

Gene-specific oligonucleotide PCR primers (Table II) were designed using Beacon Designer 4 (Premier Biosoft International) and obtained from a commercial supplier (Sigma-Genosys). Quantitative PCR (qPCR) was performed in an MX3000*p* Multiplex Quantitative PCR system (Stratagene) using QuantiTect SYBR Green PCR kits (Qiagen). qPCR reactions were carried out in duplicate 25 µL reaction volumes containing 300 nM forward and reverse primers and 10 ng template using the following program: 95°C for 15 min, and 40 cycles of 95°C for 20 s, 56°C for 30 s, and 72°C for 30 s with fluorescence acquisition at the end of the 56°C primer annealing step. Sequence-specific standard curves were generated using serial dilutions of cDNA and the threshold values noted. The efficiency of the amplification for each primer set was verified by generating standard curves over a range of 0.1 ng to 100 ng of cDNA template. All qPCR assays that generated efficiencies in the range of 96-104% were considered acceptable for our assays. The built in amplification-based proprietary algorithm (Stratagene) was used to set the fluorescence threshold value for each primer pair reaction based on the efficiency as determined by standard curve generation. The value of the fluorescence threshold for each primer pair was used to analyze data from experimental reactions. The number of cycles (*Ct*) at which the amplification-corrected normalized fluorescence (dRn) for each reaction crossed the threshold value was exported to Excel (Microsoft), PRISM (GraphPad) and GENSTAT (http://www.vsni.co.uk/products/genstat/) for further analysis. The specificity of the reaction was checked post-amplification by melt curve analysis.

Determination of reference genes

The standard deviation (SD) of Ct was determined from triplicate reactions using 10 ng of cDNA generated from 5 infected, 3 unexposed and 2 exposed, culture negative animals (Tables 1 and 3). Genes producing a SD of greater than 1.0 were considered to be inappropriate for use as reference genes as this reflects $\geq$ 2-fold change in expression level. Ct's were checked to ensure that ordering of infected and non-infected samples was not occurring (i.e. uninfected samples having closely matched Ct's, and infected samples having closely matched Ct's distinct from the uninfected Ct's). No ordering was observed during the course of these experiments. For each tissue type the reference gene with the lowest SD of Ct was used as the reference gene.

Statistical analysis

The differences in levels of TLR gene expression between groups of sheep based on deltaCt (ΔCt) were examined using restricted maximum likelihood (REML) in a linear mixed model (GenStat Release 10.1 2007, Lawes Agricultural Trust, Rothamsted Experimental Station). Sheep were grouped according to exposure to *M. ptb* (unexposed, exposed) and nested within the latter were classified as one of four exposure groups: unexposed, unaffected, early paucibacillary or multibacillary; exposure and exposure group were included as fixed effects. Property of origin was included as a random factor as a defacto for other sources of variation. To determine differences between the five tissue types (jejunum, ileum, jejunal lymph node, ileal lymph node and PBMCs), the tissue type was included as a fixed effect and animal as a random effect together with other factors as described. Post-tests for the significance of differences between predicted means were calculated in Excel (Microsoft) using a t-test applying the standard error of the difference for each pair of predicted means. Significance was assessed at the 95% level. Fold change was calculated by $2^{-\Delta\Delta Ct}$ [52] using the predicted means with the unexposed group as the reference population (control). For illustrative purposes, the Y axis was reversed in Figs 2 to 5 to show the direction in fold change obtained by $2^{-\Delta\Delta Ct}$ analysis.

Results

Establishing reference genes for ovine intestinal tissue, lymph node and PBMC samples

To determine reference genes suitable for use in relative quantitation of gene expression, qPCR primers were designed to a number of well characterized reference genes chosen from the available literature (Table II). In addition two putative reference genes, HK5.1 and H7.7, identified previously by Long Distance Differential Display PCR (LDD-PCR) on ileum and lymph nodes respectively (L. Di Fiore, personal communication) were also assessed. The SD of *Ct* was determined for each primer set using 10ng cDNA from each of 6 infected and 5 unexposed/uninfected animals per tissue type. All the genes analyzed were moderately to highly expressed, having *Ct*'s between 17 and 27 using 10ng of cDNA.

Across the intestinal samples, the transcription levels of β-actin, 18S and GAPDH showed the highest variation, followed by β2-microglobulin and α-tubulin (Table III). All had a SD greater than 1.0 indicating a greater than 2 fold change in expression level and were not suitable reference genes in this tissue and infection model. β-actin, 18S and GAPDH expression varied widely, generating a SD greater than 2.0 in most cases. This indicates a > 4-fold change in expression between animals that was not associated with *M. ptb* infection status. The putative reference gene HK5.1, isolated from DDPCR on ileal samples gave the smallest variation of Ct in both ileum and jejunum samples (SD 0.59, 0.58 respectively), reflecting its stability over the duration of infection with *M. ptb*. It also had a mid-range mean Ct value of 26 and was deemed most suitable for use as a reference gene.

In the lymph node tissues, β-actin and β2-microglobulin were highly variable in expression. The DDPCR-isolated putative reference gene, HK7-7, had the most stable expression (SD 0.32), a mid-range mean Ct value of 25 and was considered most suitable for use as a reference gene in these tissues (Table III). Despite its high variability in intestinal samples, the levels of GAPDH transcription were the most stable of the genes tested in PBMCs (SD = 0.43), unaffected by *M. ptb* exposure or disease status. GAPDH was thus used as the reference gene when analyzing gene expression in PBMC samples (Table III).

The expression level of TLRs is altered in the ileum and jejunum of sheep infected with M. ptb

To determine if the relative expression of TLR genes is altered at the sites of infection during Johne's disease, qPCR primers were designed to the 10 available ovine TLR sequences present in the GenBank database (Table II).

For the control group, 12 previously unexposed sheep were selected from 2 Johne's disease free farms to eliminate potential confounding effects of property in the statistical analysis. In addition, 18 animals were selected from 3 naturally infected flocks. The true Johne's disease status of all animals was determined by histopathology [64], radiometric culture of faeces and intestinal tissues and other standard methods (Table I). Gene expression differences between the subcategories of sheep were assessed using restricted maximum likelihood analysis in a linear mixed model which accounted for variation due to effects of property. Comparisons were made between unexposed (n=12), uninfected (n=6), early paucibacillary (n=6) and multibacillary animals (n=6).

The expression levels in the ileum and jejunum were determined by comparative quantitation following normalization to the stable reference gene HK5.1 (Table III). The levels of expression of TLRs 1to 8 were found to be relatively abundant in the intestinal tissues generating Ct's between 22 and 38 with 10ng of cDNA template, however expression of TLR9 and TLR10 could only be detected after 43 cycles of amplification with 100ng of cDNA suggesting low abundance. Detection of TLR9 and TLR10 expression by qPCR at this low level was outside of the quantitative ranges of the assays and so could not be progressed further.

REML analysis indicated the levels of expression for TLR2 (P=0.004), TLR3 (P=0.022), TLR4 (P<0.001), TLR5 (P<0.001) and TLR8 (P<0.001) were significantly higher in the ileum of infected animals relative to the uninfected animals with the largest difference in ΔCt being between uninfected and multibacillary animals in each case (Fig 1). The decrease in ΔCt value between the uninfected and infected animals indicated an increase in expression level. Both the paucibacillary and multibacillary mean ΔCt were significantly different from the uninfected animals. However, no significant difference was observed between the paucibacillary and multibacillary lesion groups (Fig 1) despite a trend for the latter to be higher. Assuming that multibacillary lesions are an extension of paucibacillary lesions, this finding may indicate relatively uniform or minor fluctuations in TLR expression following induction of the immunopathology.

The expression of TLR2, TLR4 and TLR8 also was found to be significantly increased in the jejunal tissues of infected animals (P=0.032, 0.004 and 0.008 respectively), with the greatest difference in ΔCt being between the multibacillary animals and the uninfected animals, although in contrast to the ileum, TLR2 and TLR4 expression in the paucibacillary animals was not significantly different from the uninfected group (Fig 2). In addition, the expression of TLR4 in the jejunum of multibacillary animals was significantly higher than in the paucibacillary animals with almost 3-fold higher levels (P=0.047, Fig 2).

TLR2 and TLR8 revealed the largest difference in mean expression level, in excess of 7- and 8-fold in the ileum and 16- and 8-fold in the jejunal tissues of multibacillary animals relative to the unexposed group respectively (Figs 1, 2). Despite significant up-regulation, the increase was not as great in the paucibacillary animals and although there were trends to increased expression of TLRs 1, 6 and 7 in the ileum and jejunum of infected animals, these were not significantly altered relative to uninfected animals (Figs 1 and 2).

The expression level of TLRs in the associated lymph nodes of sheep infected with M. ptb

To determine if the relative expression of TLR genes is also altered in the appropriate draining mesenteric lymph nodes during Johne's disease, cDNA was also prepared from the tissues of the animals as described above and comparative quantitation performed following normalization to

DDH7-7, whose expression was found to be stable across the infected and uninfected animals (Table III).

The expression levels of TLR1 to 8 were also relatively abundant in the lymph node tissues, generating Ct's between 21 and 37 with 10ng of cDNA template, all falling within the quantifiable ranges of the qPCR assays. The levels of TLR9 and TLR10 in lymph node were low and their amplification from 100ng of cDNA fell outside the linear range of the assays and could not be quantified reliably.

Increases in TLR gene expression levels were less in the lymph nodes than in the intestinal tissues. Significant increases in expression were found in both the ileal and jejunal lymph nodes of infected animals relative to uninfected animals for TLR1 (*P*=0.029, 0.021), TLR2 (*P*=<0.001, 0.01), TLR6 (*P*=0.01, <0.001) and TLR8 (*P*=<0.001, 0.022) (Figs 3 and 4) after allowing for variation due to property. TLR4 was significantly altered only in the ileal lymph node (*P*=0.003) (Fig 3) and TLR3 only in the jejunal lymph node (*P*=0.019) (Fig 4). TLR5 and TLR7 were not significantly altered in either lymph node of any infected groups relative to the uninfected animals. In the paucibacillary group, TLR1 and TLR6 in ileal lymph node and TLR2 in jejunal lymph node were not significantly different from the uninfected group. Graded responses were present among the animals, with the largest changes seen in the multibacillary animals relative to the unexposed animals.

There was a clear trend for the paucibacillary group to have lower expression levels of TLR than the multibacillary group, and this was significant for TLR2 in ileal lymph node (P=0.027) and TLR1, TLR3 and TLR6 in jejunal lymph node (P=0.032, 0.027 and 0.001 respectively).

TLR expression in PBMCs is not significantly altered response to infection status

There is recirculation of leucocytes between intestinal and lymph node tissues via peripheral blood. To determine if the expression of TLR transcripts in circulating monocytes is also altered during infection, we prepared cDNA from PBMCs isolated from unexposed, uninfected animals and animals in various stages of disease (Table I) and analyzed the expression following normalization to the reference gene GAPDH, the expression of which was previously found to be stable in PBMCs across the infected and uninfected animals (Table III).

TLR 1, TLR6, TLR7 and TLR8, all showed trends to increases in expression in uninfected animals relative to the unexposed group, suggesting these genes may be affected by exposure to *M. ptb*, although none were significantly altered in the PBMCs of infected animals relative to uninfected animals. The expression level of TLR1, TLR3, TLR5 and to a lesser extent TLR6 was slightly decreased in the PBMCs of infected animals relative to the uninfected animals while slight increases in expression were seen for TLR2 and TLR8, and no change of TLR6 and TLR7.

Discussion

In this study we analyzed the expression of the 10 known TLR genes in tissues from the predilection sites for Johne's disease from sheep naturally infected with *M. ptb*. Two TLRs (TLR9 and TLR10) were minimally expressed and could not be quantified. However, expression of TLR1-8 was able to be quantified enabling comparisons to be made between out bred sheep classified as non-exposed, exposed but uninfected, early paucibacillary cases and multibacillary cases after accounting statistically for variance due to property of origin.

In this study, we analyzed a panel of putative reference genes for comparative qPCR to determine those suitable for analysis of ovine ileum, jejunum, lymph node and peripheral blood mononuclear cell samples. An ideal reference gene would have constant expression levels irrespective of the infection status of the animal. A comprehensive analysis of this type has not previously been performed in sheep. A gene previously identified from a DD-PCR study on ileal tissues (L. Di Fiore,

personal communication), HK5.1, and a second gene isolated during a study on DD-PCR in lymph node samples (L. Zhong, unpublished), HK7-7, had the most stable expression in intestinal tissue and lymph node tissue, respectively. Despite high variability in intestinal samples, the levels of GAPDH transcription remained the most stable of the genes tested in PBMCs and was selected as the reference gene in these samples. A suitable reference gene is required for each experimental model, system or tissue under investigation and should not be selected solely based on its historical use [86]. Several genes are well documented as reference genes for qPCR analysis, however evidence of the unsuitability of many of these genes in some models and tissues has begun to emerge [26, 35, 69, 68, 72, 85]. GAPDH is one of the most widely used reference genes however it has been shown to be variable in different models of infection suggesting that it is not the best reference gene to use in all circumstances [68, 85]. We have shown previously that the simplest method for comparing and selecting reference genes is the evaluation of the SD and plotting of *Ct*s, allowing differences in expression to be easily determined [85]. The commonly used reference genes analyzed here showed variability in expression in intestinal tissues of greater than 1 SD in *Ct*; use of GAPDH, β-actin and 18S may be inappropriate. If gene expression data are to be reported in a biologically relevant context and subtle differences in gene expression are to be identified, the use of a suitable stably expressed reference gene is a critical consideration.

During this study, 12 previously unexposed animals from two Johne's disease free flocks and 18 animals from three naturally infected flocks were used to determine putative differences in the expression of TLR genes associated with infection. A sophisticated statistical procedure, REML (restricted maximum likelihood) in a linear mixed model, was used to remove variance associated with source of the out bred sheep to enable comparison of the effects of exposure to *M. ptb* and stage of infection as assessed histologically.

The level of several TLR varied significantly in association with the stage of infection in exposed sheep, after allowing for variation due to property. There was a clear trend for most TLRs in the paucibacillary group to have lower expression levels than the multibacillary group. Significant differences associated with the degree of infection following exposure were found in the ileum for TLR2, TLR3, TLR4, TLR5 and TLR8, and in the jejunum for TLR2, TLR4 and TLR8. In both the ileal and jejunal lymph nodes, significant increases were found for TLR1, TLR2, TLR6 and TLR8, while TLR4 was specifically increased in the ileal lymph node and TLR3 in the jejunal lymph nodes. In most cases these differences were due to differences in TLR expression between early paucibacillary and also multibacillary groups when compared to uninfected sheep.

No significant changes in TLR gene expression were observed in the peripheral blood mononuclear cells of infected animals relative to the uninfected animals despite trends to up-regulation. A larger sample size may have resulted in a significant outcome in the model used. Quantitative expression of the TLR genes in PBMCs may have use in predicting exposure to *M. ptb* as trends in up-regulation were seen in the three exposed groups relative to the unexposed animals for some genes (Fig 5). Further work on a larger group of animals will confirm whether sample size limited the power of the analysis and trends that were seen for TLR expression to be higher in exposed sheep than unexposed sheep for TLR1, TLR6, TLR7 and TLR8.

This study was conducted in an out bred population of sheep from several sources in order to identify robust differences that may have future application in investigation of disease biology with a view to disease prevention and control. A key question that arises from the study is the biological significance of the changes in TLR expression that were observed.

Pathogen recognition is dependent to a degree on the ability of TLRs to recognize a variety of molecular patterns from microbes and they display considerable target specificity [51]. Ligand recognition leads to the recruitment of MyD88 and the IL-1 receptor associated kinases IRAK-1 and IRAK-4 [42, 82], inducing a number of host genes through a complex signaling cascade resulting ultimately in the activation of acute host responses necessary to eliminate the invading mycobacteria

[50]. The detection of a broad spectrum of mycobacterial components and whole cells by TLRs is thus critical for determining the outcome of infection.

In studies of human and mouse models, agonists such as lipoproteins and glycolipoproteins, lipomannan, ara-LAM, PIM and heat shock proteins induce cell activation, apoptosis and mycobacterial killing via TLR2 and TLR4 dependent induction of TNFα, IL-12 and nitric oxide [7, 14, 16, 31, 33, 36, 43, 47, 53, 58, 63, 67, 83, 90, 94]. The protective role of TLRs in mycobacterial infection is further supported by TLR2-deficient and MyD88-deficient individuals having a higher susceptibility to challenge with *M.tb* or *M. avium* [9, 27, 29, 59, 76, 95]).

TLRs link innate and adaptive immunity through dendritic cell (DC) mediated activation of T cells. Following TLR activation, DCs increase their cell surface MHC molecules containing pathogen-derived peptide fragments, enhancing their ability to activate T cells [6, 41]. Additionally, stimulation of other DCs with TLR ligands results in the expression of IFN-α and IFN-β [39, 40] which also function in the development of adaptive immunity, including proliferation of memory T cells, inhibition of T cell apoptosis, enhanced IFN-γ secretion, B cell isotype switching and differentiation into plasma cells and NK cell activation [41].

As discussed, a number of TLR receptors have been shown to play a role in bacterial infections and their ligands have been well characterized. TLR1, TLR2, TLR4 and TLR6 recognise lipoproteins such as lipopolysaccharide (LPS) from Gram-negative bacteria and peptidoglycan from Gram-positive bacteria [2]. TLR2 has been shown to form heterodimers with TLR1 and TLR6 to discriminate a wide variety of molecules. Complexes of TLR1/2 and TLR2/6 can discriminate triacyl- and diacyl-lipopeptides respectively [2]. TLR5 recognises protein ligands such as flagellin [2, 89]. The intracellularly localized receptors TLR3, 7 and 8, detect nucleic acids derived from viruses and bacteria. TLR3 was shown to recognize double stranded RNA (dsRNA) while TLR7 and TLR8 recognize synthetic imidazoquinoline-like molecules and single stranded RNA (ssRNA) [2]. Activation of TLR3, TLR5, TLR7 and TLR8 have not been demonstrated thus far in mycobacterial infections although under normal conditions they have been shown to be expressed in cells that can be infected by mycobacteria such as epithelial cells in the lungs and skin [32, 84] and dendritic cells where TLR7 and TLR8 respond to small anti-viral compounds to activate immune cells [38]. This present study demonstrated that TLR3, TLR5 and TLR8 were significantly up-regulated in response to infection with *M. ptb* in ovine Johne's disease. The mechanism for this remains unknown and further work will be required to determine if this is a specific up-regulation or a result of redundancy within the TLR signalling pathways. Elucidating the mycobacterial recognition and signalling pathway will reveal the fundamental immunological processes induced by *M. ptb*.

In eukaryotes, gene expression is controlled predominantly at the level of protein translation so it will be important to determine if the increases in transcript level of the TLR genes seen here by qPCR are also reflected in the proteome of the animals. In the case of gene expression in peripheral blood, it may be possible to detect significant differences in expression of the receptors at the protein level that may subsequently facilitate the diagnosis of *M. ptb* infection by colorimetric techniques such as flow cytometry or ELISA.

Another area which may warrant future investigation is whether the expression levels of the TLR transcripts or translated protein receptors in PBMCs from infected animals increases significantly in response to stimulation *in vitro* with purified antigen, Johnin-PPD or whole mycobacteria. Precedents for this approach include the early cell mediated immune (CMI) response detected by measurements of *in vitro* antigen-induced peripheral blood lymphocyte proliferation and cytokine secretion [10, 17, 46].The Bovigam® assay was developed to detect and quantify release of the cytokine IFN-γ when whole blood is cultured with bovine tuberculins [73]. The lymphocyte stimulation test (LST) is another assay of CMI and is sensitive for the detection of early stages of infection in cattle and sheep, responses being reduced in sheep with severe multibacillary lesions [15, 18, 49,

56]. *In vitro* stimulation of PBMCs from infected cows with *M. ptb* and microarray analysis revealed a rapid and transient activation of numerous genes within 2-4 hours of exposure [25].

The increases in expression determined here are from heterogenous populations of cells present in the native tissues of sheep. From this, we cannot determine what physiological event is responsible for the expression changes. For example, the changes may be due to up-regulation in resident cells in that tissue, or to cellular infiltration of subsets of mononuclear cells that have a constant expression of the TLR which results in an apparent up-regulation. The latter event could be a distinct possibility, as mild to moderate cellular infiltration was seen in cases of Johne's disease. This is a limitation of all approaches to the study of gene expression during inflammation in whole tissues, including by microarray. Further research at sub-gross level is clearly warranted to establish the location of increased TLR expression in Johne's disease.

Acknowledgements

The authors would like to thank Mrs. Reena Mehta, Mr.Craig Kristo, and Mrs. Anna Waldron for animal husbandry and laboratory support, Dr Lyrissa Di Fiore for the HK5.1 primers and Dr. Peter Thomson for advice on statistical analysis. This work was funded by Meat and Livestock Australia.

References

Aderem A., Underhill D.M., Mechanisms of phagocytosis in macrophages, Annu Rev Immunol (1999) 17:593-623.

Akira S., Uematsu S., Takeuchi O., Pathogen recognition and innate immunity, Cell (2006) 124:783-801.

Aliprantis A.O., Weiss D.S., Zychlinsky A., Toll-like receptor-2 transduces signals for NF-kappa B activation, apoptosis and reactive oxygen species production, J Endotoxin Res (2001) 7:287-291.

Armstrong J.A., Hart P.D., Phagosome-lysosome interactions in cultured macrophages infected with virulent tubercle bacilli. Reversal of the usual nonfusion pattern and observations on bacterial survival, J Exp Med (1975) 142:1-16.

Bafica A., Scanga C.A., Feng C.G., Leifer C., Cheever A., Sher A., TLR9 regulates Th1 responses and cooperates with TLR2 in mediating optimal resistance to Mycobacterium tuberculosis, J Exp Med (2005) 202:1715-1724.

Banchereau J., Steinman R.M., Dendritic cells and the control of immunity, Nature (1998) 392:245-252.

Basu S., Pathak S.K., Banerjee A., Pathak S., Bhattacharyya A., Yang Z., Talarico S., Kundu M., Basu J., Execution of macrophage apoptosis by PE_PGRS33 of Mycobacterium tuberculosis is mediated by Toll-like receptor 2-dependent release of tumor necrosis factor-alpha, J Biol Chem (2007) 282:1039-1050.

Bech-Nielsen S., Jorgensen J.B., Ahrens P., Feld N.C., Diagnostic accuracy of a Mycobacterium phlei-absorbed serum enzyme-linked immunosorbent assay for diagnosis of bovine paratuberculosis in dairy cows, J Clin Microbiol (1992) 30:613-618.

Ben-Ali M., Barbouche M.R., Bousnina S., Chabbou A., Dellagi K., Toll-like receptor 2 Arg677Trp polymorphism is associated with susceptibility to tuberculosis in Tunisian patients, Clin Diagn Lab Immunol (2004) 11:625-626.

Bendixen P.H., Immunological reactions caused by infection with Mycobacterium paratuberculosis. A review, Nord Vet Med (1978) 30:163-168.

Bermudez L.E., Young L.S., Natural killer cell-dependent mycobacteriostatic and mycobactericidal activity in human macrophages, J Immunol (1991) 146:265-270.

Bermudez L.E., Parker A., Goodman J.R., Growth within macrophages increases the efficiency of Mycobacterium avium in invading other macrophages by a complement receptor-independent pathway, Infect Immun (1997) 65:1916-1925.

Bhardwaj N., Nash T.W., Horwitz M.A., Interferon-gamma-activated human monocytes inhibit the intracellular multiplication of Legionella pneumophila, J Immunol (1986) 137:2662-2669.

Brightbill H.D., Libraty D.H., Krutzik S.R., Yang R.B., Belisle J.T., Bleharski J.R., Maitland M., Norgard M.V., Plevy S.E., Smale S.T., Brennan P.J., Bloom B.R., Godowski P.J., Modlin R.L., Host defense mechanisms triggered by microbial lipoproteins through toll-like receptors, Science (1999) 285:732-736.

Buergelt C.D., DeLisle G., Hall C.E., Merkal R.S., Duncan J.R., In vitro lymphocyte transformation as a herd survey method for bovine paratuberculosis, Am J Vet Res (1978) 39:591-595.

[16] Bulut Y., Michelsen K.S., Hayrapetian L., Naiki Y., Spallek R., Singh M., Arditi M., Mycobacterium tuberculosis heat shock proteins use diverse Toll-like receptor pathways to activate pro-inflammatory signals, J Biol Chem (2005) 280:20961-20967.

Burrells C., Inglis N.F., Davies R.C., Sharp J.M., Detection of specific T cell reactivity in sheep infected with Mycobacterium avium subspecies silvaticum and paratuberculosis using two defined mycobacterial antigens, Vet Immunol Immunopathol (1995) 45:311-320.

Burrells C., Clarke C.J., Colston A., Kay J.M., Porter J., Little D., Sharp J.M., A study of immunological responses of sheep clinically-affected with paratuberculosis (Johne's disease). The relationship of blood, mesenteric lymph node and intestinal lymphocyte responses to gross and microscopic pathology, Vet Immunol Immunopathol (1998) 66:343-358.

Cheville N.F., Hostetter J., Thomsen B.V., Simutis F., Vanloubbeeck Y., Steadham E., Intracellular trafficking of Mycobacterium avium ss. paratuberculosis in macrophages, Dtsch Tierarztl Wochenschr (2001) 108:236-243.

Clarke C.J., Patterson I.A., Armstrong K.E., Low J.C., Comparison of the absorbed ELISA and agar gel immunodiffusion test with clinicopathological findings in ovine clinical paratuberculosis, Vet Rec (1996) 139:618-621.

Clarke C.J., The pathology and pathogenesis of paratuberculosis in ruminants and other species, J Comp Pathol (1997) 116:217-261.

Clemens D.L., Horwitz M.A., Characterization of the Mycobacterium tuberculosis phagosome and evidence that phagosomal maturation is inhibited, J Exp Med (1995) 181:257-270.

Coccia E.M., Passini N., Battistini A., Pini C., Sinigaglia F., Rogge L., Interleukin-12 induces expression of interferon regulatory factor-1 via signal transducer and activator of transcription-4 in human T helper type 1 cells, J Biol Chem (1999) 274:6698-6703.

Corpa J.M., Garrido J., Garcia Marin J.F., Perez V., Classification of lesions observed in natural cases of paratuberculosis in goats, J Comp Pathol (2000) 122:255-265.

Coussens P.M., Jeffers A., Colvin C., Rapid and transient activation of gene expression in peripheral blood mononuclear cells from Johne's disease positive cows exposed to Mycobacterium paratuberculosis in vitro, Microb Pathog (2004) 36:93-108.

Dheda K., Huggett J.F., Bustin S.A., Johnson M.A., Rook G., Zumla A., Validation of housekeeping genes for normalizing RNA expression in real-time PCR, Biotechniques (2004) 37:112-114, 116, 118-119.

[27] Feng C.G., Scanga C.A., Collazo-Custodio C.M., Cheever A.W., Hieny S., Caspar P., Sher A., Mice lacking myeloid differentiation factor 88 display profound defects in host resistance and immune responses to Mycobacterium avium infection not exhibited by Toll-like receptor 2 (TLR2)- and TLR4-deficient animals, J Immunol (2003) 171:4758-4764.

Flynn J.L., Goldstein M.M., Chan J., Triebold K.J., Pfeffer K., Lowenstein C.J., Schreiber R., Mak T.W., Bloom B.R., Tumor necrosis factor-alpha is required in the protective immune response against Mycobacterium tuberculosis in mice, Immunity (1995) 2:561-572.

Fremond C.M., Yeremeev V., Nicolle D.M., Jacobs M., Quesniaux V.F., Ryffel B., Fatal Mycobacterium tuberculosis infection despite adaptive immune response in the absence of MyD88, J Clin Invest (2004) 114:1790-1799.

Gao J.J., Zuvanich E.G., Xue Q., Horn D.L., Silverstein R., Morrison D.C., Cutting edge: bacterial DNA and LPS act in synergy in inducing nitric oxide production in RAW 264.7 macrophages, J Immunol (1999) 163:4095-4099.

Gehring A.J., Dobos K.M., Belisle J.T., Harding C.V., Boom W.H., Mycobacterium tuberculosis LprG (Rv1411c): a novel TLR-2 ligand that inhibits human macrophage class II MHC antigen processing, J Immunol (2004) 173:2660-2668.

Gewirtz A.T., Navas T.A., Lyons S., Godowski P.J., Madara J.L., Cutting edge: bacterial flagellin activates basolaterally expressed TLR5 to induce epithelial proinflammatory gene expression, J Immunol (2001) 167:1882-1885.

Gilleron M., Quesniaux V.F., Puzo G., Acylation state of the phosphatidylinositol hexamannosides from Mycobacterium bovis bacillus Calmette Guerin and mycobacterium tuberculosis H37Rv and its implication in Toll-like receptor response, J Biol Chem (2003) 278:29880-29889.

Gonzalez J., Geijo M.V., Garcia-Pariente C., Verna A., Corpa J.M., Reyes L.E., Ferreras M.C., Juste R.A., Garcia Marin J.F., Perez V., Histopathological classification of lesions associated with natural paratuberculosis infection in cattle, J Comp Pathol (2005) 133:184-196.

Hamalainen H.K., Tubman J.C., Vikman S., Kyrola T., Ylikoski E., Warrington J.A., Lahesmaa R., Identification and validation of endogenous reference genes for expression profiling of T helper cell differentiation by quantitative real-time RT-PCR, Anal Biochem (2001) 299:63-70.

Heldwein K.A., Fenton M.J., The role of Toll-like receptors in immunity against mycobacterial infection, Microbes Infect (2002) 4:937-944.

Hemmi H., Takeuchi O., Kawai T., Kaisho T., Sato S., Sanjo H., Matsumoto M., Hoshino K., Wagner H., Takeda K., Akira S., A Toll-like receptor recognizes bacterial DNA, Nature (2000) 408:740-745.

Hemmi H., Kaisho T., Takeuchi O., Sato S., Sanjo H., Hoshino K., Horiuchi T., Tomizawa H., Takeda K., Akira S., Small anti-viral compounds activate immune cells via the TLR7 MyD88-dependent signaling pathway, Nat Immunol (2002) 3:196-200.

Honda K., Sakaguchi S., Nakajima C., Watanabe A., Yanai H., Matsumoto M., Ohteki T., Kaisho T., Takaoka A., Akira S., Seya T., Taniguchi T., Selective contribution of IFN-alpha/beta signaling to the maturation of dendritic cells induced by double-stranded RNA or viral infection, Proc Natl Acad Sci U S A (2003) 100:10872-10877.

Hoshino K., Kaisho T., Iwabe T., Takeuchi O., Akira S., Differential involvement of IFN-beta in Toll-like receptor-stimulated dendritic cell activation, Int Immunol (2002) 14:1225-1231.

Iwasaki A., Medzhitov R., Toll-like receptor control of the adaptive immune responses, Nat Immunol (2004) 5:987-995.

Janssens S., Beyaert R., Functional diversity and regulation of different interleukin-1 receptor-associated kinase (IRAK) family members, Mol Cell (2003) 11:293-302.

Jung S.B., Yang C.S., Lee J.S., Shin A.R., Jung S.S., Son J.W., Harding C.V., Kim H.J., Park J.K., Paik T.H., Song C.H., Jo E.K., The mycobacterial 38-kilodalton glycolipoprotein antigen activates the mitogen-activated protein kinase pathway and release of proinflammatory cytokines through Toll-like receptors 2 and 4 in human monocytes, Infect Immun (2006) 74:2686-2696.

Kawai T., Akira S., TLR signaling, Semin Immunol (2007) 19:24-32.

Koets A.P., Adugna G., Janss L.L., van Weering H.J., Kalis C.H., Wentink G.H., Rutten V.P., Schukken Y.H., Genetic variation of susceptibility to Mycobacterium avium subsp. paratuberculosis infection in dairy cattle, J Dairy Sci (2000) 83:2702-2708.

[Kreeger J.M., Snider T.G., 3rd, Measurement of lymphoblast proliferative capacity of stimulated blood mononuclear cells from cattle with chronic paratuberculosis, Am J Vet Res (1992) 53:392-395.

Krutzik S.R., Ochoa M.T., Sieling P.A., Uematsu S., Ng Y.W., Legaspi A., Liu P.T., Cole S.T., Godowski P.J., Maeda Y., Sarno E.N., Norgard M.V., Brennan P.J., Akira S., Rea T.H., Modlin R.L., Activation and regulation of Toll-like receptors 2 and 1 in human leprosy, Nat Med (2003) 9:525-532.

Krutzik S.R., Modlin R.L., The role of Toll-like receptors in combating mycobacteria, Semin Immunol (2004) 16:35-41.

Kurade N.P., Tripathi B.N., Rajukumar K., Parihar N.S., Sequential development of histologic lesions and their relationship with bacterial isolation, fecal shedding, and immune responses during progressive stages of experimental infection of lambs with Mycobacterium avium subsp. paratuberculosis, Vet Pathol (2004) 41:378-387.

Lasker M.V., Nair S.K., Intracellular TLR signaling: a structural perspective on human disease, J Immunol (2006) 177:11-16.

Liew F.Y., Xu D., Brint E.K., O'Neill L.A., Negative regulation of toll-like receptor-mediated immune responses, Nat Rev Immunol (2005) 5:446-458.

Livak K.J., Schmittgen T.D., Analysis of relative gene expression data using real-time quantitative PCR and the 2(-Delta Delta C(T)) Method, Methods (2001) 25:402-408.

MacMicking J.D., North R.J., LaCourse R., Mudgett J.S., Shah S.K., Nathan C.F., Identification of nitric oxide synthase as a protective locus against tuberculosis, Proc Natl Acad Sci U S A (1997) 94:5243-5248.

Means T.K., Lien E., Yoshimura A., Wang S., Golenbock D.T., Fenton M.J., The CD14 ligands lipoarabinomannan and lipopolysaccharide differ in their requirement for Toll-like receptors, J Immunol (1999) 163:6748-6755.

Menzies M., Ingham A., Identification and expression of Toll-like receptors 1-10 in selected bovine and ovine tissues, Vet Immunol Immunopathol (2006) 109:23-30.

Milner A.R., Wilks C.R., Borland R., In vitro responses of lymphocytes from cattle with advanced Mycobacterium paratuberculosis infection to homologous and heterologous antigens, Res Vet Sci (1981) 31:93-99.

Morris K.R., Lutz R.D., Choi H.S., Kamitani T., Chmura K., Chan E.D., Role of the NF-kappaB signaling pathway and kappaB cis-regulatory elements on the IRF-1 and iNOS promoter regions in mycobacterial lipoarabinomannan induction of nitric oxide, Infect Immun (2003) 71:1442-1452.

Noss E.H., Pai R.K., Sellati T.J., Radolf J.D., Belisle J., Golenbock D.T., Boom W.H., Harding C.V., Toll-like receptor 2-dependent inhibition of macrophage class II MHC expression and antigen processing by 19-kDa lipoprotein of Mycobacterium tuberculosis, J Immunol (2001) 167:910-918.

Ogus A.C., Yoldas B., Ozdemir T., Uguz A., Olcen S., Keser I., Coskun M., Cilli A., Yegin O., The Arg753GLn polymorphism of the human toll-like receptor 2 gene in tuberculosis disease, Eur Respir J (2004) 23:219-223.

Okamura H., Kashiwamura S., Tsutsui H., Yoshimoto T., Nakanishi K., Regulation of interferon-gamma production by IL-12 and IL-18, Curr Opin Immunol (1998) 10:259-264.

Pai R.K., Pennini M.E., Tobian A.A., Canaday D.H., Boom W.H., Harding C.V., Prolonged toll-like receptor signaling by Mycobacterium tuberculosis and its 19-kilodalton lipoprotein inhibits gamma interferon-induced regulation of selected genes in macrophages, Infect Immun (2004) 72:6603-6614.

Parker L.C., Prince L.R., Sabroe I., Translational mini-review series on Toll-like receptors: networks regulated by Toll-like receptors mediate innate and adaptive immunity, Clin Exp Immunol (2007) 147:199-207.

Pecora N.D., Gehring A.J., Canaday D.H., Boom W.H., Harding C.V., Mycobacterium tuberculosis LprA is a lipoprotein agonist of TLR2 that regulates innate immunity and APC function, J Immunol (2006) 177:422-429.

Perez V., Garcia Marin J.F., Badiola J.J., Description and classification of different types of lesion associated with natural paratuberculosis infection in sheep, J Comp Pathol (1996) 114:107-122.

Perez V., Tellechea J., Badiola J.J., Gutierrez M., Garcia Marin J.F., Relation between serologic response and pathologic findings in sheep with naturally acquired paratuberculosis, Am J Vet Res (1997) 58:799-803.

Perez V., Tellechea J., Corpa J.M., Gutierrez M., Garcia Marin J.F., Relation between pathologic findings and cellular immune responses in sheep with naturally acquired paratuberculosis, Am J Vet Res (1999) 60:123-127.

Quesniaux V.J., Nicolle D.M., Torres D., Kremer L., Guerardel Y., Nigou J., Puzo G., Erard F., Ryffel B., Toll-like receptor 2 (TLR2)-dependent-positive and TLR2-independent-negative regulation of proinflammatory cytokines by mycobacterial lipomannans, J Immunol (2004) 172:4425-4434.

Radonic A., Thulke S., Mackay I.M., Landt O., Siegert W., Nitsche A., Guideline to reference gene selection for quantitative real-time PCR, Biochem Biophys Res Commun (2004) 313:856-862.

[69] Radonic A., Thulke S., Bae H.G., Muller M.A., Siegert W., Nitsche A., Reference gene selection for quantitative real-time PCR analysis in virus infected cells: SARS corona virus, Yellow fever virus, Human Herpesvirus-6, Camelpox virus and Cytomegalovirus infections, Virol J (2005) 2:7.

Roach D.R., Bean A.G., Demangel C., France M.P., Briscoe H., Britton W.J., TNF regulates chemokine induction essential for cell recruitment, granuloma formation, and clearance of mycobacterial infection, J Immunol (2002) 168:4620-4627.

Rock F.L., Hardiman G., Timans J.C., Kastelein R.A., Bazan J.F., A family of human receptors structurally related to Drosophila Toll, Proc Natl Acad Sci U S A (1998) 95:588-593.

Rodriguez-Mulero S., Montanya E., Selection of a suitable internal control gene for expression studies in pancreatic islet grafts, Transplantation (2005) 80:650-652.

Rothel J.S., Jones S.L., Corner L.A., Cox J.C., Wood P.R., A sandwich enzyme immunoassay for bovine interferon-gamma and its use for the detection of tuberculosis in cattle, Aust Vet J (1990) 67:134-137.

Rothermel C.D., Rubin B.Y., Murray H.W., Gamma-interferon is the factor in lymphokine that activates human macrophages to inhibit intracellular Chlamydia psittaci replication, J Immunol (1983) 131:2542-2544.

Russell D.G., Dant J., Sturgill-Koszycki S., Mycobacterium avium- and Mycobacterium tuberculosis-containing vacuoles are dynamic, fusion-competent vesicles that are accessible to glycosphingolipids from the host cell plasmalemma, J Immunol (1996) 156:4764-4773.

Scanga C.A., Bafica A., Feng C.G., Cheever A.W., Hieny S., Sher A., MyD88-deficient mice display a profound loss in resistance to Mycobacterium tuberculosis associated with partially impaired Th1 cytokine and nitric oxide synthase 2 expression, Infect Immun (2004) 72:2400-2404.

Schnare M., Barton G.M., Holt A.C., Takeda K., Akira S., Medzhitov R., Toll-like receptors control activation of adaptive immune responses, Nat Immunol (2001) 2:947-950.

Shiratsuchi H., Krukovets I., Ellner J.J., Role of T cell subsets in the modulation of Mycobacterium avium growth within human monocytes, Cell Immunol (2000) 202:6-12.

Sockett D.C., Conrad T.A., Thomas C.B., Collins M.T., Evaluation of four serological tests for bovine paratuberculosis, J Clin Microbiol (1992) 30:1134-1139.

Stabel J.R., Cytokine secretion by peripheral blood mononuclear cells from cows infected with Mycobacterium paratuberculosis, Am J Vet Res (2000) 61:754-760.

Sturgill-Koszycki S., Schlesinger P.H., Chakraborty P., Haddix P.L., Collins H.L., Fok A.K., Allen R.D., Gluck S.L., Heuser J., Russell D.G., Lack of acidification in Mycobacterium phagosomes produced by exclusion of the vesicular proton-ATPase, Science (1994) 263:678-681.

Suzuki N., Suzuki S., Yeh W.C., IRAK-4 as the central TIR signaling mediator in innate immunity, Trends Immunol (2002) 23:503-506.

Sweet L., Schorey J.S., Glycopeptidolipids from Mycobacterium avium promote macrophage activation in a TLR2- and MyD88-dependent manner, J Leukoc Biol (2006) 80:415-423.

Takeuchi J., Watari E., Shinya E., Norose Y., Matsumoto M., Seya T., Sugita M., Kawana S., Takahashi H., Down-regulation of Toll-like receptor expression in monocyte-derived Langerhans cell-like cells: implications of low-responsiveness to bacterial components in the epidermal Langerhans cells, Biochem Biophys Res Commun (2003) 306:674-679.

Taylor D.L., Thomson P.C., de Silva K., Whittington R.J., Validation of endogenous reference genes for expression profiling of RAW264.7 cells infected with Mycobacterium avium subsp. paratuberculosis by quantitative PCR, Vet Immunol Immunopathol (2007) 115:43-55.

Thellin O., Zorzi W., Lakaye B., De Borman B., Coumans B., Hennen G., Grisar T., Igout A., Heinen E., Housekeeping genes as internal standards: use and limits, J Biotechnol (1999) 75:291-295.

Thoma-Uszynski S., Stenger S., Takeuchi O., Ochoa M.T., Engele M., Sieling P.A., Barnes P.F., Rollinghoff M., Bolcskei P.L., Wagner M., Akira S., Norgard M.V., Belisle J.T., Godowski P.J., Bloom B.R., Modlin R.L., Induction of direct antimicrobial activity through mammalian toll-like receptors, Science (2001) 291:1544-1547.

Thorel M.F., Vialard J., Manfroni F., Bernardot J., Ostyn A., Vandevelde J., [Experimental paratuberculosis in sheep after intravenous or oral inoculation: pathogenicity and biologic diagnosis], Ann Rech Vet (1992) 23:105-115.

Uematsu S., Jang M.H., Chevrier N., Guo Z., Kumagai Y., Yamamoto M., Kato H., Sougawa N., Matsui H., Kuwata H., Hemmi H., Coban C., Kawai T., Ishii K.J., Takeuchi O., Miyasaka M., Takeda K., Akira S., Detection of pathogenic intestinal bacteria by Toll-like receptor 5 on intestinal CD11c+ lamina propria cells, Nat Immunol (2006) 7:868-874.

Underhill D.M., Ozinsky A., Smith K.D., Aderem A., Toll-like receptor-2 mediates mycobacteria-induced proinflammatory signaling in macrophages, Proc Natl Acad Sci U S A (1999) 96:14459-14463.

Verna A.E., Garcia-Pariente C., Munoz M., Moreno O., Garcia-Marin J.F., Romano M.I., Paolicchi F., Perez V., Variation in the immuno-pathological responses of lambs after experimental infection with different strains of Mycobacterium avium subsp. paratuberculosis, Zoonoses Public Health (2007) 54:243-252.

Welsh M.D., Cunningham R.T., Corbett D.M., Girvin R.M., McNair J., Skuce R.A., Bryson D.G., Pollock J.M., Influence of pathological progression on the balance between cellular and humoral immune responses in bovine tuberculosis, Immunology (2005) 114:101-111.

Whittington R.J., Marsh I., McAllister S., Turner M.J., Marshall D.J., Fraser C.A., Evaluation of modified BACTEC 12B radiometric medium and solid media for culture of Mycobacterium avium subsp. paratuberculosis from sheep, J Clin Microbiol (1999) 37:1077-1083.

Wieland C.W., Knapp S., Florquin S., de Vos A.F., Takeda K., Akira S., Golenbock D.T., Verbon A., van der Poll T., Non-mannose-capped lipoarabinomannan induces lung inflammation via toll-like receptor 2, Am J Respir Crit Care Med (2004) 170:1367-1374.

Yim J.J., Lee H.W., Lee H.S., Kim Y.W., Han S.K., Shim Y.S., Holland S.M., The association between microsatellite polymorphisms in intron II of the human Toll-like receptor 2 gene and tuberculosis among Koreans, Genes Immun (2006) 7:150-155.

Table I. Experimental animals used in this study

Property	Animal ID	Infection status	Histological lesion[a]				Tissue Culture[b]	Faecal Culture[b]	Tissue[c]	Lymph node[c]	PBMC[c]	Reference gene[d]
			TI-A	*TI-D*	*LN-A*	*LN-D*						
A	2	Unexposed	0	0	0	0	-	-			✓	PB
	3	Unexposed	0	0	0	0	-	-	✓	✓		T, LN
	4	Unexposed	0	0	0	0	-	-	✓	✓	✓	
	5	Unexposed	0	0	0	0	-	-	✓	✓		T, LN
	6	Unexposed	0	0	0	0	-	-	✓	✓		
	7	Unexposed	0	0	0	0	-	-	✓	✓	✓	PB
	8	Unexposed	0	0	0	0	-	-	✓	✓	✓	
	10	Unexposed	0	0	0	0	-	-			✓	PB
B	6-3	Unexposed	0	0	0	0	-	-	✓	✓		
	6-4	Unexposed	0	0	0	0	-	-	✓	✓		
	6-6	Unexposed	0	0	0	0	-	-	✓	✓		
	6-7	Unexposed	0	0	0	0	-	-	✓	✓		
	6-8	Unexposed	0	0	0	0	-	-	✓	✓		
	6-9	Unexposed	0	0	0	0	-	-	✓	✓		
C	981	Uninfected	0	0	0	0	-	-	✓	✓		T, LN
	982	Uninfected	0	0	0	0	-	-	✓	✓	✓	
	983	Uninfected	0	0	0	0	-	-	✓	✓	✓	PB
	988	Early Pauci	3a	3a	2	1	+	-	✓	✓		T, LN
	989	Early Pauci	3a	3a	2	2	+	+	✓	✓	✓	PB
	990	Multibacilliary	3b	3a	2	2	+	+	✓	✓	✓	T, LN
	986	Multibacilliary	3b	3b	2	1	+	+	✓	✓		
D	10/9	Uninfected	0	0	0	0	-	-	✓	✓		T, LN
	31/23	Uninfected	0	0	0	0	-	-	✓	✓	✓	T, LN, PB
	52/18	Uninfected	0	0	0	0	-	-	✓	✓	✓	
	30/14	Early Pauci	3a	3a	2	1	+	-	✓	✓	✓	T, LN, PB
	48/16	Early Pauci	3a	0	2	1	+	-	✓	✓	✓	T, LN
	50/7	Early Pauci	3a	0	1	0	-	-	✓	✓	✓	
	87/28	Early Pauci	3a	0	ND	0	+	-	✓	✓		
	14/33	Multibacilliary	3b	3b	1	2	+	+	✓	✓	✓	T, LN, PB
	35/8	Multibacilliary	3b	3b	2	1	+	-	✓	✓	✓	T, LN, PB
	55/15	Multibacilliary	3b	0	1	1	+	-	✓	✓	✓	
	76/2	Multibacilliary	3b	3a+	2	1	+	+	✓	✓	✓	
E	4-1	Uninfected	0	0	0	0	-	-			✓	PB
	4-3	Uninfected	0	0	0	0	-	-			✓	
	4-4	Uninfected	0	0	0	0	-	-			✓	
	4-2	Early Pauci	3a	0	2	1	+	-			✓	PB

[a] Perez et al, 1996. TI-A, terminal ileum immediately adjacent to ileo-caecal junction; LN-A, TI-A associated draining lymph node; TI-D, terminal jejunum, 3m proximal to ileo-caecal junction; LN-D, TI-D associated draining lymph node.

[b] Determined by growth in radiometric culture medium (modified BACTEC 12B, BD) at 37°C for 12 weeks or until maximum Growth Index (GI) of 999. Presence of *M. ptb* at completion of culture was verified by IS*900* PCR amplification; -, negative; +, positive.
[c] ✓ indicates samples used for gene expression analysis.
[d] indicated samples used to determine reference genes; T tissue, LN lymph node, PB peripheral blood mononuclear cells. ND = not determined for this sample.

Table II. Primers used during this study

Primer	Gene	Sequence (5′-3′)	Genbank Accession
Q5 OvB2M	β2-microglobulin	CTGCTGTCGCTGTCTGGA	**AY549962**
Q3 OvB2M		CAGTTCAGGTAATTTGGCTTTCC	
Q5 OvBact	β-actin	CATCCTGACCCTCAAGTACC	**U39357**
Q3 OvBact		TCGTTGTAGAAGGTGTGGTG	
Q5 Ovtub	α-tubulin	CCAGATGGTGAAATGTGACC	**AF251146**
Q3 Ovtub		GCATTGACATCTTTGGGAAC	
Q5 OvPPIA	PPIA	TGAGCACTGGAGAGAAAGGATTTG	**AY251270**
Q3 OvPPIA		AGTCACCACCCTGGCACATAA	
Q5 Ov18S	18S	GCAATTATTCCCCATGAACG	**DQ013885**
Q3 Ov18S		CAAAGGGCAGGGACTTAATC	
Q5 GAPDH	GAPDH	TTCCAGTATGATTCCACCCATG	**AF035421**
Q3 GAPDH		GCCTTTCCATTGATGACGAG	
Q5 HK5.1	Putative SFRS6	TTAACAAAGTGGGAGAAAGATACC	Unpublished[a]
Q3 HK5.1		TAACATGCCATAGTGCCTTTATG	
Q5 H7-7	COPG2	GTGTTCCCTCTTTGCTTCTGAC	Unpublished[a]
Q3 H7-7		AGGTGGCTATGATTTATTGGTGAG	
Q5 TLR1	TLR 1	GGTTGAGTGCCACACAGTTAC	**AY957612**[b]
Q3 TLR1		TCTCTTTCCCCATAAGTATCTCCTAA	
Q5 TLR2	TLR 2	TCACACGGTGGAGGAAGATTC	**AY957613**[b]
Q3 TLR2		TGAACCAGGAAGATGATAAGTTAGAT	
Q5 TLR3	TLR 3	TATAAACTGAACCACGCACTCTG	**AY957614**[b]
Q3 TLR3		AAGCATTTACCCGTTCTTTCTGAA	
Q5 TLR4	TLR 4	TGCGGAATGAACTGGTAAAGAAC	**AY957615**[b]
Q3 TLR4		GATGATATTGGCGGCGATGG	
Q5 TLR5	TLR 5	ACCACATCGCCAACATCCAG	**AY957616**[b]
Q3 TLR5		ACCCGTCTCTAAGGAAGTGTCT	
Q5 TLR6	TLR 6	GGCTGGTGCTGGCTGTTG	**AY957617**[b]
Q3 TLR6		CGGGTCTGCGTCCACTGA	
Q5 TLR7	TLR 7	TGACAGAAATTCCTGGAGGTATTC	**AY957618**[b]
Q3 TLR7		TGGAGAGATGCCTGCTATGTG	
Q5 TLR8	TLR 8	CAGACTTTCTACGATGCTTACG	**AY957619**[b]
Q3 TLR8		GTTCTTGTCCTCACTCTCTTCC	
Q5 TLR9	TLR 9	AACCGCATCCACCACTTG	**AY957620**[b]
Q3 TLR9		GGGCAGTTCCACTTGAGG	
Q5 TLR10	TLR 10	CAATTACAACCACACTGGATTTATC	**AY957621**[b]
Q3 TLR10		TGGCATAGAATCAGAACTTTCAG	

[a] Unpublished sequence, primers provided by L. Zhong and L. Di Fiore; [b] Menzies and Ingham, 2006.

Table III. Determination of reference genes in intestinal, lymph node and PBMC samples. HK5.1, H7.7 and GAPDH had the small SD in Ct in the tissues, lymph nodes and PBMCs respectively, and were chosen as reference genes for these samples.

	Ileum		Jejunum		Lymph node		PBMC	
Gene	Ct	SD	Ct	SD	Ct	SD	Ct	SD
α-tubulin	20.15	1.00	19.17	1.12	19.98	0.59	21.28	0.80
β-actin	24.26	2.29	22.92	2.53	21.06	1.19	17.88	0.84
β-2m	19.26	1.05	19.45	1.11	22.19	1.04	ND	ND
GAPDH	23.59	1.95	22.00	2.55	23.12	0.63	22.77	0.43
PPIA	20.04	0.93	19.53	0.83	24.80	0.55	22.52	1.07
18S	20.33	2.34	17.06	2.22	ND	ND	18.79	0.54
HK5.1	25.60	0.59	26.28	0.58	ND	ND	27.43	0.69
H7-7	26.62	0.62	25.05	0.68	25.00	0.36	ND	ND

ND - not determined

Figure 1. Mean ΔCt of TLR1-8 expression in the ileum of sheep infected with M. ptb. TLR2, TLR3, TLR4, TLR5 and TLR8 were significantly higher in the ileum of infected animals relative to the uninfected animals. Error bars show standard error. Numbers show mean fold change in expression relative to unexposed animals calculated using ΔCt. a significantly different from the uninfected animals. For illustrative purposes, the Y axis is reversed to show the direction in fold change obtained by 2-ΔΔCt analysis.

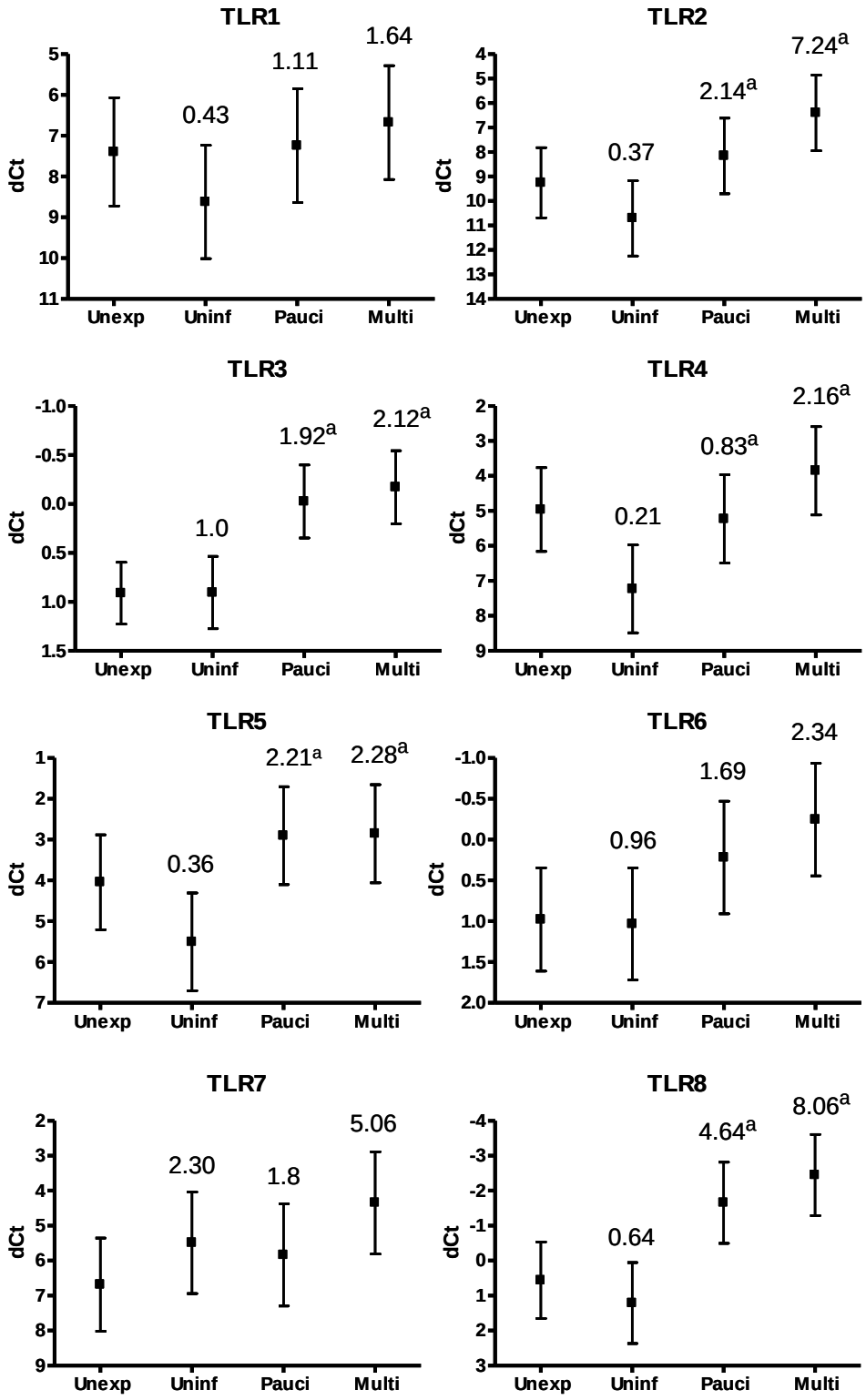

Figure 2. Mean ΔCt of TLR1-8 expression in the jejunum of sheep infected with M. ptb. TLR2, TLR4 and TLR8 were significantly increased in the jejunal tissues of infected animals. Error bars show standard error. Numbers show mean fold change in expression relative to unexposed animals. [a] significantly different from the uninfected animals calculated using ΔCt. [b] significantly different from paucibacillary animals. For illustrative purposes, the Y axis is reversed to show the direction in fold change obtained by $2^{-\Delta\Delta Ct}$ analysis.

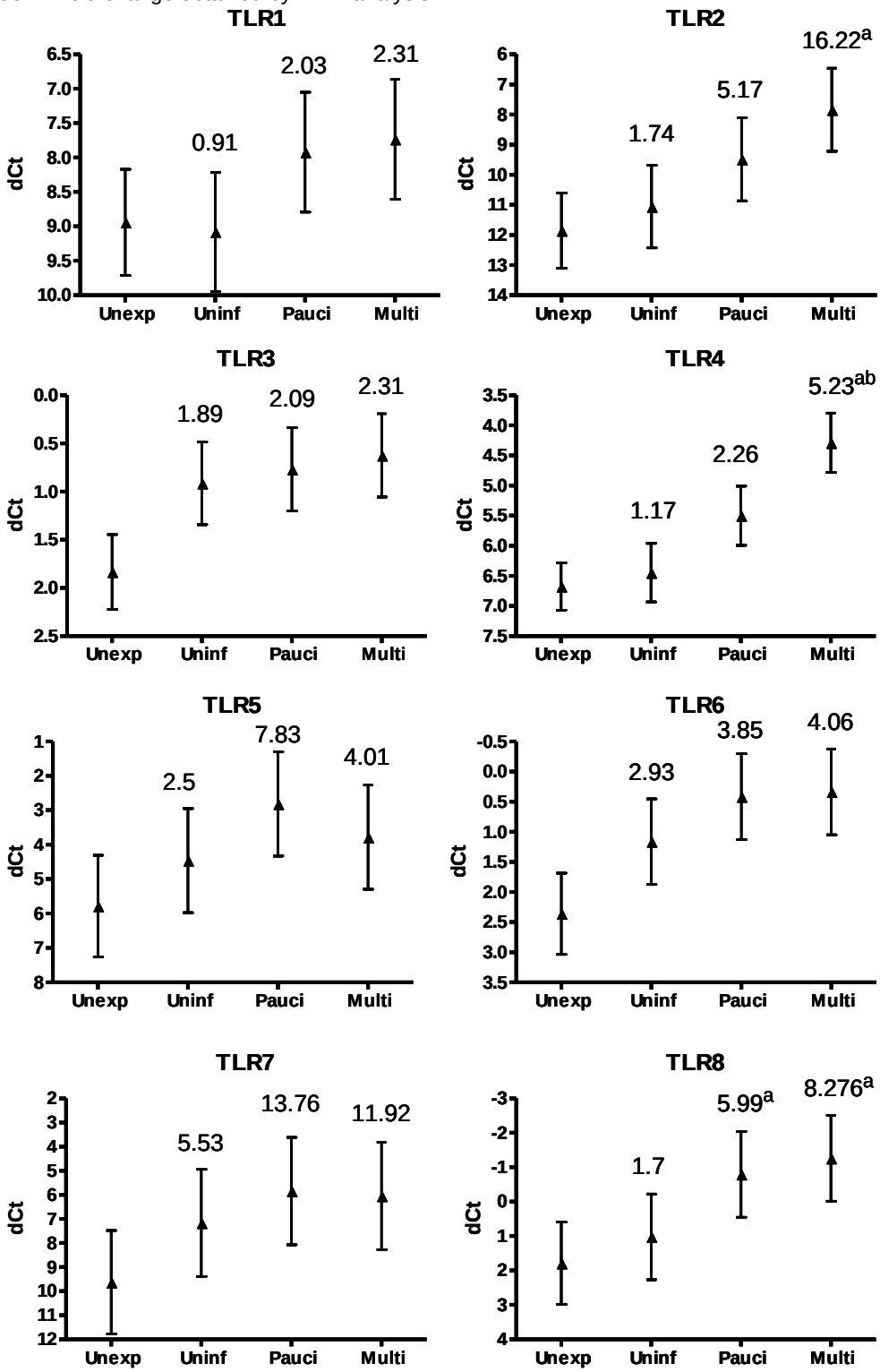

Figure 3. Mean ΔCt of TLR1-8 expression in the ileal lymph nodes of sheep infected with M. ptb. Significant increases in expression of TLR1, TLR2, TLR4, TLR6 and TLR8 were found in the ileal lymph nodes of infected animals relative to uninfected animals. Error bars show standard error. Numbers show mean fold change in expression relative to unexposed animals calculated using ΔCt. [a] significantly different from the uninfected animals. [b] significantly different from paucibacillary animals. For illustrative purposes, the Y axis is reversed to show the direction in fold change obtained by $2^{-\Delta\Delta Ct}$ analysis.

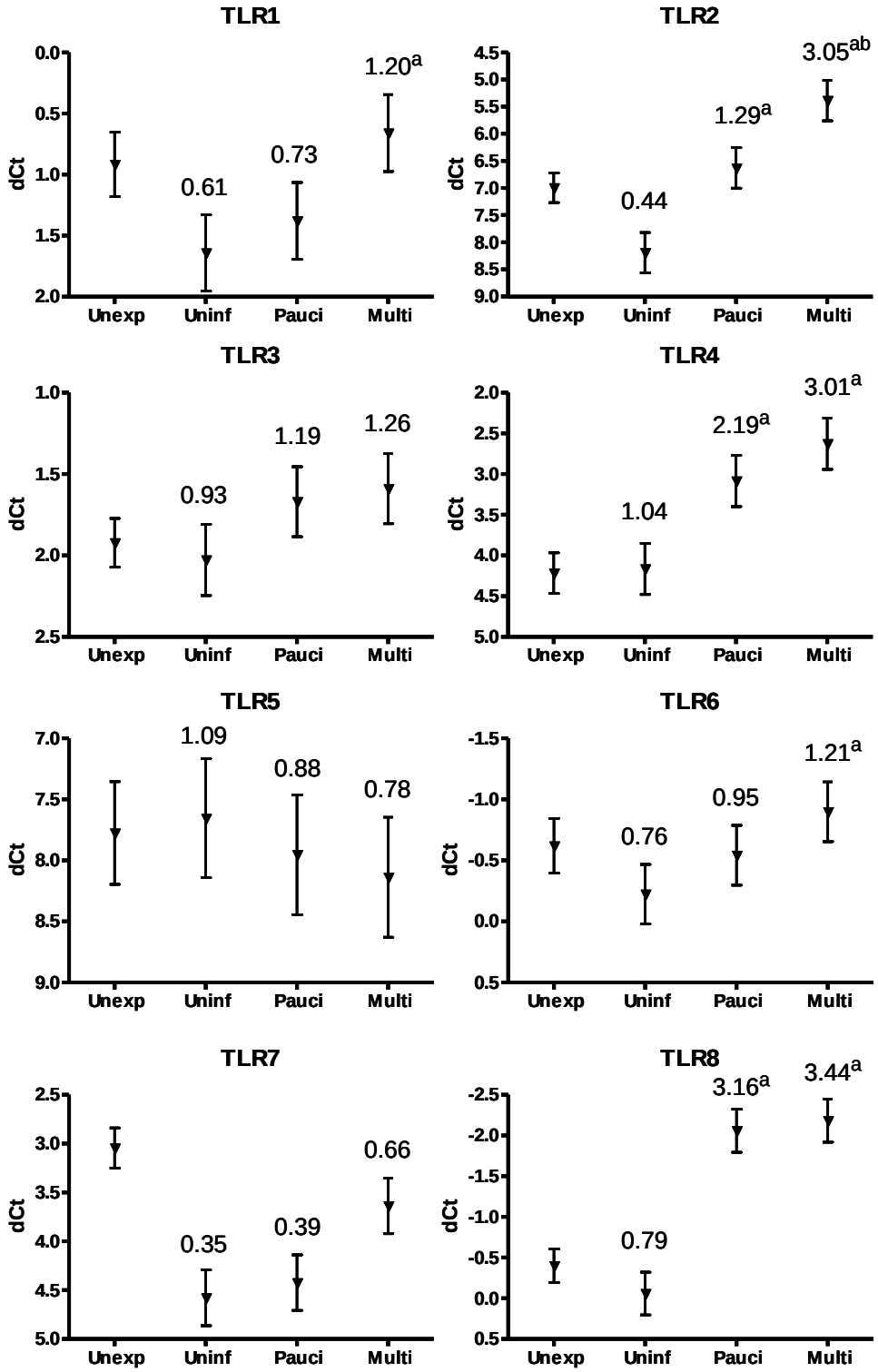

Figure 4. Mean ΔCt of TLR1-8 expression in the jejunal lymph nodes of sheep infected with M. ptb. Significant increases in expression were found in the jejunal lymph nodes of infected animals relative to uninfected animals for TLR1, TLR2, TLR3, TLR6 and TLR8. Error bars show standard error. Numbers show mean fold change in expression relative to unexposed animals calculated using ΔCt. [a] significantly different from the uninfected animals. [b] significantly different from paucibacillary animals. For illustrative purposes, the Y axis is reversed to show the direction in fold change obtained by $2^{-\Delta\Delta Ct}$ analysis.

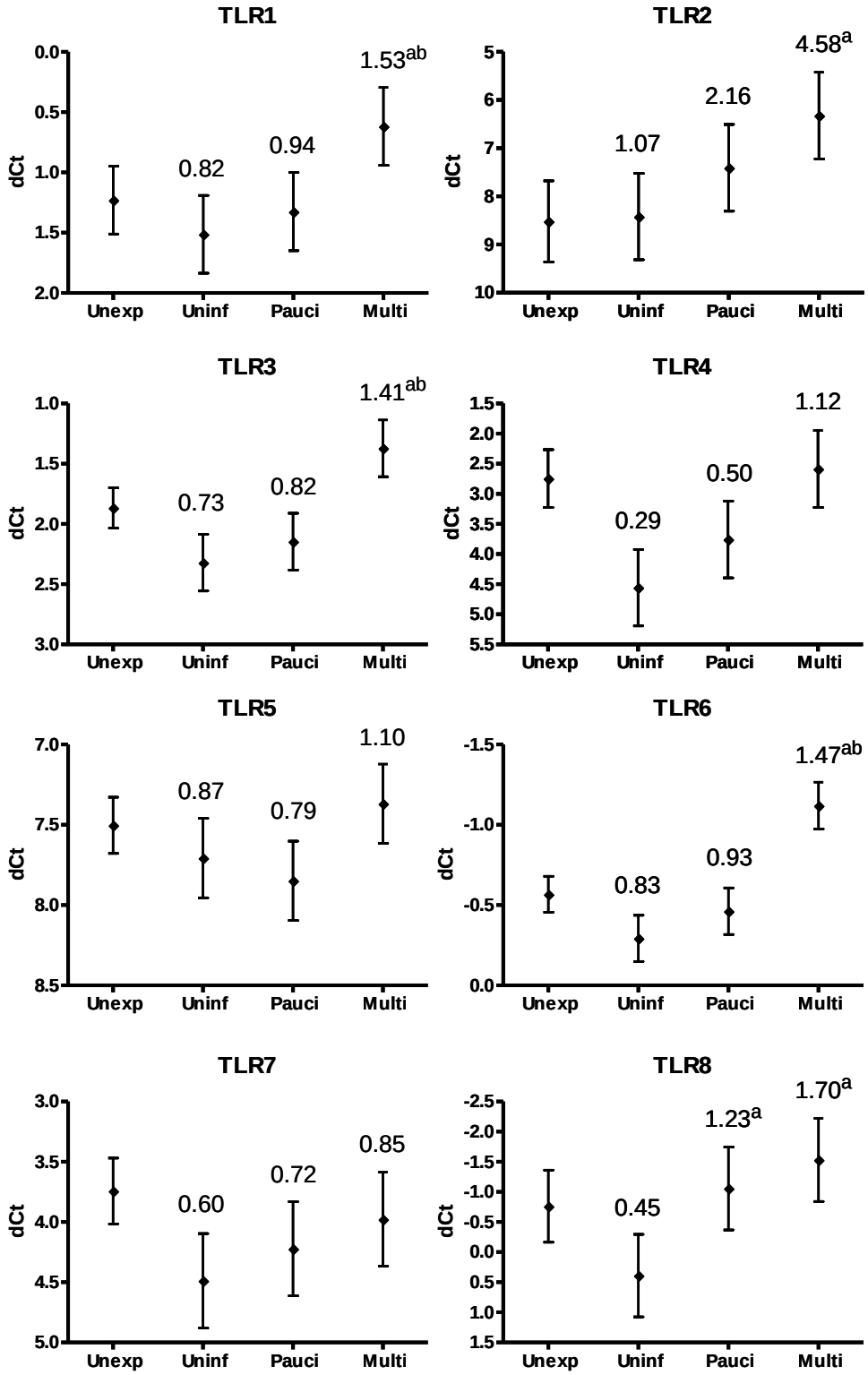

Figure 5. Mean ΔCt of TLR1-8 expression in PBMCs of sheep infected with M. ptb. None of the TLR genes analyzed were significantly altered in the PBMCs of infected animals relative to uninfected animals. TLR 1, TLR6, TLR7 and TLR8 showed trends to increases in expression in uninfected animals relative to the unexposed group. Error bars show standard error. Numbers show mean fold change in expression relative to unexposed animals calculated using ΔCt. For illustrative purposes, the Y axis is reversed to show the direction in fold change obtained by $2^{-\Delta\Delta Ct}$ analysis

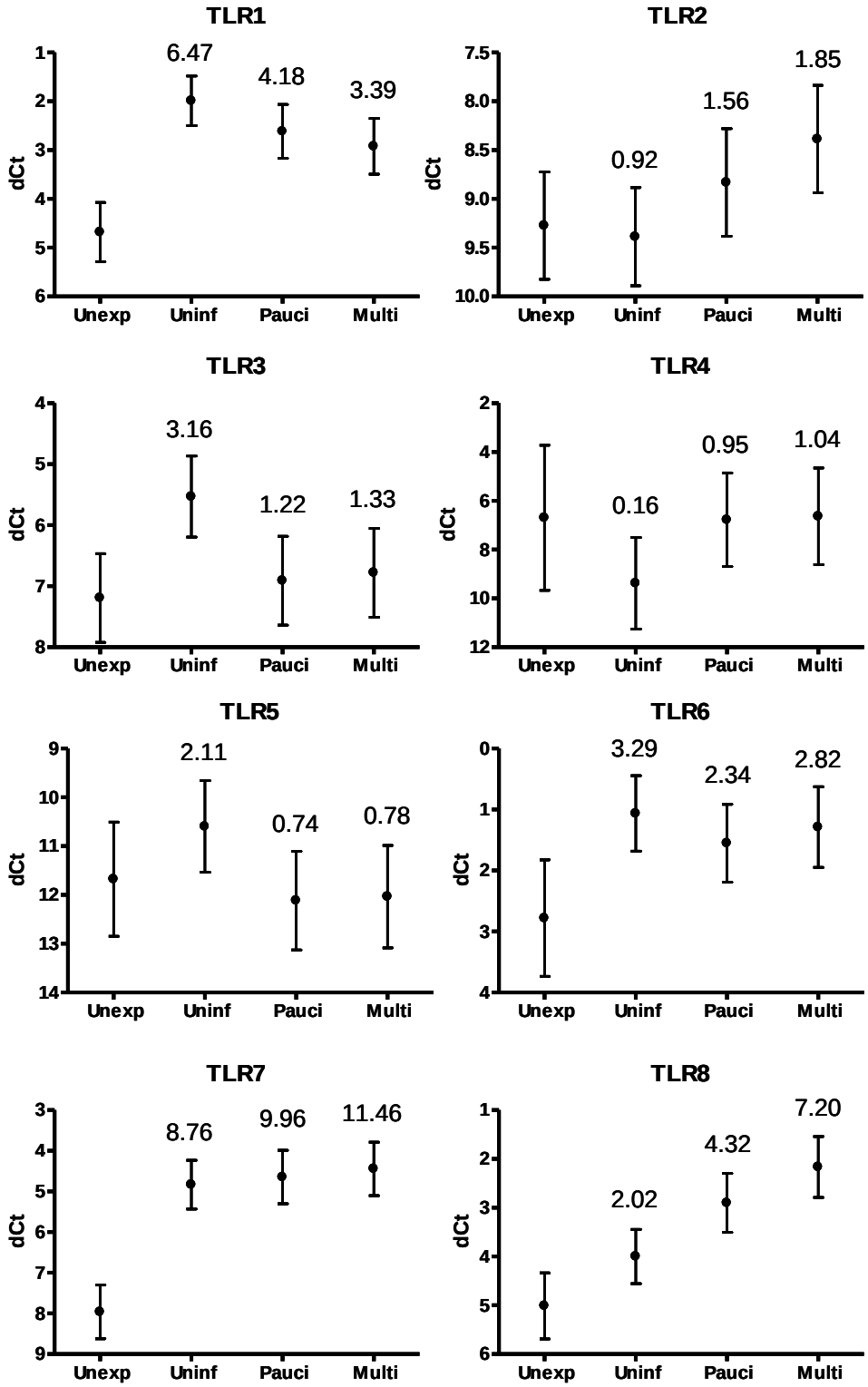

9.21 Appendix 3B-4 Subprogram 3 Proteomic profiling of ovine serum by SELDI-TOF MS: optimization, reproducibility and feasibility

Introduction

Physiological and pathological processes modify the composition and abundance of proteins in serum (the serum proteome) and may generate a unique signature, known as a *proteomic signature*, or *disease signature* (Rocken et al., 2004). This approach has yet to be applied in animal health, if for no other reason than proteomic research in animals to define the normal serum proteome has been limited. However, there are many possible applications. Examples from human medicine include serum proteomic diagnosis of cryptic diseases such as ovarian, prostate, head and neck, breast and pancreatic cancers (Conrads et al., 2004; Koopmann et al., 2004; Li et al., 2004; Petricoin et al., 2002; Petricoin and Liotta, 2004; Wadsworth et al., 2004; Wulfkuhle et al., 2001). Although genomic approaches are now being used in animal health research, protein structure and the dynamics of protein expression cannot be predicted from them with certainty as the proteome is a dynamic collection of proteins that vary over time and between cells, tissue types, individuals, and between entities with different pathological or physiological conditions (Clarke et al., 2003). Downstream measurement of gene expression at the level of mRNA is not necessarily related to protein expression level and cannot predict the key signaling molecules in a protein network. However, the emerging field of proteomics provides a mass-screening approach to analyze overall distribution and abundance of proteins, and identify and characterize individual proteins of interest.

The low-molecular-weight (LMW) region of the serum proteome is an assortment of intact proteins and fragments of larger proteins, including components of both the innate and adaptive immune systems, and so potentially contains an abundance of information (Liotta et al., 2003). Recent studies have revealed that proteomic profiling of serum using an application of mass spectrometry (MS) called surface-enhanced laser desorption ionisation time-of-flight (SELDI-TOF) MS is useful for the early detection of a wide range of human malignancies. The application of this technology to animal health research could allow the discovery of potential biomarkers for the early diagnosis of disease, or monitoring disease progression and recovery. Blood is readily collected and so is a practical sample for analysis in all of the domestic animal species and many animal serum archives exist worldwide. However, to date SELDI-TOF MS appears not to have been applied in veterinary medicine. This method is analogous to affinity chromatography, where proteins are retained on a chip surface on the basis of charge, surface hydrophobicity, or biospecific interaction with ligand molecules. This enables fractionation of serum in a variety of ways prior to ionisation and analysis by MS, thereby simplifying the sample and facilitating discovery of novel and useful signals.

The aim of this study was to determine the feasibility of examination of whole ovine serum using SELDI-TOF MS for biomarker discovery. We proposed to establish optimal protein binding and spectral acquisition conditions to facilitate future studies of immunological responses in infectious disease in sheep. Criteria that would need to be met for such an application include: i) production of complex spectra containing many well-resolved peaks, as the greater the number of peaks resolved, the greater the likelihood of detecting a pattern of interest; ii) practical optimisation of experimental conditions so that data can be obtained reliably; iii) a high level of reproducibility between and within experiments so that biological differences can be distinguished from experimental error. These factors were evaluated using blood samples from outbred sheep to assess application to a real-world setting.

Material and methods

Experimental animals

Nine Merino sheep aged 3 years were obtained from a property at Bathurst, New South Wales and housed in a pen at Camden for two weeks prior to collection of blood samples. They were fed a mixture of lucern chaff and lupins, and had ad libitum access to water. Four other Merino sheep were selected for a serum storage experiment. These sheep were obtained from a property at Armidale New South Wales. In addition, four adult female Merino sheep were obtained from the university farm "Arthursleigh" at Marulan, New South Wales for a biomarker discovery experiment. They were administered one dose of an oil adjuvant bivalent recombinant Dichelobacter nodosus fimbrial antigen (1 mL) subcutaneously at 10 months of age and a booster vaccine was administered one month later. Serum samples were collected before and two months after vaccination. Serum agglutinative tests confirmed an antibody response post vaccination.

Sample preparation

Peripheral blood was collected into plain red-topped vacutainers (BD) containing a gel serum separator with silica activator. Serum samples routinely collected for the footrot vaccine biomarker discovery experiment were allowed to clot at room temperature for 2 hours and other sera were allowed to clot for 30 minutes at room temperature. Samples were centrifuged at 3000 xg for 10 minutes and the serum was removed to a 15 mL polypropylene tube (Falcon, BD). At this point, serum samples collected for the footrot biomarker discovery experiment were stored at -20°C until use. The other sera were centrifuged again at 3000 xg for 10 minutes to pellet cellular debris and 2 mL was taken to a fresh 15 mL tube. Serum samples collected for storage experiments were then stored at -20°C until use. For the other samples, 3 mL of reducing buffer (8M urea, 1% CHAPS in PBS) was added, vortexed and 100µL aliquots were snap frozen on liquid nitrogen in 1.5 mL polypropylene screw cap tubes (Interpath). These samples were stored at -80°C until required. Each aliquot was thawed only once for SELDI-TOF MS analysis and any unused sample was discarded. Protein concentrations of samples were determined using a Bradford protein assay reagent (BIO-RAD) according to the manufacturer's instructions, and spectrophotometry at 595 nm (BioPhotometer, Eppendorf).

Selection of optimal experimental settings for SELDI-TOF MS

A range of experimental variables related to matrix (energy absorbing molecule, EAM), array surface and binding buffer combination, sample load and instrument settings were evaluated (Table 1). The spectra generated were judged by the peak evaluation criteria described in section 2.5.

Generation of SELDI-TOF MS spectra

Serum samples were thawed briefly at room temperature and centrifuged for two minutes at 16,000 xg. . Serum samples stored at -20°C were thawed at room temperature for around 30 minutes then reduced with reducing buffer added in 1: 2 ratio, briefly vortexed and incubated on ice for 20 minutes. A further 1:2 dilution of all sera was made by adding binding buffer and samples were kept on ice prior to analysis, which was conducted within 30 minutes of thawing. Arrays were processed according to the manufacturer's instructions (Ciphergen). Prior to processing, IMAC-30 arrays were loaded with either 100mM $NiSO_4$ or 100mM $CuSO_4$ (2 x 5 µl x 5 min). Briefly, the arrays were pre-equilibrated with 5 µL binding buffer (3 x 5 minutes) in a humidity chamber with gentle agitation, a 5 µL sample was then applied and incubated for 60 minutes. The spots were washed three times with binding buffer (5 µL, 5 min) and twice with HEPES (1mM, pH 7.0, 5 µL, 5 min). Array surfaces were allowed to dry and 2 applications of 1 µL of 50% EAM (50% sinapinic acid (SPA) (Ciphergen) dissolved in 50% v/v acetonitrile, 0.5% trifluoroacetic acid (Sigma) was applied to each spot on the array, allowing the solution to dry between applications. The EAM alpha-cyano-4-hydroxycinnamic acid (CHCA) was prepared in the same manner.

Arrays were analysed on the Protein Biology System II (PBS II) mass spectrometer (Ciphergen Biosystems, Freemont, CA, USA). For low energy readings, chips were analysed manually with a high mass of 25 kDa, optimized from 2 to 20 kDa. Mass to charge ratio (*m/z*) was calibrated externally using a peptide standard (All-in-one peptide calibration ProteinChip® array, Ciphergen) and a mass/charge (*m/z)* accuracy of 0.1% was achieved. Baseline subtraction was performed, and spectra normalized to total ion current with a minimum *m/z* of 2000 Da. Peaks were then detected with a built-in peak detection system using default settings and data were exported to Excel (Microsoft), Prism (GraphPad) or Minitab 12.21 (Minitab Inc.) for analysis.

Evaluation of spectra

The number of peaks (NP) per spectrum as well as peak resolution and amplitude were evaluated. Resolution was defined by two indices, PC1 and PC2 as defined previously (Cordingley et al., 2003). PC1 describes the shape of the peaks: the average broadness of the peak relative to the mass as defined by the formula $1/NP\sum(M/W^{1/2})$ where M is the mass of a peak, and $W^{1/2}$ is its width at half-height. The aim is to maximize this value. PC2 measures the lowest resolution of two consecutive peaks per spectrum, that is, how well two consecutive peaks are separated, using the formula $2(M_2-M_1)/ W_1^{1/2} + W_2^{1/2}$. Higher values denote better peak resolution. The amplitude (intensity) of peaks was considered in evaluation of spectrum quality, as intensities above 40 can saturate the detector preventing accurate quantification of peaks.

Reproducibility of individual peaks and spectra

Spectral reproducibility was evaluated according to relative intensity, *m/z*, PC1 and PC2 using up to 18 identified peaks (see below). Only peaks with an *m/z* larger than 2000 Da were included. All sera were diluted 1:4, all spectra were acquired with the same instrument settings in experiments conducted over 3 days, baseline was subtracted and peak intensity was normalised, unless otherwise stated.

To evaluate within-chip reproducibility, sera from eight animals were applied in duplicate on one 16-spot CM10 chip on day 1. Seven peaks (*m/z* 4074.5, 4627.9, 7939.3, 8505.1, 8728.8, 9257.8, 18585.7) that appeared in all eight samples with comparable intensities were selected. In a second experiment, one serum sample was applied to all eight spots on each of three IMAC-30 chips on days 1, 2 and 3, respectively, using a fresh aliquot of serum each day. Eighteen peaks (*m/z* 4357.3, 4623.5, 4724.6, 7442.9, 7524.0, 7931.5, 8000.6, 8493.0, 8719.1, 9252.4, 9459.0, 11564.1, 13753.1, 14890.0, 15048.1, 15256.9, 16005.1, 16073.4) were selected for analysis.

To evaluate between-chip reproducibility, the data obtained from the 3 chips in the second experiment were analysed. In a third experiment, sera from eight animals were applied without replication to one spot on an IMAC-3 chip on day 2 and this was repeated another chip on day 3 using a fresh aliquot of each serum. The IMAC-3 array has the same chemical surface as IMAC-30 but lacks a built-in hydrophobic border. The hydrophobic barrier is created manually by encircling with a hydrophobic pen. The seven peaks selected in the first experiment were used.

To assess the effect of protein concentration on reproducibility, spectra from the third experiment in which sera were diluted 1:4 were compared with those from a fourth experiment in which an IMAC-30 chip was prepared with undiluted sera from the same eight animals.

Long term stability of samples on chips and drift of the mass spectrometer was determined by re-acquisition of spectral data from a CM10 chip that had been probed with serum applied undiluted or diluted 1:4, 1:8 or 1:25 and spectra acquired from it three months prior, using the same instrument. The chip was stored at room temperature in a sealed tube in the dark. Six peaks ranging from 4,000 to 10,000 Da were selected based on their presence in all spectra regardless of the dilution of the sample.

Statistical analysis

Coefficient of variation (CV) was calculated for peak intensity, *m/z*, PC1 and PC2. In addition, the concordance correlation coefficient (CCC), developed by Lin (1989) for assessment of concordance between continuous data, was calculated (http://www.niwascience.co.nz/services/statistical/concordance) to reflect the agreement between replicates within and between chips for data from the second experiment: values larger than 0.99 indicate perfect agreement; values between 0.95 and 0.99 indicate substantial agreement; values between 0.90 and 0.95 indicate moderate agreement; values less than 0.90 indicate poor agreement. For the second experiment, analysis of variance (ANOVA) was conducted on the intensity of each of the 18 peaks with the chip as a fixed factor, with a P value of 0.05 regarded as significant.

To evaluate potential relations between reproducibility and the mass or intensity of peaks, least squares linear regressions of standard deviation (SD) of *m/z* on peak intensity, SD of *m/z* on *m/z*, SD of intensity on *m/z* and SD of intensity on intensity were conducted for the eighteen peaks selected in the second experiment.

Effect of serum collection protocol and storage

To evaluate the effect of different serum sample collection protocols and storage temperatures on protein profile, four serum samples (23, 53, 54 and 55) which had been divided and stored at -20°C and -80°C were compared. Sera from each animal were applied with replication on two IMAC-30 chips: chip 1 had the four samples stored at -20°C and on chip 2 -80°C stored samples were applied. Six peaks (m/z 4636.7, 7943.1, 8311.4, 8730.2, 9262.3, 11575.3) were selected to assess reproducibility between samples stored at different temperatures. The peak resolution indices PC1 and PC2 were also calculated to evaluate the spectra quality.

Pilot biomarker discovery experiment

The nickel immobilized IMAC-30 ProteinChip array and SPA as the EAM were selected for this experiment. Biomarker Wizard software (Ciphergen) was used to assign signals from proteins of equal masses into common clusters between contrasting animal populations: before and after footrot vaccination. Routinely collected sera stored at -20°C were used. The normalized peak intensity of each peak detected in the vaccinated sheep was compared with the same sheep before vaccination by a non-parametric two-sample Mann-Whitney U-test (Krauth, 1983). The following settings were chosen for automatic peak detection in Biomarker Wizard: (i) auto-detect peaks to cluster, (ii) first pass: signal/noise ratio 5, (iii) minimal peak threshold: 50% of all spectra, (iv) cluster mass window: 0.5% of mass and (v) second pass: signal/noise ratio 5. As a quality control procedure, all peak clusters generated from Biomarker Wizard were visually inspected and manually relabelled if necessary.

Results

Selection of optimal experimental settings for SELDI-TOF MS

There were substantial differences in spectra associated with choice of matrix. CHCA generated very sharp peaks under 15 kDa but very few peaks of larger mass were obtained (Fig. 1). In contrast SPA provided acceptable spectra up to 20 kDa and there was less reduction in peak intensity with increasing sample dilution compared to CHCA. This is a useful feature for SPA, which may reduce the need for protein standardization in a sample prior to analysis. SPA was used in subsequent experiments.

To evaluate which combination of array surface, binding buffer, sample concentration, matrix and detector sensitivity/laser intensity setting generated the best overall spectrum as determined by NP, PC1, PC2 and amplitude criteria, the parameters listed in Table 1 were used to acquire spectra. Substantial differences in spectra were observed. As an example, the spectra generated with instrument settings 7-220, 6-230, 7-230 and 8-220 using a CM10 array with low stringency binding buffer and undiluted serum had 13 to 24 peaks, PC1 ranging from 225 to 302, PC2 from 0.9 to 2.7 and between 5 and 12 peaks with amplitude >5. The optimum settings for four array types, CM10, Q10, H50 and IMAC-30 were determined and found to vary between chip type (Table 2). The IMAC-30 array had enhanced spectral quality when charged with Ni^{2+} ions compared with Cu^{2+} ions. For all array types, better spectra were generated with either undiluted serum (about 26 mg/ml) or serum diluted 1:4 (about 6.5 mg/ml) than with higher dilutions of serum.

Reproducibility of individual peaks and spectra

In general there was a very high degree of reproducibility of estimates of mass (m/z) and moderate reproducibility of estimates of intensity for replicate samples. For example, the average within-chip CV for m/z among seven peaks was 0.01% while that for intensity was 13.1% (sera from 8 animals evaluated in duplicate on one chip, Table 3). The sera from some animals generated spectra with greater inherent variation in mass and amplitude of peaks than did sera from other animals; this is illustrated by the range of values for mean CV among animals (m/z range 0.01 to 0.03%; intensity range 5.9 - 36.8%) (Table 3). Furthermore, some peaks displayed greater inherent variability than others, particularly for intensity.

The same features were observed where one sample was replicated 8 times on each of three chips (Table 4). The mean within-chip CVs for peak intensity over 18 peaks were 13.9, 18.0 and 15.2% on chips 1, 2 and 3, respectively. The corresponding values for CV for m/z were 0.012, 0.023 and 0.016%. CCC values for intensity were all greater than 0.9 indicating substantial to perfect agreement between replicates while the CCC values for m/z were all greater than 0.99 indicating

almost perfect agreement between replicates. Some peaks were less reproducible than others, with up to 25% CV for intensity and 0.038% for m/z of individual peaks within chip.

Reproducibility of mass and intensity was only slightly lower between chips (Table 4). CCC and CV were computed for positional replicates of a single serum sample applied to different chips, for example chip 1, spot 1 paired with chip 2, spot 1. The mean CV for peak intensity from 18 peaks was <15% between any two consecutive days (1 and 2, or 2 and 3) while the mean CV between day 1 and day 3 was 23%. There were significant differences between means of peak intensity associated with chip for 5 of the 18 peaks (m/z 7442, 13753, 14890, 16005,16073 Da). Between chip mean CV for m/z from 18 peaks ranged from 0.015% to 0.022% for comparisons between day 1 and 2, 2 and 3 and 1 and 3 and there was no significant difference in mean m/z for any peak between any two days. The CCC values for intensity mostly exceeded 0.95 indicating substantial to perfect agreement, while agreement for m/z was perfect.

Relations between reproducibility and m/z and intensity of peaks

Possible relations between variability in m/z or intensity and either the mass of the peak or its intensity were explored by regression analysis (Fig 3). There was no relation between the degree of variability in intensity of a peak and its m/z. However, peaks of high intensity tended to have more variable intensity than peaks of lower intensity. Similarly, proteins with high m/z tended to have greater variation in m/z than smaller proteins. In addition, m/z estimates appeared to be more variable for some peaks of low intensity compared to those of more abundant proteins, but the relationship was not linear.

Sample dilution intuitively would have a large impact on spectra and in fact comparing 1:4 dilution with undiluted sample there were dramatic changes in peak intensity with mean CV for seven peaks for one animal (982) being 56.6% (range 7.2 to 71.1%); the CCC showed a very poor correlation especially for peaks with lower intensity (data not shown). However, the mean CV and CCC of m/z were 0.041% and 0.9899, respectively, demonstrating that a 4-fold dilution of the sample did not significantly alter the estimates of m/z of these peaks.

Sample stability and potential drift of the mass spectrometer was determined by re-acquisition of spectral data from a CM10 array that had been analysed three months prior, using identical instrument settings. The number of peaks in re-acquired spectra was almost the same as the number originally seen except for one serum dilution 1:8 (16 compared to 17). Interestingly, undiluted serum generated more peaks during re-acquisition (21 compared with 20); unexpectedly, many of these peaks had visibly increased intensities when re-acquired (Fig. 4). As expected, the mean CV for peak intensity across all sample dilutions for the 5 selected peaks was high (42.21%) but there was little variation in m/z (mean CV 0.017%). The CV of PC1 for undiluted, 1:4, 1:8 and 1:25 were 0.11%, 0.26%, 7.03% and 14.14% respectively, indicating an increase in variation of PC1 with dilution. However, the pattern of variation in PC2 with dilution was unclear (21.15%, 0.99%, 10.21% and 17.34%).

Impact of sample collection protocols and storage on serum protein profiles

Protein profiles generated from serum samples stored at -20°C and -80°C were compared. Among four samples, peptides with higher mass range, in particular two peptides with m/z of 8728 and 9261 Da had reduced peak intensity in samples stored at -20°C compared with same samples stored at -80°C (Fig. 5). In addition, the protein profiles of samples stored at -20°C revealed a greater number of peaks in the low mass range (range from 3000 to 5000 Da) than the same samples stored at -80°C (Fig. 6). Spectral reproducibility was evaluated based on relative intensity and m/z of six peaks that were common to all samples regardless of storage (Table 5). In general, three of four -80°C stored samples (23, 53, and 54) had a higher reproducibility of estimates of relative intensity than

the same samples stored at -20°C. There was no significant difference in reproducibility of estimates of m/z due to storage temperature. The samples stored at -80°C had slightly better peak resolution (PC1 and PC2) than the same samples stored at -20°C except sample 53, which had a peak separation index PC2 lower than the same sample stored at -20°C (Table 5).

Pilot biomarker discovery

In the pilot biomarker discovery experiment, serum protein profiles generated from four Merino sheep were compared before and after footrot vaccination. The sera were collected routinely and stored at -20°C. Data were generated from IMAC-30 Ni^{2+} ProteinChip arrays. Coupled with Biomarker Wizard software, the serum protein profile in the molecular weight range from 3000 to 25000 Da was analysed. Four putative biomarkers (m/z of 8502, 8727, 9261, 14894 Da) were identified. Three biomarkers (m/z of 8502, 8727, 9261 Da) were significantly down-regulated while a biomarker with m/z of 14894 Da was significantly up-regulated in footrot vaccinated sheep compared to the same sheep before vaccination (Table 6). Fig. 7 shows a representative pseudo gel view of one differentially expressed protein (Fig. 7).

Discussion

The low molecular mass region of the serum proteome presents an opportunity for biomarker discovery, as it may contain information for diagnosis, prognosis and monitoring the progression of disease. SELDI-TOF MS analysis of serum has repeatedly been shown to have the discriminative power to reveal putative biomarkers to diagnose a wide range of malignancies, some in the early stages of progression, and so it follows that it may have application to early detection of immune responses to microbial infection. Application of this novel technology to the study of animal proteomes in health and disease has been uncommon. It has been used only to explore proteomic fingerprints in mice as a model for human diseases and combined with two-dimensional polyacrylamide gel electrophoresis to analyse ovine lymph (Leak et al., 2004). Consequently there are very few data or protocols available. In this investigation we proposed to establish optimal protocols for analysis of ovine serum to facilitate future studies of infectious diseases in sheep. The feasibility of this was demonstrated using an optimised protocol to find biomarkers in footrot vaccinated sheep.

It is crucial to perform stringent assessment and quality control measures prior to application of novel technologies to ensure that experimental variability is minimised and that differences observed result from biological rather than experimental variation. This validation of experimental procedure and data quality is a necessary pre-requisite for identification of biomarker expression patterns. Using four sample dilutions, three ProteinChip® array surfaces, two MS matrices in combination with seven binding buffers, we have determined the most favourable combinations for generating SELDI-TOF MS spectra from ovine serum based on objective peak quality and reproducibility criteria. The IMAC–30 array loaded with Ni^{2+} and the Q10 anion exchange array with Tris-HCl pH 7.5 produced the best overall results, generating the highest number of peaks with acceptable values for peak sharpness and separation.

It was important to select the optimal matrix for generating spectra with ovine serum. According to Ciphergen, the CHCA molecule has previously been shown to be a more effective matrix for smaller peptides, but can promote multi-protonated protein ions, while SPA is more effective for larger proteins and works reasonably well for peptides. However, our results with ovine serum suggested that SPA provided acceptable spectra up to 20 kDa with less reduction in peak intensity with increasing sample dilution compared to CHCA.

The reproducibility of SELDI-TOF MS spectra was high. Both within- and between-chip CVs were below 20% for peak intensity and below 0.03% for *m/z* for most peaks. While concordance

correlation analysis showed high agreement between replicates both within- and between chip, analysis of variance revealed that five peaks had significant differences in intensity between chips. Variation in absolute peak intensity was not related to the mass of the peptide but variations in intensity and mass estimates were related to protein abundance and mass, respectively. This is in contrast to other reports which found increasing variation in peak intensity with decreasing peak mass. However, these studies measured the relation of mass to the CV of peak intensity, in other words to a normalised value for intensity, so small changes in low intensity peaks will have a large influence on the calculated CV. When endeavouring to identify putative biomarkers, software for univariate or multivariate analysis such as Biomarker Wizard or Biomarker Pattern (Ciphergen), use differences in absolute peak intensity to determine clusters of putative biomarkers. As there can be substantial variation in peak intensity associated with experimental error we suggest that in determining putative biomarkers, greater importance should be placed on the presence or absence of peaks rather than on differences in intensity of peaks. However, assessment of the presence or absence of a minor peak may be difficult due to the inherent variation in peak intensity, regardless of molecular size. For these reasons, and where there is the luxury of choice, it may be advantageous to select peaks of moderate intensity and mass. The repeatability of mass estimates was very high so that identification of peaks in spectra from different samples, in order that their intensities can be compared, is likely to be very reliable.

Quality control combined with standard operating procedures allows production of high quality spectra using SELDI-TOF MS. Our data suggest the use at least 2 replicates per sample, a uniform drying procedure, and a frequent performance check of the spectrometer. Future studies on sample collection and handling prior to preparation for SELDI-TOF MS will reveal the robustness of putative biomarkers of disease in ovine serum. It is largely unknown to what degree the quality and reproducibility of SELDI-TOF MS protein profiles might be influenced by varying sample parameters, such as clotting time, number of freeze-thaw cycles, and haemolysis. Aivado and co-workers have recently evaluated the effects of freeze-thaw cycles of human serum on spectral variation (Aivado et al., 2005). They found that up to five cycles did not significantly influence the CV. Likewise, varying the clotting time between 30 min and 12 h did not lead to statistically significant differences in peak intensity or mass.

Absolute signal intensity depends on the amount of sample. However, use of the matrix SPA for ovine serum resulted in spectra that were not particularly sensitive to relatively large changes in protein load on the chip. If the sample preparation conditions are carefully optimised, standardised and monitored, good reproducibility can be achieved.

Storing serum samples at -80°C places a burden on most laboratories in terms of cost and space requirement. In addition, many previously collected serum samples that are potentially valuable resources for disease biomarker discovery research likely have had less stringent sample collection protocols and are stored at -20°C. The main objective of the serum storage experiment was to investigate the usefulness of sera that had been stored at -20°C. There was decreased peak intensity for two major proteins and a greater number of low mass range proteins compared to the same samples stored at -80°C. It is likely that low mass range peaks were degradation products generated as a result of proteolysis due to -20°C storage, although other factors may contribute. In general, the estimate of reproducibility of intensity for -80°C stored samples was slightly better than the same samples stored at -20°C. However there was no significant difference in reproducibility for *m/z* between samples stored at the two temperatures. This finding suggested that the samples collected using a less stringent protocol and stored at -20°C can be used for biomarker identification provided that all samples in the collection are handled in a similar manner. It would be good practice to develop an optimized and standardized protocol initially and take into account the factors such as transit time, clotting time and tube type.

Using routinely collected serum samples stored at -20°C, together with the optimal protocol on IMAC-30 Ni^{2+} arrays, a biomarker discovery experiment was conducted. The protein profiles of four

one year old Merino sheep before and after vaccination with a bacterial antigen differed and a panel of four putative biomarkers was identified. In conclusion, these results indicate the potential of the technology to detect immunological responses in infectious disease in sheep. Further studies are required to identify novel immunological biomarkers in livestock.

References

Aivado, M., Spentzos, D., Alterovitz, G., Otu, H.H., Grall, F., Giagounidis, A.A., Wells, M., Cho, J.Y., Germing, U., Czibere, A., Prall, W.C., Porter, C., Ramoni, M.F., Libermann, T.A., 2005. Optimization and evaluation of surface-enhanced laser desorption/ionization time-of-flight mass spectrometry (SELDI-TOF MS) with reversed-phase protein arrays for protein profiling. Clin Chem Lab Med 43, 133-140.

Clarke, W., Zhang, Z., Chan, D.W., 2003. The application of clinical proteomics to cancer and other diseases. Clin Chem Lab Med 41, 1562-1570.

Conrads, T.P., Hood, B.L., Issaq, H.J., Veenstra, T.D., 2004. Proteomic patterns as a diagnostic tool for early-stage cancer: a review of its progress to a clinically relevant tool. Mol Diagn 8, 77-85.

Cordingley, H.C., Roberts, S.L., Tooke, P., Armitage, J.R., Lane, P.W., Wu, W., Wildsmith, S.E., 2003. Multifactorial screening design and analysis of SELDI-TOF ProteinChip array optimization experiments. Biotechniques 34, 364-365, 368-373.

Koopmann, J., Zhang, Z., White, N., Rosenzweig, J., Fedarko, N., Jagannath, S., Canto, M.I., Yeo, C.J., Chan, D.W., Goggins, M., 2004. Serum diagnosis of pancreatic adenocarcinoma using surface-enhanced laser desorption and ionization mass spectrometry. Clin Cancer Res 10, 860-868.

Krauth, J., 1983. The interpretation of significance tests for independent and dependent samples. J Neurosci Methods 9, 269-281.

Leak, L.V., Liotta, L.A., Krutzsch, H., Jones, M., Fusaro, V.A., Ross, S.J., Zhao, Y., Petricoin, E.F., 3rd, 2004. Proteomic analysis of lymph. Proteomics 4, 753-765.

Li, J., White, N., Zhang, Z., Rosenzweig, J., Mangold, L.A., Partin, A.W., Chan, D.W., 2004. Detection of prostate cancer using serum proteomics pattern in a histologically confirmed population. J Urol 171, 1782-1787.

Liotta, L.A., Ferrari, M., Petricoin, E., 2003. Clinical proteomics: written in blood. Nature 425, 905.

Petricoin, E.F., Ardekani, A.M., Hitt, B.A., Levine, P.J., Fusaro, V.A., Steinberg, S.M., Mills, G.B., Simone, C., Fishman, D.A., Kohn, E.C., Liotta, L.A., 2002. Use of proteomic patterns in serum to identify ovarian cancer. Lancet 359, 572-577.

Petricoin, E.F., Liotta, L.A., 2004. SELDI-TOF-based serum proteomic pattern diagnostics for early detection of cancer. Curr Opin Biotechnol 15, 24-30.

Rocken, C., Ebert, M.P., Roessner, A., 2004. Proteomics in pathology, research and practice. Pathol Res Pract 200, 69-82.

Wadsworth, J.T., Somers, K.D., Cazares, L.H., Malik, G., Adam, B.L., Stack, B.C., Jr., Wright, G.L., Jr., Semmes, O.J., 2004. Serum protein profiles to identify head and neck cancer. Clin Cancer Res 10, 1625-1632.

Wulfkuhle, J.D., McLean, K.C., Paweletz, C.P., Sgroi, D.C., Trock, B.J., Steeg, P.S., Petricoin, E.F., 3rd, 2001. New approaches to proteomic analysis of breast cancer. Proteomics 1, 1205-1215.

Table 1. Summary of chip array surfaces, binding buffer and instrument settings combinations.

Chip type	*General description*	*Chromatographic function*	*Wash/ Binding buffer*	*Sample Dilution*	*EAM*	*Instrument Setting*[a]
Q10	Strong anion exchange	Analysis of negative charged residues	Tris-HCl pH 7.5, pH9.0	neat, 1:4, 1:8, 1:15, 1:25	SPA	7-220, 7-230, 8-230, 8-235
CM10	Weak cation exchange	Analysis of positive charged residues	Tris-HCl pH 7.0, pH 4.0, High stringency buffer	neat, 1:4, 1:8, 1:15, 1:25	SPA	7-220, 7-230, 6-230, 8-220, 6-190, 7-190
			Low stringency Buffer[b]		SPA & CHCA	
IMAC-30	Immobilized metal affinity capture	Analysis of residues binding divalent metal ions	Ni^{2+} PBS	neat, 1:4, 1:8, 1:15, 1:25	SPA & CHCA	6-175, 6-180, 7-220, 7-230, 6-230, 6-220
			Cu^{2+} PBS		SPA	7-220, 7-230, 6-230, 6-220
H50	Hydrophobic/ reversed phase	Capture of large proteins through hydrophobic or reversed phase interaction	10% ACN, 0.1% TFA	neat, 1:4, 1:8, 1:15, 1:25	SPA	7-220, 7-230, 8-220, 8-230, 9-230, 9-220

[a] detector sensitivity - laser intensity; [b]Ciphergen.

Table 2. Spectral characteristics in the range 2 to 25 kDa for Protein Chip arrays under optimal conditions

Chip type	*Binding Buffer*	*Sample Dilution*	*Instrument Setting*	*NP*[1]	*PC1*	*PC2*	*NP*[a] *with intensity >10*	*NP*[a] *with intensity >5*
CM10	High Stringency	1:4	7-220	17	485.24	1.38	7	10
Q10	Tris-HCl pH 7.5	1:4	7-220	21	355.94	0.86	3	5
H50	Tris-HCl pH 9.0	Neat	9-230	15	236.90	0.57	7	11
IMAC30 Cu^{2+}	PBS	1:4	7-220	12	216.24	0.96	4	6
IMAC30 Ni^{2+}	PBS	1:4	6-220	26	293.81	1.00	2	7

[a] NP – number of peaks

Table 3. Reproducibility of peak intensity and mass/charge for 7 peaks in the spectra of serum samples from eight sheep. Data are coefficient of variation (CV).

Animal	*Within chip* *Experiment 1*[a]				*Between chip* *Experiment 3*[b]			
	Peak intensity		Mass/charge		Peak intensity		Mass/charge	
	Mean[b]	Rang[d]	Mean[b]	Range[d]	Mean[b]	Range[d]	Mean[b]	Range[d]
982	36.83	15.20 - 46.30	0.02	0.001 - 0.029	10.46	2.55-21.05	0.027	0.010-0.051
984	13.45	0.60 - 28.75	0.03	0.011 - 0.061	25.69	8.84-32.12	0.028	0.015-0.058
986	7.90	0.25 - 24.38	0.00	0.001 - 0.005	20.60	11.28-34.50	0.023	0.009-0.042
987	9.46	5.51 - 15.55	0.01	0.000 - 0.028	17.79	1.88-43.54	0.050	0.045-0.078
989	5.92	0.11 - 13.43	0.01	0.001 - 0.028	15.55	2.09-36.43	0.038	0.007-0.047
990	9.21	1.38 - 34.72	0.01	0.001 - 0.024	21.98	2.57-59.43	0.026	0.000-0.066
991	11.39	4.19 - 17.79	0.01	0.004 - 0.017	9.13	0.44-26.77	0.019	0.000-0.064
992	10.97	1.97 - 15.02	0.01	0.004 - 0.039	12.41	0.67-20.92	0.013	0.009-0.032
Overall	13.14	0.11 - 46.30	0.01	0.000 - 0.039	16.70	0.67-59.43	0.028	0.000-0.078

[a] two replicates of each sample on one CM10 chip; [b] one replicate of each sample on two IMAC chips; [v] average CV for 7 peaks; [d] extreme values of the CV among 7 peaks;

Table 4. Reproducibility of peak intensity and mass/charge for 18 peaks in the spectra of one serum sample applied to all spots of three IMAC chips. Data are coefficient of variation (CV).

Within chip					*Between chip*				
	Intensity		Mass/charge			Intensity		Mass/charge	
Chip	Mean[a]	Range[a]	Mean	Range	Chips	Mean	Range	Mean	Range
1	13.9	10.5-19.9	0.012	0.006-0.019	1 and 2	12.7	6.5-20.2	0.022	0.007-0.034
2	18.0	11.6-23.4	0.023	0.012-0.038	2 and 3	14.9	7.5-23.7	0.017	0.009-0.034
3	15.2	9.2-24.7	0.016	0.012-0.031	1 and 3	22.8	10.5-41.5	0.015	0.009-0.022

[a] mean and range for 18 peaks among eight replicates of the sample on each chip

Table 5. Reproducibility of peak intensity and mass/charge, and mean peak resolution of 6 peaks in the spectra of four serum samples stored either at -20° C or -80°C.

	Reproducibility (CV)				*Peak resolution*	
	Intensity[a]		Mass/charge[a]		PC1	PC2
Sample	Mean	Range	Mean	Range		
23 (-20°C)	19.5	3.93-52.74	0.037	0.031-0.046	418.06	14.81
23 (-80°C)	15.2	4.31-23.31	0.037	0.035-0.043	437.48	19.21
53 (-20°C)	13.4	1.65-26.58	0.008	0.001-0.018	393.6.	12.35
53 (-80°C)	19.0	2.79-40.94	0.008	0.001-0.014	404.47	7.61
54 (-20°C)	23.5	0.72-62.5	0.018	0.013-0.02	477.42	17.05
54 (-80°C)	5.8	0.53-18.84	0.007	0.0001-0.013	489.78	24.32
55 (-20°C)	38.2	5.25-70.5	0.019	0.01-0.023	443.21	14.45
55 (-80°C)	12.8	2.19-22.96	0.003	0.0001-0.003	452.56	19.66

[a] mean and range for 6 peaks

Table 6. Putative serum biomarkers significantly down- or up-regulated in footrot vaccinated sheep compared to sheep before vaccination.

Biomarker Number	*m/z (Da)*	*Vaccination effect*	*Fold change*	*P value*[a]
1	8502	Down-regulated	3.1	1.73×10^{-5}
2	8727	Down-regulated	2	5.9×10^{-3}
3	9261	Down-regulated	2.4	4.7×10^{-3}
4	14894	Up-regulated	2.8	2.8×10^{-5}

[a]P-values were obtained by Mann-Whitney U-test comparing the normalized peak intensities of 4 vaccinated sheep to the same sheep before vaccination.

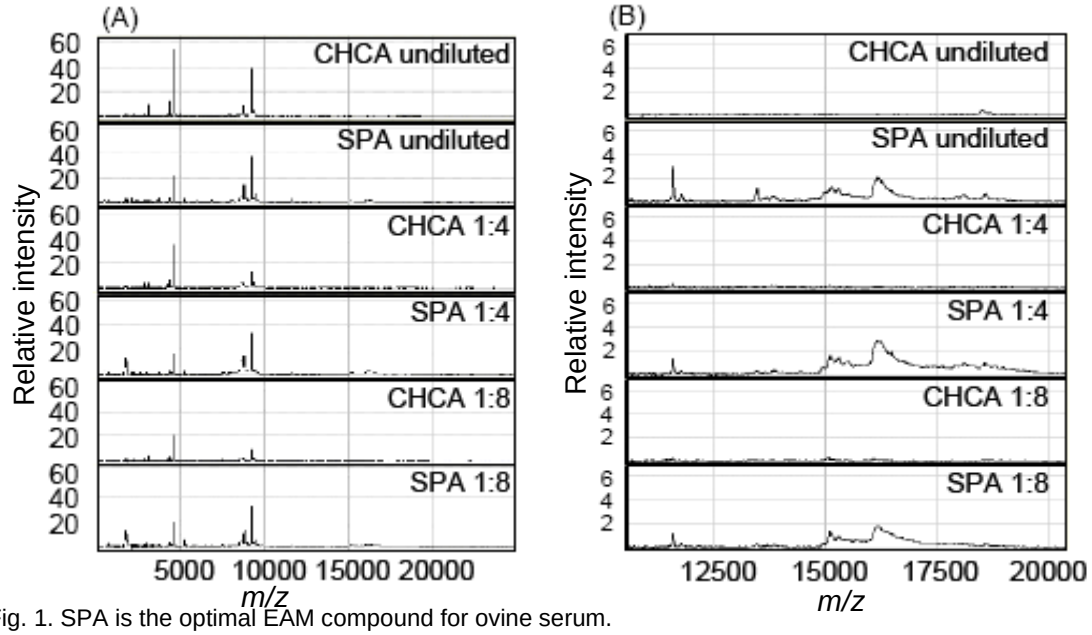

Fig. 1. SPA is the optimal EAM compound for ovine serum.

Spectra generated with SPA had less reduction in peak intensity compared to CHCA. A: Mass acquisition from 2000 - 20000 Da; B: enlargement of peaks from A at 10000 - 20000 Da. Spectra were generated using IMAC-30 Cu^{2+} arrays with CHCA or SPA at three sample dilutions; undiluted, 1:4 and 1:8.

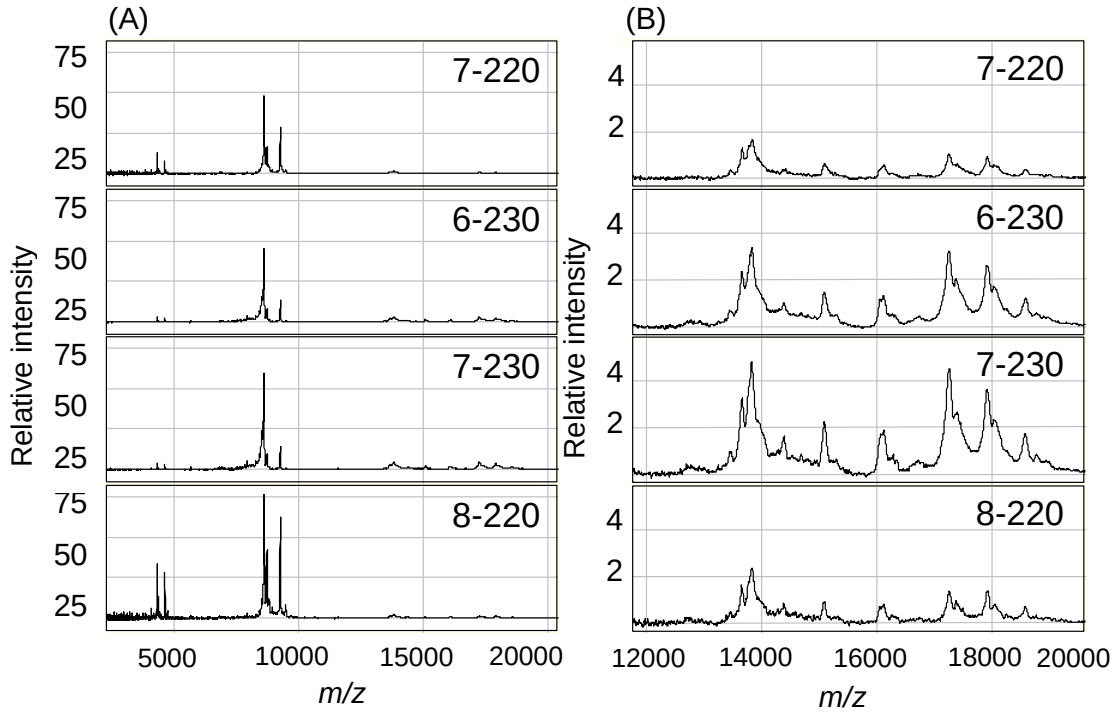

Fig. 2. The effect of instrument settings on spectral acquisition. - Detector sensitivity of 7 and laser intensity of 230 generated the optimal SELDI-TOF MS spectra. (A) Mass acquisition of 2000 - 20000Da; (B) Enlargement of peaks from A from 12000 – 19000 Da. Spectra were generated using the CM10 array, low stringency buffer and undiluted serum.

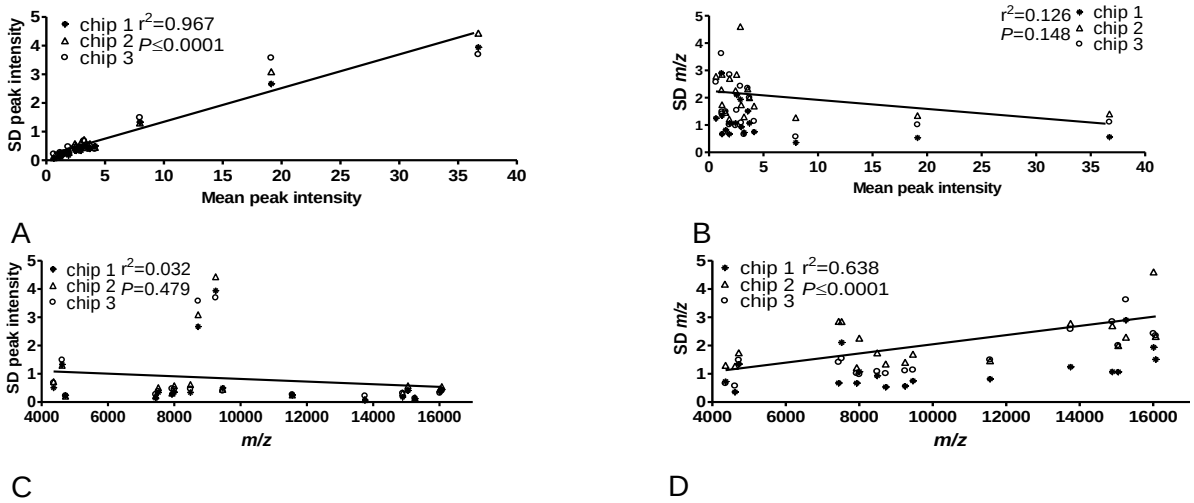

Fig. 3. Linear regression analysis of the relation between variability in peak intensity and mass.

Linear regression analysis of the relation between variability in peak intensity and mass and absolute values for these parameters for 18 peaks between *m/z* 4357.3 and 16073.4 across eight replicates on three chips. Panels A and B, variability of intensity; panels C and D , variability of *m/z.*

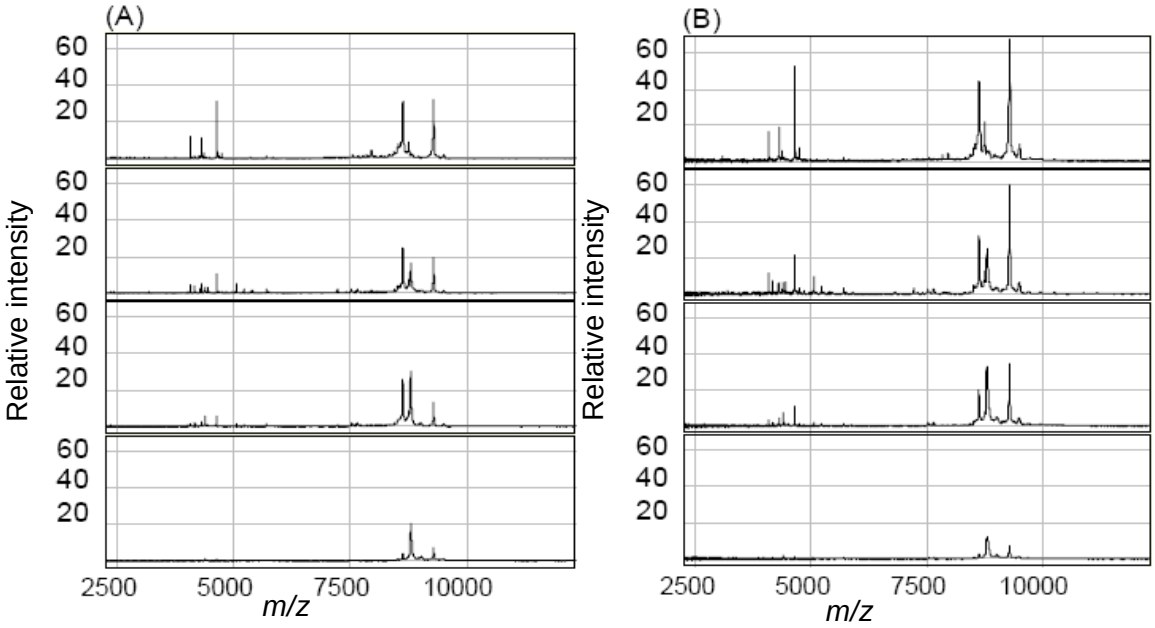

Fig. 4. Effects on spectral generation of array storage and machine drift.
(A) Spectra generated using 7-220, CM10 array, Tris-HCL pH 4.0 and 4 sample dilutions (top to lower panel: undiluted, 1:4, 1:8 and 1:25); (B) Spectra from the same chip as in (A) re-acquired following three months storage, with the same instrument settings.

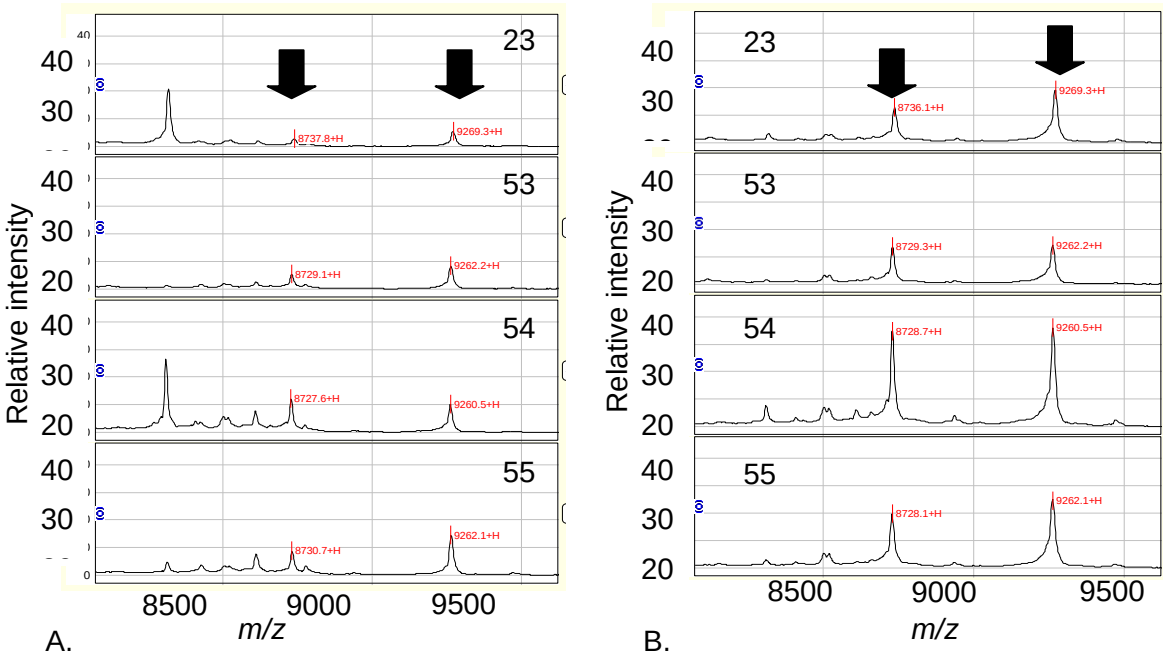

Fig. 5. Impact of sample storage on serum protein profile.
(A) Representative protein profiles of four serum samples: 23, 53, 54 and 55, which were stored at -20°C showing the reduced peak intensity of two proteins (arrowed peaks with m/z of 8728 and 9261 Da). (B) The protein profiles of the same four serum samples stored at -80°C showing higher intensity of the same two proteins.

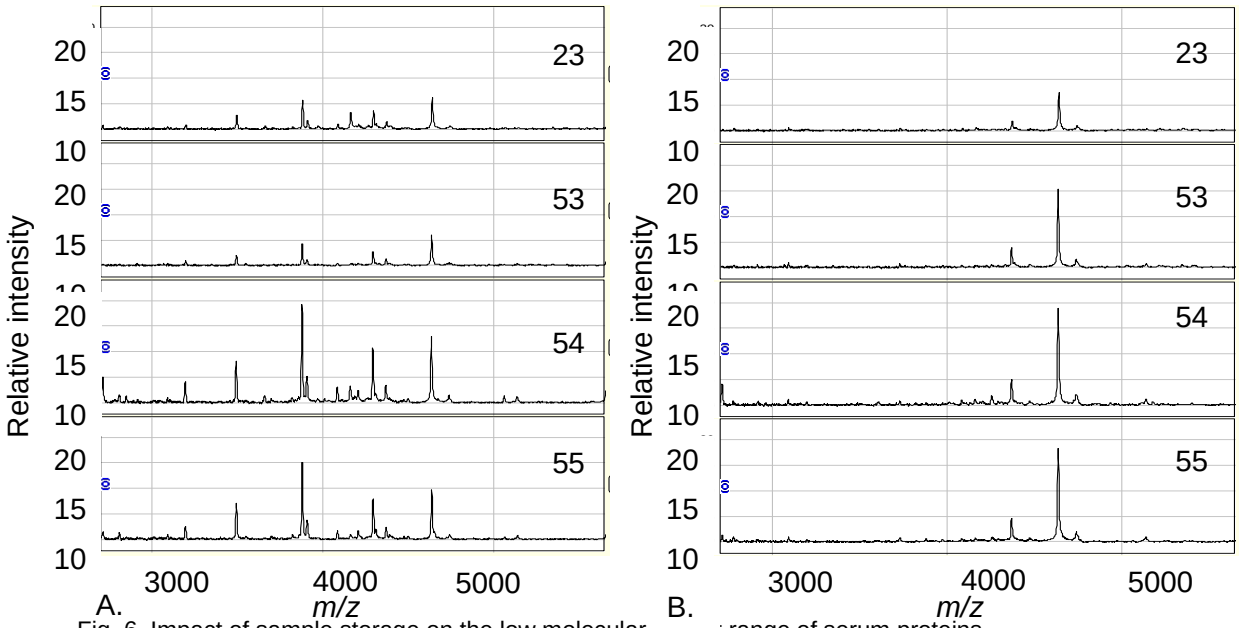

Fig. 6. Impact of sample storage on the low molecular weight range of serum proteins.
(A) Spectra generated from four serum samples stored at -20°C, processed on IMAC 30 – Ni^{2+} chip surface, showing more proteins detected in the range 3000 to 5000 Da. (B) Spectra generated from same serum samples stored at -80°C.

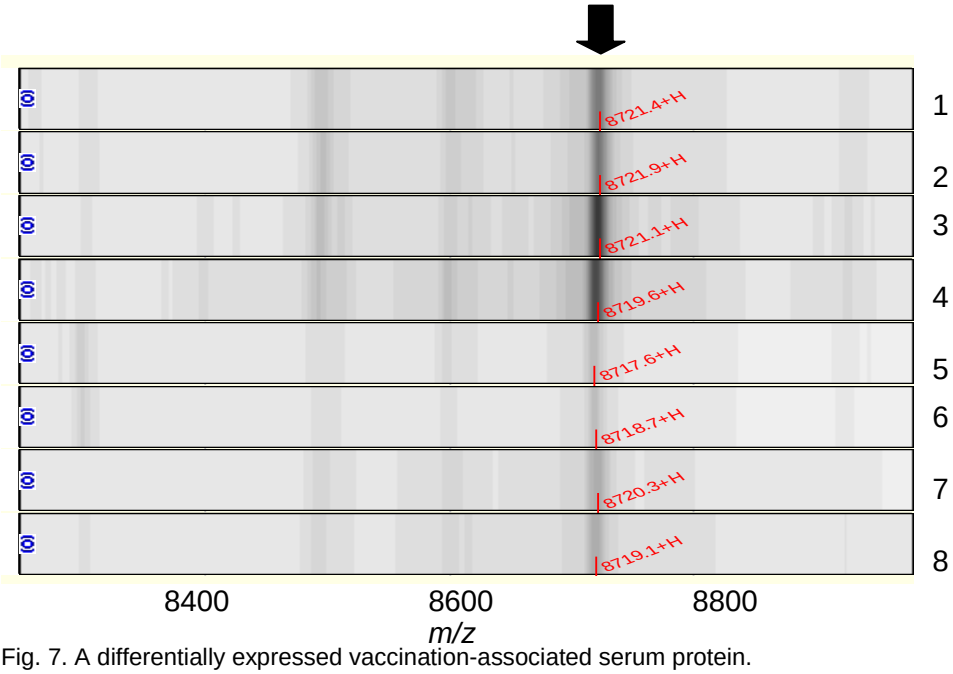

Fig. 7. A differentially expressed vaccination-associated serum protein.
A representative pesudogel view of SELDI-TOF MS analysis of serum samples from 4 sheep, processed on IMAC 30- Ni^{2+} chip surfaces. The upper four protein profiles are serum from footrot vaccinated sheep and the bottom four spectra are from the same sheep before vaccination. The arrow indicates a protein with increased expression in vaccinated sheep. Lanes 1 to 4, vaccinated sheep. Lanes 5 to 8, pre-vaccination.

9.22 Appendix 3B-5 Subprogram 3 Identification of serum biomarkers for Ovine Johne's Disease using SELDI-TOF-MS

Introduction

Johne's Disease (paratuberculosis) caused by *Mycobacterium avium* subsp. *paratuberculosis*, is characterized by chronic lesions of granulomatous enteritis, lymphadenitis and progressive emaciation. Paratuberculosis has become widespread in domestic ruminants in Australia. The disease has been reported in cattle in Australia since 1925 but only recently recognized in sheep [1]. The first report of paratuberculosis in sheep in Australia was in 1980 [16] and the first outbreak reported in New South Wales in 1981 [26].

Paratuberculosis typically progresses through three distinct stages and the division of the stage is based on the detection of host immune responses to *M .a. paratuberculosis* antigen, detection of faecal shedding of mycobacteria and existence of clinical signs. In the first and second stages of infection, which are considered subclinical stages, the animals are infected but asymptomatic. Animals can remain in the subclinical stages for a number of years before progressing into clinical disease or can remain asymptomatic without developing outward clinical signs of disease. In the first stage of infection, fecal shedding cannot be detected by culture, while in the second stage shedding can be intermittent. The third or clinical stage of disease is characterized by shedding high numbers of bacteria into the environment and progressive weight loss of the infected animals [9].

Current diagnostic tests for paratuberculosis include indirect detection of the host immune response to infection or direct tests to detect the microorganism by culture. During the early stages of infection the host response is primarily cell mediated, with little or no humoral immune response [29]. Therefore, serologic tests of host immune response such as enzyme-linked immunosorbent assays (ELISA) and agar gel immunodiffusion (AGID) assays which rely on detection of antibodies produced during the humoral response are more useful at a later stage of infection. In addition, the sensitivity of these tests vary with the different stages of disease [15]. In the early stage of infection, no single diagnostic test can definitively diagnose infection although the gamma interferon test (Bovigam™) has shown some promise for early detection in cattle and sheep but with moderate sensitivity and specificity [28, 30]. Another complication with immunological tests is interference from prior vaccination. Vaccines based on mineral oil adjuvants are normally administered subcutaneously to sheep from 2 weeks to 4 months of age. This sensitization from vaccines has caused interference with diagnosis of paratuberculosis in naturally infected animals and also causes sensitization in tuberculosis test.

The faecal culture test is the definitive diagnostic test for paratuberculosis and is the only method that can transverse both sub-clinical and clinical stages of disease [31]. However, this test is limited to detecting animals that are already shedding the organism into the environment and are in the later subclinial stages of the disease. In addition, culturing of *M. a. paratuberculosis* requires a lengthy incubation time to demonstrate growth. Current methods for the culturing of *M.a. paratuberculosis* from faecal samples require 8 to 16 weeks on solid medium and up to 12 weeks in sheep is standard in liquid medium using the Bactec detection system [34]. Methods based on detection of nucleic acids by PCR amplification, particularly the application of real-time PCR, nested PCR and immuno-magnetic bead separation assays have made the detection of *M.a. paratuberculosis* more rapid and semi quantitative, but they are less sensitive than culture [4, 6, 10, 11, 18]. However, the majority of tests are based on amplification of the *M. a. paratuberculosis* IS*900* element. This has now been reported to have moderate specificity due to the high degree of similarity between *M.a. paratuberculosis* and environmental mycobacteria that contain IS*900*-like insertion sequences [6, 17]. There is need for a new diagnostic test for JD to be developed that has better sensitivity and specificity than current tests, and especially that has better capacity to detect animals in the early stage of infection.

Theoretically, various physiological and pathological processes could modify the proteome in a protein reservoir such as serum, generating a unique disease-specific signature, known as a *proteomic signature*, or *disease signature* [25]. Due to the lack of any specific or sensitive diagnostic tests for the early detection of Johne's disease, there is a critical need for serum markers to aid in the early detection of this disease. The first part of this chapter, a small scale biomarker discovery experiment was conducted and demonstrated that two ProteinChip array surfaces, IMAC-30 activated with $NiSO_4$ and the strong anion exchange array (Q10) both can generate a panel of potential biomarkers. In the second part of the study, the sample size was increased to include 30 sheep in various subclinical stages of infection and 29 unexposed sheep to determine putative serum biomarkers for infection. In addition, 30 sheep vaccinated with Gudair® were also sampled and compared with the unexposed group of animals in order to identify potential 'vaccination biomarkers' in serum. Two independent multivariate statistics algorithms: Classification and Regression Tree and Linear Discriminant Analysis were employed to identify a panel of serum biomarkers for *M. a. paratuberculosis* infection and vaccination.

Materials and methods

Animal sample characteristics

In the pilot scale biomarker discovery study, a total of 11 sheep were selected and divided into two groups: uninfected and infected. The uninfected group included 4 female adult Merino sheep and the infected group comprised 7 naturally infected female adult sheep. They both selected from O31.A trial and were sourced from the property 'Jamyca Caloola' in the New England Rural Lands Protection Board and arrived at Camden in April 2005. The disease status of both groups was evaluated by faecal and tissue culture, ELISA, AGID test and histology examination.

In the large scale biomarker discovery study, a total of 89 sheep aged from 2 to 4 years were carefully selected and were divided into three different groups: unexposed, infected and vaccinated (Table 1). Unexposed sheep (Group 1, n = 29) were adult female Merino sheep selected from a property at Armdale in the New England Rural Lands Protection Board, New South Wales from a flock in which no Johne's disease had been previously reported. The negative disease status was confirmed by faecal and tissue culture, ELISA, AGID test and histology examination.

Vaccinated sheep (Group 2, n = 30) were two to three years old adult female Merino sheep selected from a University Farm "Arthursleigh" at Marulan, New South Wales. They were administered one dose of oil adjuvant Gudair™ vaccine (1 mL) subcutaneously at three months of age. Faecal culture, ELISA and AGID tests were performed to confirm the absence of Johne's disease infection of the sheep. The serum samples were collected on farm (Table 1).

The infected sheep (Group 3, n = 30) were comprised of 26 naturally infected female adult Merino sheep, which included nineteen sheep selected from the O31.E trial, seven animals from the O31.A trial and another four experimentally infected cross-breed sheep from the O31.3 trial (Table 1). The O31.E sheep were naturally infected and were obtained from a property at Bathurst, New South Wales. They were selected after an on-farm pre-selection procedure. In the pre-selection process, faecal and serum samples from one hundred sheep were collected. Faecal smear, ELISA and AGID tests were conducted to evaluate the potential infection status of each sheep. After pre-selection, a total of 33 sheep were included in the O31.E trial. These 33 sheep were housed in a pen at Camden for a number of weeks and serum samples were collected one week prior to necropsy. The final selection of nineteen naturally infected adult female sheep from the O31.E trial for this large scale biomarker discovery study was based on the results of faecal culture, tissue culture, ELISA, AGID tests and histological examination. The seven naturally infected female adult sheep from the O31.A trial were sourced from the same property as in the pilot scale biomarker study. The four female adult experimentally infected cross-breed sheep (O31.3) were obtained from a property at Armidale

New South Wales and challenged with $1X10^7$ *M. a. paratuberculosis* strain Telford 9.2 at weekly intervals three times at four months of age. The serum samples were collected 20 months after last challenge. The infection status of seven O31.A and four O31.3 sheep were evaluated using faecal and tissue culture, ELISA, AGID test and histological examination. Based on the Perez classification, the infected group comprised ten sheep with multibacillary lesions (3b); 12 sheep with early paucibacillary lesions (3a) and 8 with late paucibacillary lesions (3c) (Table 1)

.

Table 1. Animal population characteristics

Group	*Trial Code*	*No. of Animals*	*Animal ET number*	*Age*	*Sex*	*Breed*	*Histological examination*				*Tissue culture*	*Faecal culture*	*ELISA % (S/P)*	*GDP T*	*Faecal Smear*
							Histology Category	**Perez**	**No. of gut sections with JD lesion**	**No. of LN sections with JD lesion**					
Unifec	031.D	N = 29	3.	3+	Femal	Merin	All negative	N/	N/A	N/A	All -ve	All –ve	N/A	N/A	N/A
Vacci	031.F	N = 30		2+	Femal	Merin	N/A	N/	N/A	N/A	N/A		N/A	N/A	N/A
Infect	031.E	N=19	2412	3+	All	All	pos	3a	5	4			285	-	neg
			2476				pos	3b	6	6			258	3+	+/-
			2484		Femal	Merin	pos	3a	3	4			256	2+	+/-
			2428		e	o	inc	3a	2	1			206	-	+/-
			2450				pos	3a	3	2			202	-	+/-
			2435				pos	3b	6	6			198	3+	+
			2458				pos	3c	5	5			155	2+	+
			2430				pos	3a	6	5			150	wk	+/-
			2455				pos	3b	3	4			147	-	+/-
			2448				pos	3a	2	5			144	-	+/-
			2403				inc	3a	1	4			118	-	Ne
			2440				pos	3c	2	2			110	-	+/-
			2420				inc	3a	1	3			96	1+	+/-
			2477				pos	3a	2	1			93	-	Ne
			2451				inc	3a	2	1			88	-	+/-
			2487				pos	3a	3	2			83	-	+/-
			2427				pos	3a	4	4			80	-	Ne
			2405				inc	3a	1	1			79	-	+
			2414				pos	3b	6	6			71	-	+
Infect	031.A	N=7	985	3+	Femal	Merin	pos	3d	2	2	+	+	210	1+	2
			986				pos	3b	6	6	+	+	117	3+	1
			988				pos	3a	5	4	+	-	32	-	0.5
			989				pos	3a	6	5	+	+	149	2+	1
			990				pos	3b	6	6	+	+	123	2+	1
			992				pos	3a	5	5	+	-	223	3+	1
			994				pos	3d	3	3	+	-	172	-	1
	031.3	N=4	1002	2+	Femal	cross-	pos	3b	6	6					
			1014				pos	3b	6	6					
			1021				pos	3b	6	6					
			1022				pos	3b	6	6					

A number of tests were used to evaluate the disease status of each sheep used in the experiment. Faecal culture, ELISA and AGID tests were conducted for all animals [27, 35]. The infection status was confirmed post necropsy by intestine tissue culture and histological examination of terminal ileum (3 sections), jejunum (3 sections) and mesenteric lymph nodes corresponding to each level of ileum and jejunum. Tissues were fixed in 10% buffered formalin at the time of necropsy, embedded in paraffin, sectioned at 5 um and stained with hematoxylin and eosin and by a Ziehl-Neelsen method [13]. According to the classification developed by Perez [19], the paratuberculosis lesions in naturally infected sheep were classified histologically into three types. Type 1 lesions consisted of small granulomas located exclusively in the ileocecal Peyer's patches. Type 2 lesions consisted of granulomata in the mucosa associated with Peyer's patches. Type 3 lesions were characterized by granulomas in the area of mucosa associated with Peyer's patches and other mucosal areas [19]. The type 3 lesion was further sub-categorized into three sub-types: 3a (early paucibacillary lesion), 3c (late paucibacillary lesion) and 3b (multibacillary lesion).

Sample preparation for SELDI analysis

For unexposed and infected groups, peripheral blood was collected into plain red-topped vacutainers (BD) containing a gel serum separator with silica activator and allowed to clot at room temperature for 30 minutes [2]. For vaccinated group, serum samples were allowed to clot at room temperature for 2 to 3 hours before processing due to the distance travelled between farm and laboratory. Samples were centrifuged at 3000 xg for 10 minutes and the serum was removed to a 15 mL polypropylene tube (Falcon, BD). The serum was centrifuged again at 3000 xg for 10 minutes to pellet cellular debris and 2 mL was taken to a fresh 15 mL tube. 3 mL of reducing buffer (8M urea, 1% CHAPS in PBS) was added, vortexed and 100µL aliquots were snap frozen on liquid nitrogen in 1.5 mL polypropylene screw cap tubes (Interpath). Samples were stored at -80°C until required. Each aliquot was thawed only once for SELDI-TOF MS analysis and any unused sample was discarded. Protein concentrations of samples were determined using a Bradford protein assay reagent (BIO-RAD) according to the manufacturer's instructions, and spectrophotometry at 595 nm (BioPhotometer, Eppendorf).

ProteinChip Array analysis

Serum samples were thawed briefly on wet ice and centrifuged for two minutes at 16,000 xg. The serum samples were profiled on immobilized metal affinity capture (IMAC-30) ProteinChip Arrays and on strong anion exchange (Q10) ProteinChip Arrays according to the manufacturer's instructions (Ciphergen Biosystems). Briefly, samples were first diluted 1:4 by adding binding buffer (1x PBS for IMAC array, 50mM Tris-HCl pH7.5 for Q10 array) and kept on ice for approximately 30 minutes prior to analysis. Prior to processing, IMAC-30 arrays were loaded with 100mM $NiSO_4$ (2 × 5µL × 5 min). Then the arrays were pre-equilibrated with 5 µL binding buffer (3 × 5 min) in a humidity chamber with gentle agitation. 5 µL of sample was then applied and incubated for 60 minutes. The spots were washed with binding buffer three times (5 µL, 5 min) and twice with HEPES (1mM, pH 7.0, 5 µL, 1 min). Array surfaces were allowed to dry for seven minutes and 1uL of 50% sinapinic acid (3,5-dimethoxy-4-hydroxycinnamic acid) (Ciphergen) dissolved in 50% (v/v) acetonitrile, 0.5% trifuluroacetic acid (both Sigma) was applied twice to each spot on the array and allowed to dry for five minutes between applications.

SELDI data acquisition

Arrays were analysed on the Protein Biology System II (PBSII) mass spectrometer (Ciphergen Biosystems, Freemont, CA, USA). Peak detection was performed using the ProteinChip software version 3.0 (Ciphergen). Spectra were collected from 2000 to 100,000 Da for analysis. Using IMAC ProteinChip arrays, only low molecular weight spectra were collected. Using the Q10 ProteinChip surface, both low and high molecular weight spectra were collected. For data acquisition of low molecular weight proteins, the detection size range was between 2 and 20 kDa, with a maximum size of 25 kDa. The detector sensitivity was set at 5, and laser intensity was set at 210. For acquisition of high molecular weight proteins on the Q10 array, the detection size range was 20 to 80 kDa, with a maximum size of 100 kDa. The detector sensitivity was set at 5, and the laser intensity was set at 230. The mass to charge ratio (m/z) was calibrated externally using the all-in-one peptide calibration kit: [Arg8]-Vasopressin (1084.25+1H), Somatostatin (1637.9+1H), Insulin B-chain (bovine) (3495.94+1H), Insulin (human recombinant) (5807.65+1H), Hirudin BKHV(7033.61+1H) (Ciphergen) and a mass/charge (m/z) accuracy of 0.1% was achieved before the test arrays were read. Spectra smaller than 2 KDa were not collected due to possible energy absorbing molecular artefacts. The spectra were subjected to baseline subtraction and were normalized to total ion current with a minimum m/z of 2000 Da for the low molecular weight range and 20kDa for the high molecular weight range.

Pilot scale biomarker discovery experiment and cluster generation

Five different ProteinChip array types and buffers, Q10 with Tris-HCl pH7.5 buffer, CM10 with Tris-HCl pH 7.0 buffer and low stringency buffer (Ciphergen), IMAC-30 Ni^{2+} with PBS and IMAC-30 Cu^{2+} with PBS, were examined in the pilot scale biomarker discovery experiment to determine which array type and buffer gave the largest number of putative differentially expressed proteins between uninfected and infected animals (Table 2). Following this stage, Biomarker Wizard software (Ciphergen) was used to detect common proteins (clusters) between contrasting animal populations: infected vs. unexposed animals and vaccinated vs. unexposed animals. The following settings were chosen for automatic peak detection in Biomarker Wizard: (i) auto-detect peaks to cluster, (ii) first pass: signal/noise ratio 5, (iii) minimal peak threshold: 50% of all spectra, (iv) cluster mass window: 0.5% of mass and (v) second pass: signal/noise ratio 5. As a quality control procedure, all peak clusters generated from Biomarker Wizard were visually inspected and manually relabelled if necessary. After relabelling, the intensity values for replicates were exported to Microsoft Excel for further data analysis.

Reproducibility

A single serum sample from an unexposed sheep was used as a QC sample and was added to one spot of each array tested. A total of 26 QC spots were then generated from 26 arrays in this study. The spot location of the QC serum was determined on a rolling basis; it was moved from spot one to spot eight and back to spot one in each consecutive run (Figure 1). As there were a large number of samples, each array was loaded with samples from different groups to avoid clustering of group with array [8], see Appendix II for array work sheets. Duplicates of all samples were processed (Appendix II).

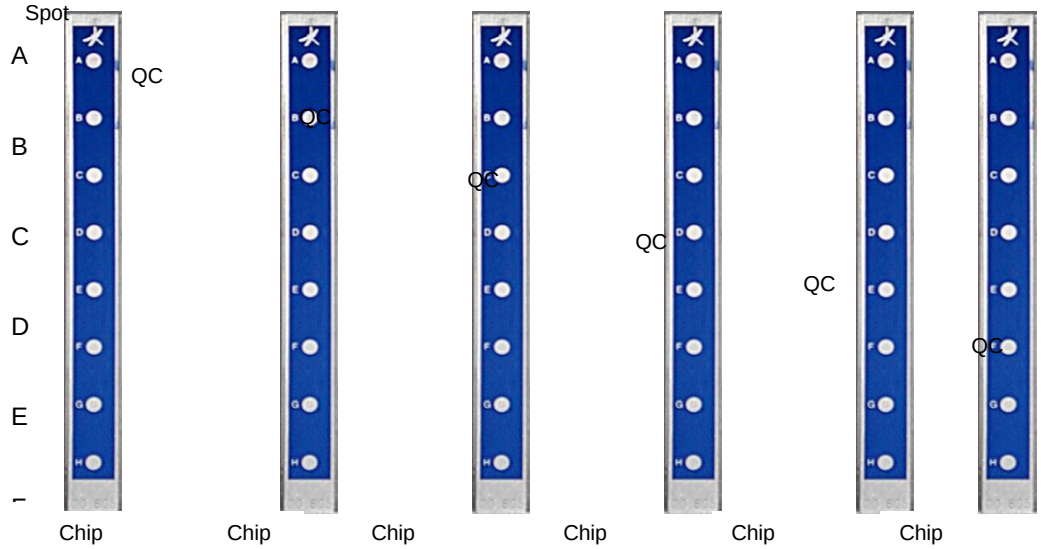

Figure 1 Schematic diagram showing the spot location of QC samples.
The spot location of QC serum with respect to case and control samples was determined on a rolling basis; it was moved systematically from spot A chip 1 to Spot H on Chip 8 and then back to spot A in each consecutive run.

As described in previous chapter, between-run and within-run reproducibility was evaluated by applied a control serum to all eight spots of three arrays over three days and within-chip reproducibility were examined. The between-chip reproducibility was also evaluated using the data generated from the three QC chips. In addition, the same eighteen peaks (with molecular mass of 4357.3, 4623.5, 4724.6, 7442.9, 7524.0, 7931.5, 8000.6, 8493.0, 8719.1, 9252.4, 9459.0, 11564.1, 13753.1, 14890.0, 15048.1, 15256.9, 16005.1, 16073.4 Da) were selected from the spectra generated from each QC spot on every individual chip and spectra derived from all 26 chips were evaluated for between-chip reproducibility.

Coefficient of variation (CV) was calculated for peak intensity and *m/z*. In addition, the concordance correlation coefficient (CCC), developed by Lin (1989) for assessment of concordance between continuous data, was calculated (http://www.niwascience.co.nz/services/statistical/concordance) to reflect the agreement between pairs of replicates within and between chips: values larger than 0.99 indicate perfect agreement; values between 0.95 and 0.99 indicate substantial agreement; values between 0.90 and 0.95 indicate moderate agreement; values less than 0.90 indicate poor agreement. The between-spot CCC values were computed by randomly selecting five pairs of spots from 26 chips, for example, spot 1 on chip 1 paired with spot 3 on chip 3.

Univariate analysis

The Significance Analysis of Microarray (SAM) algorithm (Stanford University) [23, 22] was used for univariate analysis to identify significant proteomic features between contrasting animal populations. Given the group identity, the data type was selected as “two class unpaired data” and 5000 permutations were performed. The false significant discovery rate was set to zero to avoid the identification of false significant proteomic features caused by multiple comparisons. The mean and median of transformed intensities were compared using t tests and Wilcoxon rank sum tests.

Classification and Regression Tree (CART) model

Construction of a decision tree classification and regression algorithm was performed using Biomarker Pattern Software (BPS) version 5.0.2 (Ciphergen), as described by Breiman *et.al* with

modifications. The clusters generated from Biomarker Wizard were included as a learning sample to build decision trees. A decision tree is an inverted flow-chart, which consists of repeat splitting of data sets into subsets according to a given classification task. The decision tree starts from a root node, which contains all the samples, by selecting Gini as diversity index, favouring an even split from 0.00 to 2.00 and varied by 0.2 each time. The classification tree splits the data into two nodes, using one rule at a time in the form of a yes/no question (Figure 4.2). Thus, the BPS methodology is a binary recursive partitioning tool. The binary process means that the parent nodes are always split into exactly two child nodes while it is recursive because the process can be repeated by treating each child node as a parent. The ends of the 'branches' of the tree are terminal nodes, meaning that the final classification has been reached, while other nodes continue to be split until terminal nodes are reached.

The splitting decision was defined by the presence or absence of a specific peak or changing of its expression level (intensity). In the schematic diagram of Figure 2, peptide A in node 1 and peptide B in node 2 are two peptides that were selected. Peptide A is the main splitter in this decision tree. The splitting rule is used to split the node into two child nodes and BPS always asks questions with a 'yes' or 'no' answer. The Gini rule, which is a measure of how well the splitting rule can separate the classes contained in the node, was used to evaluate the quality of the splitter. Once a best split has been found, the algorithm repeats the process for each child node, until further splitting is impossible or has no gain and is stopped. The classification of each terminal node was determined by the group that represented the majority of samples in that node.

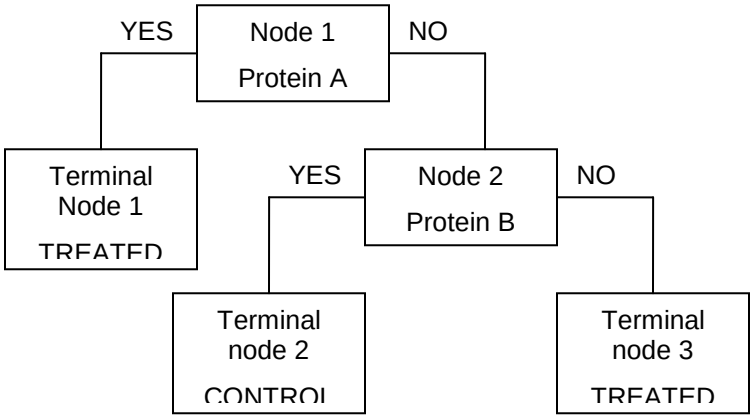

Figure 2 Schematic diagram illustrating a decision tree generated from CART analysis.
Node 1 is the root node, which contains all the samples, and through a process of yes/no questions child nodes are generated. The terminal nodes indicate that the final classification has been reached. One SELDI peptide/peak is used to split the data. Protein A is the main splitter in this example.

The V-fold cross-validation function was used to evaluate the accuracy of each decision tree. Cross-validation is a statistical practice of partitioning a sample of the data into subsets, so that the analysis is initially performed on a single subset, while the other subsets are retained for validating the initial analysis. In V-fold cross-validation, the original samples are partitioned into V sub-samples. Of the V sub-samples, a single subset of samples is retained as the validation data for testing the model, and the remaining V-1 sub-samples are used as learning samples or training samples. In the BPS mode, the program firstly builds up a maximal tree using all the learning samples and then subsequently prunes back. Then BPS randomly divides the learning sample into roughly 10 equal parts, each containing a similar distribution of dependent variables. BPS then re-constructs the largest tree by taking 9 parts of the data, and uses the remaining $1/10^{th}$ of the data to

obtain estimates of error rate of selected sub-trees. The same process is then repeated until each part of the data has been reserved one time as a test sample. By following this procedure, a number of parameters, such as the Favor Even Factor (ranged from 0 to 2), number of V-fold cross validation and number of parent node minimum cases, and a variety of predictors (peaks) were used to generate the optimal classification tree; in most cases this is the tree with the lowest 'cost' or misclassification rate. Each tree was read as a specific pattern of peptides for classifying contrasting groups.

Linear Discriminant Analysis (LDA) model

Multivariate linear discriminant analysis was used to determine which protein or peptide could best discriminate between infected and unexposed or between vaccinated and unexposed animal populations. Discriminant analysis was conducted in a stepwise manner. Firstly, the selection of candidate variables used to build up the model was performed using a stepwise regression algorithm and guided by the respective F value. The F value for a variable indicates its statistical significance in the discrimination between groups and is a measure of the extent to which a variable makes a unique contribution to the predication of group membership. Secondly, the candidate variables were tested in a two-group discriminant algorithm and a discriminant function created. The model classification accuracy was determined by cross-validation. The discriminant analysis was performed in MIniTab and S-plus software.

Clustering analysis

In order to identify the possible existence of sub-groups within the infected animal populations, two standard clustering methods: K-means and hierarchical clustering analysis using a three-cluster option were attempted on the spectral data generated from IMAC-30 ProteinChip arrays. In hierarchical clustering analysis, three different linkage algorithms were tested and compared: single linkage, complete linkage and group average clustering. Based on clustering results, the infected animals were re-sub-grouped and Biomarker Wizard used to discover the spectral differences between these sub-groups. Finally, the sub-grouping results were compared to the histological classification of individual infected animals. The clustering analysis was performed in S-plus software.

Results

Pilot scale biomarker discovery

In the pilot biomarker discovery experiment, five different ProteinChip array types and buffers were evaluated to determine which combination generated the largest number of putative biomarkers between uninfected versus infected sheep. Among the five ProteinChip array types examined, the strong ion exchange array (Q10) with Tris-HCl pH7.5 buffer generated the greatest number of different proteomic features between contrasting animals: eight potential biomarkers were identified in total, six down-regulated and two up-regulated (Table 2). Five significantly down-regulated proteins were identified using the IMAC 30-Ni^{2+} array and three were identified with the IMAC-30 Cu^{2+} array, two up-regulated and one down-regulated. No significant proteomic feature was identified using cation exchange array (CM10) with either buffer (Table 2). Therefore, two ProteinChip arrays, Q10 and IMAC-30 Ni^{2+} were selected for the large scale biomarker discovery experiment to identify potential biomarkers with a larger sample size.

Table 2. Summary of ProteinChip array types and buffers evaluated in pilot scale biomarker discovery experiment

ProteinChip array	*Buffers*	*Total No. of putative differentially expressed*	*No. of up-regulated*	*No. of down-*

		proteins	*proteins*	*regulated proteins*
Strong anion exchanger (Q10)	Tris-HCl, pH 7.5	8	6	2
Weak cation exchanger (CM10)	Tris-HCl, pH 7.0	0	0	0
	Low stringency buffer	0	0	0
IMAC-30 Ni^{2+}	PBS	5	5	0
IMAC-30 Cu^{2+}	PBS	3	2	1

Large scale biomarker discovery

In the large scale biomarker discovery experiment, SELDI-TOF MS (Ciphergen) was used to identify proteomic features between contrasting animal populations: (1) infected sheep versus unexposed sheep and (2) sheep vaccinated with Gudair™ vaccine versus unexposed sheep. In the unexposed group, 22 of 29 sheep were used to generate spectra on the IMAC 30 ProteinChip array; all 29 unexposed sheep were used on the Q10 ProteinChip array. Using SAM at a median false discovery rate of zero, a panel of significantly differentially expressed proteomic features were identified between contrasting populations (see below). A representative pseudogel view of one differentially expressed protein generated from the IMAC-30 ProteinChip array between unexposed animals and vaccinated animals is shown in Figure 3.

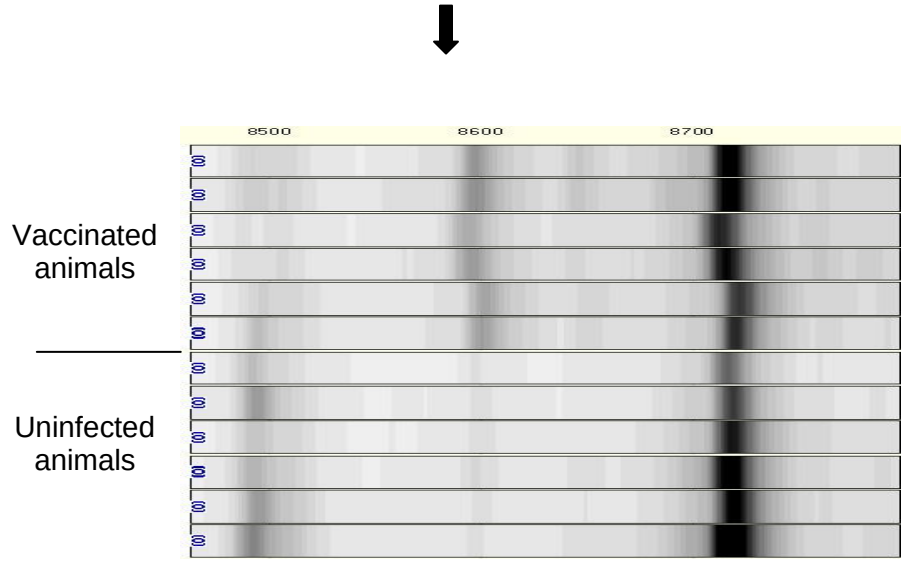

Figure 3 A differentially expressed vaccination-associated serum protein.
A representative pseudogel view of SELDI-TOF MS analysis of serum samples, processed on the IMAC 30 – Ni $^{2+}$ chip surface, shows the relative abundance of a differentially expressed protein (arrow) associated with Gudair™ vaccination in sheep. The peptide has a maximum fold change (>5) as determined by SAM data analysis. The upper six spectral protein profiles are sera from six sheep vaccinated with Gudair™ and the bottom six spectral profiles are from unexposed sheep.

Comparison of infected versus unexposed animals

Univariate analysis

Analysis of samples from infected and unexposed animals revealed twenty-one differentially expressed peptides among two ProteinChip array types. Of these 11 peptides (with molecular mass of 5188, 7936, 8496, 8595, 8651, 8702, 9260, 9320, 10231, 38902 and 77495 Da, respectively) were found to be up-regulated 1.6 to 3.2 fold in infected sheep. Another ten peptides (with molecular mass of 8263, 8305, 8353, 8725, 11570, 13753, 13812, 44534, 47115, and 74786 Da respectively) were down-regulated between 1.7 to 4.3 fold in infected sheep relative to the unexposed sheep (Table 3). In the infected animals, the total numbers of up- and down-regulated peptidess were similar: 11 up-regulated compared to 10 down-regulated peptides (Table 3). A peptide from the Q10 ProteinChip array with a mass of 8263 Da had the greatest fold change detected: 4.6 fold down-regulation.

Table 3. Differentially expressed proteomic features between unexposed and infected animals from two ProteinChip array types by univariate analysis in order of *m/z*.

No.	*m/z*	*Fold change*	*Infection effect*	*q-value(%)*[1]	*ProteinChip array*	*Peaks used*	
						CART	**LDA**
1	5188.2	1.79	Up	0	IMAC 30		
2	7936.8	1.64	Up	0	IMAC 30		
3	**8263.0**	**-4.63**	**Down**	**0**	**Q10**	X	X
4	**8305.**4	-2.65	Down	0	IMAC 30	X	X
5	**8353.2**	**-1.91**	**Down**	**0**	**Q10**		
6	**8496.5**	**1.70**	**Up**	**0**	**Q10**		X
7	**8595.9**	1.50	Up	**0**	**IMAC 30**		
8	**8651.0**	**2.91**	**Up**	**0**	**IMAC 30**	X	X
9	8702.1	1.82	Up	0	Q10		
10	8725.5	-1.85	Down	0	IMAC 30		
11	9259.9	1.95	Up	0	Q10		
12	9320.6	1.73	Up	0	IMAC 30		
13	10230.6	2.16	Up	0	IMAC 30		X
14	11569.9	-2.18	Down	0	IMAC 30		
15	**13752.7**	**-3.49**	**Down**	**0**	**IMAC 30**	X	X
16	13812.2	-3.06	Down	0	IMAC 30		
17	38901.8	3.20	Up	0	Q10		
18	44534.4	-2.44	Down	0	Q10		
19	47114.7	-1.70	Down	0	Q10		
20	**74786.4**	**-2.23**	**Down**	**0**	**Q10**		
21	**77494.6**	**2.52**	**Up**	**0**	**Q10**		

1 q-value: this is the lowest False Discovery Rate at which the peptide is called significant in the SAM analysis. It is like the P-value, but adapted to the analysis of a large number of peptides.

Classification and Regression Tree (CART) model

The Biomarker Pattern Software (Ciphergen) was used to simultaneously find peaks and identify protein patterns that separated infected sheep or vaccinated sheep from unexposed animals.

IMAC-30 ProteinChip array serum profiling

Firstly, spectra derived from IMAC-30 ProteinChip arrays were considered. CART model I was generated using 104 spectra derived from 52 serum samples (duplicates of 30 infected and 22 unexposed sheep). This model had five decision nodes, based on the intensity of three peptides with masses of 13753, 8651 and 8302 Da. The 13753 Da peptide was used as the root decision node in this classification model (Figure 4). The infected sheep were allocated into terminal nodes 1 and 3, while the unexposed sheep were allocated into terminal nodes 2 and 4. In the ten-fold cross-validation, the program randomly divided the total 52 spectra into 10 sub-sets and regenerated the model using 9 subsets of samples. The last subset sample was then used as the testing sample to test the accuracy of model. This random division process was repeated until every sample had participated in the test set at least once. By this manner, this model achieved a sensitivity of 90.0% in identifying infected animals (27 of 30) and a specificity of 90.9% in identifying unexposed animals (20 of 22) in cross-validation (Table 4).

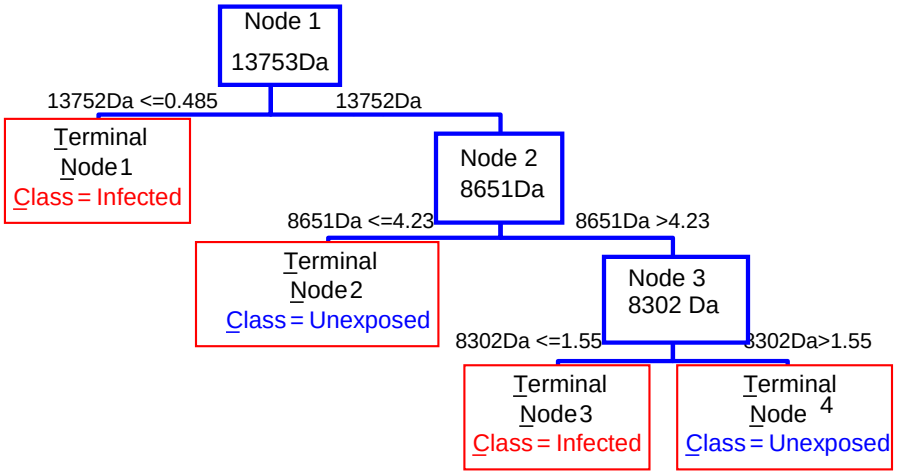

Figure 4. CART model I: infected versus unexposed samples

This classification decision tree was generated from IMAC 30 ProteinChip array spectra. Spectra from 52 serum samples were used as a learning set to generate a decision tree to distinguish sera obtained from sheep infected with paratuberculosis from unexposed sheep. There are three decision nodes, based on the intensity of three different peptides with mass of 13752, 8651 and 8302 Da. Terminal nodes determine whether a sample is classified as unexposed or vaccinated.

Q10 ProteinChip array serum profiling

To identify potential serum biomarkers using spectra generated from the Q10 ProteinChip array, CART model II was developed to distinguish unexposed animals from infected animals. CART model II was developed using 118 spectra obtained from 59 serum samples (duplicates of 30 infected and 29 unexposed sheep) to differentiate infected from unexposed animals. Surprisingly, this model included only one decision node based upon a peptide of 8262 Da and this peptide was 4.6 fold down-regulated in the infected animals (Figure 5). Using this decision algorithm, 27 of 29 unexposed animals and 25 of 30 infected animals were correctly classified following 10-fold cross validation (Table 4).

Table 4. CART models: infected vs. unexposed samples

	Unexposed		*Infected*	
	Correct/Total	***Percent***	***Correct/Total***	***Percent***
CART model I – using spectra generated from IMAC 30 ProteinChip array				
Training set resubstitution results				
	21/22	***95.45***	***28/30***	***93.33***
Training set cross-validation results				
	20/22	***90.91***	***27/30***	***90.00***
CART model II – using spectra generated from Q10 ProteinChip array				
Training set learning results				
	27/29	***93.10***	***25/30***	***83.3***
Training set cross-validation results				
	27/29	***93.10***	***25/30***	***83.3***

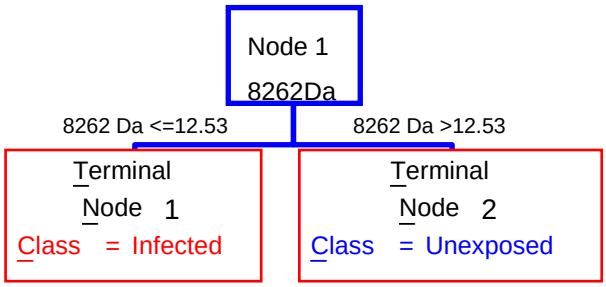

Figure 5 CART model II: infected versus unexposed samples

This classification decision tree was generated from Q10 ProteinChip array spectra. Spectra from 59 serum samples were used as a learning set to generate a decision tree to distinguish sera obtained from sheep infected with paratuberculosis from unexposed sheep. There is one decision node, based on the intensity of one peptide with mass of 8262 Da. Terminal nodes determine whether a sample is classified as unexposed or infected.

Linear Discriminant Analysis model

Discriminant analysis was used as an alternative to CART analysis to identify a subset of peptides that could discriminate infected sheep from unexposed sheep. Initially, all significant peptides identified by univariate analysis, which used the same training set as CART analysis were evaluated as potential predictors and subjected to stepwise regression analysis. The discriminant function was created using the peptides selected from stepwise regression analysis. The accuracy of the discriminant model was then tested using cross-validation. Again the spectra were generated using IMAC 30 ProteinChip arrays (104 spectra derived from sera of 30 infected and 22 unexposed animals in duplicate).

Discriminant model I was generated to distinguish sheep infected with paratuberculosis from unexposed sheep and identified five peptides of mass: 13753, 10231, 8302, 16074 and 8651 Da. Among these five peptides, the 13753, 8302 and 8651 Da peptides were also identified in the CART classification model (Figure 4). Again, peptide 13753 Da was the best discriminator in this model,

and was also selected as the root decision node in CART model I. However, in Discriminant model I, two peptides 10231 and 16074 Da were used that were not included in the CART model. The discriminant model correctly identified 20 of 22 unexposed animals and 27 of 30 infected animals in the cross-validation (Table 5), which was the same accuracy as the CART model.

Table 5. Discriminant models: infected vs. unexposed samples

	Unexposed		***Infected***	
	Correct/Total	***Percent***	***Correct/Total***	***Percent***
Discriminant model I – using spectra generated from IMAC 30 ProteinChip array				
Training set resubstitution results				
	20/22	***90.91***	***29/30***	***96.97***
Training set cross-validation results				
	20/22	***90.91***	***27/30***	***90.00***
Discriminant function :				
Scores = 10.67 + 0.80 M8302 – 0.11 M8651 -2.40 M10231 + 3.19M13752 – 0.28 M16074				
Discriminant model II – using spectra generated from Q10 ProteinChip array				
Training set resubstitution results				
	28/29	***96.55***	***26/30***	***86.67***
Training set cross-validation results				
	28/29	***96.55***	***26/30***	***86.67***
Discriminant function:				
Scores = 9.08 + 0.22M8262 – 0.12 M8494				

Similarly, a discriminant model was generated using spectra derived from the Q10 ProteinChip array. There were 118 spectra in total derived from 30 infected sheep and 29 unexposed animals. Discriminate model II was used to differentiate between infected and unexposed sheep and consisted of two peptides with masses of 8262 and 8494 Da. The first peptide had the greatest discriminatory power, and was also selected as the root decision node in the CART model II (Figure 5). Upon cross-validation, this model correctly identified 26 of 30 infected sheep and 28 of 29 unexposed animals (Table 5). The accuracy of Discriminant Model II was close to that of the classification model generated by CART analysis (25 of 30 infected sheep and 27 of 29 unexposed animals correctly identified during cross-validation), which contained only one decision node using a peptide of mass 8262 Da (Figure 5).

Comparison of vaccinated versus unexposed animals

Univariate analysis

The univariate analysis between unexposed and Gudair™ vaccinated sheep revealed that there were a total of 20 peptides with increased or decreased expression in the vaccinated animals. Of these, 16 were up-regulated (with molecular mass of 2184, 5212, 7937, 8496, 8595, 8651, 8702, 9254, 9320, 9461, 9691, 10231, 28513, 38902, 74786 and 77495 Da, respectively) and 4 were down-regulated (with molecular mass of 5167, 11570, 13753, and 13812Da, respectively) with a minimum of 1.5 fold change (Table 6). The analysis showed that in vaccinated sheep the majority of differentially expressed peptides were up-regulated: 16 were up-regulated compared to 4 down-regulated (Table 6). A peptide with a mass of 8595 Da showed the maximum fold change at 6.5 fold up-regulation. The peptides that were significantly down-regulated were generated using the IMAC 30 ProteinChip array.

There were a number of differentially expressed peptides common to both infected and vaccinated animals relative to the control group but with a slightly different fold change in each group. The peptides with masses of 8496, 8595, 8651, 8702, 9320, 10231, 38902 and 777495 Da were all up-regulated to similar levels in both infected and vaccinated animals. Among these, two peptides (with mass of 8651 and 10231 Da) had apparent higher levels of fold change in infected animals compared to vaccinated animals (2.9 fold vs. 2.58 fold, 2.16 fold vs. 1.77 fold, respectively). All the other peptides had higher expression levels in the vaccinated animals than in infected animals and when compared to unexposed animals. One cluster of two proteins with masses of 13753 and 13812 Da were both down-regulated in vaccinated and infected animals with an average of 4.5 and 3.5 fold change, respectively.

Table 6. Differentially expressed proteomic features between unexposed and vaccinated animals from two ProteinChip array types by univariate analysis

No.	*m/z*	Fold change	Vaccination Effect	q- value[1] (%)	ProteinChip Array	Peaks used	
						CART	LDA
1	2184.2	2.56	Up	0	Q10		
2	5167.0	-1.97	Down	0	IMAC-30		
3	5212.2	2.57	Up	0	IMAC-30		
4	7936.8	2.08	Up	0	IMAC-30		
5	**8496.5**	**2.94**	**Up**	**0**	**Q10**	**X**	**X**
6	**8595.0**	**6.50**	**Up**	**0**	**IMAC-30**	**X**	**X**
7	8651.0	2.58	Up	0	IMAC-30		
8	8702.1	2.79	Up	0	Q10		
9	9253.8	1.76	Up	0	IMAC-30		
10	9320.6	1.79	Up	0	IMAC-30		**X**
11	9461.3	1.69	Up	0	IMAC-30		
12	9691.6	1.95	Up	0	IMAC-30		**X**
13	10230.6	1.77	Up	0	IMAC-30		
14	11569.9	-1.73	Down	0	IMAC-30		
15	**13752.7**	**-4.96**	**Down**	**0**	**IMAC-30**	**X**	**X**
16	13812.2	-4.09	Down	0	IMAC-30		
17	28513.6	1.70	Up	0	Q10		
18	38901.8	3.74	Up	0	Q10		
19	74786.4	1.21	Up		Q10	**X**	
20	77494.6	3.81	Up	0	Q10	**X**	**X**

1 q-value: this is the lowest False Discovery Rate at which the peptide is called significant in the SAM analysis. It is like the P-value, but adapted to the analysis of a large number of peptides.

Classification and Regression Tree (CART) model

IMAC-30 ProteinChip array serum profiling

CART model III was based on 104 spectra generated from 52 serum samples: duplicates of 30 vaccinated and 22 unexposed samples. This classification tree had two decision nodes (Figure 6). The root node was a peptide of mass 8596 Da that was 6.5 fold up-regulated in univariate data analysis when vaccinated animals were compared to unexposed animals (Table 6) and the second decision node was a peptide of mass 13753 Da that was 5 fold down-regulated in univariate data analysis (Table 4). The vaccinated animals were classified in terminal node 2 while terminal nodes one and three contained the unexposed animals. With the peptide of mass 8595 Da as the parent node, a sample with an intensity of this peptide lower than 1.84 went to the left terminal node 1 and was classified as unexposed, otherwise it went to node 2. Samples in node 2 were further classified based on the intensity of the second peptide with a mass of 13753 Da. A sample was classified as a vaccinated sample with intensity lower than 0.595 in terminal node 2, otherwise it was classified as an unexposed sample in terminal node 3. All 52 spectra were used as the learning set. In the learning set, classification model IV correctly identified 100% of the unexposed samples and 96.7% of the vaccinated samples. This classification model correctly identified 21 of 22 unexposed animals and 29 of 30 vaccinated animals in the ten-fold cross-validation (Table 7).

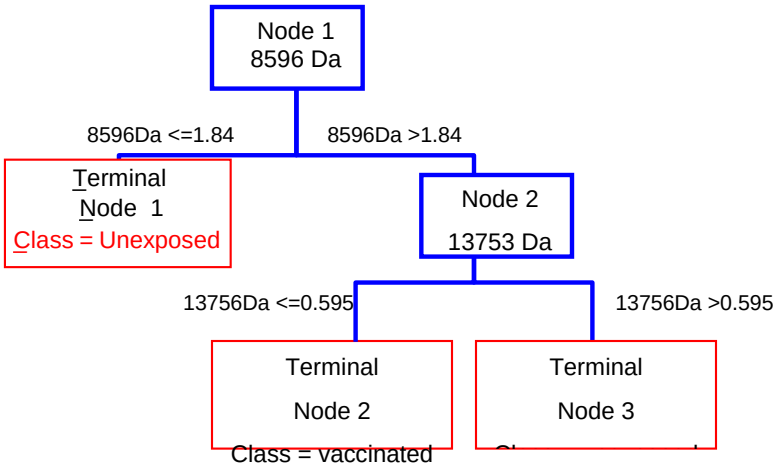

Figure 6 CART model III: vaccinated versus unexposed samples.

This classification decision tree was generated from IMAC 30 ProteinChip array spectra. Spectra from 52 serum samples were used as a learning set to generate a decision tree to distinguish sera obtained from sheep vaccinated with Gudair™ vaccine from unexpoesd, un-vaccinated sheep. There are two decision nodes, node 1 and node 2, based on intensity of two different peptides with mass of 8595 and 13753 Da. Terminal nodes determine whether a sample is classified as unexposed or vaccinated.

Notably, the 13753 Da peptide was involved in both CART models I and III. Peptide 13753 Da was used as the root biomarker in CART model I and was 3.5 fold and 5 fold down-regulated in the infected animals and vaccinated animals respectively, in comparison with unexposed animals by univariate analysis (Tables 3 and 6). In comparison to CART model III, CART model I utilized two additional peptides, 8651 and 8302 Da, as additional decision nodes to enhance the discriminatory power for infected versus unexposed animals.

Table 7. CART models: vaccinated vs. unexposed samples

	Unexposed		*Vaccinated*	
	Correct/Total	***Percent***	***Correct/Total***	***Percent***
CART model III – using spectra generated from IMAC 30 ProteinChip array				
Training set resubstitution results				
	22/22	***100***	***29/30***	***96.67***
Training set cross-validation results				
	21/22	***95.45***	***29/30***	***96.67***
CART model IV – using spectra generated from Q10 ProteinChip array				
Training set learning results				
	29/29	***100.00***	***27/30***	***90.00***
Training set cross-validation results				
	24/29	***82.76***	***24/30***	***80.00***

Q10 ProteinChip array serum profiling

CART model IV was generated using 118 spectra derived from 59 serum samples (30 vaccinated and 29 unexposed sheep) to discriminate sheep vaccinated with Gudair™ vaccine from unexposed, un-vaccinated sheep. The classification algorithm generated by this analysis had five decision nodes based on intensity of five peptides with masses of 8496, 74786, 77494, 8262 and 8353 Da (Figure 7). This classification model split vaccinated animals into nodes 2, 3, 5 and 7 and unexposed animals into nodes 1, 4 and 6. It correctly classified 24 of 30 vaccinated sheep and 22 of 29 unexposed animals following cross-validation (Table 7). The root biomarker in CART model IV was a 8496 Da peptide, which was 2.9 fold up-regulated in the vaccinated animals in the univariate analysis (Table 3 and 6).

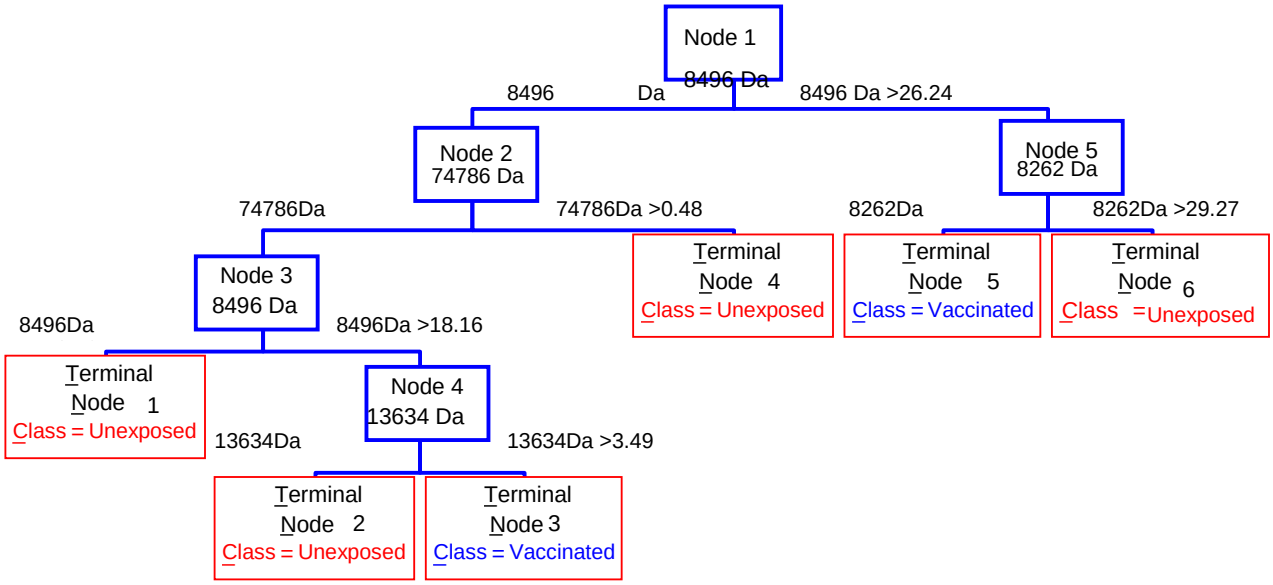

Figure 7. CART model IV: vaccinated versus unexposed

This classification decision tree was generated from Q10 ProteinChip array spectra. Spectra from 59 serum samples were used as a learning set to generate a decision tree to distinguish sera obtained from sheep vaccinated with Gudair™ vaccine from unexposed sheep. There are five decision nodes, based on the intensity of four peptides with mass of 8496, 74786, 8262 and 13634 Da. Terminal nodes determine whether a sample is classified as vaccinated or unexposed.

Linear Discriminant Analysis model

To differentiate between unexposed, un-vaccinated sheep and Gudair vaccinated animals, Discriminant model III was developed using a linear combination of four peptides of masses: 8595, 13753, 9691 and 9320 Da. The peptide of mass 8595 Da was identified as having the maximum contribution to the model, and notably was also selected as the root node in the CART analysis (Figure 6). Peptide of mass 13753 Da was also selected in both models. This discriminant model correctly identified 20 of 22 unexposed animals and all vaccinated animals during the cross-validation process (Table 8).

Discriminant model IV to distinguish vaccinated sheep from unexposed sheep was developed using a linear combination of four peaks, with masses of 8496, 93973, 8353 and 77494 Da. In comparison to classification model IV generated by CART analysis (Figure 4.7), the best discriminator (peptide 8496 Da) was same as the root decision node while the other three peaks were different to those used in CART analysis. In addition, two peptides selected in the Discriminant model IV (93973 and 8353 Da) were not significantly different in univariate analysis. In the cross-validation, this model correctly identified 26 of 30 (86.7%) vaccinated sheep and 27 of 29 (93.1%) unexposed sheep (Table 8).

Table 8 Discriminant models: vaccinated vs. unexposed samples

	Unexposed		*Vaccinated*	
	Correct/Total	***Percent***	***Correct/Total***	***Percent***
Discriminant model III – using spectra generated from IMAC 30 ProteinChip array				
Training set resubstitution results				
	20/22	***90.91***	***30/30***	***100***
Training set cross-validation results				
	20/22	***90.91***	***30/30***	***100***
Discriminant function :				
Scores = 11.79 + 0.39M8595 – 1.31 M9320 + 5.26 M9691 – 4.62 M13752				
Discriminant model IV – using spectra generated from Q10 ProteinChip array				
Training set resubstitution results				
	27/29	***93.10***	***26/30***	***86.67***
Training set cross-validation results				
	27/29	***93.10***	***26/30***	***86.67***
Discriminant function :				
Scores = 10.14 + 0.23 M8496 – 8.78 M93793 -0.91 M8353 + 1.31 M77494				

Clustering analysis on infected animals

Histological examination of the infected sheep demonstrated differences in the stage of disease of the infected animals. Twelve sheep were found to have early paucibacillary lesions (3a), 8 had later paucibacillary lesions (3c) and 10 sheep had multibacillary disease (3b). To identify the possible existence of serum biomarkers for these histological sub-groups within the infected animals, clustering analysis was performed on the spectra derived from 30 infected animals using IMAC-30 ProteinChip arrays. The spectra between 2000 and 13000 Da were used to create the data matrix for clustering analysis. The K-means clustering analysis and complete linkage based hierarchical clustering method generated similar results with the three-cluster option and the results from this analysis suggested that three sub-groups might exist within infected animals (Table 9). Analysis using Biomarker Wizard based on sub-groups generated from clustering analysis revealed that there were distinct spectral differences between sub-groups. These differences mainly focused on the presence or absence of two peptides: 8650 Da and 8720 Da (Figure 8). Sub-group one consisted of two animals 2412 and 2440. The protein profile from these animals contained only one of these peptides, 8650 Da. Sub-group two, which contained 13 animals, contained only peptide 8720 Da. However the spectra from sub-group three, which contained 15 animals, had both peptides.

As mentioned previously, the infected animals had been classified based on histological examination (see Table 1) and these different histological lesions have been demonstrated to be associated with disease progression. We speculated that the clustering results generated from spectral of infected sheep may associate with the individual animal histological classification. But the close observation of the Table 9 clustering result didn't reveal this correlation. In order to further identify whether a pattern exists within infected animals, a SAM analysis was performed. The infected animals were re-grouped based on number of acid fast bacilli (AFB) in the gut into two groups: paucibacillary group (AFB <2) and multibacillary group (AFB ≥2). The SAM analysis revealed that no peptide was significantly different (more than 2 fold) between two groups and it suggested that the clustering results observed were not related to the individual animal histology classification.

Table 9. Clustering analysis on spectra generated from infected animals using IMAC 30 ProeinChip array

Sub-group 1			*Sub-group 2*			*Sub-group 3*		
Animal ID	***Lesion type***	***No. of AFB in the gut***	***Animal ID***	***Lesion type***	***No. of AFB in the gut***	***Animal ID***	***Lesion type***	***No. of AFB in the gut***
2412	***3a-c***	***1***	***2430***	***3a***	***1***	***2403***	***3a***	***0***
2440	***3c***	***1***	***2448***	***3a***	***0-1***	***2420***	***3a***	***0***
			2450	***3a***	***1***	***2428***	***3a***	***0***
			2477	***3a***	***1***	***2405***	***3a***	***0***
			2484	***3a***	***1***	***2451***	***3c***	***0***
			2487	***3a***	***1-2***	***2427***	***3a-c***	***0-1***
			988	***3a***	***1***	***2458***	***3a-c***	***1***
			989	***3a***	***0-1***	***994***	***3c***	***0-1***
			2455	***3b***	***2***	***992***	***3c***	***0-1***
			986	***3b***	***4***	***1022***	***3b***	***3***
			990	***3b***	***2-3***	***2435***	***3b***	***3***
			985	***3d***	***1***	***2476***	***3b***	***2***
			1014	***3b***	***3+***	***1002***	***3b***	***3***
						1021	***3b***	***4***
						2414	***3b***	***2-3***

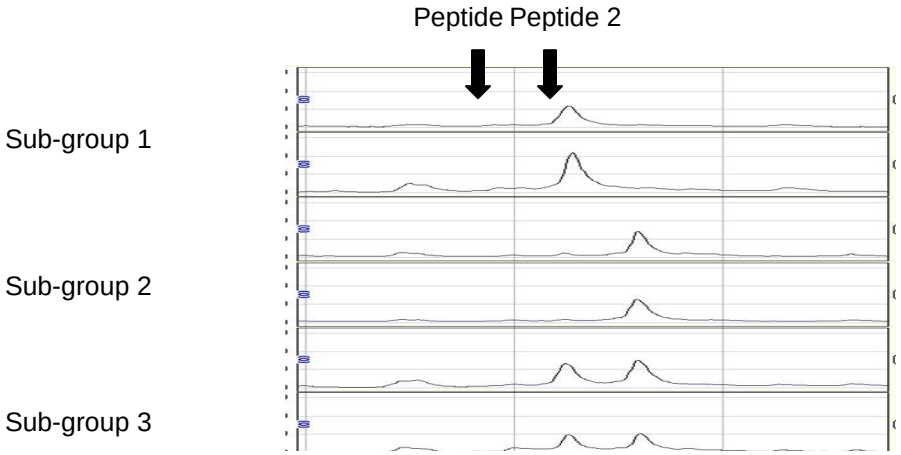

Figure 8 Sub-grouping within infected animals. The animal grouping based on clustering result generated from spectra of infected animals using IMAC 30 ProteinChip array. The top panel is representing the animals in subgroup one with only peptide 1 present. The middle panel is representing the animals of subgroup 1 with only peptide 2 while the bottom panel is representing the subgroup 3 animals with both peptide 1 and 2 present. The peptide 1 represents the peptide with mass of 8651 Da and the peptide 2 represents the peptide with mass of 8725 Da.

Reproducibility of study

The details of within-chip and between QC chip reproducibility can be found in Chapter 3. To determine the reproducibility between QC spots, the CV for peak intensity and *m/z* was computed using 18 peaks across one spot on each of 26 arrays. The average CV for intensity was 15.8% (range 9.7% to 33.9%) and the average CV for m/z was 0.028% (range 0.024% to 0.035%). The average CCC value for intensity across five randomly selected pairs of spots was 0.981 and ranged from 0.960 to 0.996 and the value for m/z of same five pairs were all greater than 0.99 indicating perfect agreement between spots (Table 10).

Table 10 Between– QC spot reproducibility

Peak intensity				*Mass/charge*			
Mean CV (%)[1]	Range of CV[2]	Mean CCC[1]	Range of CCC[2]	Mean CV (%)[1]	Range of CV[2]	Mean CCC[1]	Range of CCC[2]
15.8	9.7-33.9	0.981	0.960-0.996	0.028	0.024-0.035	0.999	0.999-0.999

[1] Means from positional replicates on 26 arrays for 18 peaks; [2] Extreme values among 18 peaks from positional replicates on 26 arrays.

Discussion

Comparison of infected and vaccinated animals with unexposed controls

Currently there are no reliable methods for the early detection of Ovine Johne's Disease. Widely used antibody-based serological tests are only useful at later stages of infection and with moderate sensitivity and specificity [7, 24]. Faecal culture has been used as the definitive diagnostic test, and may be useful in both sub-clinical and clinical stages of infection. However, this test requires 12 weeks incubation time to conclude a negative result. In addition, the faecal shedding of bacteria by the animals in the early sub-clinical stages may be intermittent, making the test somewhat unreliable. Recently, the use of SELDI-TOF MS for high-throughput protein profiling of human serum has facilitated the identification of panels of peptides and proteins that may be indicative of early disease for several types of cancers [12, 20, 21]. Here, a similar approach has been exploited, and a

number of proteins and peptides have been identified in this study that may be capable of distinguishing infected or vaccinated sheep from unexposed individuals.

A total of 89 serum samples, representing 30 sheep infected with Johne's disease, 30 sheep vaccinated with Gudair™ vaccine and 29 unexposed, un-vaccinated sheep, were used to generate protein profiles by SELDI-TOF MS. To enhance the selection of peptides with biological relevance, two independent multivariate tools, CART and multivariate linear discriminant analysis, were used in addition to the univariate analysis of SAM. In each method, a small subset of peptides that could distinguish between contrasting sample populations was identified. Although comparison of different statistical tools was not the main purpose of this study, as an alternative to linear discriminant analysis, the tree based classification tool was used in addition as it has a number of advantages over parametric techniques [32]. The major advantage is that it is a nonparametric algorithm. Secondly, no advance variable selection is required since the variable is selected automatically to reduce classification errors and bias. In addition, those variables that do not contribute to the classification success are not used. In discriminant analysis, the stepwise procedure will capitalize on chance because the variables have to be 'chosen' by the user to be included in the model. Thus, caution is needed and one cannot entirely rely on the *F* value to determine the entry or removal of variables. Thirdly, it is robust with outliers and the variable transformation does not change the tree structure. However, the classification tree has its own disadvantages. The main disadvantage is the possibility of growing an over-sized, over-fitted tree, and in some cases the overall tree may not be optimal since the methodology assures the local splitter will be optimal [14].

A comparison of the peptides selected by the two methods showed that the primary discriminator or the root decision nodes were the same in both methods, and the accuracy of both methods in cross-validation was very similar. Using the data generated from the IMAC-30 ProteinChip array, the CART model III correctly identified 21 of 22 unexposed cases and 29 of 30 vaccinated animals, while the discriminant model III correctly identified 20 of 22 unexposed animals and all 30 vaccinated sheep (Tables 7 and 8). These observations provide confidence that these peptides may be genuine disease or vaccination related serum biomarkers. An examination of the peptides utilized in both models revealed both increases and decreases in intensity when the serum of infected and vaccinated sheep was compared to unexposed animals (Tables 3 and 4). This suggests that the disease or vaccination status of the animal can elevate or diminish the circulating serum proteins or peptides, and these changes could be used to detect the presence of disease or vaccination.

Based on the pilot study results, two ProteinChip array types were selected for this trial, IMAC-30 and Q10, and both revealed panels of potential serum biomarkers. The IMAC-30 ProteinChip array worked well in the low molecular weight range while the Q10 revealed peaks in both low and high molecular weight ranges. The models generated from spectra derived from IMAC-30 Proteinchip array (infected or vaccinated versus unexposed) using two statistical methods had similar accuracy (Tables 4, 5 and Tables 7, 8). The models for discriminating vaccinated from unexposed sheep generated by both methods were slightly better than the models differentiating infected from unexposed animals. However the model created from spectra derived from the Q10 ProteinChip array that was used to discriminate vaccinated sheep from unexposed animals did not achieve satisfactory results. The CART model identified 24 of 29 unexposed sheep and 24 of 30 vaccinated animals while the discriminant model identified 27 of 29 unexposed sheep and 26 of 30 vaccinated sheep (Tables 7 and 8).

Clustering analysis on spectral of infected animals

In parallel an attempt was made to identify potential serum biomarkers for the infection status of animals based on the histological classification system developed by Perez *et. al* [19]. In paratuberculosis, the different types of granulomatous lesion observed have been associated with

stages of disease progression. Paucibacillary lesions, which occur in the early stage of paratuberculosis, consist of many lymphocytes, plasma cells and macrophages and small numbers of epithelioid cells, with no or few visible of mycobacteria [3, 5]. In contrast, multibacillary lesions which in most cases occur at later stages of disease, consist mainly of macrophages and epithelioid cells and bear large numbers of mycobacteria [33]. The close examination of spectra within infected animals, in particular the spectra generated from IMAC-30 ProteinChip arrays has shown that variation or patterns might be present within the infected group of animals. This was the hypothesis behind the clustering analysis on spectra of infected animals derived from IMAC-30 ProteinChip array, to attempt to look for a potential relationship that may exist between the sub-groups and lesion types.

As an un-supervised tool, clustering analysis helped to discover the potential relationships among infected animals based on individual spectra. To select the optimal method and obtain the best separation was not an easy task. The K-means method worked well with the continuous data set, while for hierarchical clustering methods, three different ways of calculating dissimilarity had their own advantages and disadvantages. Single linkage can often give unsatisfactory results if 'intermediates' are present between relatively distinct clusters, while the average and complete linkage tend to impose a structure on the data rather than uncover the actual structure present. In contrast, when data contain the true cluster structure masked by the addition of noise, single linkage gave poor results, with average and complete methods being far superior [14]. Since it has been demonstrated that no single method could be claimed to be the best for all types of data, the comparison of clustering results using different methods against SELDI spectra was of critical importance to find the optimal method and discover the group separation that had biological relevance.

In this study, the K-means and hierarchical clustering with average linkage generated similar results with three subgroups identified. The spectral differences between sub-groups revealed using Biomarker Wizard mainly focused on two peptides: peptide one with mass of 8650 Da and peptide two with mass of 8720 Da. However, the clustering results observed in the infected animals had no obvious connection to the individual animal histology classification. This was further demonstrated by the SAM analysis that showed no significant differences existed between paucibacillary and multibacillary groups and the two-peptides-clustering within infected sheep is not related to histological category.

The potential disease-related biomarkers identified so far are based on cross-validation and a separate testing sample set is clearly needed to further validate these biomarkers in a wider population of infected and vaccinated sheep. Ideally, a separate testing sample should include infected animals at different stages of disease progression. Within infected group, it would be interesting to monitor at which stage 'peptide 1' or 'peptide 2' starts to appear in the protein profile. In addition, another future task of this study is to identify the potential biomarkers discovered during this study. One of the advantages of using SELDI TOF-MS technology is that one can achieve a good classification rate without knowing the identity of these proteins. However, the characterization and identification of these biomarkers could provide invaluable insight into the physiology and pathophysiology of Ovine Johne's Disease.

References

Albison H.E., Talbot R.J.d., Johne's disease in Victoria, Aust Vet J (1936) 12:125-138.

Banks R.E., Stanley A.J., Cairns D.A., Barrett J.H., Clarke P., Thompson D., Selby P.J., Influences of Sample Processing on Low-Molecular-Weight Proteome Identified by Surface-Enhanced Laser Desorption/Ionization Mass Spectrometry, Clin Chem (2005).

Buergelt C.D., Hall C., McEntee K., Duncan J.R., Pathological evaluation of paratuberculosis in naturally infected cattle, Vet Pathol (1978) 15:196-207.

Christopher-Hennings J., Dammen M.A., Weeks S.R., Epperson W.B., Singh S.N., Steinlicht G.L., Fang Y., Skaare J.L., Larsen J.L., Payeur J.B., Nelson E.A., Comparison of two DNA extractions and nested PCR, real-time PCR, a new commercial PCR assay, and bacterial culture for detection of Mycobacterium avium subsp. paratuberculosis in bovine feces, J Vet Diagn Invest (2003) 15:87-93.

Cocito C., Gilot P., Coene M., de Kesel M., Poupart P., Vannuffel P., Paratuberculosis, Clin Microbiol Rev (1994) 7:328-345.

Cousins D.V., Whittington R., Marsh I., Masters A., Evans R.J., Kluver P., Mycobacteria distenct from Mycobacterium avium subsp. paratuberculosis isolated from the faeces of ruminants possess IS900-like sequences detectable IS900 polymerase chain reaction: implications for diagnosis, Mol Cell Probes (1999) 13:431-442.

Eamens G.J., Whittington R.J., Marsh I.B., Turner M.J., Saunders V., Kemsley P.D., Rayward D., Comparative sensitivity of various faecal culture methods and ELISA in dairy cattle herds with endemic Johne's disease, Vet Microbiol (2000) 77:357-367.

Hu J., Coombes K.R., Morris J.S., Baggerly K.A., The importance of experimental design in proteomic mass spectrometry experiments: some cautionary tales, Brief Funct Genomic Proteomic (2005) 3:322-331.

Khalifeh M.S., Stabel J.R., Effects of gamma interferon, interleukin-10, and transforming growth factor beta on the survival of Mycobacterium avium subsp. paratuberculosis in monocyte-derived macrophages from naturally infected cattle, Infect Immun (2004) 72:1974-1982.

Khare S., Ficht T.A., Santos R.L., Romano J., Ficht A.R., Zhang S., Grant I.R., Libal M., Hunter D., Adams L.G., Rapid and sensitive detection of Mycobacterium avium subsp. paratuberculosis in bovine milk and feces by a combination of immunomagnetic bead separation-conventional PCR and real-time PCR, J Clin Microbiol (2004) 42:1075-1081.

Kim S.G., Shin S.J., Jacobson R.H., Miller L.J., Harpending P.R., Stehman S.M., Rossiter C.A., Lein D.A., Development and application of quantitative polymerase chain reaction assay based on the ABI 7700 system (TaqMan) for detection and quantification of Mycobacterium avium subsp. paratuberculosis, J Vet Diagn Invest (2002) 14:126-131.

Koopmann J., Zhang Z., White N., Rosenzweig J., Fedarko N., Jagannath S., Canto M.I., Yeo C.J., Chan D.W., Goggins M., Serum diagnosis of pancreatic adenocarcinoma using surface-enhanced laser desorption and ionization mass spectrometry, Clin Cancer Res (2004) 10:860-868.

Luna L.G., Manual of histologic staining methods of the armed forces institute of pathology (Ed.^Eds.), McGraw-Hill Book Company, New York, N. Y., 1968, p.^pp.

Maindonald J., Braun J., Data analysis and graphics using R: an example based approach (Ed.^Eds.), Cambridge University Press, 2003, p.^pp.

Marshall J., Kupchak P., Zhu W., Yantha J., Vrees T., Furesz S., Jacks K., Smith C., Kireeva I., Zhang R., Takahashi M., Stanton E., Jackowski G., Processing of serum proteins underlies the mass spectral fingerprinting of myocardial infarction, J Proteome Res (2003) 2:361-372.

McCausland I.P., Apparent Johne's disease in a sheep, Aust Vet J (1980) 56:564.

Naser S.A., Felix J., Liping H., Romero C., Naser N., Walsh A., Safranek W., Occurrence of the IS900 gene in Mycobacterium avium complex derived from HIV patients, Mol Cell Probes (1999) 13:367-372.

O'Mahony J., Hill C., Rapid real-time PCR assay for detection and quantitation of Mycobacterium avium subsp. paratuberculosis DNA in artificially contaminated milk, Appl Environ Microbiol (2004) 70:4561-4568.

Perez V., Garcia Marin J.F., Badiola J.J., Description and classification of different types of lesion associated with natural paratuberculosis infection in sheep, J Comp Pathol (1996) 114:107-122.

Petricoin E.F., Ardekani A.M., Hitt B.A., Levine P.J., Fusaro V.A., Steinberg S.M., Mills G.B., Simone C., Fishman D.A., Kohn E.C., Liotta L.A., Use of proteomic patterns in serum to identify ovarian cancer, Lancet (2002) 359:572-577.

Petricoin E.F., Liotta L.A., SELDI-TOF-based serum proteomic pattern diagnostics for early detection of cancer, Curr Opin Biotechnol (2004) 15:24-30.

Poon T.C., Yip T.T., Chan A.T., Yip C., Yip V., Mok T.S., Lee C.C., Leung T.W., Ho S.K., Johnson P.J., Comprehensive proteomic profiling identifies serum proteomic signatures for detection of hepatocellular carcinoma and its subtypes, Clin Chem (2003) 49:752-760.

Poon T.C., Chan K.C., Ng P.C., Chiu R.W., Ang I.L., Tong Y.K., Ng E.K., Cheng F.W., Li A.M., Hon E.K., Fok T.F., Lo Y.M., Serial analysis of plasma proteomic signatures in pediatric patients with severe acute respiratory syndrome and correlation with viral load, Clin Chem (2004) 50:1452-1455.

Reichel M.P., Kittelberger R., Penrose M.E., Meynell R.M., Cousins D., Ellis T., Mutharia L.M., Sugden E.A., Johns A.H., de Lisle G.W., Comparison of serological tests and faecal culture for the detection of Mycobacterium avium subsp. paratuberculosis infection in cattle and analysis of the antigens involved, Vet Microbiol (1999) 66:135-150.

Rocken C., Ebert M.P., Roessner A., Proteomics in pathology, research and practice, Pathol Res Pract (2004) 200:69-82.

Seaman J.T., Gardner I.A., Dent C.H., Johne's disease in sheep, Aust Vet J (1981) 57:102-103.

Sergeant E.S., Marshall D.J., Eamens G.J., Kearns C., Whittington R.J., Evaluation of an absorbed ELISA and an agar-gel immuno-diffusion test for ovine paratuberculosis in sheep in Australia, Prev Vet Med (2003) 61:235-248.

Stabel J.R., Production of gamma-interferon by peripheral blood mononuclear cells: an important diagnostic tool for detection of subclinical paratuberculosis, J Vet Diagn Invest (1996) 8:345-350.

Stabel J.R., Cytokine secretion by peripheral blood mononuclear cells from cows infected with Mycobacterium paratuberculosis, Am J Vet Res (2000) 61:754-760.

Stabel J.R., Whitlock R.H., An evaluation of a modified interferon-gamma assay for the detection of paratuberculosis in dairy herds, Vet Immunol Immunopathol (2001) 79:69-81.

Stabel J.R., Bannantine J.P., Development of a nested PCR method targeting a unique multicopy element, ISMap02, for detection of Mycobacterium avium subsp. paratuberculosis in fecal samples, J Clin Microbiol (2005) 43:4744-4750.

Steinberg D., Colla P., CART: tree-structured non-parametric data analysis, In: (Ed.^Eds.), San Diego, Salford Systems, 1997, p.^pp.

Tanaka S., Sato M., Onitsuka T., Kamata H., Yokomizo Y., Inflammatory cytokine gene expression in different types of granulomatous lesions during asymptomatic stages of bovine paratuberculosis, Vet Pathol (2005) 42:579-588.

Whittington R.J., Marsh I., Turner M.J., McAllister S., Choy E., Eamens G.J., Marshall D.J., Ottaway S., Rapid detection of Mycobacterium paratuberculosis in clinical samples from ruminants and in spiked environmental samples by modified BACTEC 12B radiometric culture and direct confirmation by IS900 PCR, J Clin Microbiol (1998) 36:701-707.

Whittington R.J., Eamens G.J., Cousins D.V., Specificity of absorbed ELISA and agar gel immuno-diffusion tests for paratuberculosis in goats with observations about use of these tests in infected goats, Aust Vet J (2003) 81:71-75.

9.23 Appendix 4A-1 Subprogram 4 Culture of *Mycobacterium avium* subsp. *paratuberculosis* from blood samples

Introduction

Culture of pathogenic mycobacteria from blood is of increasing importance to human medicine due to the tendency for these pathogens to cause disease in HIV positive patients. While the growth requirements of *M. tuberculosis* and *M. avium* complex differ from *M. ptb*, sample processing and culture techniques for these pathogens may be adaptable for culture of *M. ptb*.

Culture using Bactec Myco/F lytic, Bactec 13 A, Bactec 12 B and BacT/Alert FA culture media has successfully grown both *M. tuberculosis* and *M. avium* complex from whole blood [1-6]. Concentrate from Isolator tubes (Wampole Laboratories, Cranbury, N.J., previously manufactured by Du Pont Co., Wilmington, Del.), which lyses leucocytes and erythrocytes and neutralize the bactericidal properties of blood, have been successfully inoculated onto a variety of solid and liquid media to isolate mycobacteria [4-9].

Bactec Myco/F lytic and MGIT systems both utilize fluorescence-based detection methods which fluoresce when oxygen levels in the media decrease in response to oxygen consumption during growth of the bacteria. Early testing of MGIT for growth of *M. ptb* has shown that supplementation of the media with egg yolk interferes with detection [10]. Further work has suggested that egg yolk can be used in this media (2005, colloquium) The MGIT media contains high concentrations of Vancomycin to reduce contamination with unwanted bacteria, however this is inhibitory to growth of the sheep strains present in Australia (Gumber and Whittington, 2006).

The Bactec TB 460 system, which measures radioactive CO_2 generation to detect growth, has successfully been used to culture ovine strains of *M. ptb* from faeces, tissues and milk using Bactec 12B media [11, 12]. The limitation of using Bactec 12B media for culture from blood is the small volume of sample that can be used for inoculation; 0.2mls was used in one study [5]. Bactec 12B media is suitable for inoculation with Isolator concentrate [5, 7]. However inhibition of growth of organisms by components of the Isolator tube has been demonstrated in liquid media.

The Bactec 13A media, which also uses the Bactec TB 460 radiometric detection system, is formulated specifically for the culture of mycobacteria directly from blood allowing larger volumes to be inoculated. However, it has not yet been tested for suitability for blood culture of animals infected with paratuberculosis.

Aims:

To develop a spiking method that resembles natural infection so that different methods of processing blood samples can be compared.

To compare different methods of processing blood samples for culture.

To develop a method of culturing blood samples which enables detection of mycobacteraemia in infected sheep.

Materials and Methods

Spiking blood with M. ptb

To determine the time required for uptake of the mycobacteria by the white blood cells 1 x 10^6 mycobacteria, enumerated using the MPN method, were added to 9mls of blood in a 50ml tube (Falcon, BD). Blood was incubated at 37ºC on a rotating mixer for 1 and 4 hours.

After 1 and 4 hours red cell lysis buffy coats were obtained. Viable cells were counted using Typan blue staining and heat fixed smears were stained using Diff Quick and ZN stains. This was repeated with using 3 blood tubes and including a zero hour control with no mycobacteria added.

Experiment 1

Various methods of processing blood prior to culture were compared using blood from an uninfected sheep with a known number of *M. ptb* added. These included: whole blood culture using the Bactec 13A media; whole blood lysis using the ISOLATOR 10® tube (Oxoid) and a 5% saponin lysis buffer; and white blood cell, or "buffy coat" preparations unprocessed, processed with a red cell lysis buffer and processed using Ficoll gradient centrifugation.

300ml blood in CPDA (Baxter) was collected from an uninfected sheep. Serial ten fold dilutions of bacterial suspension were prepared to give final concentrations of: 10^6, 10^5, 10^4 *M. ptb* /ml, enumerated using the MPN method. Telford sheep strain 2636-2 a pure clonal S strain of *M. ptb,* was used. 0.7ml bacterial suspension was inoculated into 70ml blood for each dilution, producing final concentrations of 10^4, 10^3 and 10^2 mycobacteria /ml of blood. One negative control was included (100ml blood with no mycobacteria added). The inoculated blood was then incubated at 37°C for 4 hrs on a rotary mixer (2 rev /min) in 50ml Falcon tubes. Each dilution was then subdivided into 10ml aliquots which were processed using the Isolator tube method, Lysis pellet method, red cell lysis buffy coat method, Ficoll buffy coat method, crude buffy coat method and Whole blood culture method.

Experiment 2

From the results seen in Experiment 1, it was decided that the Crude buffy coat method, and the whole blood in 13A media method be eliminated due to poor performance. The lysis pellet method was done only at the slower centrifugation speeds for ease of processing. The Isolator method was adapted to include a wash step. The Ficoll method was eliminated as the red cell lysis buffy coat method was found to be technically easier and performed marginally better.

The addition of mycobacteria was performed similarly to produce final concentrations of 10^2, 10 and 1 of mycobacteria /ml of blood. 120 ml aliquots were processed using the Isolator tube method, Lysis pellet method, red cell lysis buffy coat method and CB18 methods.

Experiment 3

Due to difficulty processing the CB 18 pellet and the inhibition experiment results, CB 18 was excluded from further experiments. The performance of red cell lysis buffy coat and the saponin lysis pellets were using 10mls of blood with 10^2, 10, 1 *M. ptb*/ml added.

Experiment 4

An experiment was conducted to examine any difference in growth between samples inoculated directly into Bactec 12B media, to those which were frozen at -80C prior to inoculation. The samples in this experiment were processed using the red cell lysis method.

Inhibition of Culture by CB 18, Blood and Processed samples

The delay in growth of some samples such as the crude buffy coat, indicated that some component of the blood or processed sample may be inhibitory to growth. The potentially inhibitory substance was added to a culture vial before adding 100 *M. ptb* enumerated using the MPN method. The samples tested were: 100ul, 300ul and 500ul of CB 18 pellet, 100ul, 300ul and 500ul of blood, a red cell lysis pellet, a saponin lysis pellet and for volume controls 100ul, 300ul and 500ul of MQW. Days to CGI 1000 were calculated to determine any inhibitory effect.

Animal Experiments

Samples were taken for culture from Animals Trials OJD 031.3, 4, 5, 6, B, E as previously described. 230 samples were processed using the red cell lysis method and culture in modified Bactec 12B media to evaluate the method on real samples.

Antibiotics and HPC decontamination

The effect of antibiotics and decontamination with HPC was examined on environmental contaminates and *M. ptb.*

Antimicrobial sensitivity was done using solid and liquid media on a number of contaminants. The effect of the antibiotics on the growth of *M. ptb* was assessed using a modified Bactec 12B media. The effect of HPC decontamination using 0.3%, and 0.75% for 6, 16, 24, and 72 hrs on *M. ptb* was assessed using modified 12B media.

Results

Spiking blood with *M .ptb*

There was no decrease in viable white blood cells obtained between 1 and 4 hour incubations (1.5×10^5 and 1.8×10^5 cells respectively) in the initial experiment and 0, 1 and 4 hour incubations (2.8×10^6, 6.2×10^6 and 3.0×10^6 cells respectively) in the repeat experiment. In both experiments the ZN staining showed a greater uptake of AFB after 4 hours incubation than 1 hour. However the cytoplasm was not clearly visible so it could not be determined if the AFB were intracellular, attached to the cell walls or extracellular. The mycobacteria were, however, closely associated with the cells. Based on these results in was decided that subsequent incubations be done for 4 hours.

Experiment 1

Growth of all isolates was confirmed as *M. ptb* by conventional IS*900* PCR and *Mse*1 REA on ethanol cleaned Bactec samples

Whole Blood

The two highest concentrations of *M.ptb* showed a substantial delay in growth, while the lowest concentration of *M. ptb* did not grow (Fig 1)

Lysis Pellets

The pellet that was produced in the fast lysis method was approximately 500 – 1000ul in size produced difficulties in inoculation, while the slow lysis method produced a pellet of approximately 200ul in size. The improved growth of the slow lysis method compared to the fast lysis method most likely reflects more efficient inoculation of the pellet.

The positive control at each number of *M. ptb* added grew faster than any of the processed samples indicating possible loss of bacteria during processing or carry over of inhibitory substances (Fig 1). However, as this data was not replicated there is no indication of variation of growth, and of processing.

Isolator ® Tube

Unwashed Isolator concentrate resulted in a substantial delay in growth particularly with the lower concentrations of *M. ptb*. This delay was reduced by washing the concentrate with PBS prior to inoculation (Fig 1).

Buffy Coats Preparations

Crude buffy coat preparations produced a delay in growth that was greatest in the lowest concentration of *M. ptb* added.

The red cell lysis and Ficoll buffy coats both resulted in a small delay in growth with a trend for slower growth with Ficoll buffy coats compared to red cell lysis buffy coats which tended to grow marginally slower than lysis pellets (Fig 1).

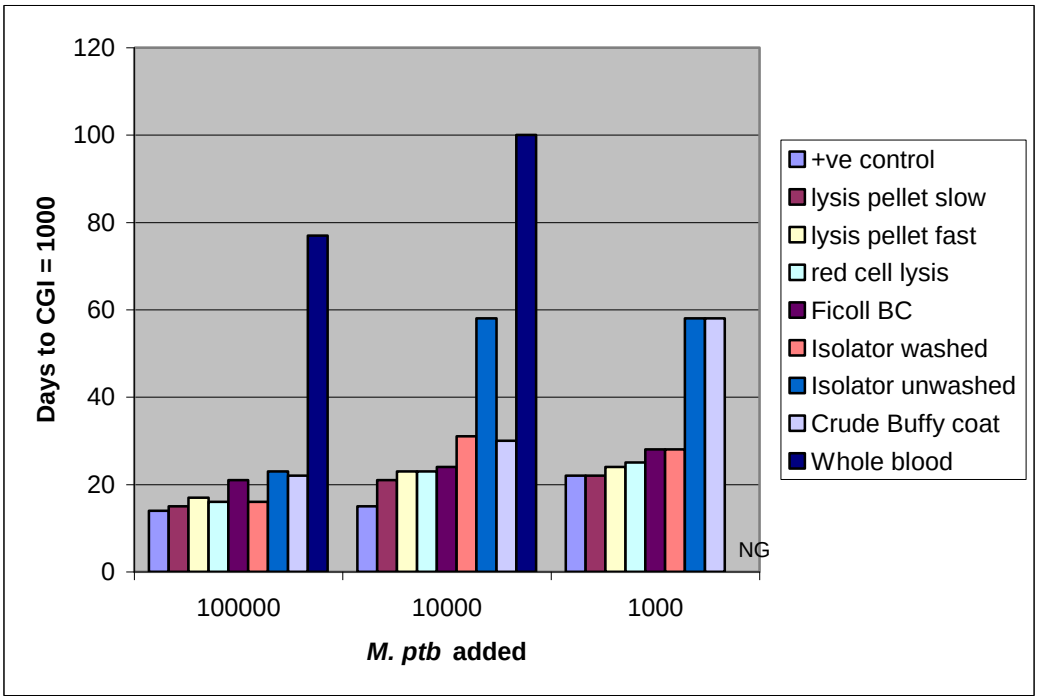

.

Figure 1. Comparison of methods for processing blood. Number of days to a cumulative growth index of 1000 using different numbers of *M. ptb* and processing methods. NG = no growth. An increase in the number of days to CGI =1000 indicates a less effective method. Unwashed Isolator concentrate, Crude buffy coat and whole blood showed a substantial delay in growth. The slow lysis pellet method tended to grow marginally quicker than the fast lysis pellet and red cell lysis pellet methods, which tended to grow marginally quicker than the Ficoll buffy coat method.

Experiment 2

The culture from the Isolator method with 100 Mycobacteria added was contaminated thus no result is shown. The red cell lysis and saponin lysis pellets showed comparable results at all concentrations (Fig 2). The Isolator and CB18 methods show a trend to delayed growth at all concentrations tested. This was greatest in the lowest concentration using the Isolator method with a delayed growth of 6 days compared to the red cell lysis and saponin lysis methods (Fig 2). Using the CB 18 method the delay was greatest in the two lowest concentrations, with a delayed growth of 11 and 9 days compared to the red cell and saponin lysis methods (Fig 2). The CB18 pellets were approximately 200 – 500ul in size which hampered inoculation and increases the risk of carry over of substances inhibitory to growth.

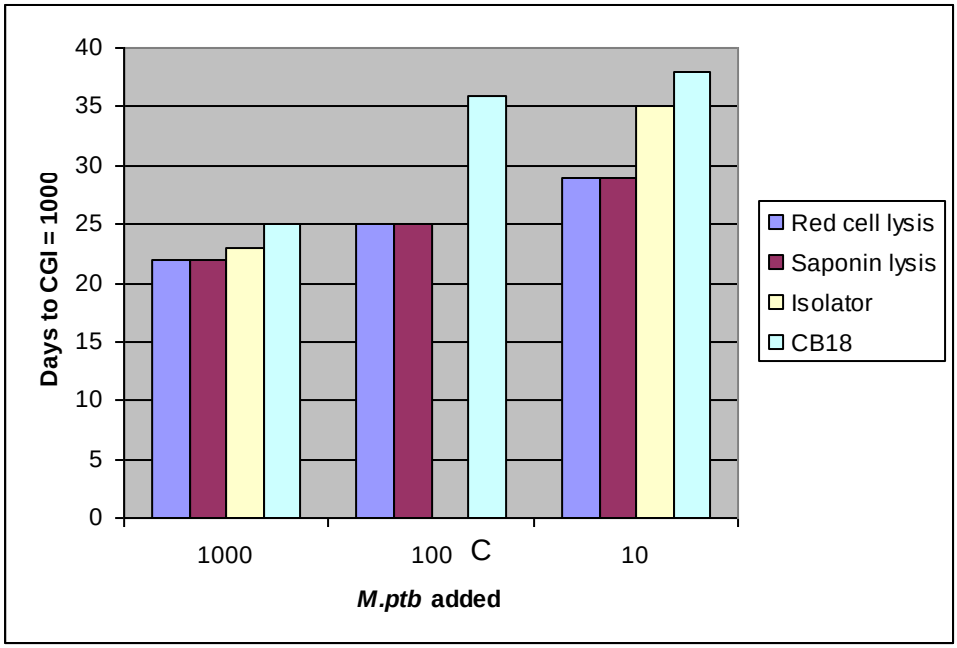

Figure 2. Further comparison of methods for processing blood. Number of days to a cumulative growth index of 1000 using different numbers of *M. ptb* and processing methods. An increase in the number of days to CGI =1000 indicates a less effective method. C = contaminated culture.

Experiment 3

The red cell lysis and saponin lysis methods performed similarly with a trend to decreased days to a cumulative growth index of 1000 using the red cell lysis method (Fig 3).

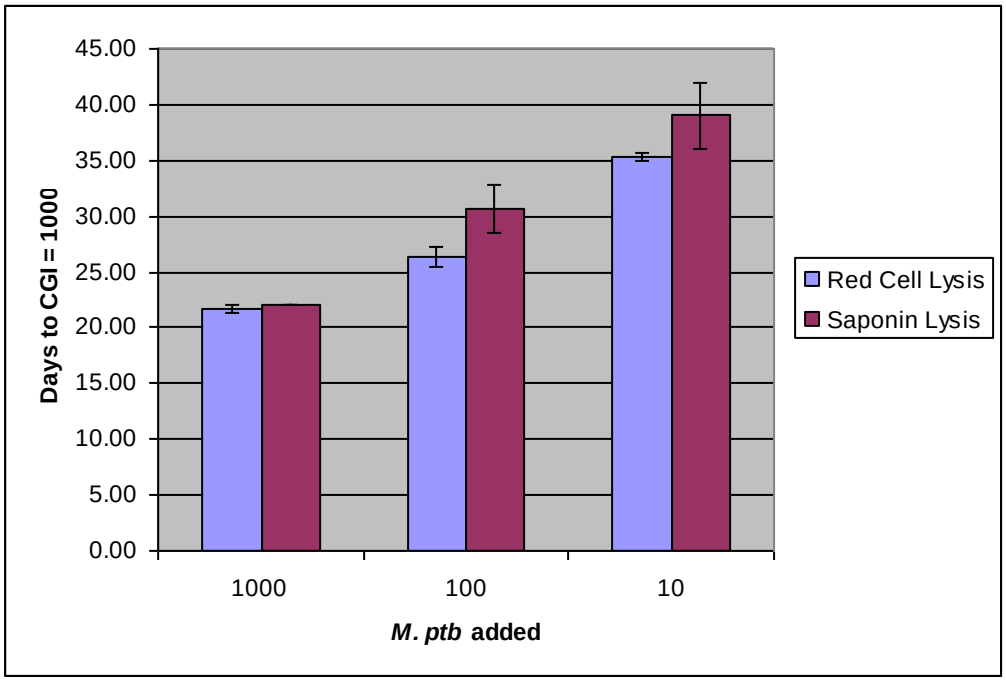

Figure 3. Further comparison of methods for processing blood. Number of days to a cumulative growth index of 1000 using different numbers of *M. ptb* and different processing methods. An increase in the number of days to CGI =1000 indicates a less effective method.

Experiment 4

There was a delay in growth of 2 days to CGI of 1000 with frozen samples compared to fresh with 1000 or 100 *M. ptb* added, however this was reversed with frozen samples reaching CGI of 1000 2 days faster with 10 *M. ptb* added (Fig 4). Therefore freezing the samples is unlikely to cause a decrease in detection as it does not appear to be detrimental at low numbers of organisms.

Figure 4. Effect of freezing and thawing. Number of days to a cumulative growth index of 1000 using different numbers of *M. ptb* and different processing methods. An increase in the number of days to CGI =1000 indicates a less effective method.

Inhibition of Culture by CB 18, Blood and Processed samples

Blood delayed growth at all volumes added. The CB 18 pellet delayed growth with 300ul added and there was no growth with 500ul of pellet added (Fig 5). Saponin and red cell lysis pellets caused a minimal delay in growth (1.3 and 0.3 days respectively, Fig 5) which is unlikely to prevent detection of the organism from a sample.

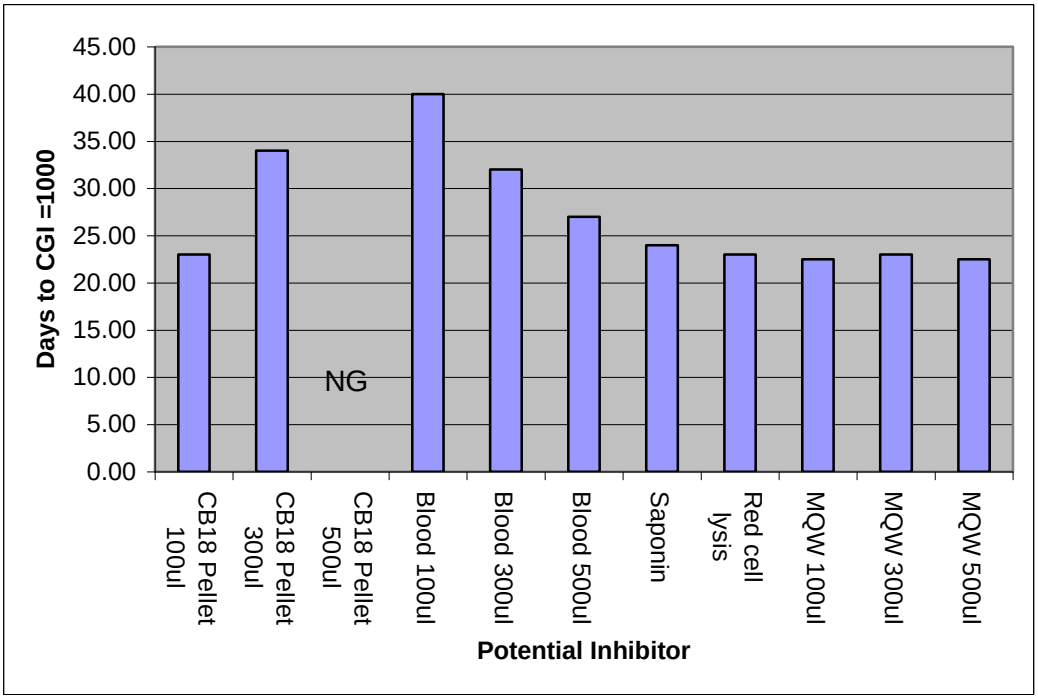

Figure 5. Effect of inhibitors. Number of days to a Cumulative Growth Index of 1000 of cultures with different potential inhibitors and 100 *M. ptb* added. NG = no growth. An increase number of days to CGI =1000 indicates a delay in growth due to the additive.

In further experiments blood and red blood cells resulted in a greater delay in growth than white blood cells or plasma (3.8,3.3, 1.5 and 0.7 days respectively).

Animal Experiments

1/30 late subclinically or clinically infected animals from 031.A or 031.E were blood culture positive. 11/12 of the IV infected animals from 031.B were culture positive. Of the 11 infected animals from 031.3, 2 were blood culture positive at their final bleed. 2/26 infected animals from 031.6 were blood culture positive on their final bleed. 12/230 culture were contaminated with a non specific contaminant, most likely due to environmental contamination of the skin prior to venipuncture.

Antibiotics and HPC decontamination

All contaminants tested were sensitive to Amoxicillan clavulanate, Tetracycline and Enrofloxacin in solid and liquid media. All antibiotics at all concentrations tested delayed or inhibited the growth of the S- strain of *M. ptb.*

0.3% and 0.75% HPC appears to cause a minimal delay in growth when low numbers of organisms are added.

Discussion

A method of artificially spiking blood has been shown to result in mycobacteria closely associated with white blood cells, thus resembling the hypothesised naturally infected blood, with mycobacteria

within phagocytic cells within the blood. Using this method different processing techniques have been compared with a known number of mycobacteria added initially.

The 13A media was discontinued by the manufacturer and we were unable to determine the cause of the poor results with this media. Further work conducted on inhibition of growth by blood and processed samples indicates that blood in a potent inhibitor of growth of *M. ptb* in Bactec 12B liquid media. The blood was also anticogulated with CPDA which may also have contributed to the inhibition. The carry over of blood and anticoagulant in the Crude buffy coats may have caused the inhibition of growth apparent in this method. The unwashed Isolator concentrate performed poorly which may have been due, in part, to the smaller proportion of the concentrate inoculated. However it is also likely that some of the inhibition is due to carry over of growth inhibitors from the processing of the samples as the 0.2ml washed concentrate performed better than its unwashed counterpart. Inhibition of culture may be due to carry over of the propylene glycol in the ISOLATOR10 ® tubes. Washing the concentrate appears necessary to remove growth inhibitors. The commercially available isolator method will be discarded due to poor performance at low concentrations of mycobacteria and due to the high cost of the blood tubes.

Saponin Lysis pellet and AMCO buffy coats performed well at all concentrations. However there is no data on the repeatability of these results. As both methods performed well with low numbers of *M. ptb* added, factors such as ease of processing, contamination rates and potential inhibition of growth must be considered when determining the optimal method.

There is a possibility that CB18 may help concentrate the mycobacteria at very low numbers of organisms; however due to the inhibitory nature of the pellet, it is unlikely to be effective in its current form.

The inhibition experiments showed that blood and red blood cells caused a delay in growth, thus the red cell lysis method was chosen for the animal trials as it effectively removed this inhibitor prior to culture.

Conclusion

A method for detecting viable organisms in blood of infected animals by culture has been developed and evaluated on 230 samples. A small number of infected animals appear to have bacteraemia detectable by this method. A method for reducing environmental contamination from field samples, while causing a minimal effect on *M. ptb,* has been developed.

References

Archibald, L.K., et al., Utility of paired BACTEC MYCO/F LYTIC blood culture vials for detection of bacteremia, mycobacteremia, and fungemia. J Clin Microbiol, 2001. **39**(5): p. 1960-2.

Esteban, J., et al., Usefulness of the BACTEC MYCO/F lytic system for detection of mycobacteremia in a clinical microbiology laboratory. J Microbiol Methods, 2000. **40**(1): p. 63-6.

Hanscheid, T., et al., Growth of *Mycobacterium tuberculosis* in conventional BacT/ALERT FA blood culture bottles allows reliable diagnosis of Mycobacteremia. J Clin Microbiol, 2005. **43**(2): p. 890-1.

Witebsky, F.G., et al., Comparison of BACTEC 13A medium and Du Pont isolator for detection of mycobacteremia. J Clin Microbiol, 1988. **26**(8): p. 1501-5.

Gill, V.J., et al., Use of lysis-centrifugation (isolator) and radiometric (BACTEC) blood culture systems for the detection of mycobacteremia. J Clin Microbiol, 1985. **22**(4): p. 543-6.

Archibald, L.K., et al., Comparison of BACTEC MYCO/F LYTIC and WAMPOLE ISOLATOR 10 (lysis-centrifugation) systems for detection of bacteremia, mycobacteremia, and fungemia in a developing country. J Clin Microbiol, 2000. **38**(8): p. 2994-7.

Kiehn, T.E. and R. Cammarata, Laboratory diagnosis of mycobacterial infections in patients with acquired immunodeficiency syndrome. J Clin Microbiol, 1986. **24**(5): p. 708-11.

Havlir, D., C.A. Kemper, and S.C. Deresinski, Reproducibility of lysis-centrifugation cultures for quantification of *Mycobacterium avium* complex bacteremia. J Clin Microbiol, 1993. **31**(7): p. 1794-8.

David, S.T., et al., Detecting mycobacteraemia for diagnosing tuberculosis. Indian J Med Res, 2004. **119**(6): p. 259-66.

Stitt, D.T., K.M. Sturm, and P.A. Hagemann. Preliminary methods for growing *Mycobacterium paratuberculosis* using the BBL MGIT Mycobateria Growth Indicator Tube. in *Fifth International Colloquium on Paratuberculosis*. 1996.

Whittington, R.J., et al., Evaluation of Modified BACTEC 12 B Radiometric Medium and Solid Media for Culture of *Mycobacterium avium* subsp. *paratuberculosis* from Sheep. J Clin Microbiol, 1999. **37**(4): p. 1077-1083.

Lambeth, C., et al., Intrauterine and transmammary transmission of *Mycobacterium avium* subsp *paratuberculosis* in sheep. Aust Vet J, 2004. **82**(8): p. 504-8.

9.24 Appendix 4A-2 Subprogram 4 Evaluation of the expression of surface receptors on cells

Introduction

Changes in the proportions of cells of specific phenotype (i.e. cell type and within type the kind of specific cell surface receptors) have been recorded at the site of infection in sheep with Johne's disease. Sheep with multibacillary lesions have been shown to have an increase in the proportion of macrophages while animals with paucibacillary lesions have an increase of CD-4 T cells (Clarke and Little, 1996; Clarke, 1997). *Mycobacterium avium* subspecies *paratuberculosis* (*M.ptb*) experimentally inoculated animals found to have survived the infection have an increased number of B cells within their intestinal lymph nodes (Begg and Griffin, 2005). Therefore changes in cell populations during infection may provide useful information regarding the immune response occurring within an infected animal and possibly provide a way of diagnosing diseased sheep. Furthermore, methods exist to concentrate specific types of cells, and if blood cells infected with *Mptb* could be concentrated, would enable more sensitive diagnosis from blood samples using methods such as culture. The aim of this study was to measure cell surface phenotype populations in peripheral blood to help determine if there are changes in response to infection with *M.ptb*. Any populations of cells that do change significantly during *M.ptb* infection may be of diagnostic potential.

Methods

Animals

All animals in these experiments were used with the approval of the University of Sydney Animal Care and Ethics Committee. The Merino sheep were maintained at pasture unless otherwise stated.

Experimentally infected sheep

Preparation of the Telford *Mycobacterium avium* subspecies *paratuberculosis* inoculum.

Myobacterium paratuberculosis strain Telford 9.2, a pure clonal culture at passage level 5 (including its primary isolation from sheep faeces) was reconstituted from lyophilised stock and inoculated into a BACTEC vial supplemented with egg yolk and mycobactin J (MJ) (Whittington et al., 1999). After culture in BACTEC to achieve maximal growth, the vial was subcultured to 7H10+MJ slopes and incubated for 4-6 weeks at 37^{o}C. Telford 9.2 is an IS1311 S strain, IS900 RFLP type S1 (Marsh et al., 2006; Marsh and Whittington, 2007).

The slopes were harvested into single cell suspensions prepared in PBS with 0.1% V/V Tween 80. Enumeration was conducted using a visual count in a Thoma-ruled counting chamber and by end point titration in BACTEC medium (using a standard three tube most probable number [MPN] method) (Reddacliff et al., 2003). The visual counts were used to prepare the inoculation doses at 10^9 *M.ptb* organisms/mL of undiluted suspension. One millilitre aliquots of this stock suspension was diluted in 10 mL of PBS for each of the animals to be infected as shown in Table 1.

The remaining undiluted suspension (stock) was retained at 4°C in order to repeat the inoculation one week later. Another MPN was set up on the day of the second dose from the stock suspension stored at 4^{o}C to confirm the viable dose after storage. IS*900* and IS*1311* PCR assays conducted on the stock solution were used to confirm that the infectious material was *M.ptb* S strain. A fresh suspension was prepared for further inoculation doses (typically one month later).

Preparation of gut homogenate inoculum.

Using the method of Begg et al 2005 (Begg et al., 2005), gut tissue from animal 986 (sourced from a farm in the Southern Tablelands of NSW, Australia) with multibacillary lesions, shown to be infected by culture and *IS*900 PCR with the ovine strain confirmed by *IS*1311 PCR was stored at -80^{o}C until required. The tissue was defrosted and homogenized using a mortar and pestle in an equal volume of sterile distilled water. The homogenate was filtered through a funnel lined with 2 layers of sterile gauze followed by a 70um cell strainer. The sample was homogenized by vortexing for 30 minutes and passed through a 26 gauge needle 2 times. The number of *M.ptb* cells was enumerated to calculate the number of organisms/mL. This was done using direct visual counts using 4 uL of a 10^{-3} dilution of the homogenate smeared onto 5mm x 5mm square grid which was divided into equal quarters, the smears were then ZN stained and the acid fast bacilli were counted. A BACTEC MPN was also carried out on the sample. The sample was then frozen at -80^{o}C. The MPN showed the gut homogenate (total volume 54mL) to be at $2.3x10^{8}$ CFU/mL with direct visual count showing $3.67x10^{8}$ bacteria per mL. On the day prior to the first inoculation the homogenate was thawed diluted with 11mL of PBS giving a total volume of 65mL at $1.9x10^{8}$CFU/mL. One in ten dilutions of the homogenate was spread onto TSA plates to enumerate the amount of contaminating bacteria in the sample. The plates were incubated at 37^{o}C for 3 days. Fewer than 1000 CFU/mL of contaminating bacteria were observed. Twenty two millilitres was then frozen at -80^{o}C to be held as the 3rd and final inoculation a further 22mLs was stored for one week at 4^{o}C for the second inoculation. The remaining 21 mLs of suspension were put into 1mL aliquots and were mixed with 9mL of PBS for the first challenge dose and the animals were inoculated as shown in Table 1. The same procedure was done with the stored doses, either refrigerated or frozen stocks, when required.

Table 1: Experimental inoculations of sheep

Trial	Sheep breed	Age of animals at challenge	No of sheep	Strain of *M.ptb*	First dose	Second dose	Third dose
031.6	Merino	4 months	20	Telford 9.2	9.3×10^{7}	9.3×10^{7}	1.5×10^{8}
031.6	Merino	4 months	20	Gut isolate	1.9×10^{8}	9.3×10^{7}	9.3×10^{7}
031.6	Merino	4 months	20	None given			

Naturally exposed or Johne's disease free sheep

Animals were selected from farms in NSW, Australia on which ovine Johne's disease had been previously identified. The diseased animals were transported to the University of Sydney OJD quarantine shed and held for 2 weeks prior to necropsy. The animals were fed lucerne chaff and grain once daily with water supplied *ad libitum.* Sheep from the OJD free property remained on farm until the day of the necropsy due to their close proximity. A blood sample was taken from each animal prior to being necropsied.

Necropsy: All animals were euthanased using an intravenous injection of barbiturate into the jugular vein. The intestines from the duodenum to the rectum were removed from the animal and placed in a clean tray. The trays were cleaned with warm water and a virucidal disinfectant, Trigene 2 (Medichem International, UK). Samples were then taken from the following sections of the small intestine terminal ileum, posterior jejunum, mid distal jejunum, middle jejunum, mid proximal jejunum and anterior jejunum and ileocecal lymph node. The ileocaecal lymph node and jejunal lymph nodes corresponding to the sections of jejunum sampled were also collected.

Isolation of *M. paratuberculosis* from faeces and tissue: Samples collected from animals were frozen at -80^{o}C until they were processed. Faecal samples and tissue samples were processed for BACTEC culture as described previously (Whittington et al., 1999). Briefly after decontamination samples were inoculated into Bactec Vials and cultured for 12 weeks at 37^{o}C. After culture any positive samples were confirmed by PCR and REA as previously described (Whittington et al., 1998a; Whittington et al., 1998b).

Isolation of white blood cells for FACS analysis

Hepranised whole blood was centrifuged at 1455 x g for 20 minutes to obtain buffy coats. These were lysed in 5ml AMCO red blood cell lysis buffer (0.83% NH_4Cl in 0.1% $KHCO_3$ –0.01M EDTA**)** for 5 minutes at room temperature. The Addition of 5ml of FACS buffer (0.1%azide, 1.0% Bovine serum in PBS) occurred before centrifugation at 233 x g for 5 minutes. The resultant cell pellet was resuspended in 5ml of FACS buffer and centrifuged at 233 x g for 5 minutes Washed again in 5 ml of FACS buffer and resuspended in 2ml of FACS buffer. Cells were counted and adjusted to 4 x 10^{6}cells/mL by addition of FACS buffer.

Isolation and culture of ovine monocytes for FACS analysis

For each experiment, blood was collected into EDTA blood tubes. The monocyte-rich fraction of the blood was separated through an OptiPrep (Nycomed Pharma, Oslo, Norway) density gradient, as described by Berger & Griffin 2006 (Berger and Griffin, 2006). The Monocytes were harvested, washed once with PBS and resuspend in 2 mL pre-warmed Macrophage Culture Medium. The cells were enumerated using trypan blue and resuspended at 1x106 cells/mL. The cells were placed in a flask and incubated for 1 hr at 37oC in 5% CO2. The culture medium was then discarded and the flask rinsed with RPMI. Macrophage Culture Medium was added again containing 10% autologous serum + 1 ng/mL rhMCSF. Adherent cells were left to proliferate for 1 week, with changes of the media every 3-4 days.

FACS staining method

Staining was carried out in 96 well round bottom plates at room temperature. All antibodies were diluted in FACS buffer. 50µL of FACS buffer or antibody was added to the wells at the appropriate concentrations;.CD4(17D) 0.5 µg/ml, CD5(CC17) 1.0 µg/ml, CD6(CC38) 40µg/ml, CD8$\alpha\alpha$ (CC63) 0.2 µg/ml , CD8$\alpha\beta$ (CC58) 0.25 µg/ml, CD11a (F10-150) 10 µg/ml, CD45R (CC76) 1/1000 of 20 x tissue culture supernatant, $\gamma\delta$TCR(86D) 1/16 of tissue culture supernatant, $\gamma\delta$TCR(WC1) 0.25µg/ml, WC4 200 µg/ml and CD14-FITC (TUK4) (Miltenyi) 1/15. 50µL of cells were added and left to incubate in the dark for 10 minutes. To remove unbound antibodies 100µL of FACS buffer was added to all wells and the plates were centrifuged for 3 minutes at 233 x g. The supernatants were flicked off and the cells were resuspended by vortexing. A further150µL of FACS buffer was then added and the process repeated. 50µL of FACS buffer (CD14 FITC wells) or 50µL of Donkey anti-mouse IgG FITC (Jackson Immunochemicals) at 1/175 as a secondary was added to the cells stained with unlabelled antibodies and incubated for 10 minutes in the dark. Unbound antibody was removed as described earlier. 150µL of 1% paraformaldehyde in PBS was added to each well and plates were left at 4^{o}C before reading on a FACSCalibur HTS (Becton & Dickinson). The results were analysed using Cellquest pro.

Results

The proportion of cells in each of the phenotypes did not change significantly regardless of whether a sheep was challenged with *M.ptb* or left un-inoculated (Figure 1). A spike in the number of CD-14 cells was observed in the unchallenged control group at 8 months post infection, although this

dropped back to the levels of the gut homogenate and Telford inoculated groups at necropsy (Figure 1). In some cell populations such as CD-8aa, the control group of animals had an increased number of cells, although this was consistent across the entire sampling period. Other cell phenotypes such as CD11a had a varied response over time from the different treatment groups, although it is difficult to attribute this to a challenge treatment as the responses were not consistent.

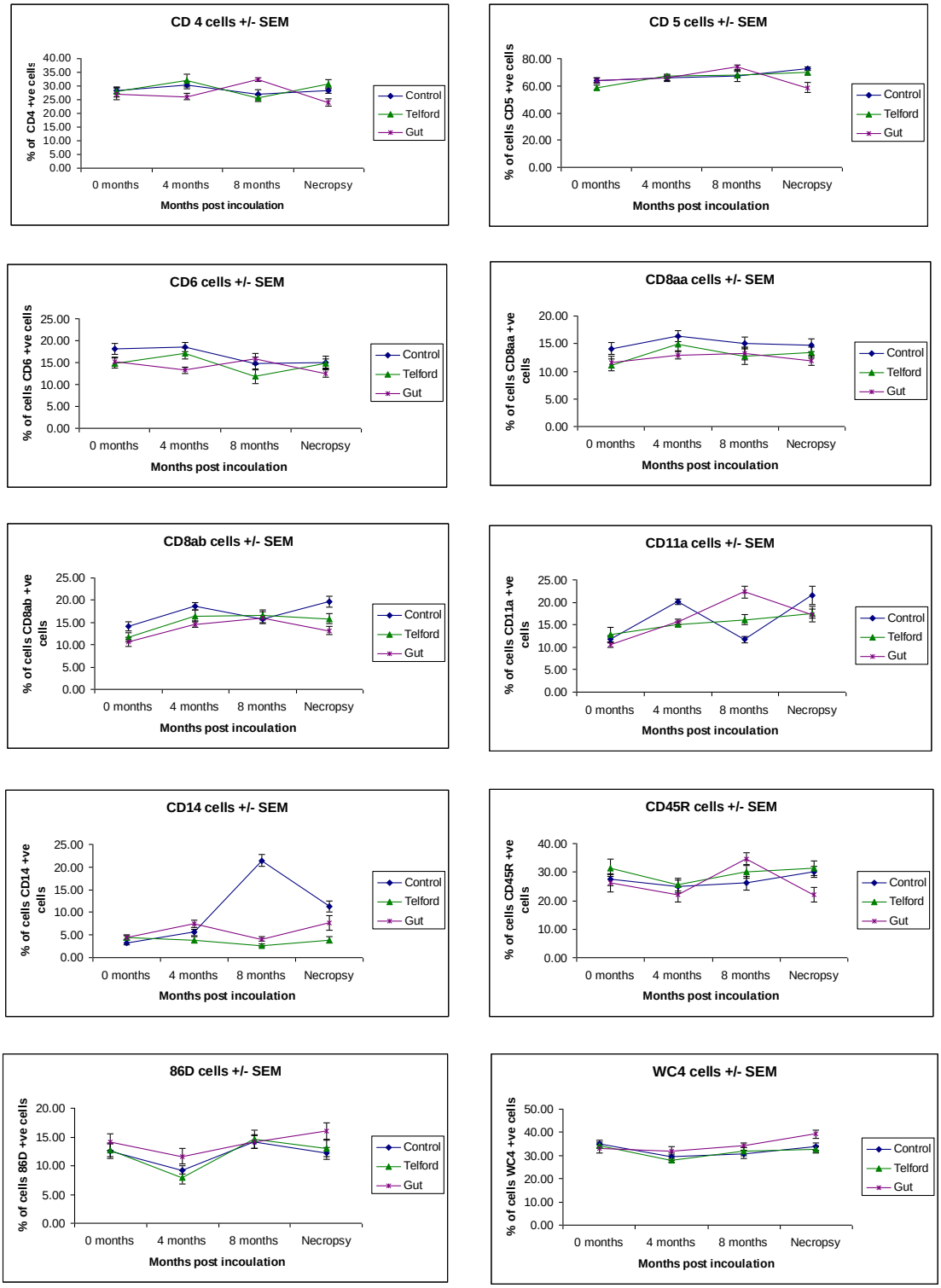

Figure 1: The proportion of different cell phenotypes as measured by FACS analysis in white blood cells from experimentally infected sheep in trial 031.6. The sheep were either unexposed, challenged with a gut homogenate or Telford 9.2 pure clonal strains of *M.ptb*. The data are the mean response +/- standard error.

Initial investigations into the cell surface maker CD-6 in naturally infected animals identified a difference in expression between diseased and uninfected sheep (Figure 2). To further investigate this observation, expression of CD6 was assessed in other sheep with and without Johne's disease, both experimentally infected (Figure 3) and naturally infected. The experimentally infected sheep showed no differences in CD6 expression between infected or uninfected animals (Figure 3). Later examination of more naturally infected sheep showed a greater variation than seen in the initial studies.

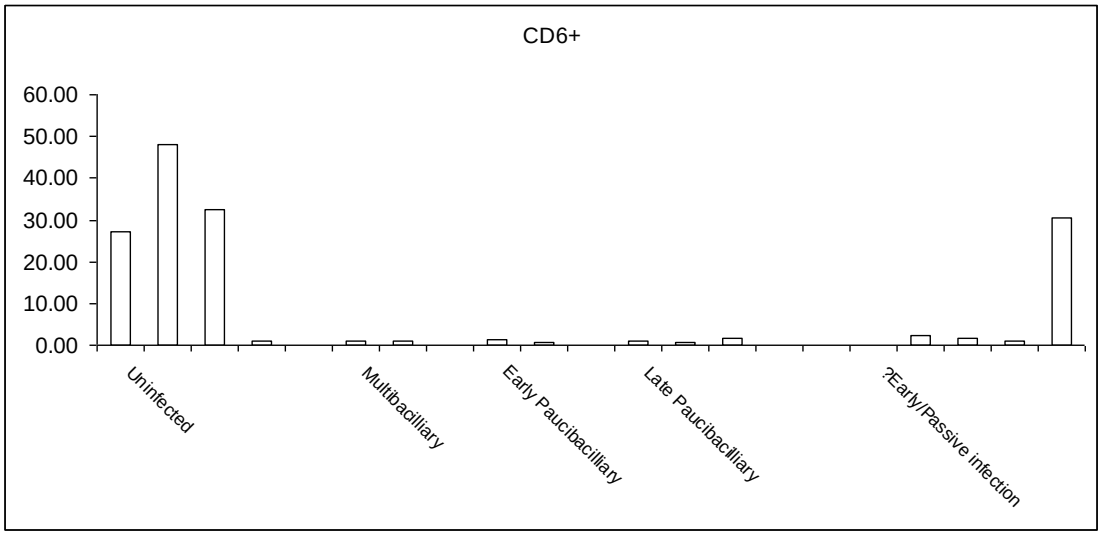

Figure 2. CD6 expression on lymphocytes in animals with and without Johne's disease acquired naturally. Expression of CD6 was determined by flow cytometric analysis.

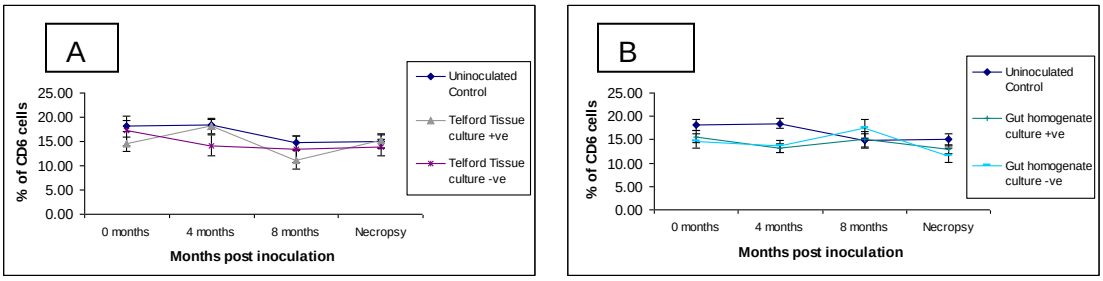

Figure 3. Average CD6 expression on lymphocytes in experimentally inoculated animals with and without *M.ptb* infection in trial 031.6. A: sheep infected with Telford 9.2 pure clonal strain of *M.ptb*. B: sheep infected with gut homogenate *M.ptb* strain. Data are mean and standard error.

The phenotype of ovine monocytes was also examined. Cell markers such as CD14 and CD11a were high as would be expected (Figure 4). Unfortunately this analysis could only be done on uninfected cell populations as not enough cells could be isolated from a single sheep at one time to enable a comparison to be done between *M.ptb* infected and uninfected cells.

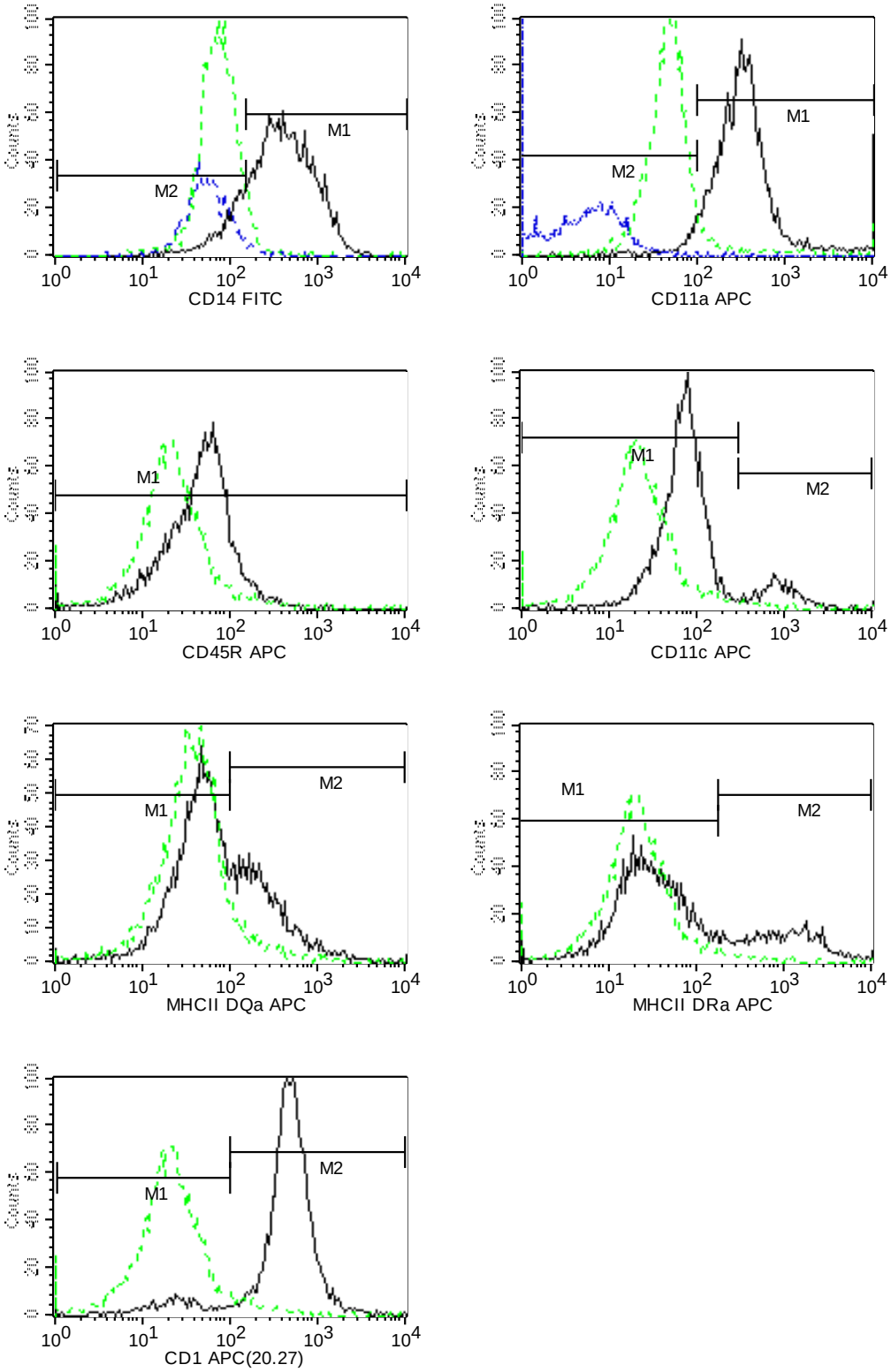

Figure 4. FACS analysis of the different phenotypes from uninfected monocytes. The Y axis shows the number of cells counted while the X axis shows the fluorescent intensity for the different phenotypes and the fluorochrome used. The solid black line shows macrophages stained with the different phenotypic markers. The dotted green line (or light grey if seen in black and white) shows the negative fluorchrome control stained monocytes. The blue dotted line (Black if seen in back and white) represents unstained cells.

Discussion

Very few differences could be seen in the proportion of cells with specific phenotypes in OJD infected and uninfected sheep in this study. While there were individual time points where there were some differences, there was no consistent pattern that would allow for the identification of infected animals. The cell surface maker CD-6 initially looked promising as an indicator of susceptibility to infection in a group of naturally infected sheep although later experimental work on both experimentally and naturally infected sheep showed that this phenotypic maker could not be used to determine the infection status.

While this was a reasonably detailed investigation, a lack of antibody reagents specific for sheep meant that not all of the known mammalian cell surface markers could be examined. It is also possible that several different phenotypic markers may need to be examined on a cell at one time to determine the infection status of a sheep. Other variables that could be examined concurrently include cytokines and ability of the cells to proliferate in response to *M.ptb* antigens.

The difficulty in isolating large numbers of purified monocytes from peripheral blood of sheep has severely hampered in-depth examination of changes in the phenotype of monocytes and macrophages after infection of these cells with *M.ptb*. These studies may be easier in cattle where larger numbers of cells are present, and larger volumes of blood can be collected without harming the animal.

References

Begg, D. J. and Griffin, J. F. 2005. Vaccination of sheep against M. paratuberculosis: immune parameters and protective efficacy. Vaccine.

Begg, D. J., O'Brien, R., Mackintosh, C. G. and Griffin, J. F. 2005. Experimental Infection Model for Johne's Disease in Sheep. Infection and Immunity 73, 5603-11.

Berger, S. T. and Griffin, F. T. 2006. A comparison of ovine monocyte-derived macrophage function following infection with Mycobacterium avium ssp. avium and Mycobacterium avium ssp. paratuberculosis. Immunol Cell Biol.

Clarke, C. J. 1997. The pathology and pathogenesis of paratuberculosis in ruminants and other species. Journal of Comparative Pathology 116, 217-61.

Clarke, C. J. and Little, D. 1996. The pathology of ovine paratuberculosis: gross and histological changes in the intestine and other tissues. Journal of Comparative Pathology 114, 419-37.

Marsh, I. B., Bannantine, J. P., Paustian, M. L., Tizard, M. L., Kapur, V. and Whittington, R. J. 2006. Genomic comparison of Mycobacterium avium subsp. paratuberculosis sheep and cattle strains by microarray hybridization. J Bacteriol 188, 2290-3.

Marsh, I. B. and Whittington, R. J. 2007. Genomic diversity in Mycobacterium avium: single nucleotide polymorphisms between the S and C strains of M. avium subsp. paratuberculosis and with M. a. avium. Mol Cell Probes 21, 66-75.

Reddacliff, L. A., Nicholls, P. J., Vadali, A. and Whittington, R. J. 2003. Use of Growth Indices from Radiometric Culture for Quantification of Sheep Strains of Mycobacterium avium subsp. paratuberculosis. Applied and Environmental Microbiology 69, 3510-6.

Whittington, R., Marsh, I., Choy, E. and Cousins, D. 1998a. Polymorphisms in IS1311, an insertion sequence common to Mycobacterium avium and M. avium subsp. paratuberculosis, can be used to distinguish between and within these species. Mol Cell Probes 12, 349-58.

Whittington, R. J., Marsh, I., McAllister, S., Turner, M. J., Marshall, D. J. and Fraser, C. A. 1999. Evaluation of modified BACTEC 12B radiometric medium and solid media for culture of

Mycobacterium avium subsp. paratuberculosis from sheep. Journal of Clinical Microbiology 37, 1077-83.

Whittington, R. J., Marsh, I., Turner, M. J., McAllister, S., Choy, E., Eamens, G. J., Marshall, D. J. and Ottaway, S. 1998b. Rapid detection of Mycobacterium paratuberculosis in clinical samples from ruminants and in spiked environmental samples by modified BACTEC 12B radiometric culture and direct confirmation by IS900 PCR. J Clin Microbiol 36, 701-7.

9.25 Appendix 4B-1 Subprogram 4 Migration of sheep white blood cells *in vitro* and *in vivo*

Introduction

It is known that *Mycobacterium avium* subspecies *paratuberculosis* (*M.ptb*) move from the gut to extra intestinal tissues such as the mammary gland (Koenig et al., 1993; Lambeth et al., 2004), foetal tissue, (Lambeth et al., 2004), spleen (Ayele et al., 2004), liver (Gwozdz et al., 1997; Gwozdz et al., 2000; Barrington et al., 2003) and lymph nodes not associated with the gut (Koenig et al., 1993; Ayele et al., 2004; Lambeth et al., 2004), and blood (Koenig et al., 1993; Gwozdz et al., 1997; Gwozdz et al., 2000; Barrington et al., 2003; Buergelt and Williams, 2004; Juste et al., 2005) and milk (Barrington et al., 2003; Buergelt and Williams, 2004; Lambeth et al., 2004). The movement of *M.ptb* to these areas is thought to be via macrophages. Tracking of the white blood cells possibly carrying *M.ptb* around the body may provide an alternative method to diagnose the infection. To do this an improved understanding of sheep macrophages and other white blood cells and their migration is required. It was decided to determine if sheep white blood cells migrate after infection with *M.ptb in vivo,* to determine where in the body *M.ptb* traffic to when injected intravenously (IV) and to determine if *M.ptb* infected PBMCs will take the bacteria to different places in the body compared to IV injected *M.ptb*. We also attempted to deduce if it is possible to track the movement of PBMCs labelled with CFSE in the body of a sheep.

Methods

Animals

All animals in these experiments were used with the approval of the University of Sydney Animal Care and Ethics Committee. The Merino sheep for the cell migration *in vivo* experiment were maintained in pens. The animals were feed lucerne chaff and grain once daily with water supplied *ad libitum.* The sheep for the *in vitro* cell migration experiment were maintained at pasture.

Preparation of the Telford *Mycobacterium avium* subspecies *paratuberculosis* inoculum

Myobacterium paratuberculosis strain Telford 9.2, a pure clonal culture at passage level 5 (including its primary isolation from sheep faeces) was reconstituted from lyophilised stock and inoculated into a BACTEC vial supplemented with egg yolk and mycobactin J (MJ) (Whittington et al., 1999). After culture in BACTEC to achieve maximal growth, the vial was subcultured to 7H10+MJ (Company) slopes and incubated for 4-6 weeks at 37^{o}C. Telford 9.2 is an IS1311 S strain, IS900 RFLP type S1 (Marsh et al., 2006; Marsh and Whittington, 2007).

The slopes were harvested into single cell suspensions prepared in PBS with 0.1% V/V Tween 80. Enumeration was conducted using a visual count in a Thoma-ruled counting chamber and by end point titration in BACTEC medium (using a standard three tube most probable number [MPN] method) (Reddacliff et al., 2003). The visual counts were used to prepare the inoculation doses at 10^{9} *M.ptb* organisms/mL of undiluted suspension. One millilitre aliquots of this stock suspension were made and the suspensions were frozen at -80^{o}C until required.

Cell migration *in vitro*

Vaccinated sheep

Sheep No W1 0596 had been vaccinated with a dose of Gudair® vaccine (1 mL) subcutaneously to the anterior part of the neck as instructed by the manufacturer.

Stimulation of the blood samples

Heparinized blood was collected from animal W1 0596. 0.5 mL of heparinised blood was placed into wells and stimulated with 0.5 mL of *M.ptb* 316v antigen at 20µg/mL. A negative control consisted of the blood having 0.5 mL of media added while the positive control had 0.5 mL PWM added at 10ug/mL. There were 12 replicates for each of the different stimulations. After 48 hours of culture at 37^{o}C with 5% CO_2 the plasma supernatant was collected and stored at -20^{o}C until required.

Heparinized blood was collected from animal W1 0596 and centrifuged at 1,455 x *g* for 20 min. The buffy coat of white blood cells was removed and layered on to 2 mL of ficoll paque (GE Healthcare, Sweden δ = 1.077) and centrifuged at 754 x *g* for 30 minutes with no brake. The cloudy layer of white blood cells was removed and washed twice by centrifugation in 10 ml of phosphate buffered saline (PBS). The cells were resuspended in 5 ml of 10% fetal calf serum (Gibco BRL, Grand Island, NY) made up in RPMI 1640 (Gibco BRL) supplemented with L-glutamine and penicillin/streptomycin (Gibco BRL) (complete media). The cells were enumerated using trypan blue and suspended at 2.5 x 10^6 viable cells/mL

The white blood cells were divided into 2 lots of 8mL. Into lot one *M.ptb* were added at a multiplicity of infection of 10:1. In lot two PBS was added at an equal volume to that of the *M.ptb* added in lot one.

The two tubes containing the *M.ptb* infected white blood cells and non infected white blood cells were placed into a 37^{0}C incubator and rotated for 4 hours.

After the incubation the cells were washed twice by centrifugation in 10 ml of phosphate buffered saline (PBS). The cells were enumerated using trypan blue and suspended at 2 x 10^6 viable cells/mL

At this time the white blood cells and stored plasma supernatant were used in a CytoSelect 24 well cell migration assay (Cell Biolabs INC). Following the instructions of the kit, in the lower chamber one of following stored plasma samples was placed into the well as required; serum free RPMI 1640 (Gibco BRL) supplemented with L-glutamine and penicillin/streptomycin (Gibco BRL) (incomplete media); sheep plasma from W1 0596 stimulated with media (unstimulated) made to 10% with incomplete media; sheep plasma from W1 0596 stimulated with *M.ptb* antigen made to 10% with incomplete media; or 10% Fetal calf serum (complete media). In the upper chambers the white blood cells isolated from W1 0596 either infected with *M.ptb* or uninfected cells were used.

The cells and the media were allowed to incubate for 21 hours at 37^{o}C with 5% CO_2. After which time the cells that moved from the upper chamber to the lower (migrating cells) were measured following the manufacture's instructions. Briefly the cells from the upper chamber were discarded. The cells attached to the underside of the upper chamber and in the lower chamber were lysed and then stained with CyQuant GR dye solution. After a 20 minute incubation the fluorescence reaction was measured at an excitation and emission wavelengths of 492nm/516nm in a Stratagene MX3000p QPCR machine.

Cell migration *in vivo*

Five Merino ewes were sourced from an OJD MAP MN3 property in the New England Rural Lands Protection Board. The ewes had been used as breeding animals on the Camden farms for the

previous year and were known to be free of *M.ptb* by ELISA and faecal culture. The animals were 3 - 4 years of age. 200mL of heparinised blood was collected from each of three sheep and was centrifuged at 1,455 x *g* for 20 min. The buffy coat of white blood cells was removed and layered on to 2x 10 mL of ficoll paque (GE Healthcare, Sweden δ = 1.077) and centrifuged at 754 x *g* for 30 minutes with no brake. The cloudy layer of white blood cells was removed and washed twice by centrifugation in 30 ml of phosphate buffered saline (PBS). The cells were resuspended in 10 mL of PBS. The cells were enumerated using trypan blue. The white blood cells from the sheep were stained with CFSE for 5 minutes, then were washed 2 times in PBS supplemented with 5% Fetal Calf Serum. The cells were resuspended at $5x10^6$ cells per mL into 28mLs of complete RPMI media. (Giving a total cell count of $1.4x10^8$ cells).

The cells from two of the sheep 1mL of *M.ptb* at $1x10^{10}$ CFU/mL were added while the cells from the third animal received 1 mL of PBS. The tubes containing the *M.ptb* infected white blood cells and non infected white blood cells were placed into a 37^0C rotatory incubator for 6 hours. The cells were then washed 3 times in 30mL of PBS and then resuspended in 10mL of PBS and put into a 10mL syringe. The cells were then injected back into the same animal from which they were taken using an 18 gauge needle via the jugular vein. The remaining 2 animals from which no blood was taken were injected IV via the jugular vein with 1 x 10^{10} CFU *M.ptb* in PBS. Over the following 2 days 30 mL blood samples were taken for culture of the *M.ptb* and FACS analysis of the blood to detect the CFSE stained cells.

Necropsy

On the third day all animals were euthanased using an intravenous injection of barbiturate into the jugular vein. The intestines from the duodenum to the rectum were removed from the animal and placed in a clean tray. The trays were cleaned with warm water and a virucidal disinfectant, Trigene 2 (Medichem International, UK) Samples were taken from the prescapular lymph node, muscle, mammary tissue, pre femorals (suprmammary ln) popliteals, hepatic, mediastinal, heart , lung, liver, spleen, anterior and posterior jejunal lymph nodes, ileocaecal lymph node, anterior and posterior jejunum, ileocaecal valve and a faecal sample. All samples were processed for tissue culture and histology while sections of the lymph nodes were used for FACS analysis by maceration using a scalpel blade and forceps, the cells were washed in PBS then analysed in the FACS machine.

Isolation of *M. paratuberculosis* from faeces and tissue

Samples collected from animals were frozen at -80^{o}C until they were processed. Faecal samples and tissue samples were processed for BACTEC culture as described previously (Whittington et al., 1999). Briefly after decontamination samples were inoculated into Bactec Vials and cultured for 12 weeks at 37^{o}C. After culture any positive samples were confirmed by PCR and REA as previously described (Whittington et al., 1998a; Whittington et al., 1998b).

Isolation of *M. paratuberculosis* from blood

Heparinised blood was collected daily from each sheep and centrifuged at 1,455 x *g* for 20 min. The buffy coat of white blood cells was transferred to a red blood cell lysis buffer for 5 mins. 5mls of PBS was added to stop the reaction and the white blood cells pelleted by centrifugation at 233 x g for 10 mins. The resultant pellet was washed with 1 ml PBS before storage at -80ºC prior to culture in a modified BACTEC 12B medium described previously for faecal and tissue culture (Whittington et al., 1998b).

FACS analysis of CFSE stained cells

Heparinised whole blood was centrifuged at 1455 x g for 20 minutes to obtain buffy coats. These were lysed in 5ml AMCO red blood cell lysis buffer (0.83% NH_4Cl in 0.1% $KHCO_3$ –0.01M EDTA**)** for 5 minutes at room temperature. The addition of 5ml of FACS buffer (0.1%azide, 1.0% Bovine serum in PBS) occurred before centrifugation at 233 x g for 5 minutes. The resultant cell pellet was resuspended in 5ml of FACS buffer and centrifuged at 233 x g for 5 minutes Washed again in 5 ml of FACS buffer and resuspended in 2ml of FACS buffer. The lymph nodes were macerated using a scalpel blade and forceps and passed through a 70µm cell strainer. The cells were washed in PBS and resuspended in 2mL of FACS buffer. Blood and lymph node cells were counted and adjusted to 4 x 10^6cells/mL by addition of FACS buffer. The cells were then spun down resuspended in 1% paraformaldehyde in PBS and read on a FACSCalibur HTS (Becton & Dickinson). The results were analysed using Cellquest pro.

Results

Cell migration *in vitro*

The *in vitro* cell migration experiment showed that fetal calf serum inhibited migration of cells uninfected with *M.ptb*. When *M.ptb* was present in the cells the migration of the cells was unaffected. Infection of the white blood cells with *M.ptb* or using sheep plasma either stimulated with *M.ptb* or unstimulated did not increased the amount of migration over that of uninfected cells drawn towards serum free media (Figure 1).

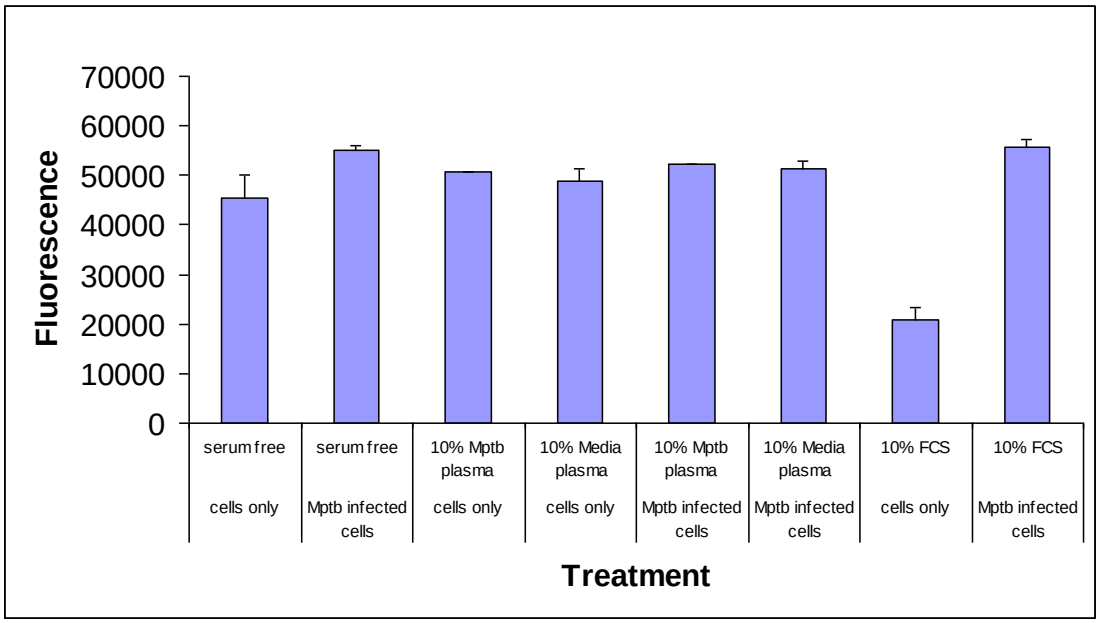

Figure 1: In vitro sheep white blood cell migration. The amount of white blood cells from a vaccinated sheep either uninfected (cells only) or infected with *M.ptb* were measured moving towards different stimuli which included serum free media (a control), 10% Mtpb serum (blood stimulated with *M.ptb* with the plasma collected and diluted to 10%), 10% RPMI serum (blood stimulated with media with the plasma collected and diluted to 10%), and 10% fetal calf serum (FCS). The amount of fluorescence on the Y axis corresponds to the amount o cells migrating: higher fluorescence indicates greater cell migration. Error bars show the standard error of the mean.

Cell migration *in vivo* and fate of IV injected Mptb

The results as shown in Figure 2 suggest that it is not feasible to track *ex vivo* CFSE labelled cells reintroduced into the blood circulatory system as very few CFSE labelled cells could be detected in the blood or lymph nodes examined.

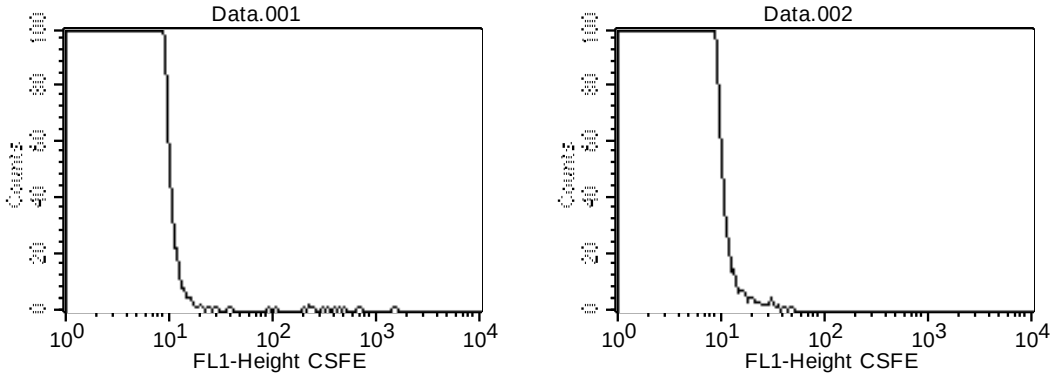

Figure 2. FACS analysis of the blood samples from an animal with injected CFSE labelled cells (Data.001) and from an animal with no labelled CFSE cells (Data.002). The Y axis represents the number of cells counted while the X axis represents fluorescent intensity of the cell. In this case most of the cells are negative for CFSE (ie below 10^1 on the x axis).

Results from the histology and tissue culture (Table 1) of the 5 sheep showed that the animals given the CFSE labelled cells only did not have any *M.ptb*. Tissue culture results indicate the sheep which received white blood cells infected with the *M.ptb* (CFSE labelled cells infected with *M.ptb*) compared to those that had *M.ptb* intravenously injected had a similar pattern of *M.ptb* tracking. The

only tissue in which a difference could be detected between the two treatments was the hepatic lymph node, to which *M.ptb* within white blood cells moved but not when the *M.ptb* was injected directly into the blood. Numerous tissues were found to be free from *M.ptb* infection these included all the gut associated tissues and mammary tissue, kidney and heart.

Table 1: Tissues found to have *M.ptb* present after necropsy of five sheep

Sheep	1	2	3	4	5
Treatment	CFSE labelled cells - no *M.ptb*	CFSE labelled cells infected with *M.ptb*	CFSE labelled cells infected with *M.ptb*	IV injection with *M.ptb*	IV injection with *M.ptb*
Hepatic LN*		+	+		
Mediastinal LN		+	+	+	+
Retropharyngeal LN				+	+
Popliteal LN			+		
Prescapular LN			+	+	+
Supramammary LN				+	+
Liver		+		+	+
Spleen		+	+	+	+
Lung		+	+	+	+

* LN = Lymph node

M. ptb was recovered from the blood by culture in all infected sheep at 1 and 2 days post inoculation, and 3 of the 4 infected sheep at 3 days post inoculation (Table 2).

Table 2: Blood samples found to have *M.ptb* present by culture

Blood sample	CFSE labelled cells No *M.ptb*	CFSE labelled cells Infected with *M.ptb*	CFSE labelled cells Infected with *M.ptb*	IV injection With *M.ptb*	5 IV injection With *M.ptb*
Day 1		+	+	+	+
Day 2		+	+	+	+
Day 3		+		+	+

Discussion

The *in vitro* cell movement experiment provided a surprise result with the inhibition of the sheep white blood cell migration by fetal calf serum (FCS). This inhibition of migration was overcome by infection of the cells with *M.ptb*, indicating the infected cells produced the factors required to restore cell migration. The movement of cells with or without *M.ptb* infection was the same in the other treatments. This indicates that infection or that the factors released into plasma after *M.ptb* stimulation does not induce migration of sheep white blood cells.

The *in vivo* cell movement experiment was a small scale study, which was designed to track both the peripheral blood mononuclear cells (PBMC) and *M.ptb*. The five animals were split into three treatment groups. PBMCs were removed from one sheep and labelled with a dye (CFSE) then were injected intravenously back into the same animal. PBMCs were removed from another two sheep, labelled with CFSE and infected with *Mpt* and then reinjected intravenously. The last group of two sheep was infected intravenously with *M.ptb* only. This experimental design allowed the possible tracking of the CFSE labelled PBMCs to different lymph nodes and in the blood by FACs analysis and to identify where the *M.ptb* moved to in the body by culture of the bacteria from tissues. The design would also identify whether infected PBMCs track to different places in the body compared to “naked” bacteria.

The FACS analysis of the white blood cells labelled with CFSE showed the cells did not go to any particular place in the body. There were very few CFSE labelled cells detected in any of the tissues examined. A dilution effect is responsible for this. From the 200 ml sample of blood we removed from each of the sheep it was possible to inject 1.4×10^8 CFSE labelled PBMCs. In each litre of blood the normal range of white blood cells is $4\text{-}12 \times 10^9$ and in a 40 Kg animal as used in this experiment there would be an estimated 3.2 litres of blood. This means the number of CFSE labelled cells was very low compared to the total number of white blood cells in the animal. Unless *M.ptb* caused migration to a specific lymph node (which it did not) it was unlikely that the cells could be detected.

Tissue culture and histology indicated that only the hepatic lymph node could be used to detect differences between animals injected with *M.ptb* intravenously or those which had infected white blood cells reintroduced. Surprisingly the gut was found to be free of infection. This is the site of the natural infection so it was expected the white blood cells would traffic there especially as experimental infections via the intravenous route have resulted in disease formation in the gut (Brotherston et al., 1961). The result also shows that when *M.ptb* gains access to the blood (Koenig et al., 1993; Gwozdz et al., 1997; Gwozdz et al., 2000; Barrington et al., 2003; Buergelt and Williams, 2004; Juste et al., 2005) it may traffic to many tissues within the animal allowing for detection of the bacteria as has been seen in previous research.

References

Ayele, W. Y., Bartos, M., Svastova, P. and Pavlik, I. 2004. Distribution of Mycobacterium avium subsp. paratuberculosis in organs of naturally infected bull-calves and breeding bulls. Vet Microbiol 103, 209-17.

Barrington, G. M., Gay, J. M., Eriks, I. S., Davis, W. C., Evermann, J. F., Emerson, C., O'Rourke, J. L., Hamilton, M. J. and Bradway, D. S. 2003. Temporal patterns of diagnostic results in serial samples from cattle with advanced paratuberculosis infections. J Vet Diagn Invest 15, 195-200.

Brotherston, J. G., Gilmour, N. J. and Samuel, J. 1961. Quantitative Studies of *Mycobacterium johnei* in the Tissues of Sheep. Journal of Comparative Pathology 71, 286 - 299.

Buergelt, C. D. and Williams, J. E. 2004. Nested PCR on blood and milk for the detection of Mycobacterium avium subsp paratuberculosis DNA in clinical and subclinical bovine paratuberculosis. Aust Vet J 82, 497-503.

Gwozdz, J. M., Reichel, M. P., Murray, A., Manktelow, W., West, D. M. and Thompson, K. G. 1997. Detection of *Mycobacterium avium* subsp. *paratuberculosis* in ovine tissues and blood by the polymerase chain reaction. Veterinary Microbiology 57, 233-44.

Gwozdz, J. M., Thompson, K. G., Murray, A., West, D. M. and Manktelow, B. W. 2000. Use of the polymerase chain reaction assay for the detection of *Mycobacterium avium* subspecies *paratuberculosis* in blood and liver biopsies from experimentally infected sheep. Australian Veterinary Journal 78, 622-4.

Juste, R. A., Garrido, J. M., Geijo, M., Elguezabal, N., Aduriz, G., Atxaerandio, R. and Sevilla, I. 2005. Comparison of blood polymerase chain reaction and enzyme-linked immunosorbent assay for detection of Mycobacterium avium subsp. paratuberculosis infection in cattle and sheep. J Vet Diagn Invest 17, 354-9.

Koenig, G. J., Hoffsis, G. F., Shulaw, W. P., Bech-Nielsen, S., Rings, D. M. and St-Jean, G. 1993. Isolation of Mycobacterium paratuberculosis from mononuclear cells in tissues, blood, and mammary glands of cows with advanced paratuberculosis. Am J Vet Res 54, 1441-5.

Lambeth, C., Reddacliff, L. A., Windsor, P., Abbott, K. A., McGregor, H. and Whittington, R. J. 2004. Intrauterine and transmammary transmission of Mycobacterium avium subsp paratuberculosis in sheep. Aust Vet J 82, 504-8.

Marsh, I. B., Bannantine, J. P., Paustian, M. L., Tizard, M. L., Kapur, V. and Whittington, R. J. 2006. Genomic comparison of Mycobacterium avium subsp. paratuberculosis sheep and cattle strains by microarray hybridization. J Bacteriol 188, 2290-3.

Marsh, I. B. and Whittington, R. J. 2007. Genomic diversity in Mycobacterium avium: single nucleotide polymorphisms between the S and C strains of M. avium subsp. paratuberculosis and with M. a. avium. Mol Cell Probes 21, 66-75.

Reddacliff, L. A., Nicholls, P. J., Vadali, A. and Whittington, R. J. 2003. Use of Growth Indices from Radiometric Culture for Quantification of Sheep Strains of *Mycobacterium avium* subsp. *paratuberculosis*. Applied and Environmental Microbiology 69, 3510-6.

Whittington, R., Marsh, I., Choy, E. and Cousins, D. 1998a. Polymorphisms in IS1311, an insertion sequence common to Mycobacterium avium and M. avium subsp. paratuberculosis, can be used to distinguish between and within these species. Mol Cell Probes 12, 349-58.

Whittington, R. J., Marsh, I., McAllister, S., Turner, M. J., Marshall, D. J. and Fraser, C. A. 1999. Evaluation of modified BACTEC 12B radiometric medium and solid media for culture of *Mycobacterium avium* subsp. *paratuberculosis* from sheep. Journal of Clinical Microbiology 37, 1077-83.

Whittington, R. J., Marsh, I., Turner, M. J., McAllister, S., Choy, E., Eamens, G. J., Marshall, D. J. and Ottaway, S. 1998b. Rapid detection of Mycobacterium paratuberculosis in clinical samples from ruminants and in spiked environmental samples by modified BACTEC 12B radiometric culture and direct confirmation by IS900 PCR. J Clin Microbiol 36, 701-7.

9.26 Appendix 4B-2 Subprogram 4 Development of a QPCR assay for blood samples

Introduction

As there may be technical difficulties with routine culture of Mptb from blood, a real time quantitative PCR assay (QPCR) was also developed. A number of QPCR assay formats were assessed for analytical sensitivity and specificity. These assays utilized the *M. paratuberculosis* specific sequences: IS*900*, IS*mav2*, f57, and IS*MAP2.*

Materials & Methods

Analytical sensitivity and specificity

An IS*900* Taqman assay (IS*900*T) was developed to attempt to exclude the organisms containing IS*900*-like sequences. The Sweden strain, Strain 2333, which contains a IS*900*-like sequence with 94% homology was detected with this assay. The Strain 2333 sequence was homologous with the K10 strain sequence at the primer and probe site for this assay. An Australian mycobacterial isolate containing an IS*900*-like sequence (P99-4609 AgWA D Cousins) was also detected using this assay; however no sequence data was available for this isolate. An IS*900* SYBR Green assay developed in Japan, (RT-J) was also assessed. The RT-J assay reliably detected 1 fg of genomic DNA and was specific for all isolates tested.

SYBR assays were developed for the IS*mav2*, f57, and IS*MAP2* sequences. The IS*mav2* assay produced non specific amplification with a number of isolates tested. The IS*mav2*B assay detected 10fg of genomic DNA and was specific with all isolates tested. The f57 assay detected 100fg of genomic DNA and was specific with all isolates tested. The f57B assay detected 10fg genomic DNA and was specific with all isolates tested. The IS*MAP2* assay detected 10fg of genomic DNA and detected 3 non-*M. ptb* isolates; *M. parafortuitum* ATCC 19686; *M. scrofulaceum* ATCC 19981; and *M. avium* St 16 (serovar 6).

The IS*mav2*B, f57B and IS*MAP2* were designed to allow for multiplexing with the RT-J assay in a Taqman assay.

These results are summarised in Table 1.

Table 1: Specificity of QPCR assays and conventional P90-91 PCR tested using IS*900*-like isolates and other Mycobacterial species.

Isolate	P90-91	IS*900*T	RT-J	IS*mav2*	IS*mav2*B	f57	f57B	IS*MAP2*
M.paratuberculosis -316V	+	+	+	+	+	+	+	+
Mycobacterium sp AM1 (AgWA)	+	-	-	+	-	-	-	-
Mycobacterium sp AM3 (AgWA)	+	-	-	+	-	-	-	-
Mycobacterium sp AM4 (AgWA)	+	-	-	+	-	-	-	-
Mycobacterium sp AM5 (AgWA)	+	-	-	+	-	-	-	-
M. scrofulaceum-like CM97/1703/1 (VIAS)	+	-	-	+	-	-	-	-
M. scrofulaceum-like CM97/1703/2 (VIAS)	+	-	-	+	-	-	-	-
Mycobacterium sp IWGMT90236 (Qld Health)	+	-	-	+	-	-	-	-
Mycobacterium sp JD00/266 (VIAS)	+	-	-	+	-	-	-	-
Mycobacterium sp P99-4609 (AgWA)	+	+	-	+	-	-	-	-
Mycobacterium sp Strain 2333 (Sweden)	+	+	-	+	-	-	-	-
M. chitae ATCC 19627	ND	-	-	ND	-	-	-	-
M. flavescens ATCC 14474	ND	-	-	ND	-	-	-	-
M. gordonae ATCC 14470	ND	-	-	ND	-	-	-	-
M. intracellulare ATCC 13950	ND	-	-	ND	-	-	-	-
M. kansasii ATCC 12478	ND	-	-	ND	-	-	-	-
M. nonchromogenicum ATCC 19530	ND	-	-	ND	-	-	-	-
M. parafortuitum ATCC 19686	ND	-	-	ND	-	-	-	+
M. pheli ATCC 11758	ND	-	-	ND	-	-	-	-
M. scrofulaceum ATCC 19981	ND	-	-	ND	-	-	-	+
M. terrae ATCC 15755	ND	-	-	ND	-	-	-	-
M. thermoresistibile ATCC 23292	ND	-	-	ND	-	-	-	-
M. avium TMC 715	ND	-	-	ND	-	-	-	-
M. avium St 1 (serovar 1)	ND	-	-	ND	-	-	-	-
M. avium St 9 (serovar 11)	ND	-	-	ND	-	-	-	-
M. avium St 11 (serovar 21)	ND	-	-	ND	-	-	-	-
M. avium St 12 (serovar 10)	ND	-	-	ND	-	-	-	-
M. avium St 15 (serovar 5)	ND	-	-	ND	-	-	-	-
M. avium St 16 (serovar 6)	ND	-	-	ND	-	-	-	+
M. avium St 18 (serovar 9)	ND	-	-	ND	-	-	-	-
M. avium St 19 (serovar 2)	ND	-	-	ND	-	-	-	-
M. avium St 26 (serovar 3)	ND	-	-	ND	-	-	-	-
M. avium St 29 (serovar 8)	ND	-	-	ND	-	-	-	-

Table 2 Analytical Sensitivity using 316V genomic DNA

Assay	Analytical Sensitivity (fg)
IS*900*T	10
RT-J	1
IS*mav2*	10
IS*mav2* B	10
f 57	100
f 57 B	10
IS*MAP2*	10

Extraction of *M. ptb* DNA from Blood

Commercial and in-house DNA extraction methods were compared using a suspension of *M. ptb* enumerated using the Helber visual method.

Comparison of different extraction methods applied to spiked Buffy Coat samples - Preliminary Study

Two types of protocols were compared:

1. Easy DNA, QIAamp DNA Mini Kit and Boiling/Freezing
2. PLG tubes as described by Naser et al., 2004.

The PLG method failed to amplify any product on conventional PCR. The other methods amplified product with 10 000 and 1000 *M. ptb* added. All samples produced a large amount of DNA assumed to have originated from the white blood cells. This DNA was suspected of inhibiting the PCR, thus decreasing the sensitivity of detecting *M. ptb*.

Bacterial suspension extractions

A number of methods including mechanical lysis by the fast prep method and boiling were compared using 10^4 and 10^2 *M. ptb* added. The results are summarised in Table 1.

Table 3. Summary of extraction methods from bacterial suspensions. Conventional PCR results are given indicating the presence and intensity (trace to 4+) of the band. QPCR results are shown with the number of cycles (Ct) at which the threshold florescence is crossed. The lower the Ct the more effective the extraction method.

M.ptb added	10^4		10^2	
Method	PCR	QPCR Ct	PCR	QPCR Ct
Easy DNA	2+	25.9	-ve	30.74
QIAamp DNA Mini Kit	3+	24.2	-ve	30.36
Boiled Lysate	2+	26.4	trace	29.02*
Fast Prep +Qiagen	1+	28.9	ND	
Fast Prep	3+	no Ct	2+	25.91
Microlysis	trace	38.8	ND	

*Tm (melting temperature on dissociation curve) different to +ve control

The Fast Prep mechanical lysis method was the most effective method in this experiment, so all further work was conducted using this method and the commercially available mechanical lysis method, Johne Prep, which also uses mechanical lysis.

The commercially available Johne Prep method was more repeatable than the Fast Prep method with similar sensitivity; both detecting 10 organisms enumerated using the Helber visual method.

Removal of Somatic DNA

Two published methods for removing excess white blood cells from buffy coat preps prior to extraction and amplification of mycobacterial DNA were compared with no processing to remove white blood cell DNA.

Method A, (Roth et al., 1999), involved a 10min incubation at 56°C with Proteinase K in 1% Triton X-100 followed by washing with Tris HCL. This resulted in good reduction in the size of the cell pellet.

Method B,(Restrepo et al., 2006) used a WBC lysis buffer which did not reduce the size of the cell pellet.

Method C, there was no additional step to remove WBC DNA. The results are shown in Figure 1.

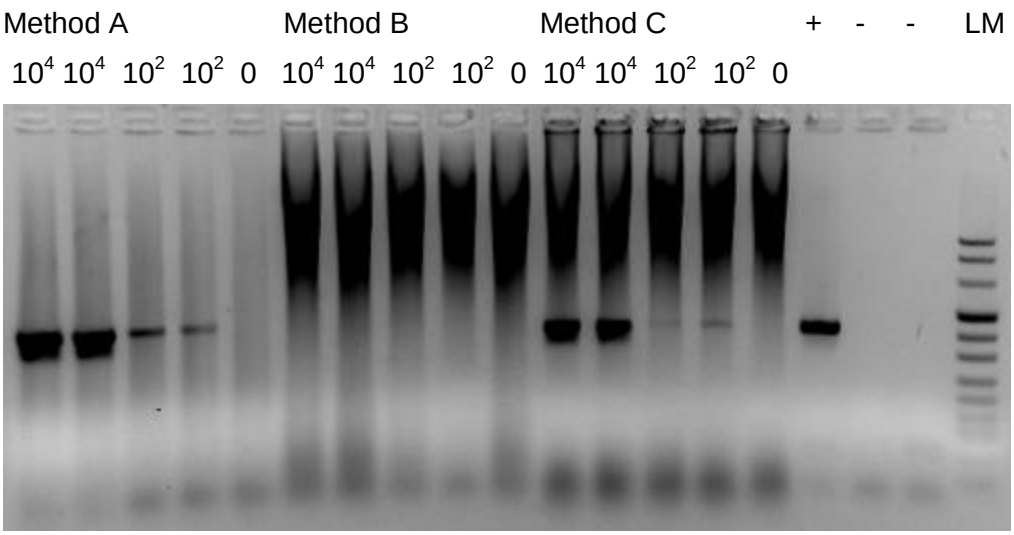

Figure 1. Lanes 1-5 were processed using method A, lanes 6-10 were processed using Method B, lanes 11-15 were processed using Method C, lane 16 is PCR +ve control and lanes 17 and 18 and PCR –ve controls, lane 19 is LMVIII(Roche). Lanes 1,2,6,7,11, and 12 had 10^4 mycobacteria added prior to processing, lanes 3,4,8,9,13, and 14 had 10^2 mycobacteria added prior to processing, and lanes 5, 10, and 15 were –ve process controls.

The large black smear visible at the top of lanes 6-15 indicate a large amount of non specific DNA, in this case the WBC DNA. This is visibly reduced in method A.

Further experiments found that a concentration of 0.1%Trition X-100 was more effective than 1% Trition X-100. The incubation time was extended to 30mins.

Conclusion

A method for processing blood to detect *M. ptb* DNA has been optimised, including processing, extraction and amplification. This method can detect 10 organisms in 10 mls of blood. This method is now available for application to stored samples from animal trials. However, it needs to be compared to a gold standard test; the most appropriate test is culture. As the results of culture using BACTEC suggest that the rate of bacteraemia in sheep is very low, except perhaps at the end of the disease process, additional samples need to be acquired in order to validate the PCR test as it is applied to blood samples. When this has been done the test can be evaluated in archived samples to determine whether it is capable of detecting circulating M. ptb that are not apparent to culture-based methods.

References

Naser, S. A., Ghobrial, G., Romero, C. and Valentine, J. F. (2004) *Lancet,* **364,** 1039-44.

Restrepo, B. I., Gomez, D. I., Shipley, G. L., McCormick, J. B. and Fisher-Hoch, S. P. (2006) *J Microbiol Methods,* **67,** 220-9.

Roth, A., Fischbach, F., Arasteh, K. N., Futh, U. and Mauch, H. (1999) *Scand J Infect Dis,* **31,** 393-8.